NOTES TO POLARIZATION STUDIES

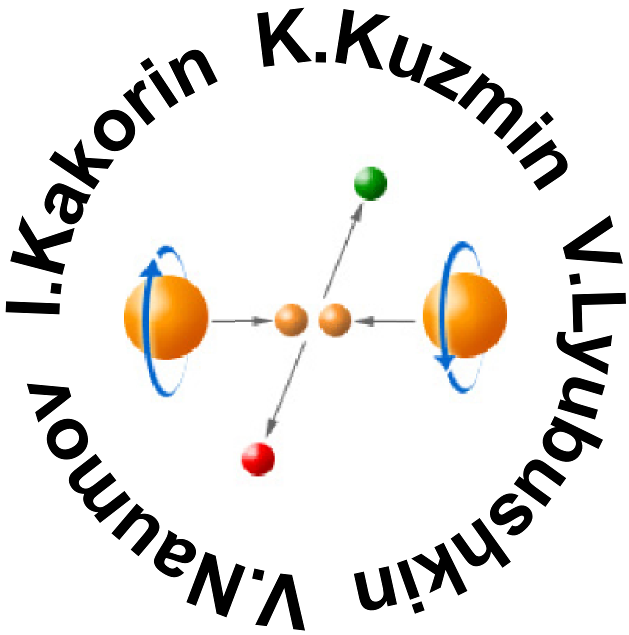

13/03/2022

JINR, Dubna

These haphazard notes (= drafts) were written long ago and are for internal use only. In the present form and for the time being, the notes are mainly needed to refer to some results that we have not published (and probably never will publish) but are used in the codes within the GENIE project. Some sections are partially outdated and will be updated as needed.

FOR INTERNAL USE!

Contents

List of Figures

List of Tables

Chapter 1

Mean lepton polarization

1.1 Lepton polarization vector

The lepton polarization vector $\boldsymbol{\mathcal{P}} = (\mathcal{P}_1, \mathcal{P}_2, \mathcal{P}_3)$ is defined through the polarization density matrix

$$\frac{d^2\boldsymbol{\sigma}_{\nu\to\ell}}{dE_\ell d\cos\theta} = \frac{1}{2}\left(1+\boldsymbol{\sigma}\boldsymbol{\mathcal{P}}\right)\frac{d^2\sigma_{\nu\to\ell}}{dE_\ell d\cos\theta} \tag{1.1}$$

whose matrix elements are given by contracting the leptonic tensor $L_{\alpha\beta}^{\lambda\lambda'}$ with the spin-averaged hadronic tensor $W^{\alpha\beta}$,

$$\frac{d^2\sigma_{\nu\to\ell}^{\lambda\lambda'}}{dE_\ell d\cos\theta} = \frac{G_F^2 P_\ell \kappa^2}{4\pi M E_\nu} L_{\alpha\beta}^{\lambda\lambda'} W^{\alpha\beta}. \tag{1.2}$$

Here $d^2\sigma_{\nu\to\ell}/dE_\ell d\cos\theta$ is the differential cross section for *unpolarized* lepton production in νN collisions. Both $d^2\boldsymbol{\sigma}_{\nu\to\ell}/dE_\ell d\cos\theta$ and $d^2\sigma_{\nu\to\ell}/dE_\ell d\cos\theta$ are defined for each subprocess – QES, RES, DIS, or for the sum over all three subprocesses (QES+RES+DIS) – subject to circumstances. According to Eq. (1.1), the *perpendicular* ($\mathcal{P}_1$), *transverse* ($\mathcal{P}_2$), and *longitudinal* ($\mathcal{P}_3$) components of the polarization vector are given by

$$\begin{aligned}
\mathcal{P}_1 \equiv \mathcal{P}_P &= \quad \rho_{+-} + \rho_{-+} \quad = \frac{d^2\sigma_{\nu\to\ell}^{+-} + d^2\sigma_{\nu\to\ell}^{-+}}{d^2\sigma_{\nu\to\ell}}, \\
\mathcal{P}_2 \equiv \mathcal{P}_T &= i\left(\rho_{+-} - \rho_{-+}\right) = i\,\frac{d^2\sigma_{\nu\to\ell}^{+-} - d^2\sigma_{\nu\to\ell}^{-+}}{d^2\sigma_{\nu\to\ell}}, \\
\mathcal{P}_3 \equiv \mathcal{P}_L &= \quad \rho_{++} - \rho_{--} \quad = \frac{d^2\sigma_{\nu\to\ell}^{++} - d^2\sigma_{\nu\to\ell}^{--}}{d^2\sigma_{\nu\to\ell}},
\end{aligned}$$

where $\rho_{\lambda\lambda'}$ are defined by

$$\boldsymbol{\rho} = \begin{pmatrix} \rho_{++} & \rho_{+-} \\ \rho_{-+} & \rho_{--} \end{pmatrix} = \frac{1}{2}\left(1+\boldsymbol{\sigma}\boldsymbol{\mathcal{P}}\right),$$

and

$$d^2\sigma_{\nu\to\ell} = d^2\sigma_{\nu\to\ell}^{++} + d^2\sigma_{\nu\to\ell}^{--}.$$

Clearly $d^2\sigma_{\nu\to\ell}^{++}/dE_\ell d\cos\theta$ ($d^2\sigma_{\nu\to\ell}^{--}/dE_\ell d\cos\theta$) is the cross section for production of right (left) handed lepton. Since the components $\mathcal{P}_i$ (as well as the cross section for unpolarized lepton production) must be real, we have

$$\begin{aligned}
&\mathrm{Im}\, d^2\sigma_{\nu\to\ell}^{++} = \mathrm{Im}\, d^2\sigma_{\nu\to\ell}^{--} = 0, \\
&\mathrm{Re}\, d^2\sigma_{\nu\to\ell}^{+-} = \mathrm{Re}\, d^2\sigma_{\nu\to\ell}^{-+}, \\
&\mathrm{Im}\, d^2\sigma_{\nu\to\ell}^{+-} = -\mathrm{Im}\, d^2\sigma_{\nu\to\ell}^{-+}.
\end{aligned}$$

Taking account for these equations and the condition

$$0 \le \mathcal{P}^2 = \mathcal{P}_1^2 + \mathcal{P}_2^2 + \mathcal{P}_3^2 \le 1$$

yields the following inequalities:

$$0 \le d^2\sigma_{\nu\to\ell}^{++} d^2\sigma_{\nu\to\ell}^{--} - \left|d^2\sigma_{\nu\to\ell}^{+-}\right|^2 \le \frac{1}{4}\left(d^2\sigma_{\nu\to\ell}^{++} + d^2\sigma_{\nu\to\ell}^{--}\right)^2,$$

providing a useful numerical test.

NOTE I: Once more: $\mathcal{P}_L$ and $\mathcal{P}_P$ are the components of $\boldsymbol{\mathcal{P}}$ parallel to $\mathbf{p}_\ell$ and perpendicular to $\mathbf{p}_\ell$ in the production plane, while $\mathcal{P}_T$ is perpendicular to the production plane. Why this is so? Let us show that $\boldsymbol{\rho}$ is actually the polarization density matrix. First, we remind ourselves that $\frac{1}{2}\sigma_i$ are the operators of the lepton spin projections and therefore, taking into account that

$$\text{Tr}\,(\boldsymbol{\rho}) = 1 \quad \text{and} \quad [\sigma_i, \sigma_j]_+ = 2\delta_{ij},$$

we have

$$\text{Tr}\left(\boldsymbol{\rho}\frac{\sigma_i}{2}\right) = \frac{\mathcal{P}_i}{2}.$$

that is $\mathcal{P}_i$ are indeed the components of the lepton polarization vector defined relative to the lepton momentum. Note also that the density matrix $\boldsymbol{\rho}$ is relativistic covariant, since the ratios $d^2\sigma^{\lambda\lambda'}_{\nu\to\ell}/d^2\sigma_{\nu\to\ell}$ are the ratios of tensor convolutions. Moreover,

$$\langle\mathcal{P}^2\rangle = (\boldsymbol{\sigma}\boldsymbol{\mathcal{P}})^2 = \mathcal{P}_1^2 + \mathcal{P}_2^2 + \mathcal{P}_3^2 \equiv \mathcal{P}^2$$

is a relativistic scalar.

NOTE II: Let us denote $\boldsymbol{\mathcal{P}} = \mathcal{P}\boldsymbol{\xi}$, where $\boldsymbol{\xi} = \left(\xi_1, \xi_2, \xi_3\right)$ is a unit (pseudo)vector. In order to understand its transformation properties we introduce the axial 4-vector $s = (s_0, \mathbf{s})$ whose spatial component, $\mathbf{s}$, coincides with the vector $\boldsymbol{\xi}$ in the lepton rest frame (LRF). Below, we will mark that frame by symbol *; then, by definition, $\mathbf{s}^\star = \boldsymbol{\xi}^\star$. Since the scalar product of the polar 4-vector p and the axial 4-vector s must vanish,

$$sp = s_0 E_\ell - \mathbf{s}\mathbf{p}_\ell = 0 \quad \text{or} \quad s_0 = \frac{\mathbf{s}\mathbf{p}_\ell}{E_\ell}.$$

Therefore

$$s_0^\star = 0 \quad \text{and} \quad s^2 = (s^\star)^2 = -\left(\boldsymbol{\xi}^\star\right)^2 = -1.$$

Let us now represent the 3-vector $\mathbf{s}$ in the form

$$\mathbf{s} = \boldsymbol{\xi} + \alpha\left(\boldsymbol{\xi}\mathbf{p}_\ell\right)\mathbf{p}_\ell,$$

where α is an unknown function. According to the above relations it satisfies the equation

$$m_\ell^2 P_\ell^2 \alpha^2 + 2m_\ell^2\alpha - 1 = 0$$

which has two solutions,

$$\alpha_\pm = \frac{\pm 1}{m_\ell\left(E_\ell \pm m_\ell\right)}.$$

Only one of these solutions (α_+) provides the condition $\mathbf{s}^\star = \boldsymbol{\xi}^\star$. Indeed,

$$\alpha_-\left(\boldsymbol{\xi}\mathbf{p}_\ell\right)\mathbf{p}_\ell = -\left(\boldsymbol{\xi}\mathbf{n}_\ell\right)\left(E_\ell/m_\ell + 1\right)\mathbf{n}_\ell$$

(where $\mathbf{n}_\ell = \mathbf{p}_\ell/|\mathbf{p}_\ell|$) does not vanish as $P_\ell \equiv |\mathbf{p}_\ell| \to 0$ while

$$\alpha_+\left(\boldsymbol{\xi}\mathbf{p}_\ell\right)\mathbf{p}_\ell = \left(\boldsymbol{\xi}\mathbf{n}_\ell\right)\left(E_\ell/m_\ell - 1\right)\mathbf{n}_\ell \to 0$$

as $P_\ell \to 0$. Finally we arrive at the well-known formula for the components of the spin 4-vector:

$$\mathbf{s} = \boldsymbol{\xi} + \frac{\left(\boldsymbol{\xi}\mathbf{p}_\ell\right)\mathbf{p}_\ell}{m_\ell\left(E_\ell + m_\ell\right)}, \quad s_0 = \frac{\left(\boldsymbol{\xi}\mathbf{p}_\ell\right)}{m_\ell}.$$

An obvious while very important feature of the vector $\boldsymbol{\xi}$ is in its invariance relative to Lorentz boosts. Indeed, the boost from LRF to lab. frame gives

$$s_3 = \frac{E_\ell}{m_\ell}\,\xi_3^\star, \quad s_{1,2} = \xi_{1,2}^\star.$$

On the other hand,

$$s_3 = \xi_3 + \frac{\xi_3 P_\ell^2}{m_\ell\left(E_\ell + m_\ell\right)} = \frac{E_\ell}{m_\ell}\,\xi_3, \quad s_{1,2} = \xi_{1,2}.$$

Therefore

$$\boldsymbol{\xi} = \boldsymbol{\xi}^\star.$$

This *does not mean* at all that $\boldsymbol{\xi}$ is invariant relative to *any* Lorentz transformation. Let us consider, for example, a spatial rotation given by a 3×3 matrix $\mathbf{T}$. Under such a transformation,

$$\mathbf{s} \mapsto \mathbf{s}' = \mathbf{T}\mathbf{s} = \mathbf{T}\boldsymbol{\xi} + \frac{\left(\boldsymbol{\xi}\mathbf{p}_\ell\right)\mathbf{T}\mathbf{p}_\ell}{m_\ell\left(E_\ell + m_\ell\right)}.$$

On the other hand,

$$\mathbf{s}' = \boldsymbol{\xi}' + \frac{\left(\boldsymbol{\xi}'\mathbf{p}'_\ell\right)\mathbf{p}'_\ell}{m_\ell\left(E'_\ell + m_\ell\right)}.$$

Since

$$E'_\ell = E_\ell, \quad \mathbf{p}'_\ell = \mathbf{T}\mathbf{p}_\ell, \quad \text{and} \quad \boldsymbol{\xi}\mathbf{p}'_\ell = \boldsymbol{\xi}\mathbf{T}\mathbf{p}_\ell = \mathbf{T}^T\boldsymbol{\xi}\mathbf{p}_\ell,$$

we have

$$\boldsymbol{\xi} \mapsto \boldsymbol{\xi}' = \mathbf{T}\boldsymbol{\xi}.$$

Therefore $\boldsymbol{\xi}$ and $\mathbf{p}_\ell$ are transformed similar way and thus $\boldsymbol{\xi}\mathbf{p}_\ell$ is invariant. It is also clear that vector $\boldsymbol{\xi}$ will be (in general) transformed by a superposition of a spatial rotation and Lorentz boost.

1.2 Lepton generation functions

Let us now introduce two *generation functions*

$$G_\ell^\pm\left(E_\ell,\vartheta_\ell,\varphi_\ell,h\right)=\frac{1}{\lambda_\nu\left(E_\ell\right)}\int dE_\nu d\cos\vartheta_\nu d\varphi_\nu W_{\nu\to\ell}^\pm\left(E_\nu,E_\ell,\theta\right)\mathit{\Phi}_\nu\left(E_\nu,\vartheta_\nu,\varphi_\nu,h\right) \tag{1.3}$$

which enter into the full transport equations and describe production of fully polarized leptons with helicity ±1. Here $\mathit{\Phi}_\nu\left(E_\nu,\vartheta_\nu,\varphi_\nu,h\right)$ is the neutrino differential energy spectrum along the direction defined by the *nadir* angle ϑ_ν and *azimuthal* angle φ_ν on the oblique depth h (a function of ϑ_ν); λ_ν is the neutrino interaction length; and the functions $W_{\nu\to\ell}^\pm\left(E_\nu,E_\ell,\theta\right)$ are defined by

$$W_{\nu\to\ell}^+\left(E_\nu,E_\ell,\theta\right)\equiv\frac{d^3N_{\nu\to\ell}^+\left(E_\nu,E_\ell,\theta\right)}{dE_\ell d\cos\vartheta_\ell d\varphi_\ell}=\frac{1}{2\pi\sigma_{\nu N}^{\rm tot}\left(E_\ell\right)}\left[\frac{d^2\sigma_{\nu\to\ell}^{++}\left(E_\nu,E_\ell,\theta\right)}{dE_\ell d\cos\theta}\right], \tag{1.4a}$$

$$W_{\nu\to\ell}^-\left(E_\nu,E_\ell,\theta\right)\equiv\frac{d^3N_{\nu\to\ell}^-\left(E_\nu,E_\ell,\theta\right)}{dE_\ell d\cos\vartheta_\ell d\varphi_\ell}=\frac{1}{2\pi\sigma_{\nu N}^{\rm tot}\left(E_\ell\right)}\left[\frac{d^2\sigma_{\nu\to\ell}^{--}\left(E_\nu,E_\ell,\theta\right)}{dE_\ell d\cos\theta}\right]. \tag{1.4b}$$

NOTE III: Let $\mathbf{x}$ be a n dimensional vector and $\mathbf{T}$ be a linear and unimodular transformation: $\mathbf{x}'=\mathbf{T}\mathbf{x}$, $\det\mathbf{T}=1$. Then

$$\prod_i dx_i'=\frac{\partial\left(x_1',\ldots,x_n'\right)}{\partial\left(x_1,\ldots,x_n\right)}\prod_i dx_i.$$

Since

$$\frac{\partial\left(x_1',\ldots,x_n'\right)}{\partial\left(x_1,\ldots,x_n\right)}=\det\left\|\frac{\partial x_i'}{\partial x_j}\right\|=\det\left\|T_{ij}\right\|=1,$$

the differential form $\prod dx_i$ is invariant by the $\mathbf{T}$ transformation:

$$\prod_i dx_i'=\prod_i dx_i.$$

This is in particular true for any $3D$ rotation and hence $d\cos\vartheta_\ell d\varphi_\ell=d\cos\theta d\psi$, where ψ is the azimuthal angle of the lepton momentum in the frame whose z axis is directed along the neutrino momentum. Eqs. (1.4) therefore holds true considering that the elements of the polarization density matrix are independent of the angle ψ.

The sum

$$G_\ell\left(E_\ell,\vartheta_\ell,\varphi_\ell,h\right)=G_\ell^+\left(E_\ell,\vartheta_\ell,\varphi_\ell,h\right)+G_\ell^-\left(E_\ell,\vartheta_\ell,\varphi_\ell,h\right) \tag{1.5}$$

then defines the generation function for unpolarized leptons and (as we shall show later on) the ratio

$$\langle\mathbf{n}_\ell\boldsymbol{\mathcal{P}}\rangle\equiv\langle\mathcal{P}_3\rangle=\frac{G_\ell^+\left(E_\ell,\vartheta_\ell,\varphi_\ell,h\right)-G_\ell^-\left(E_\ell,\vartheta_\ell,\varphi_\ell,h\right)}{G_\ell^+\left(E_\ell,\vartheta_\ell,\varphi_\ell,h\right)+G_\ell^-\left(E_\ell,\vartheta_\ell,\varphi_\ell,h\right)} \tag{1.6}$$

defines the mean longitudinal lepton polarization.

1.3 New angular variables

The integration in the right side of Eq. (1.3) is over the kinematically allowed range. Clearly in terms of the angles ϑ_ν and φ_ν it is quite intricate. But we can essentially simplify the integration by an appropriate change of variables. Let us consider this change carefully in order to avoid misunderstanding.

The momenta of neutrino ν_ℓ and lepton ℓ in lab. frame (K) are written as

$$\mathbf{p}_\nu=|\mathbf{p}_\nu|\begin{pmatrix}\sin\vartheta_\nu\cos\varphi_\nu\\ \sin\vartheta_\nu\sin\varphi_\nu\\ \cos\vartheta_\nu\end{pmatrix},\quad \mathbf{p}_\ell=|\mathbf{p}_\ell|\begin{pmatrix}\sin\vartheta_\ell\cos\varphi_\ell\\ \sin\vartheta_\ell\sin\varphi_\ell\\ \cos\vartheta_\ell\end{pmatrix},$$

where ϑ_ν and ϑ_ℓ are the *nadir* angles, and φ_ν and φ_ℓ are the *azimuthal* angles (Fig. 1.1). The scattering angle θ (the angle between the vectors $\mathbf{p}_\nu$ and $\mathbf{p}_\ell$) is given by

$$\cos\theta=\sin\vartheta_\nu\sin\vartheta_\ell\cos\left(\varphi_\nu-\varphi_\ell\right)+\cos\vartheta_\nu\cos\vartheta_\ell.$$

Let us define the frame K' whose polar axis z' is directed along the lepton momentum, $\mathbf{p}_\ell$, the x' axis lies in the plane formed by the vector $\mathbf{p}_\ell$ and z axis, and the y' axis is orthogonal to that plane as is schematically shown in Fig. 1.1. The corresponding unit vectors are

$$\mathbf{e}_x'=\begin{pmatrix}\cos\vartheta_\ell\cos\varphi_\ell\\ \cos\vartheta_\ell\sin\varphi_\ell\\ -\sin\vartheta_\ell\end{pmatrix},\quad \mathbf{e}_y'=\begin{pmatrix}-\sin\varphi_\ell\\ \cos\varphi_\ell\\ 0\end{pmatrix},\quad \mathbf{e}_z'=\begin{pmatrix}\sin\vartheta_\ell\cos\varphi_\ell\\ \sin\vartheta_\ell\sin\varphi_\ell\\ \cos\vartheta_\ell\end{pmatrix}.$$

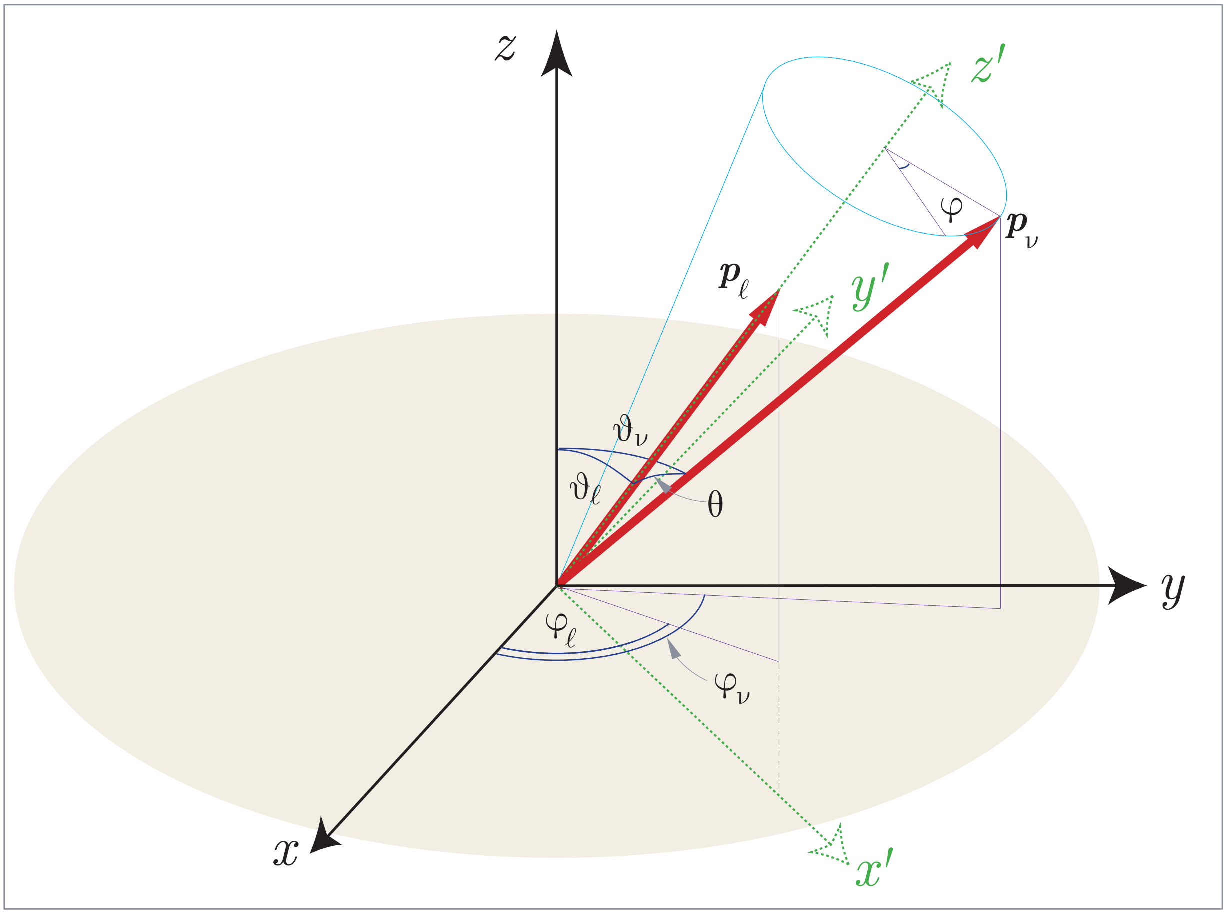

Figure 1.1: Definition of angular variables.

The explicit form of the vectors $\mathbf{e}'_x$ and $\mathbf{e}'_z$ follows directly from their definition while $\mathbf{e}'_y$ is obtained from the relation $\mathbf{e}'_y = \mathbf{e}'_z \times \mathbf{e}'_x$. As is seen, vector $\mathbf{e}'_y$ lies in the (x, y) plane and thus the transformation from K to K' may be described as the anticlockwise rotation with angle φ_ℓ about the z axis and subsequent rotation of the z axis about the new y axis with angle θ.

The transformation matrix from the frame K' to frame K therefore is

$$\mathbf{T} = \left(\mathbf{e}'_x, \mathbf{e}'_y, \mathbf{e}'_z\right) = \begin{pmatrix} \cos\vartheta_\ell \cos\varphi_\ell & -\sin\varphi_\ell & \sin\vartheta_\ell \cos\varphi_\ell \\ \cos\vartheta_\ell \sin\varphi_\ell & \cos\varphi_\ell & \sin\vartheta_\ell \sin\varphi_\ell \\ -\sin\vartheta_\ell & 0 & \cos\vartheta_\ell \end{pmatrix}$$

and the inverse transformation (from K to K') is

$$\mathbf{T}^{-1} = \mathbf{T}^T = \begin{pmatrix} \cos\vartheta_\ell \cos\varphi_\ell & \cos\vartheta_\ell \sin\varphi_\ell & -\sin\vartheta_\ell \\ -\sin\varphi_\ell & \cos\varphi_\ell & 0 \\ \sin\vartheta_\ell \cos\varphi_\ell & \sin\vartheta_\ell \sin\varphi_\ell & \cos\vartheta_\ell \end{pmatrix}.$$

Since $\det \mathbf{T} = 1$, we have

$$d\cos\vartheta_\nu d\varphi_\nu = d\cos\theta d\varphi. \tag{1.7}$$

NOTE IV: This is quite clear from NOTE III (Sect. 1.2, p. 11). However it seems instructive to verify Eq. (1.7) by direct calculation. From Eqs. (1.8) it follows that

$$\begin{pmatrix} \dfrac{\partial\cos\vartheta_\nu}{\partial\theta} & \dfrac{\partial\varphi_\nu}{\partial\theta} \\ \dfrac{\partial\cos\vartheta_\nu}{\partial\varphi} & \dfrac{\partial\varphi_\nu}{\partial\varphi} \end{pmatrix} = \begin{pmatrix} -\cos\vartheta_\ell \sin\theta - \sin\vartheta_\ell \cos\theta \cos\varphi & \dfrac{\sin\vartheta_\ell}{\sin\varphi} - \dfrac{\cos\vartheta_\ell}{\tan\theta \tan\varphi} \\ \sin\vartheta_\ell \sin\theta \sin\varphi & \cos\vartheta_\ell \end{pmatrix}$$

Therefore,

$$\frac{\partial\left(\cos\vartheta_\nu, \varphi_\nu\right)}{\partial\left(\cos\theta, \varphi\right)} = 1 \quad \text{and} \quad d\cos\vartheta_\nu d\varphi_\nu = d\cos\theta d\varphi.$$

The neutrino and lepton momenta in the K' frame are written as

$$\mathbf{p}'_\nu = |\mathbf{p}_\nu| \begin{pmatrix} \sin\theta\cos\varphi \\ \sin\theta\sin\varphi \\ \cos\theta \end{pmatrix}, \quad \mathbf{p}'_\ell = |\mathbf{p}_\ell| \begin{pmatrix} 0 \\ 0 \\ 1 \end{pmatrix}.$$

From equation $\mathbf{p}_\nu = \mathbf{T}\mathbf{p}'_\nu$ we can find the angles ϑ_ν and φ_ν as functions of θ and φ:

$$\cos\vartheta_\nu = \cos\vartheta_\ell\cos\theta - \sin\vartheta_\ell\sin\theta\cos\varphi, \tag{1.8a}$$
$$\sin\vartheta_\nu\cos\varphi_\nu = (\sin\vartheta_\ell\cos\theta + \cos\vartheta_\ell\sin\theta\cos\varphi)\cos\varphi_\ell - \sin\theta\sin\varphi\sin\varphi_\ell, \tag{1.8b}$$
$$\sin\vartheta_\nu\sin\varphi_\nu = (\sin\vartheta_\ell\cos\theta + \cos\vartheta_\ell\sin\theta\cos\varphi)\sin\varphi_\ell + \sin\theta\sin\varphi\cos\varphi_\ell. \tag{1.8c}$$

Eqs. (1.8b) and (1.8c) can be rewritten to a more compact form through the substitution

$$\varphi_\nu = \varphi_\ell + \alpha. \tag{1.9}$$

The parameter $\alpha = \alpha(\vartheta_\ell; \theta, \varphi)$ does not depend of the angle φ_ℓ and is defined by the following equations:

$$\sin\vartheta_\nu\cos\alpha = \sin\vartheta_\ell\cos\theta + \cos\vartheta_\ell\sin\theta\cos\varphi, \tag{1.10a}$$
$$\sin\vartheta_\nu\sin\alpha = \sin\theta\sin\varphi. \tag{1.10b}$$

Now, by applying the above definitions, we can rewrite Eq. (1.3) as

$$G_\ell^\pm(E_\ell, \vartheta_\ell, \varphi_\ell, h) = \frac{1}{\lambda_\nu(E_\ell)} \int dE_\nu \int d\cos\theta\, W^\pm_{\nu\to\ell}(E_\nu, E_\ell, \theta) \int_0^{2\pi} d\varphi\, \Phi_\nu(E_\nu, \vartheta_\nu, \varphi_\nu, h). \tag{1.11}$$

Here, the integration bounds are defined only through kinematic variables E_ν and $\cos\theta$, and only the neutrino flux in the integrand of Eq. (1.11) remains dependent of the angle φ_ℓ (through the angle φ_ν).

The next simplifying step is in averaging the generation functions over the lepton azimuthal angle. So let us define

$$\overline{G}_\ell^\pm(E_\ell, \vartheta_\ell, h) = \frac{1}{2\pi} \int_0^{2\pi} d\varphi_\ell\, G_\ell^\pm(E_\ell, \vartheta_\ell, \varphi_\ell, h). \tag{1.12}$$

Consider the integral

$$\int_0^{2\pi} d\varphi_\ell \int_0^{2\pi} d\varphi\, \Phi_\nu(E_\nu, \vartheta_\nu, \varphi_\nu, h) = \int_0^{2\pi} d\varphi \int_0^{2\pi} d\varphi_\ell\, \Phi_\nu(E_\nu, \vartheta_\nu, \varphi_\nu, h).$$

According to Eq. (1.9), $d\varphi_\ell = d\varphi_\nu$ and, considering that $\Phi_\nu(E_\nu, \vartheta_\nu, \varphi_\nu, h)$ is a periodic function of φ_ν, the above integral becomes

$$2\pi \int_0^{2\pi} d\varphi\, \overline{\Phi}_\nu(E_\nu, \vartheta_\nu, h),$$

where $\overline{\Phi}_\nu(E_\nu, \vartheta_\nu, h)$ is the neutrino differential energy spectrum averaged over the azimuth angle.

Finally,

$$\overline{G}_\ell^\pm(E_\ell, \vartheta_\ell, h) = \frac{1}{\lambda_\nu(E_\ell)} \int dE_\nu \int d\cos\theta\, W^\pm_{\nu\to\ell}(E_\nu, E_\ell, \theta) \int_0^{2\pi} d\varphi\, \overline{\Phi}_\nu(E_\nu, \vartheta_\nu, h) \tag{1.13}$$

and the ratio

$$\langle \mathbf{n}_\ell \boldsymbol{\mathcal{P}} \rangle_{\varphi_\ell} \equiv \langle \mathcal{P}_3 \rangle_{\varphi_\ell} = \frac{\overline{G}_\ell^+(E_\ell, \vartheta_\ell, h) - \overline{G}_\ell^-(E_\ell, \vartheta_\ell, h)}{\overline{G}_\ell^+(E_\ell, \vartheta_\ell, h) + \overline{G}_\ell^-(E_\ell, \vartheta_\ell, h)} \tag{1.14}$$

defines the mean longitudinal lepton polarization averaged over the azimuthal angle. Just this quantity is necessary for our aims.

NOTE V: The FORTRAN code CORTout returns just the azimuth-averaged atmospheric neutrino fluxes, $\overline{\Phi}_\nu(E_\nu, \vartheta_\nu, 0)$, *near the earth's surface*. In order to calculate the function $\Phi_\nu(E_\nu, \vartheta_\nu, \varphi_\nu, 0)$, the full code CORT has to be used. Since it is rather problematic task to interpolate within a 3D array, the using of the full code would be extremely time-consuming.

Unfortunately, it's not over yet. There are several nuances which are not very simple. But, with the above formulas we can immediately calculate the mean quantity polarization for the *contained* τ events. In this case, all angular variables and the depth h are explicitly defined.

Chapter 2

Atmospheric neutrino induced muons (CLA)

2.1 General comments

In this section, we consider the fluxes of *unpolarized* muons generated by atmospheric neutrinos in earth. We deal with the fluxes *averaged over the azimuth angle* and, for simplicity, omit the overline from hereon.

A few more notes.

1. We neglect the muon range straggling that is we use the 1D Continuous Loss Approximation (CLA).
2. We also neglect the multiple Coulomb scattering of muons.
3. The muon stopping power $\beta_\mu(E_\mu) = -dE_\mu/dh$ is the sum over all essential subprocesses:
   - ionization and excitation of atoms (including production of knock-on electrons) [405],
   - direct e^+e^- and $\mu^+\mu^-$ pair production [409–412],
   - bremsstrahlung [415–417],
   - photonuclear interactions [420, 421].

   Note that the stopping power is, generally speaking, different for μ^+ and μ^- (due to different diffractive corrections) and also is dependent of muon polarization. In absence of any information about the latter effect, we are obliged to neglect it. This is a very plaguy flaw of our study. The former effect has been investigated by Kelner and Fedotov [418, 419] for muon bremsstrahlung and will be taken into account here, of course.
4. We do not take into account the muon finite lifetime. This is permissible for ultrarelativistic energies and/or for dense enough media like the earth. Indeed, the average decay range of a muon of energy E_μ is given by

   $$\frac{\tau_\mu P_\mu}{m_\mu}\,\rho \simeq 6.23\times 10^5\ \text{g/cm}^2\left(\frac{\rho}{1\ \text{g/cm}^3}\right)\left(\frac{P_\mu}{1\ \text{GeV/c}}\right),$$

   where m_μ, τ_μ and P_μ are the muon mass, lifetime and momentum, respectively. It is clear that the decay range is much larger[1] than the muon interaction range

   $$\mathfrak{R}_\mu(E_\mu) = \int_{m_\mu}^{E_\mu} \frac{dE'_\mu}{\beta_\mu(E'_\mu)}$$

   in a dense medium; hence the muon decay effect is completely negligible in all instances of our interest.

2.2 A simple model

Let us first examine the simplest scenario as a good starting-point which is also useful for a normalization of more advanced results. Namely we will deal here with *unmixed* muon neutrino propagation through matter without absorption and regeneration. Therefore the muon generation function is independent of h and equal to

$$G_\mu(E_\mu,\vartheta_\mu) = \frac{1}{\lambda_{\nu_\mu}(E_\mu)}\int dE_\nu \left[\frac{dN_\mu(E_\nu,E_\mu)}{dE_\mu}\right]\mathit{\Phi}_{\nu_\mu}(E_\nu,\vartheta_\mu,0),$$

where

$$\frac{dN_\mu(E_\nu,E_\mu)}{dE_\mu} = \frac{1}{\sigma^{\text{tot}}_{\nu_\mu N}(E_\mu)}\left[\frac{d\sigma_{\nu_\mu N}(E_\nu,E_\mu)}{dE_\mu}\right].$$

[1] Typically of about 3 orders of magnitude (see, for example, Refs. [3, 404]).

Note that $\varPhi_{\nu_\mu}(E_\nu, \vartheta_\mu, 0)$ is the muon neutrino energy spectrum *at production* and, according to the 1D approximation, $\vartheta_{\nu_\mu} = \vartheta_\mu$. We assume also that the matter background is *chemically homogeneous* and hence the muon stopping power is also depth independent. Since the neutrino energy spectrum from any source (including cosmic ray interactions in the atmosphere) has a cutoff at high enough energy, we have

$$\lim_{E_\mu \to \infty} G_\mu(E_\mu, \vartheta_\mu) = 0. \tag{2.1}$$

Within all these assumptions, the 1D transport equation and the boundary condition are

$$\frac{\partial \varPhi_\mu(E_\mu, \vartheta_\mu, h)}{\partial h} = \frac{\partial}{\partial E_\mu}\left[\beta_\mu(E_\mu)\,\varPhi_\mu(E_\mu, \vartheta_\mu, h)\right] + G_\mu(E_\mu, \vartheta_\mu), \tag{2.2}$$

$$\varPhi_\mu(E_\mu, \vartheta_\mu, 0) = 0. \tag{2.3}$$

From Eq. (2.1) it immediately follows that

$$\lim_{E_\mu \to \infty} \varPhi_\mu(E_\mu, \vartheta_\mu, h) = 0. \tag{2.4}$$

2.2.1 Equilibrium spectrum

At large enough depths, h, the differential muon spectrum does not depend of h that is $\partial\varPhi_\mu/\partial h \to 0$ as $h \to \infty$. Let us call this asymptotic equilibrium spectrum,

$$\varPhi_\mu^{\rm eq}(E_\mu, \vartheta_\mu) = \lim_{h \to \infty} \varPhi_\mu(E_\mu, \vartheta_\mu, h).$$

By integrating the transport equation for the differential equilibrium spectrum

$$\frac{\partial}{\partial E_\mu}\left[\beta_\mu(E_\mu)\varPhi_\mu^{\rm eq}(E_\mu, \vartheta_\mu)\right] + G_\mu(E_\mu, \vartheta_\mu) = 0$$

over the muon energy and taking into account Eq. (2.4) we find

$$\varPhi_\mu^{\rm eq}(E_\mu, \vartheta_\mu) = \frac{1}{\beta_\mu(E_\mu)} \int_{E_\mu}^{\infty} G_\mu(E_\mu, \vartheta_\mu)\, dE'_\mu. \tag{2.5}$$

Then the integral equilibrium muon spectrum is given by

$$\varPhi_\mu^{\rm eq}(\geq E_\mu, \vartheta_\mu) = \int_{E_\mu}^{\infty} \varPhi_\mu^{\rm eq}(E'_\mu, \vartheta_\mu)\, dE'_\mu = \int_{E_\mu}^{\infty} G_\mu(E'_\mu, \vartheta_\mu)\, R_\mu(E'_\mu, E_\mu)\, dE'_\mu, \tag{2.6}$$

where the function R_μ is defined by

$$R_\mu(E_1, E_2) = \int_{E_2}^{E_1} \frac{dE'}{\beta_\mu(E')} = \mathfrak{R}_\mu(E_1) - \mathfrak{R}_\mu(E_2)$$

and

$$\mathfrak{R}_\mu(E) = \int_{m_\mu}^{E} \frac{dE'}{\beta_\mu(E')} = \int_0^{E_{\rm kin}} \frac{dE'_{\rm kin}}{\beta_\mu(E'_{\rm kin} + m_\mu)}.$$

is the *mean range* of a muon with initial energy E. Therefore $R_\mu(E_1, E_2)$ may be treated as the mean range of a muon with initial energy E_1 and final energy E_2 (it is assumed of course that $E_1 \geq E_2$).

NOTE VI: For rough estimations, one can assume that $G_\mu(E_\mu, \vartheta_\mu) \propto E_\mu^{-\gamma}$ with $\gamma > 1$. Then

$$\varPhi_\mu^{\rm eq}(E_\mu, \vartheta_\mu) = \frac{E_\mu G_\mu(E_\mu, \vartheta_\mu)}{(\gamma - 1)\beta_\mu(E_\mu)}.$$

At high energies one can neglect the muon ionization energy loss and approximate the stopping power by the linear function, $\beta_\mu(E_\mu) = bE_\mu$ (see Note VII, p. 16). Then the formulas (2.5) and (2.6) for the differential and integral spectra become extremely simple:

$$\varPhi_\mu^{\rm eq}(E_\mu, \vartheta_\mu) = \frac{G_\mu(E_\mu, \vartheta_\mu)}{(\gamma - 1)b} \quad \text{and} \quad \varPhi_\mu^{\rm eq}(\geq E_\mu, \vartheta_\mu) = \frac{E_\mu G_\mu(E_\mu, \vartheta_\mu)}{(\gamma - 1)^2 b} = \frac{E_\mu \varPhi_\mu^{\rm eq}(E_\mu, \vartheta_\mu)}{(\gamma - 1)}.$$

2.2.2 Exact solution to Eq. (2.2)

Let us define the function $\mathcal{E}_\mu\left(E_\mu, h\right)$ as (the only) root of equation

$$R_\mu\left(\mathcal{E}_\mu, E_\mu\right) = h. \tag{2.7}$$

This function has the obvious physical meaning: it is the energy which a muon must have at the boundary of the medium in order to reach depth h having energy E_μ. Differentiating Eq. (2.7) over E_μ and h then gives:

$$\frac{\partial \mathcal{E}_\mu\left(E_\mu, h\right)}{\partial E_\mu} = \frac{\beta_\mu\left(\mathcal{E}_\mu\left(E_\mu, h\right)\right)}{\beta_\mu\left(E_\mu\right)}, \qquad \frac{\partial \mathcal{E}_\mu\left(E_\mu, h\right)}{\partial h} = \beta_\mu\left(\mathcal{E}_\mu\left(E_\mu, h\right)\right). \tag{2.8}$$

Therefore $\mathcal{E}_\mu\left(E_\mu, h\right)$ is the solution to the following differential equation

$$\frac{\partial \mathcal{E}_\mu\left(E_\mu, h\right)}{\partial h} = \beta_\mu\left(E_\mu\right) \frac{\partial \mathcal{E}_\mu\left(E_\mu, h\right)}{\partial E_\mu} \tag{2.9}$$

with the boundary condition $\mathcal{E}_\mu\left(E_\mu, 0\right) = E_\mu$.

NOTE VII: For completeness, we enumerate here some useful properties of the functions $\mathcal{E}_\mu(E, h)$ and $R_\mu\left(E_1, E_2\right)$.

1. One can prove that for $h' \leq h$ and $E' \geq E$ the following identities take place:

$$\mathcal{E}_\mu\left(\mathcal{E}_\mu(E, h'), h - h'\right) = \mathcal{E}_\mu\left(E', h - R_\mu(E', E)\right) = \mathcal{E}_\mu(E, h),$$
$$\int_0^h f\left(\mathcal{E}_\mu(E, h - h'), h'\right) dh' = \int_E^{\mathcal{E}_\mu(E,h)} f\left(E', h - R_\mu(E', E)\right) \frac{dE'}{\beta_\mu(E')}.$$

   The later one is valid for arbitrary integrable function $f(E, h)$.

2. For small depths, h, the following expansion of $\mathcal{E}_\mu(E, h)$ in series in powers of h may be of some utility:

$$\mathcal{E}_\mu(E, h) = E + \sum_{k=1}^{\infty} \beta_\mu^k(E) \frac{h^k}{k!},$$

$$\beta_\mu^k(E) = \beta_\mu(E) \frac{d\beta_\mu^{k-1}(E)}{dE} \quad \text{for} \quad k > 0 \quad \text{and} \quad \beta_\mu^0(E) = E.$$

3. (A toy model.) Let us consider a simple but useful model in which the stopping power is a linear function of energy, $\beta_\mu = a + bE$. Such a formula roughly represents the real energy dependence of the muon stopping power for energies above some hundreds of MeV (where a represents ionization and bE – radiative and photonuclear muon energy loss; actually both a and b are functions of energy). In this model, it is easy to find the exact formulas:

$$R_\mu\left(E_1, E_2\right) = \frac{1}{b} \ln\left(\frac{a + bE_1}{a + bE_2}\right), \quad \mathcal{E}_\mu(E, h) = Ee^{bh} + \frac{a}{b}\left(e^{bh} - 1\right).$$

   Thus, for small depths ($h \ll 1/b$) $\mathcal{E}_\mu$ is a linear function of h while for large depths ($h \gg 1/b$) it is an exponentially increasing function:

$$\mathcal{E}_\mu(E, h) \approx \begin{cases} E + (a + bE)h, & \text{if} \quad bh \ll 1, \\ (E + a/b)\, e^{bh}, & \text{if} \quad bh \gg 1. \end{cases}$$

Taking into account Eqs. (2.8) and (2.9) one can prove that the exact solution to the transport equation (2.2) is given by

$$\Phi_\mu\left(E_\mu, \vartheta_\mu, h\right) = \int_0^h \frac{\beta_\mu\left(\mathcal{E}_\mu(E_\mu, h - h')\right)}{\beta_\mu\left(E_\mu\right)} G_\mu\left(\mathcal{E}_\mu\left(E_\mu, h - h'\right), \vartheta_\mu\right) dh'. \tag{2.10}$$

By change to the new variable of integration $E'_\mu = \mathcal{E}_\mu\left(E_\mu, h - h'\right)$ and taking into account that

$$dE'_\mu = -\frac{\partial \mathcal{E}_\mu\left(E_\mu, h - h'\right)}{\partial h} dh' = -\beta_\mu\left(\mathcal{E}_\mu\left(E_\mu, h - h'\right)\right) dh' = -\beta_\mu\left(E'_\mu\right) dh',$$

solution (2.10) can be rewritten as

$$\Phi_\mu\left(E_\mu, \vartheta_\mu, h\right) = \frac{1}{\beta_\mu\left(E_\mu\right)} \int_{E_\mu}^{\mathcal{E}_\mu(E_\mu,h)} G_\mu\left(E'_\mu, \vartheta_\mu\right) dE'_\mu \tag{2.11a}$$

$$= \Phi_\mu^{\text{eq}}\left(E_\mu, \vartheta_\mu\right) - \int_{\mathcal{E}_\mu(E_\mu,h)}^{\infty} G_\mu\left(E'_\mu, \vartheta_\mu\right) dE'_\mu \tag{2.11b}$$

Since $\mathcal{E}_\mu\left(E_\mu,h\right)$ is a monotonically increasing function of both arguments (and, as a consequence, $\mathcal{E}_\mu\left(E_\mu,h\right)\to\infty$ as $h\to\infty$ or $E_\mu\to\infty$), $\varPhi_\mu\left(E_\mu,\vartheta_\mu,h\right)\approx\varPhi_\mu^{\rm eq}\left(E_\mu,\vartheta_\mu\right)$ at large depths.[2]

For the integral energy spectrum

$$\varPhi_\mu\left(\geq E_\mu,\vartheta_\mu,h\right)=\int_{E_\mu}^\infty\varPhi_\mu\left(E'_\mu,\vartheta_\mu,h\right)dE'_\mu$$

(a measurable quantity in the present day underground experiments) we have

$$\begin{aligned}
\varPhi_\mu\left(\geq E_\mu,\vartheta_\mu,h\right) &= \int_{E_\mu}^\infty\frac{dE'_\mu}{\beta_\mu\left(E'_\mu\right)}\int_{E'_\mu}^{\mathcal{E}_\mu\left(E'_\mu,h\right)}G_\mu\left(E''_\mu,\vartheta_\mu\right)dE''_\mu \\
&= \int_{E_\mu}^\infty\frac{dE'_\mu}{\beta_\mu\left(E'_\mu\right)}\int_{E_\mu}^\infty\theta\left(E''_\mu-E'_\mu\right)\theta\left(\mathcal{E}_\mu\left(E'_\mu,h\right)-E''_\mu\right) \\
&\quad\times G_\mu\left(E''_\mu,\vartheta_\mu\right)dE''_\mu \\
&= \int_{E_\mu}^\infty G_\mu\left(E'_\mu,\vartheta_\mu\right)dE'_\mu\int_{E_\mu}^{E'_\mu}\theta\left(\mathcal{E}_\mu\left(E''_\mu,h\right)-E'_\mu\right)\frac{dE''_\mu}{\beta_\mu\left(E''_\mu\right)} \\
&= \int_{E_\mu}^\infty G_\mu\left(E'_\mu,\vartheta_\mu\right)dE'_\mu\int_{\mathcal{E}_\mu(E_\mu,h)}^{\mathcal{E}_\mu\left(E'_\mu,h\right)}\theta\left(E''_\mu-E'_\mu\right)\frac{dE''_\mu}{\beta_\mu\left(E''_\mu\right)} \\
&= \int_{E_\mu}^{\mathcal{E}_\mu(E_\mu,h)}G_\mu\left(E'_\mu,\vartheta_\mu\right)dE'_\mu\int_{E_\mu}^{E'_\mu}\frac{dE''_\mu}{\beta_\mu\left(E''_\mu\right)}+\int_{\mathcal{E}_\mu(E_\mu,h)}^\infty G_\mu\left(E'_\mu,\vartheta_\mu\right)dE'_\mu\int_{E'_\mu}^{\mathcal{E}_\mu\left(E'_\mu,h\right)}\frac{dE''_\mu}{\beta_\mu\left(E''_\mu\right)} \\
&= \int_{E_\mu}^{\mathcal{E}_\mu(E_\mu,h)}G_\mu\left(E'_\mu,\vartheta_\mu\right)R_\mu\left(E'_\mu,E_\mu\right)dE'_\mu+h\int_{\mathcal{E}_\mu(E_\mu,h)}^\infty G_\mu\left(E'_\mu,\vartheta_\mu\right)dE'_\mu.
\end{aligned}$$

The following useful identity

$$\int_{\mathcal{E}_\mu(E_\mu,h)}^{\mathcal{E}_\mu\left(E'_\mu,h\right)}\frac{dE''_\mu}{\beta_\mu\left(E''_\mu\right)}=\int_{E_\mu}^{E'_\mu}\frac{dE''_\mu}{\beta_\mu\left(E''_\mu\right)}$$

had been applied several times in the above chain of transformations. Finally we arrive at the following formula for the integral spectrum:

$$\varPhi_\mu\left(\geq E_\mu,\vartheta_\mu,h\right)=\varPhi_\mu^{\rm eq}\left(\geq E_\mu,\vartheta_\mu\right)-\int_{\mathcal{E}_\mu(E_\mu,h)}^\infty G_\mu\left(E'_\mu,\vartheta_\mu\right)\left[R_\mu\left(E'_\mu,E_\mu\right)-h\right]dE'_\mu. \tag{2.12}$$

The nonequilibrium correction on the right of Eq. (2.12) is negative (that is the exact integral spectrum is always less than the equilibrium one) since

$$R_\mu\left(E'_\mu,E_\mu\right)-h=R_\mu\left(E'_\mu,\mathcal{E}_\mu\left(E_\mu,h\right)\right)\geq 0,\quad\text{for}\quad E'_\mu\geq\mathcal{E}_\mu\left(E_\mu,h\right).$$

It is obvious that $\varPhi_\mu\left(\geq E_\mu,\vartheta_\mu,h\right)\to\varPhi_\mu^{\rm eq}\left(\geq E_\mu,\vartheta_\mu\right)$ as $h\to\infty$. In fact, for low energy thresholds, the correction is numerically small everywhere except for a narrow band of circumhorizontal directions ($\vartheta_\mu\simeq\pi/2$).

2.3 Account for neutrino mixing, absorption and regeneration

Here we consider for the moment the simplest case of neutrino mixing, $\nu_\mu\leftrightarrow\nu_\tau$, supported by the Super-Kamiokande, MACRO and SOUDAN 2 atmospheric neutrino data. Neutrino oscillations of this type can be treated as vacuum. The experimental bounds on Δm_{23}^2 suggest[3] that neutrino oscillations and interactions inside the earth are well separated in the following sense: below a few TeV neutrino interactions are negligible while above this energy the neutrino oscillations are negligible. Moreover, above $1-10$ TeV one can neglect the difference between the ν_μ and ν_τ total CC cross sections. As a result we can neglect the quantum interference between neutrino mixing and absorption [485] and write the survival and transition probabilities as product of the vacuum probabilities,

$$\mathcal{P}_{\nu_\mu\to\nu_\mu}\left(E_\nu,\vartheta_\nu,h\right)\quad\text{or}\quad\mathcal{P}_{\nu_\mu\to\nu_\tau}\left(E_\nu,\vartheta_\nu,h\right)=1-\mathcal{P}_{\nu_\mu\to\nu_\mu}\left(E_\nu,\vartheta_\nu,h\right),$$

[2] Considering the toy model, $G_\mu\propto E_\mu^{-\gamma}$, $\gamma>1$, $\beta_\mu=a+bE_\mu$ (see NOTE VI, p. 16), one can show that the relative nonequilibrium correction to the differential energy spectrum exponentially decays with increasing depth:

$$\frac{\left|\varPhi_\mu-\varPhi_\mu^{\rm eq}\right|}{\varPhi_\mu^{\rm eq}}=\left[\frac{E_\mu}{\mathcal{E}_\mu\left(E_\mu,h\right)}\right]^{\gamma-1}\overset{h\to\infty}{\longrightarrow}\frac{e^{-b(\gamma-1)h}}{\left[1+a/\left(bE_\mu\right)\right]^{\gamma-1}}.$$

For the real (rather steep) spectrum of atmospheric neutrinos, the nonequilibrium correction is actually small for all directions, except for almost horizontal ones.

[3] In the 99.73% C.L. the bounds are $1.4\times10^{-3}{\rm eV}^2<\Delta m_{23}^2<5.1\times10^{-3}{\rm eV}^2$ with the best-fit value of $2.6\times10^{-3}{\rm eV}^2$ [490]. In the same C.L., the best-fit (effective) mixing angle is maximal ($\theta_{23}=\pi/4$) with the lower bound given by $\sin^2 2\theta_{23}>0.86$ [490]. The fraction $\sin^2\theta_s$ of atmospheric muon neutrinos that transform into sterile states ($\nu_\mu\to\cos\theta_s\nu_\tau+\sin\theta_s\nu_s$) is limited by $\sin^2\theta_s<0.19$ (90% C.L.) [487].

and the factor $\exp\left[-h/\mathit{\Lambda}_\nu\left(E_\nu,h\right)\right]$, where $\mathit{\Lambda}_\nu\left(E_\nu,h\right)=\lambda_\nu\left(E_\nu\right)/\left[1-Z_\nu\left(E_\nu,h\right)\right]$ is the effective absorption length and the function $Z_\nu\left(E_\nu,h\right)$ takes into account the neutrino regeneration due to neutral current interactions [486]. We can therefore write the muon and τ neutrino fluxes in the earth as

$$\mathit{\Phi}_{\nu_\mu}\left(E_\nu,\vartheta_\nu,h\right)=\mathcal{P}_{\nu_\mu\to\nu_\mu}\left(E_\nu,\vartheta_\nu,h\right)\exp\left[-\frac{h}{\mathit{\Lambda}_\nu\left(E_\nu,h\right)}\right]\mathit{\Phi}_{\nu_\mu}\left(E_\nu,\vartheta_\nu,0\right),$$
$$\mathit{\Phi}_{\nu_\tau}\left(E_\nu,\vartheta_\nu,h\right)=\mathcal{P}_{\nu_\mu\to\nu_\tau}\left(E_\nu,\vartheta_\nu,h\right)\exp\left[-\frac{h}{\mathit{\Lambda}_\nu\left(E_\nu,h\right)}\right]\mathit{\Phi}_{\nu_\mu}\left(E_\nu,\vartheta_\nu,0\right).$$

2.3.1 Fluxes of fully polarized τ leptons

Let $\mathit{\Phi}_\tau^\pm\left(E_\tau,\vartheta_\tau,h\right)$ be the fluxes of fully polarized with helicity ±1 τ leptons *of the same charge* generated in $\nu_\tau N$ interactions in the earth. Then the sum $\mathit{\Phi}_\tau^+ + \mathit{\Phi}_\tau^-$ represents the unpolarized flux and the ratio $\left(\mathit{\Phi}_\tau^+ - \mathit{\Phi}_\tau^-\right)/\left(\mathit{\Phi}_\tau^+ + \mathit{\Phi}_\tau^-\right)$ is the mean longitudinal polarization of the τ lepton beam. At all energies of our interest, the τ lepton decay length $L_\tau^{\mathrm{d}}\left(E_\tau\right)=\tau_\tau P_\tau/m_\tau$ (where τ_τ, m_τ and P_τ are the lifetime, mass and momentum of τ lepton) is small in comparison with its interaction length (in contrast to the case of muon). Therefore the interactions of τ with matter are completely negligible and the transport equation for $\mathit{\Phi}_\tau^\pm\left(E_\tau,\vartheta_\tau,h\right)$ is very simple:

$$\frac{\partial\mathit{\Phi}_\tau^\pm\left(E_\tau,\vartheta_\tau,h\right)}{\partial h}=-\frac{\mathit{\Phi}_\tau^\pm\left(E_\tau,\vartheta_\tau,h\right)}{L_\tau^{\mathrm{d}}\left(E_\tau\right)\rho\left(R\left(h,\vartheta_\tau\right)\right)}+G_\tau^\pm\left(E_\tau,\vartheta_\tau,h\right). \tag{2.13}$$

Here $\rho(R)$ is the radial density distribution in the earth and $G_\tau^\pm\left(E_\tau,\vartheta_\tau,h\right)$ is the generation function, those explicit form will be discussed in detail below.

The formal solution to Eq. (2.13) can be found straightforwardly:

$$\mathit{\Phi}_\tau^\pm\left(E_\tau,\vartheta_\tau,h\right)=\int_0^h\exp\left[-\int_{h'}^h\frac{dh''}{L_\tau^{\mathrm{d}}\left(E_\tau\right)\rho\left(R\left(h'',\vartheta_\tau\right)\right)}\right]G_\tau^\pm\left(E_\tau,\vartheta_\tau,h'\right)dh'. \tag{2.14}$$

NOTE VIII: Within the 1D approximation ($\vartheta_\tau=\vartheta_\nu$), the oblique depth $h=h\left(L,\vartheta_\nu\right)$ is defined by equation $dh=\rho(R)dL$, where

$$R=R\left(L,\vartheta_\nu\right)=\sqrt{L^2-2R_\oplus L\cos\vartheta_\nu+R_\oplus^2}$$

is the distance of the neutrino interaction point from the center of the earth, L is the distance between the interaction point and the neutrino ingress point and $R_\oplus$ is the earth radius. Thus

$$h=\int_0^L\rho\left(R\left(L',\vartheta_\nu\right)\right)dL'.$$

The radius R is uniquely determined from this equation as a function of h and ϑ_τ (see "UHECR Lectures", Sect. 3.1.2 for more details).

According to the definition for the oblique depth h,

$$\int_{h'}^h\frac{dh''}{\rho\left(R\left(h'',\vartheta_\tau\right)\right)}=L-L',$$

where L and L' are the corresponding spatial distances. Since $L_\tau^{\mathrm{d}}\left(E_\tau\right)$ is extremely small, the integral on right of Eq. (2.14) is saturated at $L=L'$. Therefore, with very good accuracy we can write

$$\mathit{\Phi}_\tau^\pm\left(E_\tau,\vartheta_\tau,h\right)=\rho\left(R\left(h,\vartheta_\tau\right)\right)G_\tau^\pm\left(E_\tau,\vartheta_\tau,h\right)\int_0^L\exp\left[\frac{L'-L}{L_\tau^{\mathrm{d}}\left(E_\tau\right)}\right]dL'$$

and finally,

$$\mathit{\Phi}_\tau^\pm\left(E_\tau,\vartheta_\tau,h\right)=\rho\left(R\left(h,\vartheta_\tau\right)\right)L_\tau^{\mathrm{d}}\left(E_\tau\right)G_\tau^\pm\left(E_\tau,\vartheta_\tau,h\right). \tag{2.15}$$

According to Eq. (2.15), the mean longitudinal polarization is

$$\frac{G_\tau^+\left(E_\tau,\vartheta_\tau,h\right)-G_\tau^-\left(E_\tau,\vartheta_\tau,h\right)}{G_\tau^+\left(E_\tau,\vartheta_\tau,h\right)+G_\tau^-\left(E_\tau,\vartheta_\tau,h\right)}. \tag{2.16}$$

The generation functions $G_\tau^\pm$ appearing in the above formulas are defined by (see Sect. 1.2)

$$G_\tau^\pm\left(E_\tau,\vartheta_\tau,h\right)=\frac{1}{\lambda_{\nu_\tau}\left(E_\tau\right)}\int dE_\nu d\cos\vartheta_\nu d\varphi_\nu\left[\frac{d^2N_{\nu_\tau\to\tau}^\pm\left(E_\nu,E_\tau,\theta\right)}{dE_\tau d\cos\theta}\right]\mathit{\Phi}_{\nu_\tau}\left(E_\nu,\vartheta_\nu,h\right), \tag{2.17}$$

where

$$\frac{d^2N^{+}_{\nu_\tau\to\tau}(E_\nu,E_\tau,\theta)}{dE_\tau d\cos\theta} = \frac{1}{2\pi\sigma^{\text{tot}}_{\nu_\tau N}(E_\tau)}\left[\frac{d^2\sigma^{++}_{\nu_\tau\to\tau}(E_\nu,E_\tau,\theta)}{dE_\tau d\cos\theta}\right]$$

and

$$\frac{d^2N^{-}_{\nu_\tau\to\tau}(E_\nu,E_\tau,\theta)}{dE_\tau d\cos\theta} = \frac{1}{2\pi\sigma^{\text{tot}}_{\nu_\tau N}(E_\tau)}\left[\frac{d^2\sigma^{--}_{\nu_\tau\to\tau}(E_\nu,E_\tau,\theta)}{dE_\tau d\cos\theta}\right]$$

are the normalized double differential cross section for production of fully polarized τ leptons.

NOTE IX: Strictly speaking, the angles ϑ_τ and ϑ_ν in Eq. (2.17) must be replaced with the corresponding nadir angles $\widetilde{\vartheta}_\tau$ and $\widetilde{\vartheta}_\nu$ defined in the *neutrino interaction point* (point C in Fig. 2.1). It is easy to see however that this amendment can be neglected. Indeed,

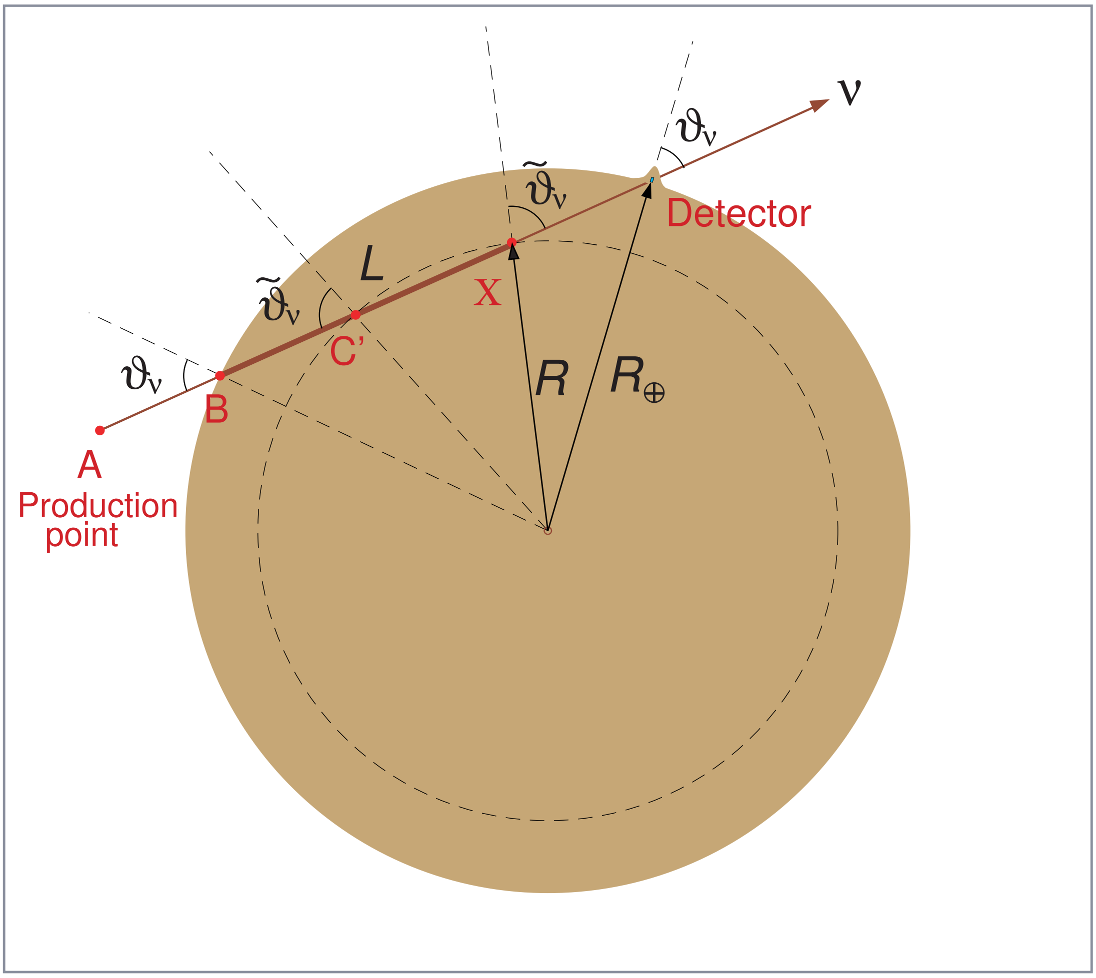

Figure 2.1: Definition of some geometric variables.

$$\frac{\sin\vartheta_\nu}{\sin\widetilde{\vartheta}_\nu} = \frac{R}{R_\oplus},$$

where

$$R = \sqrt{L^2 - 2R_\oplus L\cos\vartheta_\nu + R_\oplus^2} = \sqrt{X^2 - 2R_\oplus X\cos\vartheta_\nu + R_\oplus^2}$$

and

$$X = 2R_\oplus\cos\vartheta_\nu - L$$

is the distance between the neutrino interaction point and egress point. Since the muons originated from τ lepton decay can only reach the earth surface from the distances $X \lesssim 15\,\text{km} \ll R_\oplus$, the effective values of R can be approximated by

$$R \approx R_\oplus\left(1 - \frac{X}{R_\oplus}\cos\vartheta_\nu\right)$$

and thus the difference

$$\widetilde{\vartheta}_\nu - \vartheta_\nu \approx \frac{X}{R_\oplus}\sin\vartheta_\nu \lesssim 2.4\times10^{-3}\sin\vartheta_\nu \lesssim 0.14^\circ$$

is really negligible. The same arguments are valid for the angle ϑ_τ.

By applying the results of Sect. 1.3 we can transform Eq. (2.17) to

$$G_\tau^\pm\left(E_\tau,\vartheta_\tau,h\right)=\frac{1}{\lambda_{\nu_\tau}(E_\tau)}\int dE_\nu d\cos\theta\left[\frac{d^2N^\pm_{\nu_\tau\to\tau}\left(E_\nu,E_\tau,\theta\right)}{dE_\tau d\cos\theta}\right]\int_0^{2\pi}d\varphi\,\varPhi_{\nu_\tau}(E_\nu,\vartheta_\nu,h)\,. \tag{2.18}$$

Unfortunately this formula is still too complicated for numerical calculations. Let us rewrite it in the collinear approximation. Within this approximation, we have to put $\vartheta_\nu=\vartheta_\tau$ in the integrand on right of Eq. (2.18). Then

$$\int_0^{2\pi}d\varphi\,\varPhi_{\nu_\tau}(E_\nu,\vartheta_\nu,h)\approx 2\pi\varPhi_{\nu_\tau}(E_\nu,\vartheta_\tau,h)$$

and

$$G_\tau^\pm\left(E_\tau,\vartheta_\tau,h\right)\approx\frac{1}{\lambda_{\nu_\tau}(E_\tau)}\int dE_\nu\left[\frac{dN^\pm_{\nu_\tau\to\tau}\left(E_\nu,E_\tau\right)}{dE_\tau}\right]\varPhi_{\nu_\tau}(E_\nu,\vartheta_\tau,h)\,. \tag{2.19}$$

NOTE X: The applicability of the collinear approximation is in fact doubtful since the polarization is a strong function of θ and the angular dependence of the low-energy ν_τ flux may also be rather strong due to the oscillating factor $\mathcal{P}_{\nu_\mu\to\nu_\tau}\left(E_\nu,\vartheta_\nu,h\right)$ and geomagnetic effects. At low energies, the mean scattering angle, $\langle\theta\rangle$, is large providing additional aggravating factor. Moreover, in case of quasielastic contribution, there is the rigid constraint between the scattering angle and energies; hence the collinear approximation is artificial for this contribution. At high energies, when both oscillations and geomagnetic effects are small, the "intrinsic" angular asymmetry is still essential. On the other hand, at high energies, the mean scattering angle becomes small and thus the 1D approach becomes more satisfactory. But (ALAS!) high-energy contribution is by itself small just because the transition probability, $\mathcal{P}_{\nu_\mu\to\nu_\tau}\left(E_\nu,\vartheta_\nu,h\right)$, vanishes... Nonetheless, within the problem under consideration, the 1D approximation seems to be satisfactory everywhere, since the corresponding effect by itself is rather small. This is a "poor man" argument. Therefore, in order to estimate the error introduced by the 1D approximation, it is *necessary* to compare numerically the outputs of Eqs. (2.19) and Eq. (2.18) just in the earth surface ($X=0$).

2.3.2 Fluxes of unpolarized muons

Now we can write the 1D transport equation for muons generated in $\nu_\mu N$ CC interactions and in decay of the neutrino induced τ leptons:

$$\frac{\partial\varPhi_\mu(E_\mu,\vartheta_\mu,h)}{\partial h}=\frac{\partial}{\partial E_\mu}\left[\beta_\mu\left(E_\mu\right)\varPhi_\mu\left(E_\mu,\vartheta_\mu,h\right)\right]+G_\mu\left(E_\mu,\vartheta_\mu,h\right), \tag{2.20}$$

$$\varPhi_\mu(E_\mu,\vartheta_\mu,0)=0. \tag{2.21}$$

Here

$$G_\mu\left(E_\mu,\vartheta_\mu,h\right)=G_{\mu\mu}\left(E_\mu,\vartheta_\mu,h\right)+G^+_{\tau\mu}\left(E_\mu,\vartheta_\mu,h\right)+G^-_{\tau\mu}\left(E_\mu,\vartheta_\mu,h\right),$$

$$G_{\mu\mu}\left(E_\mu,\vartheta_\mu,h\right)=\frac{1}{\lambda_{\nu_\mu}\left(E_\mu\right)}\int dE_\nu\left[\frac{dN_{\nu_\mu\to\mu}\left(E_\nu,E_\mu\right)}{dE_\mu}\right]\varPhi_{\nu_\mu}\left(E_\nu,\vartheta_\mu,h\right), \tag{2.22}$$

$$G^\pm_{\tau\mu}\left(E_\mu,\vartheta_\mu,h\right)=B_{\tau\mu}\int dE_\tau\frac{\left[f_0\left(E_\tau,E_\mu\right)\pm f_1\left(E_\tau,E_\mu\right)\right]\varPhi_\tau^\pm\left(E_\tau,\vartheta_\mu,h\right)}{L_\tau\left(E_\tau\right)\rho\left(r\left(h,\vartheta_\tau\right)\right)}, \tag{2.23a}$$

$f_{0,1}\left(E_\tau,E_\mu\right)$ are the $\tau_{\mu3}$ decay spectral functions (their explicit form will be written later on) and $B_{\tau\mu}=\Gamma\left(\tau_{\mu3}\right)/\Gamma_\tau^{\rm tot}$ is the fraction of the $\tau_{\mu3}$ decay mode. According to PDG [3], $B_{\tau\mu}=(17.36\pm0.05)\%$ and the fraction of the radiative decay mode $\tau^-\to\mu^-\overline{\nu}_\mu\nu_\tau\gamma$ with hard γ[4] is $(0.36\pm0.04)\%$. We do not include the radiative mode separately.[5]

Substituting Eq. (2.15) into Eq. (2.23a) then gives

$$G^\pm_{\tau\mu}\left(E_\mu,\vartheta_\mu,h\right)=B_{\tau\mu}\int dE_\tau\left[f_0\left(E_\tau,E_\mu\right)\pm f_1\left(E_\tau,E_\mu\right)\right]G_\tau^\pm\left(E_\tau,\vartheta_\mu,h\right). \tag{2.23b}$$

The exact solution to Eq. (2.20) can be found similar to one for Eq. (2.2). It is

$$\varPhi_\mu\left(E_\mu,\vartheta_\mu,h\right)=\int_0^h\frac{\beta_\mu\left(\mathcal{E}_\mu(E,h-h')\right)}{\beta_\mu\left(E_\mu\right)}G_\mu\left(\mathcal{E}_\mu\left(E,h-h'\right),\vartheta_\mu,h'\right)dh' \tag{2.24a}$$

$$=\frac{1}{\beta_\mu\left(E_\mu\right)}\int_{E_\mu}^{\mathcal{E}_\mu(E_\mu,h)}G_\mu\left(E'_\mu,\vartheta_\mu,h-R_\mu\left(E'_\mu,E_\mu\right)\right)dE'_\mu. \tag{2.24b}$$

However the integral energy spectrum

$$\varPhi_\mu\left(\geq E_\mu,\vartheta_\mu,h\right)=\int_{E_\mu}^\infty\varPhi_\mu\left(E'_\mu,\vartheta_\mu,h\right)dE'_\mu$$

cannot be transformed to a simple formula similar to Eq. (2.12) owing to the h dependence of the generation function conditioned by the oscillation and (to a lesser extend) by the absorption factors.

[4]For example, in the recent CLEO experiment [422], the requirements imposed on detected γ's correspond to a τ-rest-frame energy cutoff $E^*_\gamma>10\,\mathrm{MeV}$.

[5]In fact, it is not quite clear from Ref. [3] whether the radiative mode is included into the main one (as it is for the μ_{e3} decay). Probably it is not. So there is an uncertainty (of about 0.4%) in $B_{\tau\mu}$ as well as in the spectral functions, $f_{0,1}$, that is however completely negligible in our study.

Chapter 3

Kinematics of νN scattering

3.1 Quasielastic scattering

Let us write here a summary of useful kinematic formulas for the reaction $\nu + N \to \ell + N'$ taking into account the difference between the masses of initial and final nucleons (M_i and M_f, respectively). We use the following notation for the kinematic variables in the lab. frame:

$$k \equiv p_\nu = (E_\nu, \mathbf{p}_\nu)\,, \quad k' \equiv p_\ell = (E_\ell, \mathbf{p}_\ell)\,, \quad p \equiv p_i = (E_i, \mathbf{p}_i)\,, \quad p' \equiv p_f = (E_f, \mathbf{p}_f)\,.$$

The particle energies in the center-of-mass frame (CMF) are

$$E_\nu^* = \frac{s - M_i^2}{2\sqrt{s}}, \quad E_\ell^* = \frac{s + m^2 - M_f^2}{2\sqrt{s}},$$
$$E_i^* = \frac{s + M_i^2}{2\sqrt{s}}, \quad E_f^* = \frac{s - m^2 + M_f^2}{2\sqrt{s}},$$

where

$$s = (k+p)^2 = (k'+p')^2 = M_i\,(2E_\nu + M_i)\,.$$

The energy–momentum conservation provides the equation[1]

$$E_\nu P_\ell \cos\theta = E_\ell\,(E_\nu + M_i) - \sqrt{s}E_\ell^* \tag{3.1}$$

where θ is the scattering angle ($\mathbf{p}_\nu \mathbf{p}_\ell = E_\nu P_\ell \cos\theta$). It is useful to define the following dimensionless parameter:

$$\zeta = \frac{\sqrt{s}P_\ell^*}{mE_\nu} = \frac{2M_i\sqrt{s}P_\ell^*}{m\,(s - M_i^2)} = \frac{M_i\sqrt{\left(s + m^2 - M_f^2\right)^2 - 4m^2 s}}{m\,(s - M_i^2)}.$$

The solutions to Eq. (3.1) can be written in terms of the lepton momentum ($P_\ell \equiv |\mathbf{p}_\ell| = P_\ell^\pm(\theta)$) or energy ($E_\ell = E_\ell^\pm(\theta)$):

$$P_\ell^\pm(\theta) = \frac{E_\nu\left[\sqrt{s}E_\ell^*\cos\theta \pm m\,(E_\nu + M_i)\sqrt{\zeta^2 - \sin^2\theta}\right]}{s + E_\nu^2\sin^2\theta} \tag{3.2a}$$

$$= \frac{E_\nu^*\left(M_i E_\ell^*\cos\theta \pm m E_i^*\sqrt{\zeta^2 - \sin^2\theta}\right)}{M_i^2 + (E_\nu^*)^2\sin^2\theta}, \tag{3.2b}$$

$$E_\ell^\pm(\theta) = \frac{\sqrt{s}E_\ell^*\,(E_\nu + M_i) \pm mE_\nu^2\cos\theta\sqrt{\zeta^2 - \sin^2\theta}}{s + E_\nu^2\sin^2\theta} \tag{3.2c}$$

$$= \frac{M_i E_\ell^* E_i^* \pm m\,(E_\nu^*)^2\cos\theta\sqrt{\zeta^2 - \sin^2\theta}}{M_i^2 + (E_\nu^*)^2\sin^2\theta}, \tag{3.2d}$$

where θ is the scattering angle ($\mathbf{p}_\nu \mathbf{p}_\ell = E_\nu P_\ell \cos\theta$) and

$$\zeta = \frac{\sqrt{s}P_\ell^*}{mE_\nu} = \frac{2M_i\sqrt{s}P_\ell^*}{m\,(s - M_i^2)} = \frac{M_i\sqrt{\left(s + m^2 - M_f^2\right)^2 - 4m^2 s}}{m\,(s - M_i^2)}.$$

According to Eq. (3.2a),

$$P_\ell^+(\theta)P_\ell^-(\theta) = m^2E_\nu^2\left(1 - \zeta^2\right). \tag{3.3}$$

Therefore for $\zeta \le 1$ there are two solutions, $P_\ell^+(\theta)$ and $P_\ell^-(\theta)$, while for $\zeta > 1$ there is only one solution, $P_\ell^+(\theta)$.

[1] In fact it can be found from the equation $(k - k')^2 = (p - p')^2$.

NOTE XI:

Let us prove the above statement.

- $\zeta < 1$: It is obvious that $P_\ell^+(0) > 0$. Thus, according to Eq. (3.3), $P_\ell^-(0) > 0$. Since

$$P_\ell^+(\theta) = P_\ell^-(\theta) = \frac{m^2 E_\nu \sqrt{1-\zeta^2}}{\sqrt{s} E_\ell^*} \quad \text{if and only if} \quad \sin\theta = \zeta,$$

both $P_\ell^+(\theta)$ and $P_\ell^-(\theta)$ are positive for $0 \leq \theta < \arcsin\zeta$. It is also clear that $\cos\theta > 0$ (otherwise $P_\ell^\pm(\theta)$ would be negative at $\sin\theta = \zeta$). Therefore, there are two *physical* solutions, $P_\ell^+(\theta) > 0$ and $P_\ell^-(\theta) > 0$, for

$$0 \leq \theta < \min\left(\arcsin\zeta, \pi/2\right) \equiv \theta_\ell(E_\nu)$$

and there is no physical solution for $\theta \geq \theta_\ell(E_\nu)$.

- $\zeta > 1$: The signs of the *formal* solutions $P_\ell^+(\theta)$ and $P_\ell^-(\theta)$ are opposite. Since, according to Eq. (3.2a), $P_\ell^+(\theta) \geq P_\ell^-(\theta)$, we have $P_\ell^+(\theta) \geq 0$ and thus $P_\ell^-(\theta) \leq 0$. So for any θ there is the only *physical* solution, $P_\ell^+(\theta)$.

- $\zeta = 1$: In this special case

$$P_\ell^* = \frac{mE_\nu}{\sqrt{s}}, \quad E_\ell^* = \frac{m\left(E_\nu + M_i\right)}{\sqrt{s}},$$

and therefore

$$\begin{aligned} P_\ell^-(\theta) &= 0, \quad P_\ell^+(\theta) = \frac{2m\left(E_\nu + M_i\right)E_\nu\cos\theta}{s + E_\nu^2\sin^2\theta}, \\ E_\ell^-(\theta) &= m, \quad E_\ell^+(\theta) = m + \frac{2mE_\nu^2\cos^2\theta}{s + E_\nu^2\sin^2\theta}. \end{aligned}$$

The case is only possible for $0 \leq \theta \leq \pi/2$ since $P_\ell^-(\theta) < 0$ as $\theta > \pi/2$. The two solutions are different everywhere except for the angle $\theta = \pi/2$.

One more useful identity can be found from Eq. (3.3):

$$P_\ell^+\frac{\partial P_\ell^-}{\partial\theta} + P_\ell^-\frac{\partial P_\ell^+}{\partial\theta} = 0.$$

It is clear therefore that $P_\ell^+(\theta)$ ($P_\ell^-(\theta)$ is a monotonically decreasing (increasing) function of θ within the two-branch region $\zeta < 1$, $\theta > \theta_\ell(E_\nu)$. From this it follows that the scattering angle θ is a single-valued function of P_ℓ the for any ζ. Of course this trivial fact immediately follows from Eq. (3.1).

Taking into account the conditions $\zeta \geq \sin\theta$ and $\sin\theta \geq 0$ we have

$$\begin{aligned} &P_\ell = P_\ell^+(\theta), \quad E_\ell = E_\ell^+(\theta), \quad 0 \leq \theta \leq \pi, && \text{if} \quad \zeta > 1, \\ &P_\ell = P_\ell^\pm(\theta), \quad E_\ell = E_\ell^\pm(\theta), \quad 0 \leq \theta < \arcsin\zeta, && \text{if} \quad \zeta \leq 1. \end{aligned}$$

The asymptotic value of $\arcsin\zeta$ at $E_\nu \to \infty$ is given by

$$\arcsin\zeta \to \arcsin\left(\frac{M_i}{m}\right) \quad \text{if} \quad M_i \leq m.$$

The condition $\zeta = 1$ defines the neutrino energy at which the second solution, P_ℓ^-, disappears. It can be rewritten in terms of the neutrino energy as

$$\left(E_\nu - \epsilon_\nu^-\right)\left(E_\nu - \epsilon_\nu^+\right) = 0 \tag{3.4}$$

with

$$\epsilon_\nu^\pm = \frac{M_f^2 - \left(M_i \mp m\right)^2}{2\left(M_i \mp m\right)} \quad \text{and} \quad \epsilon_\nu^+ - \epsilon_\nu^- = m\left(1 + \frac{M_f^2}{M_i^2 - m^2}\right).$$

In general, Eq. (3.4) may have 0, 1 or 2 solutions. The latter possibility is in fact excluded since ϵ_ν^- is either negative or, as in the case of e^+ production, positive but is below the reaction threshold,

$$E_\nu^{\text{th}} = \frac{\left(M_f + m\right)^2 - M_i^2}{2M_i}. \tag{3.5}$$

The nontrivial solutions, ϵ_ν^+, together with the thresholds and the differences $\epsilon_\nu^+ - E_\nu^{\text{th}}$ are shown in Table 3.1. The same quantities evaluated for the isoscalar nucleon target by putting $M_i \approx M_f \approx \left(M_i + M_f\right)/2$ are shown in Table 3.2.

Comparing the tables, one can conclude that the isoscalar target approximation is appropriate for $\mu^\pm$ and $\tau^\pm$ production slightly above the reaction thresholds and becomes appropriate also for $e^\pm$ production at $E_\nu > (40 - 50)$ MeV.

Table 3.1: E_ν^{th}, ϵ_ν^+ and $\epsilon_\nu^+ - E_\nu^{\text{th}}$ for 6 QE reactions.

Reaction	E_ν^{th} (MeV)	ϵ_ν^+ (MeV)	$\epsilon_\nu^+ - E_\nu^{\text{th}}$
$\nu_e + n \to e^- + p$	0	–	–
$\overline{\nu}_e + p \to e^+ + n$	1.8060638	1.8060648	0.94537 eV
$\nu_\mu + n \to \mu^- + p$	110.16137	110.89578	734.41 keV
$\overline{\nu}_\mu + p \to \mu^+ + n$	113.04730	113.82083	773.53 keV
$\nu_\tau + n \to \tau^- + p$	3453.6527	–	–
$\overline{\nu}_\tau + p \to \tau^+ + n$	3463.4511	–	–

Table 3.2: The same quantities as in Table 3.1 but for the isoscalar target.

ℓ	E_ν^{th} (MeV)	ϵ_ν^+ (MeV)	$\epsilon_\nu^+ - E_\nu^{\text{th}}$
e	0.51114	0.51114	0.0757 eV
μ	111.603	112.357	753.8 keV
τ	3458.55	–	–

The exact kinematics suggests that the condition $\zeta = 1$ is never satisfied for electron production (the reaction with no threshold, $\zeta > 1$) and for $\tau^\pm$ production ($\zeta < 1$) while for production of e^+ and $\mu^\pm$ the values of ϵ_ν^+ are slightly above the reaction thresholds. However the two-branch energy gap

$$\epsilon_\nu^+ - E_\nu^{\text{th}} = \frac{m\left(M_f - M_i + m\right)^2}{2M_i\left(M_i - m\right)}$$

for e^+ and $\mu^\pm$ production is extremely narrow since both $m_{e,\mu}$ and $M_n - M_p$ are small in comparison with the nucleon mass.

One can prove that the parameter ζ is a *decreasing* function of s for electron production and an *increasing* function for all the rest reactions (Fig. 3.1). In the last case,

$$0 \le \zeta < \frac{M_i}{m}.$$

Since $m_\tau > M_{p,n}$, we conclude that for τ lepton production there are two branches of solutions at any neutrino energy above the reaction threshold. The maximum scattering angle for τ production is[2]

$$\theta_\tau^{\max} = \begin{cases} \arcsin(M_n/m_\tau) \approx 31.9203^\circ & \text{for} \quad \tau^- \\ \arcsin(M_p/m_\tau) \approx 31.8712^\circ & \text{for} \quad \tau^+. \end{cases}$$

At a fixed neutrino energy, the lepton energy and momentum satisfy the conditions

$$E_\ell^{\min} \le E_\ell \le E_\ell^{\max} \quad \text{and} \quad P_\ell^{\min} \le P_\ell \le P_\ell^{\max}, \tag{3.6}$$

where

$$\begin{aligned} E_\ell^{\min} &= \frac{E_\ell^*\left(E_\nu + M_i\right) - P_\ell^* E_\nu}{\sqrt{s}}, \quad & E_\ell^{\max} &= \frac{E_\ell^*\left(E_\nu + M_i\right) + P_\ell^* E_\nu}{\sqrt{s}}, \\ P_\ell^{\min} &= \frac{\left|E_\ell^* E_\nu - P_\ell^*\left(E_\nu + M_i\right)\right|}{\sqrt{s}}, \quad & P_\ell^{\max} &= \frac{E_\ell^* E_\nu + P_\ell^*\left(E_\nu + M_i\right)}{\sqrt{s}}. \end{aligned} \tag{3.7}$$

Proof: Let's write down the Lorentz transformation for the lepton energy from CMF to LF:

$$E_\ell = \varGamma\left(E_\ell^* - \mathbf{v}\mathbf{p}_\ell^*\right).$$

Since CMF moves relative to LF with the velocity $\mathbf{v}$ equal in magnitude to that of the initial nucleon, and directed along the neutrino velocity, we have

$$E_\ell = \frac{E_i^*}{M_i}\left(E_\ell^* - \frac{P_i^*}{E_i^*}P_\ell^*\cos\theta_\ell^*\right) = \frac{1}{M_i}\left(E_i^* E_\ell^* - P_i^* P_\ell^*\cos\theta_\ell^*\right),$$

where θ_ℓ^* is the lepton scattering angle in CIF. Since this angle is arbitrary we obtain

$$E_\ell^{\max/\min} = \frac{1}{M_i}\left(E_i^* E_\ell^* \pm P_i^* P_\ell^*\right)$$

[2]For the isoscalar nucleon target with the mass of $\left(M_p + M_n\right)/2$, it is about 31.896°.

(note that $P_i^* = E_\nu^*$). It is not difficult to check that these formulas match Eq. (3.6).

Similar way we find:

$$E_f^{\max/\min} = \frac{1}{M_i}\left(E_i^* E_f^* \pm P_i^* P_f^*\right).$$

Considering that $P_\ell^* = P_f^*$, it is easy to veryfy that

$$E_\ell^{\max} + E_f^{\min} = E_\ell^{\min} + E_f^{\max} = E_\nu + M_i.$$

The corresponding boundaries for the Bjorken variable $y = (pq)/(pk) = 1 - E_\ell/E_\nu$ and $Q^2 = -q^2$ are

$$y^{\min} = 1 - \frac{1}{\sqrt{s}}\left[E_\ell^*\left(1+\frac{M_i}{E_\nu}\right) + P_\ell^*\right],$$
$$y^{\max} = 1 - \frac{1}{\sqrt{s}}\left[E_\ell^*\left(1+\frac{M_i}{E_\nu}\right) - P_\ell^*\right],$$

and

$$Q_\pm^2 = 2E_\nu^*\left(E_\ell^* \pm P_\ell^*\right) - m^2 = \frac{\left(s-M_i^2\right)\left(E_\ell^* \pm P_\ell^*\right)}{\sqrt{s}} - m^2 = m^2\left[\frac{s-M_i^2}{\left(E_\ell^* \mp P_\ell^*\right)\sqrt{s}} - 1\right],$$

Therefore

$$y^{\max} - y^{\min} = \frac{2P_\ell^*}{\sqrt{s}},$$
$$Q_+^2 - Q_-^2 = 4E_\nu^* P_\ell^* = \frac{\left(s-M_i^2\right)P_\ell^*}{\sqrt{s}} = 2M_i E_\nu\left(y^{\max} - y^{\min}\right).$$

NOTE XII:

For better understanding the behavior of the parameter ζ let us investigate the derivative

$$\frac{d\zeta}{ds} = \frac{1}{2\zeta}\left(\frac{d\zeta^2}{ds}\right) = \frac{M_i^2 \varXi}{m^2\left(s-M_i^2\right)^3\zeta},$$
$$\varXi = \left(m^2 + M_f^2 - M_i^2\right)s + \left(M_f^2 - m^2\right)\left(m^2 - M_f^2 + M_i^2\right).$$

Since $s \geq \max\left[M_i^2, (M_f+m)^2\right]$, we have

- $M_f < M_i - m$:

$$\varXi < -\left(M_i^2 - M_f^2\right)^2 + m^2\left(2M_f^2 - m^2\right) < -M_f\left(M_i - M_f\right)^2\left(2M_i + M_f\right) - m^4;$$

- $M_f > M_i - m$:

$$\varXi > 2m\left(M_f + m\right)\left[M_f\left(M_f + m\right) - M_i^2\right] > 2mM_i\left(M_f+m\right)\left(M_f - M_i\right);$$

- $M_f = M_i - m$:

$$\varXi = -2M_i^2\left(M_i - M_f\right)^2.$$

Therefore $d\zeta/ds < 0$ for the e^- production and $d\zeta/ds > 0$ for the rest QE reactions. Since ζ vanishes on the thresholds of these 5 reactions, $d\zeta/ds \to \infty$ as $E_\nu \to E_\nu^{\text{th}}$. This behavior is clearly seen in Fig. 3.1.

NOTE XIII:

Let us consider the kinematics of the thresholdless reaction $\nu_e + n \to e^- + p$ with more details. Since

$$\frac{dE_e^*}{d\sqrt{s}} = \frac{E_p^*}{\sqrt{s}} > 0 \quad \text{and} \quad \frac{dE_\nu^*}{d\sqrt{s}} = \frac{E_n^*}{\sqrt{s}} > 0,$$

we have

$$E_e^* \geq \frac{m_n^2 - m_p^2 + m_e^2}{2m_n} \simeq 1.292578811 \text{ MeV}, \quad P_e^* \gtrsim 1.187282648 \text{ MeV}/c \quad \text{and} \quad E_\nu^* \geq 0.$$

$$\frac{dQ_\pm}{d\sqrt{s}} = \frac{2\left(E_e^* \pm P_e^*\right)\left(E_n^* P_e^* \pm E_p^* E_\nu^*\right)}{\sqrt{s}P_e^*}.$$

According to the last equation, $dQ_+^2/d\sqrt{s} > 0$ that is Q_+^2 is a monotonically increasing function of neutrino energy. Let us prove that the same is also true for Q_-^2. Indeed, after some manipulations we can find that

$$\frac{dQ_-^2}{d\sqrt{s}} = \frac{\left(E_e^* - P_e^*\right)A_+ A_-}{8s\sqrt{s}P_e^*\left(E_n^* P_e^* + E_p^* E_\nu^*\right)},$$

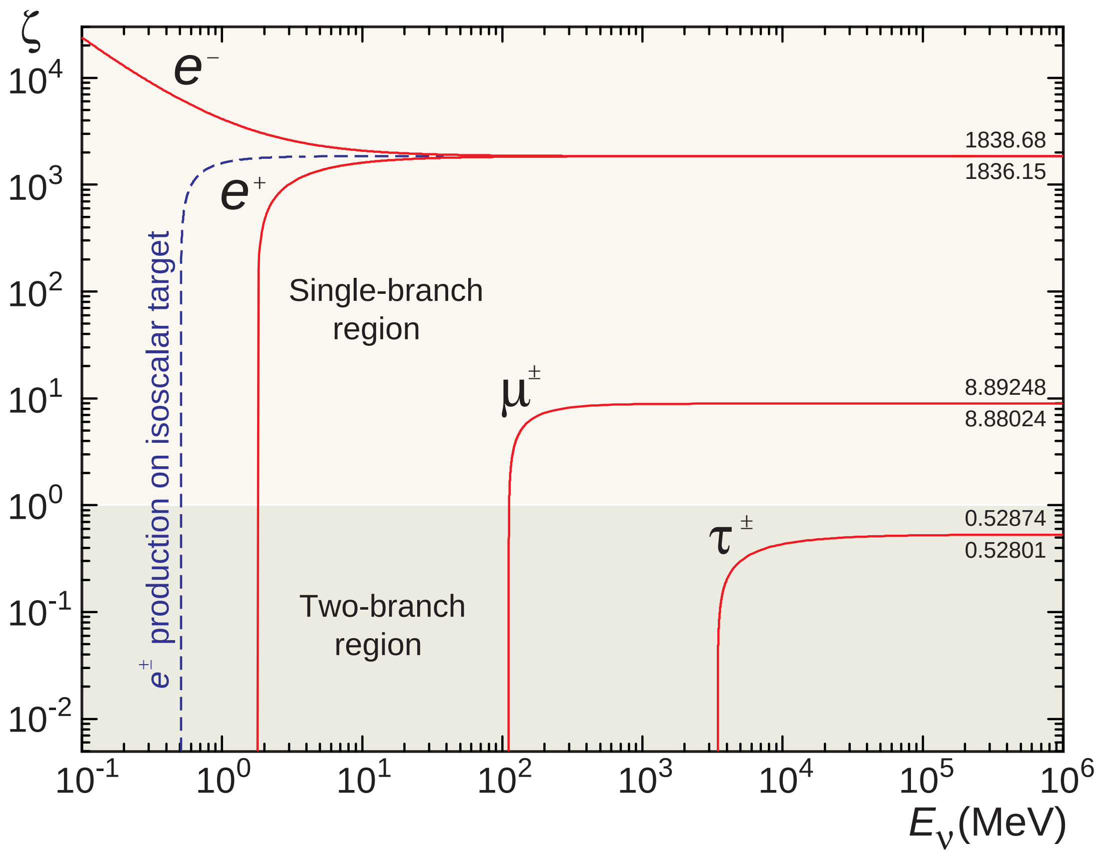

Figure 3.1: Parameter ζ as a function of neutrino energy for production of $e^\pm$, $\mu^\pm$ and $\tau^\pm$. The differences between the curves for production of muons and τ leptons of different charges are undistinguished in this scale. Asymptotic values of the function ζ are shown near the curves.

where

$$A_\pm = (m_n \pm m_p)\, s + m_n \left(m_p^2 - m_e^2 \pm m_p m_n\right).$$

Taking into account that $s \geq m_n^2$ we have

$$A_\pm \geq m_n \left[(m_n \pm m_p)^2 - m_e^2\right]$$

and therefore $dQ_-^2/d\sqrt{s} > 0$.

Finally,

$$\frac{d\left(Q_+^2 - Q_-^2\right)}{d\sqrt{s}} = \frac{4\left[E_e^* E_p^* E_\nu^* + (P_e^*)^2 E_n^*\right]}{\sqrt{s} P_e^*} > 0.$$

Several important facts follow from the above consideration:

- at $E_\nu = 0$

$$Q_-^2 = Q_+^2 = -m_e^2 \simeq -0.2611199 \text{ MeV}^2$$

and, at very low energies, the Q^2 interval linearly squeezes when energy decreases:

$$\begin{aligned} Q_+^2 - Q_-^2 &\sim 2\sqrt{\left(m_n^2 - m_p^2 + m_e^2\right)^2 - 4m_e^2 m_n^2}\left(\frac{E_\nu}{m_n}\right) \\ &\simeq 4.7491306 \times 10^{-6} \left(\frac{E_\nu}{1 \text{ MeV}}\right) \text{ MeV}^2; \end{aligned}$$

- Q_-^2 is *negative at all energies* while Q_+^2 changes its sign at

$$s = m_n^2\left(1 + \frac{m_e^2}{m_n^2 - m_p^2}\right) \quad \text{or} \quad E_\nu = \frac{m_n m_e^2}{2\left(m_n^2 - m_p^2\right)} \simeq 50.5091 \text{ keV};$$

- the asymptotic behavior of the lower bound at high energies is given by

$$Q_-^2 \sim -\frac{m_e^2\left(m_n^2 - m_p^2\right)}{s} \simeq -\frac{6.341723 \times 10^{-4} \text{ MeV}^2}{s}.$$

To obtain the latter formula we took into accopnt that

$$P_e^* = \frac{\sqrt{s}}{2}\left[1 - \frac{m_p^2 + m_e^2}{s} - \frac{2m_e^2 m_p^2}{s^2} + \mathcal{O}\left(\frac{1}{s^3}\right)\right]$$

and

$$E_e^* - P_e^* = \frac{m_e^2}{\sqrt{s}}\left[1 + \frac{m_p^2}{s} + \mathcal{O}\left(\frac{1}{s^2}\right)\right].$$

Some of the mentioned features of the $\nu_e + n \to e^- + p$ reaction are illustrated in Fig. 6.1 (see Sect. 6.3.3).

NOTE XIV:

It is useful to investigate the behavior of Q_-^2 for all QE reactions. Exactly the same way as in previous Note we can derive

$$\frac{dQ_-^2}{d\sqrt{s}} = \frac{\left(E_\ell^* - P_\ell^*\right) A_+ A_-}{8s\sqrt{s}P_\ell^*\left(E_i^* P_\ell^* + E_f^* E_\nu^*\right)} \quad \text{with} \quad A_\pm = \left(M_i \pm M_f\right)s + M_i\left[M_f\left(M_f \pm M_i\right) - m^2\right].$$

For the threshold value $s = s^{\text{th}} = (M_f + m)^2$ we have

$$A_\pm = A_\pm^{\text{th}} = \pm M_f\left(m + M_f \pm M_i\right)^2 \quad \text{and} \quad A_-^{\text{th}} A_+^{\text{th}} = -M_f\left[(m + M_f)^2 - M_i^2\right]^2.$$

By using these relations one can prove that

- $Q_-^2 < 0$ for e^- production,
- $Q_-^2 > 0$ for e^+, μ^+ and τ^+ production,
- Q_-^2 changes its sign for μ^- and τ^- production at

$$s = m_n\left(1 + \frac{m^2}{m_n^2 - m_p^2}\right) \quad \text{or} \quad E_\nu = \frac{m^2 m_n}{2\left(m_n^2 - m_p^2\right)}.$$

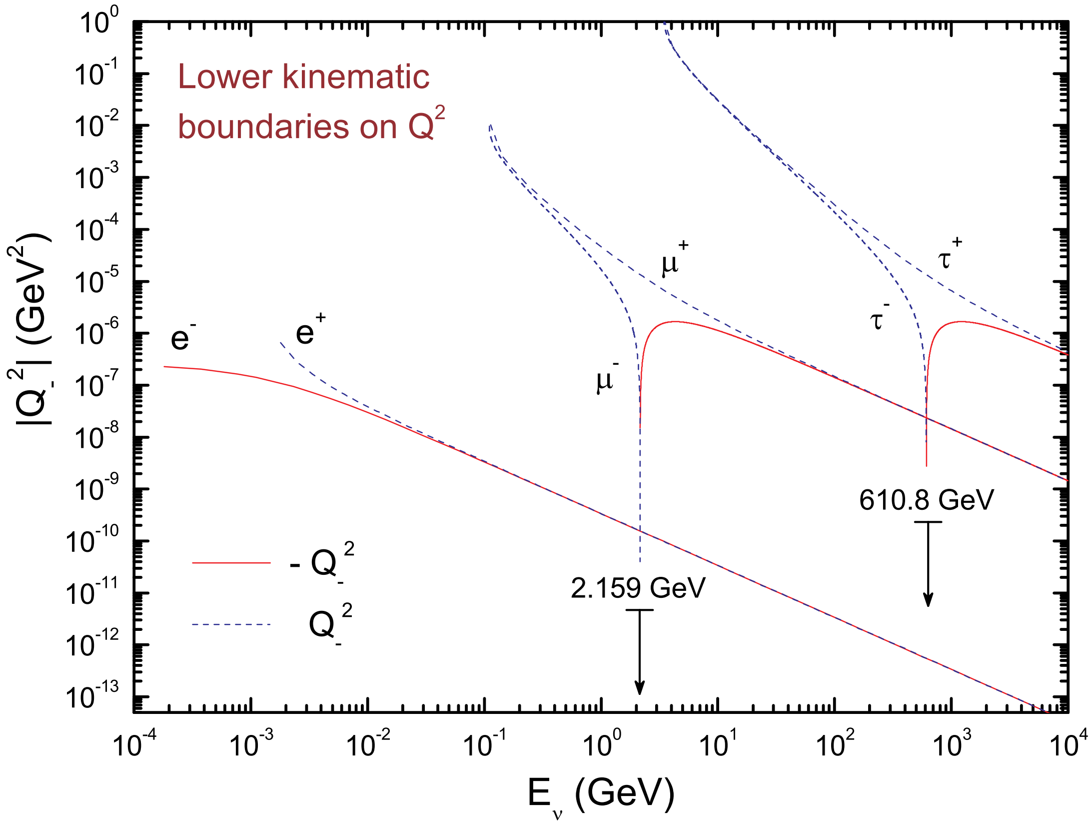

Figure 3.2: Absolute value of the lower kinematic boundary Q_-^2 vs (anti)neutrino energy for the six $\Delta Y = 0$ QE reactions. The energies at which the Q_-^2 changes its sign are also shown.

These features are illustrated in Fig. 3.2. Unfortunately it is seen no observational consequences of these nontrivial facts.

NOTE XV:

Let us derive the transformation from the double differential to single differential cross section. For simplicity we first consider only the main one-solution branch. Then

$$\frac{d\sigma}{dQ^2} = 2\pi \int_{-1}^{1} d\cos\theta \left|\frac{dQ^2}{dE_\ell}\right|^{-1} \frac{d^2\sigma}{dE_\ell d\cos\theta}. \tag{3.8}$$

From the definition

$$Q^2 = -q^2 = -(p_\nu - p_\ell)^2 = -m^2 + 2\left(E_\ell E_\nu - P_\ell P_\nu \cos\theta\right) \tag{3.9}$$

(where, as above, $m = m_\ell$) we obtain

$$\frac{dQ^2}{dE_\ell} = 2E_\ell \left(1 - \frac{E_\nu}{P_\ell}\cos\theta\right).$$

Formal solution of Eq. (3.9) relative to variable E_ℓ is

$$E_\ell^\pm = E_\ell^\pm(Q^2,\theta) = \frac{Q^2+m^2}{2E_\nu \sin^2\theta}\left[1 \pm \cos\theta\sqrt{1 - \left(\frac{2mE_\nu \sin\theta}{Q^2+m^2}\right)^2}\,\right]. \tag{3.10}$$

First of all we note that only one solution E_ℓ^- is free from the singularity at $\theta = 0$ [similarly one can investigate the case $\theta = \pi$. Let's omit...]. It is easy to find that

$$E_\ell^-(Q^2,0) = \frac{m^2 E_\nu}{Q^2+m^2} + \frac{Q^2+m^2}{4E_\nu}. \tag{3.11}$$

Since $\partial E_\ell^-(Q^2,\theta)/\partial\theta\big|_{\theta=0} = 0$ and $\partial^2 E_\ell^-(Q^2,\theta)/\partial\theta^2\big|_{\theta=0} > 0$, Eq. (3.11) provides the minimum of $E_\ell^-(Q^2,\theta)$. The positivity of the discriminant introduces the obvious θ-function into the integral (3.8). Similar way we obtain

$$P_\ell^\pm = P_\ell^\pm(Q^2,\theta) = \frac{Q^2+m^2}{2E_\nu \sin^2\theta}\left[\cos\theta \pm \sqrt{1 - \left(\frac{2mE_\nu \sin\theta}{Q^2+m^2}\right)^2}\,\right]. \tag{3.12}$$

Only the solution P_ℓ^- is appropriate because only in this case $\left(E_\ell^-\right)^2 - \left(P_\ell^-\right)^2 = m^2$. Clearly

$$P_\ell^-(Q^2,0) = \frac{m^2 E_\nu}{Q^2+m^2} - \frac{Q^2+m^2}{4E_\nu}. \tag{3.13}$$

Of course this is the minimum of $P_\ell^-(Q^2,\theta)$. One more θ-function is $\theta(P_\ell^-)$.

All this is realized in the current code for the SM RFG model implementation but in fact we could forget about the above formulas since the transformation (3.8) can be performed in very trivial way:

$$\frac{d\sigma}{dQ^2} = 2\pi \int_{E_\ell^{\min}}^{E_\ell^{\max}} dE_\ell \left|\frac{dQ^2}{d\cos\theta}\right|^{-1} \frac{d^2\sigma(E_\nu,E_\ell,\theta)}{dE_\ell d\cos\theta} = \frac{\pi}{E_\nu}\int_{E_\ell^{\min}}^{E_\ell^{\max}} \frac{dE_\ell}{P_\ell}\frac{d^2\sigma(E_\nu,E_\ell,\theta)}{dE_\ell d\cos\theta} \tag{3.14}$$

$$= 2\pi \int_{P_\ell^{\min}}^{P_\ell^{\max}} dP_\ell \left|\frac{dQ^2}{d\cos\theta}\right|^{-1} \frac{d^2\sigma(E_\nu,P_\ell,\theta)}{dP_\ell d\cos\theta} = \frac{\pi}{E_\nu}\int_{P_\ell^{\min}}^{P_\ell^{\max}} \frac{dP_\ell}{P_\ell}\frac{d^2\sigma(E_\nu,P_\ell,\theta)}{dP_\ell d\cos\theta}, \tag{3.15}$$

where the boundaries $E_\ell^{\min}$, $E_\ell^{\max}$, etc. are given by Eq. (3.7) and it was taken into account that

$$\frac{dQ^2}{d\cos\theta} = -2P_\ell E_\nu, \quad \cos\theta = \frac{E_\ell}{P_\ell} - \frac{Q^2+m^2}{2P_\ell E_\nu}.$$

3.1.1 Kinematics of the SM RFG model

Let's find the threshold neutrino energy for the case when the initial nucleon moves with momentum $\mathbf{p}_i = \mathbf{p}$. Since

$$s = (p_\nu + p_i)^2 = M_i^2 + 2\left(E_\nu E_{\mathbf{p}} - \mathbf{p}_\nu \mathbf{p}\right) = M_i^2 + 2E_\nu\left(E_{\mathbf{p}} - \mathrm{p}\cos\theta\right), \tag{3.16}$$

(where $E_{\mathbf{p}} = E_i = \sqrt{\mathbf{p}^2 + M_i^2}$, $\mathrm{p} = |\mathbf{p}|$, and θ is the angle between the neutrino and initial nucleon momenta), we have

$$E_\nu^{\text{th}} = \frac{\left(M_f + m\right)^2 - M_i^2}{2\left(E_{\mathbf{p}} - \mathrm{p}\cos\theta\right)}. \tag{3.17}$$

For pedagogical purposes, let's derive this formula using the Lorentz transformation. Let $\tilde{E}_\nu^{\text{th}}$ denote the neutrino energy threshold in the rest frame of the nucleon, (see Eq. (3.5)),

$$\tilde{E}_\nu^{\text{th}} = \frac{\left(M_f + m\right)^2 - M_i^2}{2M_i}.$$

Boost from the lab. frame gives

$$\tilde{E}_\nu^{\text{th}} = \frac{E_{\mathbf{p}}}{M_i}\left(E_\nu^{\text{th}} - \frac{\mathbf{p}}{E_{\mathbf{p}}}\mathbf{p}_\nu^{\text{th}}\right) = \frac{1}{M_i}E_\nu^{\text{th}}\left(E_{\mathbf{p}} - \mathrm{p}\cos\theta\right)$$

whence we get Eq. (3.17). Obviously, Eq. (3.17) turns into Eq. (3.5) when $\mathrm{p} = 0$. The effect is illustrated in Fig. 3.3 for the reactions $\nu_\mu n \to \mu^- p$ and $\nu_\tau n \to \tau^- p$.

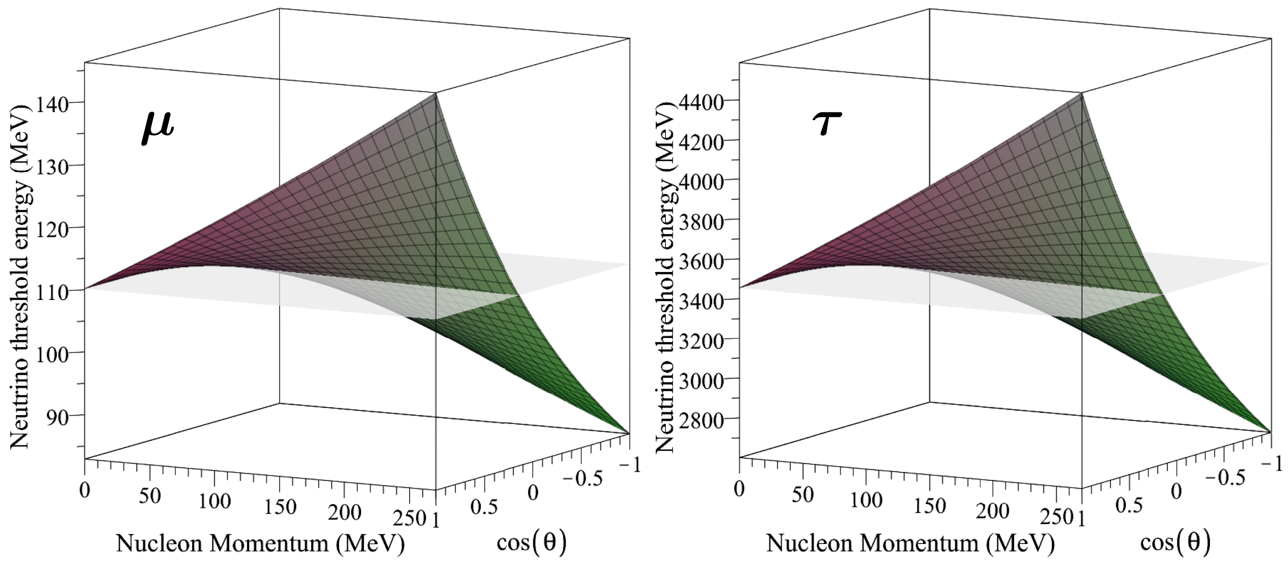

Figure 3.3: Neutrino energy thresholds for the rections $\nu_\mu n \to \mu^- p$ and $\nu_\tau n \to \tau^- p$ vs. neutron momentum p and $\cos\theta$. The gray planes show the thresholds for p=0.

Well, how do you account for the binding energy of the nucleon in the nucleus? Naive substitution

$$E_{\mathbf{p}} \longmapsto E'_{\mathbf{p}} = E_{\mathbf{p}} - E_b$$

in Eq. (3.16) yields

$$\left(E_{\mathbf{p}} - E_b\right)^2 - \mathbf{p}^2 + 2\left[E_\nu\left(E_{\mathbf{p}} - E_b\right) - \mathbf{pk}\right] = \left(M_f + m\right)^2$$

and therefore

$$E_\nu^{\text{th}} = \frac{\left(M_f + m\right)^2 + \mathrm{p}^2 - \left(E_{\mathbf{p}} - E_b\right)^2}{2\left(E_{\mathbf{p}} - E_b - \mathrm{p}\cos\theta\right)}. \tag{3.18}$$

Unfortunately this formaula violates Lorentz invariantce and Lorentz boost is inapplicable. Let's try to "relativize" the SM RFG model by introducing the effective mass of the bound nucleon, $M_i' = M_i - \epsilon$, as follows:

$$\sqrt{\mathrm{p}^2 + (M_i - \epsilon)^2} = E_{\mathbf{p}} - E_b.$$

The formal solution to this equation

$$\epsilon = M_i - \sqrt{M_i^2 - 2E_{\mathbf{p}}E_b + E_b^2}$$

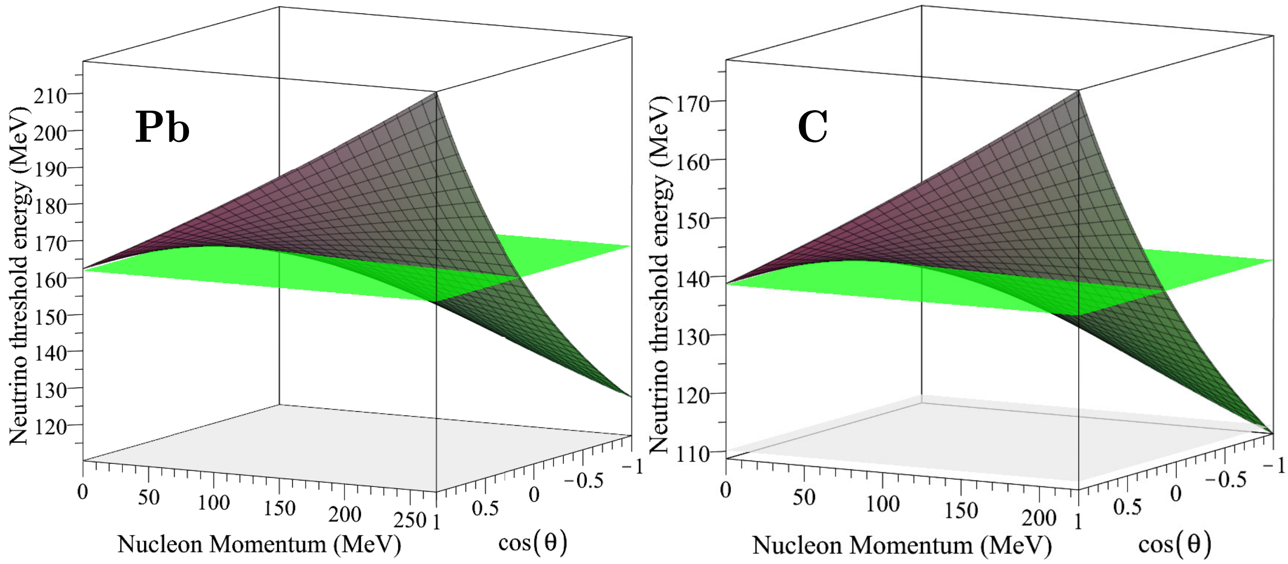

Figure 3.4: Neutrino energy thresholds for the rection $\nu_\mu n_b \to \mu^- p$ on bound neutron vs. neutron momentum p and $\cos\theta$ for lead and carbon. The green planes show the corresponding thresholds for p=0. The gray planes show the same, but for a free neutron.

can be expanded in inverse powers of M_i:

$$\epsilon = E_b\left[1 + \frac{\mathrm{p}^2}{2M_i^2} + \frac{E_b\mathrm{p}^2}{2M_i^3} - \frac{\mathrm{p}^2\left(\mathrm{p}^2 - 4E_b^2\right)}{8M_i^4} + O\left(\frac{1}{M^5}\right)\right]. \tag{3.19}$$

The maximum possible corrections $\propto M^{-n}$ are as follows:

$$n = 2: \quad 4.1\%, \quad n = 3: \quad 0.2\%, \quad n = 4: \quad 0.08\%.$$

So, only the first correction is essential. But it violates relativistic covariance. Given that the momentum distribution is uniform, we can approximately replace p $\longmapsto p_F/2$. Then

$$\epsilon \approx E_b\left(1 + \frac{p_F^2}{8M_i^2}\right). \tag{3.20}$$

with an accuracy of about 2%. But for that price, it gives us a relativistically covariant theory. Since, moreover, the values of E_b used in our calculation have nothing to do with the real binding energies and are themselves obtained within a 5% accuracy (if not worser), we can accept the inaccuracy of the formula (3.20). Finally, the dispersion law in the covariant SM RFG model can be written as

$$E_{\mathbf{p}} = \sqrt{\mathrm{p}^2 + (M_i - \epsilon)^2} \tag{3.21}$$

with the parameter ϵ given by (3.20). Figure 3.4 shows examples for ν_μ CCQE scattering on neutrons bound in lead and carbon.

This exercise also sheds some light on the effective mass M^* in the SuSAM* model. Namely, a part of this effective mass is responsible for the binding energy. In fact, we (and even more so the authors of the model) have known this for a long time. How neatly does this all work? Figure (3.5) shows the differences, Δ, between the threshold neutrino energies given by Eq. (3.18) (noncovariant) and approximate (but covariant) formula

$$E_\nu^{\mathrm{th}} = \frac{(M_f + m)^2 - (M_i - \epsilon)^2}{2\left(\sqrt{(M_i - \epsilon)^2 + \mathrm{p}^2} - \mathrm{p}\cos\theta\right)}. \tag{3.22}$$

As is seen, the difference is practically negligible. Calculations show that for nuclei lighter than the lead nucleus, the difference is even smaller. Do we need to rewrite the program and recalculate everything? God forbid!!! It is enough to realize that it is not difficult in principle to make the theory covariant, but we know that this will not change anything. So, in all subsequent calculations we will use Eq. (3.18).

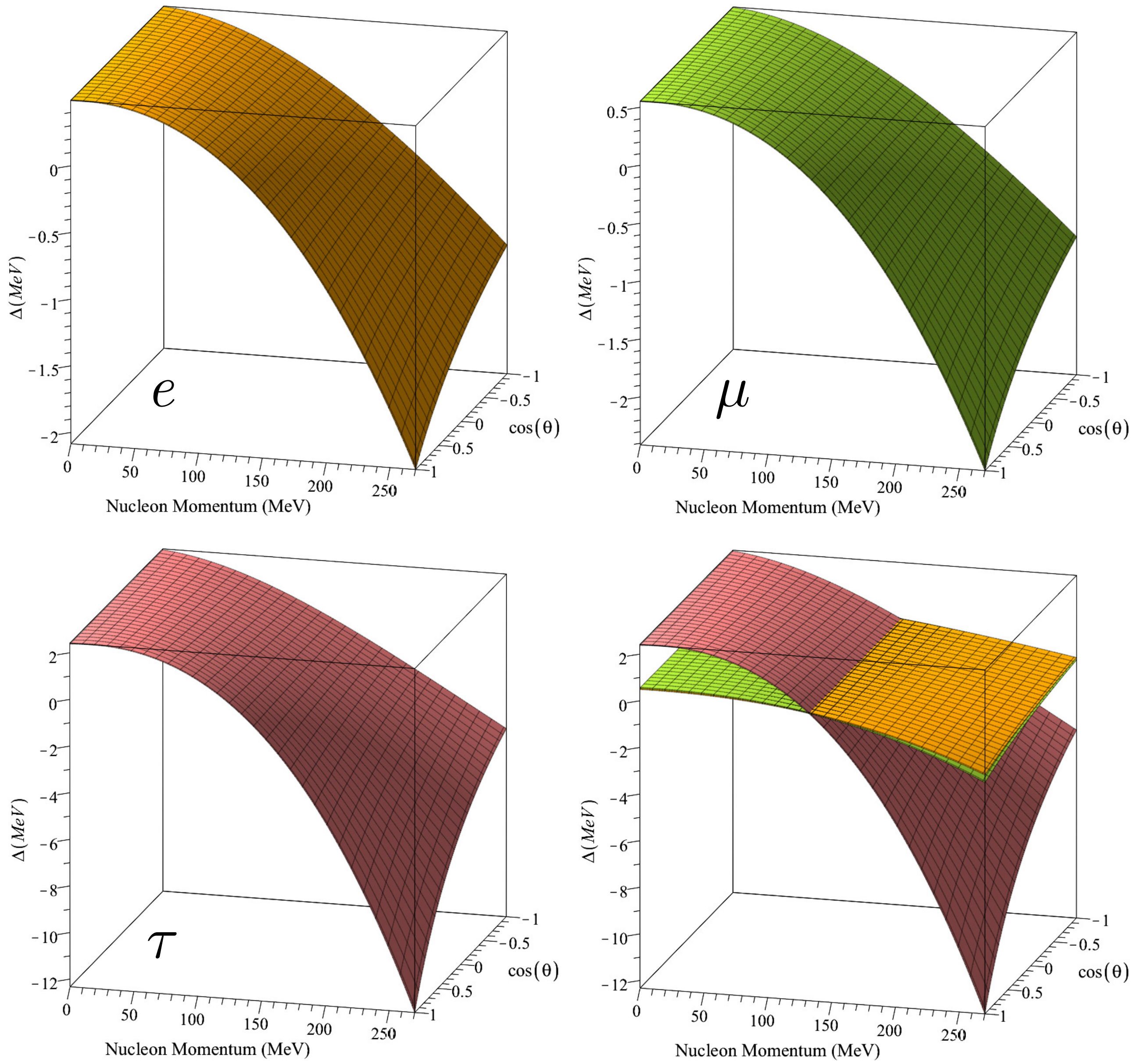

Figure 3.5: Difference between the threshold neutrino energies, calculated with the exact (noncovariant) and approximate (covariant) formulas for the reactions $\nu_\mu n_b \to \ell^- p$ ($\ell = e, \mu, \tau$) on neutron bound in lead. The bottom right panel shows all three Δs. Although at first glance the effect for the reaction with ν_τ seems noticeable, it is not at all so; due to the huge reaction threshold, the relative difference is negligible: $-0.0025 \lesssim \Delta/E_\nu^{\rm th} \lesssim 0.0005$ for lead and $-0.0008 \lesssim \Delta/E_\nu^{\rm th} \lesssim 0.0002$ for carbon.

3.1.2 Kinematics of CC0π scattering on nuclei

Let's start with interesting facts about the energy thresholds.

Weizsäcker mass formula

Below, for numerical illustrations we'll use the well-known Weizsäcker formula for the binding energy:

$$B(Z,A) = A\epsilon(Z,A) = a_V A - a_S A^{2/3} - a_C Z^2 A^{-1/3} - a_A (A-2Z)^2 A^{-1} + a_P A^{-3/4}, \tag{3.23}$$

where[3]

$$a_V = 15.76, \quad a_S = 17.81, \quad a_C = 0.711, \quad a_A = 23.7, \quad a_P = 34 \times \begin{cases} +1 & Z,N \text{ even } (A \text{ even}), \\ 0 & A \text{ odd}, \\ -1 & Z,N \text{ odd } (A \text{ even}). \end{cases}$$

Also, we'll use the empirical formula for the valley of stability (VS). From the Weizsäcker formula (3.23) it can be derived that in the VS

$$\frac{N}{Z} \approx a + bA^{2/3}, \quad a = 1, \quad b = \frac{a_c}{2a_A} = 0.015, \tag{3.24}$$

but empirically it is better to use $a = 0.98$. Figure 3.6 shows comparison of Eq. (3.23) against the data. Calculations are done using Eq. (3.24). It can be seen that the Weizsäcker approximation is quite suitable for not too precise estimates. For our purposes it is quite sufficient. From Eq. (3.24) it can be derived

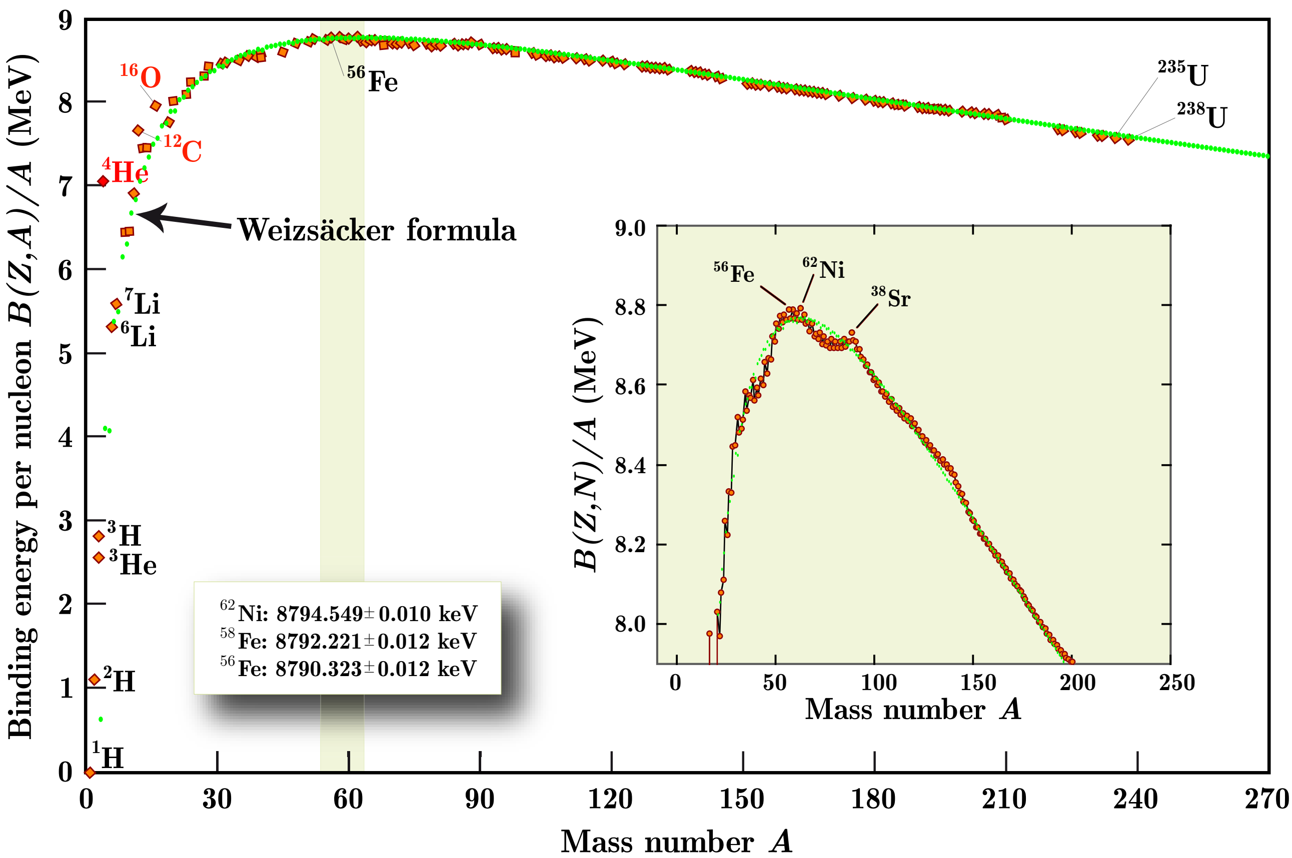

Figure 3.6: Test of the Weizsäcker formula for valley of stability; Eqs. (3.23) and (3.24) were formally applied to all A.

$$\begin{aligned} \frac{A}{Z} &= \frac{bX}{6} + b^2 Z^2 \left[\frac{4}{X}\left(\frac{b^3 Z^2}{6} + a + 1\right) + \frac{b}{3}\right] + a + 1, \\ X &= Z^{2/3}\left[8b^6 Z^4 + 72(a+1)b^3 Z^2 + 108(a+1)^2 + 12\sqrt{3(a+1)^3(4b^3 Z^2 + 27a + 27)}\right]^{1/3}. \end{aligned} \tag{3.25}$$

These cumbersome formulas are useful for drawing some figures in Maple.

[3]All values are given in MeV. The numerical values of the coefficients a_i may differ from author to author, but for our purposes this is not important. In real calculations we use the experimental values for E_b and the masses of the nuclei.

The thresholds

Here we consider the neutrino and antineutrino energy thresholds for the $0p0h$, $1p1h$, and $2p2h$ reactions:[4]

$$
\begin{aligned}
&\mathbf{0p0h}: \begin{cases} 1-\ \nu_\ell + (Z,A) \to \ell^- + (Z+1,A), \\ 2-\ \overline{\nu}_\ell + (Z,A) \to \ell^+ + (Z-1,A), \end{cases} \\
&\mathbf{1p1h}: \begin{cases} 3-\ \nu_\ell + (Z,A) \to \ell^- + (Z,A-1) + p, \\ 4-\ \overline{\nu}_\ell + (Z,A) \to \ell^+ + (Z-1,A-1) + n, \end{cases} \\
&\mathbf{2p2h}: \begin{cases} 5-\ \nu_\ell + (Z,A) \to \ell^- + (Z-1,A-2) + p + p, \\ 6-\ \nu_\ell + (Z,A) \to \ell^- + (Z,A-2) + p + n, \\ 7-\ \overline{\nu}_\ell + (Z,A) \to \ell^+ + (Z-1,A-2) + n + n, \\ 8-\ \overline{\nu}_\ell + (Z,A) \to \ell^+ + (Z-2,A-2) + n + p, \end{cases}
\end{aligned}
\tag{3.26}
$$

The reactions are numbered from 1 to 8 for easy for easy reference. The corresponding thresholds are

$$
E_\nu^{\text{th}} = \begin{cases}
\dfrac{[M(Z+1,A) - A\epsilon(Z+1,A) + m_\ell]^2}{2M'(Z,A)} - \dfrac{M'(Z,A)}{2} & \mathbf{0p0h} \\
\dfrac{[M(Z+1,A) - (A-1)\epsilon(Z,A-1) + m_\ell]^2}{2M'(Z,A)} - \dfrac{M'(Z,A)}{2} & \mathbf{1p1h} \\
\dfrac{[M(Z+1,A) - (A-2)\epsilon(Z-1,A-2) + m_\ell]^2}{2M'(Z,A)} - \dfrac{M'(Z,A)}{2} & \mathbf{2p2h}\ (pp) \\
\dfrac{[M(Z+1,A) - (A-2)\epsilon(Z,A-2) + m_\ell]^2}{2M'(Z,A)} - \dfrac{M'(Z,A)}{2} & \mathbf{2p2h}\ (pn)
\end{cases}
$$

$$
E_{\overline{\nu}}^{\text{th}} = \begin{cases}
\dfrac{[M(Z-1,A) - A\epsilon(Z-1,A) + m_\ell]^2}{2M'(Z,A)} - \dfrac{M'(Z,A)}{2} & \mathbf{0p0h} \\
\dfrac{[M(Z-1,A) - (A-1)\epsilon(Z-1,A-1) + m_\ell]^2}{2M'(Z,A)} - \dfrac{M'(Z,A)}{2} & \mathbf{1p1h} \\
\dfrac{[M(Z-1,A) - (A-2)\epsilon(Z-1,A-2) + m_\ell]^2}{2M'(Z,A)} - \dfrac{M'(Z,A)}{2} & \mathbf{2p2h}\ (nn) \\
\dfrac{[M(Z-1,A) - (A-2)\epsilon(Z-2,A-2) + m_\ell]^2}{2M'(Z,A)} - \dfrac{M'(Z,A)}{2} & \mathbf{2p2h}\ (np)
\end{cases}
$$

where

$$
M(Z,A) = ZM_p + (A-Z)M_n \quad \text{and} \quad M'(Z,A) = M(Z,A) - A\epsilon(Z,A).
$$

It can be proved analytically that the threshold of τ lepton production in (anti)neutrino-nucleus collisions is always lower than in (anti)neutrino-nucleon collisions. But the proof is very cumbersome and it is much easier to show it numerically.

All of these thresholds are shown (as functions of Z) in the left panels of Figs. 3.7–3.14 for electron, muon, and tau neutrinos and antineutrinos (from top to bottom). The binding energies are calculated according to Eq. (3.23) in which A is fixed by the VS relation (3.25) (filled circles) or the isoscalar condition $A = 2Z$ (open circles); the latter are shown just for comparison.[5] The right panels show the ratios of E_ν^{th} and $E_{\overline{\nu}}^{\text{th}}$ to the corresponding energy threshold on bare nucleons. The only exception is the case of ν_e scattering for which the reaction $\nu_e n \to ep$ is thresholdless.

Figure 3.15 shows a comparison of the thresholds for the reactions under consideration. In the figure, the binding energies are calculated according to Eq. (3.23) in which A is fixed by the VS relation (3.25). The numbering correspond to the sequence of the reactions in list (3.26).

Conclusions are quite obvious. A possible application of the effect is as follows: assume we have a ν_τ or $\overline{\nu}_\tau$ beam with energies below the τ production threshold for the bare nucleon, but higher than that for a given nuclear target. Then the observation of τ in the detector will indicate a production mechanism (diffractive, coherent) beyond the impulse approximation. That seems potentially interesting. So it makes sense to develop an appropriate theory.

Let's look at some more helpful illustrations. Figure 3.16 shows a comparison of the τ lepton kinetic energy and momentum ranges in the reaction $\nu_\tau + (Z,A) \to \tau^- + (Z+1,A)$ (the reaction that has the lowest threshold) for three nuclei ($Z = 7$, 10, and 20). Again, the binding energies are calculated according to Eq. (3.23) in which A is fixed by the VS relation (3.25). Later we use more realistic inputs. Figure 3.17 shows the same but for the reaction $\overline{\nu}_\ell + (Z,A) \to \ell^+ + (Z-1,A)$.

[4] So far, we are not considering reactions

$$
\nu_\ell + (Z,A) \to \ell^- + (Z,A-2) + D \ \text{ and } \ \overline{\nu}_\ell + (Z,A) \to \ell^+ + (Z-2,A-2) + D.
$$

[5] It is clear that most isoscalar nuclei (especially at large Z) are either unstable or do not exist at all.

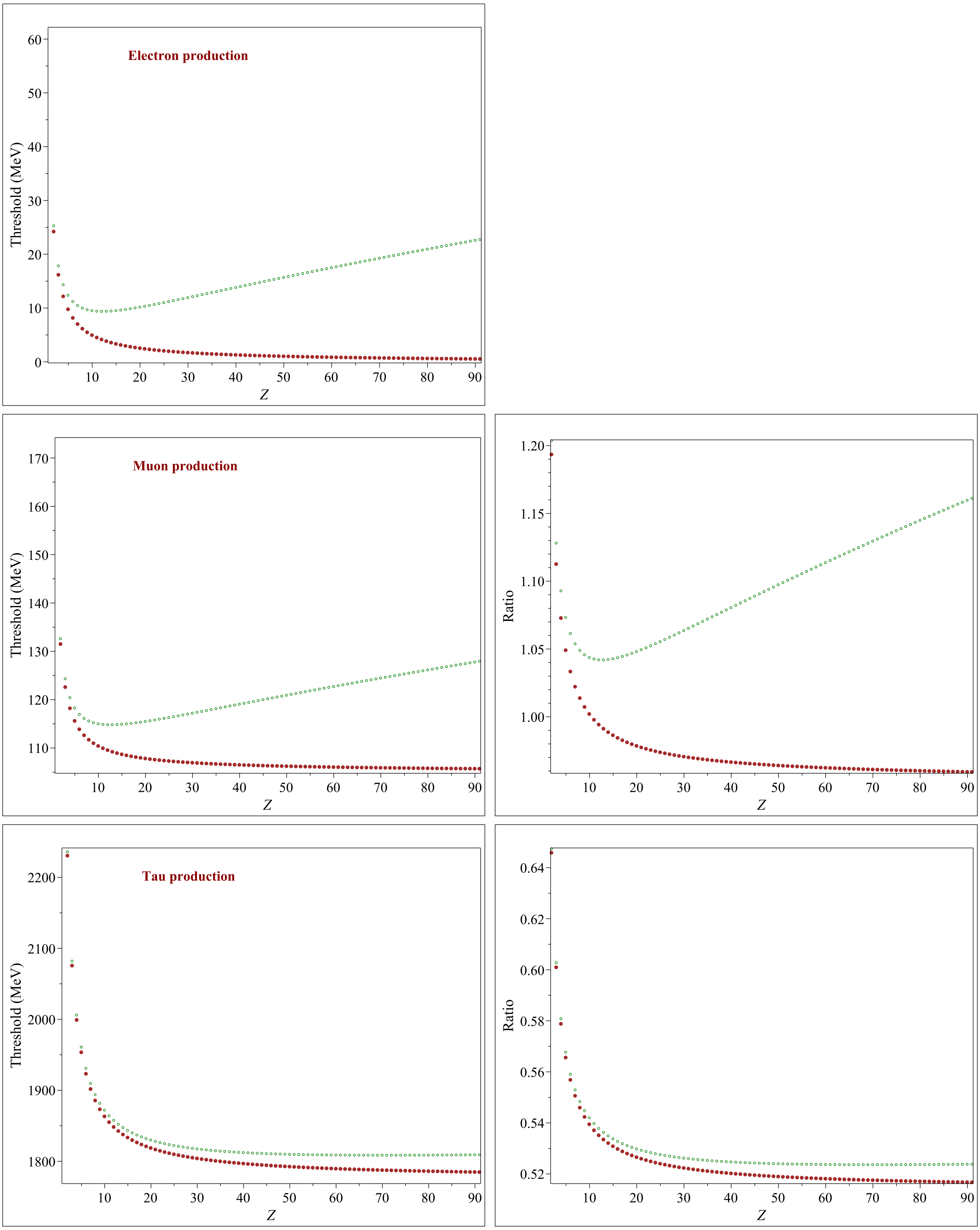

Figure 3.7: Neutrino energy thresholds for the reactions $\nu_\ell + (Z, A) \to \ell^- + (Z+1, A)$ (left panels) and ratios of these thresholds to the thresholds for the corresponding reactions on bare neutron (right panels). The binding energies are calculated according to Eq. (3.23) in which A is fixed by the VS relation (3.25).

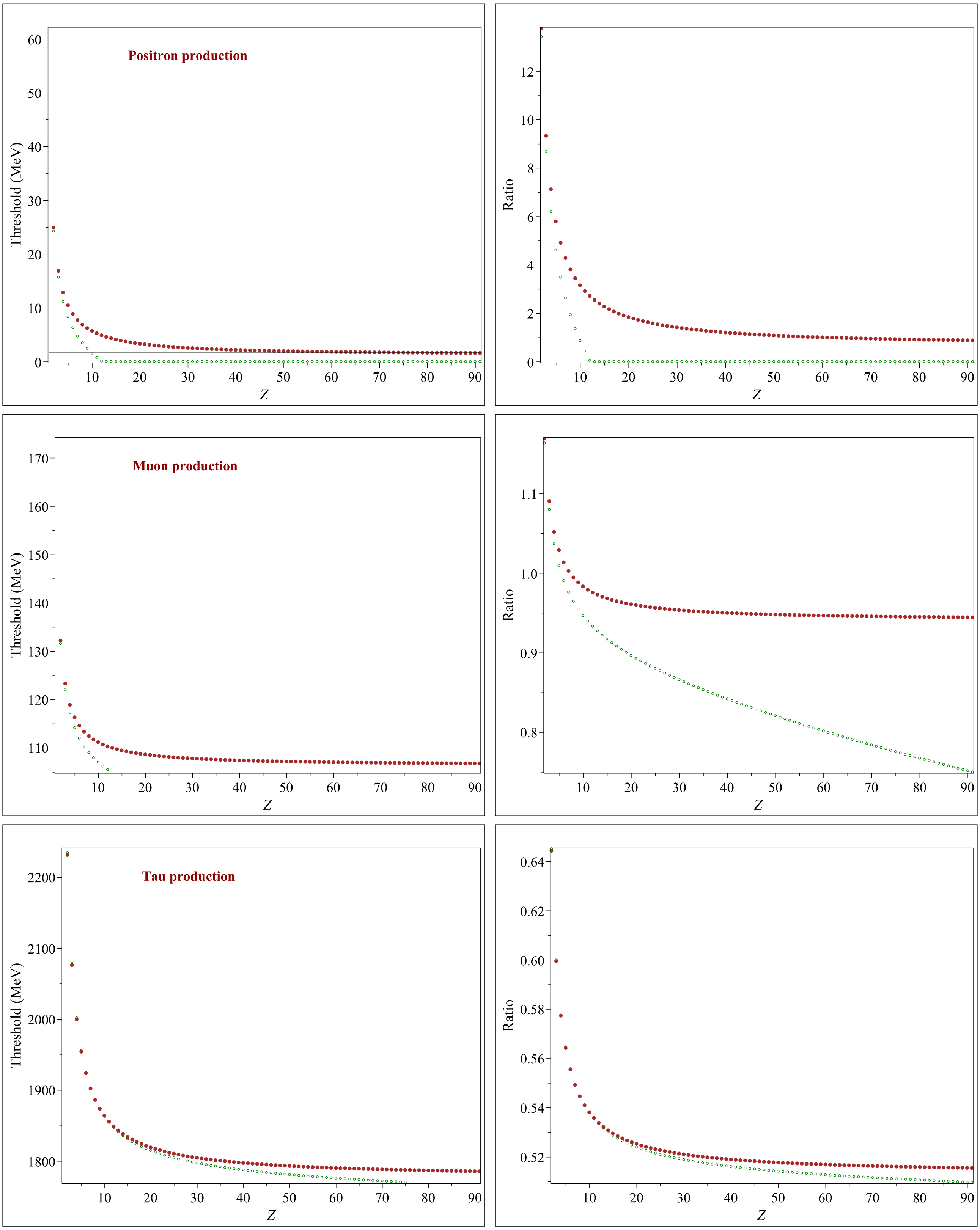

Figure 3.8: Antineutrino energy thresholds for the reactions $\overline{\nu}_\ell + (Z, A) \to \ell^+ + (Z-1, A)$ (left panels) and ratios of these thresholds to the thresholds for the corresponding reactions on bare proton (right panels). The binding energies are calculated according to Eq. (3.23) in which A is fixed by the VS relation (3.25).

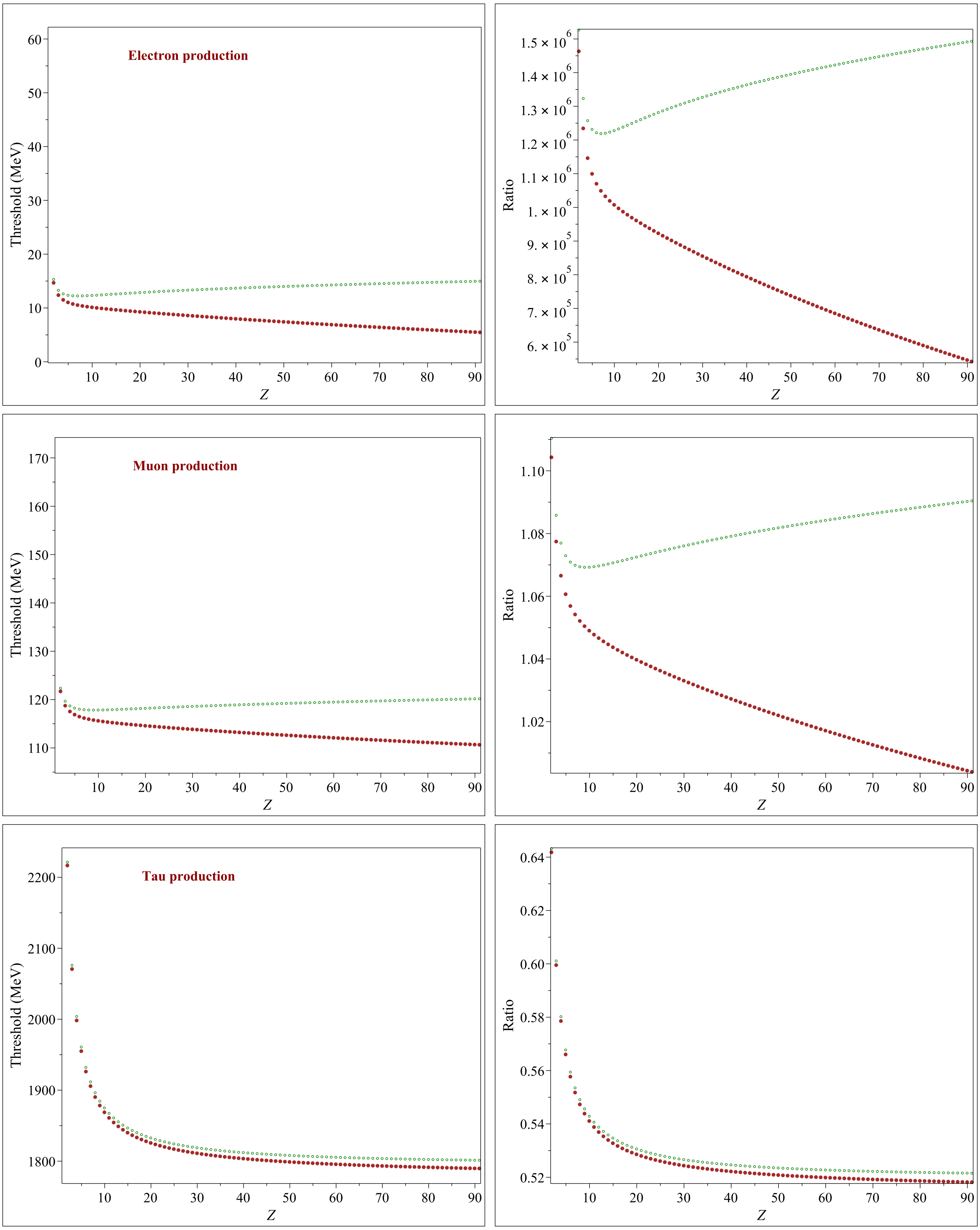

Figure 3.9: The same as in Fig. 3.7 but for the reactions $\nu_\ell + (Z, A) \to \ell^- + (Z, A-1) + p$.

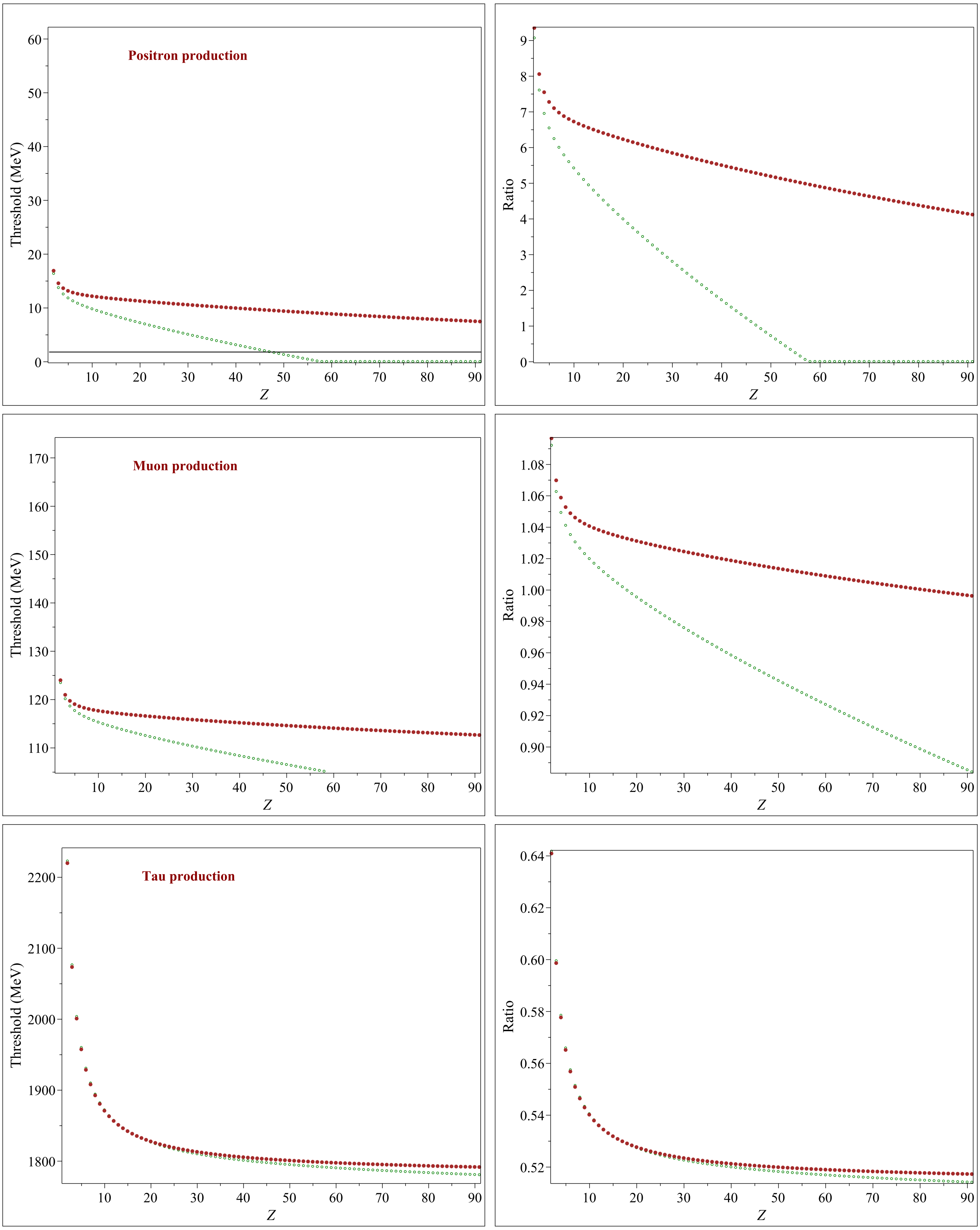

Figure 3.10: The same as in Fig. 3.8 but for the reactions $\overline{\nu}_\ell + (Z, A) \to \ell^+ + (Z-1, A-1) + n$.

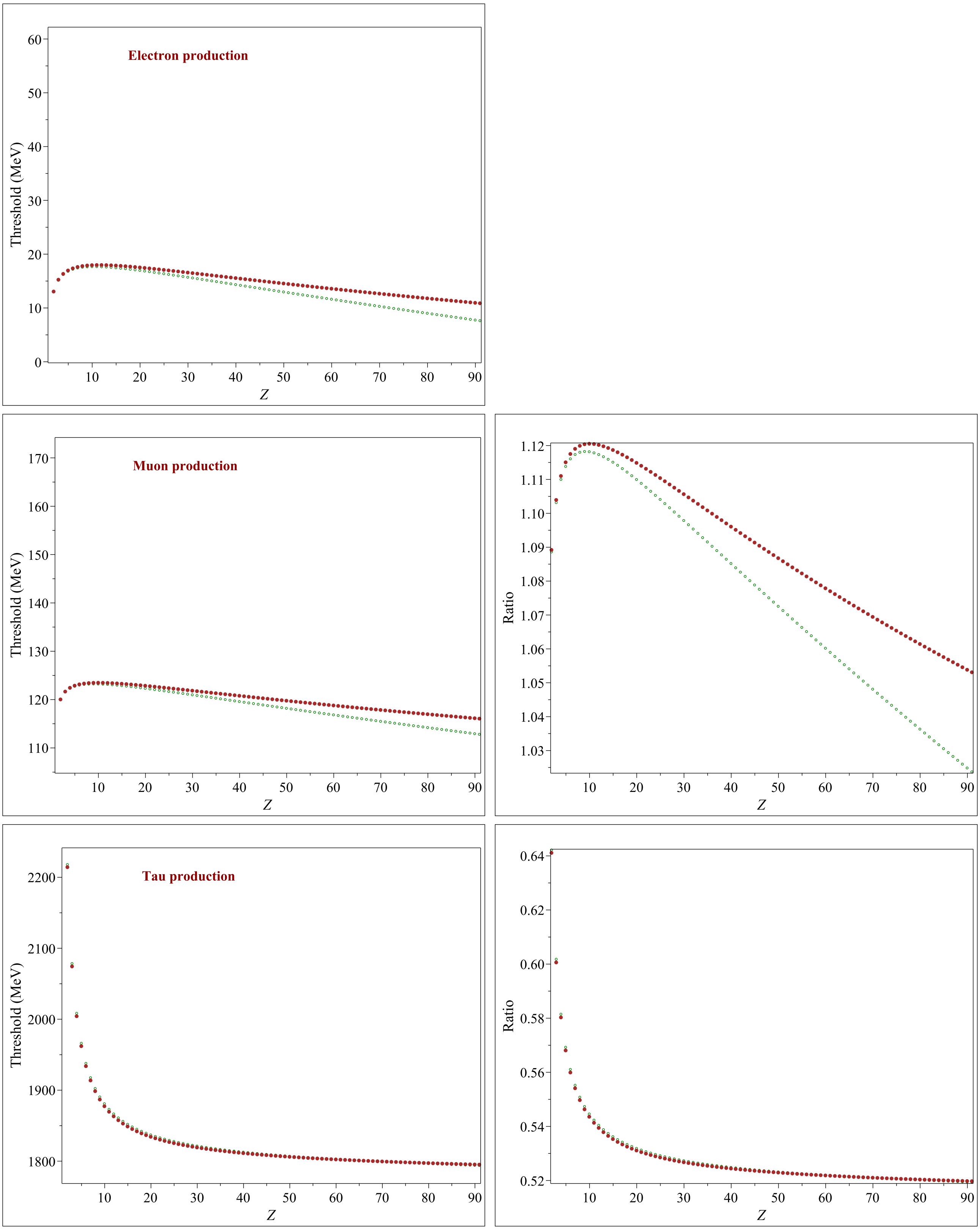

Figure 3.11: The same as in Fig. 3.7 but for the reactions $\nu_\ell + (Z, A) \to \ell^- + (Z-1, A-2) + p + p$.

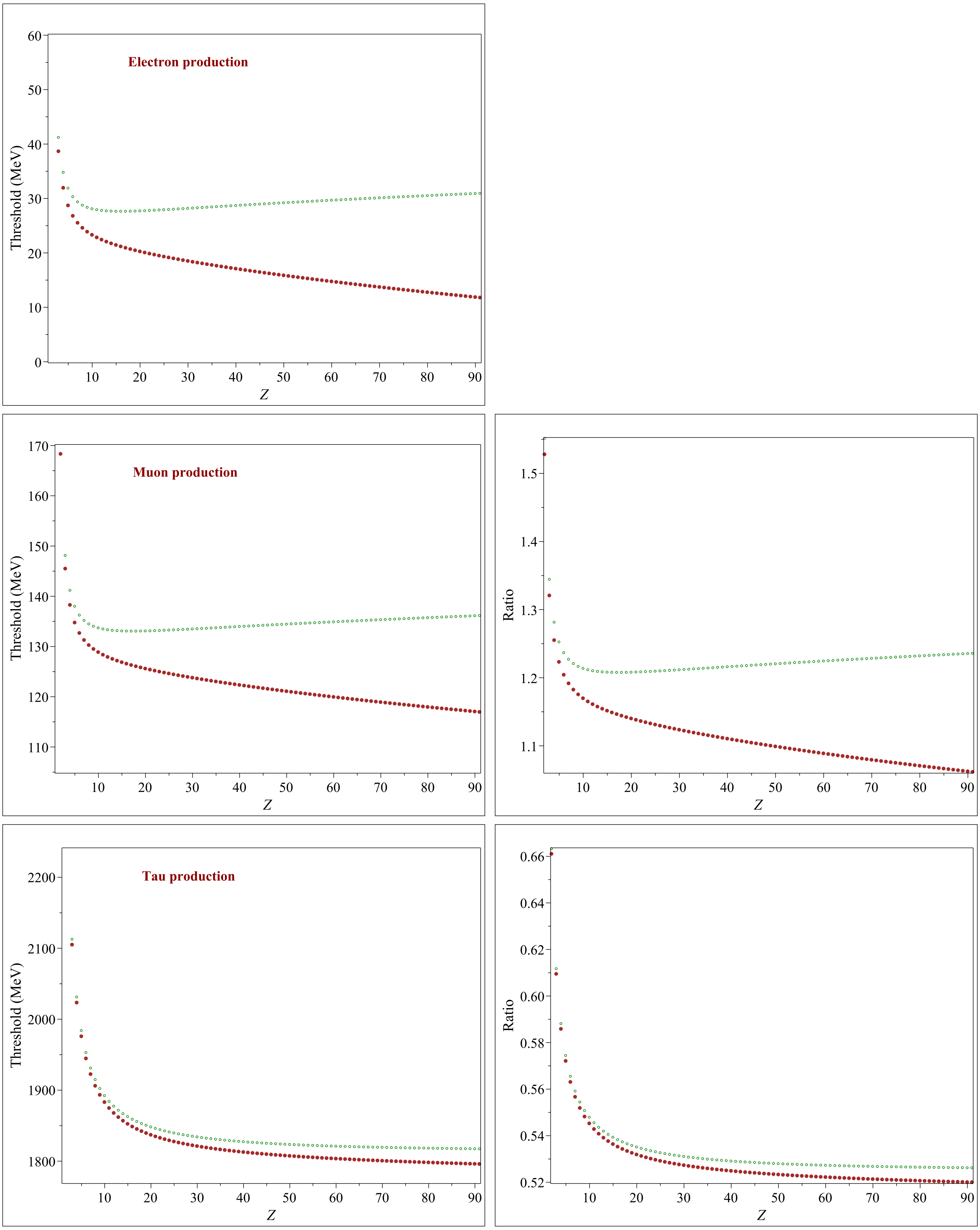

Figure 3.12: The same as in Fig. 3.7 but for the reactions $\nu_\ell + (Z, A) \to \ell^- + (Z, A-2) + p + n$.

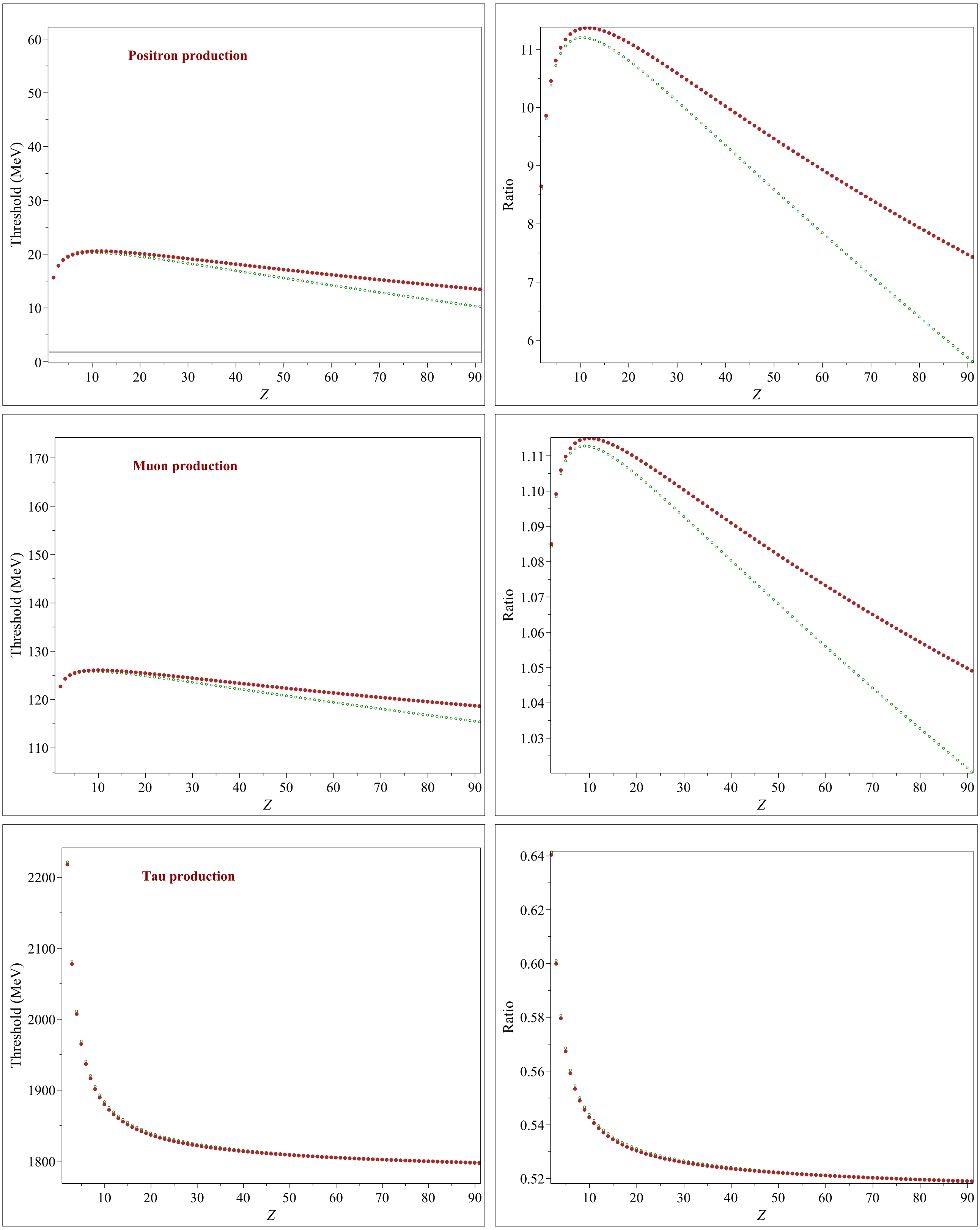

Figure 3.13: The same as in Fig. 3.8 but for the reactions $\overline{\nu}_\ell + (Z, A) \to \ell^+ + (Z-1, A-2) + n + n$.

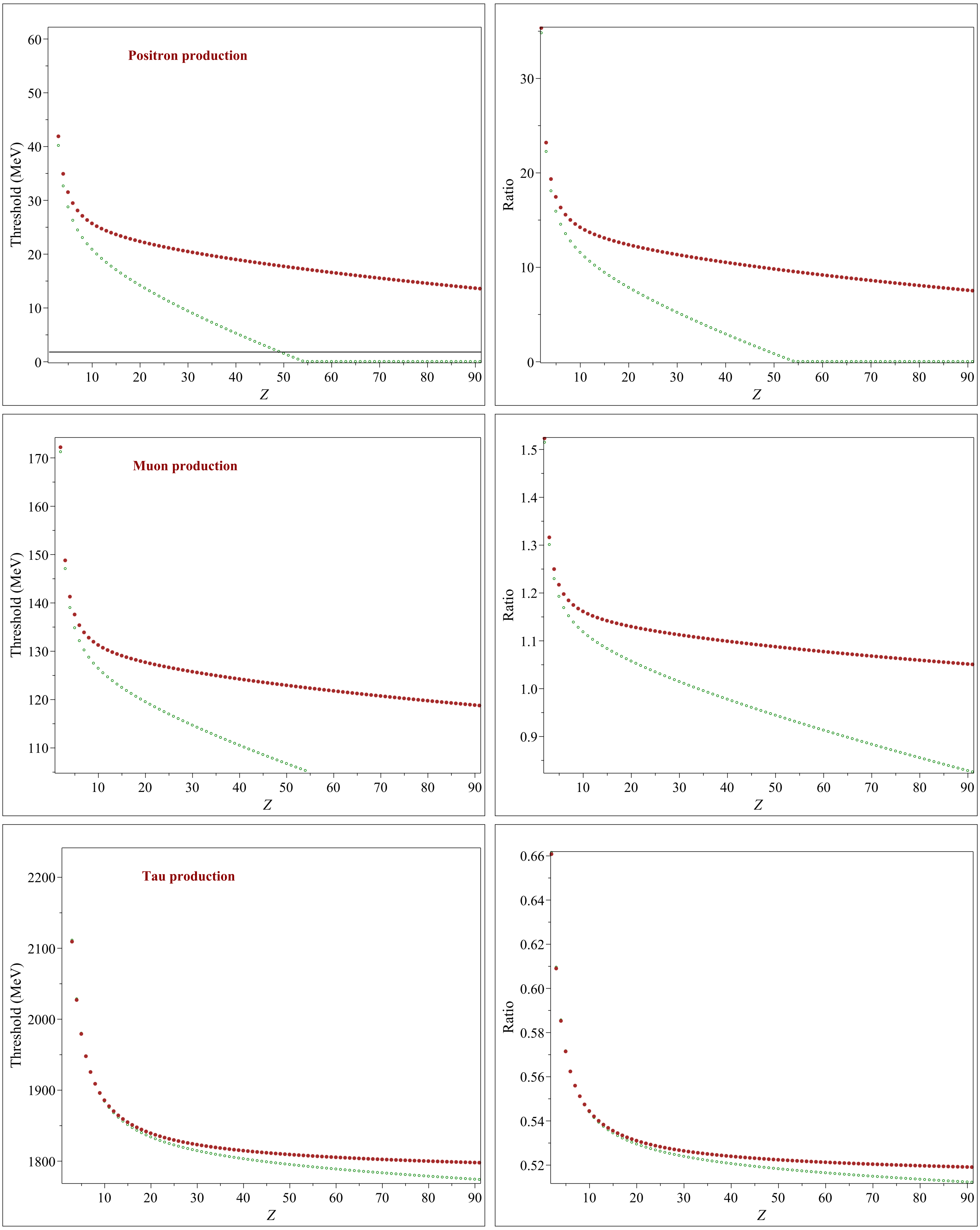

Figure 3.14: The same as in Fig. 3.8 but for the reactions $\overline{\nu}_\ell + (Z, A) \to \ell^+ + (Z-2, A-2) + n + p$.

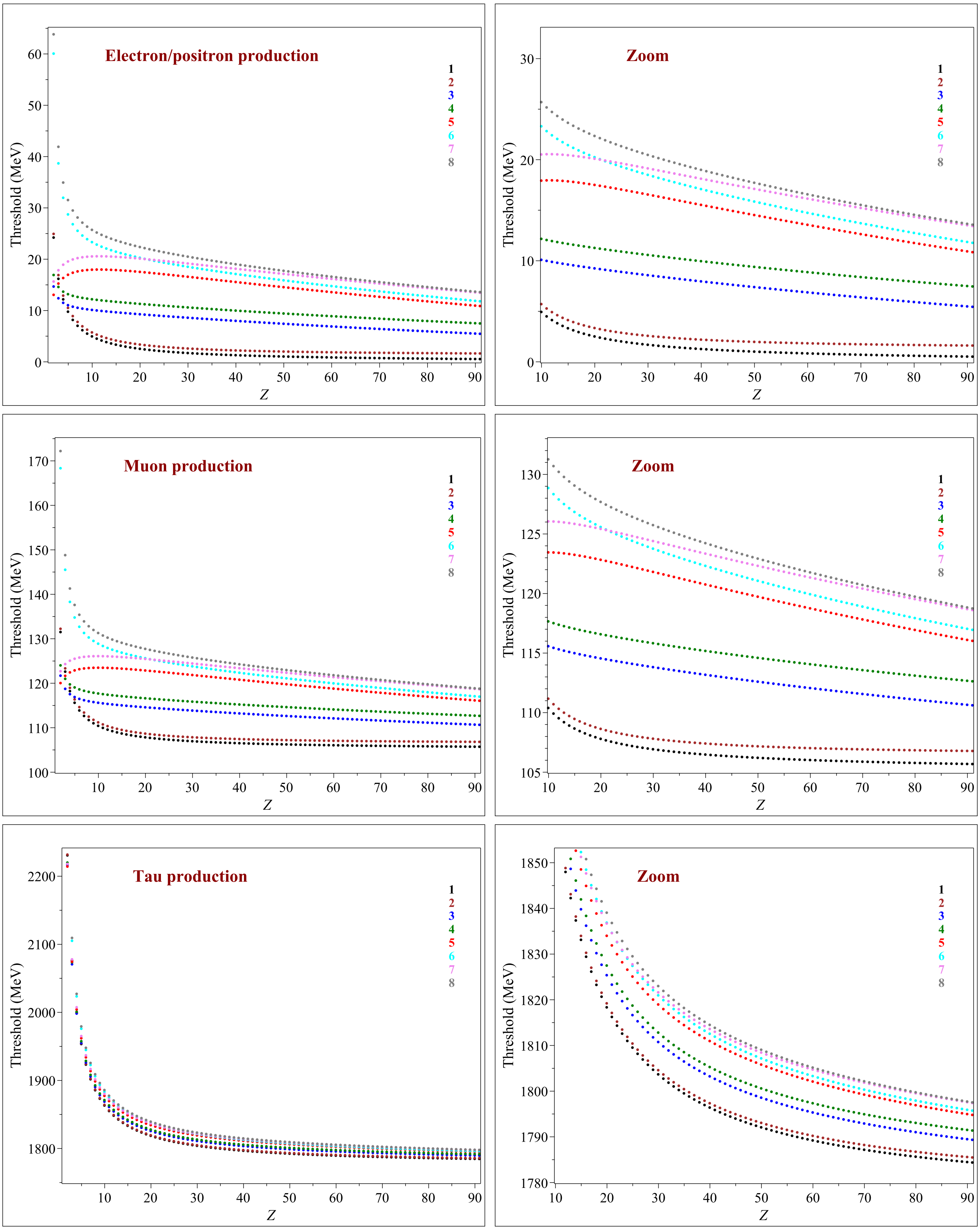

Figure 3.15: A comparison of the thresholds for the reactions under consideration. The binding energies are calculated according to Eq. (3.23) in which A is fixed by the VS relation (3.25) (as filled circles in Figs. 3.7–3.14). The numbering corresponds to the sequence of reactions in the (3.26) list, and the color corresponds to the color of the curves.

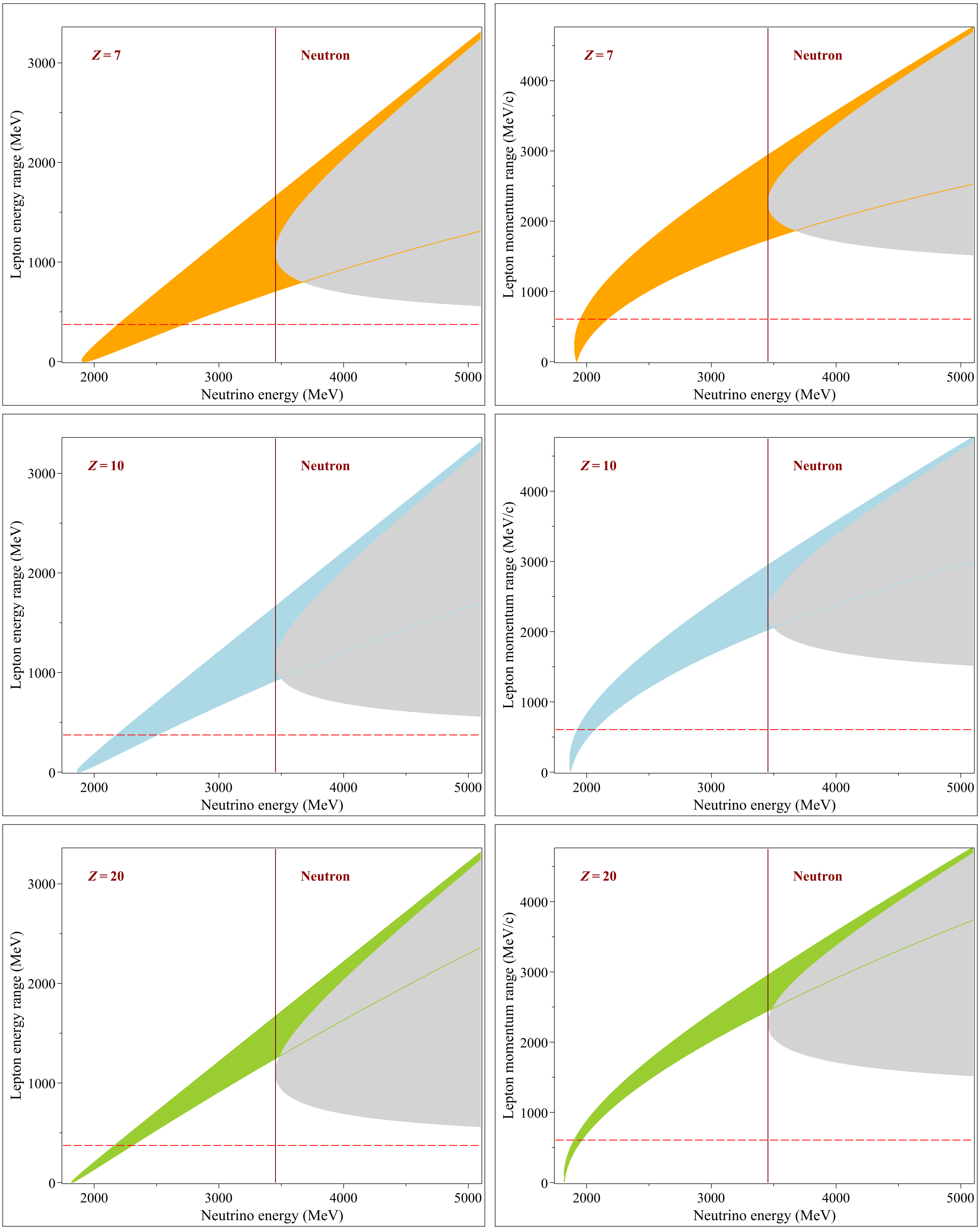

Figure 3.16: Comparison of the τ lepton kinetic energy and momentum ranges in the reaction $\nu_\tau + (Z, A) \to \tau^- + (Z + 1, A)$ for nuclei with $Z = 7$, 10, and 20. The binding energies are calculated according to Eq. (3.23) in which A is fixed by the VS relation (3.25). Vertical lines show the neutrino energy thresholds for reaction $\nu_\tau + n \to \tau^- + p$. Gray areas to the right of these lines show the τ lepton kinetic energy and momentum ranges for this reaction. Horizontal dashed lines show the minimum possible kinetic energy and momentum of the τ lepton in the reaction $\nu_\tau + n \to \tau^- + p$.

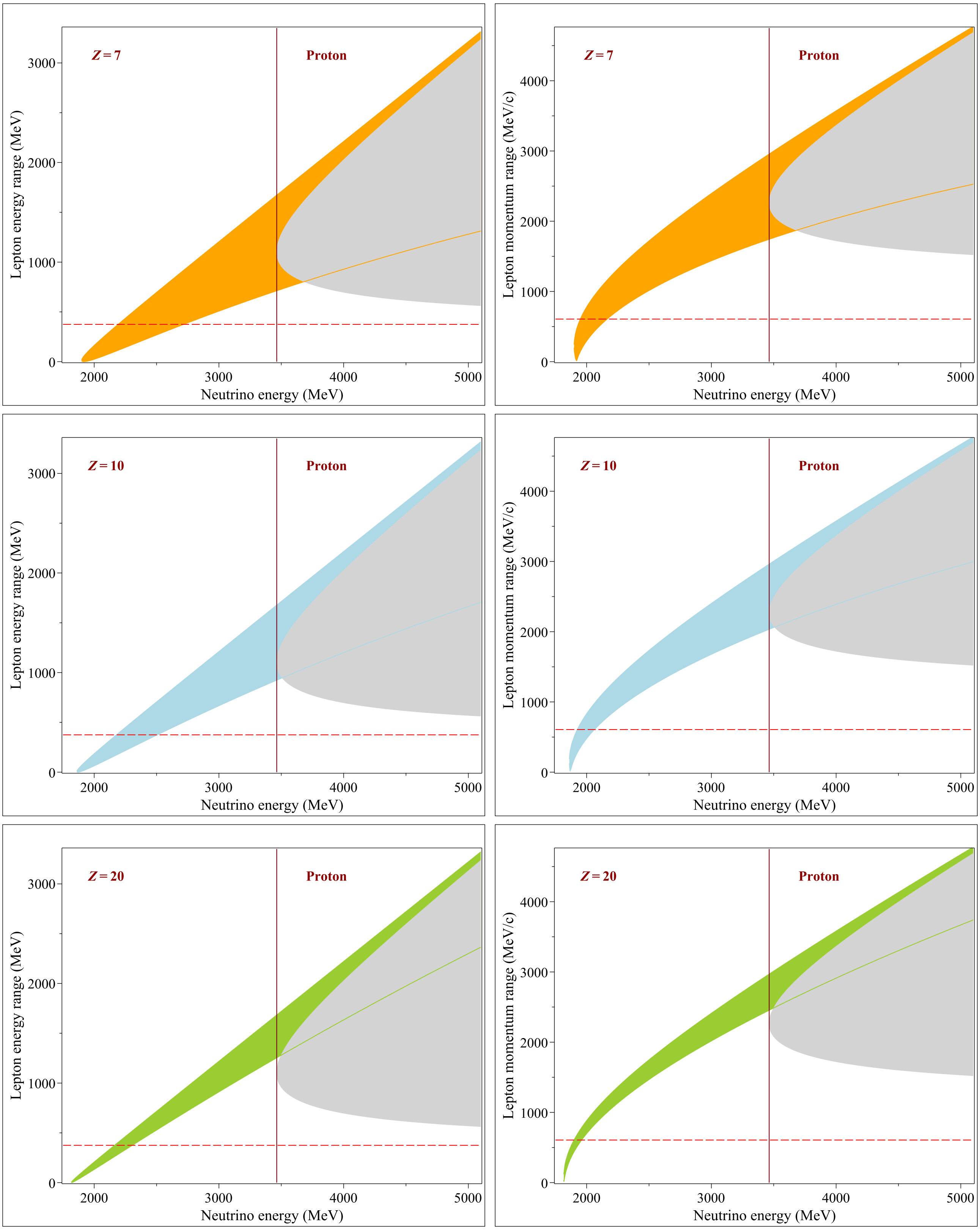

Figure 3.17: Comparison of the τ lepton kinetic energy and momentum ranges in the $0p0h$ reaction $\overline{\nu}_\ell + (Z, A) \to \ell^+ + (Z-1, A)$ for nuclei with $Z = 7$, 10, and 20. The binding energies are calculated according to Eq. (3.23) in which A is fixed by the VS relation (3.25). Vertical lines show the neutrino energy thresholds for reaction $\overline{\nu}_\tau + p \to \tau^+ + n$. Gray areas to the right of these lines show the τ lepton kinetic energy and momentum ranges for this reaction. Horizontal dashed lines show the minimum possible kinetic energy and momentum of the τ lepton in the reaction $\overline{\nu}_\tau + p \to \tau^+ + n$.

Horizontal dashed lines in Figs. 3.16 and 3.17 show the minimum possible kinetic energy (T_τ) and momentum (P_τ) of the τ lepton in the corresponding reactions on bare nucleon. These are given by the following relations:

$$T_\tau^{\rm ass} = \frac{(m_\tau - m_n)^2}{2m_n} \approx 373.23\ \text{MeV}, \quad P_\tau^{\rm ass} = \frac{m_\tau^2 - m_n^2}{2m_n} \approx 605.35\ \text{MeV}/c, \ \text{ for } \ \nu_\tau + n \to \tau^- + p;$$
$$T_\tau^{\rm ass} = \frac{(m_\tau - m_p)^2}{2m_p} \approx 374.90\ \text{MeV}, \quad P_\tau^{\rm ass} = \frac{m_\tau^2 - m_p^2}{2m_p} \approx 606.83\ \text{MeV}/c \ \text{ for } \ \overline{\nu}_\tau + p \to \tau^+ + n.$$

In fact, these are the asymptotic values of functions $T_\tau^{\min} = E_\tau^{\min} - m_\tau$ and $P_\tau^{\min}$ given by Eqs. (3.6) at $E_\nu \to \infty$. We see that in reactions at nuclei the τ lepton energies/momenta can be smaller (up to zero). Unfortunately, this does not provide an experimentally valuable additional signature, since the decay products of τ involve (invisible) neutrinos. But this could be used as an additional criterion in the case of a sharply decaying above 3.5 GeV (anti)neutrino spectrum.

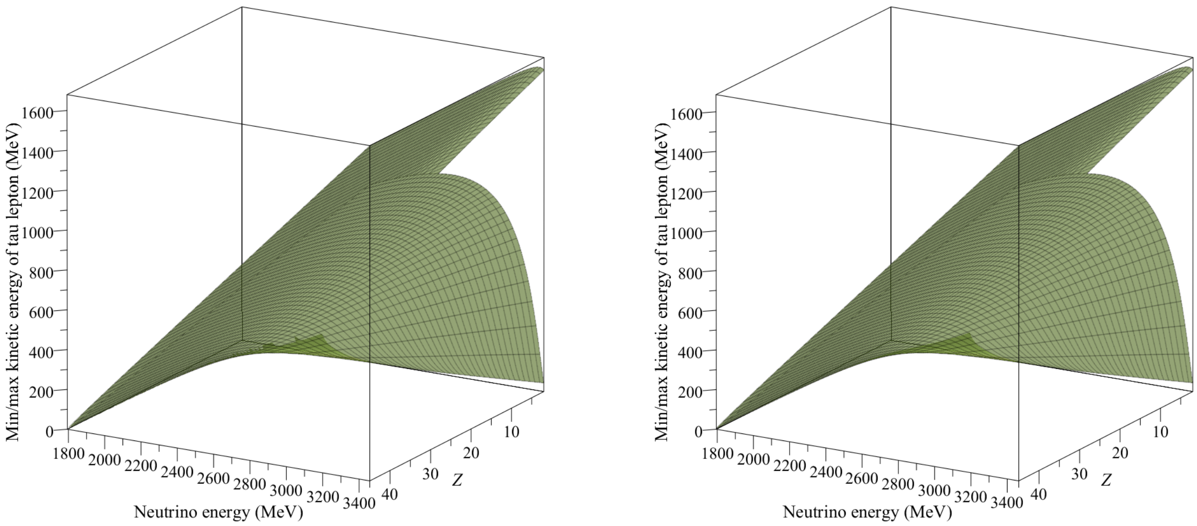

Figure 3.18: Minimum and maximum τ lepton kinetic energies vs. neutrino energy and Z for the $0p0h$ reactions $\nu_\tau + (Z, A) \to \tau^- + (Z+1, A)$ (left panel) and $\overline{\nu}_\ell + (Z, A) \to \ell^+ + (Z-1, A)$ (right panel). It is in particular seen that the maximum energy almost independent of Z.

Now let's consider the realistic calculations that use experimental data on the binding energies of the nuclides in question.

Reaction on Specific Nuclei

Here we consider reactions at a few selected nuclei, particularly Carbon and Oxigen, for which the measured binding energies are poorly described by the Weizsäcker formula (see Fig. 3.6). These nuclei are also important as components of many modern neutrino detectors.

Reactions on Bromine are interesting in at least two aspects. First, Bromine is relatively heavy and therefore the corresponding reactions have lower ν_τ and $\overline{\nu}_\tau$ energy thresholds than those for C and O. Second, Bromine is a component of Freon, a popular scintillator used in past (and perhaps future) neutrino detectors.

The input data are shown in Figs. 3.19, 3.20, and 3.21.

R	NUCLIDE	BINDING ENERGY PER NUCLEON IN MeV	TOTAL BINDING ENERGY IN MeV	PERCENTAG ABUNDANCE	HALF LIFE	U#NITS
1	6−Carbon−12	7.6801459166667	92.161751	98.889999	stable	
2	6−Carbon−14	7.520322	105.284508	0.000000	5730	years
3	6−Carbon−13	7.469851	97.108063	1.110000	stable	
RELEVANT NUCLIDES						
1	7−Nitrogen−12	6.1701100833333	74.04132	0.000000	0.011	seconds
3	7 − Nitrogen − 13	7.2388669230769	94.10527	0.000000	9.956	minutes
1	5 − Boron − 12	6.6312669166667	79.575203	0.000000	0.0202	seconds
3	5 − Boron − 13	6.4964013076923	84.453217	0.000000	0.01736	seconds

Figure 3.19: Stable Carbon isotopes listed in order of binding energy per nucleon. Also listed are the nuclides that can be the final state nuclei in the reactions in question.

R	NUCLIDE	BINDING ENERGY PER NUCLEON IN MeV	TOTAL BINDING ENERGY IN MeV	PERCENTAG ABUNDANCE	HALF LIFE	U#NITS
1	8 − Oxigen − 16	7.9762086875	127.619339	99.762001	stable	
2	8 − Oxigen − 18	7.7670585	139.807053	0.200000	stable	
3	8 − Oxigen − 17	7.750745	131.762665	0.038000	stable	
RELEVANT NUCLIDES						
1	9 − Fluorine − 16	6.96373275	111.419724	0.000000	1.1e-20	seconds
2	9 − Fluorine − 18	7.6316223333333	137.369202	0.000000	11.163	seconds
3	9 − Fluorine − 17	7.5423296470588	128.219604	0.000000	64.49	seconds
1	7 − Nitrogen − 16	7.373828875	117.981262	0.000000	7.13	seconds
2	7 − Nitrogen − 18	7.0383445	126.690201	0.000000	0.624	seconds
3	7 − Nitrogen − 17	7.286188	123.865196	0.000000	4.173	seconds

Figure 3.20: Stable Oxigen isotopes listed in order of binding energy per nucleon. Also listed are the nuclides that can be the final state nuclei in the reactions in question.

R	NUCLIDE	BINDING ENERGY PER NUCLEON IN MeV	TOTAL BINDING ENERGY IN MeV	PERCENTAG ABUNDANCE	HALF LIFE	U#NITS
1	35 − Bromine − 81	8.6959153209877	704.369141	49.310001	stable	
2	35 − Bromine − 83	8.6933314337349	721.546509	0.000000	2.4	hours
3	35 − Bromine − 79	8.6875965696203	686.320129	50.689999	stable	
RELEVANT NUCLIDES						
1	36 − Krypton − 81	8.6827912469136	703.306091	0.000000	229000	years
3	36 − Krypton − 79	8.6571137594937	683.911987	0.000000	35.04	hours
1	34 − Selenium − 81	8.6860027530864	703.566223	0.000000	18.45	minutes
3	34 − Selenium − 79	8.6955875443038	686.951416	0.000000	0	seconds

Figure 3.21: Stable Bromine isotopes listed in order of binding energy per nucleon. Also listed are the nuclides that can be the final state nuclei in the reactions in question.

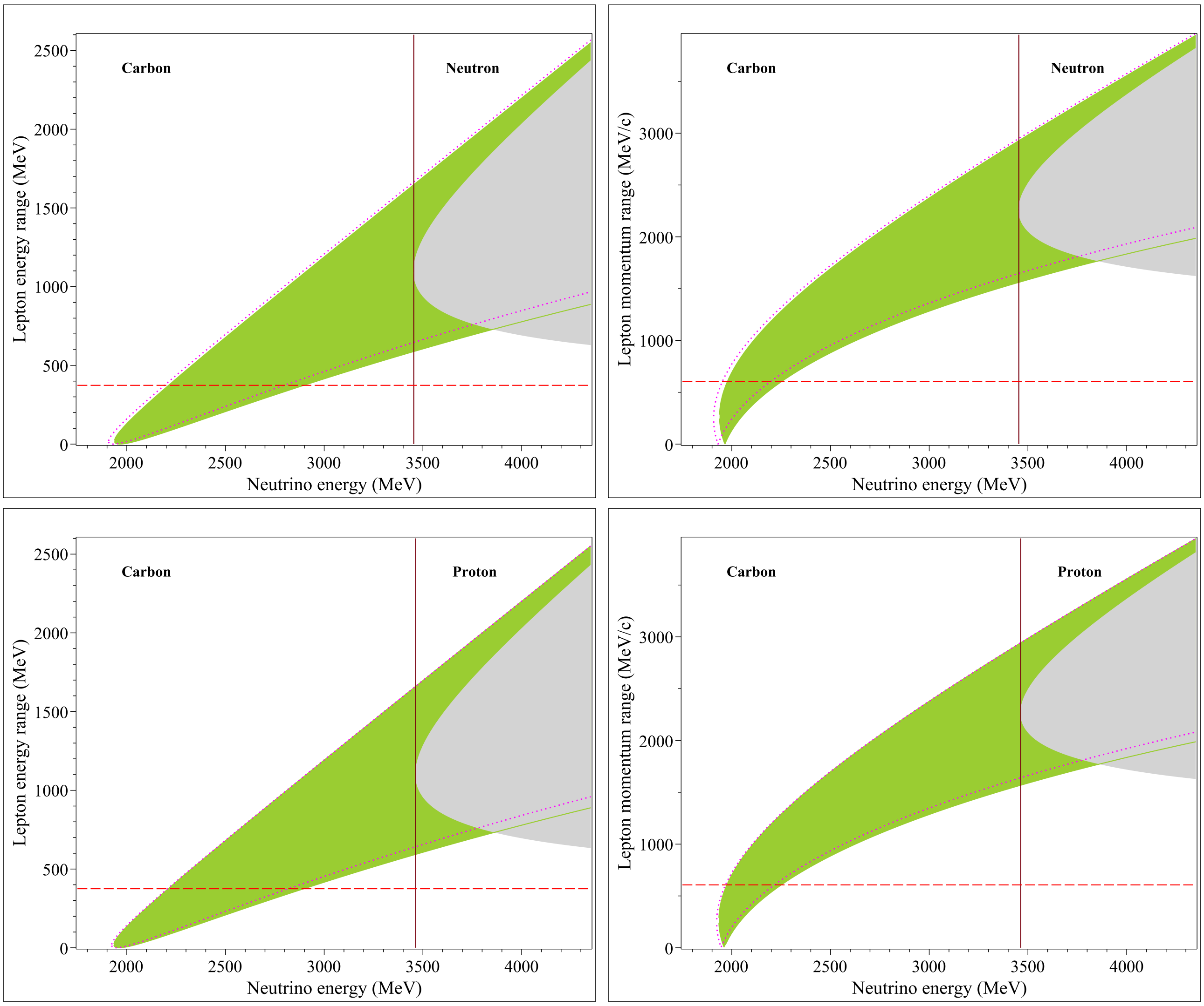

Figure 3.22: The τ lepton kinetic energy and momentum ranges in the $0p0h$ reactions $\nu_\tau + {}^{12}_{6}\mathrm{C} \to \tau^- + {}^{12}_{7}\mathrm{N}$ (top panels) and $\overline{\nu}_\tau + {}^{12}_{6}\mathrm{C} \to \tau^+ + {}^{12}_{5}\mathrm{B}$ (bottom panels). The dotted curves represent the corresponding ranges for the reactions $\nu_\tau + {}^{13}_{6}\mathrm{C} \to \tau^- + {}^{13}_{7}\mathrm{N}$ (top) and $\overline{\nu}_\tau + {}^{13}_{6}\mathrm{C} \to \tau^+ + {}^{13}_{5}\mathrm{B}$ (bottom). Other notations are the same as in Fig. 3.16.

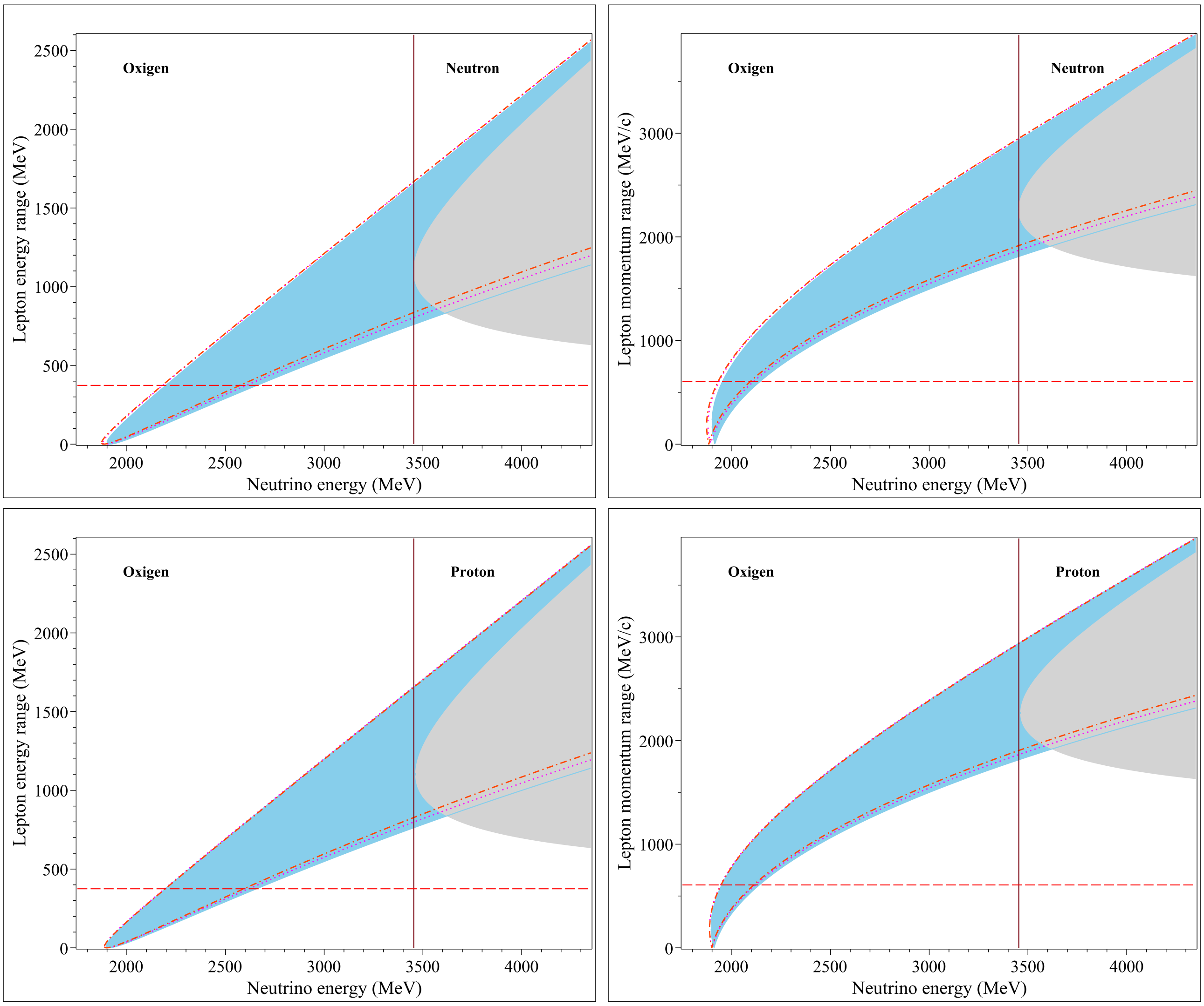

Figure 3.23: The τ lepton kinetic energy and momentum ranges in the $0p0h$ reactions $\nu_\tau + {}^{16}_{8}\mathrm{O} \to \tau^- + {}^{16}_{9}\mathrm{F}$ (top panels) and $\overline{\nu}_\tau + {}^{16}_{8}\mathrm{O} \to \tau^+ + {}^{16}_{7}\mathrm{N}$ (bottom panels). The dotted curves represent the corresponding ranges for the reactions $\nu_\tau + {}^{17}_{8}\mathrm{O} \to \tau^- + {}^{17}_{9}\mathrm{F}$ and $\nu_\tau + {}^{18}_{8}\mathrm{O} \to \tau^- + {}^{18}_{9}\mathrm{F}$ (top) and $\overline{\nu}_\tau + {}^{17}_{8}\mathrm{O} \to \tau^+ + {}^{17}_{7}\mathrm{N}$ and $\overline{\nu}_\tau + {}^{18}_{8}\mathrm{O} \to \tau^+ + {}^{18}_{7}\mathrm{N}$ (bottom). Other notations are the same as in Fig. 3.16.

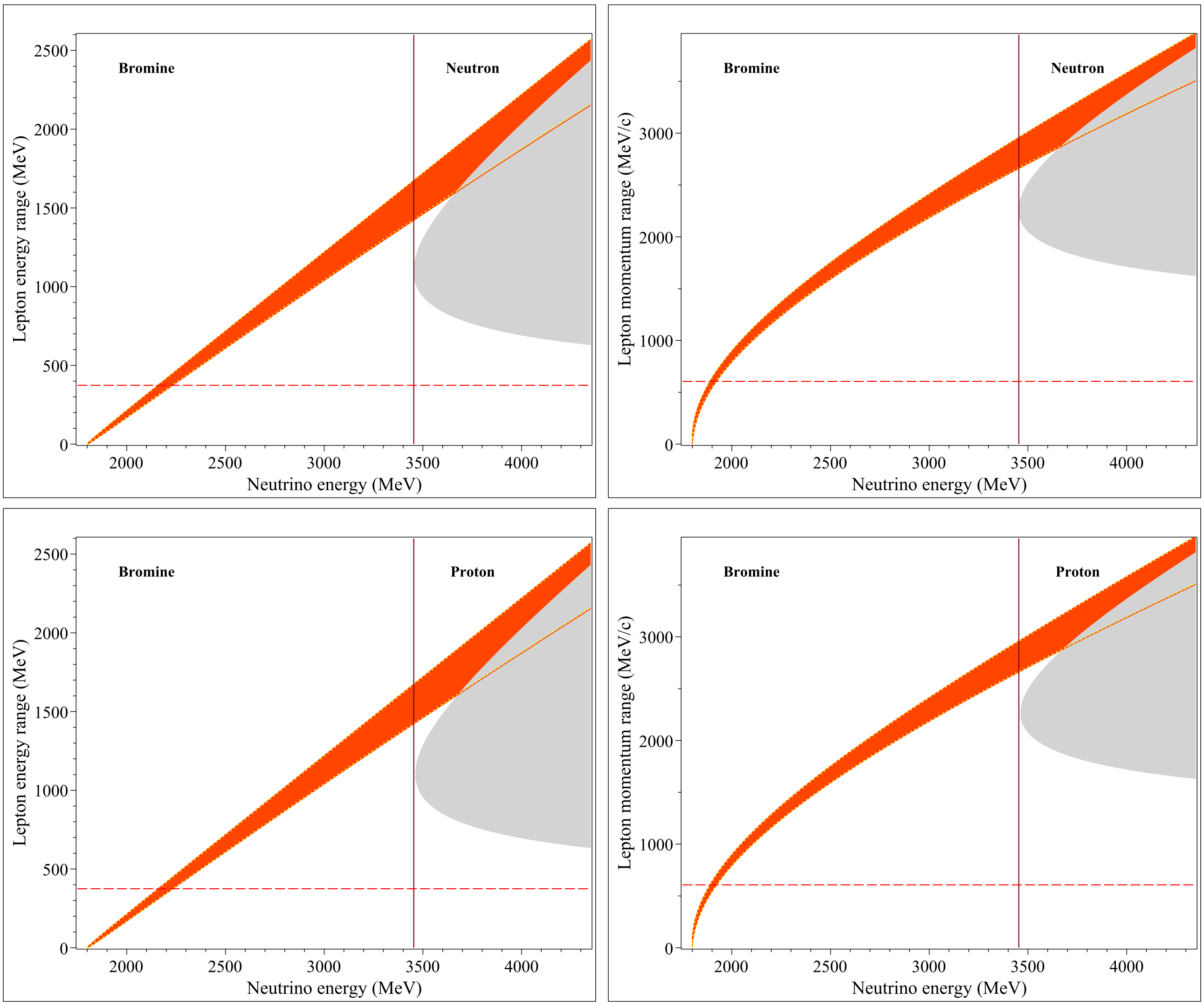

Figure 3.24: The τ lepton kinetic energy and momentum ranges in the $0p0h$ reactions $\nu_\tau + {}^{79}_{35}\mathrm{Br} \to \tau^- + {}^{79}_{36}\mathrm{Kr}$ (top panels) and $\overline{\nu}_\tau + {}^{79}_{35}\mathrm{Br} \to \tau^+ + {}^{79}_{34}\mathrm{Se}$ (bottom panels). The dotted curves represent the corresponding ranges for the reactions $\nu_\tau + {}^{81}_{35}\mathrm{Br} \to \tau^- + {}^{81}_{36}\mathrm{Kr}$ (top) and $\overline{\nu}_\tau + {}^{81}_{35}\mathrm{Br} \to \tau^+ + {}^{81}_{34}\mathrm{Se}$ (bottom). Other notations are the same as in Fig. 3.16.

3.2 Single pion production

Let us consider now the kinematics of the CC induced single pion production by neutrino or antineutrino,

$$\nu_\ell + N_i \to \ell^- + N_f + \pi \quad \text{or} \quad \overline{\nu}_\ell + N_i \to \ell^+ + N_f + \pi, \tag{3.27}$$

taking into account the mass of outgoing lepton m as well as the masse difference for the initial and final nucleons. The reaction threshold is given by $s^{\text{th}} = (M_f + m + m_\pi)^2$. Therefore the neutrino energy threshold is

$$E_\nu^{\text{th}} = \frac{s^{\text{th}} - M_i^2}{2M_i} = \frac{(M_f + m + m_\pi)^2 - M_i^2}{2M_i}.$$

The neutrino and lepton energies in the center-of-mass frame (CMF) of the neutrino-nucleon initial state are, respectively,

$$E_\nu^* = \frac{s - M_i^2}{2\sqrt{s}} \quad \text{and} \quad E_\ell^* \equiv E_\ell^*(W) = \frac{s + m^2 - W^2}{2\sqrt{s}}; \tag{3.28}$$

the target nucleon and the final hadronic state (resonance) energies are, respectively,

$$E_i^* = \frac{s + M_i^2}{2\sqrt{s}} \quad \text{and} \quad E_f^* \equiv E_f^*(W) = \frac{s - m^2 + W^2}{2\sqrt{s}}, \tag{3.29}$$

where

$$W^2 = (p+q)^2 = M_i^2 - Q^2 + 2M_i\,(E_\nu - E_\ell) \tag{3.30}$$

is the invariant mass square of the final hadronic state ($N_f + \pi$). Clearly

$$W_-^2 \leq W^2 \leq W_+^2, \quad \text{where} \quad W_- = M_f + m_\pi \quad \text{and} \quad W_+ = \sqrt{s} - m;$$

and the upper limit is obtained from the condition $E_\ell^* \geq m$.

The bounds for the variable

$$Q^2 \equiv -q^2 = 2\,(kk') - m^2 = 2E_\nu\,(E_\ell - P_\ell \cos\theta) - m^2 \tag{3.31}$$

can be found in terms of variable W by rewriting Eq. (3.31) in the CMF,

$$Q^2 = 2E_\nu^*\,(E_\ell^* - P_\ell^* \cos\theta^*) - m^2,$$

and putting $\cos\theta^* = \pm 1$. In this way, we have

$$Q_-^2 \leq Q^2 \leq Q_+^2, \quad \text{where} \quad Q_\pm^2 = 2E_\nu^*\,(E_\ell^* \pm P_\ell^*) - m^2. \tag{3.32}$$

In complete analogy to the QE case, by combining Eqs. (3.46), (3.30) and (3.31), we can derive the equation

$$E_\nu P_\ell \cos\theta = E_\ell\,(E_\nu + M_i) - \sqrt{s} E_\ell^*(W). \tag{3.33}$$

The formal solution to Eq. (3.33) is given by

$$P_\ell^\pm(\theta, W) = \frac{E_\nu\left[\sqrt{s}E_\ell^* \cos\theta \pm m\,(E_\nu + M_i)\sqrt{\zeta^2 - \sin^2\theta}\right]}{s + E_\nu^2 \sin^2\theta} \tag{3.34a}$$

$$= \frac{E_\nu^*\left(M_i E_\ell^* \cos\theta \pm m E_i^* \sqrt{\zeta^2 - \sin^2\theta}\right)}{M_i^2 + (E_\nu^*)^2 \sin^2\theta}, \tag{3.34b}$$

$$E_\ell^\pm(\theta, W) = \frac{\sqrt{s}E_\ell^*\,(E_\nu + M_i) \pm m E_\nu^2 \cos\theta \sqrt{\zeta^2 - \sin^2\theta}}{s + E_\nu^2 \sin^2\theta} \tag{3.34c}$$

$$= \frac{M_i E_\ell^* E_i^* \pm m\,(E_\nu^*)^2 \cos\theta \sqrt{\zeta^2 - \sin^2\theta}}{M_i^2 + (E_\nu^*)^2 \sin^2\theta}, \tag{3.34d}$$

where θ is the scattering angle ($\mathbf{p}_\nu \mathbf{p}_\ell = E_\nu P_\ell \cos\theta$) and

$$\zeta \equiv \zeta(W) = \frac{2M_i\sqrt{s}P_\ell^*}{m\,(s - M_i^2)} = \frac{M_i\sqrt{(s + m^2 - W^2)^2 - 4m^2 s}}{m\,(s - M_i^2)}.$$

Since, according to Eq. (3.34a),

$$P_\ell^+(\theta, W) P_\ell^-(\theta, W) = m^2 E_\nu^2 \left[1 - \zeta^2(W)\right]. \tag{3.35}$$

Therefore, for given θ and W, there are two solutions, P_ℓ^+ and P_ℓ^-, when $\zeta(W) \le 1$ and the only solution, P_ℓ^+, when $\zeta(W) > 1$. Finally, taking into account the conditions $\zeta(W) \ge \sin\theta$ and $\sin\theta \ge 0$ we conclude that

$$
\begin{aligned}
&P_\ell = P_\ell^+(\theta, W), \quad E_\ell = E_\ell^+(\theta, W), \quad 0 \le \theta \le \pi, && \text{if } \zeta(W) > 1, \\
&P_\ell = P_\ell^\pm(\theta, W), \quad E_\ell = E_\ell^\pm(\theta, W), \quad 0 \le \theta < \arcsin\zeta(W), && \text{if } \zeta(W) \le 1.
\end{aligned}
$$

The asymptotic value of the limiting angle at $s \gg W^2$ is given by

$$\arcsin\zeta(W) \to \arcsin\left(\frac{M_i}{m}\right) \quad \text{if} \quad M_i \le m.$$

The condition $\zeta = 1$ defines the neutrino energy at which the second solution, P_ℓ^-, disappears. It can be rewritten in terms of the neutrino energy as

$$\left[E_\nu - \epsilon_\nu^-(W)\right]\left[E_\nu - \epsilon_\nu^+(W)\right] = 0 \tag{3.36}$$

with

$$\epsilon_\nu^\pm(W) = \frac{W^2 - (M_i \mp m)^2}{2\,(M_i \mp m)} \quad \text{and} \quad \epsilon_\nu^+ - \epsilon_\nu^- = m\left(1 + \frac{W^2}{M_i^2 - m^2}\right).$$

In terms of variable s Eq. (3.36) reads:

$$\left[s - s^-(W)\right]\left[s - s^+(W)\right] = 0, \tag{3.37}$$

where

$$s^\pm(W) = M_i\left[2\,\epsilon_\nu^\pm(W) + M_i\right] = \frac{M_i\left[W^2 - m\,(m \mp M_i)\right]}{M_i \mp m}.$$

NOTE XVI:

- At high neutrino energies, namely at $s \gg W^2 + m^2$, one can write:

$$Q_-^2 = m^2\left(\frac{2E_\nu^*}{E_\ell^* + P_\ell^*} - 1\right) \simeq m^2\left(\frac{W^2 - M_i^2}{s - W^2}\right).$$

- The following identities may be of utility to simplify the numerical calculations:

$$\left(Q_-^2 + m^2\right)\left(Q_+^2 + m^2\right) = 4m^2\left(E_\nu^*\right)^2, \quad Q_+^2 - Q_-^2 = 4E_\nu^* P_\ell^*.$$

- $Q_+^2 = Q_-^2 = m\,(2E_\nu^* - m)$ in the point $W = W_+$, while $Q_+^2 > Q_-^2$ for $W < W_+$.

NOTE XVII: Eq. (3.33) can be rewritten in the form of equation of ellipse in the plane of $P_\ell \sin\theta$ versus $P_\ell \cos\theta$:

$$\left(P_\ell \sin\theta\right)^2 + \varrho^2\left(P_\ell \cos\theta - P_\ell^c\right)^2 = \left(P_\ell^*\right)^2,$$

where

$$\varrho = \frac{\sqrt{s}}{E_\nu + M_i} \quad \text{and} \quad P_\ell^c = \frac{E_\nu E_\ell^*}{\sqrt{s}}.$$

The eccentricity and the focal parameter of the ellipse are, respectively,

$$\sqrt{1 - \varrho^2} = \frac{E_\nu}{E_\nu + M_i} \quad \text{and} \quad \frac{P_\ell^*}{\sqrt{1 - \varrho^2}} = \frac{P_\ell^* \sqrt{s}}{E_\nu}.$$

NOTE XVIII:

Let us now consider the derivative (cf. NOTE XI)

$$\frac{d\zeta}{ds} = \frac{1}{2\zeta}\left(\frac{d\zeta^2}{ds}\right) = \frac{M_i^2 \varXi}{m^2\left(s - M_i^2\right)^3 \zeta},$$

where

$$\varXi = \left(W^2 - M_i^2 + m^2\right)s - \left(W^2 - M_i^2 - m^2\right)\left(W^2 - m^2\right).$$

Since $s \ge (W + m)^2$ and $W \ge M_f + m_\pi$ one can prove that $\varXi > 2m\,(W + m)\left[W\,(W + m) - M_i^2\right] > 0$. Hence $d\zeta/ds > 0$ that is ζ is a *monotonically increasing* function of s for any W. It's also clear that ζ is a *monotonically decreasing* function of W for any s.

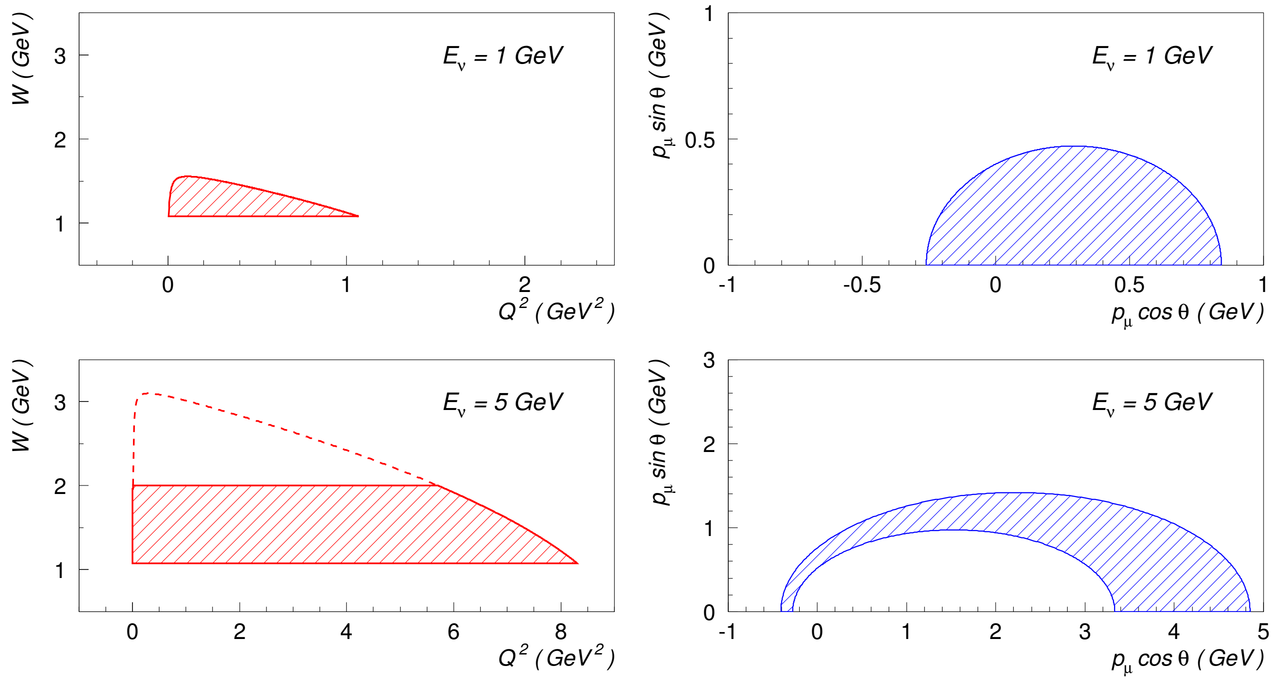

Figure 3.25: Kinematically allowed regions for the process $\nu_\mu + p \to \mu^- + p + \pi^+$ in terms of variables $\left(Q^2, W\right)$ (left) and $(P_\mu \cos\theta, P_\mu \sin\theta)$ (right) for two values of neutrino energy, E_ν. The shaded areas correspond to the W cutoff of 2 GeV.

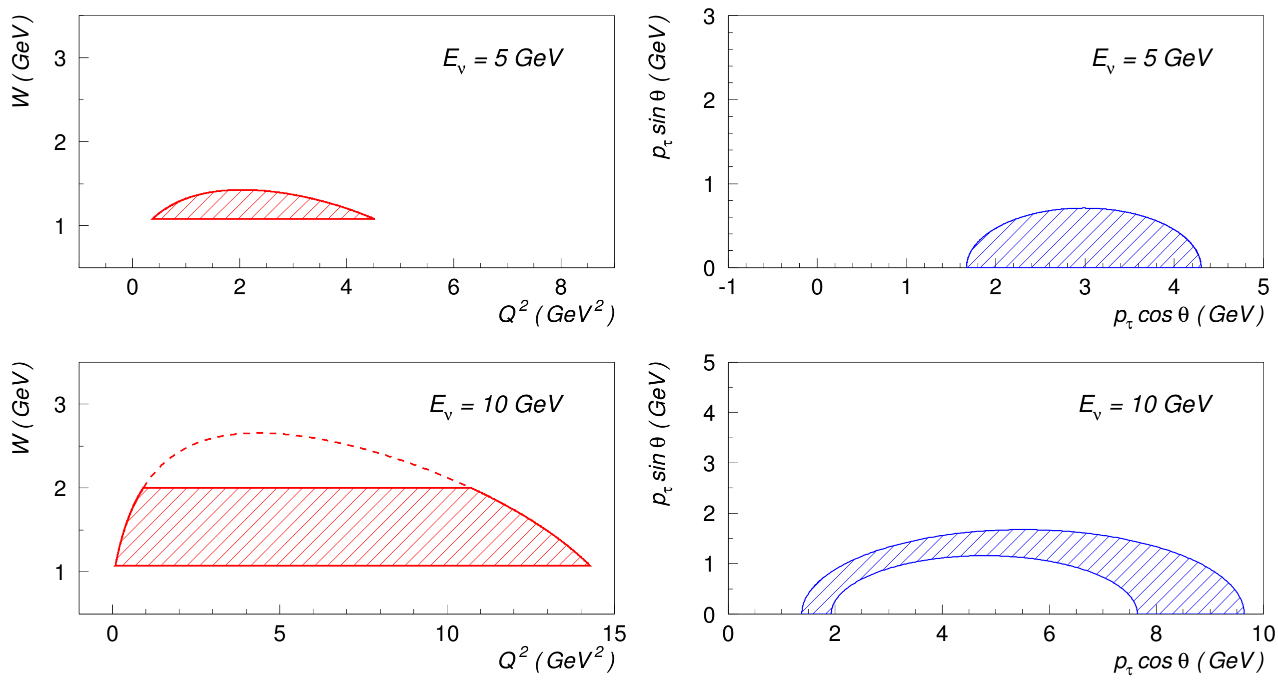

Figure 3.26: The same as in Fig. 3.25 but for the process $\nu_\tau + p \to \tau^- + p + \pi^+$.

With the actual values of the masses of particles involved into the reactions under consideration, we can conclude that the condition $\zeta = 1$ is never satisfied for $\tau^\pm$ production ($\zeta(W) < 1$ for any W, "two-branch case") while for production of $e^\pm$ and $\mu^\pm$ the values of $\epsilon_\nu^+(W)$ may be above the reaction thresholds and thus there are both single- and two-branch kinematics. The corresponding energy gap, $\epsilon_\nu^+(W) - E_\nu^{\text{th}}$ grows with W and moreover, the gap between the $\epsilon_\nu^+(W)$ and the "quasithreshold",[6]

$$\epsilon_\nu^{\text{th}}(W) = \frac{(W+m)^2 - M_i^2}{2M_i},$$

also expands with increasing W since

$$\epsilon_\nu^+(W) - \epsilon_\nu^{\text{th}}(W) = \frac{m\,(W - M_i + m)^2}{2M_i\,(M_i - m)}$$

is a monotonically increasing function of W for $M_i > m$. These statements are illustrated by numerical examples given in Table 3.3.

Table 3.3: E_ν^{th}, $\epsilon_\nu^+(W)$ and $\epsilon_\nu^+(W) - E_\nu^{\text{th}}(W)$ for 12th reactions of single pion production, evaluated with $W = M_f + m_\pi$ and with $W = 1.6$ GeV (shown in parentheses). The reactions $\overline{\nu}_\ell + n \to \ell^+ + n + \pi^-$ and $\nu_\ell + p \to \ell^- + p + \pi^+$ are not included since their kinematics is identical to that of $\nu_\ell + n \to \ell^- + n + \pi^+$ and $\overline{\nu}_\ell + p \to \ell^+ + p + \pi^-$, respectively.

Reaction	E_ν^{th} (MeV)	ϵ_ν^+ (MeV)	$\epsilon_\nu^+ - E_\nu^{\text{th}}$
$\nu_e + n \to e^- + p + \pi^0$	143.777478	143.782693	5.21483 keV
$\nu_e + n \to e^- + n + \pi^+$	150.523633	150.529316	5.68240 keV
		(893.546256)	(126.504 keV)
$\overline{\nu}_e + p \to e^+ + n + \pi^0$	146.750864	146.756297	5.43276 keV
$\overline{\nu}_e + p \to e^+ + p + \pi^-$	150.538028	150.543726	5.69808 keV
		(896.072828)	(127.350 keV)
$\nu_\mu + n \to \mu^- + p + \pi^0$	241.425537	273.688632	3.86248 MeV
$\nu_\mu + n \to \mu^- + n + \pi^+$	242.769170	281.285937	4.05482 MeV
		(1117.98991)	(39.5724 MeV)
$\overline{\nu}_\mu + p \to \mu^+ + n + \pi^0$	242.057837	277.076219	3.95799 MeV
$\overline{\nu}_\mu + p \to \mu^+ + p + \pi^-$	242.812601	281.341947	4.06671 MeV
		(1121.02086)	(39.8226 MeV)
$\nu_\tau + n \to \tau^- + p + \pi^0$	3853.41862	–	–
$\nu_\tau + n \to \tau^- + n + \pi^+$	3871.29542	–	–
$\overline{\nu}_\tau + p \to \tau^+ + n + \pi^0$	3863.95416	–	–
$\overline{\nu}_\tau + p \to \tau^+ + p + \pi^-$	3873.98986	–	–

TO BE CONTINUED

[6] That is the two-branch region.

3.2.1 Kinematics of CC1π scattering on nuclei

The thresholds

Consider the neutrino and antineutrino energy thresholds for the “trully” coherent reactions

$$\nu_\ell + (Z,A) \to \ell^- + (Z,A) + \pi^+ \quad \text{and} \quad \overline{\nu}_\ell + (Z,A) \to \ell^+ + (Z,A) + \pi^-. \tag{3.38}$$

These reactions (of course, not with τ neutrinos) have long been studied intensively experimentally, and there is some theory. But we are not so much interested in the pion in the final state, as in the τ lepton. It is clear that it is impossible to study this topic in the current experiments. Our task is to propose possible new experiments and estimate the subleading (coherent CC1pi) contributions to HK, DUNE, PINGU, ORCA.

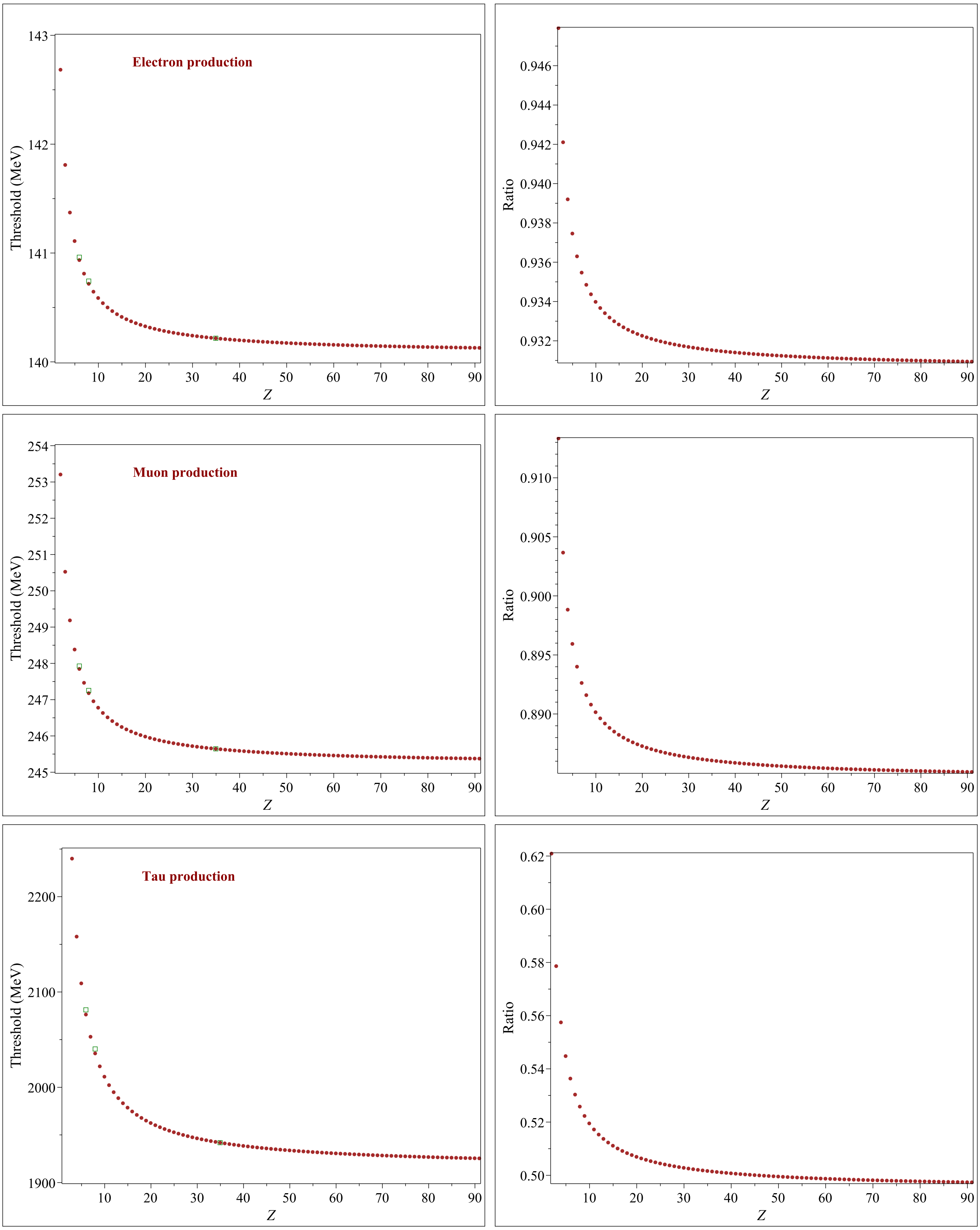

Figure 3.27: Neutrino energy thresholds for the reaction $\nu_\ell + (Z, A) \to \ell^- + (Z, A) + \pi^+$ (left panels) and ratios of these thresholds to the thresholds for the CC1π reactions on bare neutron (right panels). The binding energies are calculated according to Eq. (3.23) in which A is fixed by the VS relation (3.25). For comparison, the thresholds for the reactions on $^{12}_{6}$C, $^{16}_{8}$O, and $^{79}_{35}$Br, calculated using the measured values of B, are also shown.

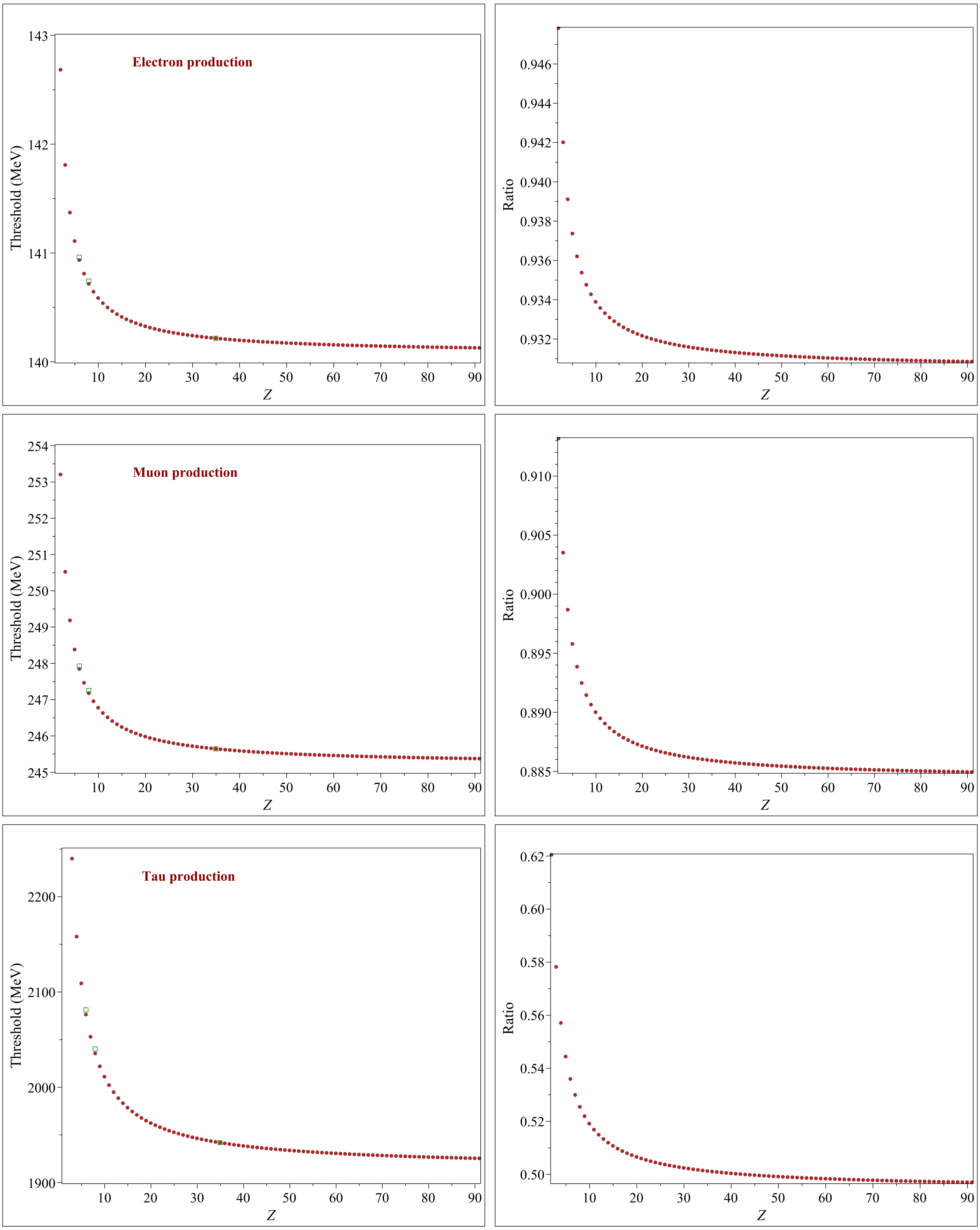

Figure 3.28: Antineutrino energy thresholds for the reaction $\overline{\nu}_\ell + (Z, A) \to \ell^+ + (Z, A) + \pi^-$ (left panels) and ratios of these thresholds to the thresholds for the CC1π reactions on bare proton (right panels). The binding energies are calculated according to Eq. (3.23) in which A is fixed by the VS relation (3.25). For comparison, the thresholds for the reactions on ${}^{12}_{6}$C, ${}^{16}_{8}$O, and ${}^{79}_{35}$Br, calculated using the measured values of B, are also shown.

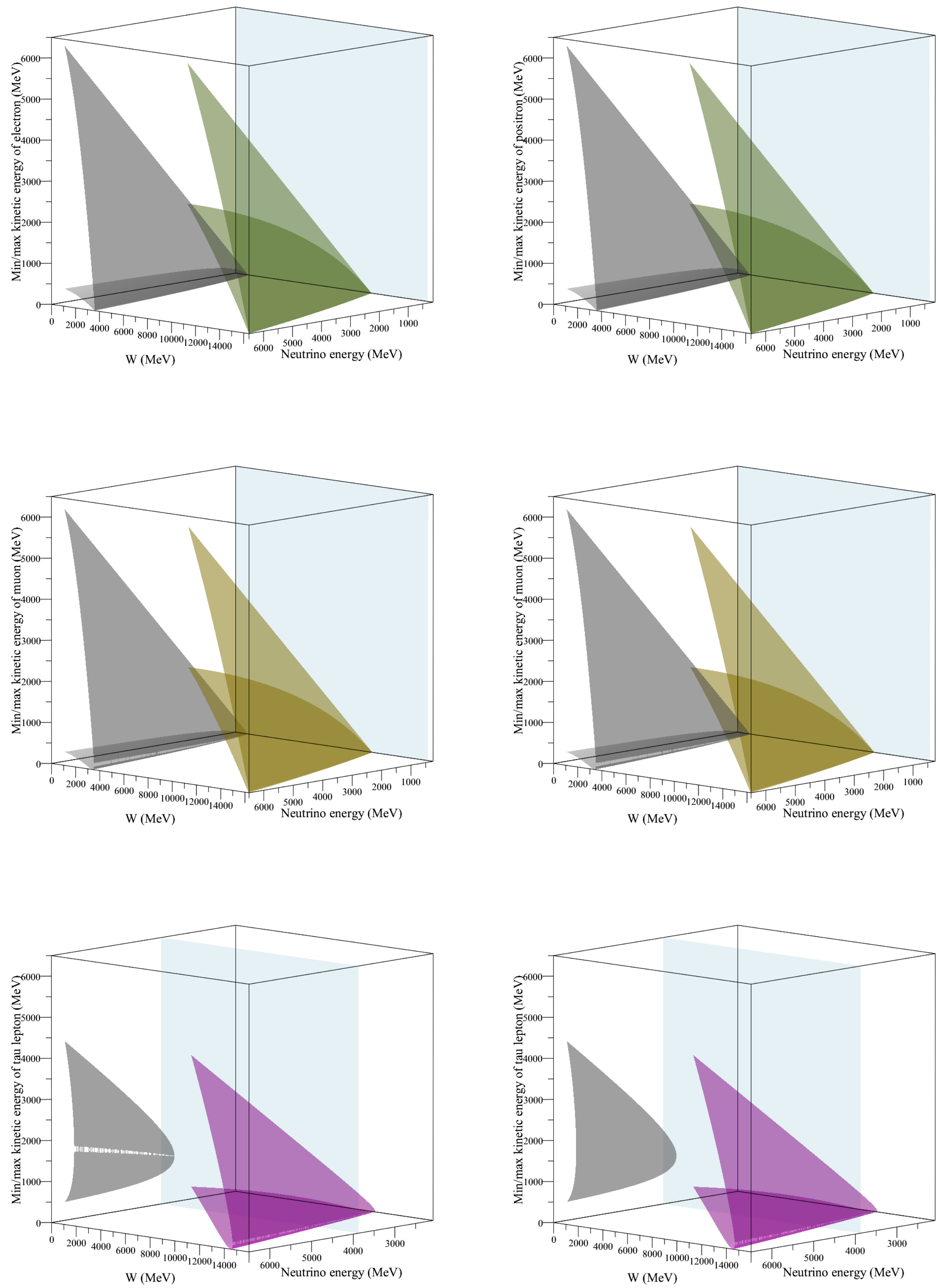

Figure 3.29: Minimum and maximum lepton kinetic energies vs. (anti)neutrino energy and W for the reactions $\nu_\ell + {}^{12}_{6}\mathrm{C} \to \ell^- + {}^{12}_{6}\mathrm{C} + \pi^+$ (left panels) and $\overline{\nu}_\ell + {}^{12}_{6}\mathrm{C} \to \ell^+ + {}^{12}_{6}\mathrm{C} + \pi^-$ (right panels), where $\ell = e, \mu, \tau$ (from top to bottom). The binding energies are calculated according to Eq. (3.23) in which A is fixed by the VS relation (3.25). The corresponding boundaries for CC1π reactions on bare nucleons are also shown (gray surfaces). In all cases, the surfaces are depicted in the boundaries $W^- \leq W < W^+$. Vertical planes show the (anti)neutrino energy thresholds in the reactions on bare nucleons.

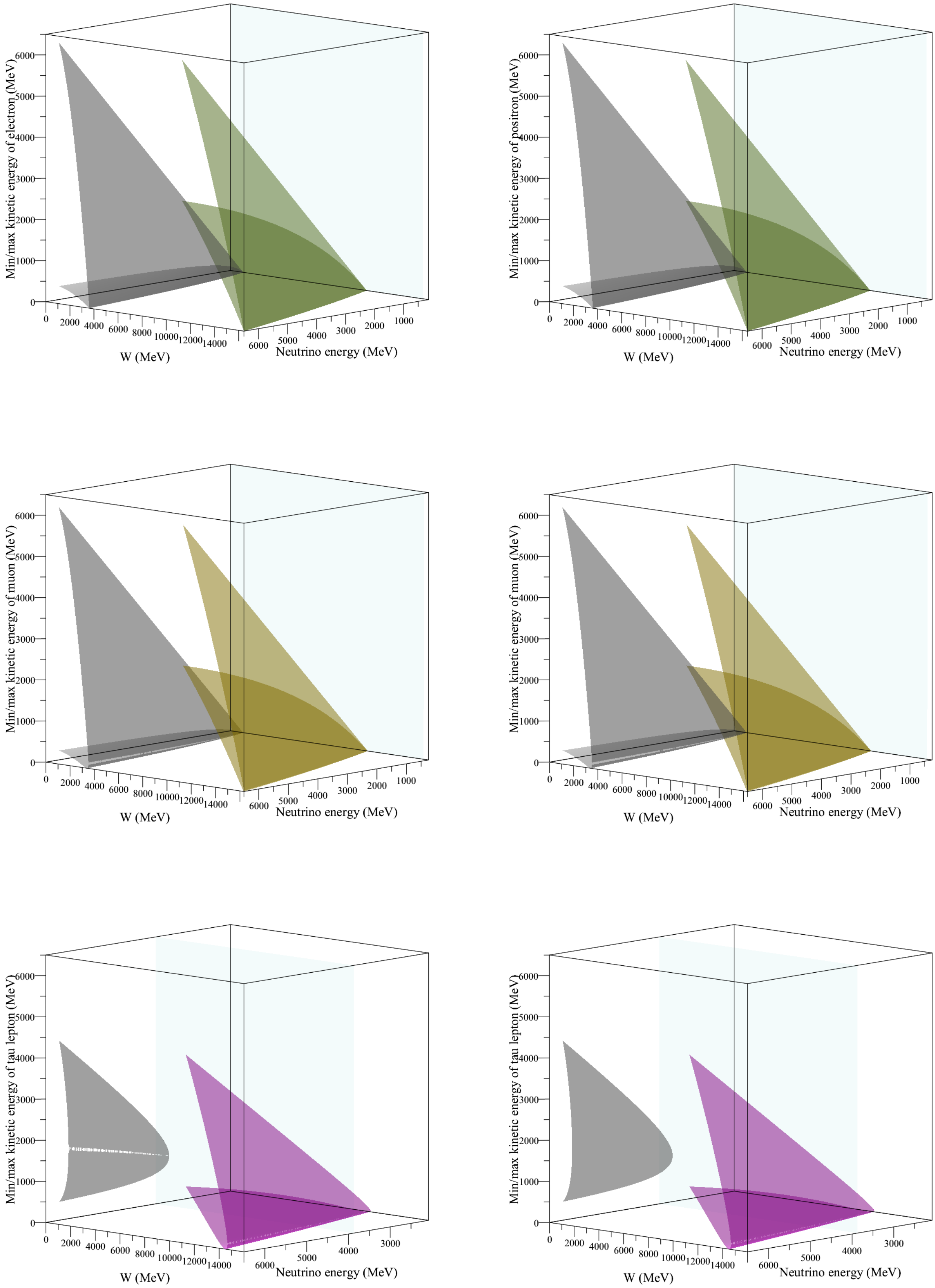

Figure 3.30: Minimum and maximum lepton kinetic energies vs. (anti)neutrino energy and W for the reactions $\nu_\ell + {}^{12}_{6}\mathrm{C} \to \ell^- + {}^{12}_{6}\mathrm{C} + \pi^+$ (left panels) and $\overline{\nu}_\ell + {}^{12}_{6}\mathrm{C} \to \ell^+ + {}^{12}_{6}\mathrm{C} + \pi^-$ (right panels), where $\ell = e, \mu, \tau$ (from top to bottom). The corresponding boundaries for CC1π reactions on bare nucleons are also shown (gray surfaces). In all cases, the surfaces are depicted in the boundaries $W^- \leq W < W^+$. Vertical planes show the (anti)neutrino energy thresholds in the reactions on bare nucleons. It is seen that the difference with Fig. 3.29 is almost imperceptible.

The total cross section can be obtained by integrating within the kinematical bounds:

$$\sigma\left(E_\nu\right)=\int\limits_{M_f+m_\pi}^{\min(\sqrt{s}-m,W_{\text{cut}})} dW \int\limits_{Q_-^2\left(s,W^2\right)}^{Q_+^2\left(s,W^2\right)} dQ^2\ \frac{d^2\sigma}{dW dQ^2}. \tag{3.39}$$

If the differential cross section

$$\frac{d^4\sigma}{dW dQ^2 d\cos\hat{\theta}_\pi d\hat{\varphi}_\pi}$$

is known, where $\hat{\theta}_\pi$ and $\hat{\varphi}_\pi$ are the angles of the final-state pion in the isobaric (πN center-of-mass) frame, then the total cross section can be obtained as

$$\sigma\left(E_\nu\right)=\int\limits_{M_f+m_\pi}^{\min(\sqrt{s}-m,W_{\text{cut}})} dW \int\limits_{Q_-^2\left(s,W^2\right)}^{Q_+^2\left(s,W^2\right)} dQ^2 \int\limits_{-1}^{1} d\cos\hat{\theta}_\pi \int\limits_{0}^{2\pi} d\hat{\varphi}_\pi\ \frac{d^4\sigma}{dW dQ^2 d\cos\hat{\theta}_\pi d\hat{\varphi}_\pi}. \tag{3.40}$$

Sometimes the following four measurables are needed:

$$\frac{d\sigma}{dW},\quad \frac{d\sigma}{d\hat{\varphi}_\pi},\quad \frac{d\sigma}{d\cos\hat{\theta}_\pi},\quad \text{and}\quad \frac{d\sigma}{dQ^2}.$$

The first three of these can be found quite easily:

$$\frac{d\sigma}{dW}\left(E_\nu,W\right)=\int\limits_{Q_-^2\left(s,W^2\right)}^{Q_+^2\left(s,W^2\right)} dQ^2 \int\limits_{-1}^{1} d\cos\hat{\theta}_\pi \int\limits_{0}^{2\pi} d\hat{\varphi}_\pi\ \frac{d^4\sigma}{dW dQ^2 d\cos\hat{\theta}_\pi d\hat{\varphi}_\pi}, \tag{3.41}$$

$$\left(M_f+m_\pi\le W\le\min(\sqrt{s}-m,W_{\text{cut}})\right)$$

$$\frac{d\sigma}{d\cos\hat{\theta}_\pi}\left(E_\nu,\cos\hat{\theta}_\pi\right)=\int\limits_{M_f+m_\pi}^{\min(\sqrt{s}-m,W_{\text{cut}})} dW \int\limits_{Q_-^2\left(s,W^2\right)}^{Q_+^2\left(s,W^2\right)} dQ^2 \int\limits_{0}^{2\pi} d\hat{\varphi}_\pi\ \frac{d^4\sigma}{dW dQ^2 d\cos\hat{\theta}_\pi d\hat{\varphi}_\pi}, \tag{3.42}$$

$$\frac{d\sigma}{d\hat{\varphi}_\pi}\left(E_\nu,\hat{\varphi}_\pi\right)=\int\limits_{M_f+m_\pi}^{\min(\sqrt{s}-m,W_{\text{cut}})} dW \int\limits_{Q_-^2\left(s,W^2\right)}^{Q_+^2\left(s,W^2\right)} dQ^2 \int\limits_{-1}^{1} d\cos\hat{\theta}_\pi\ \frac{d^4\sigma}{dW dQ^2 d\cos\hat{\theta}_\pi d\hat{\varphi}_\pi}. \tag{3.43}$$

To find $d\sigma/dQ^2$ we introduce an auxiliary quantity $W_0(Q^2)$ which is the root of Eq. (3.32)

$$\text{if } Q^2\ge 2E_\nu^* m-m^2:\ \ Q_+^2(W_0)=Q^2,\quad \text{if } Q^2\le 2E_\nu^* m-m^2:\ \ Q_-^2(W_0)=Q^2. \tag{3.44}$$

It turns out that $W_0^2(Q^2)=s+m^2-\sqrt{s}(B+m^2/B)$, where $B=(Q^2+m^2)/2E_\nu^*$, so

$$\frac{d\sigma}{dQ^2}\left(E_\nu,Q^2\right)=\int\limits_{M_f+m_\pi}^{\min(W_0(Q^2),W_{\text{cut}})} dW \int\limits_{-1}^{1} d\cos\hat{\theta}_\pi \int\limits_{0}^{2\pi} d\hat{\varphi}_\pi\ \frac{d^4\sigma}{dW dQ^2 d\cos\hat{\theta}_\pi d\hat{\varphi}_\pi}, \tag{3.45}$$

$$\left[Q_-^2\left(s,W^2=(M_f+m_\pi)^2\right)\le Q^2\le Q_+^2\left(s,W^2=(M_f+m_\pi)^2\right)\right].$$

NOTE XIX:

- At high neutrino energies, namely at $s\gg W^2+m^2$, one can write:

$$Q_-^2=m^2\left(\frac{2E_\nu^*}{E_\ell^*+P_\ell^*}-1\right)\simeq m^2\left(\frac{W^2-M_i^2}{s-W^2}\right).$$

- The following identities may be of utility to simplify the numerical calculations:

$$\left(Q_-^2+m^2\right)\left(Q_+^2+m^2\right)=4m^2\left(E_\nu^*\right)^2,\quad Q_+^2-Q_-^2=4E_\nu^* P_\ell^*.$$

- $Q_+^2=Q_-^2=m\left(2E_\nu^*-m\right)$ in the point $W=W_+$, while $Q_+^2>Q_-^2$ for $W<W_+$.

NOTE XX: Eq. (3.33) can be rewritten in the form of equation of ellipse in the plane of $P_\ell \sin\theta$ versus $P_\ell \cos\theta$:

$$(P_\ell \sin\theta)^2 + \varrho^2 \left(P_\ell \cos\theta - P_\ell^c\right)^2 = \left(P_\ell^*\right)^2,$$

where

$$\varrho = \frac{\sqrt{s}}{E_\nu + M_i} \quad \text{and} \quad P_\ell^c = \frac{E_\nu E_\ell^*}{\sqrt{s}}.$$

The eccentricity and the focal parameter of the ellipse are, respectively,

$$\sqrt{1-\varrho^2} = \frac{E_\nu}{E_\nu + M_i} \quad \text{and} \quad \frac{P_\ell^*}{\sqrt{1-\varrho^2}} = \frac{P_\ell^*\sqrt{s}}{E_\nu}.$$

3.3 Deep inelastic scattering (DIS)

The following set of invariant variables is conventionally in use for description of the neutrino-nucleon DIS:[7]

$$s = (k+p)^2 = \left(k' + p_X\right)^2 = 2ME_\nu + M^2,$$
$$Q^2 = -q^2 = -\left(k - k'\right)^2 = 2MxyE_\nu,$$
$$W^2 = p_X^2 = (p+q)^2 = 2M(1-x)yE_\nu + M^2,$$
$$\nu = \frac{(pq)}{M} = yE_\nu = E_\nu - E_\ell, \quad x = \frac{Q^2}{2(pq)} = \frac{Q^2}{2MyE_\nu}, \quad y = \frac{(pq)}{(pk)} = 1 - \frac{E_\ell}{E_\nu}.$$

The center-of-mass neutrino and lepton energies are

$$E_\nu^* = \frac{s - M^2}{2\sqrt{s}} \quad \text{and} \quad E_\ell^* = \frac{s + m^2 - W^2}{2\sqrt{s}}. \tag{3.46}$$

Clearly the reaction threshold energy is given by

$$E_\nu^{\text{th}} = \frac{s^{\text{th}} - M^2}{2M} = \frac{\left(m + W_{\text{cut}}\right)^2 - M^2}{2M},$$

where W_{cut} is the conventional W cutoff.[8] The physical boundaries for the W are

$$W_{\text{cut}} \le W \le \sqrt{s} - m,$$

where the upper limit is obtained from the condition $E_\ell^* \ge m$.

3.3.1 Properties of vector N and kinematic boundaries

The 4-vector N is defined by

$$N_\alpha = \epsilon_{\alpha\beta\gamma\delta} p^\beta k^\gamma q^\delta = \epsilon_{\alpha\beta\gamma\delta} (p+k)^\beta p^\gamma q^\delta.$$

Let us consider this vector in the center-of-mass frame. Since $\mathbf{p}^* + \mathbf{k}^* = 0$ we have

$$N^* = (0, \mathbf{N}^*), \quad \text{where} \quad \mathbf{N}^* = \sqrt{s}\left(\mathbf{k}^* \times \mathbf{k}'^*\right), \quad |\mathbf{N}^*| = \sqrt{s} E_\nu^* P_\ell^* \sin\theta^*.$$

Therefore

$$N^2 = -s\left(E_\nu^* P_\ell^* \sin\theta^*\right)^2 = -\frac{\left(s - M^2\right)^2}{16}\left[\left(s - W^2 + m^2\right)^2 - 4m^2 s\right]\sin^2\theta^*. \tag{3.47a}$$

On the other hand

$$N^2 = p^2(qk)^2 - 2(kp)(pq)(qk) + q^2(kp)^2. \tag{3.47b}$$

[7] Of course, we assume here $M_i = M_f = M \equiv (m_p + m_n)/2$.

[8] We will use normally $W_{\text{cut}} = M + 2m_\pi$ assuming that the range $M \le W < M + 2m_\pi$ is saturated by the QE scattering and single pion neutrinoproduction.

NOTE XXI: To derive Eq. (3.47b) we have used the identity

$$g^{\alpha\alpha'}\epsilon_{\alpha\beta\gamma\delta}\,\epsilon_{\alpha'\beta'\gamma'\delta'} = -\begin{vmatrix} g_{\alpha\beta'} & g_{\alpha\gamma'} & g_{\alpha\delta'} \\ g_{\beta\beta'} & g_{\beta\gamma'} & g_{\beta\delta'} \\ g_{\gamma\beta'} & g_{\gamma\gamma'} & g_{\gamma\delta'} \end{vmatrix}.$$

which follows from

$$\epsilon_{\alpha\beta\gamma\delta}\,\epsilon_{\alpha'\beta'\gamma'\delta'} = -\begin{vmatrix} g_{\alpha\alpha'} & g_{\alpha\beta'} & g_{\alpha\gamma'} & g_{\alpha\delta'} \\ g_{\beta\alpha'} & g_{\beta\beta'} & g_{\beta\gamma'} & g_{\beta\delta'} \\ g_{\gamma\alpha'} & g_{\gamma\beta'} & g_{\gamma\gamma'} & g_{\gamma\delta'} \\ g_{\delta\alpha'} & g_{\delta\beta'} & g_{\delta\gamma'} & g_{\delta\delta'} \end{vmatrix}.$$

By substituting

$$(qk) = -\frac{1}{2}\left(Q^2+m^2\right), \quad (kp) = \frac{1}{2}\left(s-M^2\right), \quad (qp) = \frac{1}{2}\left(Q^2+W^2-M^2\right),$$

we find

$$N^2 = \frac{s}{4}\left(Q^2-Q_-^2\right)\left(Q^2-Q_+^2\right) \quad \text{with} \quad Q_\pm^2 = Q_\pm^2(s,W) = 2E_\nu^*\left(E_\ell^* \pm P_\ell^*\right) - m^2.$$

The following identities are of some utility:

$$Q_-^2 + Q_+^2 = 2\left(2E_\nu^*E_\ell^* - m^2\right), \quad Q_-^2Q_+^2 = m^2\left[4E_\nu^*\left(E_\nu^* - E_\ell^*\right) + m^2\right].$$

Taking into account that $0 \leq \sin\theta^* \leq 1$, we arrive at the following inequalities:

$$\left(Q^2-Q_-^2\right)\left(Q^2-Q_+^2\right) \leq 0, \qquad \left(2Q^2-Q_-^2-Q_+^2\right)^2 \geq 0.$$

The latter one provides no restriction while the first inequality yields

$$Q_-^2 \leq Q^2 \leq Q_+^2. \tag{3.48}$$

The same also follows from the trivial consideration discussed in Sect. 3.2.

NOTE XXII: The inequalities (3.48) can be rewritten in terms of variables y and E_ν. Since

$$\left(Q^2+m^2\right)^2 + 4yE_\nu^2\left(Q^2+m^2\right) - 4Q^2E_\nu^2 \leq 0, \tag{3.49}$$

we have

$$Q_-^2\left(y,E_\nu\right) \leq Q^2 \leq Q_+^2\left(y,E_\nu\right), \qquad Q_\pm^2\left(y,E_\nu\right) = 2E_\nu^2\left[1-y-\frac{m^2}{2E_\nu^2} \pm \sqrt{(1-y)^2-\frac{m^2}{E_\nu^2}}\right].$$

It is clear that $Q_-^2\left(y,E_\nu\right) \geq 0$ for $y \geq -E_\nu^2/(2m^2)$ that is for any y.

Let us rewrite inequality (3.49) in terms of variables y and x:

$$\left(1+\frac{Mx}{2E_\nu}\right)y^2 - \left[1-\frac{m^2}{2E_\nu^2}\left(1+\frac{E_\nu}{Mx}\right)\right]y + \frac{m^4}{8MxE_\nu^3} \leq 0.$$

3.3.2 Nachtmann and Feynman variables

The Nachtmann variable [186] is defined by

$$x_N = \frac{Q^2}{2M^2x}\left(\sqrt{1+\frac{4M^2x^2}{Q^2}}-1\right) = \frac{2x}{1+\sqrt{1+4M^2x^2/Q^2}}. \tag{3.50}$$

where x is the standard Bjorken scaling variable. Clearly $x_N \approx x$ when $Q^2 \gg 4M^2x^2$ but in general case $x_N < x$. How to use the Nachtmann variable? The recipe is

$$\frac{d\sigma}{dxdy} = K\sum_{i=1}^{5} A_i\left(x,y,E_\nu\right)F_i\left(x_N,Q^2\right)$$

TO BE CONTINUED

However, the Nachtmann variable is not the *fraction of the nucleon momentum carried by the struck parton in the Breit frame*. Let us call the latter Feynman variable, x_F. Under assumption that the struck and final partons are on shell the Feynman variable is defined by[9] [187, 189]

$$\frac{x_F}{x_N} = \frac{Q_{fi}^2}{Q^2}, \tag{3.51}$$

where

$$2Q_{fi}^2 = Q^2 + m_f^2 - m_i^2 + \sqrt{Q^4 + 2\left(m_f^2 + m_i^2 + 2k_T^2\right)Q^2 + \left(m_f^2 - m_i^2\right)^2},$$

m_i and m_f are the masses of the struck and final partons, and k_T is the transverse momentum of the struck parton in the Breit frame. For NC scattering $m_f = m_i$. Thus

$$x_F = \frac{x_N}{2}\left[1 + \sqrt{1 + \frac{4(m_i^2 + k_T^2)}{Q^2}}\right]$$

and neglecting k_T^2/Q^2 or taking some "effective" value for k_T^2, x_F may be used the same way as x_N. Well, but how to use the Feynman variable for CC scattering? In general this is not a trivial question, because x_F is now different for different quark transitions and well above the t quark production threshold all transitions (with electric charge change of ± 1) become possible.

Let us write the $1/Q^2$ expansion

$$\frac{Q_{fi}^2}{Q^2} = 1 + \frac{m_f^2 + k_T^2}{Q^2} - \frac{2\left(m_i^2 + k_T^2\right)\left(m_f^2 + k_T^2\right)}{Q^4} + \ldots.$$

We can slightly simplify our life by neglecting the $\mathcal{O}\left(k_T^2/Q^2\right)$ and $\mathcal{O}\left(m_{i,f}^4/Q^4\right)$. It would be nice to write

$$\frac{d\sigma}{dxdy} = K\sum_{i=1}^{5} A_i\left(x, y, E_\nu\right) F_i\left(x'_F, Q^2\right),$$

where

$$x'_F = x_N\left(1 + \frac{m_f^2}{Q^2}\right) \approx x_F.$$

But which f must be used in every PDF $q\left(x'_F, Q^2\right)$? Another problem is in bad behavior of x'_F for small Q^2. Indeed, x'_F behaves like $\left(m_f^2/M^2\right)x^{-1}$ as $Q^2 \to 0$. Therefore it can be large.

3.3.3 Derivation of Eq. (3.51)

Here we will follow the approach of Ref. [192]. We mark the physical values in the Breit frame (BF) with tilde over the symbol. Thus $\tilde{q} = \left(\tilde{q}^0, 0, 0, \tilde{q}^3\right)$, $\tilde{p}_N = \left(\tilde{p}^0, 0, 0, \tilde{p}^3\right)$ and $\tilde{p}^3 \to -\infty$. Let k_i and k_f are the 4-momenta of initial (struck) and final partons. By definition,

$$\tilde{k}_i^3 = x_F\tilde{p}^3 \tag{3.52}$$

and thus

$$\tilde{k}_i^0 = \sqrt{\left(x_F\tilde{p}^3\right)^2 + k_T^2 + m_i^2}, \tag{3.53}$$

where $k_T^2 = \tilde{k}_T = \left(\tilde{k}_i^1\right)^2 + \left(\tilde{k}_i^2\right)^2$ (that is k_T is the part of $\tilde{k}_i$ transverse to $\tilde{p}_N$ and $\tilde{q}$). From the conservation law

$$\tilde{q} + \tilde{k}_i = \tilde{k}_f$$

we have

$$2\tilde{q}\tilde{k}_i = 2\left(\tilde{q}^0\tilde{k}_i^0 - \tilde{q}^3\tilde{k}_i^3\right) = Q^2 + m_f^2 - m_i^2. \tag{3.54}$$

Velocity of the BF in the lab. frame is $\mathbf{v}_{\mathrm{BF}} = -\tilde{\mathbf{p}}_N/\tilde{p}^0$. Therefore

$$|\mathbf{v}_{\mathrm{BF}}| = -\frac{\tilde{p}^3}{\tilde{p}^0}, \quad \sqrt{1 - |\mathbf{v}_{\mathrm{BF}}|^2} = \frac{\tilde{p}^0}{M},$$

and Lorentz transformation of q can be written as

$$\begin{aligned}\tilde{q}^0 &= \frac{1}{M}\left(q^0\tilde{p}^0 + q^3\tilde{p}^3\right),\\ \tilde{q}^3 &= \frac{1}{M}\left(q^3\tilde{p}^0 + q^0\tilde{p}^3\right).\end{aligned}$$

[9] For a recent discussion of the problem in case of lepton-proton inelastic scattering see Ref. [192].

Substituting these equations into Eq. (3.54), taking into account Eqs. (3.52) and (3.53) and finding the limit as $\tilde{p}^3 \to -\infty$ we arrive at the following *exact* equation for x_F:

$$\left(q^0 + q^3\right) M x_F + \frac{\left(m_i^2 + k_T^2\right)\left(q^0 - q^3\right)}{M x_F} = Q^2 + m_f^2 - m_i^2. \tag{3.55}$$

Its solution yields Eq. (3.51).

Useful formulas:

$$q^3 = \nu\sqrt{1 + \frac{2Mx}{\nu}} = \nu\sqrt{1 + \frac{4M^2x^2}{Q^2}}.$$

Here we assume that $q^0 = \nu \geq 0$. This is true if $M' \geq M$ In fact we *must* assume that $m_p = m_n$ to have x varying between 0 and 1. This approximation seems natural if we neglect the transverse momentum k_T (which may be much larger then the $n - p$ mass difference) and light quark masses.

3.3.4 Threshold Conditions

We *define* the differential cross sections for the inclusive CC DIS reaction

$$\nu N \to lX \tag{3.56}$$

by

$$\frac{d\sigma^{\text{DIS}}_{\nu N \to lX}}{dy} = \int_{x^-}^{1} dx\, \theta\left(W^2 - M_h^2\right) \frac{d^2\sigma_{\nu N \to lX}}{dxdy}, \tag{3.57}$$

where

$$W^2 = p_X^2 = (q + p)^2 = Q^2\left(\frac{1}{x} - 1\right) - M^2$$

and M_h is the total mass of the hadron system h.

Let us find out the points of intersection between the curves

$$(1 - x)Q^2 = \left(M_h^2 - M^2\right)x \tag{3.58}$$

and

$$\left(Q^2 + m^2\right)^2 + \frac{2Q^2E_\nu}{Mx}\left(Q^2 + m^2\right) - 4Q^2E_\nu^2 = 0. \tag{3.59}$$

The solution is

$$x = x_h^{\pm}\left(E_\nu\right) = \frac{a_h\left(E_\nu\right) \pm \sqrt{b_h\left(E_\nu\right)}}{2c_h\left(E_\nu\right)}, \tag{3.60}$$

where

$$a_h\left(E_\nu\right) = 1 - \frac{\left(M_h^2 - M^2 - m^2\right)\left[\left(M_h^2 - M^2\right)E_\nu + m^2M\right]}{2M\left(M_h^2 - M^2\right)E_\nu^2},$$

$$b_h\left(E_\nu\right) = \left[1 - \frac{\left(M_h - m\right)^2 - M^2}{2ME_\nu}\right]\left[1 - \frac{\left(M_h + m\right)^2 - M^2}{2ME_\nu}\right],$$

$$c_h\left(E_\nu\right) = 1 + \frac{\left(M_h^2 - M^2 - m^2\right)^2}{4\left(M_h^2 - M^2\right)E_\nu^2}.$$

Clearly $b_h\left(E_\nu\right) \geq 0$ (and thus the solution does exist) at

$$E_\nu \geq E_\nu^h = \frac{\left(M_h + m\right)^2 - M^2}{2M},$$

where E_ν^h is exactly the *threshold neutrino energy* for the reaction (3.56).

Clearly, for the quasielastic threshold ($M_h = M$) the solution degenerates to $x_h^{\pm} = 1$ providing no additional cutoff for the physical region

$$y^- \leq y \leq y^+, \quad x^- \leq x \leq 1.$$

For very high neutrino energies we have

$$x_h^- \approx \frac{m^2}{2ME_\nu} \approx x^-, \quad x_h^+ \approx 1 - \frac{M_h^2 - M^2}{2ME_\nu}.$$

We assume from here that $M_h > M$.

Let us now *define* the differential and total cross sections for the inclusive reaction (3.56) by

$$\frac{d\sigma^{\text{DIS}}_{\nu N \to lhX}}{dy} = \int_{x^-}^{x_h^+} dx\, \theta\left(y - y_h^{\text{min}}\right)\theta\left(y^+ - y\right) \frac{d^2\sigma_{\nu N \to l + \text{anything}}}{dxdy}, \tag{3.61}$$

$$y^{-}\left(x_h^{-}, E_\nu\right) \leq y \leq y^{+}\left(x_h^{+}, E_\nu\right), \qquad E_\nu \geq E_\nu^h,$$

and

$$\begin{aligned} \sigma_{\nu N\to lhX}^{\text{DIS}} &= \int dy \int_{x^-}^{x_h^+} dx\, \theta\left(y - y_h^{\text{min}}\right) \theta\left(y^+ - y\right) \frac{d^2\sigma_{\nu N\to l+\text{anything}}}{dxdy} \\ &= \int_0^1 dy' \int_{x^-}^{x_h^+} dx\, \left(y^+ - y_h^{\text{min}}\right) \frac{d^2\sigma_{\nu N\to l+\text{anything}}}{dxdy}, \end{aligned} \tag{3.62}$$

where

$$y_h^{\text{min}} = y_h^{\text{min}}\left(x, E_\nu\right) = \max\left[y^-\left(x, E_\nu\right), \frac{M_h^2 - M^2}{2M(1-x)E_\nu}\right],$$

$$y^{\pm}\left(x_h^{\pm}, E_\nu\right) = \frac{M_h^2 - M^2}{2M\left(1 - x_h^{\pm}\right)E_\nu},$$

and the new variable y' in Eq. (3.62) is defined by

$$y = \left(y^+ - y_h^{\text{min}}\right) y' + y_h^{\text{min}}.$$

For the moment we'll assume that the *minimal* hadron system h of the DIS is $N + 2\pi$. Therefore $M_h = M + 2m_\pi$,

$$y_h^{\text{min}} = \max\left[y^-, \frac{2m_\pi\left(M + m_\pi\right)}{M(1-x)E_\nu}\right],$$

and the *total* CC cross section is

$$\sigma_{\nu N}^{\text{tot}} = \sigma_{\nu N}^{\text{QES}} + \sigma_{\nu N}^{\text{Res}} + \sigma_{\nu N\to \ell + N + 2\pi + X}^{\text{DIS}}.$$

Needless to say that $\sigma_{\nu N\to \ell hX}^{\text{DIS}} = 0$ as $E_\nu \leq E_\nu^h$ and that the corresponding results for the NC inclusive reaction

$$\nu\left(\overline{\nu}\right) N \to \nu\left(\overline{\nu}\right) + h + X \tag{3.63}$$

can be obtained by putting $m = 0$ in the above equations.

Chapter 4

Nucleon form factors (obsolete!)

In this Chapter, we consider explicit formulae for the nucleon form factors used in our numerical calculations.

4.1 QE CC form factors

In terms of Sachs electric G_E and magnetic G_M form factors Dirac electromagnetic isovector F_V^{CC}, Pauli electromagnetic isovector F_M^{CC}, axial F_A^{CC} and pseudoscalar F_P^{CC} charged current form factors are [6]

$$\begin{aligned}
F_V^{CC} &= \left(1+\frac{Q^2}{4M^2}\right)^{-1}\left(G_E+\frac{Q^2}{4M^2}G_M\right),\\
F_M^{CC} &= \left(1+\frac{Q^2}{4M^2}\right)^{-1}\left(G_M-G_E\right),\\
F_A^{CC} &= \left(1+\frac{Q^2}{m_A^2}\right)^{-2}F_A^{CC}(0),\\
F_P^{CC} &= \frac{2M^2}{m_\pi^2+Q^2}F_A^{CC},
\end{aligned}$$

$F_A^{CC}(0)=-1.267$. The Sachs form factors, G_E and G_M, have more intuitive physical interpretations than F_1 and F_2. Form factors G_E and G_M can be interpreted as Fourier transforms of spatial distributions of charge and magnetization of the nucleon in the Breit frame. In this case of elastic electron-nucleon scattering the Breit frame is the center-of-mass frame of the electron-nucleon system. In this system the incoming electron and the recoil proton had a momentum of $q/2$, the initial nucleon and scattered electron had a momentum $-q/2$. Thus $q^2=-\mathbf{q}^2$, no energy transfer in this frame. For each q^2 value, there is a Breit frame in which the form factors are represented as $G_{E,M}\left(\mathbf{q}^2\right)=G_{E,M}\left(q^2\right)$, where $G_{E,M}\left(q^2\right)$ is determined in the laboratory frame. At the limit of pointlike nucleon at $Q^2=0$, form factors are normalized as

$$G_M^p(0)=\mu_p,\quad G_M^n(0)=\mu_n,\quad G_E^p(0)=1,\quad G_E^n(0)=0.$$

4.1.1 Dipole model (DM)

In this model nucleon electric and magnetic form factors is given by the standard dipole parameterization

$$G_E=\left(1+\frac{Q^2}{m_V^2}\right)^{-2},\quad G_M=(\mu_p-\mu_n)\left(1+\frac{Q^2}{m_V^2}\right)^{-2}.$$

4.1.2 Extended Gari–Krüempelmann model (GKex)

The so-called “GKex” model is given by the following set of formulas:

$$G_{M,E}=G_{M,E}^p-G_{M,E}^n,\quad G_M^{p,n}=F_1^{p,n}+F_2^{p,n},\quad G_E^{p,n}=F_1^{p,n}-\frac{Q^2}{4m_N^2}F_2^{p,n},$$

$$F_i^{p,n}=\frac{1}{2}\left(F_i^{\text{is}}\pm F_i^{\text{iv}}\right),\quad i=1,2.$$

The GKex model has the following form for the isotopic and isovector electromagnetic form factors:

$$
\begin{aligned}
F_1^{\mathrm{is}} &= \left[\frac{g_\omega}{f_\omega}\left(\frac{m_\omega^2}{m_\omega^2+Q^2}\right)+\frac{g_{\omega'}}{f_{\omega'}}\left(\frac{m_{\omega'}^2}{m_{\omega'}^2+Q^2}\right)\right]F_V^\omega+\frac{g_\phi}{f_\phi}\left(\frac{m_\phi^2}{m_\phi^2+Q^2}\right)F_V^\phi+\left(1-\frac{g_\omega}{f_\omega}-\frac{g_{\omega'}}{f_{\omega'}}\right)F_V^D,\\
F_2^{\mathrm{is}} &= \left[\kappa_\omega\frac{g_\omega}{f_\omega}\left(\frac{m_\omega^2}{m_\omega^2+Q^2}\right)+\kappa_{\omega'}\frac{g_{\omega'}}{f_{\omega'}}\left(\frac{m_{\omega'}^2}{m_{\omega'}^2+Q^2}\right)\right]F_M^\omega+\kappa_\phi\frac{g_\phi}{f_\phi}\left(\frac{m_\phi^2}{m_\phi^2+Q^2}\right)F_M^\phi\\
&\quad+\left(\kappa_s-\kappa_\omega\frac{g_\omega}{f_\omega}-\kappa_{\omega'}\frac{g_{\omega'}}{f_{\omega'}}-\kappa_\phi\frac{g_\phi}{f_\phi}\right)F_M^D,\\
F_1^{\mathrm{iv}} &= \left[\frac{C}{2}\left(\frac{A_V+B_V\left(1+Q^2/Q_{V1}^2\right)^{-2}}{1+Q^2/Q_{V2}^2}\right)+\frac{g_{\rho'}}{f_{\rho'}}\left(\frac{m_{\rho'}^2}{m_{\rho'}^2+Q^2}\right)\right]F_V^\rho+\left(1-\frac{C_V}{2}-\frac{g_{\rho'}}{f_{\rho'}}\right)F_V^D,\\
F_2^{\mathrm{iv}} &= \left[\frac{C}{2}\left(\frac{A_M+B_M\left(1+Q^2/Q_{M1}^2\right)^{-2}}{1+Q^2/Q_{M2}^2}\right)+\kappa_{\rho'}\frac{g_{\rho'}}{f_{\rho'}}\left(\frac{m_{\rho'}^2}{m_{\rho'}^2+Q^2}\right)\right]F_M^\rho+\left(\kappa_v-\frac{C_M}{2}-\kappa_{\rho'}\frac{g_{\rho'}}{f_{\rho'}}\right)F_M^D,
\end{aligned}
$$

where the pole terms are those of the ρ, ρ', ω, ω', ϕ mesons, and the final term of each equation is determined by the asymptotic properties of PQCD. The F_i^α ($\alpha = \rho, \omega, \phi$) are the meson-nucleon form factors, while the F_i^D are effectively quark-nucleon form factors.

$$
\begin{aligned}
F_V^{\alpha,D}(Q^2) &= \frac{\Lambda_{1,D}^2}{\Lambda_{1,D}^2+\widetilde{Q}^2}\frac{\Lambda_2^2}{\Lambda_2^2+\widetilde{Q}^2},\\
F_M^{\alpha,D}(Q^2) &= \frac{\Lambda_{1,D}^2}{\Lambda_{1,D}^2+\widetilde{Q}^2}\left(\frac{\Lambda_2^2}{\Lambda_2^2+\widetilde{Q}^2}\right)^2,
\end{aligned}
$$

where $\Lambda_{1,D}$ is Λ_1 for F_i^α, Λ_D for F_i^D,

$$
\begin{aligned}
F_V^\phi\left(Q^2\right) &= F_V^\alpha\left(Q^2\right)\left(\frac{Q^2}{\Lambda_1^2+Q^2}\right)^{1.5},\\
F_M^\phi\left(Q^2\right) &= F_M^\alpha\left(Q^2\right)\left(\frac{\Lambda_1^2}{\mu_\phi^2}\frac{Q^2+\mu_\phi^2}{\Lambda_1^2+Q^2}\right)^{1.5},
\end{aligned}
$$

$$
\widetilde{Q}^2 = Q^2\frac{\ln\left[\left(\Lambda_D^2+Q^2\right)/\Lambda_{\mathrm{QCD}}^2\right]}{\ln\left(\Lambda_D^2/\Lambda_{\mathrm{QCD}}^2\right)}.
$$

Table 4.1: Parameters of the GKex models $A_V = 1.0317$, $A_M = 5.7824$, $B_V = 0.0875$, $B_M = 0.3907$, $Q_{V1}^2 = 0.3176\,\mathrm{GeV}^2$, $Q_{M1}^2 = 0.1422\,\mathrm{GeV}^2$, $Q_{V2}^2 = 0.5496\,\mathrm{GeV}^2$, $Q_{M2}^2 = 0.5362\,\mathrm{GeV}^2$, $C_V = 1.1192$, $C_M = 6.1731$, $\kappa_v = \mu_p - \mu_n$.

Parameter	GKex(02L)	GKex(02S)
$g_{\rho'}/f_{\rho'}$	0.0608	0.0401
$g_{\omega'}/f_{\omega'}$	0.2346	0.2552
g_ω/f_ω	0.6896	0.6739
g_ϕ/f_ϕ	-0.1852	-0.1676
κ_s	-0.1200	-0.1200
$\kappa_{\rho'}$	5.3038	6.8190
$\kappa_{\omega'}$	18.2284	1.4916
κ_ω	-2.8585	0.8762
κ_ϕ	13.0037	7.0172
μ_ϕ	0.6848	0.8544
Λ_1	0.9441	0.9407
Λ_2	2.8268	2.7891
Λ_D	1.2350	1.2111
Λ_{QCD}	0.1500	0.1500
C	1.0000	1.0000

4.1.3 "Patched" Budd-Bodek-Arrington 2003 fits for G_E^p, G_M^p and G_M^n.

The BBA fits for the proton electric, magnetic and neutron magnetic form factors are the inverse polynomial expressions [42]:

$$G_{M,E}^{p,n}\left(Q^2\right) = G_{M,E}^{p,n}(0)\left(1+\sum_{n=1}^{6} a_{2n}Q^{2n}\right)^{-1}.$$

The numerical values of the polynomials coefficients $a_2, \ldots, a_{12}$ are listed in Table 4.2.

Table 4.2: Coefficients for the BBA fits of the electromagnetic form factors.

	a_2	a_4	a_6	a_8	a_{10}	a_{12}
BBA (CS+PTD)						
G_E^p	3.253	1.4220	0.08582	0.331800	-0.0937100	0.01076
G_M^p	3.104	1.4280	0.11120	-0.006981	0.0003705	-0.70630$\times 10^{-5}$
BBA (CS)						
G_E^p	3.226	1.5080	-0.37730	0.610900	-0.1853000	0.01596
G_M^p	3.188	1.3540	0.15110	-0.011350	0.0005330	-0.90050$\times 10^{-5}$
BBA						
G_M^n	3.043	0.8548	0.68060	-0.128700	0.0089120	0.0

As one can see from Fig. 4.2 the BBA fit for G_M^p has unphysical behavior for $Q^2 \gtrsim 20$ GeV^2. To avoid possible troubles with the high Q^2 tail, we use the following "patch" for both BBA fits:

$$G_M^p = \mu_p G_D \left(0.304\, Q^2 - 2.5\right)^{-0.222}. \tag{4.1}$$

In Fig. 4.1 we compare the GKex(02S) and "patched" BBA fits.

4.1.4 Neutron electric form factor G_E^n

BBA do not suggest a new fitting formula for the neutron electric form factor and use the (scaled) parametrization suggested by Galster *et al.* [304] and used now by many authosrs:

$$G_E^n\left(Q^2\right) = -\mu_n \frac{a\tau}{1+b\tau} G_D\left(Q^2\right), \quad G_D\left(Q^2\right) = \left(1+\frac{Q^2}{m_V^2}\right)^{-1}, \tag{4.2}$$

where[1] $\tau = Q^2/(4m_n^2)$. Frequently used values for the parameters a and b are given in Table. 4.3. In fact the parameter

Table 4.3: Parameters involved in Eq. (4.2) used by different authors.

a	b	Ref.	a	b	Ref.
1.0	5.6	[304]	0.942	4.65	[342]
1.25	18.3	[317]	0.942	4.61	[42]
1.0	3.4	[284]	0.895	3.69	[258]

a, the slope at $Q^2 = 0$, is strongly constrained[2] by atomic measurements of the neutron charge radius $\langle r_n^2 \rangle$ (see Refs. [351, 352] and references therein) since

$$\langle r_n^2 \rangle = -6\left.\frac{dG_E^n}{dQ^2}\right|_{Q^2=0} = \frac{3a\mu_n}{2m_n^2}. \tag{4.3}$$

In our "Cookbook", we have to take into account the data collected in Ref. [352].

4.1.5 Comparison of the GKex and BBA models for the electromagnetic nucleon form factors with experimental data

---

NOTE XXIII:

Let us list the most important institutions, experimental collaborations and groups which deal with measurements of the nucleon electromagnetic form factors.

[1] Yes, the mass in this definition is the neutron mass and not M (see, e.g., Ref. [350]).

[2] Constrained but, of course, not fixed as it is stated in Ref. [258].

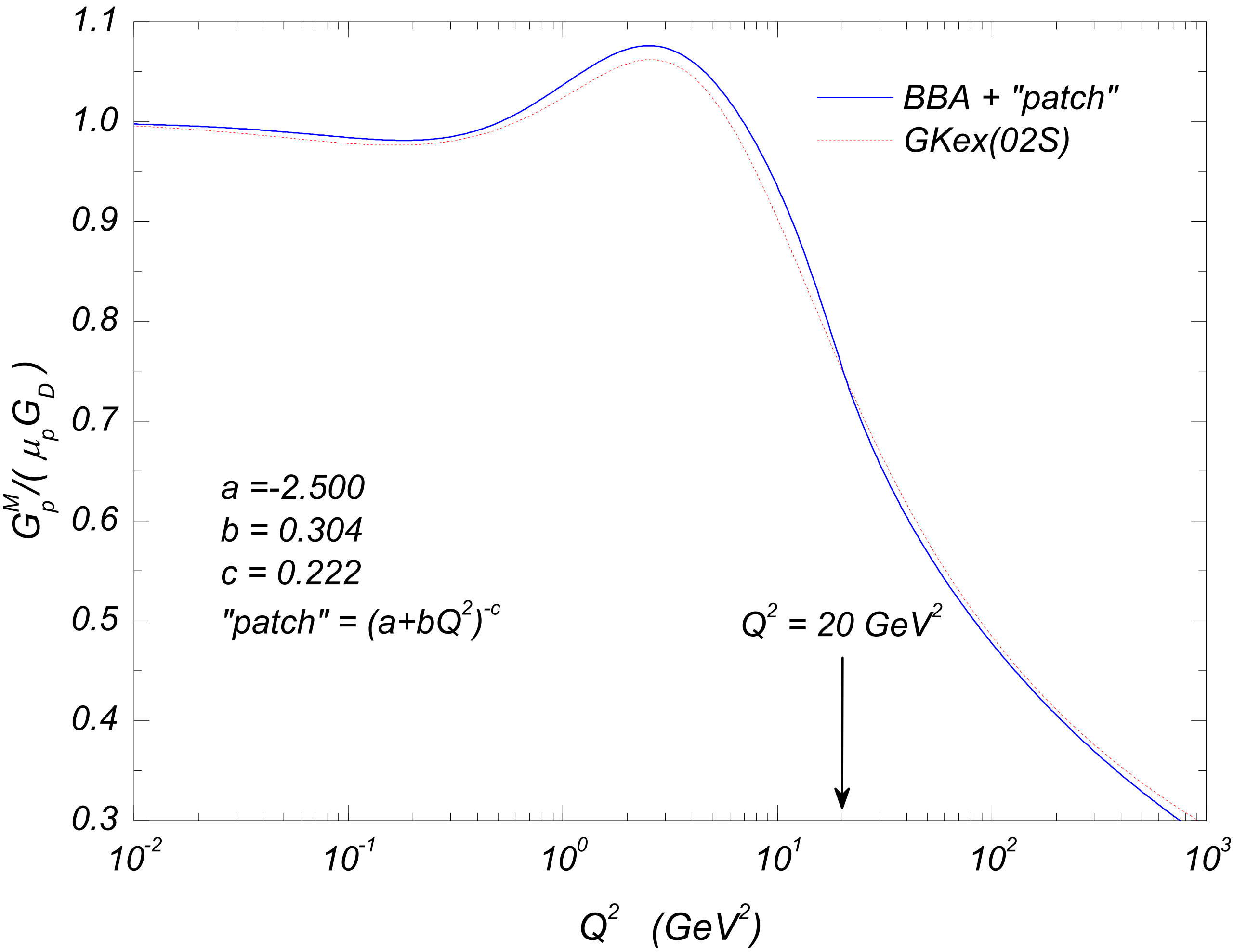

Figure 4.1: Comparison of the “patched” BBA and GKex(02S) fits for the magnetic form factor of the proton G_p^M.

- **CEA** (Cambridge Electron Accelerator), Harvard University, Cambridge, Massachusetts
- **JLab** (Thomas Jefferson National Accelerator Facility), Newport News, Virginia
  - Hall A Collaborations: E95-001, E99-007, E02-013, E01-001
  - Hall C Collaborations: E93-026, E93-038, E94-110
  - G_{Ep}(III) Collaboration: E00-114 HAPPEX-He, E01-001
- **DESY** (Deutsches Elektronen Synchrotron), Hamburg
- **ELSA** (ELectron Stretcher and Accelerator), Bonn
- **NIKHEFF** (National Institute for Nuclear and High Energy Physics), Amsterdam
- **SLAC** (Stanford Linear Accelerator Center), Stanford
- **SLEA** (Saclay Linear Electron Accelerator, Saclay
- Linear Accelerator of the Faculty of Sciences of the University of Paris
- **CES (Cornell Electron Synchrotron, Cornell University, Ithaca)**
- **Mainz ELA** (Electron Linear Accelerator)
- **MAMI** (Mainz Microtron): A1 Collaboration.

NOTE XXIV:

Let write some quotations from Refs [239] and [325], important to understanding of the nucleon electromagnetic form factors measurements.

Rosenbluth or longitudinal-transverse technique. In the Rosenbluth method separation of form factors is achieved by measuring the cross section at a fixed Q^2 value by varying the incident electron beam energy and the electron scattering angle. The measured differential cross section is plotted as a function of scattered electron angle and one can extract information on ${G_E^p}^2$ and ${G_M^p}^2$ from the slope and the intercept of the plotted curve. The G_E^p term dominates the cross section in the low Q^2 region. The G_M^p term dominates at large Q^2 values. Thus the extraction of G_M^p at low Q^2 and G_E^p at large Q^2 values becomes difficult using the Rosenbluth technique.

This method was applied in early experiments to obtaining nucleon form factors in *elastic electron-proton scattering*. In Fig. 4.2 are shown the GKex and BBA fits for the ratio $G_M^p/\left(\mu_p G_D\right)$.

Because of the lack of free neutron targets the neutron electromagnetic form factors are known with much less precision than the proton electric and magnetic form factors. They have been deduced in the past from elastic or quasielastic electron-deuteron scattering. This procedure involves considerable model dependence. Another complication arises from the fact that the net charge of the neutron is zero. As such the neutron electric form factor G_E^n is much smaller than its magnetic form factor G_M^n. Therefore, the magnetic part of the contribution dominates the cross section, which makes it very difficult to extract G_E^n from unpolarized cross section measurements using deuterium targets. In Fig. 4.3 are shown the GKex and BBA fits for the ratio $G_M^n/\left(\mu_n G_D\right)$ [3].

The original data of experiments used the Rosenbluth technique T. Janssens *et al.* [268], J. Litt *et al.* [270], C. Berger *et al.* [297], W. Bartel *et al.* [305], R. C. Walker *et al.* [279], A. F. Sill *et al.* [277] and L. Andivahis *et al.* [281] were revaluated in Ref. [338] through a new Rosenbluth analysis of the cross section measurements. The Rosenbluth data are more sensitive to systematic uncertainties and it has been suggested that the different Rosenbluth extractions are inconsistent and thus unreliable. It was demonstrated that the individual Rosenbluth measurements yield consistent results when analyzed independently, so that the normalization uncertainties between different measurements do not impact the result. The reanalysis has determined that the results cannot be made to agree with the polarization results by excluding a small set of measurements or by making reasonable modifications to the relative normalization of the various experiments. The global Rosenbluth analysis may disagree with the polarization transfer results for a variety of reasons: inclusion of bad data points or data sets in the fit, or improper constraints on the relative normalization of data sets. For each data set included in the fit, an overall normalization or scale uncertainty was determined, separate from the point-to-point systematic uncertainties. This normalization uncertainty is given in, or was estimated from, the original publication of the data. The same normalization uncertainty was applied but remove it from the total uncertainties to obtain the point-to-point uncertainties.

The experiment L. Andivahis *et al.* included data taken with more than one detector. There will therefore be different normalization factor for the data taken in the different detectors. We split the experiment into two data sets, and fit the normalization factor for each one independently. This will allow the normalization factor to be determined from both these direct measurements and the comparison to the full data set. Because we do not apply the normalization factor determined from the original analysis, we add a 2% normalization uncertainty (in quadrature) to the 1.77% uncertainty quoted in the original analysis.

The cross section for the *unpolarized elastic electron-deuteron scattering in the one-photon-exchange approximation* is described by the Rosenbluth formula. This expression contains the structure functions $A\left(Q^2\right)$ and $B\left(Q^2\right)$, which can be separated by the Rosenbluth technique. The deuteron is a spin-1 nucleus and the characterization of its charge and magnetization distribution requires three form factors: the charge monopole $F_C\left(Q^2\right)$, the magnetic dipole $F_M\left(Q^2\right)$ and the quadrupole $F_Q\left(Q^2\right)$ form factor. The $A\left(Q^2\right)$ and $B\left(Q^2\right)$ can be expressed in terms of this form factors. It is not possible to separate all three form factors of the deuteron from the unpolarized elastic electron-deuteron cross section measurement alone. The deuteron tensor moment can be expressed in terms of the deuteron form factors. Therefore, by combining the structure functions $A\left(Q^2\right)$, $B\left(Q^2\right)$ from the unpolarized cross section measurement, and the deuteron tensor moment measurement, one can separate all three deuteron form factors.

In Fig. 4.5 are shown the GKex, BBA and Warren *et al.* fits for the electric form factor of the neutron with experimental data. The structure function $A\left(Q^2\right)$ provides one of the few methods to infer the neutron electric form factor, especially in the low Q^2 region (less than 1.0 (GeV/c)^2 where theoretical descriptions of $A\left(Q^2\right)$ including relativity, meson-exchange currents (MEC), etc. are under better control compared to higher Q^2 region. The most systematic information on G_E^n at low Q^2, prior to any polarization experiment, is from the $A\left(Q^2\right)$ structure function determined from the elastic electron-deuteron scattering experiment by Platchkov *et al* [317]. However, the extraction procedure is quite complicated. First, the subtraction of $F_M^2\left(Q^2\right)$ from $A\left(Q^2\right)$ using data on $B\left(Q^2\right)$ is performed to obtain the corrected $A\left(Q^2\right)$ which contains contributions from $F_C\left(Q^2\right)$, and $F_Q\left(Q^2\right)$ only. Second, the relativistic and MEC corrections are applied to the corrected $A\left(Q^2\right)$ to obtain the corresponding $A\left(Q^2\right)$ in the impulse picture. Next, the deuteron structure is removed to obtain the nucleon isoscalar charge form factor. Finally, the proton electric form factor is subtracted from the nucleon isoscalar charge form factor and G_E^n is obtained. The extracted G_E^n values are extremely sensitive to the deuteron structure (using the Paris, Nijmegen, Argonne V14, Reid-Soft Core nucleon potentials). The large spread represents the uncertainty due to the deuteron structure, and the absolute scale of G_E^n contains a systematic uncertainty of about 50% from such an extraction. Schiavilla and Sick [339] extracted G_E^n from an analysis of the deuteron quadrupole form factor $F_Q\left(Q^2\right)$ data. State-of-the-art deuteron calculations based on a variety of different model interactions and currents show that the $F_Q\left(Q^2\right)$ form factor is relatively insensitive to the uncertain two-body operators of shorter range because the long-range one-pion exchange operator dominates the two-body contribution to $F_Q\left(Q^2\right)$.

Quasielastic electron-deuteron scattering, in which the kinematics of the electron scattering from the nucleon inside the deuteron is selected, is the other process involving the deuteron which has been used extensively in probing the electromagnetic structure of the neutron. It includes both inclusive measurements, in which only scattered electrons are detected at the quasielastic kinematics, and coincidence measurements where both the scattered electron and the knockout neutron are measured. The measured quasielastic ed cross-section per nucleon, converted to the reduced cross section is written through R_T and R_L, the transverse and longitudinal nuclear response functions, respectively. In the plane wave impulse approximation (PWIA) the quasielastic R_T response function is proportional to ${G_M^n}^2 + {G_M^p}^2$, and the R_L response function is proportional to ${G_E^n}^2 + {G_E^p}^2$. Thus, the extraction of the neutron electromagnetic form factor requires the separation of the response functions using the Rosenbluth technique followed by the subtraction of the proton contribution in PWIA. Most data on G_M^n had been deduced from quasi-elastic ed scattering. For inclusive measurements the procedure requires the separation of the longitudinal and transverse cross sections and the subsequent subtraction of a large proton contribution. Thus, it suffers from large theoretical uncertainties due in part to the deuteron model employed and in part to corrections for final-state interactions (FSI), MEC effects, and relativistic corrections.

Recoil transfer polarization method. In polarized elastic electron-proton scattering, $p(\mathbf{e}, e'\mathbf{p})$, the longitudinal P_L and transverse P_T components of the recoil final proton polarization are sensitive to different combinations of the electric and magnetic elastic form factors. In Fig. 4.4 are shown the GKex and BBA fits for the ratio $G_E^p/\left(\mu_p G_M^p\right)$ [4]. The ratio of the form factors G_E^p/G_M^p, can be directly related to the components of the recoil polarization. Because the ratio is proportional to the ratio of polarization components, the measurement does not require an accurate knowledge of the beam polarization or analyzing power of the recoil

[3] We omit for this figure the obsoleted data by D. H. Coward *et al.*, SLAC 1968 [269]; R. G. Arnold *et al.*, SLAC 1986 [see the second reference [273]]

[4] The data S. Dieterich *et al.*, MAMI 2000 [288] are omitted through the data T. Pospischil *et al.*, MAMI 2001 [291] are overlapped one.

polarimeter. Calculations of radiative corrections indicate that the effects on the recoil polarizations are small and at least partially cancel in the ratio of the two-polarization component. The polarization transfer technique allows much better measurements at high Q^2 values, there is a significant discrepancy even in the region where both techniques have comparable uncertainties. The main systematic uncertainties come from inelastic background processes and determination of the spin precession. RTPM is less sensitive to systematic uncertainties than the Rosenbluth extractions, the discrepancy appears at relatively low Q^2 values, where both techniques give equally precise results. Because almost all of the polarization transfer data come from the same experimental setup, it is in principle possible that an unaccounted for systematic error could cause a false Q2 dependence in the ratio. There are no known problems or inconsistencies in these measurements and this technique. At this time, there is no explanation for the different results obtained by the two techniques. If we do not understand this discrepancy, then it is difficult to know how to correctly combine the polarization transfer measurements with the cross section measurements in order to extract the individual form factors.

4.2 Resume for publication (fully obsolete)

In this section we compare phenomenological fits for nucleon form factors with experimental data. The GK model extended by Lomon [341] include the major vector meson pole contributions and synthesize meson-dynamics and asymptotic QCD predictions. We investigate so-called "GKex(02L)" and "GKex(02S)" sets of the model parameters. The BBA fits for proton electric, magnetic and neutron magnetic form factors are inverse polynomial expressions [42]. So-called "CS" and "CS+PTD" sets are the fits using the cross section data only and using both cross section data and the polarization transfer data, respectively. Fit for neutron electric form factor is given by Galster [304].

In previous experiments for evaluation of nucleon form factors is used the *Rosenbluth technique*. In this method for evaluating the proton form factors it is possible to extract the information on electric and magnetic form factors separately by analyzing of the differential cross sections at a fixed Q^2 value at a different electron energy and scattering angle. In the cross section the G_E^p term dominates in the low Q^2 region and the G_M^p term dominates at large Q^2 values. Thus the extraction of G_M^p at low Q^2 and G_E^p at large Q^2 values becomes difficult using the Rosenbluth technique. For evaluation of neutron form factors the technique requires the measuring the cross section for the unpolarized elastic electron-nucleus scattering described by the Rosenbluth formula. In previous analyses the thin scattering effects (the radiative corrections, Schwinger term and the additional corrections for vacuum polarization contributions from muon and quark loops) are not included. The recent experiments use the *Recoil transfer polarization method*. In polarized elastic electron-proton scattering the longitudinal and transverse components of the recoil final proton polarization are sensitive to different combinations of the electric and magnetic elastic form factors [239].

In Fig. 4.2 the GKex and BBA fits for the ratio $G_M^p/(\mu_p G_D)$ are shown. The BBA fit for G_M^p has unpredictable behavior at the range $Q^2 > 20$ GeV^2. We use the "patch" for both BBA fits:

$$\frac{G_M^p}{\mu_p G_D} = \left(0.304\,Q^2 - 2.5\right)^{-0.222}, \quad G_D\left(Q^2\right) = \left(1 + \frac{Q^2}{m_V^2}\right)^{-1}.$$

The most discrepant data are derived for the ratio $G_M^n/(\mu_n G_D)$ with uncertainty 30%. Experimental data and the GKex and BBA fits are shown in Fig. 4.3.

The ratio of the electric and magnetic form factors of the proton can be directly related to the components of the recoil polarization. In Fig. 4.4 the GKex and BBA fits for the ratio $G_E^p/(\mu_p G_M^p)$ are shown. In the range of low Q^2 values the ratio of form factors is constant and depends on normalization. The range of high Q^2 values does not contribute to the total cross sections of $e^\pm$ and $\mu^\pm$ production in neutrino-nucleon interactions. The range of Q^2 values above 1 GeV^2 is important for $\tau^\pm$ production because even at threshold of reaction Q^2 values are high. As it shown from the Figure the main mismatch between two techniques is just in this range.

In Fig. 4.5 GKex(02S) fit and Galster's fits with two sets of parameters for the G_E^n (BBA and Warren *et al.* [258]) with experimental data are shown. We omit the negative stale data of the neutron electric form factor. The positive values of data are discrepant and uncertainty achieves 10%.

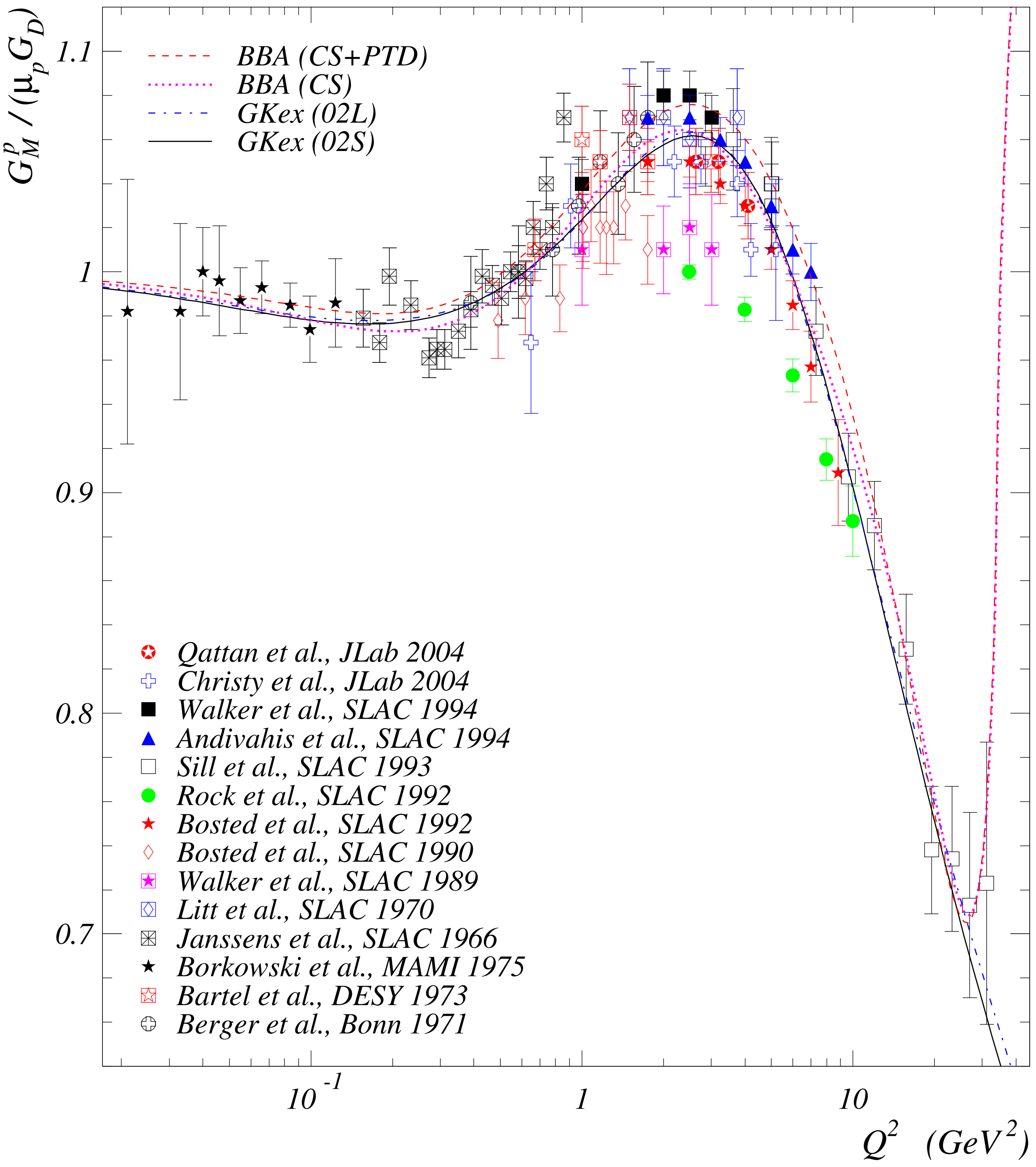

Figure 4.2: Comparison of the GKex and BBA fits for ratio $G_M^p/(\mu_p G_D)$ with experimental data. F. Borkowski *et al.* [282], P. E. Bosted *et al.* [274], P. E. Bosted *et al.* [275], M. E. Christy *et al.* [260]. The data T. Janssens *et al.* [268], J. Litt *et al.* [270], C. Berger *et al.* [297], W. Bartel *et al.* [305], R. C. Walker *et al.* [279], A. F. Sill *et al.* [277] and L. Andivahis *et al.* [281] are taken from Ref. [338]. The data R. C. Walker *et al.* [280] are taken from the figure. The dashed curve for the BBA (CS+PTD), dotted curve for the BBA (CS), dash-dotted curve for the GKex(02L) and solid curve for the GKex(02S) parametrizations.

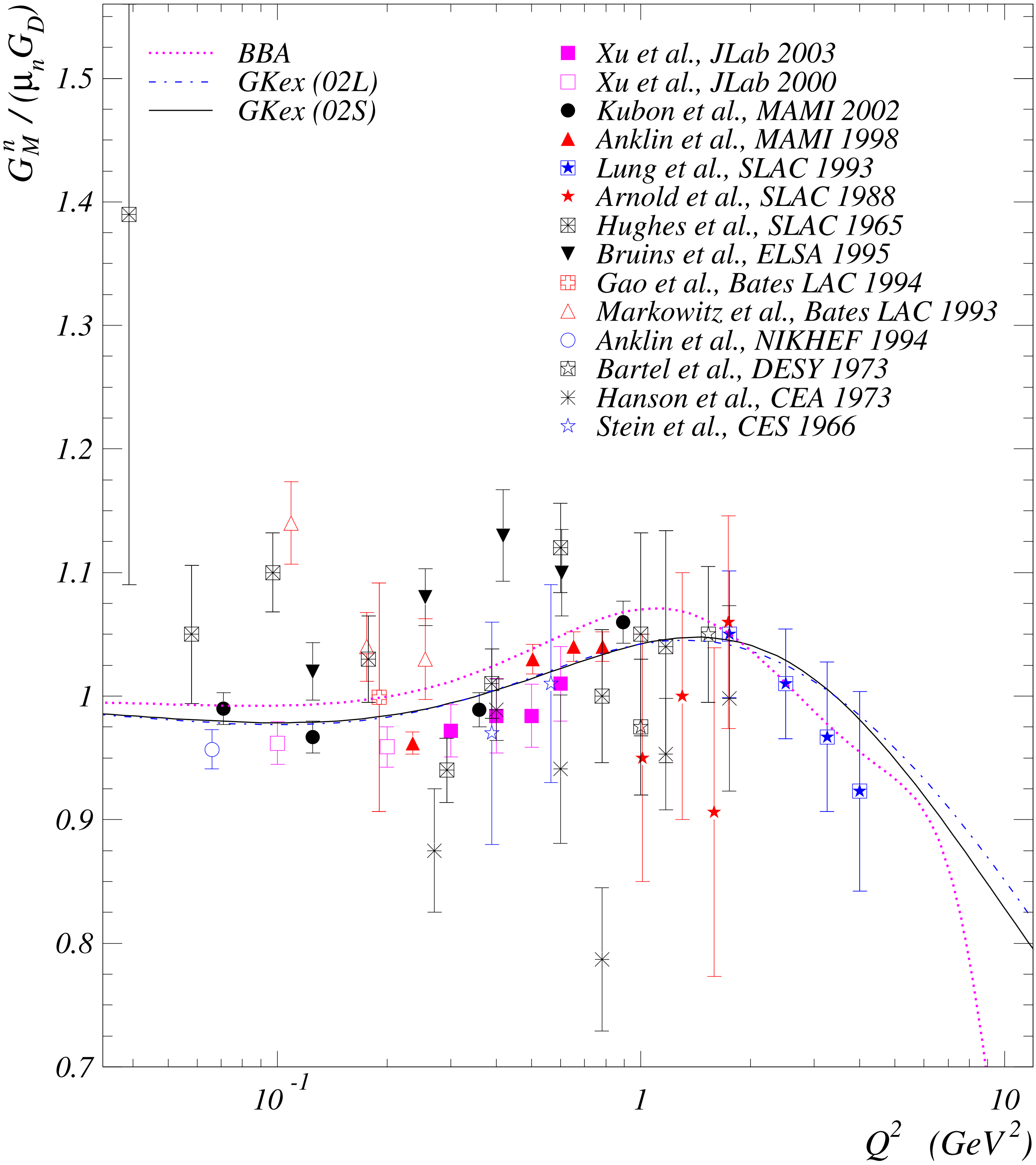

Figure 4.3: Comparison of the GKex BBA and fits for ratio $G_M^n/(\mu_n G_D)$ with experimental data. W. Bartel *et al.* [305], P. Markowitz *et al.* [278], A. Lung *et al.* [276], H. Gao *et al.* [308], H. Anklin *et al.* [311], J. Jourdan [312], E. E. W. Bruins *et al.* [298], H. Anklin *et al.* [313], W. Xu *et al.* [244], G. Kubon *et al.* [316], W. Xu *et al.* [251]. The data E. B. Hughes *et al.* [267] are taken from Ref. [305]. The data P. Stein *et al.* [318] ate taken from Ref. [305] The data R. G. Arnold *et al.* [273] are taken from the figure. The data K. M. Hanson *et al.* [266] are taken from the review [239].

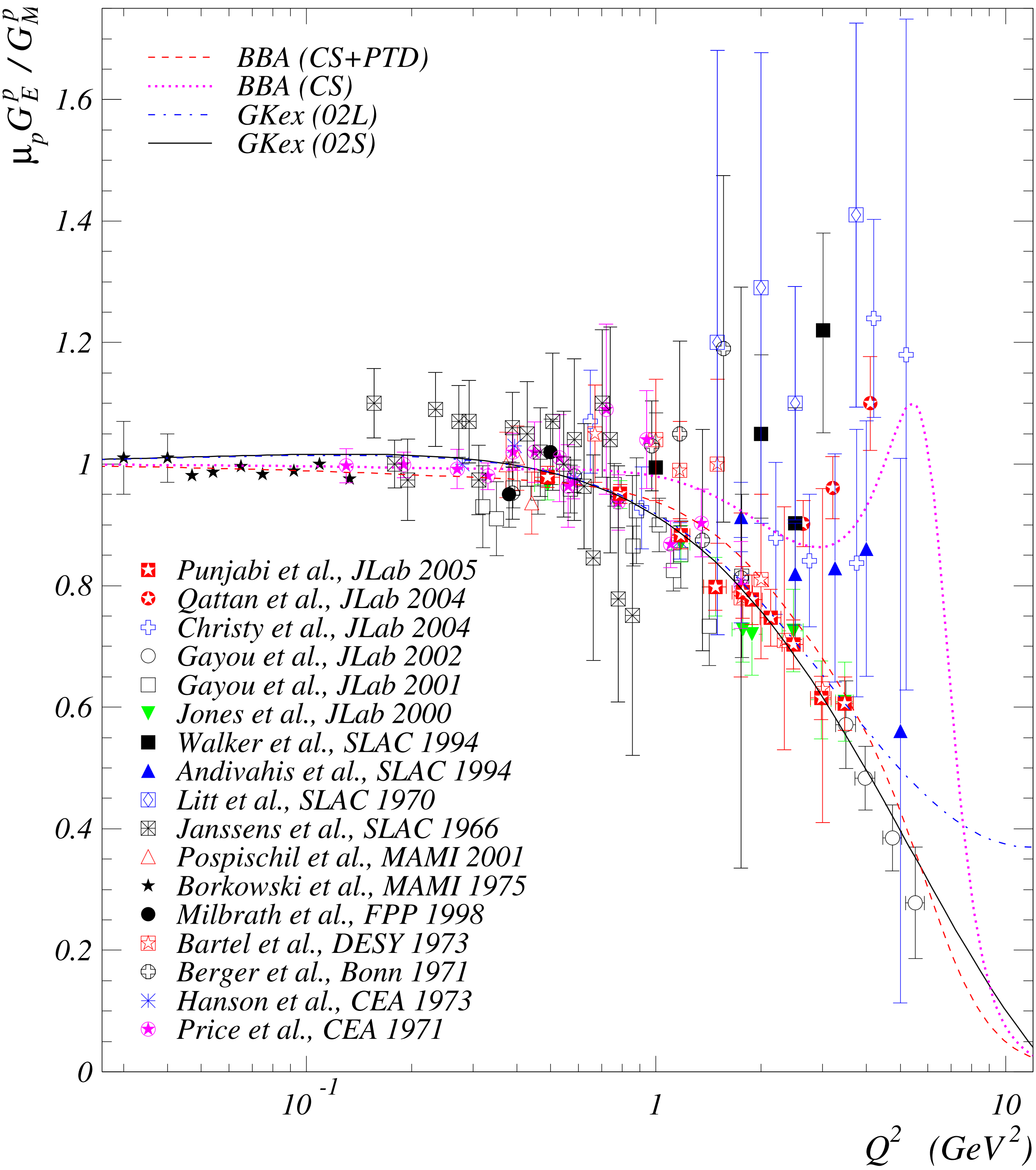

Figure 4.4: Comparison of the GKex and BBA fits for ratio $G_E^p/(\mu_p G_M)$ with experimental data. L. E. Price *et al.* [265], W. Bartel *et al.* [305], B. D. Milbrath *et al.* [309], M. K. Jones *et al.* [242], T. Pospischil *et al.* [291], O. Gayou *et al.* [247], [248], M. E. Christy *et al.* [260]. The data T. Janssens *et al.* [268], J. Litt *et al.* [270], C. Berger *et al.* [297], L. Andivahis *et al.* [281], R. C. Walker *et al.* [280], are taken from [325]. The data K. M. Hanson *et al.* [266], F. Borkowski *et al.* [282], are taken from the figure from [239].

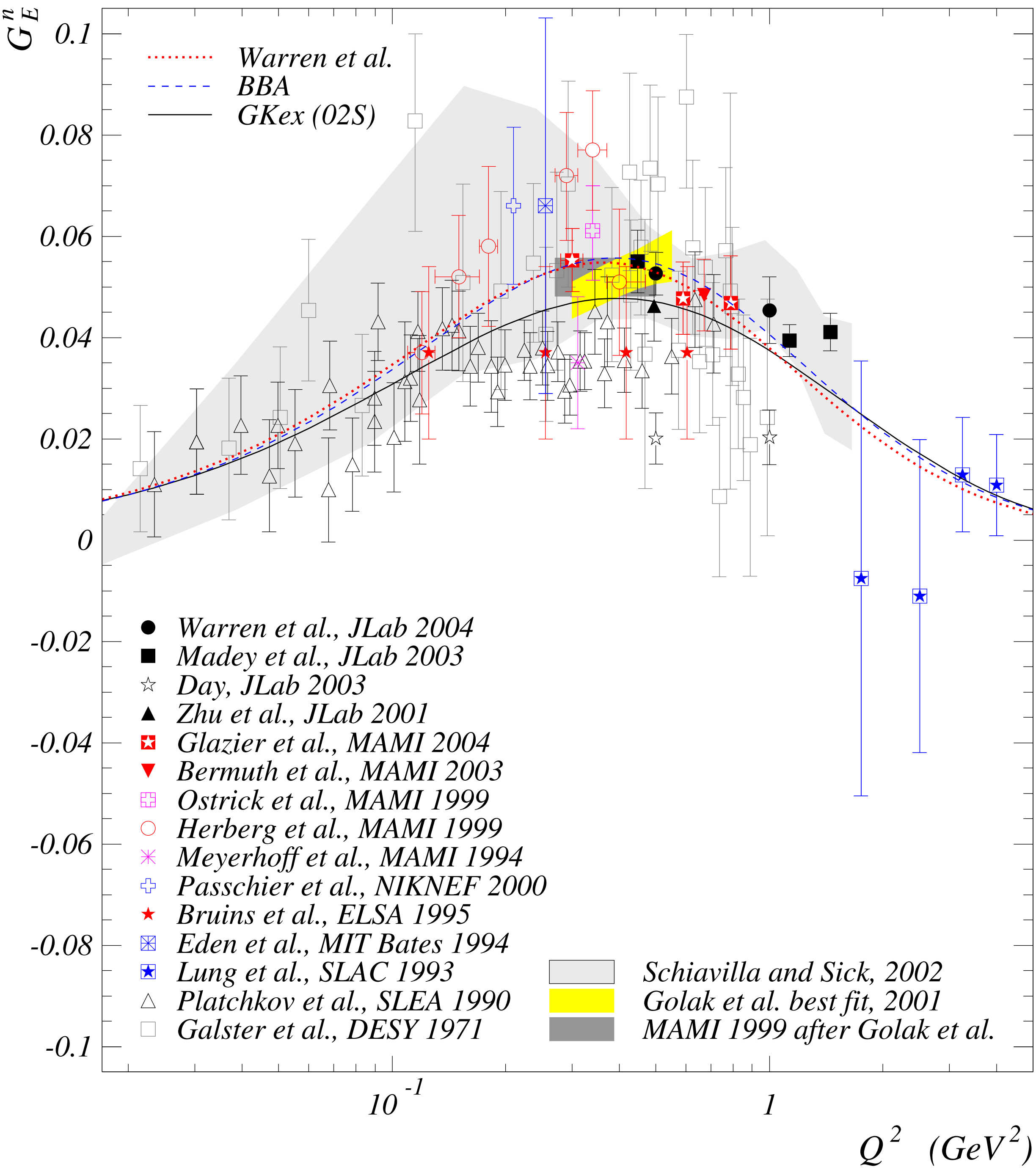

Figure 4.5: Comparison of the GKex, BBA and Warren *et al.* fits for the electric form factor of the neutron with experimental data. S. Galster *et al.* [304], D. I. Glazier *et al.* [296], M. Meyerhoff *et al.* [283], T. Eden *et al.* [307], E. E. W. Bruins *et al.* [298], C. Herberg *et al.* [284], M. Ostrick *et al.* [287], I. Passchier *et al.* [314], J. Bermuth *et al.* [295], H. Zhu *et al.* [245], R. Madey *et al.* [256], G. Warren *et al.* [258]. The data D. Day [259] are taken from a figure. The data A. Lung *et al.* [276] are taken from a figure at Ref. [348]. The data S. Platchkov *et al.* [317] are taken from a figure at Ref. [239].

Chapter 5

Nucleon structure functions

5.1 Heavy quark production thresholds

Since $q + p = p_X$ we have

$$p_X^2 = q^2 + M^2 + 2(qp) = 2M(1-x)yE_\nu + M^2.$$

Let us consider the frame (we mark it with the symbol *) in which the momentum of the system X is zero, $\mathbf{p}_X^\star = 0$. In this frame $p_X^\star = (\sum_i E_i^\star, 0)$, where $E_i^\star$ is the total energy of particle $i \in X$. Clearly $\sum_i E_i^\star$ has the minimum value when *all* particles i have zero momenta ($\mathbf{p}_i^\star = 0$). Therefore

$$2M(1-x)yE_\nu \geq M_X^2 - M^2, \tag{5.1}$$

where

$$M_X = \sum_i m_i$$

and m_i is the mass of particle i. The inequality (5.1) can be rewritten in terms of variables x and Q^2:

$$x \leq \left(1 + \frac{M_X^2 - M^2}{Q^2}\right)^{-1}. \tag{5.2}$$

Condition (5.1) or (5.2) together with the reaction threshold condition

$$2ME_\nu \geq (m + M_X)^2 - M^2 \tag{5.3}$$

and the condition $x \leq x^-$ defines the kinematic boundaries for production of any system of secondary particles X. Thus by considering the system X of hadronic (anti)quark states with the minimum value of M_X, one can find the kinematic boundary for corresponding sea (anti)quark contribution into the target nucleon structure functions. The relevant "minimal reactions" for c quark and antiquark are shown in the table. We neglect the thresholds for light (anti)quark production. The top hadrons are not discovered yet and the mass of t quark is measured with significant experimental uncertainty ($> 5M$). Thus we adopt $M_X^2 - M^2 = m_t^2$ for all relevant "minimal reactions" with top hadrons in the final state.

All the "minimal reactions" are collected in Table 5.1.

Table 5.1: Minimal reactions for charm neutrinoproduction.

Target quark	Exclusive reaction	Target quark	Exclusive reaction
d	$\nu_l + p \to l^- + \Sigma_c^{++}$	$\overline{d}$	$\overline{\nu}_l + p \to l^+ + p + D^-$
s	$\nu_l + p \to l^- + p + D_s^+$	$\overline{s}$	$\overline{\nu}_l + p \to l^+ + p + D_s^-$
d	$\nu_l + n \to l^- + \Lambda_c^+$	$\overline{d}$	$\overline{\nu}_l + n \to l^+ + n + D^-$
s	$\nu_l + n \to l^- + n + D_s^+$	$\overline{s}$	$\overline{\nu}_l + n \to l^+ + n + D_s^-$

5.2 Charm production components of $F_{2,3}$ in the BY model

Here we discuss our present-day understanding of the Bodek–Yang prescription [42, 43, 216, 217] (see also Ref. [215, Section 4.4.5]).

For the moment, let us limit ourselves with the two-generation case. The "naive" parton model formulas for the structure functions F_2 and F_3 [222] are collected in Table 5.2, where W_c^2 is the charm production threshold (see Sect. 5.1) The same may be written in a more compact form as is shown in Table 5.3. The arguments of the parton distribution functions (PDF) in both tables are x and Q^2.

Table 5.2: The "naive" parton model formulas for $F_{2,3}$.

	$W^2 < W_c^2$	$W^2 > W_c^2$
	$F_2(x,Q^2)$	
νp	$2x[d\cos^2\theta_C + s\sin^2\theta_C + \overline{u} + \overline{c}]$	$2x[d + s + \overline{u} + \overline{c}]$
$\overline{\nu} p$	$2x[u\cos^2\theta_C + c\sin^2\theta_C + \overline{d} + \overline{s}]$	$2x[u + c + \overline{d} + \overline{s}]$
νn	$2x[u\cos^2\theta_C + s\sin^2\theta_C + \overline{d} + \overline{c}]$	$2x[u + s + \overline{d} + \overline{c}]$
$\overline{\nu} n$	$2x[d\cos^2\theta_C + c\sin^2\theta_C + \overline{u} + \overline{s}]$	$2x[d + c + \overline{u} + \overline{s}]$
	$xF_3(x,Q^2)$	
νp	$2x[d\cos^2\theta_C + s\sin^2\theta_C - \overline{u} - \overline{c}]$	$2x[d + s - \overline{u} - \overline{c}]$
$\overline{\nu} p$	$2x[u\cos^2\theta_C + c\sin^2\theta_C - \overline{d} - \overline{s}]$	$2x[u + c - \overline{d} - \overline{s}]$
νn	$2x[u\cos^2\theta_C + s\sin^2\theta_C - \overline{d} - \overline{c}]$	$2x[u + s - \overline{d} - \overline{c}]$
$\overline{\nu} n$	$2x[d\cos^2\theta_C + c\sin^2\theta_C - \overline{u} - \overline{s}]$	$2x[d + c - \overline{u} - \overline{s}]$

Table 5.3: Compact form of $F_{2,3}$.

	$F_2(x,Q^2)$
νp	$2x\left[d + s + \overline{u} + \overline{c} - \theta\left(W_c^2 - W^2\right)\left(d\sin^2\theta_C + s\cos^2\theta_C\right)\right]$
$\overline{\nu} p$	$2x\left[u + c + \overline{d} + \overline{s} - \theta\left(W_c^2 - W^2\right)\left(u\sin^2\theta_C + c\cos^2\theta_C\right)\right]$
νn	$2x\left[u + s + \overline{d} + \overline{c} - \theta\left(W_c^2 - W^2\right)\left(u\sin^2\theta_C + s\cos^2\theta_C\right)\right]$
$\overline{\nu} n$	$2x\left[d + c + \overline{u} + \overline{s} - \theta\left(W_c^2 - W^2\right)\left(d\sin^2\theta_C + c\cos^2\theta_C\right)\right]$
	$xF_3(x,Q^2)$
νp	$2x\left[d + s - \overline{u} - \overline{c} - \theta\left(W_c^2 - W^2\right)\left(d\sin^2\theta_C + s\cos^2\theta_C\right)\right]$
$\overline{\nu} p$	$2x\left[u + c - \overline{d} - \overline{s} - \theta\left(W_c^2 - W^2\right)\left(u\sin^2\theta_C + c\cos^2\theta_C\right)\right]$
νn	$2x\left[u + s - \overline{d} - \overline{c} - \theta\left(W_c^2 - W^2\right)\left(u\sin^2\theta_C + s\cos^2\theta_C\right)\right]$
$\overline{\nu} n$	$2x\left[d + c - \overline{u} - \overline{s} - \theta\left(W_c^2 - W^2\right)\left(d\sin^2\theta_C + c\cos^2\theta_C\right)\right]$

In order to describe the charm production parts of the structure functions, F_i^{cp}, we note that the following charm production vertex are only possible:

$$W^+ d \to c, \quad W^- \overline{d} \to \overline{c},$$
$$W^+ s \to c, \quad W^- \overline{s} \to \overline{c}.$$

The corresponding contributions to the cross sections are proportional to $\sin^2\theta_C$ for $d, \overline{d}$ and to $\cos^2\theta_C$ for $s, \overline{s}$. Therefore the functions $F_{2,3}^{\text{cp}}$ may be written as

$$F_2^{\text{cp}}(x,Q^2) = \theta\left(W^2 - W_c^2\right)\mathcal{F}_2(\xi_c, Q^2), \tag{5.4a}$$
$$xF_3^{\text{cp}}(x,Q^2) = \theta\left(W^2 - W_c^2\right)\xi_c\mathcal{F}_3(\xi_c, Q^2), \tag{5.4b}$$

where the functions $\mathcal{F}_i(x,Q^2)$ are defined in Table 5.4 and

Table 5.4: Functions $\mathcal{F}_{2,3}$.

	$\mathcal{F}_2(x,Q^2)$	$x\mathcal{F}_3(x,Q^2)$
νp	$2x\left(d\sin^2\theta_C + s\cos^2\theta_C\right)$	$+2x\left(d\sin^2\theta_C + s\cos^2\theta_C\right)$
$\overline{\nu} p$	$2x\left(\overline{d}\sin^2\theta_C + \overline{s}\cos^2\theta_C\right)$	$-2x\left(\overline{d}\sin^2\theta_C + \overline{s}\cos^2\theta_C\right)$
νn	$2xs\cos^2\theta_C$	$+2xs\cos^2\theta_C$
$\overline{\nu} n$	$2x\overline{s}\cos^2\theta_C$	$-2x\overline{s}\cos^2\theta_C$

$$\xi_c = \frac{2x\left[1 + (M_1^2 + m_c^2)/Q^2\right]}{1 + \sqrt{1 + 4M^2x^2/Q^2} + 2xM_2^2/Q^2} = \frac{x_N\left[1 + (M_1^2 + m_c^2)/Q^2\right]}{1 + x_N M_2^2/Q^2} \tag{5.5}$$

is the Bodek-Yang scaling variable [42,43,216,217].[1]

Consequently the non charm production parts of the structure functions, $F_i^{\rm ncp}$, are

$$F_2^{\rm ncp}(x,Q^2) = F_2(\xi_0,Q^2) - \theta\left(W^2 - W_c^2\right)\mathcal{F}_2(\xi_0,Q^2), \tag{5.6a}$$
$$xF_3^{\rm ncp}(x,Q^2) = \xi_0 F_2(\xi_0,Q^2) - \theta\left(W^2 - W_c^2\right)\xi_0\mathcal{F}_2(\xi_0,Q^2), \tag{5.6b}$$

where ξ_0 is obtained from ξ_c by putting $m_c = 0$. Finally the Bodek-Yang structure functions are

$$\begin{aligned} F_2^{\rm BY}(x,Q^2) &= F_2^{\rm ncp}(x,Q^2) + F_2^{\rm cp}(x,Q^2) \\ &= F_2(\xi_0,Q^2) - \theta\left(W^2 - W_c^2\right)\left[\mathcal{F}_2(\xi_c,Q^2) - \mathcal{F}_2(\xi_0,Q^2)\right]. \\ xF_3^{\rm BY}(x,Q^2) &= xF_3^{\rm ncp}(x,Q^2) + xF_3^{\rm cp}(x,Q^2) \\ &= \xi_0 F_3(\xi_0,Q^2) - \theta\left(W^2 - W_c^2\right)\left[\xi_c\mathcal{F}_3(\xi_c,Q^2) - \xi_0\mathcal{F}_3(\xi_0,Q^2)\right]. \end{aligned}$$

5.3 Detailed properties of variables ξ_c and ξ_0.

It is easy to prove that

$$\frac{\partial x_N}{\partial x} = \frac{x_N}{x}\left(1 + \frac{4M^2x^2}{Q^2}\right)^{-1} > 0, \quad \frac{\partial \xi_c}{\partial x_N} = \frac{\xi_c}{x_N}\left(1 + \frac{M_2^2 x_N}{Q^2}\right)^{-1} > 0$$

and thus $\partial\xi_c/\partial x > 0$ that is the Bodek–Yang variable ξ_c is an increasing function of x for any Q^2. In general ξ_c can exceed 1. Indeed, the solution to equation $\xi_c = 1$ written in terms of the Bjorken x is given by

$$x = \left(1 + \frac{m_c^2 - \Delta^2}{Q^2}\right)\left[\left(1 + \frac{m_c^2 - \Delta^2}{Q^2}\right)^2 - \frac{M^2}{Q^2}\right]^{-1} \equiv x_c, \tag{5.7}$$

where $\Delta^2 = M_2^2 - M_1^2 = 0.196\,\mathrm{GeV}^2$. Since $m_c^2 - \Delta^2 > M^2$,

$$0 < x_c < 1 \quad \text{for} \quad 0 < Q^2 < \infty.$$

Finally, $0 \le \xi_c \le 1$ for $0 \le x \le x_c$ at any Q^2.

The properties of variable ξ_0 are not so simple. The solution to equation $\xi_0 = 1$ is

$$x = \left(1 - \frac{\Delta^2}{Q^2}\right)\left[\left(1 - \frac{\Delta^2}{Q^2}\right)^2 - \frac{M^2}{Q^2}\right]^{-1} \equiv x_0. \tag{5.8}$$

This function is singular and the two singular points are given by

$$Q^2 = \Delta^2 + \frac{1}{2}M^2 \pm M\sqrt{\Delta^2 + \frac{1}{4}M^2}.$$

The only point at which $x_0 = 1$ is

$$Q^2 = \frac{\Delta^4}{\Delta^2 + M^2} \equiv Q_1^2.$$

It is located between the singular points as well as the point $Q^2 = \Delta^2$ at which $x_0 = 0$ (see Table 5.5 and Fig. 5.1). Clearly $\Delta^2 - Q_1^2 = M^2\Delta^2/(\Delta^2 + M^2) > 0$.

Table 5.5: Singular points of $x_0(Q^2)$ and Q_1^2 (in GeV^2).

Q^2	proton target	neutron target	isoscalar target
left singular point	0.0309455	0.0308835	0.03091448
Q_1^2	0.0356908	0.0356105	0.00356506
right singular point	1.2414088	1.2438995	1.24265378

Finally, considering that ξ_0 is a monotonically increasing function of x, we have proved that $0 \le \xi_0 \le 1$ for $0 \le x \le x_0$ if $Q_1^2 < Q^2 < \Delta^2$ and for any x if $Q^2 \le Q_1^2$ or $Q^2 \ge \Delta^2$. We must assume therefore that the corresponding θ functions are include into the definitions of the functions $\mathcal{F}_i(\xi_0, Q^2)$.

[1] Let us ignore for the moment the (partially) obsolete recipe for the slow rescaling described in Ref. [216] and based on the GRV94 LO PDFs. The numerical values of the parameters in Eq. (5.5) obtained in Ref. [217] with the GRV98 PDFs are $M_1^2 = 0.222\,\mathrm{GeV}^2$, $M_2^2 = 0.418\,\mathrm{GeV}^2$. In more recent papers [42] and [43] these are a bit changed to $M_1^2 = 0.223\,\mathrm{GeV}^2$, $M_2^2 = 0.419\,\mathrm{GeV}^2$ while the difference $\Delta^2 = M_2^2 - M_1^2 = 0.196\,\mathrm{GeV}^2$ remains the same. The c quark mass, m_c, is taken to be 1.5 GeV. Note that the notations we use here are different from those of the original papers [42,43,216,217].

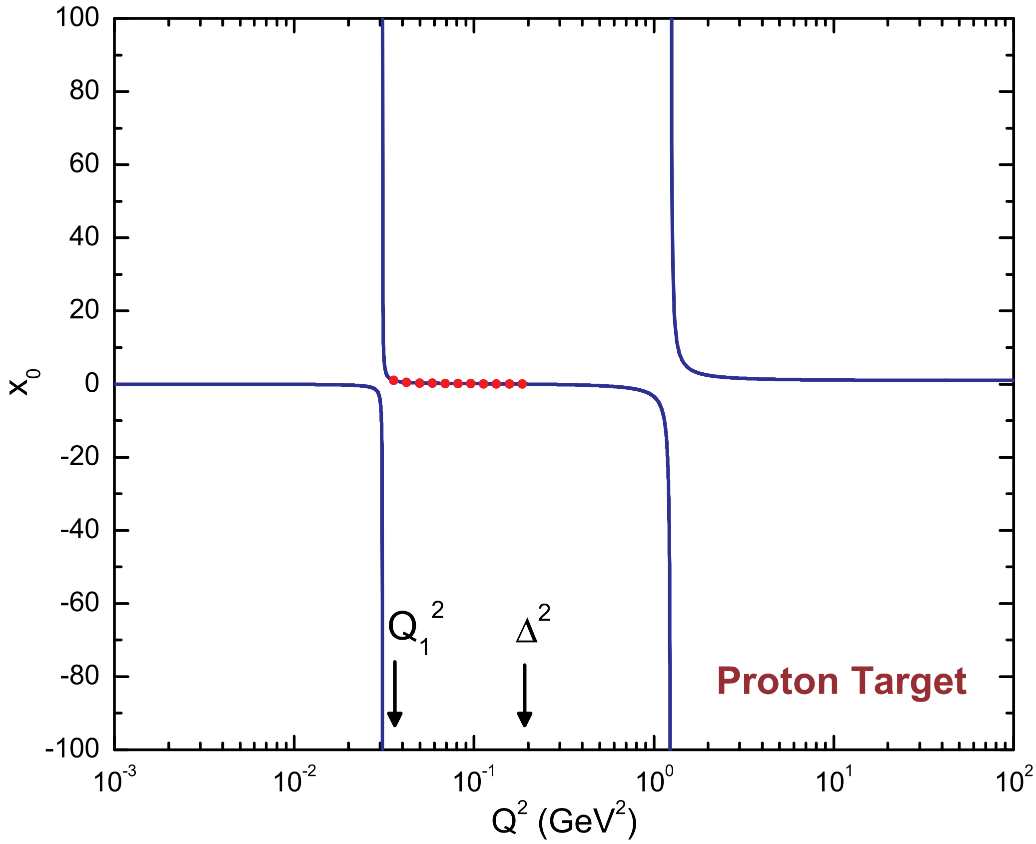

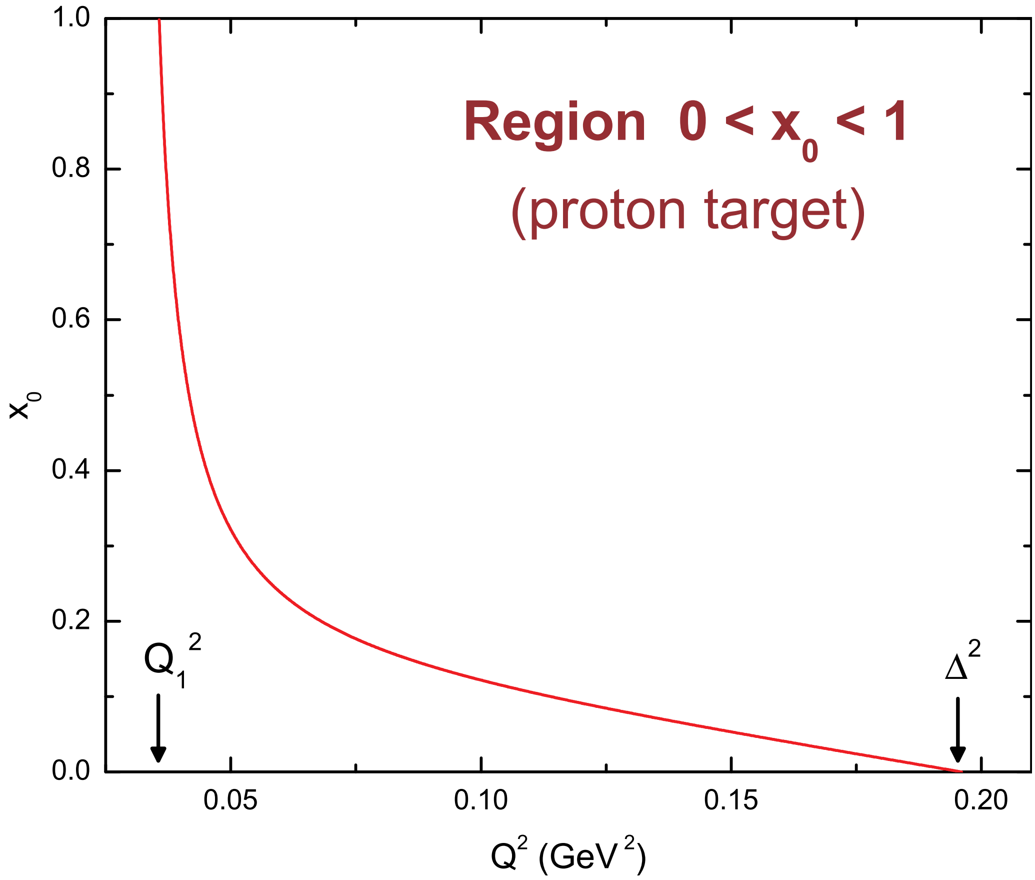

Figure 5.1: Bound x_0 as a function of Q^2 (top panel) and the zoom of the region $0 < x_0 < 1$ (bottom panel) for a proton target.

Chapter 6

Polarization density matrix

6.1 General formulas

We consider the lepton production in neutrino and antineutrino scattering from the nonpolarized nucleon target. The general form of the polarization density matrix for the reaction

$$\overset{(-)}{\nu}(k) + N(p) \to \ell(k') + X(p')$$

is given by

$$d\boldsymbol{\sigma} = \left\| d\sigma_{\lambda\lambda'} \right\| \equiv \boldsymbol{\rho} d\sigma.$$

Here k, p, k', p' are the 4-momenta of initial (anti)neutrino, target nucleon N $(= p$ or $n)$, final lepton ℓ $(= e$, μ or $\tau)$ and final hadronic system X, respectively. In the general case, the elements of that matrix are[1]

$$d\sigma_{\lambda\lambda'} = \frac{(2\pi)^4 \mathcal{M}_\lambda \mathcal{M}^*_{\lambda'} \delta\left(p_f - p_i\right)}{4\sqrt{\left(p_a p_b\right)^2 - m_a^2 m_b^2}} \prod_{j=1}^{n} \frac{d\mathbf{p}_j}{(2\pi)^3 2p_j^0}.$$

In our particular case,

$$d\sigma_{\lambda\lambda'} = \frac{(2\pi)^4 \mathcal{M}_\lambda \mathcal{M}^*_{\lambda'} \delta\left(k + p - k' - p'\right)}{4\,(kp)} \frac{d\mathbf{k}'}{(2\pi)^3 2k'_0} \frac{d\mathbf{p}'}{(2\pi)^3 2p'_0}.$$

Matrix elements are

$$\mathcal{M}_\lambda = \frac{G_F \kappa}{\sqrt{2}} \times \begin{cases} j^\alpha_\lambda\left(k, k'\right) J_\alpha\left(p, p'\right) & \text{for neutrino,} \\ \overline{j}^{\,\alpha}_\lambda\left(k, k'\right) J_\alpha\left(p, p'\right) & \text{for antineutrino.} \end{cases} \tag{6.1}$$

Here

$$\kappa = \frac{M_W^2}{M_W^2 - q^2},$$

$J_\alpha\left(p, p'\right)$ is the hadronic weak current and

$$j^\alpha_\lambda\left(k, k'\right) = \overline{u}\left(k', \lambda\right) \gamma^\alpha \left(\frac{1 - \gamma_5}{2}\right) u(k) \tag{6.2a}$$

and

$$\overline{j}^{\,\alpha}_\lambda\left(k, k'\right) = \overline{v}(k) \gamma^\alpha \left(\frac{1 - \gamma_5}{2}\right) v\left(k', \lambda\right) \tag{6.2b}$$

are the leptonic weak currents. Therefore the elements of the polarization density matrix can be written as

$$d^3\sigma_{\lambda\lambda'} = \frac{G_F^2 M \kappa^2}{16\pi^2 (kp)} L^{\alpha\beta}_{\lambda\lambda'} W_{\alpha\beta} \frac{d\mathbf{k}'}{2k'_0},$$

where

$$W_{\alpha\beta} = \frac{1}{4} \int J_\alpha\left(p, p'\right) J^*_\beta\left(p, p'\right) \delta\left(k + k' - p - p'\right) \frac{d\mathbf{p}'}{2p'_0}, \tag{6.3}$$

is the hadronic tensor and

$$L^{\alpha\beta}_{\lambda\lambda'}\left(k, k'\right) = \begin{cases} j^\alpha_\lambda\left(k, k'\right) j^{*\beta}_{\lambda'}\left(k, k'\right) & \text{for neutrino,} \\ \overline{j}^{\,\alpha}_\lambda\left(k, k'\right) \overline{j}^{\,*\beta}_{\lambda'}\left(k, k'\right) & \text{for antineutrino} \end{cases} \tag{6.4}$$

is the leptonic tensor.

[1] According to notation of Okun [1].

In the laboratory frame $d\mathbf{k}'/k'_0 = P_\ell dE_\ell d\cos\theta d\phi$ (from here, $E_\ell = k'_0$, $P_\ell = |\mathbf{k}'|$). After integrating by $d\phi$ we get the general formula for the inclusive cross section,

$$\frac{d^2\sigma_{\lambda\lambda'}}{dE_\ell d\cos\theta} = \frac{G_F^2}{4\pi}\frac{P_\ell}{ME_\nu}\kappa^2 L^{\alpha\beta}_{\lambda\lambda'}W_{\alpha\beta}. \tag{6.5}$$

The leptonic tensor summed over the final lepton helicities is given by

$$\begin{aligned} L^{\alpha\beta}(k,k') &= \sum_{\lambda\lambda'} L^{\alpha\beta}_{\lambda\lambda'}(k,k') = \frac{1}{4}\mathrm{Tr}\left[\left(\hat{k}'+m\right)\gamma^\alpha(1\mp\gamma_5)\hat{k}\gamma^\beta(1\mp\gamma_5)\right] \\ &= 2\,\mathrm{Tr}\left[k^\alpha k'^\beta + k'^\alpha k^\beta - g^{\alpha\beta}(kk') \pm \epsilon_{\alpha\beta\gamma\delta}k^\gamma k'^\delta\right], \end{aligned}$$

where the upper (lower) signs are for neutrino (antineutrino). Here we used the following formulas for the density matrices averaged over the polarization

$$u(k)\overline{u}(k) = \hat{k}, \quad \sum_{\lambda\lambda'} u(k',\lambda)\,\overline{u}(k',\lambda') = \hat{k}'+m.$$

Finally, the polarization density matrix is given by

$$\left\|\frac{d^2\sigma_{\lambda\lambda'}}{dE_\ell d\cos\theta}\right\| = \left\|\frac{G_F^2}{4\pi}\frac{P_\ell}{ME_\nu}\kappa^2 L^{\alpha\beta}_{\lambda\lambda'}W_{\alpha\beta}\right\|, \qquad \kappa = \frac{M_W^2}{M_W^2-q^2}.$$

The nucleon structure functions, W_i, are defined through the generally accepted representation of the hadronic tensor

$$\begin{aligned} W_{\alpha\beta} = &- g_{\alpha\beta}W_1 + \frac{p_\alpha p_\beta}{M^2}W_2 - i\,\frac{\epsilon_{\alpha\beta\gamma\delta}p^\gamma q^\delta}{2M^2}W_3 \\ &+ \frac{q_\alpha q_\beta}{M^2}W_4 + \frac{p_\alpha q_\beta + q_\alpha p_\beta}{2M^2}W_5 + i\,\frac{p_\alpha q_\beta - q_\alpha p_\beta}{2M^2}W_6, \end{aligned}$$

and their explicit form is defined by the particular subprocess (QE, RES or DIS). Here M is the *target nucleon mass*.[2]

The elements of the polarization density matrix are

$$\begin{aligned} \frac{d^2\sigma_{++}}{dE_\ell d\cos\theta} &= K\left(\frac{E_\ell \mp P_\ell}{2M}\right)\left\{(1\pm\cos\theta)\left(W_1 \pm \frac{E_\nu \mp P_\ell}{2M}W_3\right)\right. \\ &\left. + \frac{1\mp\cos\theta}{2}\left[W_2 + \frac{E_\ell \pm P_\ell}{M}\left(\frac{E_\ell \pm P_\ell}{M}W_4 - W_5\right)\right]\right\}, \\ \frac{d^2\sigma_{--}}{dE_\ell d\cos\theta} &= K\left(\frac{E_\ell \pm P_\ell}{2M}\right)\left\{(1\mp\cos\theta)\left(W_1 \pm \frac{E_\nu \pm P_\ell}{2M}W_3\right)\right. \\ &\left. + \frac{1\pm\cos\theta}{2}\left[W_2 + \frac{E_\ell \mp P_\ell}{M}\left(\frac{E_\ell \mp P_\ell}{M}W_4 - W_5\right)\right]\right\}, \\ \frac{d^2\sigma_{+-}}{dE_\ell d\cos\theta} &= K\left(\frac{m\sin\theta}{4M}\right)\left[\mp\left(2W_1 - W_2 - \frac{m^2}{M^2}W_4 + \frac{E_\ell}{M}W_5\right) - \frac{E_\nu}{M}W_3 + i\frac{P_\ell}{M}W_6\right], \\ \frac{d^2\sigma_{-+}}{dE_\ell d\cos\theta} &= K\left(\frac{m\sin\theta}{4M}\right)\left[\mp\left(2W_1 - W_2 - \frac{m^2}{M^2}W_4 + \frac{E_\ell}{M}W_5\right) - \frac{E_\nu}{M}W_3 - i\frac{P_\ell}{M}W_6\right], \end{aligned}$$

where the upper (lower) signs are for neutrino (antineutrino) and

$$K = \frac{G_F^2 P_\ell \kappa^2}{\pi} = \frac{G_F^2 P_\ell}{\pi}\left(1 - \frac{q^2}{M_W^2}\right)^{-2}.$$

Therefore the cross section for unpolarized lepton production is

$$\frac{d^2\sigma}{dE_\ell d\cos\theta} = \frac{d^2\sigma_{++}}{dE_\ell d\cos\theta} + \frac{d^2\sigma_{--}}{dE_\ell d\cos\theta} \equiv K\mathcal{R}, \tag{6.6}$$

where the Lorentz invariant dimensionless function $\mathcal{R}$ is given by

$$\begin{aligned} \mathcal{R} = &\left(\frac{E_\ell - P_\ell\cos\theta}{M}\right)\left(W_1 + \frac{m^2}{2M^2}W_4\right) + \left(\frac{E_\ell + P_\ell\cos\theta}{2M}\right)W_2 \\ &\pm\left[\left(\frac{E_\nu + E_\ell}{M}\right)\left(\frac{E_\ell - P_\ell\cos\theta}{2M}\right) - \frac{m^2}{2M^2}\right]W_3 - \frac{m^2}{2M^2}W_5. \end{aligned}$$

[2] This definition remains the same through the whole text even if we use some other notation for the nucleon mass like M_N or M_i.

In terms of the Bjorken scaling variables

$$x = \frac{-q^2}{2(pq)} \quad \text{and} \quad y = \frac{(pq)}{(pk')}$$

it can be rewritten as

$$\begin{aligned}\mathcal{R} = &\left(xy + \frac{m^2}{2ME_\nu}\right)W_1 + \frac{E_\nu}{M}\left\{\left(1 - y - \frac{M}{2E_\nu}xy - \frac{m^2}{4E_\nu^2}\right)W_2\right.\\ &\left.\pm y\left[x\left(1-\frac{y}{2}\right) - \frac{m^2}{4ME_\nu}\right]W_3 + \frac{m^2}{2ME_\nu}\left[\left(xy + \frac{m^2}{2ME_\nu}\right)W_4 - W_5\right]\right\}.\end{aligned}$$

The components of the polarization vector $\boldsymbol{\mathcal{P}}$ are

$$\begin{aligned}\mathcal{P}_P =& \mp\frac{m\sin\theta}{2M\mathcal{R}}\left(2W_1 - W_2 \pm \frac{E_\nu}{M}W_3 - \frac{m^2}{M^2}W_4 + \frac{E_\ell}{M}W_5\right),\\ \mathcal{P}_T =& -\frac{mP_\ell\sin\theta}{2M^2\mathcal{R}}W_6,\\ \mathcal{P}_L =& \mp 1 \pm \frac{m^2}{M^2\mathcal{R}}\left\{\left[\left(\frac{2M}{E_\ell + P_\ell}\right)W_1 \pm \left(\frac{E_\nu - P_\ell}{E_\ell + P_\ell}\right)W_3\right]\cos^2\frac{\theta}{2}\right.\\ &\left.+\left[\left(\frac{M}{E_\ell + P_\ell}\right)W_2 + \left(\frac{E_\ell + P_\ell}{M}\right)W_4 - W_5\right]\sin^2\frac{\theta}{2}\right\}.\end{aligned}$$

NOTE XXV: Another form of presentation for the longitudinal polarization

$$\begin{aligned}\mathcal{P}_L =& \mp\frac{1}{\mathcal{R}}\left\{\left(\frac{P_\ell - E_\ell\cos\theta}{M}\right)\left(W_1 - \frac{m^2}{2M^2}W_4\right) + \left(\frac{P_\ell + E_\ell\cos\theta}{2M}\right)W_2\right.\\ &\left.\pm\left[\frac{(E_\nu + E_\ell)(P_\ell - E_\ell\cos\theta) + m^2\cos\theta}{2M^2}\right]W_3 - \frac{m^2\cos\theta}{2M^2}W_5\right\}.\end{aligned}$$

is less transparent by is a little bit more convenient for numerical evaluations.

6.2 Covariant method

It can be shown (see, for example Ref. [2]) that

$$u(p_1,s_1)\,\overline{u}(p_2,s_2) = N_{12}\,\mathfrak{P}_+(p_1,s_1)\,\mathfrak{P}_+(p_2,s_2), \tag{6.7a}$$
$$v(p_1,s_1)\,\overline{v}(p_2,s_2) = N_{12}\,\mathfrak{P}_-(p_1,s_1)\,\mathfrak{P}_-(p_2,s_2), \tag{6.7b}$$

where

$$\mathfrak{P}_\pm(p_i,s_i) = \frac{1}{2}(\hat{p}_i \pm m_i)(1 + \gamma_5\hat{s}_i)$$

and N_{12} is a complex normalization constant which is expressed in terms of known quantities and of two intrinsically indeterminate phases, φ_+ and φ_-:

$$N_{12} = \frac{(1+\lambda_1\lambda_2)\,e^{i\varphi_+} + (1-\lambda_1\lambda_2)\,e^{i\varphi_-}}{2\sqrt{\upsilon_{12}}}, \tag{6.8a}$$
$$\upsilon_{12} = [m_1m_2 + (p_1p_2)]\,[1 - (s_1s_2)] + (p_1s_2)\,(p_2s_1). \tag{6.8b}$$

These formulas have to be modified if one of the particles is a neutrino or antineutrino. As is easy to prove, the neutrino and antineutrino spin 4-vectors satisfy the equation

$$m_\nu s_\nu = \mp k.$$

Accordingly, taking the limit as m_ν goes to zero, we obtain

$$\upsilon_{12} \to (kk') \pm m(ks) = (1 \mp \lambda\cos\theta)\,E_\nu\,(E_\ell \pm \lambda P_\ell) \equiv \upsilon_\lambda, \tag{6.9a}$$
$$N_{12} \to \frac{(1+\lambda)\,e^{i\varphi_+} + (1-\lambda)\,e^{i\varphi_-}}{2\sqrt{\upsilon_\lambda}} \equiv N_\lambda, \tag{6.9b}$$

and (taking into account that $\hat{k}^2 = k^2 = m_\nu^2$)

$$\mathfrak{P}_\pm (k, s_\nu) \to \frac{1}{2} (1 - \gamma_5) \hat{k}. \tag{6.10}$$

The upper (lower) sign in Eq. (6.9a) is for ν ($\overline{\nu}$), λ is the lepton helicity and we have used the indeterminacy of the phases to simplify the numerator in Eq. (6.9b). Taking these formulas into account we can calculate the weak charged currents in neutrino and antineutrino cases:

$$\begin{aligned}
j_\lambda^\alpha &= \overline{u}(k', s) \gamma^\alpha \left(\frac{1 - \gamma_5}{2} \right) u(k) \\
&= \frac{N_\lambda}{4} \mathrm{Tr} \left[\hat{k} \left(\hat{k}' + m \right) (1 + \gamma_5 \hat{s}) \gamma^\alpha (1 - \gamma_5) \right] \\
&= N_\lambda \left[m k^\alpha - s^\alpha (kk') + k'^\alpha (ks) - i \epsilon^{\alpha\beta\gamma\delta} s_\beta k_\gamma k'_\delta \right], \qquad (6.11a) \\
\overline{j}_\lambda^\alpha &= \overline{v}(k) \gamma^\alpha \left(\frac{1 - \gamma_5}{2} \right) v(k', s) \\
&= \frac{\lambda N_\lambda}{4} \mathrm{Tr} \left[\left(\hat{k}' - m \right) (1 + \gamma_5 \hat{s}) \hat{k} \gamma^\alpha (1 - \gamma_5) \right] \\
&= \lambda N_\lambda \left[-m k^\alpha - s^\alpha (kk') + k'^\alpha (ks) + i \epsilon^{\alpha\beta\gamma\delta} s_\beta k_\gamma k'_\delta \right]. \qquad (6.11b)
\end{aligned}$$

As is seen from these equations,

$$\overline{j}_\lambda^\alpha = -\lambda \left(j_{-\lambda}^\alpha \right)^*,$$

$$\begin{pmatrix} N_+ N_+^* & N_+ N_-^* \\ N_- N_+^* & N_- N_-^* \end{pmatrix} = \frac{1}{E_\nu m^2} \begin{pmatrix} \dfrac{E_\ell \mp P_\ell}{1 \mp \cos\theta} & \dfrac{m e^{i\varphi}}{\sin\theta} \\ \dfrac{m e^{-i\varphi}}{\sin\theta} & \dfrac{E_\ell \pm P_\ell}{1 \pm \cos\theta} \end{pmatrix}, \qquad \varphi = \varphi_+ - \varphi_-.$$

The leptonic tensor is given by

$$L_{\lambda\lambda'}^{\alpha\beta} = \begin{cases} j_\lambda^\alpha \left(j_{\lambda'}^\beta \right)^* & \text{for neutrino,} \\ \overline{j}_\lambda^\alpha \left(\overline{j}_{\lambda'}^\beta \right)^* & \text{for antineutrino.} \end{cases}$$

We use the generally accepted representation of the hadronic tensor (see, e.g., ref. [6])

$$\begin{aligned}
W_{\alpha\beta} = & - g_{\alpha\beta} W_1 + \frac{p_\alpha p_\beta}{M^2} W_2 - \frac{i \epsilon_{\alpha\beta\rho\sigma} p^\rho q^\sigma}{2M^2} W_3 \\
& + \frac{q_\alpha q_\beta}{M^2} W_4 + \frac{p_\alpha q_\beta + q_\alpha p_\beta}{2M^2} W_5 + i \frac{p_\alpha q_\beta - q_\alpha p_\beta}{2M^2} W_6
\end{aligned} \tag{6.12}$$

which includes 6 nucleon structure functions, W_n, whose explicit form is defined by the particular subprocess (QE, RES or DIS). Here p and M are the target nucleon 4-momentum and mass, respectively, $q = k - k'$ is the W boson 4-momentum. By applying the above results we obtain

$$\rho_{\lambda\lambda'} \propto L_{\lambda\lambda'}^{\alpha\beta} W_{\alpha\beta} = E_\nu^2 m^2 N_\lambda N_{\lambda'}^* \sum_{n=1}^{6} A_{\lambda\lambda'}^n W_n,$$

$$\begin{aligned}
A_{\lambda\lambda'}^1 &= 2 \left(\eta_{\lambda\lambda'} \mp \eta_{-\lambda\lambda'} \right) \sin^2\theta, \\
A_{\lambda\lambda'}^2 &= 4 \left(\eta_{\pm\lambda} \eta_{\pm\lambda'} \sin^4 \frac{\theta}{2} + \eta_{\mp\lambda} \eta_{\mp\lambda'} \cos^4 \frac{\theta}{2} \right) \pm \eta_{-\lambda\lambda'} \sin^2\theta, \\
A_{\lambda\lambda'}^3 &= \pm \sin^2\theta \left(\eta_{\pm\lambda} \eta_{\pm\lambda'} \frac{E_\nu - P_\ell}{M} + \eta_{\mp\lambda} \eta_{\mp\lambda'} \frac{E_\nu + P_\ell}{M} \mp \eta_{-\lambda\lambda'} \frac{E_\nu}{M} \right), \\
A_{\lambda\lambda'}^4 &= 4 \left[\eta_{\pm\lambda} \eta_{\pm\lambda'} \frac{(E_\nu + P_\ell)^2}{M^2} \sin^4 \frac{\theta}{2} + \eta_{\mp\lambda} \eta_{\mp\lambda'} \frac{(E_\nu - P_\ell)^2}{M^2} \cos^4 \frac{\theta}{2} \right] \\
&\quad \pm \eta_{-\lambda\lambda'} \frac{m^2}{M^2} \sin^2\theta, \\
A_{\lambda\lambda'}^5 &= -4 \left[\eta_{\pm\lambda} \eta_{\pm\lambda'} \frac{E_\nu + P_\ell}{M} \sin^4 \frac{\theta}{2} + \eta_{\mp\lambda} \eta_{\mp\lambda'} \frac{E_\nu - P_\ell}{M} \cos^4 \frac{\theta}{2} \right] \mp \eta_{-\lambda\lambda'} \frac{E_\ell}{M} \sin^2\theta, \\
A_{\lambda\lambda'}^6 &= i \left(\frac{\lambda - \lambda'}{2} \right) \frac{P_\ell}{M} \sin^2\theta,
\end{aligned}$$

where $\eta_\lambda = (1+\lambda)/2$. Taking into account that $\mathrm{Tr}\,\boldsymbol{\rho} = 1$, we can find the explicit formulas for the elements of the polarization density matrix in terms of variables E_ν, P_ℓ and θ:

$$\rho_{++}(E_\nu, P_\ell, \theta) = \rho_{--}(E_\nu, -P_\ell, \pi-\theta) = \frac{E_\ell \mp P_\ell}{2M\mathcal{R}}\,\mathcal{Z},$$
$$\rho_{+-}(E_\nu, P_\ell, \theta) = \rho^*_{-+}(E_\nu, P_\ell, \theta) = \frac{m\sin\theta}{4M\mathcal{R}}\,(\mathcal{X} - i\mathcal{Y})\,e^{i\varphi}.$$

Here we have introduced the following notation:

$$\begin{aligned}
\mathcal{X} &= \mp\left(2W_1 - W_2 - \frac{m^2}{M^2}W_4 + \frac{E_\ell}{M}W_5\right) - \frac{E_\nu}{M}W_3,\\
\mathcal{Y} &= -\frac{P_\ell}{M}W_6,\\
\mathcal{Z} &= (1\pm\cos\theta)\left(W_1 \pm \frac{E_\nu \mp P_\ell}{2M}W_3\right)\\
&\quad + \frac{1\mp\cos\theta}{2}\left[W_2 + \frac{E_\ell \pm P_\ell}{M}\left(\frac{E_\ell \pm P_\ell}{M}W_4 - W_5\right)\right],\\
\mathcal{R} &= \left(\frac{E_\ell - P_\ell\cos\theta}{M}\right)\left(W_1 + \frac{m^2}{2M^2}W_4\right) + \left(\frac{E_\ell + P_\ell\cos\theta}{2M}\right)W_2\\
&\quad \pm\left[\left(\frac{E_\nu + E_\ell}{M}\right)\left(\frac{E_\ell - P_\ell\cos\theta}{2M}\right) - \frac{m^2}{2M^2}\right]W_3 - \frac{m^2}{2M^2}W_5,
\end{aligned}$$

and $\varphi = \varphi_+ - \varphi_-$. Finally the projections of the lepton polarization vector are given by

$$\begin{pmatrix}\mathcal{P}_P\\ \mathcal{P}_T\end{pmatrix} = \frac{m\sin\theta}{2M\mathcal{R}}\begin{pmatrix}\cos\varphi & \sin\varphi\\ -\sin\varphi & \cos\varphi\end{pmatrix}\begin{pmatrix}\mathcal{X}\\ \mathcal{Y}\end{pmatrix}, \tag{6.13a}$$

$$\begin{aligned}
\mathcal{P}_L = \mp 1 \pm \frac{m^2}{M^2\mathcal{R}}\Bigg\{&\left[\left(\frac{2M}{E_\ell + P_\ell}\right)W_1 \pm \left(\frac{E_\nu - P_\ell}{E_\ell + P_\ell}\right)W_3\right]\cos^2\frac{\theta}{2}\\
&+ \left[\left(\frac{M}{E_\ell + P_\ell}\right)W_2 + \left(\frac{E_\ell + P_\ell}{M}\right)W_4 - W_5\right]\sin^2\frac{\theta}{2}\Bigg\}.
\end{aligned} \tag{6.13b}$$

By putting $\varphi = 0$ [3] the formulas for $\mathcal{P}_P$ and $\mathcal{P}_L$ exactly coincide with those of ref. [223] (obtained within a noncovariant approach under assumption $W_6 = 0$).

Several simple conclusions immediately follow from Eqs. (6.13). First, the perpendicular and transverse projections are unobservable quantities in contrast with the longitudinal projection of $\boldsymbol{\mathcal{P}}$ and the degree of polarization $|\boldsymbol{\mathcal{P}}|$. Second, supposing that $W_6 = 0$ (as is probably the case) one can force the polarization vector to lie in the production plane. Third, a massless lepton is fully polarized, $\boldsymbol{\mathcal{P}} = (0, 0, \mp 1)$. In particular, at the energies of our interest, electron is always fully polarized while in general, this is not the case for muon and τ lepton.

6.3 Quasielastic scattering

6.3.1 The case $M_f = M_i = M$.

In this case the hadronic weak currents are

$$J_\alpha(p,p') = \overline{u}(p')\,\Gamma_\alpha u(p), \quad \overline{J}_\alpha(p,p') = \overline{u}(p')\,\overline{\Gamma}_\alpha u(p), \tag{6.14}$$

where

$$\Gamma_\alpha = \gamma_\alpha(F_V + F_M) + \frac{2q_\alpha F_S - n_\alpha F_M}{2M} + \left(\gamma_\alpha F_A + \frac{q_\alpha F_P + n_\alpha F_T}{M}\right)\gamma_5, \tag{6.15a}$$

$$\overline{\Gamma}_\alpha = \gamma_\alpha(F_V^* + F_M^*) + \frac{2q_\alpha F_S^* - n_\alpha F_M^*}{2M} + \left(\gamma_\alpha F_A^* - \frac{q_\alpha F_P^* + n_\alpha F_T^*}{M}\right)\gamma_5, \tag{6.15b}$$

and $n = p' + p = 2p + q$.

<u>NOTE XXVI</u>: The standard definition of the vertex function for QE νN scattering is given through 6 form factors which in general are assumed to be complex:

$$\Gamma_\alpha = \Gamma_\alpha^V + \Gamma_\alpha^A = \gamma_\alpha F_V + i\sigma_{\alpha\beta}\frac{q_\beta}{2M}F_M + \frac{q_\alpha}{M}F_S + \left(\gamma_\alpha F_A + \frac{n_\alpha}{M}F_T + \frac{q_\alpha}{M}F_P\right)\gamma_5,$$

Table 6.1: Relationships between different QE form factor designations used by different authors.

This work	[6]	[222, 223]	Name
F_V	F_V^1	F_1^V	Dirac
F_M	ξF_V^2	ξF_2^V	Pauli
F_A	F_A	F_A	Axial
F_P	F_p	F_p	Pseudoscalar
F_S	F_V^3	F_3^V	Scalar
F_T	F_A^3	F_3^A	Tensor

$$F_k = \text{Re}\, F_k + i\, \text{Im}\, F_k \quad (k = V, M, S, A, T, P).$$

Some authors use a bit different notation (see Table 6.1, where $\xi = \mu_p - \mu_n$ and $\mu_{p,n}$ are the anomalous magnetic moments of p and n).

The following trivial identities are of utility for our calculations:

$$\begin{aligned}
|F_k|^2 &= F_k F_k^* = (\text{Re}\, F_k)^2 + (\text{Im}\, F_k)^2\,,\\
|F_k + F_l|^2 &= |F_k|^2 + F_k^* F_l + F_k F_l^* + |F_l|^2\\
&= |F_k|^2 + 2\,(\text{Re}\, F_k\, \text{Re}\, F_l + \text{Im}\, F_k\, \text{Im}\, F_l) + |F_l|^2\,,\\
\text{Re}\,(F_k^* F_l) &= \text{Re}\,(F_k F_l^*) = \text{Re}\, F_k\, \text{Re}\, F_l + \text{Im}\, F_k\, \text{Im}\, F_l,\\
\text{Im}\,(F_k^* F_l) &= -\text{Im}\,(F_k F_l^*) = \text{Re}\, F_k\, \text{Im}\, F_l - \text{Im}\, F_k\, \text{Re}\, F_l.
\end{aligned}$$

Every structure function W_i is of the form

$$W_i = \left|\sum_{k=1}^{6} \alpha_i^k F_k\right|^2 = \sum_{k,l=1}^{6} \alpha_i^k \left(\alpha_i^l\right)^* F_k F_l^*,$$

with some (in general complex) coefficients α_i^k. If some two coefficients, say α_i^k and α_i^l, are real, the corresponding contribution to W_i can be represented as

$$\alpha_i^k \left(\alpha_i^k - \alpha_i^l\right) \left(\alpha_i^k \left|F_k\right|^2 - \alpha_i^l \left|F_l\right|^2\right) + \alpha_i^k \alpha_i^l \left|F_k + F_l\right|^2$$

or, equivalently,

$$\alpha_i^k \left(\alpha_i^k + \alpha_i^l\right) \left(\alpha_i^k \left|F_k\right|^2 + \alpha_i^l \left|F_l\right|^2\right) - \alpha_i^k \alpha_i^l \left|F_k - F_l\right|^2.$$

If the coefficients α_i^k and α_i^l are imaginary, the same formulas may be applied after the substitution

$$\alpha_i^{k,l} \mapsto \text{Im}\left(\alpha_i^{k,l}\right).$$

These rules can be used to simplify the final formulas for W_i.

[3] We adopt this convention from here on. Therefore, according to Eq. (6.13a), $\mathcal{P}_P \propto \mathcal{X}$ and $\mathcal{P}_T \propto \mathcal{Y}$.

NOTE XXVII:
Since

$$\sigma_{\alpha\beta} = \frac{i}{2}\left(\gamma_\alpha\gamma_\beta - \gamma_\beta\gamma_\alpha\right) = -\sigma^\dagger_{\beta\alpha},$$

we have

$$\begin{aligned}\overline{u}\left(p'\right) i\sigma_{\alpha\beta}\frac{q_\beta}{2M}u(p) =& \frac{1}{4M}\overline{u}\left(p'\right)\left[\left(2g_{\alpha\beta}-\gamma_\beta\gamma_\alpha\right)p'_\beta - \gamma_\alpha\gamma_\beta p_\beta \; - p_\beta\gamma_\beta\gamma_\alpha + \left(2g_{\beta\alpha}-\gamma_\alpha\gamma_\beta\right)p_\beta\right]u(p)\\ =& \,\overline{u}\left(p'\right)\left(\gamma_\alpha - \frac{n_\alpha}{2M}\right)u(p).\end{aligned}$$

According to the Dirac equation

$$\gamma_\beta p_\beta u(p) = Mu(p), \quad \overline{u}\left(p'\right)\gamma_\beta p'_\beta = M\overline{u}\left(p'\right).$$

By definition

$$\overline{J}_\beta = \gamma_0\, J^\dagger_\beta\,\gamma_0.$$

The following well known formulas for γ matrices useful are also useful:

$$\gamma_5^\dagger = \gamma_5, \quad \gamma_\beta^\dagger = -\gamma_\beta, \quad \gamma_0\gamma_\beta = -\gamma_\beta\gamma_0, \quad \gamma_0\gamma_5 = \gamma_5\gamma_0, \quad \gamma_0\left(\gamma_\alpha\right)^\dagger\gamma_0 = -\gamma_0\gamma_\alpha\gamma_0 = \gamma_\alpha,$$
$$\gamma_0\left(\gamma_\alpha\gamma_5\right)^\dagger\gamma_0 = -\gamma_0\gamma_5^\dagger\,\gamma_\alpha^\dagger\gamma_0 = \gamma_0\gamma_5\gamma_\alpha\gamma_0 = -\gamma_0\gamma_5\gamma_0\gamma_\alpha = -\gamma_0\gamma_0\gamma_5\gamma_\alpha = \gamma_\alpha\gamma_5.$$

NOTE XXVIII: After integrating over ϕ

$$d\sigma^{CC} = \frac{G_F^2}{(2\pi)^2}\frac{M}{(k\,p)}L^{\alpha\beta}W_{\alpha\beta}\frac{d\mathbf{k}'}{E_\ell} = \frac{G_F^2}{2\pi}\frac{P_\ell}{E_\nu}L^{\alpha\beta}W_{\alpha\beta}dE_\ell d\cos\theta,$$

$$d\sigma^{CC} = \frac{G_F^2}{(2\pi)^2}\frac{M}{(k\,p)}L^{\alpha\beta}\frac{\cos^2\theta_C}{2M}\left[\int\delta\left(p'-p-q\right)\frac{d\mathbf{p}'}{E_{N'}}W_{\alpha\beta}\right]\frac{d\mathbf{k}'}{E_\ell},$$

$$\begin{aligned}W_{\alpha\beta} =& \frac{F_V^2}{2}\left[n_\alpha\,n_\beta - q_\alpha\,q_\beta - 2g_{\alpha\beta}(pq)\right] + \frac{F_A^2}{2}\left[n_\alpha\,n_\beta - q_\alpha\,q_\beta - 2g_{\alpha\beta}\left((pq)+2M^2\right)\right]\\ &+ \frac{F_M^2}{2}\left(g_{\alpha\beta}q^2 - q_\alpha\,q_\beta - n_\alpha\,n_\beta\frac{q^2}{4M^2}\right) + F_P^2\,q_\alpha\,q_\beta\frac{(pq)}{M^2}\\ &+ F_VF_M\left(g_{\alpha\beta}q^2 - q_\alpha\,q_\beta\right) - 2F_AF_P\,q_\alpha\,q_\beta + 2F_A\left(F_V+F_M\right)i\epsilon_{\alpha\beta\gamma\delta}\,p_\gamma\,p'_\delta, \quad n = p+p'.\end{aligned}$$

$$\int\delta\left(p'-p-q\right)\frac{d\mathbf{p}'}{E_{N'}} = \frac{1}{M}\delta\left(\nu+\frac{q^2}{2M}\right),$$

$$dq^2d\nu = \left|\frac{\partial\left(q^2,\nu\right)}{\partial\left(\cos\theta,E_\ell\right)}\right|dE_\ell d\cos\theta = 2E_\nu P_\ell dE_\ell d\cos\theta, \quad \frac{d\mathbf{k}'}{E_\ell} = \frac{\pi}{E_\nu}dq^2d\nu.$$

So

$$d^2\sigma^{CC} = \frac{G_F^2\cos^2\theta_C}{(2\pi)^2}\frac{M}{(kp)}\frac{1}{2M^2}\frac{\pi}{E_\nu}L^{\alpha\beta}W_{\alpha\beta}\,\delta\left(\nu+\frac{q^2}{2M}\right)dq^2d\nu,$$

and integration over ν then gives

$$\begin{aligned}\frac{d\sigma^{CC}}{d\left|q^2\right|} &= \frac{G_F^2\cos^2\theta_C}{2\pi}\frac{L^{\alpha\beta}W_{\alpha\beta}}{4M^2E_\nu^2}\\ &= \frac{G_F^2\cos^2\theta_C}{2\pi}\left[A_1F_V^2 + A_2F_A^2 + A_3F_M^2 + A_4F_P^2 \; + A_5F_VF_M - A_6F_AF_P \mp 2A_7F_A\left(F_V+F_M\right)\right],\end{aligned}$$

$$\begin{aligned}A_1 &= 1 - \left(1-\frac{y}{2}+\frac{M}{2E_\nu}\right)\left(y+\frac{m^2}{2ME_\nu}\right),\\ A_2 &= 1 - \left(1-\frac{y}{2}-\frac{M}{2E_\nu}\right)\left(y+\frac{m^2}{2ME_\nu}\right),\\ A_3 &= \frac{y}{2}\left[\frac{y}{2}+(1-y)\frac{E_\nu}{M}\right] - \frac{m^2}{4ME_\nu}\left[y\left(1-\frac{y}{4}\right)\frac{E_\nu}{M} + \frac{m^2}{4ME_\nu}\left(1-\frac{yE_\nu}{2M}\right)\right],\\ A_4 &= \frac{m^2y}{4M^2}\left(y+\frac{m^2}{2ME_\nu}\right),\\ A_5 &= \left(y+\frac{m^2}{2ME_\nu}\right)\left(y-\frac{m^2}{4ME_\nu}\right),\\ A_6 &= \frac{m^2}{2ME_\nu}\left(y+\frac{m^2}{2ME_\nu}\right),\\ A_7 &= y\left(1-\frac{y}{2}-\frac{m^2}{4ME_\nu}\right).\end{aligned}$$

NOTE XXIX:

Let us test of cross section normalization factors. Since

$$q^2 = m^2 - 2E_\nu \left(E_\ell - P_\ell \cos\theta\right) = -2MxyE_\nu = -2Mx\left(E_\nu - E_\ell\right),$$

we have

$$\frac{\partial q^2}{\partial E_\ell} = -2E_\nu\left(1 - \frac{E_\ell}{P_\ell}\cos\theta\right), \quad \frac{\partial q^2}{\partial \cos\theta} = 2E_\nu P_\ell,$$

$$\frac{\partial x}{\partial \cos\theta} = -\frac{E_\nu P_\ell}{M\left(E_\nu - E_\ell\right)}, \quad \frac{\partial x}{\partial E_\ell} = \frac{M + E_\nu\left(1 - \frac{E_\ell}{P_\ell}\cos\theta\right)}{M\left(E_\nu - E_\ell\right)},$$

and thus

$$\frac{d^2\sigma}{dE_\ell d\cos\theta} = \left|\frac{\partial\left(q^2, x\right)}{\partial\left(E_\ell, \cos\theta\right)}\right| \frac{d^2\sigma}{dq^2dx} = 2\frac{P_\ell}{y}\frac{d^2\sigma}{dq^2dx},$$

NOTE XXX:

The total QE cross section can be calculated as

$$\sigma\left(E_\nu\right) = \int_{\cos\theta_{\max}}^{1} d\cos\theta \int_{E_\ell^{\min}}^{E_\ell^{\max}} \frac{d^2\sigma\left(E_\nu, E_\ell, \theta\right)}{dE_\ell d\cos\theta} dE_\ell = \int_{\cos\theta_{\max}}^{1} \frac{d\sigma\left(E_\nu, \theta\right)}{d\cos\theta} d\cos\theta.$$

Here

$$\frac{d\sigma\left(E_\nu, \theta\right)}{d\cos\theta} = \begin{cases} \dfrac{d\sigma^+\left(E_\nu, \theta\right)}{d\cos\theta} + \dfrac{d\sigma^-\left(E_\nu, \theta\right)}{d\cos\theta}, & \text{if} \quad \zeta \le 1, \\ \dfrac{d\sigma^+\left(E_\nu, \theta\right)}{d\cos\theta}, & \text{if} \quad \zeta > 1, \end{cases}$$

$$\frac{d\sigma^\pm\left(E_\nu, \theta\right)}{d\cos\theta} = a_\pm(\theta)\widetilde{\mathcal{R}}\left(E_\nu, E_\ell^\pm(\theta), \theta\right),$$

and we took into account that the double differential QE cross section is equal to

$$K\mathcal{R}\left(E_\nu, E_\ell, \theta\right) = K\widetilde{\mathcal{R}}\left(E_\nu, E_\ell, \theta\right)\delta(1-x)$$

with

$$\delta(1-x) = a_+(\theta)\delta\left(E_\ell - E_\ell^+(\theta)\right) + a_-(\theta)\delta\left(E_\ell - E_\ell^-(\theta)\right)$$

and

$$\frac{1}{a_\pm(\theta)} = \left|\frac{\partial x}{\partial E_\ell}\right|_{E_\ell = E_\ell^\pm(\theta)}.$$

Since

$$x = \frac{-q^2}{2(pq)} = \frac{2E_\nu\left(E_\ell - P_\ell\cos\theta\right) - m^2}{2M\left(E_\nu - E_\ell\right)},$$

we have

$$a_\pm(\theta) = \left|\frac{2M\left(E_\nu - E_\ell\right)P_\ell}{MP_\ell + E_\nu\left(P_\ell - E_\ell\cos\theta\right)}\right|_{E_\ell = E_\ell^\pm(\theta)} = \frac{2M\left[E_\nu - E_\ell^\pm(\theta)\right]P_\ell^\pm(\theta)}{mE_\nu\sqrt{\zeta^2 - \sin^2\theta}}.$$

From the general formula (6.3) we have

$$\begin{aligned} W_{\alpha\beta} &= \frac{\cos^2\theta_C}{4}\int \operatorname{Tr}\left\{J_\alpha\left(\hat{p} + M\right)\overline{J}_\beta\left(\hat{p}' + M\right)\right\}\delta\left(p' - p - q\right)\frac{d\mathbf{p}'}{2E_{N'}} \\ &= \frac{\cos^2\theta_C}{4}\frac{M}{\nu}\delta\left(1 - x\right)\operatorname{Tr}\left\{J_\alpha\left(\hat{p} + M\right)\overline{J}_\beta\left(\hat{p}' + M\right)\right\}. \end{aligned}$$

Taking into account the property of δ function, $\delta\left(ax\right) = \delta\left(x\right)/|a|$, we have

$$\int \delta\left(p' - p - q\right)\frac{d\mathbf{p}_{N'}}{2E_{N'}} = \int \delta\left(p' - p - q\right)\delta\left(p'^2 - M^2\right)dp' = \delta\left(2\left(p\,q\right) + q^2\right) = \frac{\delta(1-x)}{2M\nu}.$$

So the structure functions are

$$W_n^{(\mathrm{QE})}\left(x, Q^2\right) = \cos^2\theta_C w^{-1}\omega_n\left(Q^2\right)\delta(1-x), \quad n = 1, \ldots, 6. \tag{6.16}$$

where the functions ω_n are the bilinear combinations of the electroweak form factors:

$$
\begin{aligned}
\omega_1 =& \ |F_A|^2 + x' \left(|F_A|^2 + |F_V + F_M|^2 \right), \\
\omega_2 =& \ |F_V|^2 + |F_A|^2 + x' \left(|F_M|^2 + 4\,|F_T|^2 \right), \\
\omega_3 =& \ -2\,\mathrm{Re}\left[F_A^* \left(F_V + F_M \right) \right], \\
\omega_4 =& \ \mathrm{Re}\left[F_V^* \left(F_S - \frac{1}{2} F_M \right) - F_A^* \left(F_T + F_P \right) \right] + x' \left(\frac{1}{2} |F_M - F_S|^2 + |F_T + F_P|^2 \right) \\
& - \frac{1}{4} \left(1 + x' \right) |F_M|^2 + \left(1 + \frac{1}{2} x' \right) |F_S|^2, \\
\omega_5 =& \ 2\,\mathrm{Re}\left[F_S^* \left(F_V - x' F_M \right) - F_T^* \left(F_A - 2x' F_P \right) \right] + \omega_2, \\
\omega_6 =& \ 2\,\mathrm{Im}\left[F_S^* \left(F_V - x' F_M \right) + F_T^* \left(F_A - 2x' F_P \right) \right],
\end{aligned}
$$

and we have introduced the following dimensionless variables:

$$
w = \frac{(pq)}{M^2}, \quad x' = \frac{-q^2}{4M^2}.
$$

In order to compare these formulas with the result by Llewellyn Smith [6], we consider his transformation[4]

$$
\omega'_{1,2,3,6} \equiv \omega_{1,2,3,6}, \quad \omega'_4 \equiv 4\omega_4 + \omega_2 - 2\omega_5, \quad \omega'_5 \equiv \omega_5 - \omega_2.
$$

The resulting functions

$$
\begin{aligned}
\omega'_4 =& - |F_V + F_M|^2 - |F_A + 2F_P|^2 + 4\left(1 + x' \right) \left(|F_P|^2 + |F_S|^2 \right), \\
\omega'_5 =& \ 2\,\mathrm{Re}\left[F_S^* \left(F_V - 2x' F_M \right) - F_T^* \left(F_A - 2x' F_P \right) \right]
\end{aligned}
$$

exactly match ones from Llewellyn Smith. Therefore the only difference between our result and the Llewellyn Smith's one is in the function ω_6. Clearly it disappears in the absence of the second-class currents.

By using these formulas one can transform the QE differential cross section to the standard "ABC" form

$$
\frac{d\sigma}{d\,|q^2|} = \frac{G_F^2 M^2 \cos^2_C}{8\pi E_\nu^2} \left[A\,\frac{m^2 - q^2}{M^2} + B\,\frac{s-u}{M^2} + C\,\frac{(s-u)^2}{M^4} \right],
$$

where

$$
s = (k+p)^2, \quad u = (k'-p)^2, \quad s - u = 4ME_\nu + q^2 - m^2,
$$

$$
\begin{aligned}
A =& \ \left(1 + x' \right) \left(|F_A|^2 - 4x' \,|F_T|^2 \right) - \left(1 - x' \right) \left(|F_V|^2 - x' \,|F_M|^2 \right) + 4x' \mathrm{Re}\left(F_V^* F_M \right) \\
& - \frac{m^2}{4M^2} \left[|F_V + F_M|^2 + |F_A + 2F_P|^2 - 4\left(1 + x' \right) \left(|F_S|^2 + |F_P|^2 \right) \right], \\
B =& \ \mp 4x' \mathrm{Re}\left[F_A^* \left(F_V + F_M \right) \right] - \frac{m^2}{M^2} \mathrm{Re}\left[F_S^* \left(F_V - x' F_M \right) - F_T^* \left(F_A - 2x' F_P \right) \right], \\
C =& \ \frac{1}{4} \left(|F_V|^2 + x' \,|F_M|^2 + |F_A|^2 \right) + x' \,|F_T|^2.
\end{aligned}
$$

This fits Eq. (3.22) of Ref. [6] except for the sign of the term $\propto m^2/M^2$ in the coefficient B. This difference disappears in the absence of the second-class currents ($F_S = F_T = 0$). The above formulas essentially disagree with the recent result of Paschos and Yu [222]. Namely the function A derived from Eq. (2.35) of Ref. [222] (obtained under standard assumption that form factors are real and $F_S = F_T = 0$) has the extra term

$$
\frac{m^2}{M^2} \left[\left(\frac{m^2 + q^2}{M^2} \right) F_V F_M + \left(\frac{m^2 - q^2}{2M^2} \right) F_A F_P \right]
$$

which is difficult to explain by a misprint.

[4] The inverse transformation is: $\omega_4 = \frac{1}{4} \left(\omega'_4 + \omega'_2 + 2\omega'_5 \right)$ and $\omega_5 = \omega'_5 + \omega'_2$.

Assuming all the form factors to be real we have $\omega_6 = 0$ and thus $\mathcal{P}_T = 0$.

$$
\begin{aligned}
\omega_1 &= F_A^2 + x'\left[F_A^2 + (F_V + F_M)^2\right],\\
\omega_2 &= F_A^2 + F_V^2 + x'\left(F_M^2 + 4F_T^2\right),\\
\omega_3 &= -\,2F_A\left(F_V + F_M\right),\\
\omega_4 &= -\,\frac{1}{4}\left[2F_V + (1-x')\,F_M\right]F_M - \left(F_A - x'F_P\right)F_P\\
&\quad + \left[F_V - x'F_M + (1+x')\,F_S\right]F_S - \left[F_A - x'\left(2F_P + F_T\right)\right]F_T,\\
\omega_5 &= F_A^2 + F_V^2 + x'F_M^2 + 2\left(F_V - x'F_M\right)F_S - 2\left[F_A - 2x'\left(F_P + F_T\right)\right]F_T.
\end{aligned}
$$

If we drop the form factors F_S and F_T assuming time reversal invariance and isospin symmetry (no 2nd class currents) then

$$\omega_2 = \omega_5 = F_A^2 + F_V^2 + x'F_M^2.$$

In our numerical analysis, we will investigate two models for the nucleon electromagnetic form factors, the standard dipole model and the extended model by Gari and Krüempelmann [331] updated by Lomon [341].

6.3.2 Generalization: $M_f \neq M_i$.

In this section, we consider the quasielastic νN and $\overline{\nu} N$ scattering with production of a polarized lepton and unpolarized baryon taking care for the final lepton mass and second class current (SCC) contributions. As a particular case, this of course includes the “standard” $\Delta Y = 0$ reactions $\nu_\ell n \to \ell^- p$ and $\overline{\nu}_\ell p \to \ell^+ n$ of our special interest. Let us recall here that very complete investigations of the polarization effects in the QE reactions have been performed in pioneer works of Adler [39] and Pais [5]. However a detailed comparison shows several disagreements between the formulas derived in Refs. [39] and [5] which makes it difficult to apply these results to our study. We therefore rederived the QE structure functions starting from the most general form of the weak transition current

$$J_\alpha = \langle B; p'|\widehat{J}_\alpha|N; p\rangle = \overline{u}_B\left(p'\right)\Gamma_\alpha\, u_N(p) \tag{6.17}$$

with the vertex function

$$\Gamma_\alpha = \gamma_\alpha F_V + i\sigma_{\alpha\beta}\frac{q^\beta}{2M}F_M + \frac{q_\alpha}{M}F_S + \left(\gamma_\alpha F_A + \frac{p_\alpha + p'_\alpha}{M}F_T + \frac{q_\alpha}{M}F_P\right)\gamma_5 \tag{6.18}$$

defined through the 6, in general complex, form factors $F_i = F_i\left(q^2\right)$, $i = V, M, A, P, T, S$. Here p and p' are the 4-momenta of the target nucleon N (with the mass M_N) and final baryon B (with the mass M_B), $q = k' - k = p - p'$, k and k' are the 4-momenta of (anti)neutrino and lepton, and $M = \left(M_N + M_B\right)/2$. The hadronic tensor may be written as

$$W_{\alpha\beta} = C_B \sum_{\text{spin}} J_\alpha J_\beta^*\, \delta\left(W^2 - M_B^2\right), \tag{6.19}$$

where C_B is the constant factor defined by the specific reaction,[5] $W^2 = p'^2 = (p+q)^2$, and the sum is over the nucleon and baryon spins.

From Eqs. (6.17), (6.18), and (6.19) we find the QE structure functions involved into the generic equation for the hadronic tensor (6.12):

$$W_i = 4C_B M_N M_B \omega_i\left(q^2\right)\delta\left(W^2 - M_B^2\right), \tag{6.20}$$

where the functions $\omega_{1,\ldots,6}$ are given by

$$\omega_i\left(q^2\right) = \omega_i^0\left(q^2\right) + r\,\omega_i^1\left(q^2\right) + r^2\omega_i^2\left(q^2\right); \tag{6.21}$$

the coefficient functions $\omega_i^k\left(q^2\right)$ are the following bilinear combinations of the electroweak form factors:

[5] In fact this factor may be absorbed into the definition of the form factors. For the $\Delta Y = 0$ reactions and with the standard definition of the form factors (see, e.g., Ref. [6]), $C_B = \cos^2\theta_C/4$ where θ_C is the Cabibbo mixing angle.

$$
\begin{aligned}
\omega_1^0 &= (1+x')\left|F_A\right|^2 + x'\left|F_V+F_M\right|^2, \\
\omega_1^1 &= 0, \\
\omega_1^2 &= \left|F_V+F_M\right|^2, \\
\omega_2^0 &= \left|F_A\right|^2 + \left|F_V\right|^2 + x'\left|F_M\right|^2 + 4x'\left|F_T\right|^2, \\
\omega_2^1 &= 4\,\mathrm{Re}\left(F_A^*F_T\right), \\
\omega_2^2 &= 4\left|F_T\right|^2, \\
\omega_3^0 &= -2\,\mathrm{Re}\left[F_A^*\left(F_V+F_M\right)\right], \\
\omega_3^1 &= \omega_3^2 = 0, \\
\omega_4^0 &= (1+x')\left|\tfrac{1}{2}F_M - F_S\right|^2 + x'\left|F_P+F_T\right|^2 \\
&\quad - \mathrm{Re}\left[\left(F_V^*+F_M^*\right)\left(\tfrac{1}{2}F_M - F_S\right) + F_A^*\left(F_P+F_T\right)\right], \\
\omega_4^1 &= \mathrm{Re}\left[\left(F_V^*+F_M^*\right)\left(\tfrac{1}{2}F_M - F_S\right) + F_A^*\left(F_P+F_T\right)\right], \\
\omega_4^2 &= \left|F_P+F_T\right|^2, \\
\omega_5^0 &= \omega_2^0 + 2\,\mathrm{Re}\left[F_S^*\left(F_V - x'F_M\right) - F_T^*\left(F_A - 2x'F_P\right)\right], \\
\omega_5^1 &= \omega_2^1 + \mathrm{Re}\left[F_M^*\left(F_V+F_M\right) + 2F_A^*F_P\right], \\
\omega_5^2 &= \omega_2^2 + 4\,\mathrm{Re}\left(F_P^*F_T\right), \\
\omega_6^0 &= 2\,\mathrm{Im}\left[F_S^*\left(F_V - x'F_M\right) + F_T^*\left(F_A - 2x'F_P\right)\right], \\
\omega_6^1 &= -\,\mathrm{Im}\left(F_M^*F_V + 2F_A^*F_P\right), \\
\omega_6^2 &= 4\,\mathrm{Im}\left(F_P^*F_T\right);
\end{aligned}
$$

and

$$
r = \frac{M_B - M_N}{M_B + M_N} = \frac{M_B - M_N}{2M}, \quad x' = \frac{-q^2}{4M^2}.
$$

Let us note that the traditional parametrization of the hadronic current (6.18) is not symmetric relative to transformation $F_M \leftrightarrow \gamma_5 F_T$. The more symmetric choice, $\frac{i}{2}\sigma_{\alpha\beta}q^\beta F_T'$ instead of $(p+p')_\alpha F_T$, would result in the following redefinition of the axial and tensor form factors:

$$
F_A \mapsto F_A + rF_T' \quad \text{and} \quad F_T \mapsto -2F_T'.
$$

It is easy to see that after this redefinition, the functions ω_i^k remain quadratic polynomials of r.

NOTE XXXI:

In absence of the second class currents the above formulas are a bit more compact but less insightful since some obvious symmetries of the general formulas become covert:

$$
\begin{aligned}
&\omega_1^0 = \left(1+x'\right)F_A^2 + x'\left(F_V+F_M\right)^2, \quad \omega_1^1 = 0, \quad \omega_1^2 = \left(F_V+F_M\right)^2, \\
&\omega_2^0 = F_A^2 + F_V^2 + x'F_M^2, \quad \omega_2^1 = \omega_2^2 = 0, \\
&\omega_3^0 = -2F_A\left(F_V+F_M\right), \quad \omega_3^1 = \omega_3^2 = 0, \\
&\omega_4^0 = -\tfrac{1}{2}F_M\left[F_V + \left(1-x'\right)F_M\right] - F_P\left(F_A - x'F_P\right), \\
&\omega_4^1 = \tfrac{1}{2}F_M\left(F_V+F_M\right) + F_AF_P, \quad \omega_4^2 = F_P^2, \\
&\omega_5^0 = F_A^2 + F_V^2 + x'F_M^2, \quad \omega_5^1 = F_M\left(F_V+F_M\right) + 2F_AF_P, \quad \omega_5^2 = 0, \\
&\omega_6^0 = \omega_6^1 = \omega_6^2 = 0.
\end{aligned}
$$

NOTE XXXII:

Some LS puzzles. Let us start with the expression $i\gamma_5\sigma_{\alpha\beta}q^\beta F_T/M$ in Eq. (3.13) of Ref. [6]. Considering that $\sigma_{\alpha\beta} = (i/2)\left(\gamma_\alpha\gamma_\beta - \gamma_\beta\gamma_\alpha\right)$ and $q = p_2 - p_1$ (and not $p_1 - p_2$ as is written in [6]) we have

$$
i\gamma_5\sigma_{\alpha\beta}q^\beta F_T/M = -\gamma_5\left[\left(M_2 - M_1\right)\gamma_\alpha + \left(p_2+p_1\right)_\alpha\right]F_T/M.
$$

By comparing this expression against the two contributions in Eq. (3.13) of Ref. [6]

$$
\left[-\gamma_5\gamma_\alpha\left(M_2 - M_1\right) + i\gamma_5\sigma_{\alpha\beta}q^\beta\right]F_T/M
$$

one can conclude that there are at least two misprints in that equation:

1. in the sign of the term proportional to (p_2+p_1) in the first part of Eq. (3.13) (or in the sign of the term proportional to $\sigma_{\alpha\beta}$ in its second part) and
2. in the sign of the term proportional to $\gamma_5\gamma_\alpha$ in the second part of Eq. (3.13).

Conclusion: we must start with the first definition of the vertex (the first part of Eq. (3.13)) and neglect its second form. The only significance of this second form of the vertex function is in demonstration that F_T is actually the *tensor* contribution considering that the corresponding $\gamma_5\gamma_\alpha$ term only leads to a *redefinition* of the axial form factor.

NOTE XXXIII:

Our (Llewellyn Smith's to be exact) parametrization of the vertex Γ_α is not the best one since (a) it is not symmetric relative to axial and tensor contributions and (b) our formula for the cross section becomes very cumbersome. The most concise and elegant *approximate* formula is given in Ref. [16]. It is based upon the following parametrization of the vertex:

$$\Gamma_\alpha=\gamma_\alpha g_V+i\sigma_{\alpha\beta}\frac{q_\beta}{2M}g_M+\frac{q_\alpha}{2M}g_S+\left(\gamma_\alpha g_A+i\sigma_{\alpha\beta}\frac{q_\beta}{2M}g_T+\frac{q_\alpha}{2M}g_P\right)\gamma_5. \tag{6.22}$$

Therefore

$$g_V=F_V,\quad g_M=F_M,\quad g_A=F_A+2rF_T,\quad g_T=-2F_T,\quad g_P=2F_P,\quad g_S=2F_S.$$

or

$$F_V=g_V,\quad F_M=g_M,\quad F_A=g_A+rg_T,\quad F_T=-\frac{1}{2}g_T,\quad F_P=\frac{1}{2}g_P,\quad F_S=\frac{1}{2}g_S.$$

Neglecting the $\mathcal{O}\left(m^2\right)$ contributions, the cross section written in terms of the form factors g_i is given by [16, Eq. (4.3)]

$$\frac{d\sigma}{d\left|q^2\right|}=\frac{G_F^2C^2\left|q^2\right|}{\pi E_\nu^2}\left[w_1-\frac{1}{2}\left(\frac{4E_\nu E_\ell}{q^2}+1\right)w_2\pm\left(\frac{E_\nu+E_\ell}{M_N}\right)w_3\right],$$

where

$$\begin{aligned}
w_1&=\frac{M^2}{M_N^2}\left[\left(x'+r\right)\left|g_V+g_M\right|^2+\left(x'+1\right)\left|g_A+rg_T\right|^2\right],\\
w_2&=\left|g_V\right|^2+\left|g_A\right|^2+r\left(\left|g_M\right|^2+\left|g_T\right|^2\right),\\
w_3&=\mathrm{Re}\left[\left(g_V^*+g_M^*\right)\left(g_A+rg_T\right)\right].
\end{aligned}$$

It would be worthy to compare *numerically* our "ABC" cross section against with short form. However the factor M_N in this formula seems very suspicious.

One could also rewrite our main result (formulas for ω_i) through the form factors g_i. In new terms, some of ω_i^k become slightly more symmetric and simple but other become bit more complicated instead. So I am not sure this is really a good idea.

Differential cross section.

NOTE XXXIV:

The simplest way to calculate the $d\sigma/Q^2$ is to start with the general formula for $d^2\sigma/dQ^2dW^2$,

$$\frac{d^2\sigma}{dQ^2dW^2}=\frac{G_F^2\kappa^2\mathcal{R}}{4\pi M_NE_\nu}, \tag{6.23}$$

which is obtained from Eq. (6.6) by taking into account that

$$dQ^2dW^2=\frac{\partial\left(Q^2,W^2\right)}{\partial\left(E_\ell,\cos\theta\right)}dE_\ell d\cos\theta=4M_iE_\nu P_\ell\,dE_\ell d\cos\theta.$$

Similarly, the double differential cross section for a polarized (with helicity λ) lepton production can be written as

$$\frac{d^2\sigma_\lambda}{dQ^2dW^2}=\frac{G_F^2\kappa^2L_{\lambda\lambda}^{\alpha\beta}W_{\alpha\beta}}{16\pi M_N^2E_\nu^2}=\rho_{\lambda\lambda}\frac{d^2\sigma}{dQ^2dW^2}. \tag{6.24}$$

By using the above formulas, one can rewrite the general equation for the differential cross section in terms of the form factors:

$$\frac{d\sigma}{dQ^2}=\frac{2G_F^2C_BM^2\kappa^2}{\pi E_\nu^2}\left[A\left(q^2\right)+\left(\frac{s-u}{4M^2}\right)B\left(q^2\right)+\left(\frac{s-u}{4M^2}\right)^2C\left(q^2\right)\right]. \tag{6.25}$$

Here $s=(k+p)^2$, $u=(k'-p)^2$,

$$
\begin{aligned}
A\left(q^2\right) &= \left(x'+\varkappa^2\right)a_0\left(q^2\right)-4ra_1\left(q^2\right)-r^2a_2\left(q^2\right)-4r^3a_3\left(q^2\right)-4r^4a_4\left(q^2\right),\\
B\left(q^2\right) &= 4b_0\left(q^2\right)-2rb_1\left(q^2\right)-8r^2b_2\left(q^2\right),\\
C\left(q^2\right) &= c_0\left(q^2\right)+rc_1\left(q^2\right)+r^2c_2\left(q^2\right),
\end{aligned}
$$

$$
\begin{aligned}
a_0 =\; & (1+x')\left(|F_A|^2-4x'|F_T|^2\right)-(1-x')\left(|F_V|^2-x'|F_M|^2\right)+4x'\mathrm{Re}\left(F_V^*F_M\right)\\
& -\varkappa^2\left[|F_V+F_M|^2+|F_A|^2+4\mathrm{Re}\left(F_A^*F_P\right)-4x'|F_P|^2-4(1+x')|F_S|^2\right],\\
a_1 =\; & (1+x')x'\mathrm{Re}\left(F_T^*F_A\right)+\varkappa^2\mathrm{Re}\left[\mp F_A^*\left(F_V+F_M\right)+x'F_T^*\left(F_A+2F_P\right)+(1+x')F_S^*F_V\right]\\
& +\varkappa^4\mathrm{Re}\left[F_S^*\left(F_V+F_M\right)\right],\\
a_2 =\; & (1-x')\left(|F_V|^2-x'|F_M|^2\right)-4x'\mathrm{Re}\left(F_V^*F_M\right)+(1+x')\left(|F_A|^2+8x'|F_T|^2\right)\\
& -\varkappa^2\left[|F_V+F_M|^2-(1+x')\left(|F_M|^2-4|F_P|^2\right)-|F_A+2F_P|^2-4(1+2x')|F_T|^2\right]-4\varkappa^4|F_P|^2,\\
a_3 =\; & (1+x')\mathrm{Re}\left(F_T^*F_A\right)+\varkappa^2\mathrm{Re}\left[F_T^*\left(F_A+2F_P\right)\right],\\
a_4 =\; & (1+x')|F_T|^2+\varkappa^2|F_T|^2,\\
b_0 =\; & \mp x'\mathrm{Re}\left[F_A^*\left(F_V+F_M\right)\right]+\varkappa^2\mathrm{Re}\left[F_T^*\left(F_A-2x'F_P\right)-F_S^*\left(F_V-x'F_M\right)\right],\\
b_1 =\; & \varkappa^2\left[|F_M|^2+\mathrm{Re}\left(F_V^*F_M+2F_A^*F_P\right)\right],\\
b_2 =\; & \varkappa^2\mathrm{Re}\left(F_T^*F_P\right),\\
c_0 =\; & |F_V|^2+x'|F_M|^2+|F_A|^2+4x'|F_T|^2,\\
c_1 =\; & 4\mathrm{Re}\left(F_T^*F_A\right),\\
c_2 =\; & 4|F_T|^2,
\end{aligned}
$$

and $\varkappa=m/(2M)$. As usually, the upper signs in coefficients a_1 and b_0 are to be taken for ν-induced reactions, the lower signs for $\overline{\nu}$-induced reactions. In the $M_N=M_B$ limit, these formulas fit those from Ref. [6] except for the sign of the term $\propto\varkappa^2$ in the coefficient b_0. This difference disappears in the absence of SCC ($F_S=F_T=0$ and the rest form factors are real). In the latter case, the coefficients a_i, b_i, and c_i become

$$
\begin{aligned}
a_0 =\; & \left(1+x'\right)F_A^2-\left(F_V-x'F_M\right)^2+x'\left(F_V+F_M\right)^2\\
& -\varkappa^2\left[\left(F_V+F_M\right)^2+\left(F_A+2F_P\right)^2-4\left(1+x'\right)F_P^2\right],\\
a_1 =\; & \mp\varkappa^2F_A\left(F_V+F_M\right),\\
a_2 =\; & \left(1+x'\right)F_A^2+\left(F_V-x'F_M\right)^2-x'\left(F_V+F_M\right)^2\\
& -\varkappa^2\left[\left(F_V+F_M\right)^2-\left(F_A+2F_P\right)^2-\left(1+x'\right)\left(F_M^2-4F_P^2\right)\right]-4\varkappa^4F_P^2,\\
a_3 =\; & a_4=0,\\
b_0 =\; & \mp x'F_A\left(F_V+F_M\right),\\
b_1 =\; & \varkappa^2\left(F_M^2+F_VF_M+2F_AF_P\right),\\
b_2 =\; & 0,\\
c_0 =\; & F_V^2+x'F_M^2+F_A^2,\\
c_1 =\; & c_2=0.
\end{aligned}
$$

This result exactly coincides with that of Strumia and Vissani [41] deduced recently for the inverse β decay.

Another form for the coefficients seems to be more compact and transparent (indices "1" and "2" here denote the FCC and SCC contribution, respectively): [6]

$$
A=A_1+4A_2,\quad B=B_1+4B_2,\quad C=C_1+4C_2,
$$

[6] I think just this form (maybe with some modifications) has to be used in the PRD paper.

where indices "1" and "2" mark the FCC and SCC contribution, respectively, and

$$\begin{aligned}
A_1 = &\; 2\left[\left(x'+r^2\right)\left(2x'+\varkappa^2\right)-\varkappa^4\right]\mathrm{Re}\left(F_V^*F_M\right)\\
&\mp 4r\varkappa^2\mathrm{Re}\left[F_A^*\left(F_V+F_M\right)\right]-4\varkappa^2\left(x'+r^2+\varkappa^2\right)\mathrm{Re}\left(F_A^*F_P\right)\\
&+\left[\left(x'+\varkappa^2\right)\left(x'-1+r^2-\varkappa^2\right)+r^2\right]|F_V|^2\\
&+\left[\left(x'+\varkappa^2\right)\left(x'+1-r^2-\varkappa^2\right)+r^2\right]|F_A|^2\\
&-\left[x'\left(x'+r^2\right)\left(x'-1+\varkappa^2\right)+\varkappa^4\right]|F_M|^2\\
&+4\varkappa^2\left(x'+\varkappa^2\right)\left(x'+r^2\right)\left|F_P^2\right|,\\
B_1 = &\; \mp 4x'\mathrm{Re}\left[F_A^*\left(F_V+F_M\right)\right]-2r\varkappa^2\left[|F_M|^2+\mathrm{Re}\left(F_V^*F_M+2F_A^*F_P\right)\right],\\
C_1 = &\; |F_V|^2+|F_A|^2+x'|F_M|^2;\\
A_2 = &\; -r\left(x'+r^2\right)\left[\left(x'+1+\varkappa^2\right)\mathrm{Re}\left(F_T^*F_A\right)+2\varkappa^2\mathrm{Re}\left(F_T^*F_P\right)\right]\\
&-r\varkappa^2\left[\left(x'+1+\varkappa^2\right)\mathrm{Re}\left(F_S^*F_V\right)+\varkappa^2\mathrm{Re}\left(F_S^*F_M\right)\right]\\
&-\left(x'+r^2\right)\left[\left(x'+\varkappa^2\right)\left(x'+1+r^2\right)+r^2\right]|F_T|^2\\
&+\varkappa^2\left(x'+1\right)\left(x'+\varkappa^2\right)|F_S|^2,\\
B_2 = &\; \varkappa^2\mathrm{Re}\left\{F_T^*\left[F_A-2\left(x'+r^2\right)F_P\right]-F_S^*\left(F_V-x'F_M\right)\right\},\\
C_2 = &\; r\mathrm{Re}\left(F_T^*F_A\right)+\left(x'+r^2\right)|F_T|^2.
\end{aligned}$$

6.3.3 Inverse β decay at low energies.

This case needs for a special study since it is very important for many applications, – from reactor neutrino physics to astrophysics and cosmology.

ATTENTION! Sorry for inconvenience but in this section (and only here) I'll use the following definition

$$\mathfrak{r}=\frac{m_n-m_p}{m_n+m_p}=\frac{m_n-m_p}{2M}=-r.$$

The LaTeX definitions are: `\rat` for r, `\rn` for $\mathfrak{r}$, `\rl` for $\varkappa$.

So we consider the cross section for electron production at very low neutrino energies, say $E_\nu \lesssim 1$ MeV. Therefore $E_\nu/M \lesssim \mathfrak{r}$ and $\mathfrak{r}\left(E_\nu/M\right) \lesssim \mathfrak{r}^2 \sim \varkappa^2$. The numerical values of the constants involved are:

$$\mathfrak{r} \simeq 6.8873378\times10^{-4},\quad \mathfrak{r}^2 \simeq 4.7435422\times10^{-7},\quad \varkappa^2 \simeq 7.4049818\times10^{-8}.$$

Next, variable x' varies in a wide range, as is shown in Fig. (6.1), and $x' \to -\varkappa^2$ as $E_\nu \to 0$. Hence this variable also cannot be neglected. After rewriting the kinematic factor

$$s-u=2m_n\left(E_\nu+E_e\right)-m_e^2=m_n^2-m_p^2+m_e^2+4m_nE_\nu+q^2$$

in terms of the dimensionless variables and constants we have

$$\frac{s-u}{4M^2}=\mathfrak{r}+\left(1+\mathfrak{r}\right)\frac{E_\nu}{M}-\varkappa^2-x'. \tag{6.26}$$

It is clear that all terms are essential here.

Let us forget about SCC for the moment. Then all the rest contributions into the cross section which are of the order of $\mathfrak{r}$, $\mathfrak{r}^2$ or $\varkappa^2$ (see the end of previous subsection) play the role and cannot be neglected.

Therefore, the drastic change of the behavior of σ as a function of energy at $E_\nu \ll 1$ MeV is a result of cancellation of big (order of 1 and of $\mathfrak{r}$) contributions due to "fine tuning" of the fundamental parameters involved in the exact formula for $d\sigma/dQ^2$. To demonstrate this, we perform several steps.

Variables z and z_*.

To simplify calculations, let use variable E_ν^* (the center-of-mass neutrino energy) instead of E_ν. The two variables are related to each other by

$$E_\nu^*=\frac{E_\nu}{\sqrt{1+\dfrac{2E_\nu}{m_n}}}\quad\text{and}\quad E_\nu=E_\nu^*\left[\sqrt{1+\left(\frac{E_\nu^*}{m_n}\right)^2}+\left(\frac{E_\nu^*}{m_n}\right)\right]. \tag{6.27}$$

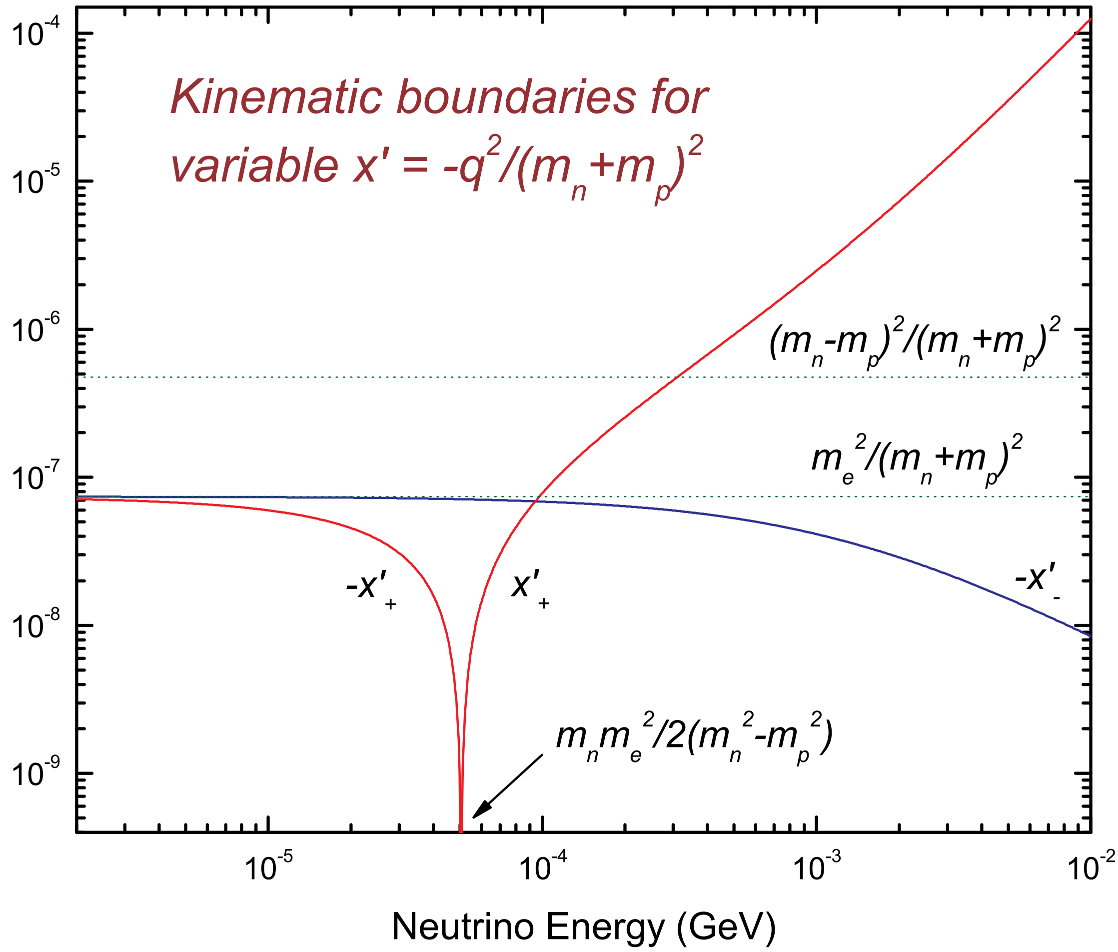

Figure 6.1: The kinematic boundaries $x'_{\mp} = Q^2_{\mp}/(4M^2)$ for variable x' in reaction $\nu n \to e^- p$ at low energies. For comparison, the values of $\mathfrak{r}^2$ and $\varkappa^2$ are also shown by dashed lines. Note that $x'_- < 0$ at all energies (and $|x'_-| < m_e^2/\left(m_n^2 - m_p^2\right)$) while x'_+ changes its sign at $E_\nu = m_n m_e^2/2\left(m_n^2 - m_p^2\right) \simeq 5.0509097 \times 10^{-5}$ GeV.

For simplification of formulas (especially in the calculations with FORTRAN and FORM), one can define the dimensionless variables

$$z = \frac{E_\nu}{m_n} = \frac{E_\nu}{(1+\mathfrak{r})M} \quad \text{and} \quad z_* = \frac{E_\nu^*}{m_n} = \frac{E_\nu^*}{(1+\mathfrak{r})M}, \tag{6.28}$$

and rewrite Eqs. (6.27) as

$$z_* = \frac{z}{\sqrt{1+2z}} = \begin{cases} z\left[1 - z + \dfrac{3z^2}{2} - \dfrac{5z^3}{2} + \mathcal{O}\left(z^4\right)\right] & \text{at} \quad z \ll 1, \\ \sqrt{\dfrac{z}{2}}\left[1 - \dfrac{1}{4z} + \dfrac{3}{32z^2} - \dfrac{5}{128z^3} + \mathcal{O}\left(\dfrac{1}{z^4}\right)\right] & \text{at} \quad z \gg 1, \end{cases} \tag{6.29a}$$

and

$$z = z_*\left(\sqrt{1+z_*^2} + z_*\right) = \begin{cases} z_*\left[1 + z_* + \dfrac{z_*^2}{2} - \dfrac{z_*^4}{8} + \mathcal{O}\left(z_*^6\right)\right] & \text{at} \quad z_* \ll 1, \\ 2z_*^2\left[1 + \dfrac{1}{4z_*^2} - \dfrac{1}{16z_*^4} + \mathcal{O}\left(\dfrac{1}{z_*^6}\right)\right] & \text{at} \quad z_* \gg 1. \end{cases} \tag{6.29b}$$

However, the energies E_ν and E_ν^* seem to be more descriptive and sometimes I'll use these together with (or instead of) the z and z_*.

The following formulas will be of utility for calculations at the low-energy range:

$$
\begin{aligned}
\sqrt{s} &= m_n\left[\sqrt{1+z_*^2}+z_*\right] = m_n\left[1+z_*+\frac{z_*^2}{2}-\frac{z_*^4}{8}+\mathcal{O}\left(z_*^6\right)\right], \\
\frac{E_e^*}{M} &= \frac{2\left(\mathfrak{r}+\varkappa^2\right)}{1+\mathfrak{r}}\sqrt{1+z_*^2}+\left(\frac{1+\mathfrak{r}^2-2\varkappa^2}{1+\mathfrak{r}}\right)z_* \\
&= \epsilon_*\left[1+\frac{\left(1+\mathfrak{r}^2-2\varkappa^2\right)}{2\left(\mathfrak{r}+\varkappa^2\right)}z_*+\frac{z_*^2}{2}-\frac{z_*^4}{8}+\mathcal{O}\left(z_*^6\right)\right], \\
\frac{P_e^*}{M} &= \sqrt{\left(\frac{E_e^*}{M}\right)^2-4\varkappa^2} \\
&= \pi_*\left\{1-\frac{\left(1+\mathfrak{r}^2-2\varkappa^2\right)\left(\mathfrak{r}+\varkappa^2\right)}{2\left(1-\varkappa^2\right)\left(\mathfrak{r}^2-\varkappa^2\right)}z_* - \left[1-\frac{\varkappa^2\left(1-\mathfrak{r}^2\right)^2}{4\left(1-\varkappa^2\right)^2\left(\mathfrak{r}^2-\varkappa^2\right)^2}\right]\frac{z_*^2}{2}+\mathcal{O}\left(z_*^3\right)\right\},
\end{aligned}
$$

where

$$
\epsilon_* = \frac{2\left(\mathfrak{r}+\varkappa^2\right)}{1+\mathfrak{r}} \simeq 1.3766675\times 10^{-3}
$$

and

$$
\pi_* = \frac{2\sqrt{\left(1-\varkappa^2\right)\left(\mathfrak{r}^2-\varkappa^2\right)}}{1+\mathfrak{r}} \simeq 1.2645213\times 10^{-3}
$$

are, respectively, the minimum energy and momentum of the electron in units of M.

Basic integrals.

Let us denote

$$
\int_{x'_-}^{x'_+}\left(-x'\right)^n dx' = \left(x'_+-x'_-\right)I_n,
$$

where

$$
x'_\pm = \frac{Q_\pm^2}{4M^2} = \frac{E_\nu^*\left(E_e^*\pm P_e^*\right)}{2M^2}-\varkappa^2 = (1+\mathfrak{r})\left(\frac{E_e^*\pm P_e^*}{2M}\right)z_*-\varkappa^2.
$$

Clearly

$$
(n+1)I_n = x_-^n + x_-^{n-1}x_+ + \cdots + x_-x_+^{n-1} + x_+^n.
$$

All integrals necessary for calculation of the cross section can be derived from the 4 basic integrals $I_0,\ldots,I_3$:

$$
\begin{aligned}
\int_{x'_-}^{x'_+}\left(-x'\right)^n\left(x'+\varkappa^2\right)dx' &= \left(x'_+-x'_-\right)\left(\varkappa^2 I_n - I_{n+1}\right), \\
\int_{x'_-}^{x'_+}\left(-x'\right)^n\left(\frac{s-u}{4M^2}\right)dx' &= \left(x'_+-x'_-\right)\left(vI_n+I_{n+1}\right), \\
\int_{x'_-}^{x'_+}\left(-x'\right)^n\left(\frac{s-u}{4M^2}\right)^2 dx' &= \left(x'_+-x'_-\right)\left(v^2I_n+2vI_{n+1}+I_{n+2}\right),
\end{aligned}
$$

where $n=0$ or 1 and

$$
v = \frac{s-u}{4M^2}+x' = \mathfrak{r}+(1+\mathfrak{r})\left(\frac{E_\nu}{M}\right)-\varkappa^2.
$$

By using the identities

$$
\begin{aligned}
x'_+ - x'_- &= \frac{P_e^* E_\nu^*}{M^2} = (1+\mathfrak{r}) \left(\frac{P_e^*}{M}\right) z_*, \\
x'_+ + x'_- &= \frac{E_e^* E_\nu^*}{M^2} - 2\varkappa^2 = -2\varkappa^2 + (1+\mathfrak{r}) \left(\frac{E_e^*}{M}\right) z_*, \\
{x'_+}^2 + {x'_-}^2 &= 2\varkappa^4 - 2\varkappa^2 \frac{E_e^* E_\nu^*}{M^2} + \frac{\left(E_e^* E_\nu^*\right)^2}{M^4}, \\
&= 2\varkappa^4 - 2\varkappa^2 (1+\mathfrak{r}) \left(\frac{E_e^*}{M}\right) z_* + (1+\mathfrak{r})^2 \left[\left(\frac{E_e^*}{M}\right)^2 - 2\varkappa^2\right] z_*^2, \\
x'_+ x'_- &= \varkappa^4 - \varkappa^2 \frac{E_\nu^* \left(E_e^* - E_\nu^*\right)}{M^2} = \varkappa^4 - \varkappa^2 (1+\mathfrak{r}) \left(\frac{E_e^*}{M}\right) z_* + \varkappa^2 (1+\mathfrak{r})^2 z_*^2, \\
{x'_+}^2 + x'_+ x_- + {x'_-}^2 &= 3\varkappa^4 - \varkappa^2 \frac{E_\nu^* \left(3E_e^* + E_\nu^*\right)}{M^2} + \frac{\left(E_e^* E_\nu^*\right)^2}{M^4} \\
&= 3\varkappa^4 - 3\varkappa^2 (1+\mathfrak{r}) \left(\frac{E_e^*}{M}\right) z_* + (1+\mathfrak{r})^2 \left[\left(\frac{E_e^*}{M}\right)^2 - \varkappa^2\right] z_*^2,
\end{aligned}
$$

and Eq. (6.26) we have

$$
\begin{aligned}
I_0 &= 1, \\
I_1 &= \varkappa^2 - \frac{E_e^* E_\nu^*}{2M^2}, \\
I_2 &= \varkappa^4 - \varkappa^2 \left[\frac{E_e^* E_\nu^*}{M^2} + \frac{\left(E_\nu^*\right)^2}{3M^2}\right] + \frac{\left(E_e^* E_\nu^*\right)^2}{3M^4}, \\
I_3 &= \varkappa^6 - \varkappa^4 \left[\frac{3E_e^* E_\nu^*}{2M^2} + \frac{\left(E_\nu^*\right)^2}{M^2}\right] + \varkappa^2 \left[\frac{\left(E_e^* E_\nu^*\right)^2}{M^4} + \frac{E_e^* \left(E_\nu^*\right)^3}{2M^4}\right] - \frac{\left(E_e^* E_\nu^*\right)^3}{4M^6}.
\end{aligned}
$$

Constant form factor approximation.

Let us now neglect the Q^2 dependence of the form factors. This is the standard assumption at low energies and usually it is also assumed that

$$F_i = F_i(0). \tag{6.30}$$

The latter approximation is appropriate since $Q^2 \sim -m_e^2$ (see fig. (6.1)) and thus the corresponding corrections are of the order of $\varkappa^2$. We however do not use Eq. (6.30) but simply assume that F_i are Q^2 independent. Then the total cross section can be written as

$$\sigma\left(E_\nu\right) = \int_{Q_-^2}^{Q_+^2} \left[\frac{d\sigma}{dQ^2}\right] dQ^2 = \left(G_F \cos\theta_C M\right)^2 \frac{2}{\pi} \left(\frac{P_e^*}{M}\right) \left(\frac{E_\nu^*}{E_\nu}\right) \left(\frac{M}{E_\nu}\right) \left[\mathfrak{A} + \mathfrak{B} + \mathfrak{C}\right], \tag{6.31}$$

where

$$
\begin{aligned}
\mathfrak{A} &= A_0 + A_1 I_1 + A_2 I_2 + A_3 I_3, \\
\mathfrak{B} &= B_0 + B_1 I_1 + B_2 I_2, \\
\mathfrak{C} &= C_0 + C_1 I_1 + C_2 I_2 + C_3 I_3.
\end{aligned}
$$

and we neglected the factor κ^2. There is no sense in writing out all the coefficients since it can be done directly in FORM or Maple.

The most important fact is that[7]

$$A_0 + B_0 + C_0 = 0.$$

Therefore

$$\sigma\left(E_\nu\right) = \frac{G_F^2 \cos^2\theta_C M^2}{2\pi} \left(\frac{P_e^*}{M}\right) \left(\frac{E_\nu^*}{E_\nu}\right) \left[c_\pm + f_\pm\left(\frac{E_\nu}{M}\right)\right], \tag{6.32}$$

where $c_\pm$ are some constants and $f_\pm(z)$ are the functions proportional to z (thus $f_\pm(0) = 0$).

TO BE CONTINUED

[7]This is a consequence of the following, more general result: for any complex form factors $F_i\left(Q^2\right)$ which are finite at small Q^2

$$\lim_{E_\nu \to 0} \left[E_\nu \sigma\left(E_\nu\right)\right] = 0 \quad \text{while} \quad \lim_{E_\nu \to 0} \left[\sigma\left(E_\nu\right)\right] = \sigma_0 \neq 0.$$

VBRT approximation.

According to Ref. [44] with the reference to Vogel [45],[8] the absorption cross section at $E_\nu \lesssim 10$ MeV is given by the following approximate expression:

$$\sigma_{\text{VBRT}}(E_\nu) = \sigma_e \left(\frac{1+3g_A^2}{4}\right)\left(\frac{E_\nu \pm \Delta}{m_e}\right)^2 \sqrt{1-\left(\frac{m_e}{E_\nu \pm \Delta}\right)^2}\left(1+\frac{a_\pm E_\nu}{m_n}\right), \tag{6.33}$$

where

$$\sigma_e = \frac{4G_F^2 \cos^2\theta_C m_e^2}{\pi} \simeq 1.674 \times 10^{-44}\ \text{cm}^2$$

is a reference neutrino cross section,

$$\Delta = m_n - m_p \simeq 1.293332\text{MeV}/c^2,$$

and $a_\pm$ are the constants which account for the correction for weak magnetism and recoil,

$$a_+ \simeq 1.1, \quad a_- \simeq -7.1.$$

In order to simplify our cumbersome result to the simple VBRT formula (6.33) we note that

$$E_e^* = \begin{cases} (E_\nu+\Delta)\left[1-\dfrac{\Delta^2-m_e^2}{m_n(E_\nu+\Delta)}\right]\left[1+\dfrac{2E_\nu}{m_n}\right]^{-1/2} & \text{for neutrino,} \\ (E_\nu-\Delta)\left[1-\dfrac{\Delta^2-m_e^2}{m_p(E_\nu-\Delta)}\right]\left[1+\dfrac{2E_\nu}{m_p}\right]^{-1/2} & \text{for antineutrino.} \end{cases}$$

Let us rewrite this as

$$E_e^* = (E_\nu \pm \Delta)(1-\alpha_\pm),$$

where

$$\begin{aligned} \alpha_+ &= \frac{\Delta^2-m_e^2}{m_n(E_\nu+\Delta)}\left(1+\frac{E_\nu}{m_n}\right) - \frac{3}{2}\left(\frac{E_\nu}{m_n}\right)^2 + \ldots, \\ \alpha_- &= \frac{\Delta^2-m_e^2}{m_p(E_\nu-\Delta)}\left(1+\frac{E_\nu}{m_p}\right) - \frac{3}{2}\left(\frac{E_\nu}{m_p}\right)^2 + \ldots. \end{aligned}$$

Then

$$P_e^* = (E_\nu \pm \Delta)\left[1-\frac{m_e^2}{(E_\nu\pm\Delta)^2}\right]^{1/2}(1-\beta_\pm),$$

where

$$\begin{aligned} \beta_\pm &= 1-\sqrt{1-2\alpha_\pm\left(1-\frac{\alpha_\pm}{2}\right)\left[1-\left(\frac{m_e}{E_\nu\pm\Delta}\right)^2\right]^{-1}} \\ &= \alpha_\pm\left[1-\left(\frac{m_e}{E_\nu\pm\Delta}\right)^2\right]^{-1}\left\{1+\frac{\alpha_\pm}{2}\left[\left(\frac{E_\nu\pm\Delta}{m_e}\right)^2-1\right]^{-1}+\ldots\right\}. \end{aligned}$$

Let us write out some numerical values. By using the exact formula for the $\alpha_\pm$ we have

$$\alpha_+ \to \alpha_+^0 \simeq +1.161636\times10^{-3} \quad \text{and} \quad \alpha_- \to \alpha_-^0 \simeq -1.163237\times10^{-3}$$

as $E_\nu \to 0$. Therefore

$$\begin{aligned} \beta_+ \to \beta_+^0 &= +10^{-3}\times \begin{cases} 1.3765 & \text{(1st approximation),} \\ 1.37666 & \text{(2nd approximation),} \\ 1.376668 & \text{(exact),} \end{cases} \\ \beta_- \to \beta_-^0 &= -10^{-3}\times \begin{cases} 1.3784 & \text{(1st approximation),} \\ 1.37828 & \text{(2nd approximation),} \\ 1.378269 & \text{(exact).} \end{cases} \end{aligned}$$

- By comparing these numbers, we can conclude that the first approximation is quite appropriate and the second one is practically exact.
- It is clear that the VBRT formula neglects the corrections $\beta_\pm$ in the factor P_e^*. Considering that the "ABC" factor is exactly proportional to E_ν, this completely explains the $\mathcal{O}\left(10^{-3}\right)$ difference between the exact and VBRT asymptotic values for the $\nu_e n$ cross section.

The following steps are quite obvious and I'll try to write out all these soon.

[8] See also Ref. [40]. In that follows, we will call this approximation "VBRT".

Asymptotics of the $\nu_e n \to e^- p$ cross section.

Since this asymptotics is important (I guess...) for cosmology, we consider it with more details here. By applying the above formulas, one can prove that

$$\lim_{E_\nu\to 0}\left[\mathfrak{A}+\mathfrak{B}+\mathfrak{C}\right]=0$$

and

$$\lim_{E_\nu\to 0}\left[\mathfrak{A}+\mathfrak{B}+\mathfrak{C}\right]\left(\frac{M}{E_\nu}\right)=\frac{\mathfrak{r}K}{1+\mathfrak{r}}\left(1+\varDelta_1+\varDelta_2\right),$$

where

$$K=\left|F_V\right|^2+3\left|F_A\right|^2,$$

the correction $\varDelta_1$ is due to the FCC only while the $\varDelta_2$ accounts for the SCC contributions and vanishes when $F_T=F_S=0$. These two corrections are given by

$$\begin{aligned}
\mathfrak{r}K\varDelta_1 = {} & \left[\mathfrak{r}^2\left(2+3\mathfrak{r}\right)-\varkappa^2\left(1+4\mathfrak{r}-\mathfrak{r}^2\right)-2\varkappa^4\right]\left|F_V\right|^2 \\
& +\left[\mathfrak{r}^2\left(2+\mathfrak{r}\right)+\varkappa^2\left(1-4\mathfrak{r}-\mathfrak{r}^2\right)-2\varkappa^4\right]\left|F_A\right|^2 \\
& +\left(\mathfrak{r}+\varkappa^2\right)\left(\mathfrak{r}^2-\varkappa^2\right)\left[\left(2+\varkappa^2\right)\left|F_M\right|^2+4\varkappa^2\left|F_P\right|^2\right] \\
& +2\left(\mathfrak{r}^2-\varkappa^2\right)\mathrm{Re}\left\{\left[2\mathfrak{r}+\varkappa^2\left(3+\mathfrak{r}\right)\right]F_V^*F_M\right. \\
& \left.-2F_A^*\left[\left(1-\varkappa^2\right)\left(F_V+F_M\right)+\varkappa^2\left(1+\mathfrak{r}\right)F_P\right]\right\}, \\
\simeq {} & \left(2\mathfrak{r}^2-\varkappa^2\right)\left|F_V\right|^2+\left(2\mathfrak{r}^2+\varkappa^2\right)\left|F_A\right|^2-4\left(\mathfrak{r}^2-\varkappa^2\right)\mathrm{Re}\left[F_A^*\left(F_V+F_M\right)\right], \\
\frac{\mathfrak{r}}{4}K\varDelta_2 = {} & \left(\mathfrak{r}^2-\varkappa^2\right)\left[\mathfrak{r}\left(1+\mathfrak{r}\right)^2-\varkappa^2\left(1+\mathfrak{r}+\mathfrak{r}^2\right)+\varkappa^4\right]\left|F_T\right|^2 \\
& +\varkappa^2\left(1-\varkappa^2\right)\left(\mathfrak{r}+\varkappa^2\right)\left|F_S\right|^2 \\
& +\mathrm{Re}\left\{\left(\mathfrak{r}^2-\varkappa^2\right)F_T^*\left[\left(1+\mathfrak{r}\right)\left(1+\mathfrak{r}-\varkappa^2\right)F_A-2\varkappa^2\left(1+\mathfrak{r}+\mathfrak{r}^2-\varkappa^2\right)F_P\right]\right. \\
& \left.+\varkappa^2\left(1-\varkappa^2\right)F_S^*\left[\left(\mathfrak{r}^2-\varkappa^2\right)F_M-\left(1+\mathfrak{r}\right)F_V\right]\right\} \\
\simeq {} & \mathrm{Re}\left[\left(\mathfrak{r}^2-\varkappa^2\right)F_T^*F_A-\varkappa^2F_S^*F_V\right].
\end{aligned}$$

Therefore the asymptotic value of the $\nu_e n \to e^- p$ cross section at $E_\nu=0$ is

$$\begin{aligned}
\sigma_0 &= \frac{4\mathfrak{r}}{\pi}\left(\frac{G_F\cos\theta_C M}{1+\mathfrak{r}}\right)^2\sqrt{\left(1-\varkappa^2\right)\left(\mathfrak{r}^2-\varkappa^2\right)}\,K\left(1+\varDelta_1+\varDelta_2\right) \\
&= \frac{G_F^2\cos^2\theta_C m_n}{2\pi}\left(1-\frac{m_p^2}{m_n^2}\right)KP_e^{\min}\left(1+\varDelta_1+\varDelta_2\right),
\end{aligned}$$

where

$$P_e^{\min}=\frac{1}{2m_n}\sqrt{\left[\left(m_n-m_p\right)^2-m^2\right]\left[\left(m_n+m_p\right)^2-m^2\right]}\simeq 1.187282648\,\mathrm{MeV}/c$$

is the minimum electron momentum.

By using the standard values

- $\cos\theta_C=0.9748\pm0.0005$, [9]
- $F_V(0)=1$,
- $F_M(0)=\mu_p-\mu_n-1=3.7058901\pm0.00000045$, [10]
- $F_A(0)=g_A=-1.267\pm0.0030$, [11]
- $F_P(0)=2g_A(M/m_\pi)^2\simeq-114.68$,

we can estimate the FCC correction as[12]

$$\varDelta_1\simeq 3.01\times10^{-3}.$$

Assuming that $F_T(0)=\eta_T g_A e^{i\phi_T}$ and $F_S(0)=\eta_S e^{i\phi_S}$ and taking into account the upper limits to η_T and η_S obtained from the nuclear structure studies [372–374] and from the BNL-AGS neutrino experiment [29], we can estimate the upper limit to the SCC correction as[13]

$$\left|\varDelta_2\right|<1.4\times10^{-4}\ll\varDelta_1.$$

[9] The error in $\cos\theta_C$ has been estimated from the PDG value $\sin\theta_C=s_{12}=0.2229\pm0.0022$ [3] as $(0.2229/0.9748)\times0.0022\simeq0.0005$.

[10] The latest PDG values are $\mu_p=2.792847337\pm0.000000029$, $\mu_n=-1.91304272\pm0.00000045$. Therefore $\mu_p-\mu_n-1=3.7058901\pm0.00000045$. However the code uses the exact value 3.705890057.

[11] This is according to PDG but both the value and the error are quite doubtful as is explained in Ref. [51, p. 1716].

[12] FORTRAN output: 3.014832393844721E-003 ($Q^2=-m_e^2$) or 3.014831917005820E-003 ($Q^2=0$).

[13] FORTRAN output: 1.3831117E-04 for maximum value and -1.3820046E-04 for minimum value. The estimation was done straightforwardly by testing 5000×5000 values of the phases η_T and η_S within the $[0,2\pi]$ interval. The calculations are done with $Q^2=0$.

The examples shown in Fig. 6.2 demonstrate variations of the correction Δ_2 when only one of the two SCC induced form factors is assumed to be nonzero. Finally, one can safely neglect this unknown correction even in comparison to Δ_1. This conclusion is important since ensures the strength of the predicted value of σ_0.[14]

Taking all these notes into account, we can estimate the asymptotic cross section as [15]

$$\sigma_0 \simeq 1.4343 \times 10^{-43}\,\text{cm}^2. \tag{6.34}$$

As we know, this value must be corrected to take into the energy-independent inner radiative corrections [47,48,50,51] According to the recent analysis by Fukugita and Kubota [51], the inner radiative corrections to Fermi and Gamov–Teller matrix elements are, respectively,

$$\delta_{\text{in}}^{\text{F}} = 0.02370 \pm 0.0008, \quad \text{and} \quad \delta_{\text{in}}^{\text{GT}} = 0.02616 \pm 0.0008.$$

So, we must replace the factor $1 + 3g_A^2$ with

$$1 + \delta_{\text{in}}^{\text{F}} + 3\left(1 + \delta_{\text{in}}^{\text{GT}}\right) g_A^2 = (1.0257 \pm 0.0008)\,(1 + 3g_A^2)$$

and thus [16]

$$\sigma_0 \simeq 1.4712 \times 10^{-43}\,\text{cm}^2. \tag{6.35}$$

Clearly, the uncertainty in the estimation of the inner radiative correction does not affect essentially to the uncertainty of σ_0, in contrast with the errors in G_F, θ_C and g_A. The maximum uncertainty is probably due to the error in g_A (considering also that the PDG value of the g_A has to be reevaluated properly taking into account the inner radiative corrections Ref. [51, p. 1716]).

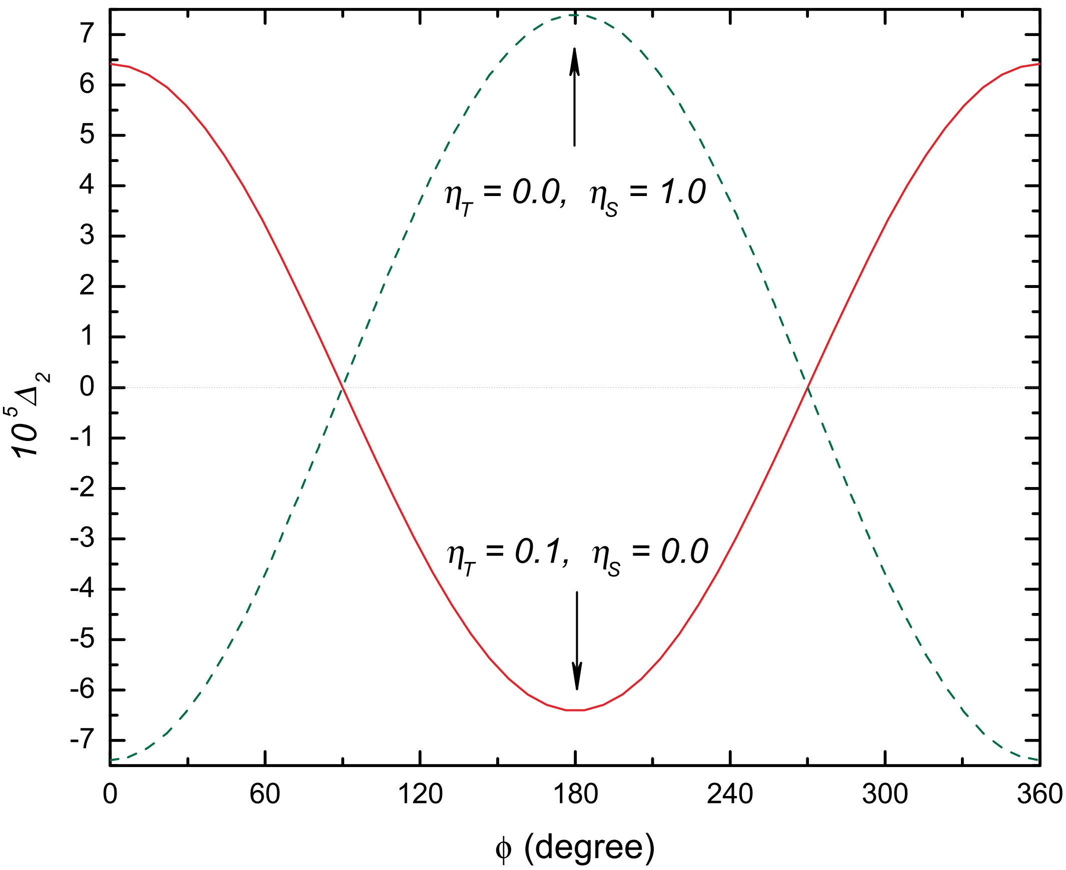

Figure 6.2: The SCC correction $\varDelta_2$ (scaled with the factor of 10^5) as a function of ϕ. The calculations are done under assumption that the SCC form factors at $Q^2 = 0$ are defined as $F_T(0) = \eta_T g_A e^{i\phi}$ and $F_S(0) = \eta_S e^{i\phi}$. Then the values $\eta_T = 0.1$ and $\eta_S = 1.0$ roughly correspond to the upper limits obtained from the nuclear structure studies [372–374] and from the BNL-AGS experiment [29], The standard FCC form factors are taken as is explained in the text. Note that $\varDelta_2$ is invariant under transformation $\phi \mapsto 2\pi - \phi$. It is also clear that $\varDelta_2 = 0$ if C invariance occurs ($\phi = \pi/2$).

[14] It can be noted that in general the FCC form factors *in the time-like region* are complex even in absence of SCC. However, due to analyticity of the form factors, this cannot essentially change the value of σ at low energies. This is an attractive fact because one can firmly estimate the impact of $\nu_e n$ interactions for the earlier stages of the primordial nucleosynthesis, at the temperatures $T = (0.1 - 1)$ MeV, when free neutrons are still abundant while electron antineutrinos do not interact with protons through CC currents.

[15] FORTRAN output: 1.434266314800469E-043 ($Q^2 = -m_e^2$) or 1.434264823913649E-043 ($Q^2 = 0$).

[16] FORTRAN output: 1.471180054501232E-043 ($Q^2 = -m_e^2$) or 1.471178525243429E-043 ($Q^2 = 0$).

Figure 6.3 shows a comparison of the numerical calculation of the total $\nu_e n$ cross section at very low energies with the exact asymptotics given by Eq. (6.34). The oscillations of the numerical curve are due to numerical arithmetics of PENTIUM IV.

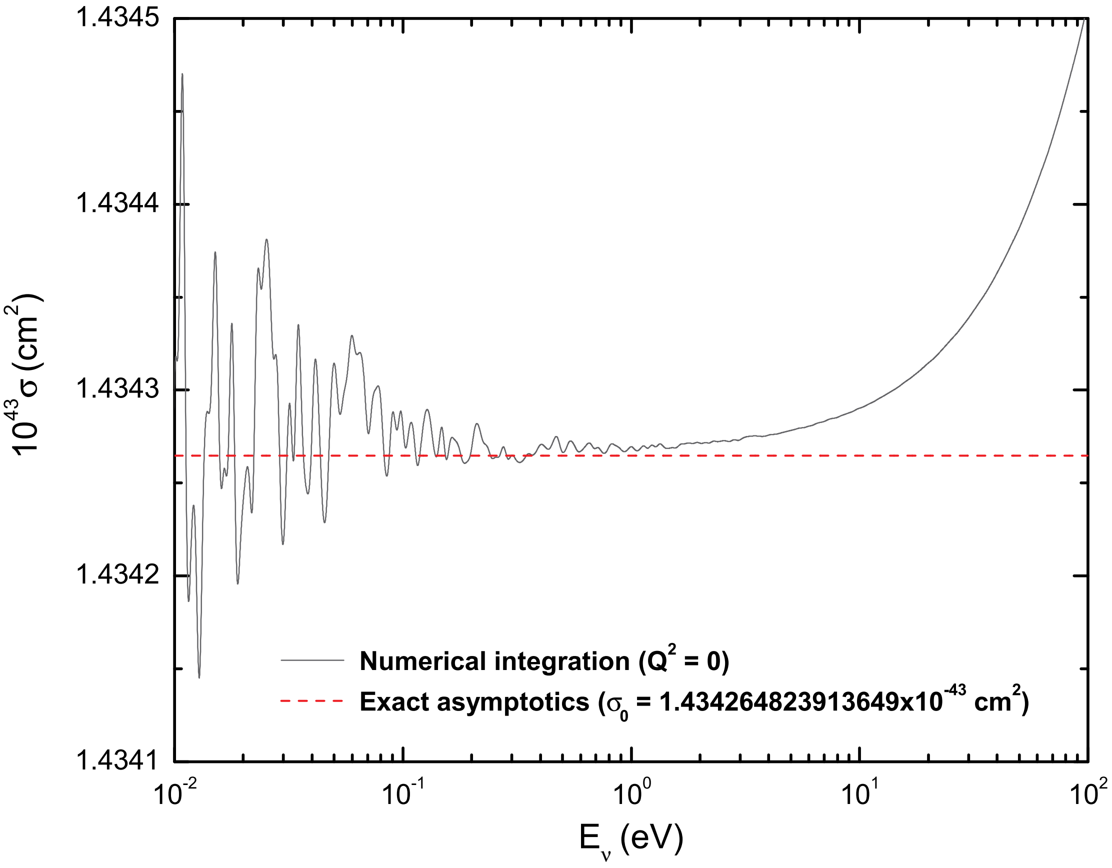

Figure 6.3: Comparison of the numerical calculation of the total $\nu_e n$ cross section at very low energies with the exact asymptotics (6.34). The oscillations of the numerical curve are due to numerical arithmetics of PENTIUM IV.

6.3.4 QES cross section in nuclear mixture.

Let's define

$\mathcal{N}_i$ is the number of nuclei (A_i, Z_i) of type i in the target, where, of course, $A_i = Z_i + N_i$ is the mass number and Z_i and N_i are the numbers of protons and neutrons in the nucleus.

$c_i = \dfrac{\mathcal{N}_i}{\sum_j \mathcal{N}_j}$ is the concentration of nuclei i.

$C_i = \dfrac{\mathcal{N}_i A_i M}{\sum_j \mathcal{N}_j A_j M} = \dfrac{\mathcal{N}_i A_i}{\sum_j \mathcal{N}_j A_j}$ is the mass concentration (mass fraction) of the nuclei i. Here M is the nucleon mass (so that $\sum_i \mathcal{N}_i A_i M$ is the full mass of the target) and we yet neglect the proton-neutron mass difference and binding energy in nuclei. As will be seen, this is an approximation quite enough for our purposes and we can not complicate the calculations by small corrections.

By definition

$$\sum_i c_i = \sum_i C_i = 1, \tag{6.36}$$

Let's find the relation of the concentrations c_i and C_i. Obviously $c_i \propto C_i/A_i$, so put $c_i = a_i C_i/A_i$ and find a_i. Since

$$\frac{c_i}{C_i} = \frac{a_i}{A_i} = \frac{\mathcal{N}_i}{\sum_j \mathcal{N}_j} \cdot \frac{\sum_j \mathcal{N}_j A_j}{\mathcal{N}_i A_i} = \frac{\sum_j \mathcal{N}_j A_j}{A_i \sum_j \mathcal{N}_j},$$

we see that a_i is a constant independent of i,

$$a_i = \frac{\sum_j \mathcal{N}_j A_j}{\sum_j \mathcal{N}_j} \equiv a,$$

so $c_i = aC_i/A_i$. Taking into account that (6.36) we obtain

$$1 = a \sum_i \frac{C_i}{A_i}, \quad 1 = \frac{1}{a} \sum_i c_i A_i$$

and therefore

$$c_i = \frac{C_i}{A_i} \left(\sum_j \frac{C_j}{A_j} \right)^{-1}, \quad C_i = c_i A_i \left(\sum_j c_j A_j \right)^{-1}. \tag{6.37}$$

Let us now find the cross sections per nucleon for the quasi-elastic scattering of neutrinos and antineutrinos on a mixture of nuclei. Let $\sigma_{\nu n}^{(i)}$ and $\sigma_{\overline{\nu} p}^{(i)}$ be the cross sections on the bound nucleons of the nucleus i. Then the cross sections (per nucleon) on the mixture are

$$\langle \sigma_{\nu n} \rangle = \frac{\sum_i N_i c_i \sigma_{\nu n}^{(i)}}{\sum_i N_i c_i} = \frac{\sum_i N_i C_i \sigma_{\nu n}^{(i)}/A_i}{\sum_i N_i C_i/A_i}, \tag{6.38a}$$

$$\langle \sigma_{\overline{\nu} p} \rangle = \frac{\sum_i Z_i c_i \sigma_{\overline{\nu} p}^{(i)}}{\sum_i Z_i c_i} = \frac{\sum_i Z_i C_i \sigma_{\overline{\nu} p}^{(i)}/A_i}{\sum_i Z_i C_i/A_i}. \tag{6.38b}$$

We will call these cross sections partial cross sections. Let us consider important partial cases.

1. Scattering on a "molecule" $(A_1, Z_1)_{n_1} (A_2, Z_2)_{n_2} \cdots (A_K, Z_K)_{n_K}$.

   Obviously $c_i = n_i / \sum_{j=1}^{K} n_i$. So from (6.38) we get

$$\langle \sigma_{\nu n} \rangle = \frac{\sum_i N_i n_i \sigma_{\nu n}^{(i)}}{\sum_i N_i n_i}, \quad \langle \sigma_{\overline{\nu} p} \rangle = \frac{\sum_i Z_i n_i \sigma_{\overline{\nu} p}^{(i)}}{\sum_i Z_i n_i}. \tag{6.39}$$

2. Scattering on an isoscalar target.

   If all the nuclei in the mixture are isoscalar ($N_i = Z_i$), it is convenient to use mass concentrations:

$$\langle \sigma_{\nu n} \rangle = \sum_i C_i \sigma_{\nu n}^{(i)}, \quad \langle \sigma_{\overline{\nu} p} \rangle = \sum_i C_i \sigma_{\overline{\nu} p}^{(i)}. \tag{6.40}$$

3. Approximation: universal nuclear effects.

   If for some reason it is possible to neglect the difference of scattering cross sections on the target nuclei, i.e. put $\sigma_{\nu n}^{(i)} = \sigma_{\nu n}$ and $\sigma_{\overline{\nu} p}^{(i)} = \sigma_{\overline{\nu} p}$,, we get the obvious result beforehand:

$$\langle \sigma_{\nu n} \rangle = \sigma_{\nu n}, \quad \langle \sigma_{\overline{\nu} p} \rangle = \sigma_{\overline{\nu} p}.$$

If the difference between the sections is small, i.e.

$$\delta\sigma_{\nu n}^{(i)} = \sigma_{\nu n}^{(i)} - \sigma_{\nu n} \quad \text{and} \quad \delta\sigma_{\overline{\nu}p}^{(i)} = \sigma_{\overline{\nu}p}^{(i)} - \sigma_{\overline{\nu}p}$$

are small compared to the sections themselves (which is almost always the case), then the differences of the partial sections from $\sigma_{\nu n}$ and $\sigma_{\overline{\nu}p}$ are small:

$$\langle\sigma_{\nu n}\rangle = \sigma_{\nu n} + \frac{\sum_i N_i c_i \delta\sigma_{\nu n}^{(i)}}{\sum_i N_i c_i}, \quad \langle\sigma_{\overline{\nu}p}\rangle = \sigma_{\overline{\nu}p} + \frac{\sum_i Z_i c_i \delta\sigma_{\overline{\nu}p}^{(i)}}{\sum_i Z_i c_i}.$$

This is also a trivial fact, but it explains why we can safely put into global fit M_A^{eff} data on any mixtures: there should be no significant difference in M_A^{eff} on different *theoretically* mixtures.

All these results explain why one does not care about taking into account such trivialities as the difference in masses of the proton and neutron and the binding energy of nucleons in nuclei.

Another important conclusion is that the presence of hydrogen in the mixture invisibly but significantly affects on the partial cross section $\langle\sigma_{\nu n}\rangle$, but only when there are at least two types of nuclei other than hydrogen. Indeed, if the mixture consists of a mixture of nuclei of type I and hydrogen, then

$$\langle\sigma_{\nu n}\rangle = \sigma_{\nu n}^{(I)},$$

i.e., the presence of hydrogen does not play any role. But if the target has two types of nuclei (plus hydrogen), then

$$\begin{aligned}\langle\sigma_{\nu n}\rangle &= \frac{N_1 c_1 \sigma_{\nu n}^{(1)} + N_2 c_2 \sigma_{\nu n}^{(2)}}{N_1 c_1 + N_2 c_2} = \frac{N_1 c_1 \sigma_{\nu n}^{(1)} + N_2 (1 - c_1 - c_H) \sigma_{\nu n}^{(2)}}{N_1 c_1 + N_2 (1 - c_1 - c_H)} \\ &= \frac{N_1 C_1 \sigma_{\nu n}^{(1)}/A_1 + N_2 C_2 \sigma_{\nu n}^{(2)}/A_2}{N_1 C_1/A_1 + N_2 C_2/A_2} = \frac{N_1 C_1 \sigma_{\nu n}^{(1)}/A_1 + N_2 (1 - C_1 - C_H) \sigma_{\nu n}^{(2)}/A_2}{N_1 C_1/A_1 + N_2 (1 - C_1 - C_H)/A_2}.\end{aligned}$$

As we can see, the presence of hydrogen manifests itself in the presence of the value c_H (or C_H) – the concentration (or mass concentration) of hydrogen. This not very obvious fact is directly related to the "mystery of T2K".[17]

[17]The puzzle taking place on December 9, 2013. I'm not sure if all of this will help us solve the problem, but at least we'll get it right. By the way, we need to take a close look at the situation with other complex targets (where there are multiple types of nuclei and hydrogen), including NOMAD – don't we have a discrepancy there? VVL obviously has a discrepancy because he only took into account the carbon. The question is – how significant is the correction and should it not be included in the data...?

6.3.5 Numerical results

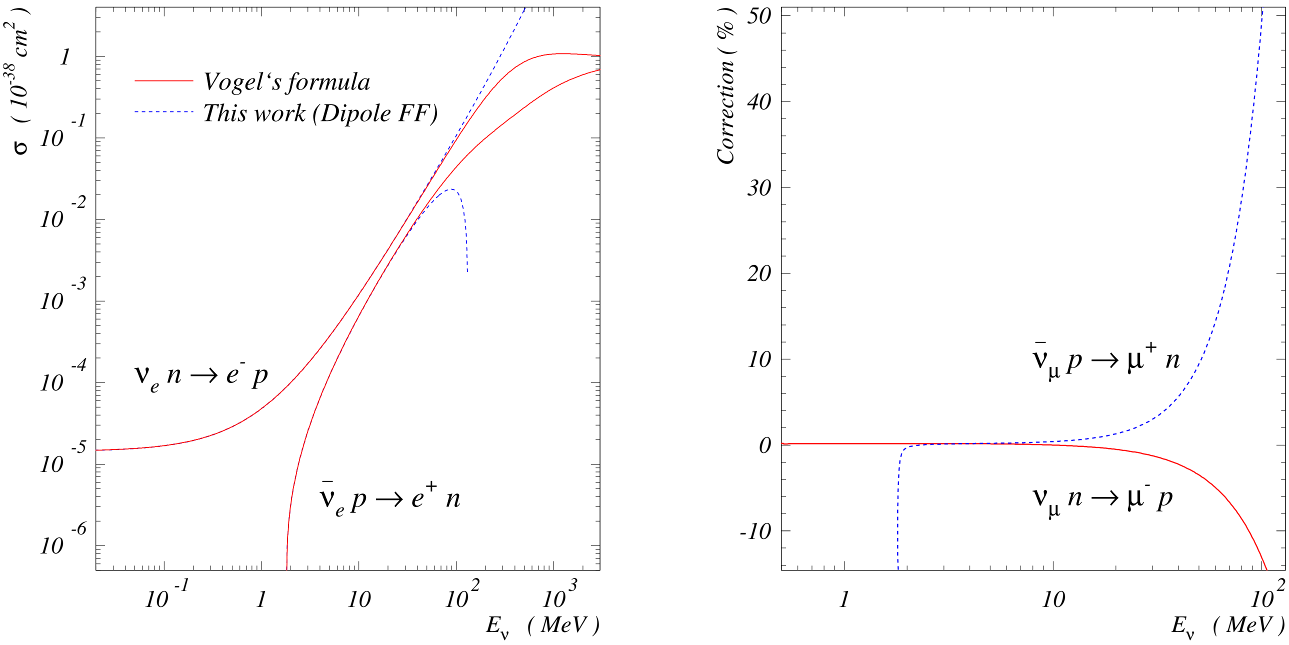

Figure 6.4: Comparison of the neutrino and antineutrino QE total cross sections with the simplified Vogel's formula given by Burrows *et al.* [44] ("VBRT approximation"; see Eq. (6.33)). Right panel shows the percentage deviations of the "VBRT" approximation from the exact result. Calculations are done with the dipole model for the electromagnetic form factors. The axial form factor is taken in the standard dipole form with $g_A = -1.267$ and $M_A = 1$ GeV$/c^2$. The SCC induced contributions are neglected.

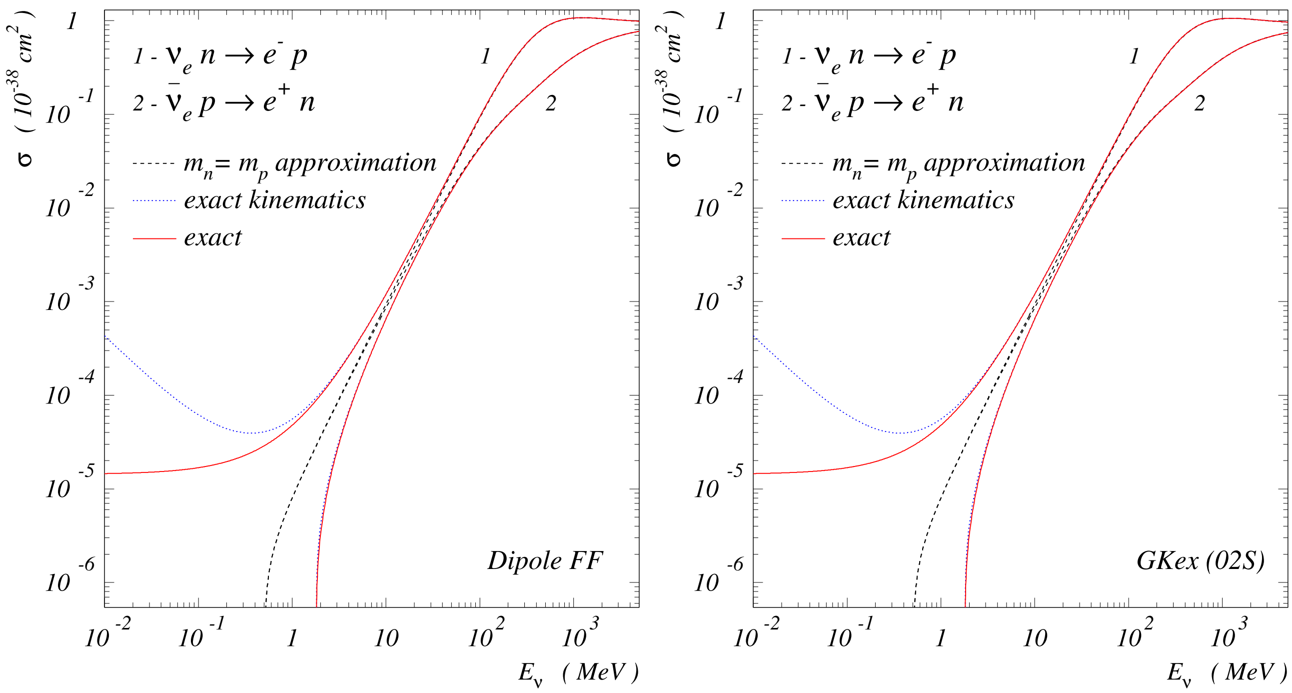

Figure 6.5: Effect of the $M_i \neq M_f$ corrections for the electron neutrino and antineutrino QE total cross sections. Calculations are done with the dipole and GKex(02S) models for the electromagnetic form factors. The axial form factor is taken in the standard dipole form with $g_A = -1.267$ and $M_A = 1$ GeV$/c^2$. The SCC induced contributions are neglected. The dotted curves show the standard approximation $M_i = M_f$, the dashed curves are calculated with the exact kinematics but neglecting the $\mathcal{O}(r^n)$ corrections in the coefficients A, B and C of Eq. (6.25), the solid curves is the result of exact calculation (all the corrections are included).

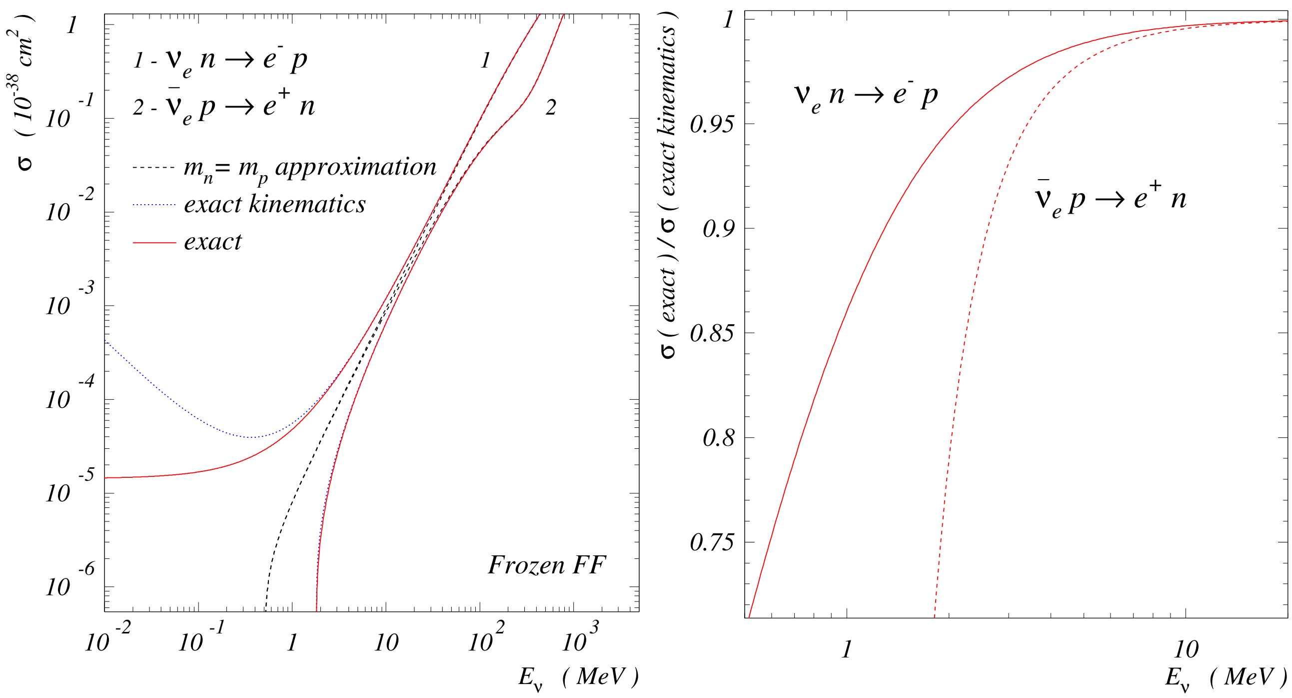

Figure 6.6: Left panel: the same as in fig. 6.5 but with the “frozen” form factors (that is means that all the form factors are taken at $Q^2 = 0$). Right panel: relative effect of the $\mathcal{O}(r^n)$ corrections to “ABC”.

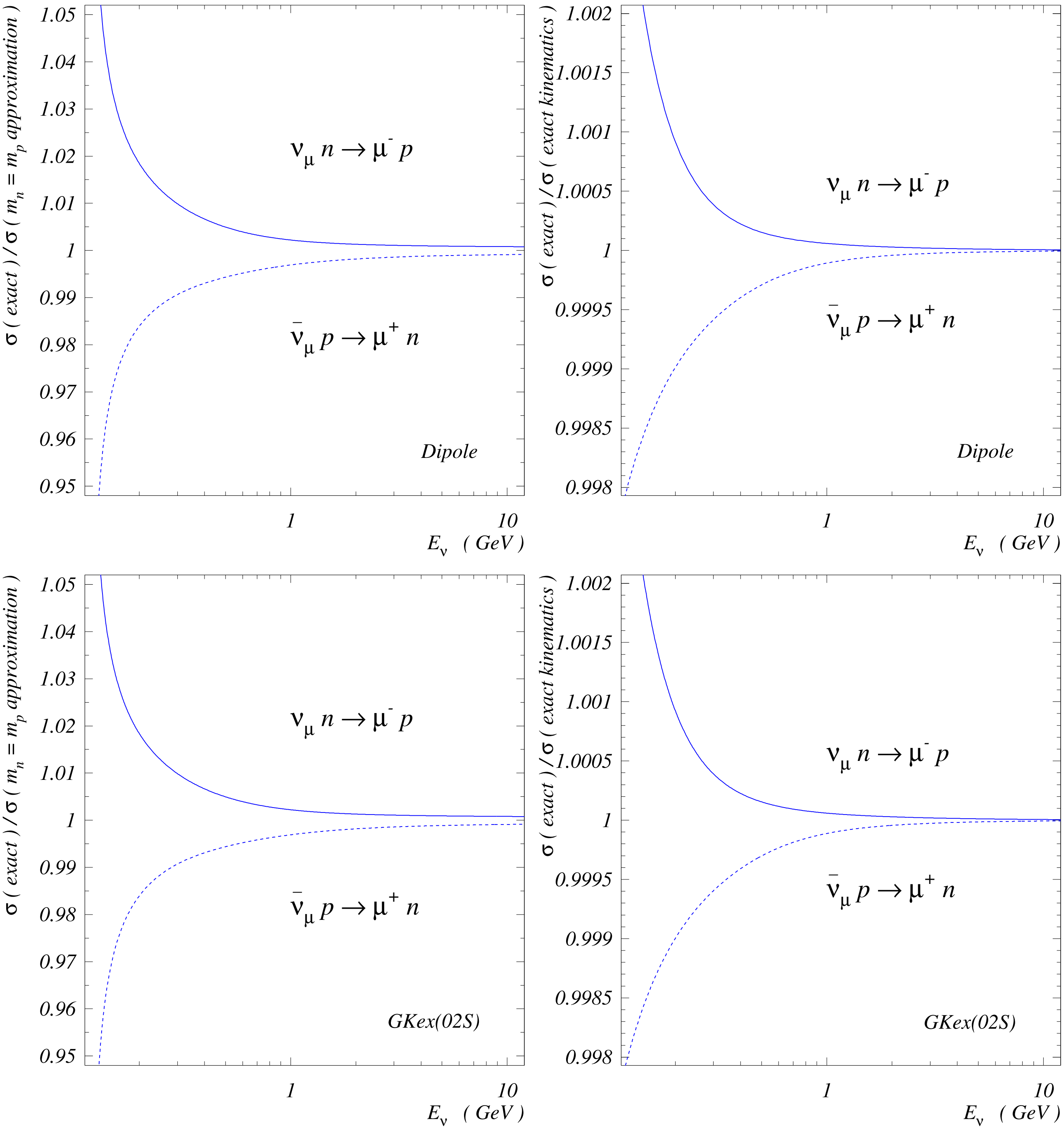

Figure 6.7: Relative effect of the corrections for muon production. Calculations are done with the dipole and GKex(02S) model for the electromagnetic form factors.

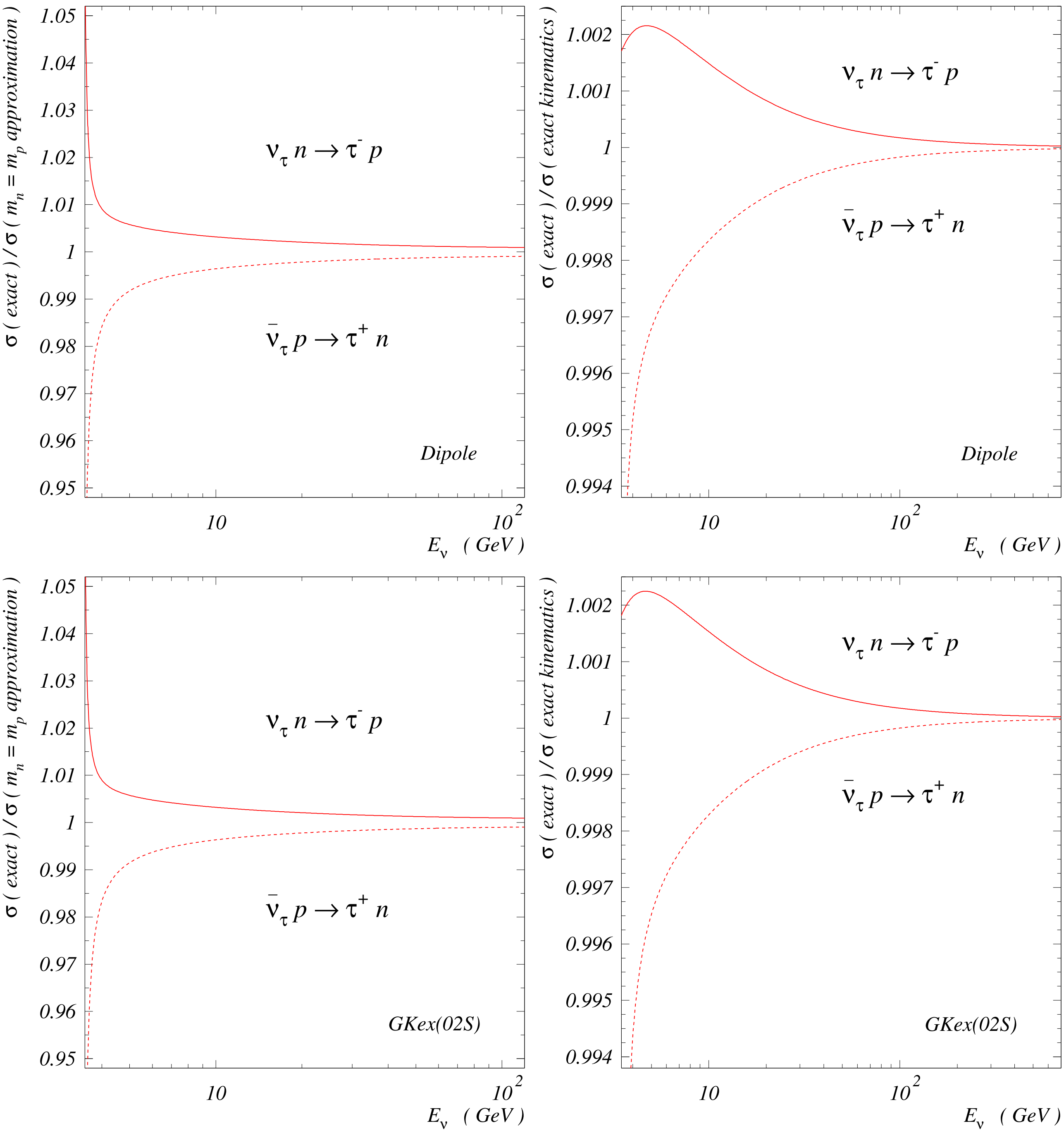

Figure 6.8: Relative effect of the corrections for tau production. Calculations are done with the dipole and GKex(02S) model for the electromagnetic form factors.

6.4 Resonance production

6.4.1 Single resonance production

In this section, we study the reactions of single nucleon resonance production,

$$\nu_\ell + p \to \ell^- + \Delta^{++}, \quad \overline{\nu}_\ell + p \to \ell^+ + \Delta^0,$$
$$\nu_\ell + n \to \ell^- + \Delta^+, \quad \overline{\nu}_\ell + n \to \ell^+ + \Delta^-.$$

In this case the hadronic weak currents are

$$\begin{aligned} J_\alpha &= \cos\theta_C \, \overline{u}^\beta (p') \, [(V_{\alpha\beta\gamma}\gamma^\gamma + V_{\alpha\beta})\gamma_5 + A_{\alpha\beta\gamma}\gamma^\gamma + A_{\alpha\beta}] \, u(p) \, , \\ \overline{J}_\alpha &= \cos\theta_C \, \overline{u}^\beta (p) \, [(V_{\alpha\beta\gamma}\gamma^\gamma - V_{\alpha\beta})\gamma_5 + A_{\alpha\beta\gamma}\gamma^\gamma + A_{\alpha\beta}] \, u(p') \, , \end{aligned}$$

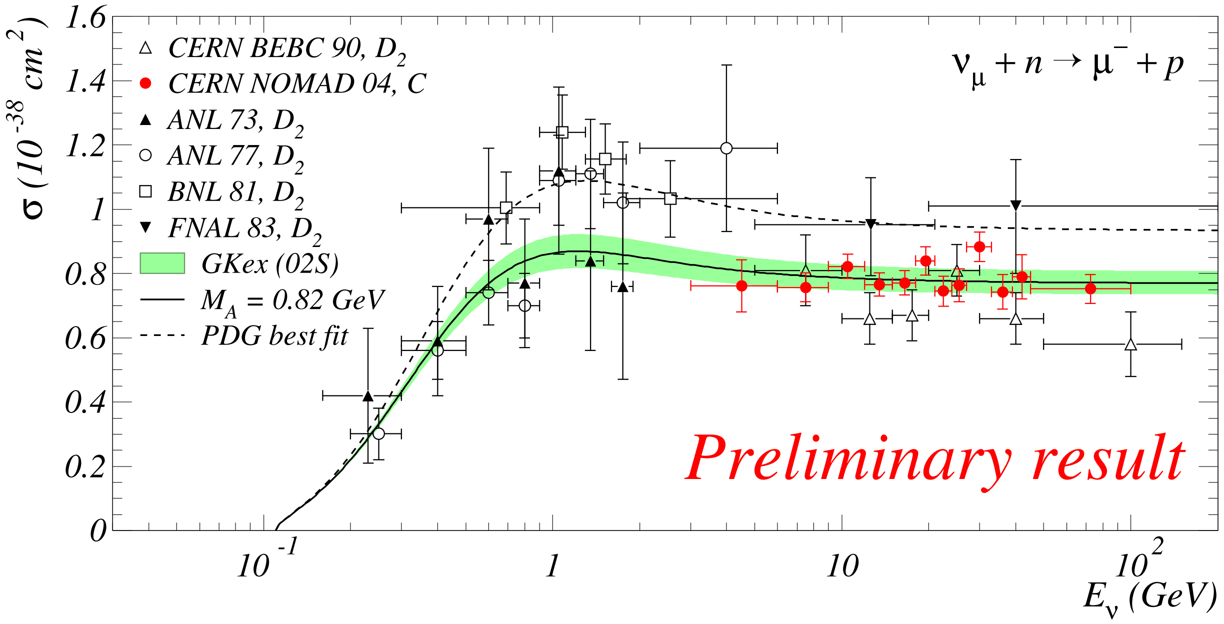

Figure 6.9: Total QE $\nu_\mu n$ cross section extracted from $\nu_\mu D$ scattering at ANL [24,25], BNL [28], FNAL [30], CERN WA-25 [17] and from recent NOMAD measurements on carbon target at CERN [22]. All the data are corrected to nuclear effects. The theoretical band corresponds to variations of M_A from 0.7 to 1.2 GeV/c^2. Solid curve is are calculated with the PDG average value $M_A = 1.03$ GeV/c^2. All calculations are done with the GKex(02S) model for the electromagnetic form factors.

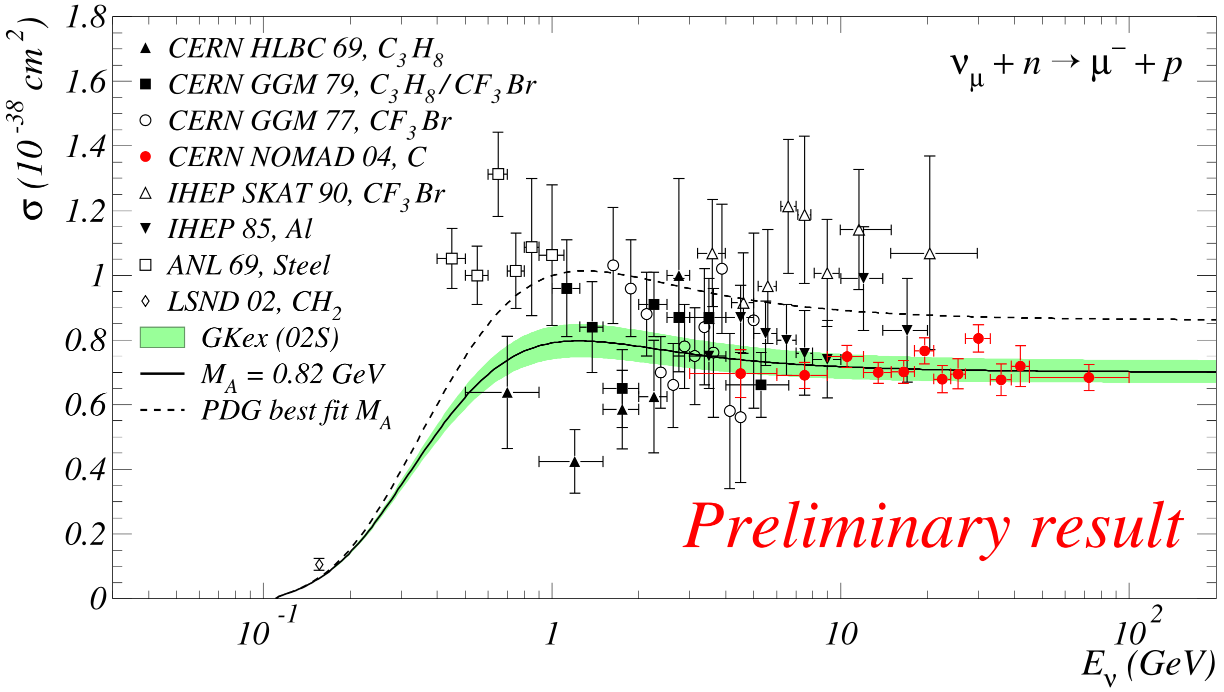

Figure 6.10: Total QE $\nu_\mu n$ cross section extracted from scattering off heavy nuclei in experiments at CERN [15] (HLBC) [18, 20] (Gargamelle), [22] (NOMAD) and at Serpukhov IHEP [34, 37]. The meaning of the band and curve is the same as in Fig. 6.9. The data of this sample (including NOMAD) are not corrected for nuclear effects; therefore these are taken into account in our calculations according to the standard relativistic Fermi gas model.

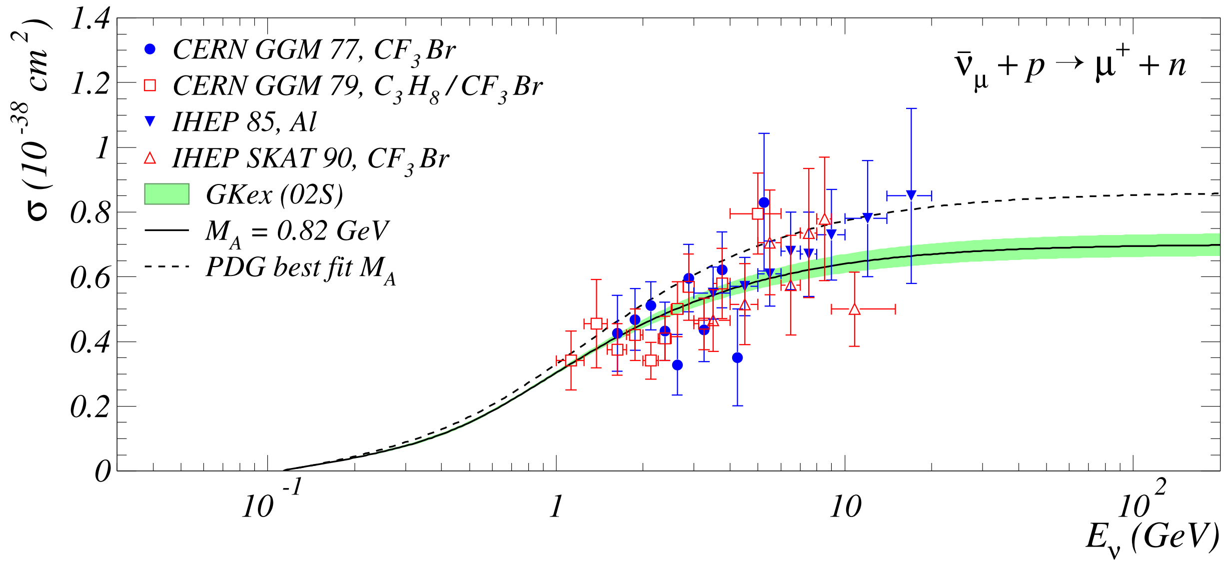

Figure 6.11: Total QE $\overline{\nu}_\mu p$ cross section extracted from scattering off heavy nuclei in experiments at CERN [18, 20] (Gargamelle) and at IHEP [34, 37]. Nuclear effects are included into the calculations according to the standard relativistic Fermi gas model. The meaning of the band and curve is the same as in Fig. 6.10. Since, as in Fig. 6.10, the data are not corrected for nuclear effects, these are taken into account in calculations according to the standard relativistic Fermi gas model.

where

$$\begin{aligned}
V_{\alpha\beta\gamma} &= C_3^V \frac{g_{\alpha\beta}q_\gamma - g_{\alpha\gamma}q_\beta}{M}, \\
A_{\alpha\beta\gamma} &= C_3^A \frac{g_{\alpha\beta}q_\gamma - g_{\alpha\gamma}q_\beta}{M}, \\
V_{\alpha\beta} &= C_4^V \frac{g_{\alpha\beta}\left(qp'\right) - p'_\alpha q_\beta}{M^2} + C_5^V \frac{g_{\alpha\beta}\left(qp\right) - p_\alpha q_\beta}{M^2} + C_6^V \frac{q_\alpha q_\beta}{M^2}, \\
A_{\alpha\beta} &= C_4^A \frac{g_{\alpha\beta}\left(qp'\right) - p'_\alpha q_\beta}{M^2} + C_5^A g_{\alpha\beta} + C_6^A \frac{q_\alpha q_\beta}{M^2},
\end{aligned}$$

$C_j^{V,A}$ are vector and axial form factors,[18] $u\left(p'\right)$ and $u^\alpha\left(p\right)$ are the Dirac spinor and the Rarita-Schwinger spin-vector, respectively

$$\sum_{spin} u\left(p\right)\overline{u}\left(p\right) = \hat{p} + M,$$

$$\sum_{spin} u^\alpha\left(p'\right)\overline{u}^\beta\left(p'\right) = \left(\hat{p}' + M'\right)\left(-g^{\alpha\beta} + \frac{2}{3}\frac{p'^\alpha p'^\beta}{M'^2} - \frac{p'^\alpha\gamma^\beta - \gamma^\alpha p'^\beta}{3M'} + \frac{\gamma^\alpha\gamma^\beta}{3}\right).$$

$$W_{\alpha\beta} = \frac{\cos^2\theta_C}{4}\int \mathrm{Tr}\left[\sum_{spin} u^\gamma\left(p'\right)\overline{u}^\delta\left(p'\right)J_{\alpha\gamma}\left(\hat{p} + M\right)\overline{J}_{\beta\delta}\right]\delta\left(p' - p - q\right)\frac{d\mathbf{p}'}{2E_{N'}},$$

$$\int \delta\left(p' - p - q\right)\frac{d\mathbf{p}'}{2E_{N'}} \to \frac{1}{\pi}\frac{W\Gamma\left(W^2\right)}{\left(W^2 - M'^2\right)^2 + W^2\Gamma\left(W^2\right)},$$

$$\Gamma\left(W^2\right) = \Gamma\left(M'\right)\frac{\lambda^{1/2}\left(W^2, M^2, m_\pi\right)}{\lambda^{1/2}\left(M'^2, M^2, m_\pi\right)},$$

here [19] $\lambda\left(a,b,c\right) = a^2 + b^2 + c^2 - 2\left(ab + bc + ca\right)$.

[18] The vertex $\Gamma_{\alpha\beta}$ for the transition $p \to \Delta^+$ is usually expressed in terms of the 8 weak form factors as

$$\begin{aligned}
\Gamma_{\alpha\beta} = {} & C_3^A \frac{g_{\alpha\beta}\hat{q} - \gamma_\alpha q_\beta}{M} + C_4^A \frac{g_{\alpha\beta}\left(qp'\right) - p'_\alpha q_\beta}{M^2} + C_5^A g_{\alpha\beta} + C_6^A \frac{q_\alpha q_\beta}{M^2} \\
& + \left(C_3^V \frac{g_{\alpha\beta}\hat{q} - \gamma_\alpha q_\beta}{M} + C_4^V \frac{g_{\alpha\beta}\left(qp'\right) - p'_\alpha q_\beta}{M^2} + C_5^V \frac{g_{\alpha\beta}\left(qp\right) - p_\alpha q_\beta}{M^2} + C_6^V \frac{q_\alpha q_\beta}{M^2}\right)\gamma_5.
\end{aligned}$$

[19] For numerical calculation is used the form $\lambda(a) = a\left(a - c_1\right) + c_2$, $c_1 = 2\left(M^2 + m_\pi^2\right)$, $c_2 = \left(M^2 - m_\pi^2\right)^2$.

The structure functions are

$$
\begin{aligned}
W_i^{(\mathrm{RES})} = & \frac{2\cos^2\theta_C}{3\zeta} M^2 \left[\frac{1}{\pi} \frac{W\Gamma(W)}{\left(W^2 - M'^2\right)^2 + W^2\Gamma^2(W)} \right] \\
& \times \sum_{jk} \left(V_i^{jk} C_j^V C_k^V + A_i^{jk} C_j^A C_k^A + K_i^{jk} C_j^V C_k^A \right),
\end{aligned}
$$

$j, k = 3, 4, 5, 6$. The nonzero coefficients V_i^{jk}, A_i^{jk} and K_i^{jk} are given in appendices.

6.4.2 Single pion production in the extended Rein–Sehgal model

In this section, we describe an extension of the famous model by Rein and Sehgal [100] for the neutrino induced single pion production (RS model from here on) in order to take account for the final lepton mass and polarization.

The charged hadronic current in the RS approach has been derived in terms of the FKR relativistic quark model [87] and its explicit form has been written in the resonance rest frame (RRF); below we will mark this frame with asterisk ($\star$). Therefore

$$
\mathbf{q}^\star = -\mathbf{p}^\star.
$$

In RRF, the energy of the incoming neutrino, outgoing lepton, target nucleon and the 3-momentum transfer are, respectively,

$$
E_\nu^\star = \frac{1}{2W}\left(2ME_\nu - Q^2 - m^2\right) = \frac{E_\nu}{W}\left[M - (E_\ell - P_\ell\cos\theta)\right], \tag{6.41a}
$$

$$
E_\ell^\star = \frac{1}{2W}\left(2ME_\ell + Q^2 - m^2\right) = \frac{1}{W}\left[ME_\ell - m^2 + E_\nu\left(E_\ell - P_\ell\cos\theta\right)\right], \tag{6.41b}
$$

$$
E_N^\star = W - (E_\nu^\star - E_\ell^\star) = \frac{M}{W}\left(M + E_\nu - E_\ell\right) \quad \text{and} \tag{6.41c}
$$

$$
\mathcal{Q}^\star = |\mathbf{q}^\star| = \frac{M}{W}\mathcal{Q}, \tag{6.41d}
$$

where

$$
\mathcal{Q} = |\mathbf{q}| = \sqrt{E_\nu^2 - 2E_\nu P_\ell\cos\theta + P_\ell^2} = \sqrt{\left(E_\nu - P_\ell\cos\theta\right)^2 + P_\ell^2\sin^2\theta}.
$$

It is convenient to direct the spatial axes of the RRF in such a way that $\mathbf{p}^\star = -\mathbf{q}^\star = (0, 0, -\mathcal{Q}^\star)$ and $k_y^\star = k_y'^\star = 0$. These conditions lead to the following system of equations:

$$
k_x^\star = k_x'^\star = \sqrt{\left(E_\nu^\star\right)^2 - \left(k_z^\star\right)^2}, \tag{6.42a}
$$

$$
k_z^\star - k_z'^\star = \mathcal{Q}^\star, \tag{6.42b}
$$

$$
k_z^\star + k_z'^\star = \frac{1}{\mathcal{Q}^\star}\left[\left(E_\nu^\star\right)^2 - \left(E_\ell^\star\right)^2 + m^2\right]. \tag{6.42c}
$$

The final equations for the neutrino and lepton 3-momenta, $\mathbf{k}^\star$ and $\mathbf{k}'^\star$ written in terms of the kinematical variables defined in the lab. frame are

$$
\begin{aligned}
k_x^\star &= k_x'^\star = \frac{E_\nu P_\ell}{\mathcal{Q}}\sin\theta, \\
k_z^\star &= \frac{E_\nu}{\mathcal{Q}W}\left[P_\ell\left(E_\nu + E_\ell - M\right)\cos\theta - E_\nu\left(E_\ell - M\right) - P_\ell^2\right], \\
k_z'^\star &= \frac{E_\nu}{\mathcal{Q}W}\left[P_\ell\left(E_\nu + E_\ell + M\right)\cos\theta - E_\nu E_\ell - P_\ell^2\left(1 + \frac{M}{E_\nu}\right)\right].
\end{aligned}
$$

By fixing the outgoing lepton helicity λ in the lab. frame we can write[20]

$$
\lambda m s = \left(P_\ell, \frac{E_\ell}{P_\ell}\mathbf{k}'\right) = \left(P_\ell, E_\ell\sin\theta, 0, E_\ell\cos\theta\right) = \frac{ME_\ell k' - m^2 p}{MP_\ell}. \tag{6.43}
$$

By using Eqs. (6.41), (6.42) and (6.43) we can determine the components of the lepton spin 4-vector in RRF:

$$
\begin{aligned}
s_0^\star &= \frac{\lambda}{mW}\left[MP_\ell + E_\nu\left(P_\ell - E_\ell\cos\theta\right)\right], \quad s_x^\star = \lambda\frac{E_\nu E_\ell}{m\mathcal{Q}}\sin\theta, \quad s_y^\star = 0, \\
s_z^\star &= \frac{\lambda}{m\mathcal{Q}W}\left[\left(E_\nu\cos\theta - P_\ell\right)\left(ME_\ell - m^2 + E_\nu E_\ell\right) - E_\nu P_\ell\left(E_\nu - P_\ell\cos\theta\right)\right].
\end{aligned}
$$

[20]Here it is assumed that the spatial axes of the lab. frame are directed in such a way that $k = (E_\nu, 0, 0, E_\nu)$ and $k' = (E_\ell, P_\ell\sin\theta, 0, P_\ell\cos\theta)$.

The general equation for leptonic weak current (for neutrino case) is:

$$\begin{aligned} j_\lambda^\alpha &= \overline{u}\left(k',s\right)\gamma^\alpha\left(\frac{1-\gamma_5}{2}\right)u(k) \\ &= N_\lambda\left[mk^\alpha + k'^\alpha(ks) - s^\alpha(kk') - i\epsilon^{\alpha\beta\gamma\delta}s_\beta k_\gamma k'_\delta\right] \end{aligned}$$

where the normalization constant N_λ is expressed in terms of the kinematic variables and of two intrinsically indeterminate phases φ_+ and φ_- (see Sect. 6.2):

$$N_\lambda = \frac{(1+\lambda)\,e^{i\varphi_+} + (1-\lambda)\,e^{i\varphi_-}}{2\sqrt{\upsilon_\lambda}}, \quad \upsilon_\lambda = (kk') + m(ks) = \frac{m^2E_\nu\left(1-\lambda\cos\theta\right)}{E_\ell - \lambda P_\ell},$$

Then, by applying the general equation, the components of the leptonic current in RRF with the lepton helicity λ measured in the lab. frame, are expressed as

$$\begin{aligned} j_0^\star &= N_\lambda m\frac{E_\nu}{W}\left(M - E_\ell - \lambda P_\ell\right)\left(1-\lambda\cos\theta\right), \\ j_x^\star &= N_\lambda m\frac{E_\nu}{\mathcal{Q}}\left(P_\ell - \lambda E_\nu\right)\sin\theta, \\ j_y^\star &= i\lambda N_\lambda m E_\nu\sin\theta, \\ j_z^\star &= N_\lambda m\frac{E_\nu}{\mathcal{Q}W}\left[\left(E_\nu + \lambda P_\ell\right)\left(M - E_\ell\right) + P_\ell\left(\lambda E_\nu + 2E_\nu\cos\theta - P_\ell\right)\right]\left(1-\lambda\cos\theta\right). \end{aligned}$$

On the other hand, in the spirit of the RS model, the leptonic current may be decomposed into three polarization 4-vectors corresponding to left-handed, right-handed and scalar polarization of the intermediate W boson:

$$j_\lambda^\alpha = \frac{1}{C}\left[c_L^\lambda e_L^\alpha + c_R^\lambda e_R^\alpha + c_S^\lambda e_{(\lambda)}^\alpha\right],$$

$$e_L^\alpha = \frac{1}{\sqrt{2}}(0,1,-i,0), \quad e_R^\alpha = \frac{1}{\sqrt{2}}(0,-1,-i,0), \quad e_{(\lambda)}^\alpha = \frac{1}{\sqrt{Q^2}}\left(\mathcal{Q}_{(\lambda)}^\star,0,0,\nu_{(\lambda)}^\star\right).$$

Here the vectors e_L^α and e_R^α are the same as in ref. [100] while $e_{(\lambda)}^\alpha$ has been modified to include the lepton mass effect. The remaining notation is

$$c_L^\lambda = \frac{C}{\sqrt{2}}\left(j_x^\star + ij_y^\star\right), \quad c_R^\lambda = -\frac{C}{\sqrt{2}}\left(j_x^\star - ij_y^\star\right), \quad c_S^\lambda = C\sqrt{|(j_0^\star)^2 - (j_z^\star)^2|},$$

$$\mathcal{Q}_{(\lambda)}^\star = \frac{C\sqrt{Q^2}}{c_S^\lambda}j_0^\star, \quad \nu_{(\lambda)}^\star = \frac{C\sqrt{Q^2}}{c_S^\lambda}j_z^\star, \quad C = \frac{\mathcal{Q}}{E_\nu\sqrt{2Q^2}}.$$

Within the extended RS model, the elements of the polarization density matrix for neutrino case may be written as the superpositions of the partial cross sections $\sigma_L^{\lambda\lambda'}$, $\sigma_R^{\lambda\lambda'}$ and $\sigma_S^{\lambda\lambda'}$:[21]

$$\frac{d\sigma_{\lambda\lambda'}}{dQ^2dW} = \frac{G_F^2\cos^2\theta_C}{\pi^2}\left(\frac{WQ^2}{M\mathcal{Q}^2}\right)\sum_{i=L,R,S}c_i^\lambda c_i^{\lambda'}\sigma_i^{\lambda\lambda'}\left(Q^2,W\right),$$

$$\sigma_{L,R}^{\lambda\lambda'} = \frac{\pi W}{2M}\left(A_{\pm3}^\lambda A_{\pm3}^{\lambda'} + A_{\pm1}^\lambda A_{\pm1}^{\lambda'}\right), \quad \sigma_S^{\lambda\lambda'} = \frac{\pi M\mathcal{Q}^2}{2WQ^2}\left(A_{0+}^\lambda A_{0+}^{\lambda'} + A_{0-}^\lambda A_{0-}^{\lambda'}\right).$$

The amplitudes $A_\varkappa^\lambda$ (with $\varkappa = \pm3,\ \pm1$ or $0\pm$) are defined by

$$\begin{aligned} A_\varkappa^\lambda\left(p\pi^+\right) &= \sqrt{3}\sum_{(I=3/2)}a_\varkappa^\lambda\left(\mathcal{N}_3^{*+}\right), \\ A_\varkappa^\lambda\left(p\pi^0\right) &= \sqrt{\frac{2}{3}}\sum_{(I=3/2)}a_\varkappa^\lambda\left(\mathcal{N}_3^{*+}\right) - \sqrt{\frac{1}{3}}\sum_{(I=1/2)}a_\varkappa^\lambda\left(\mathcal{N}_1^{*+}\right), \\ A_\varkappa^\lambda\left(n\pi^+\right) &= \sqrt{\frac{1}{3}}\sum_{(I=3/2)}a_\varkappa^\lambda\left(\mathcal{N}_3^{*+}\right) + \sqrt{\frac{2}{3}}\sum_{(I=1/2)}a_\varkappa^\lambda\left(\mathcal{N}_1^{*+}\right). \end{aligned}$$

Only those resonances are allowed to interfere which have the same spin and orbital angular momentum. Any amplitude $a_\varkappa^\lambda\left(\mathcal{N}_i^{*+}\right)$ referring to a single resonance consists of two factors which describe the production and subsequent decay of the resonance $\mathcal{N}_i^{*+}$:

$$a_\varkappa^\lambda\left(\mathcal{N}_i^*\right) = f_\varkappa^\lambda\left(\nu\mathcal{N}\to\mathcal{N}_i^*\right)\eta(\mathcal{N}_i^*\to\mathcal{N}\pi) \equiv f_\varkappa^{\lambda(\imath)}\,\eta^{(\imath)}.$$

[21] Here and below, we use the same definitions and (almost) similar notations as in ref. [100].

The resonance production amplitudes, $f_{\varkappa}^{\lambda(\imath)}$, are collected in Table II of Ref. [100]. The corresponding decay amplitudes, $\eta^{(\imath)}$, can be split into three factors,

$$\eta^{(\imath)} = \mathrm{sign}(\mathcal{N}_\imath^*)\,\sqrt{\chi_\imath}\,\eta_{BW}^{(\imath)}(W), \tag{6.44}$$

irrespective of isospin, charge or helicity. Here sign $(\mathcal{N}_\imath^*)$ is the pure sign given in Table III of ref. [100], $\chi_\imath$ is the elasticity of the resonance taking care of the branching ratio into the $\mathcal{N}\pi$ final state and

$$\eta_{BW}^{(\imath)}(W) = \sqrt{\frac{1}{2\pi N_\imath}\left[\frac{\Gamma_\imath(W)}{(W-M_\imath)^2+\Gamma_\imath^2(W)/4}\right]},$$

where

$$\begin{aligned}
\Gamma_\imath(W) &= \Gamma_\imath^0\left[\frac{\lambda(W^2,M^2,m_\pi)}{\lambda(M_\imath^2,M^2,m_\pi)}\right]^{L+1/2},\\
N_\imath &= \frac{1}{2\pi}\int_{W_-}^{W_{\max}}\left[\frac{\Gamma_\imath(W)dW}{(W-M_\imath)^2+\Gamma_\imath^2(W)/4}\right],
\end{aligned}$$

and $W_{\max} = \min\,(W_+, W_{\text{cut}})$. The kinematic limits $W_\pm$ are defined in Sect. 3.2.

It is obvious that total cross section is the sum of the partial cross sections with $\lambda = \lambda' = \pm 1$. Equation for charge conjugate antineutrino reaction can be obtained by simple interchange of $c_R^\lambda \leftrightarrow c_L^{-\lambda}$.

In the generalized RS model, the structure of the vector $e^\alpha_{(\lambda)}$ has been changed by including the lepton spin dependence. Thus we have to recalculate the inner products $J_\alpha^{V,A} e^\alpha_{(\lambda)}$, where $J_\alpha^{V,A}$ are the vector and axial hadronic currents in the FKR model. The new definitions for the structures S^V, B^A and C^A involved into the model are the following:

$$\begin{aligned}
S^V &= \left(\nu^\star_{(\lambda)}\nu^\star - \mathcal{Q}^\star_{(\lambda)}\mathcal{Q}^\star\right)\left(1+\frac{Q^2}{M^2}-\frac{3W}{M}\right)\frac{G^V(Q^2)}{6Q^2},\\
B^A &= \sqrt{\frac{\Omega}{2}}\left(\mathcal{Q}^\star_{(\lambda)} + \nu^\star_{(\lambda)}\frac{\mathcal{Q}^\star}{2Mg^2}\right)\frac{ZG^A(Q^2)}{3W\mathcal{Q}^\star},\\
C^A &= \left[\left(\mathcal{Q}^\star_{(\lambda)}\mathcal{Q}^\star - \nu^\star_{(\lambda)}\nu^\star\right)\left(\frac{1}{3}+\frac{\nu^\star}{2Mg^2}\right) + \nu^\star_{(\lambda)}\left(\frac{2}{3}W - \frac{Q^2}{2Mg^2} + \frac{n\Omega}{6Mg^2}\right)\right]\frac{ZG^A(Q^2)}{2W\mathcal{Q}^\star}.
\end{aligned}$$

We will quote the unchanged equations for the reader's convenience (don't mix that λ, used in Table II of [100] with the lepton helicity):

$$\begin{aligned}
\lambda &= \sqrt{\frac{2}{\Omega}}\frac{M}{W}\mathcal{Q},\\
T^V &= \frac{1}{3W}\sqrt{\frac{\Omega}{2}}G^V\left(Q^2\right) = T,\\
R^V &= \sqrt{2}\frac{M}{W}\left[\frac{(W+M)\mathcal{Q}}{(W+M)^2+Q^2}\right]G^V\left(Q^2\right) = R,\\
T^A &= \frac{2}{3}\sqrt{\frac{\Omega}{2}}\frac{M}{W}\left[\frac{\mathcal{Q}}{(W+M)^2+Q^2}\right]ZG^A\left(Q^2\right),\\
R^A &= \left[W+M+\frac{2N\Omega W}{(W+M)^2+Q^2}\right]\frac{\sqrt{2}ZG^A\left(Q^2\right)}{6W}.
\end{aligned}$$

6.4.3 Numerical results

Table 6.2: Nucleon Resonances with masses below 2 GeV according to PDG-2004.

1	2	3	4	5	6	7	8
✓	$P_{11}(1440)$	$[56, 0^+]_2$	a	$1430 \div 1470$	$250 \div 450\,(350)$	60–70 (0.65)	$+$
✓	$D_{13}(1520)$	$[70, 1^-]_1$	a	$1515 \div 1530$	$110 \div 135\,(120)$	50–60 (0.56)	$-$
✓	$S_{11}(1535)$	$[70, 1^-]_1$	a	$1520 \div 1555$	$100 \div 200\,(150)$	35–55 (0.45)	$-$
✓	$S_{11}(1650)$	$[70, 1^-]_1$	a	$1640 \div 1680$	$145 \div 190\,(150)$	55–90 (0.60)	$+$
✓	$D_{15}(1675)$	$[70, 1^-]_1$	a	$1670 \div 1685$	$140 \div 180\,(150)$	40–50 (0.35)	$+$
✓	$F_{15}(1680)$	$[56, 2^+]_2$	a	$1675 \div 1690$	$120 \div 140\,(130)$	60–70 (0.62)	$+$
✓	$D_{13}(1700)$	$[70, 1^-]_1$	b	$1650 \div 1750$	$50 \div 150\,(100)$	5–15 (0.10)	$-$
✓	$P_{11}(1710)$	$[70, 0^+]_2$	b	$1680 \div 1740$	$50 \div 250\,(100)$	10–20 (0.19)	$+$
✓	$P_{13}(1720)$	$[56, 2^+]_2$	a	$1650 \div 1750$	$100 \div 200\,(150)$	10–20 (0.19)	$+$
	$P_{13}(1900)$		c	$\sim \mathit{1900}$	?	$\mathit{26} \pm \mathit{6}$	
✓	$F_{17}(1990)$	$[70, 2^+]_2$	c	$\sim \mathit{1990}$	? (350)	$\mathit{6} \pm \mathit{2}$ (0.06)	$+$
✓	$P_{33}(1232)$	$[56, 0^+]_0$	a	$1230 \div 1234$	$115 \div 125\,(120)$	$> 99\,(1.)$	$+$
✓	$P_{33}(1600)$	$[56, 0^+]_2$	b	$1550 \div 1700$	$250 \div 450\,(350)$	10–25 (0.20)	$+$
✓	$S_{31}(1620)$	$[70, 1^-]_1$	a	$1615 \div 1675$	$120 \div 180\,(150)$	20–30 (0.25)	$+$
✓	$D_{33}(1700)$	$[70, 1^-]_1$	a	$1670 \div 1770$	$200 \div 400\,(300)$	10–20 (0.12)	$+$
	$P_{31}(1750)$		d	$\sim \mathit{1750}$	?	$\mathit{8} \pm \mathit{3}$	
	$S_{31}(1900)$		c	$1850 \div 1950$	$140 \div 240\,(200)$	10–30	
✓	$F_{35}(1905)$	$[56, 2^+]_2$	a	$1870 \div 1920$	$280 \div 440\,(350)$	5–15 (0.15)	$-$
✓	$P_{31}(1910)$	$[56, 2^+]_2$	a	$1870 \div 1920$	$190 \div 270\,(250)$	15–30 (0.19)	$-$
✓	$P_{33}(1920)$	$[56, 2^+]_2$	b	$1900 \div 1970$	$150 \div 300\,(200)$	5–20 (0.17)	$+$
	$D_{35}(1930)$		b	$1920 \div 1970$	$250 \div 450\,(350)$	10–20	
	$D_{33}(1940)$		d	$\sim \mathit{1940}$	?	$\mathit{18} \pm \mathit{12}$	
✓	$F_{37}(1950)$	$[56, 2^+]_2$	a	$1940 \div 1960$	$290 \div 350\,(300)$	35–40 (0.40)	$+$

1: The mark indicates that the resonance has been included into the original RS calculation (see Table II of the RS paper).

2: Resonance symbol $L_{2I,2J}\,(M_\imath)$, where $L = S, D, F, P$, the labels I and J indicate the isospin and spin, respectively, and $M_\imath$ is the (approximate) mass.

3: Quark-model assignment in terms of the flavor-spin $SU(6)$ basis $[D, L^P]_N$, where D is the dimensionality of the $SU(6)$ representation, L is the total quark orbital angular momentum, P is the total parity and N is the number of quanta of excitation.

4: Resonance status (according to PDG):

(a) existence is certain, and properties are at least fairly well explored;

(b) existence ranges from very likely to certain, but further confirmation is desirable and/or quantum numbers, branching fractions, etc. are not well determined;

(c) evidence of existence is only fair;

(d) evidence of existence is poor.

5: Resonance mass $M_\imath$ range (in MeV).

6: Breit-Wigner width $\Gamma_\imath^0$ range and, in parentheses, its mean value (in MeV).

7: Branching ratio of the resonance decay into the $\mathcal{N}\pi$ state (in %) and, in parentheses, the selected elasticity, $\chi_\imath$ (see Eq. (6.44)).

8: The pure decay sign, sign$(\mathcal{N}_\imath^*)$, involved into Eq. (6.44).

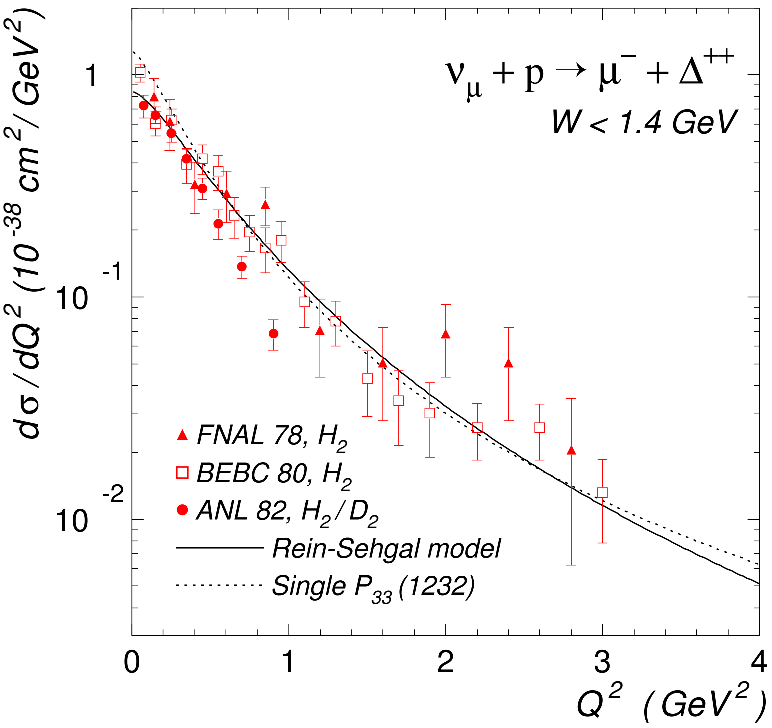

Figure 6.12: Comparison of calculations of differential cross section for the reaction $\nu_\mu p \to \mu^- \Delta^{++}$ with experimental data from FNAL [], BEBC (CERN) [66] and ANL [62]. Solid curve is for the ExRS model while the dotted curve is for the single $\Delta(1232)$ resonance production according to the Rarita-Schwinger approach.

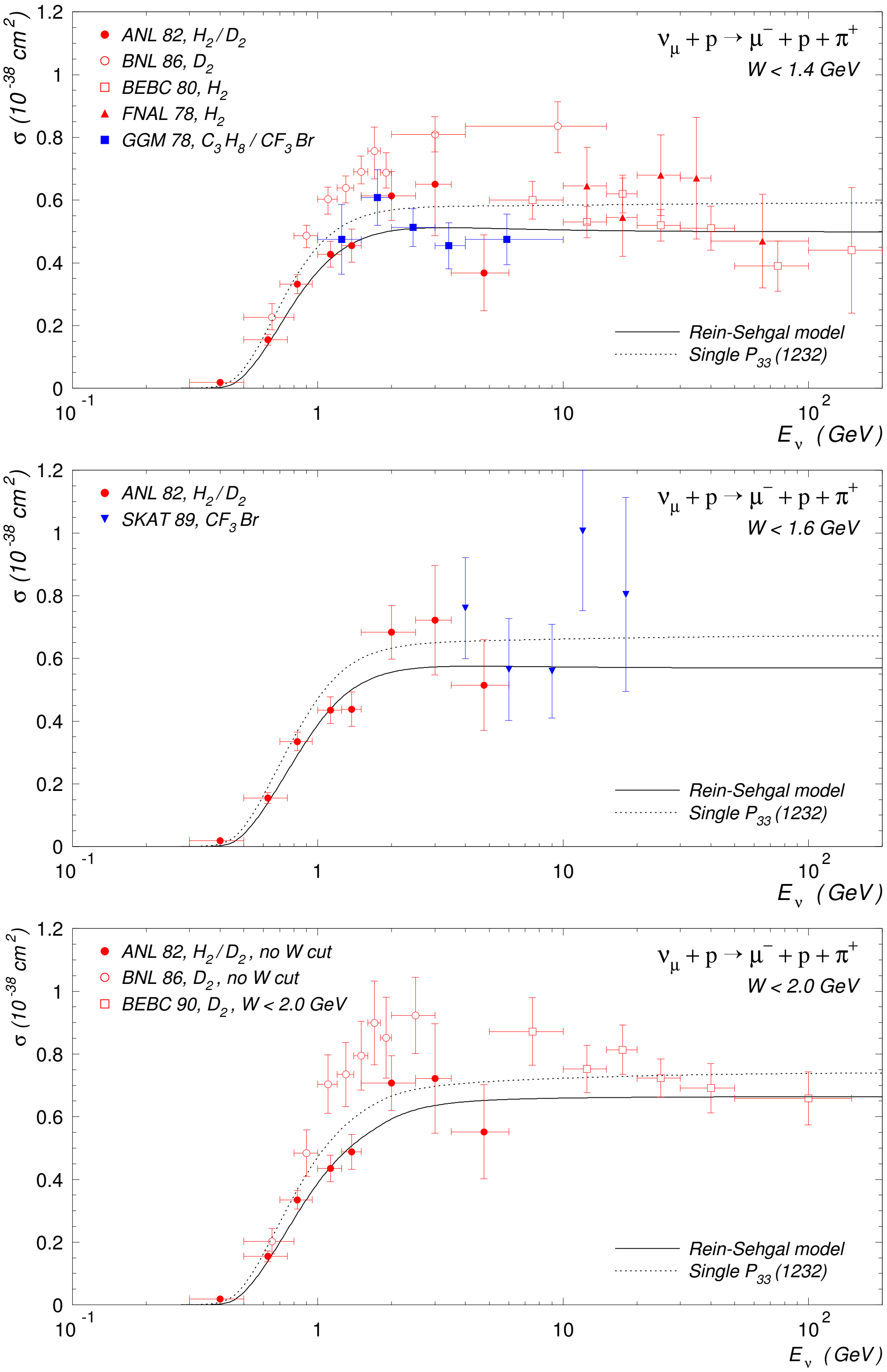

Figure 6.13: Comparison of calculations with experimental data from ANL [62], BNL [54], BEBC (CERN) [17, 66], FNAL [78], GGM (CERN) [71], SKAT (IHEP) [83], for the reaction $\nu_\mu p \to \mu^- p \pi^+$. The data and calculations are for $W < 1.4$ GeV (top panel), $W < 1.6$ GeV (central panel), $W < 2.0$ GeV and with no cutoff (bottom panel). Solid curves are for the ExRS model while the dotted curves are for the single $\Delta(1232)$ resonance production according to the Rarita-Schwinger approach.

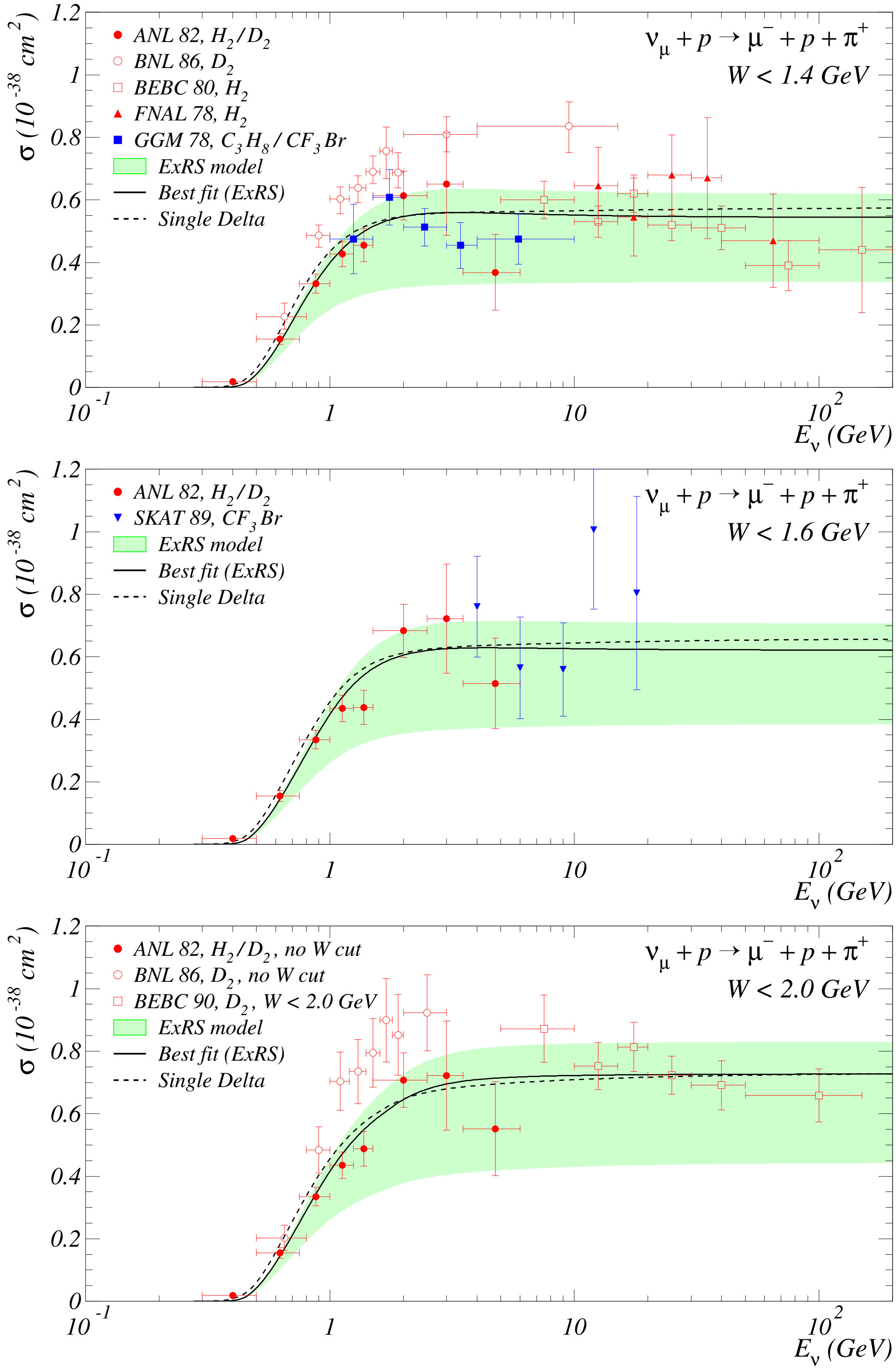

Figure 6.14: Comparison of calculations with experimental data (the same as in Fig. 6.13) for the reaction $\nu_\mu p \to \mu^- p \pi^+$ The filled bands calculated with the ExRS model correspond to variations of M_A from 0.7 to 1.2 GeV$/c^2$, solid curves are for the best global fit value $M_A = 1.09$ GeV$/c^2$. Single $\Delta(1232)$ contribution calculated within the Rarita-Schwinger approach with the best fit value $M_A = 0.99$ GeV$/c^2$ is also shown by dashed curves.

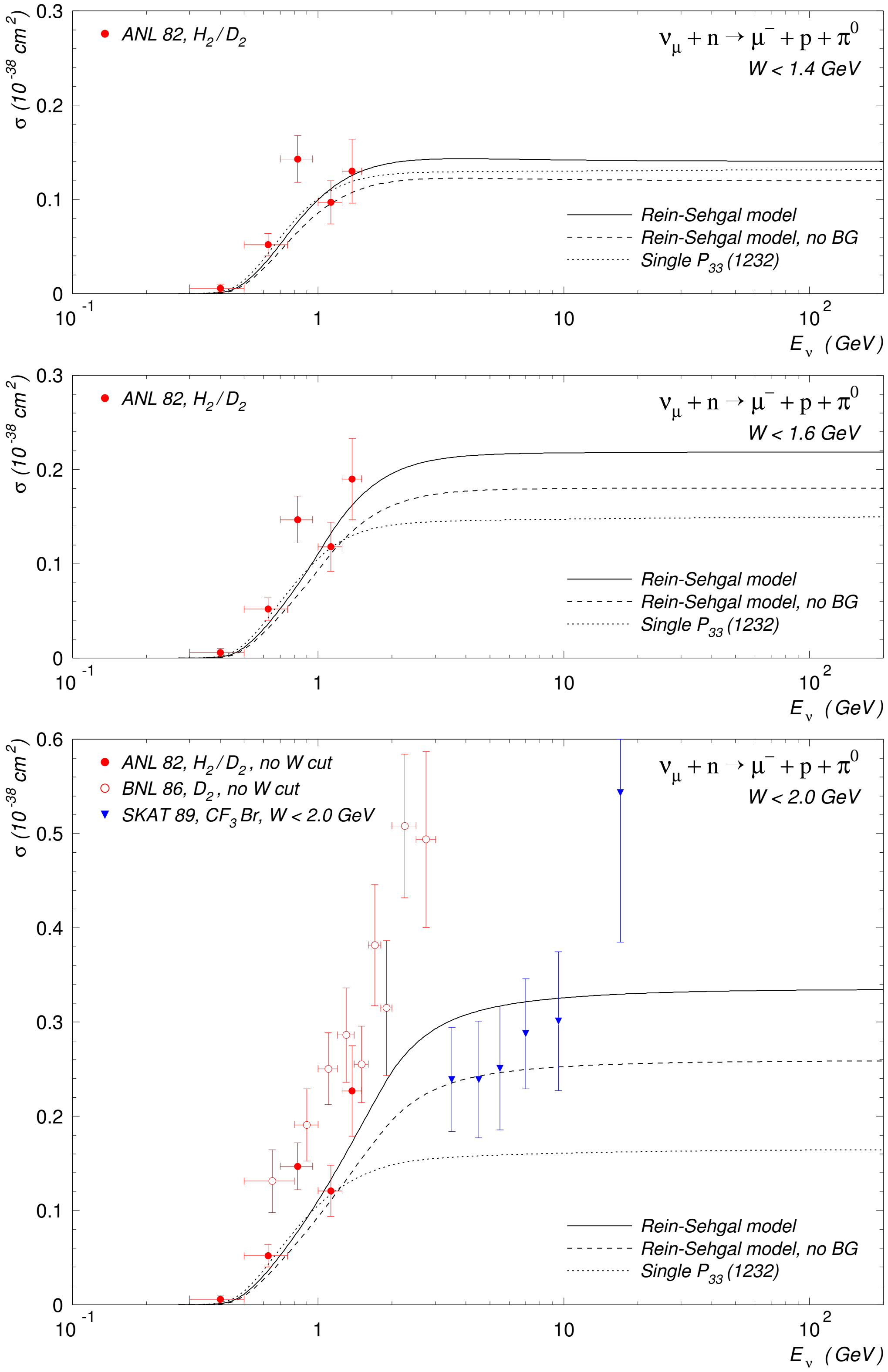

Figure 6.15: Comparison of calculations with experimental data from ANL [62], BNL [54], SKAT (IHEP) [83], for the reaction $\nu_\mu n \to \mu^- p \pi^0$. The data and calculations are for $W < 1.4$ GeV (top panel), $W < 1.6$ GeV (central panel), $W < 2.0$ GeV and with no cutoff (bottom panel). Solid and dashed curves are for the ExRS model with and without nonresonance background contribution, respectively; dotted curves are for the single $\Delta(1232)$ resonance production.

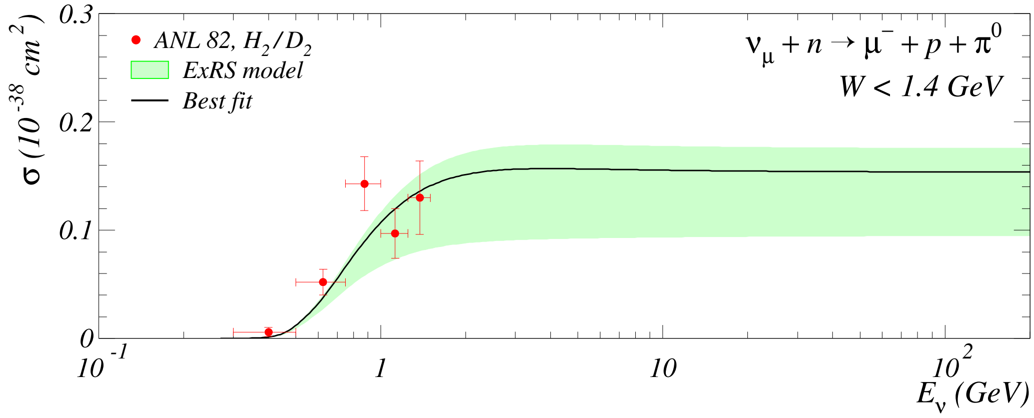

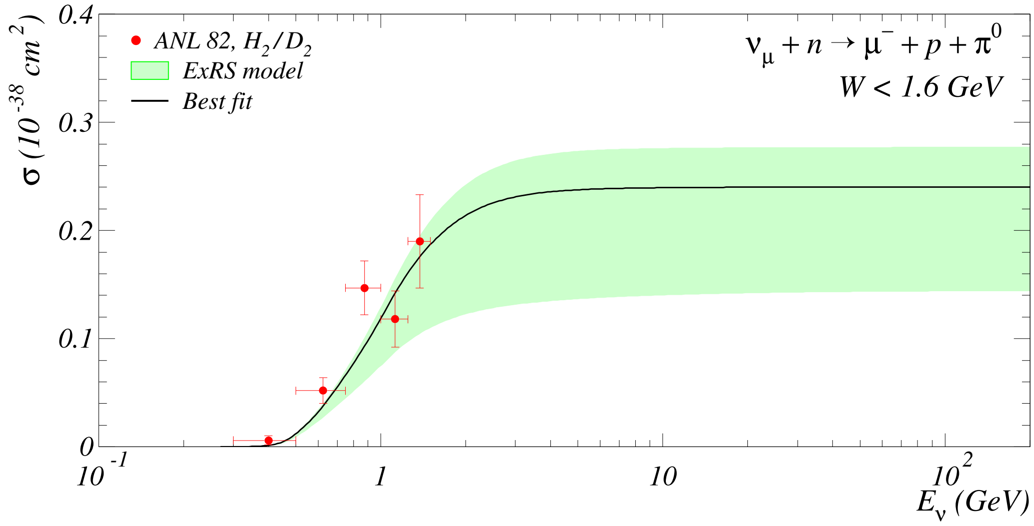

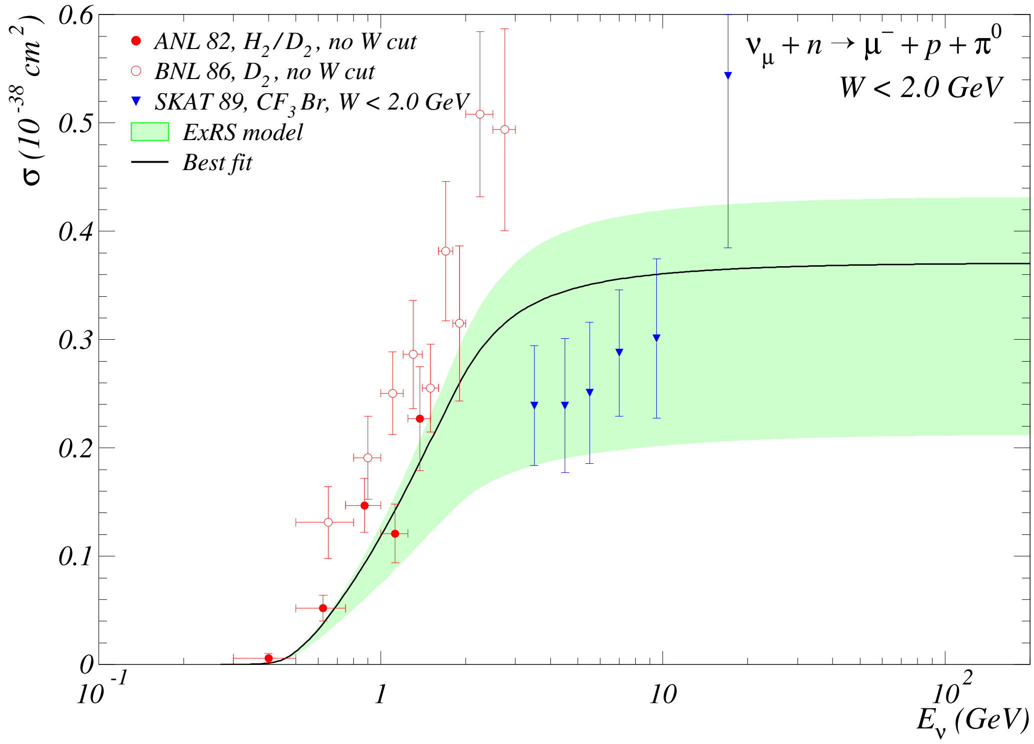

Figure 6.16: Comparison of calculations with experimental data (the same as in Fig. 6.15) for the reaction $\nu_\mu n \to \mu^- p \pi^0$. The filled bands calculated with the ExRS model correspond to variations of M_A from 0.7 to 1.2 GeV$/c^2$, solid curves are for the best global fit value $M_A = 1.09$ GeV$/c^2$.

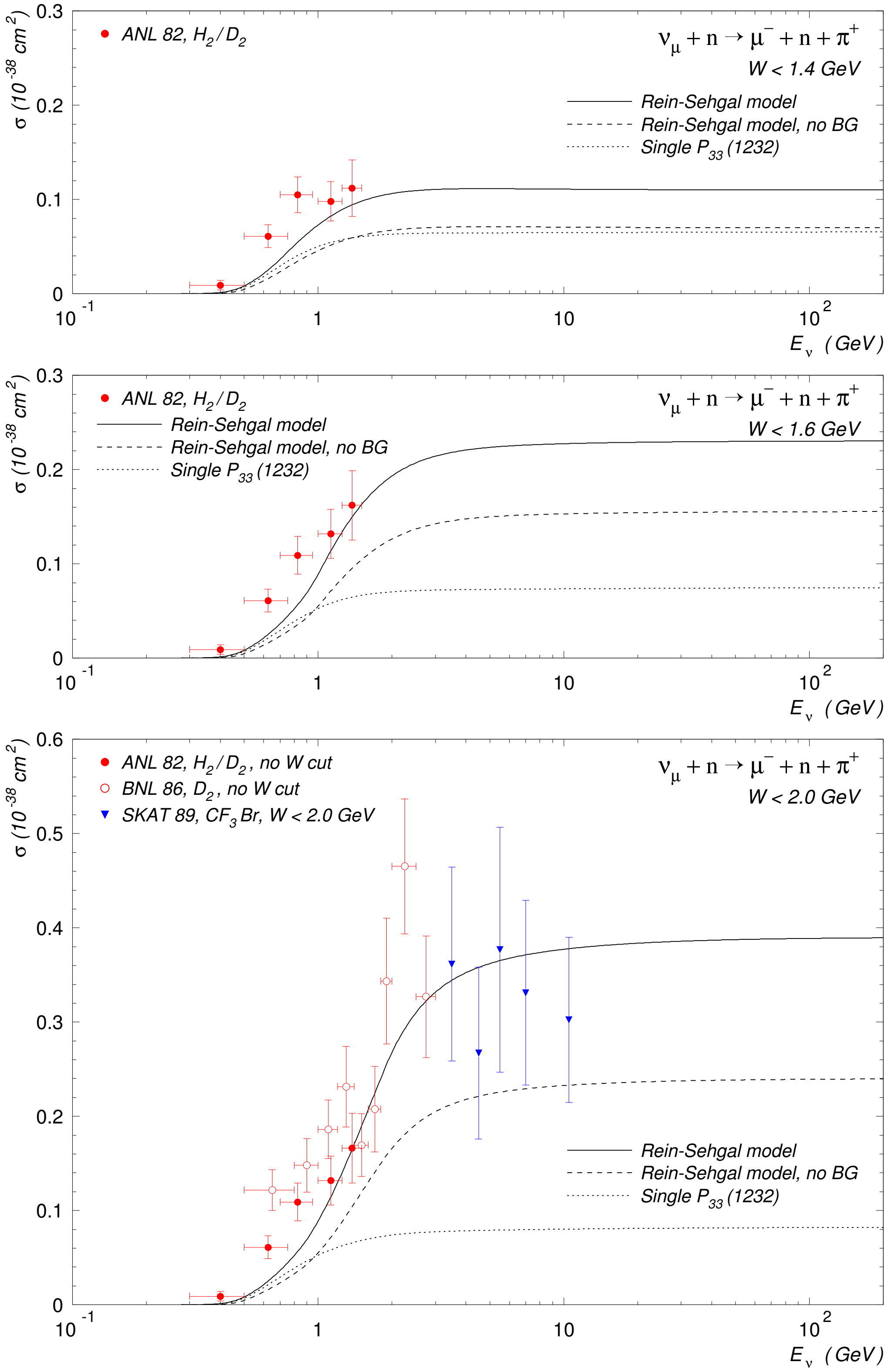

Figure 6.17: Comparison of calculations with experimental data from ANL [62], BNL [54], SKAT (IHEP) [83], for the reaction $\nu_\mu n \to \mu^- n \pi^+$. The data and calculations are for $W < 1.4$ GeV (top panel), $W < 1.6$ GeV (central panel), $W < 2.0$ GeV and with no cutoff (bottom panel). Solid and dashed curves are for the ExRS model with and without nonresonance background contribution, respectively; dotted curves are for the single $\Delta(1232)$ resonance production.

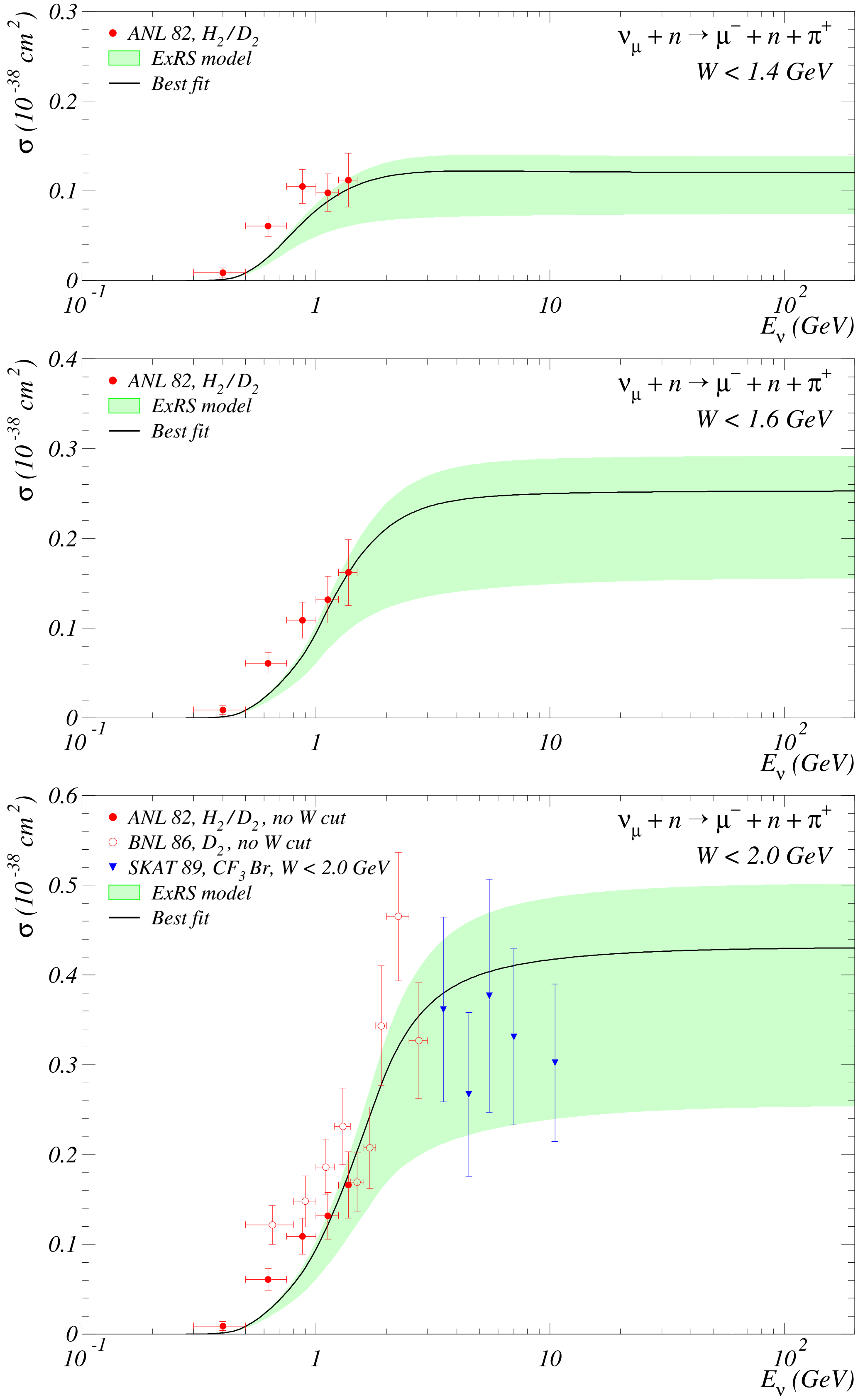

Figure 6.18: Comparison of calculations with experimental data (the same as in Fig. 6.17) for the reaction $\nu_\mu n \to \mu^- n\pi^+$. The filled bands calculated with the ExRS model correspond to variations of M_A from 0.7 to 1.2 GeV$/c^2$, solid curves are for the best global fit value $M_A = 1.09$ GeV$/c^2$.

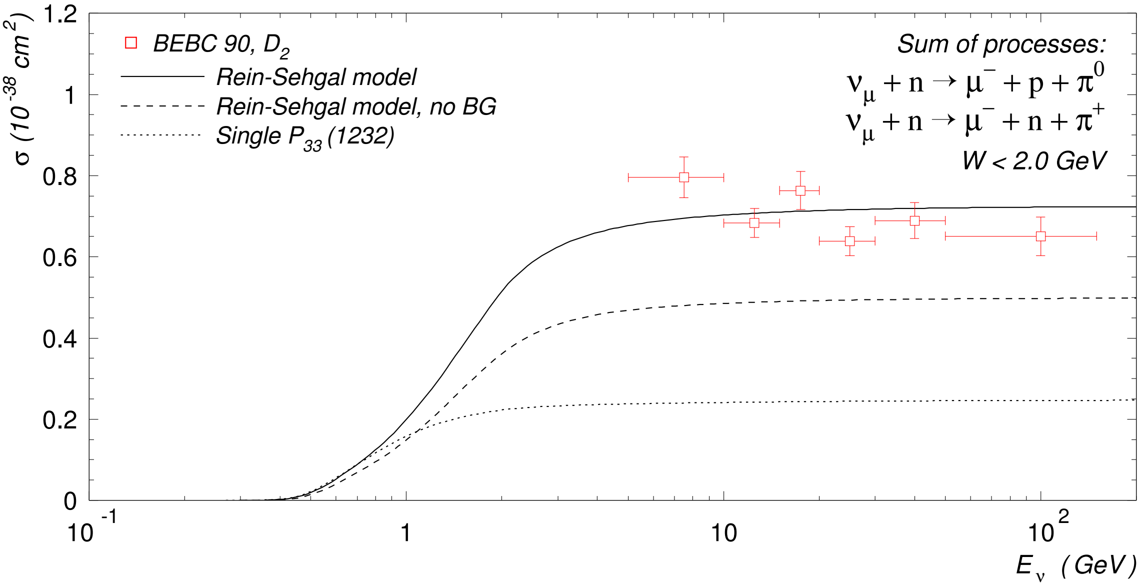

Figure 6.19: Comparison of the calculations with the experimental data from BEBC (CERN) [17] for the sum of cross sections for the reactions $\nu_\mu n \to \mu^- p\pi^0$ and $\nu_\mu n \to \mu^- n\pi^+$. The data and calculations are for $W < 2.0$ GeV. The curves have the same meaning as in Fig. 6.15.

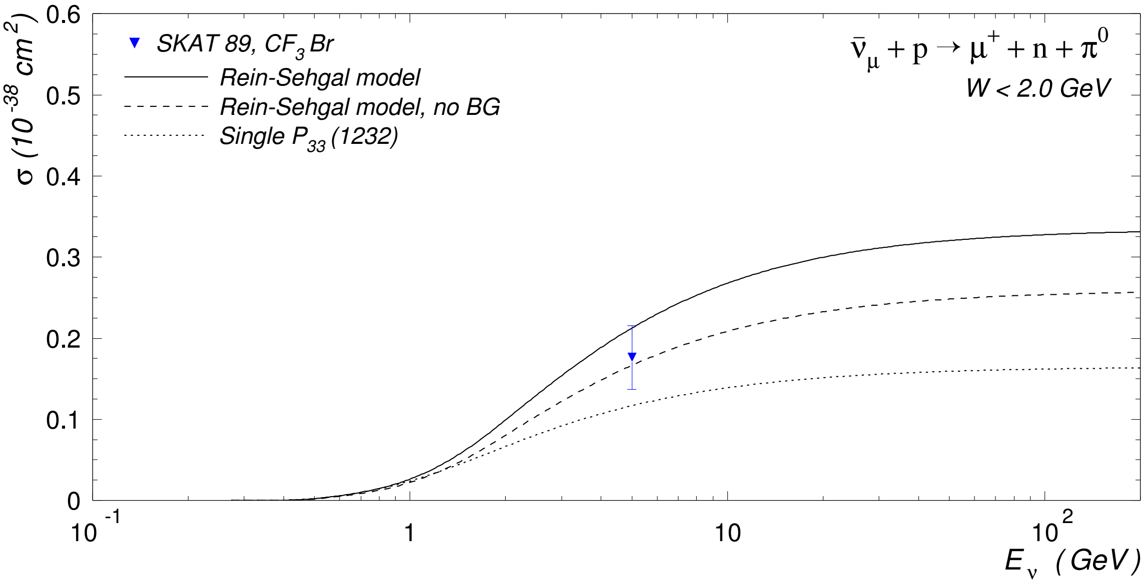

Figure 6.20: Comparison of the calculations with the experimental data from SKAT (IHEP) [83] for the reaction $\overline{\nu}_\mu p \to \mu^+ n\pi^0$. The data and calculations are for $W < 2.0$ GeV. The curves have the same meaning as in Fig. 6.15.

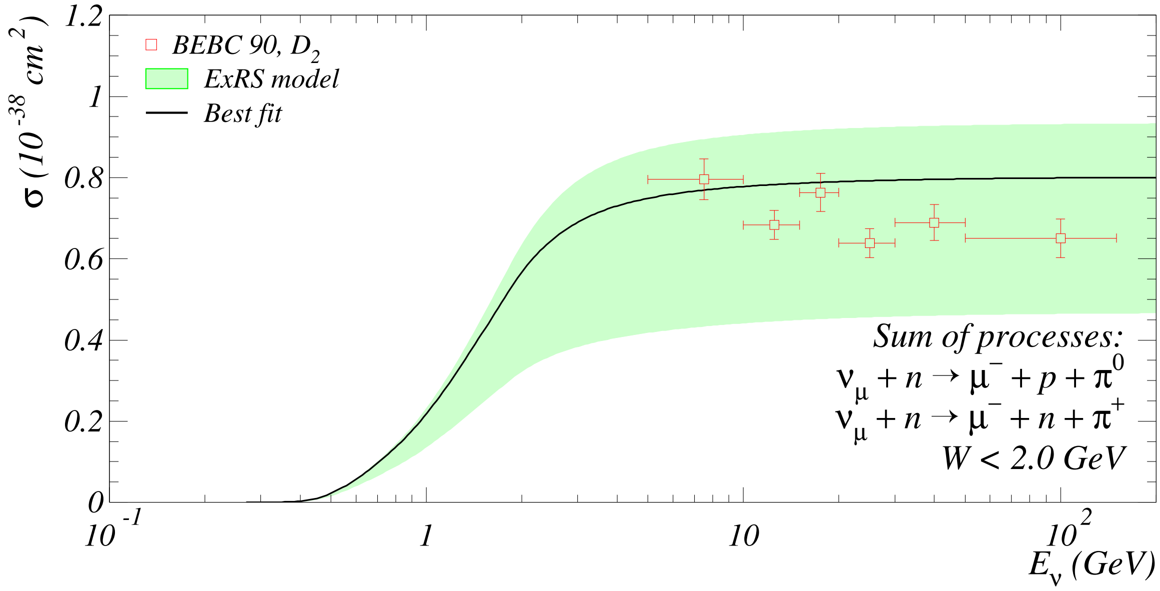

Figure 6.21: Comparison of the calculations with the experimental data (the same as in Fig. 6.20) for the sum of cross sections for the reactions $\nu_\mu n \to \mu^- p\pi^0$ and $\nu_\mu n \to \mu^- n\pi^+$. The band and curve have the same meaning as in Fig. 6.16.

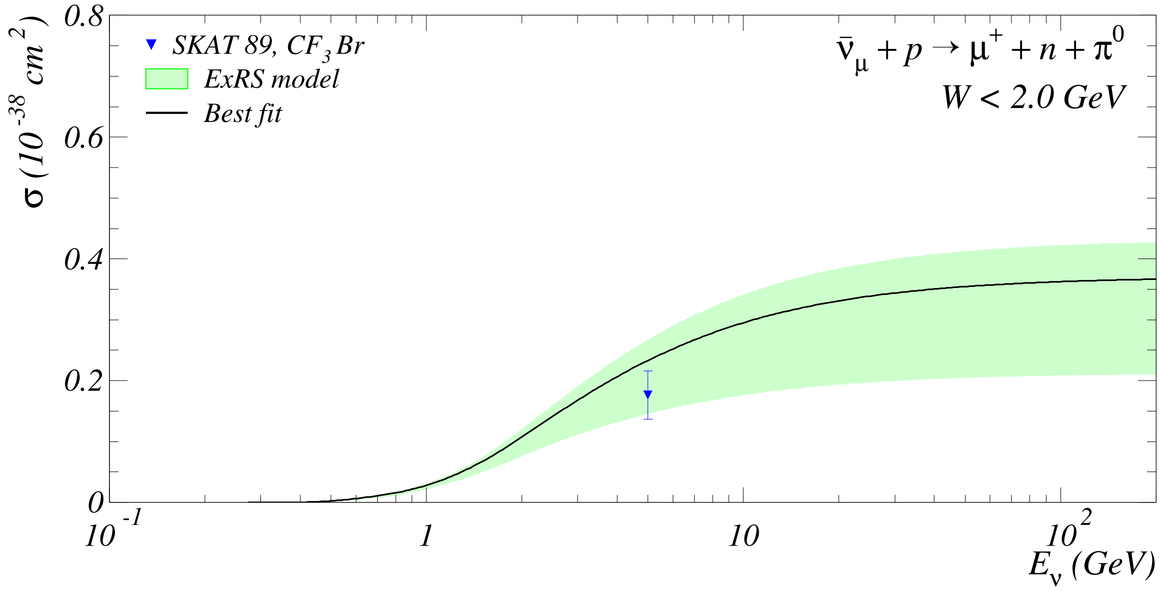

Figure 6.22: Comparison of the calculations with the experimental data (the same as in Fig. 6.20) for the reaction $\overline{\nu}_\mu p \to \mu^+ n\pi^0$. The band and curve have the same meaning as in Fig. 6.16.

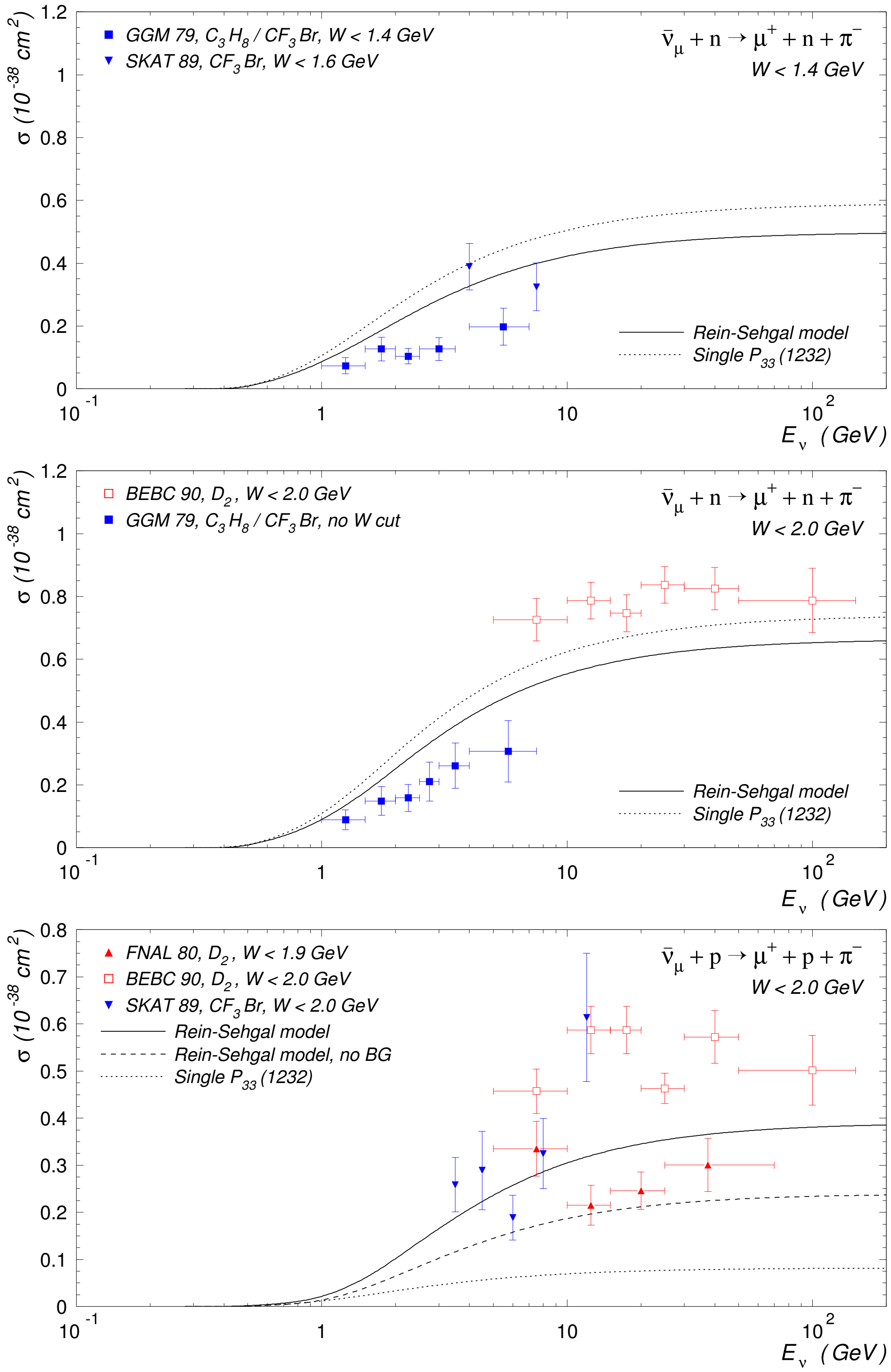

Figure 6.23: Comparison of calculations with experimental data from GGM (CERN) [73], SKAT (IHEP) [83], BEBC (CERN) [17], FNAL [80], for the reactions $\overline{\nu}_\mu n \to \mu^+ n \pi^-$ and $\overline{\nu}_\mu p \to \mu^+ p \pi^-$. The data and calculations are for $W < 1.4$ GeV (top panel) and $W < 2.0$ GeV (central panel) and $W < 1.9$ GeV and $W < 2.0$ GeV (bottom panel). Solid and dashed curves are for the ExRS model with and without nonresonance background contribution, respectively; dotted curves are for the single $\Delta(1232)$ resonance production.

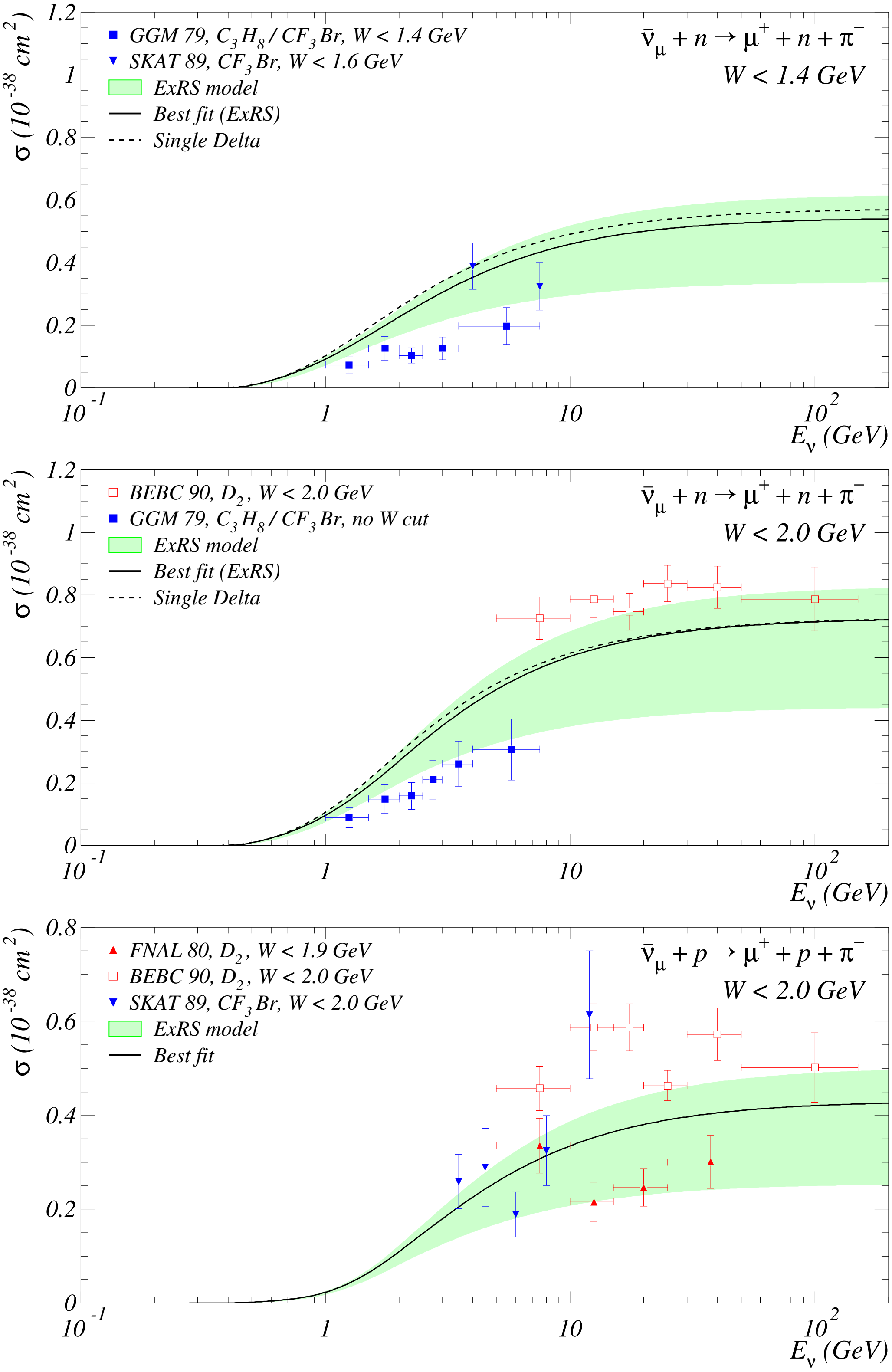

Figure 6.24: Comparison of calculations with experimental data (the same as in Fig. 6.23) for the reactions $\overline{\nu}_\mu n \to \mu^+ n\pi^-$ and $\overline{\nu}_\mu p \to \mu^+ p\pi^-$. The band and curve have the same meaning as in Fig. 6.16.

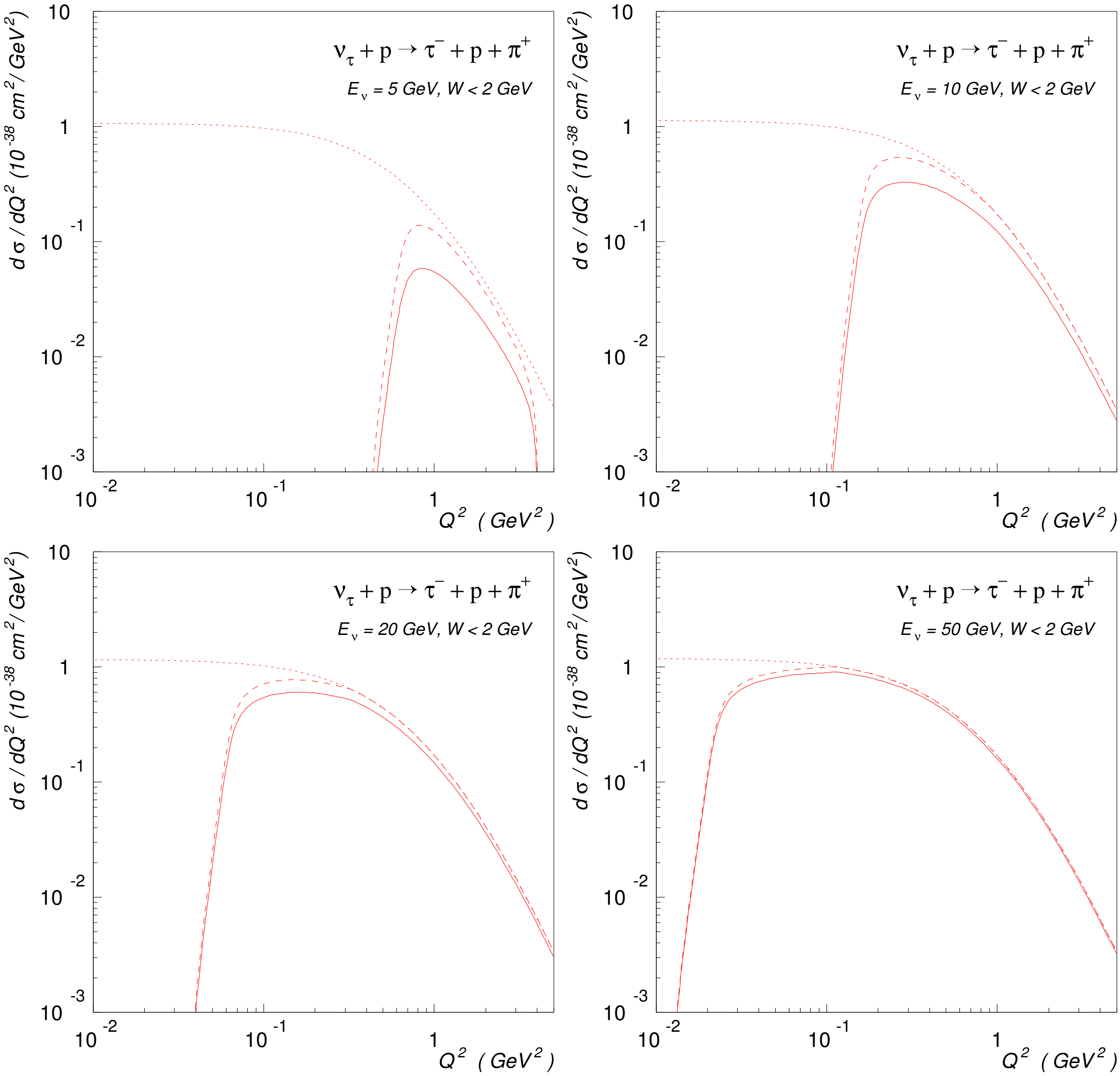

Figure 6.25: Effect of lepton mass for the differential cross section $\nu_\tau p \to \tau^- p \pi^+$ at $E_\nu = 5, 10, 20, 50$ GeV and $W < 2$ GeV. Dotted and dashed curves are, respectively, for the standard RS model with zero lepton and with the mass included only into kinematics only; solid curves are for the extended RS model in which the τ lepton mass is included in both kinematics and dynamics.

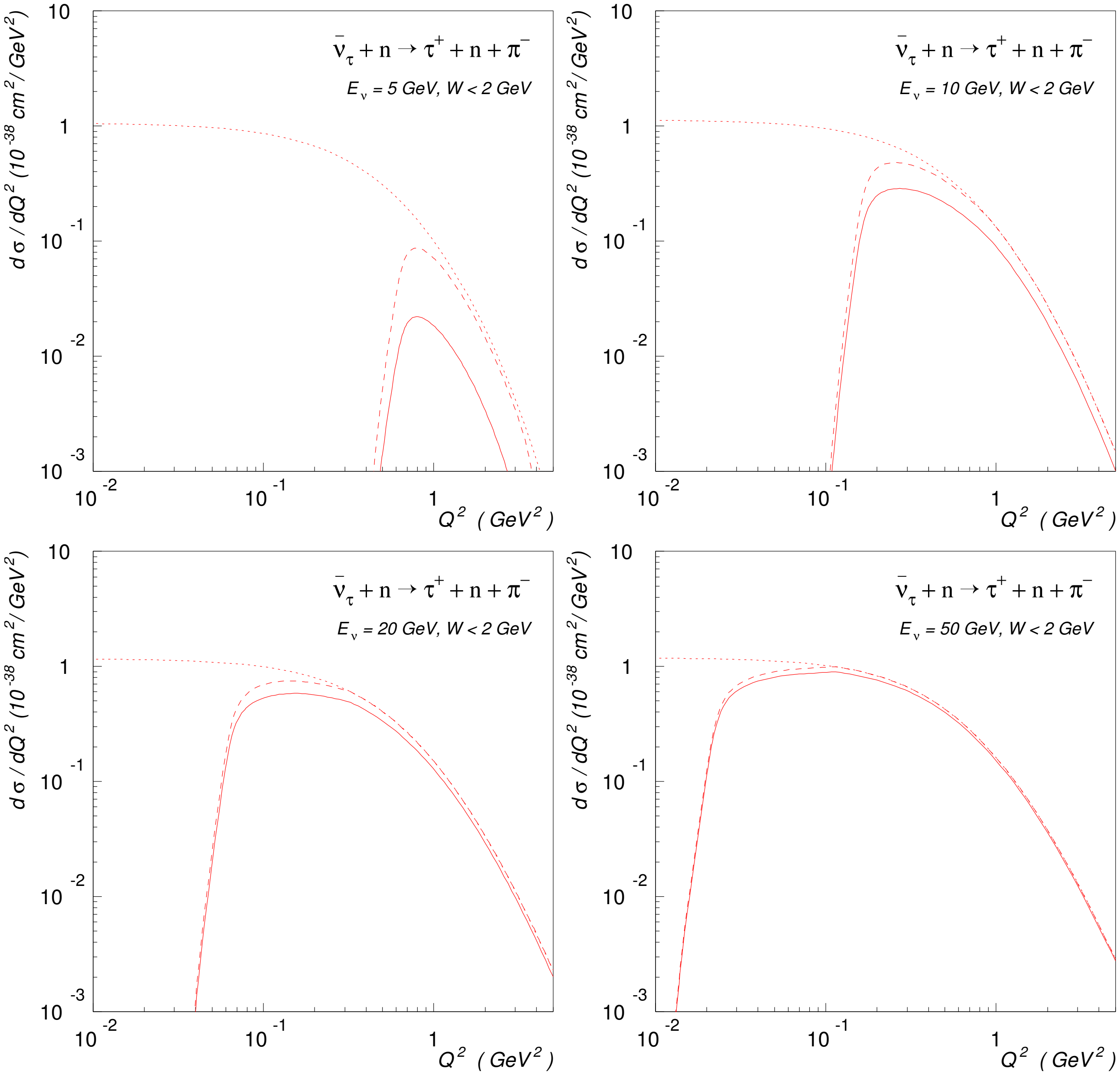

Figure 6.26: The same as in Fig. 6.25 but for the reaction $\overline{\nu}_\tau n \to \tau^- n\pi^+$.

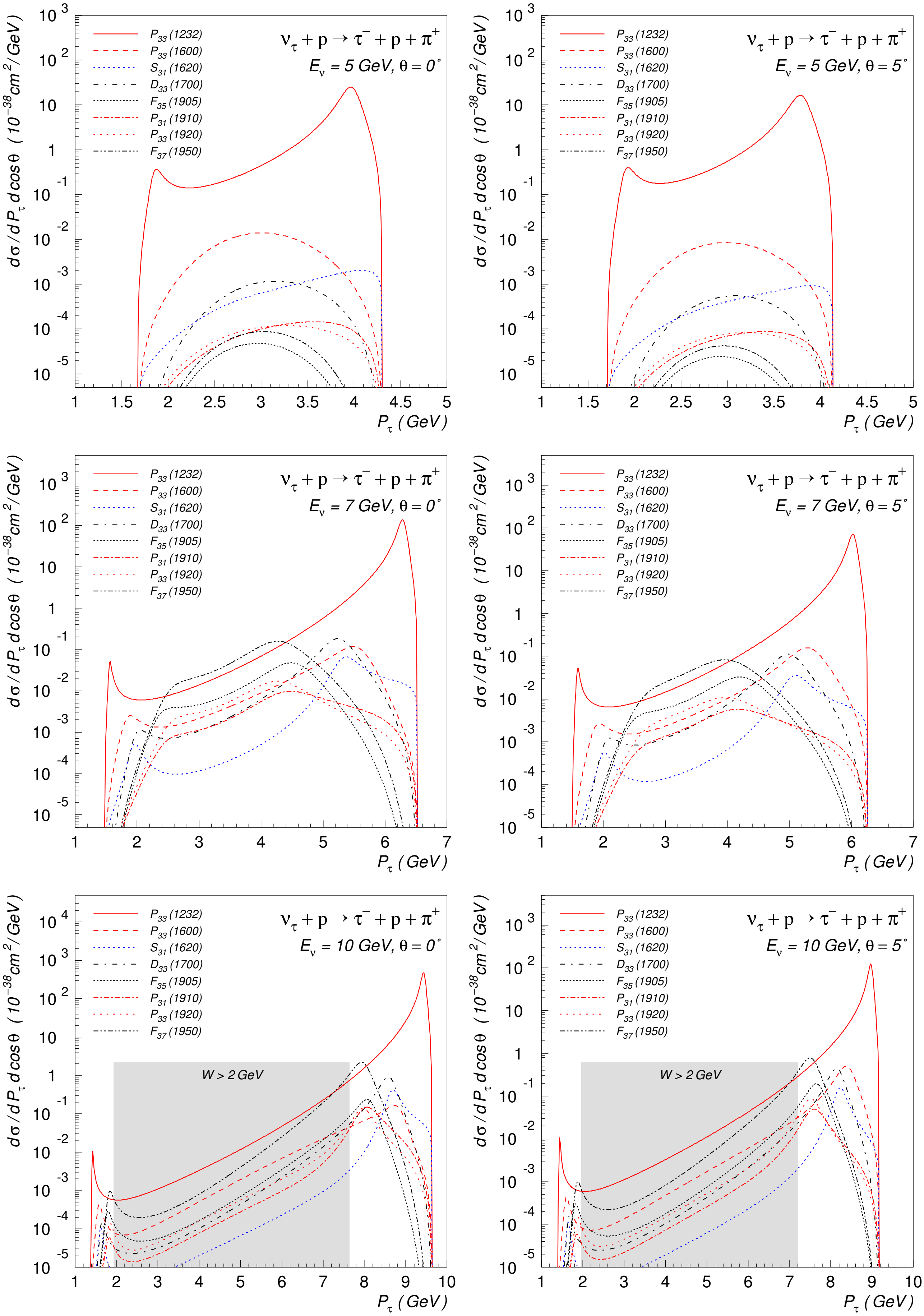

Figure 6.27: Contributions of different resonasnces to the double differential cross sections for the reaction $\nu_\tau p \rightarrow \tau^- p \pi^+$ at three neutrino energies and two scattering angles.

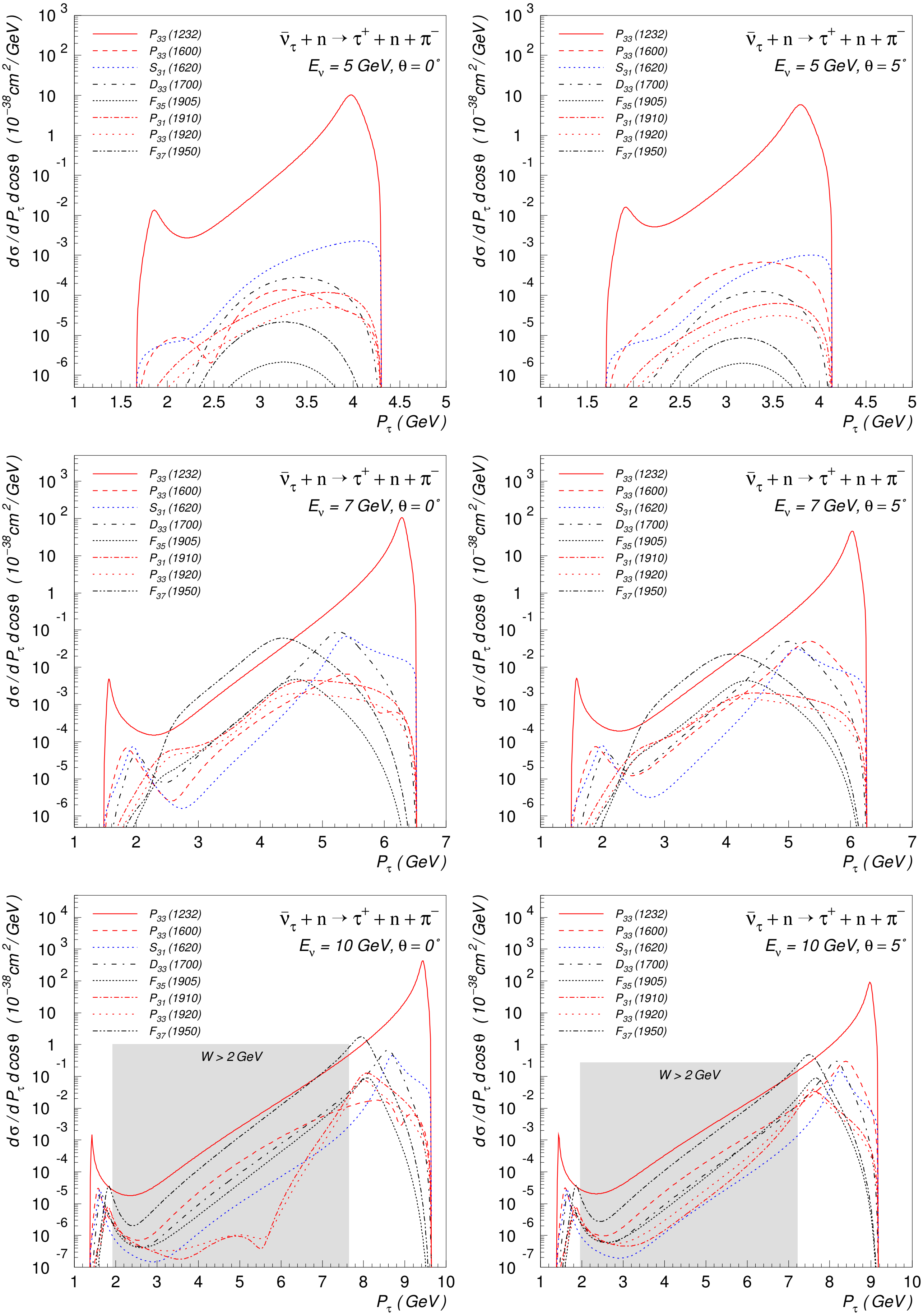

Figure 6.28: Contributions of different resonasnces to the double differential cross sections for the reaction $\overline{\nu}_\tau n \to \tau^+ n \pi^-$ at three neutrino energies and two scattering angles.

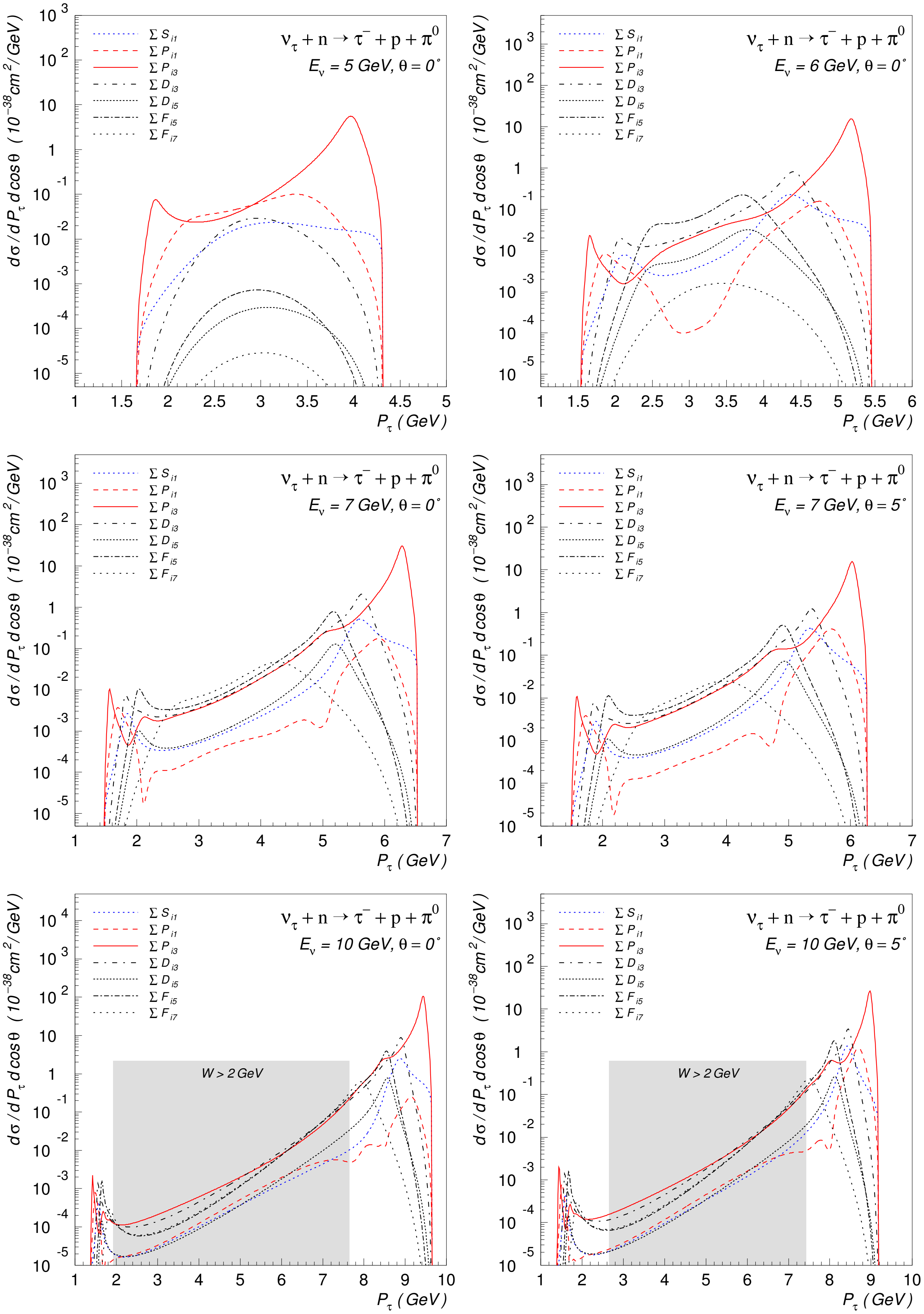

Figure 6.29: Contributions of different resonasnces to the double differential cross sections for the reaction $\nu_\tau n \to \tau^- p \pi^0$ at three neutrino energies and two scattering angles.

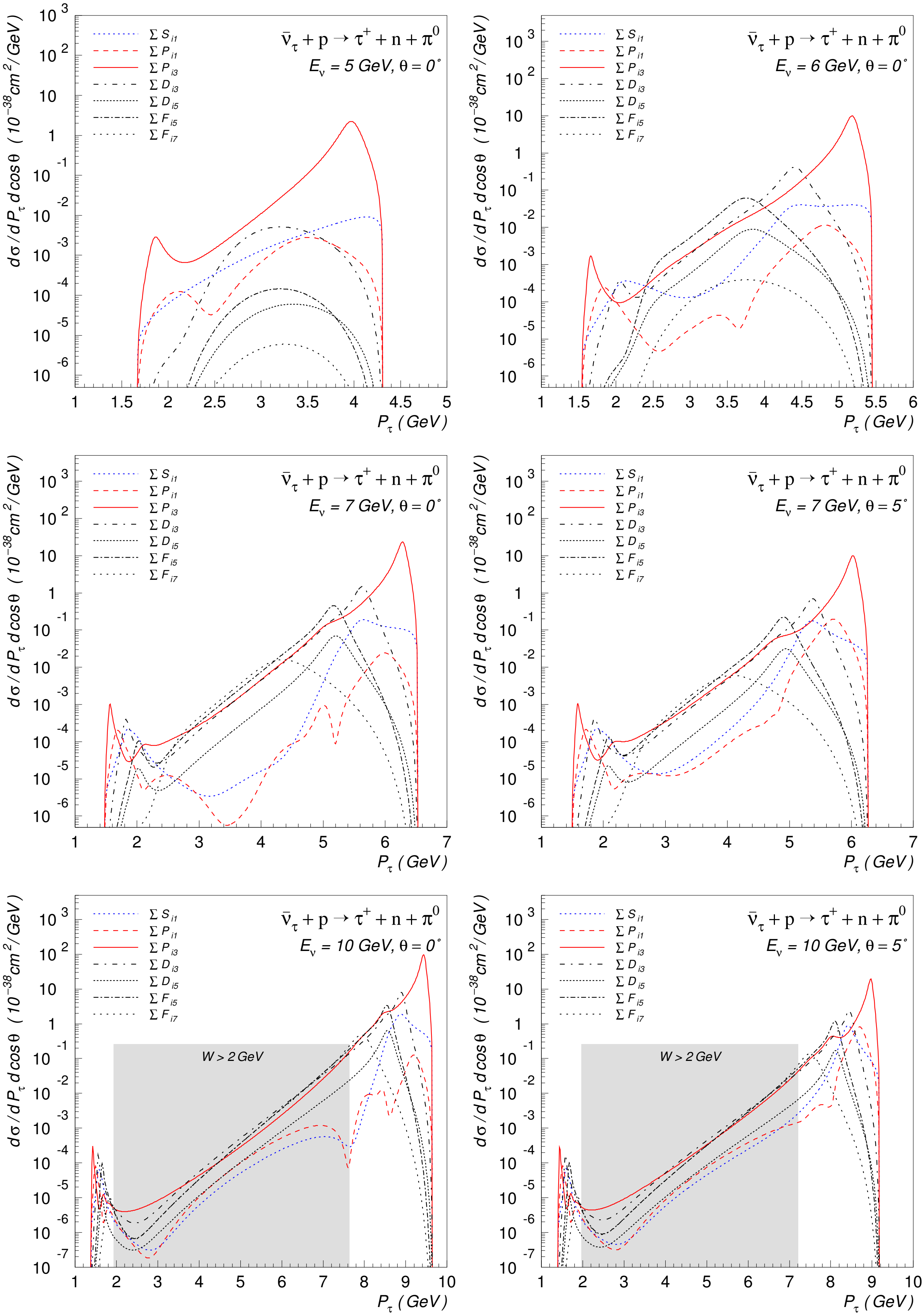

Figure 6.30: Contributions of different resonasnces to the double differential cross sections for the reaction $\overline{\nu}_\tau p \to \tau^+ n \pi^0$ at three neutrino energies and two scattering angles.

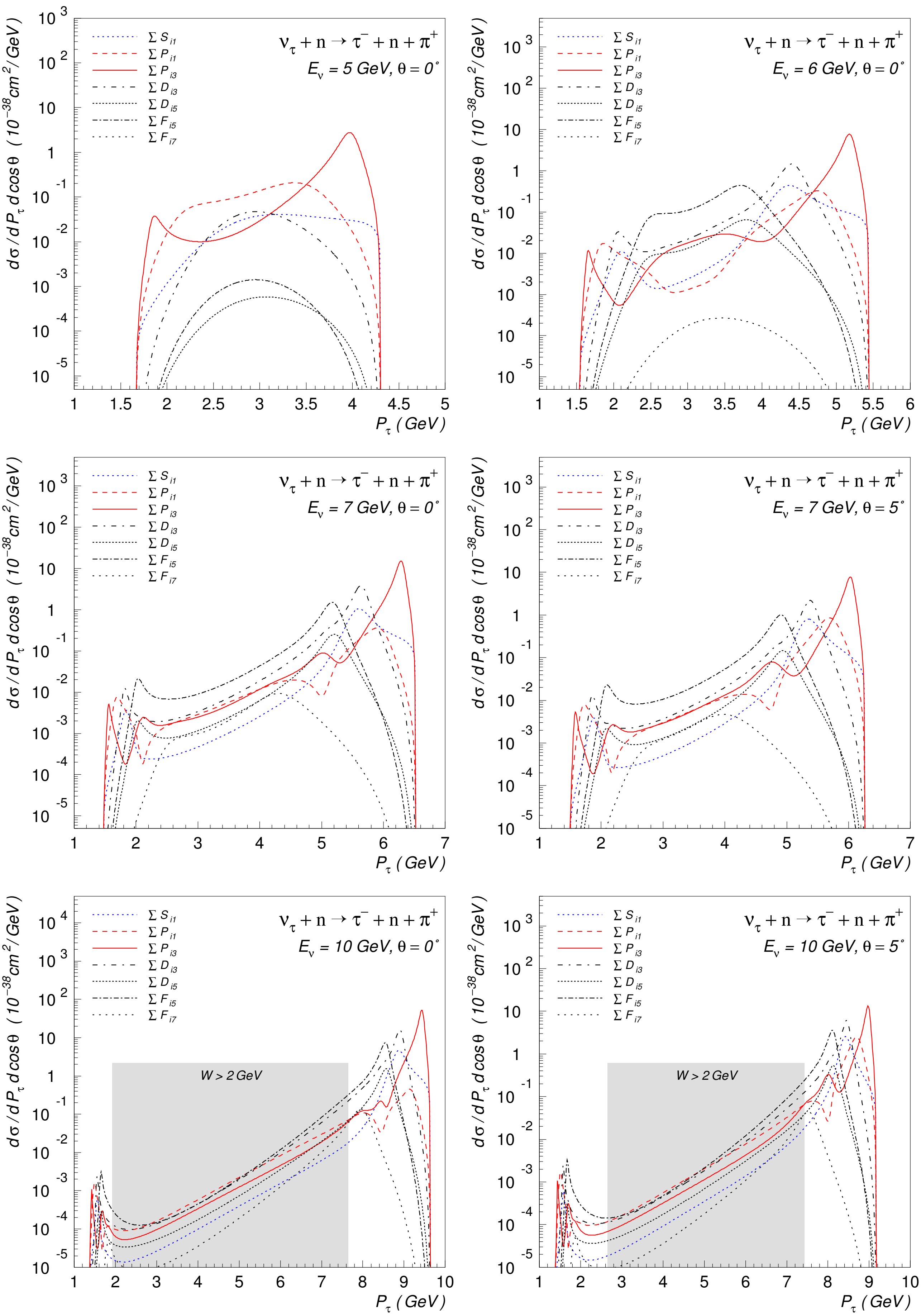

Figure 6.31: Contributions of different resonasnces to the double differential cross sections for the reaction $\nu_\tau n \rightarrow \tau^- n \pi^+$ at three neutrino energies and two scattering angles.

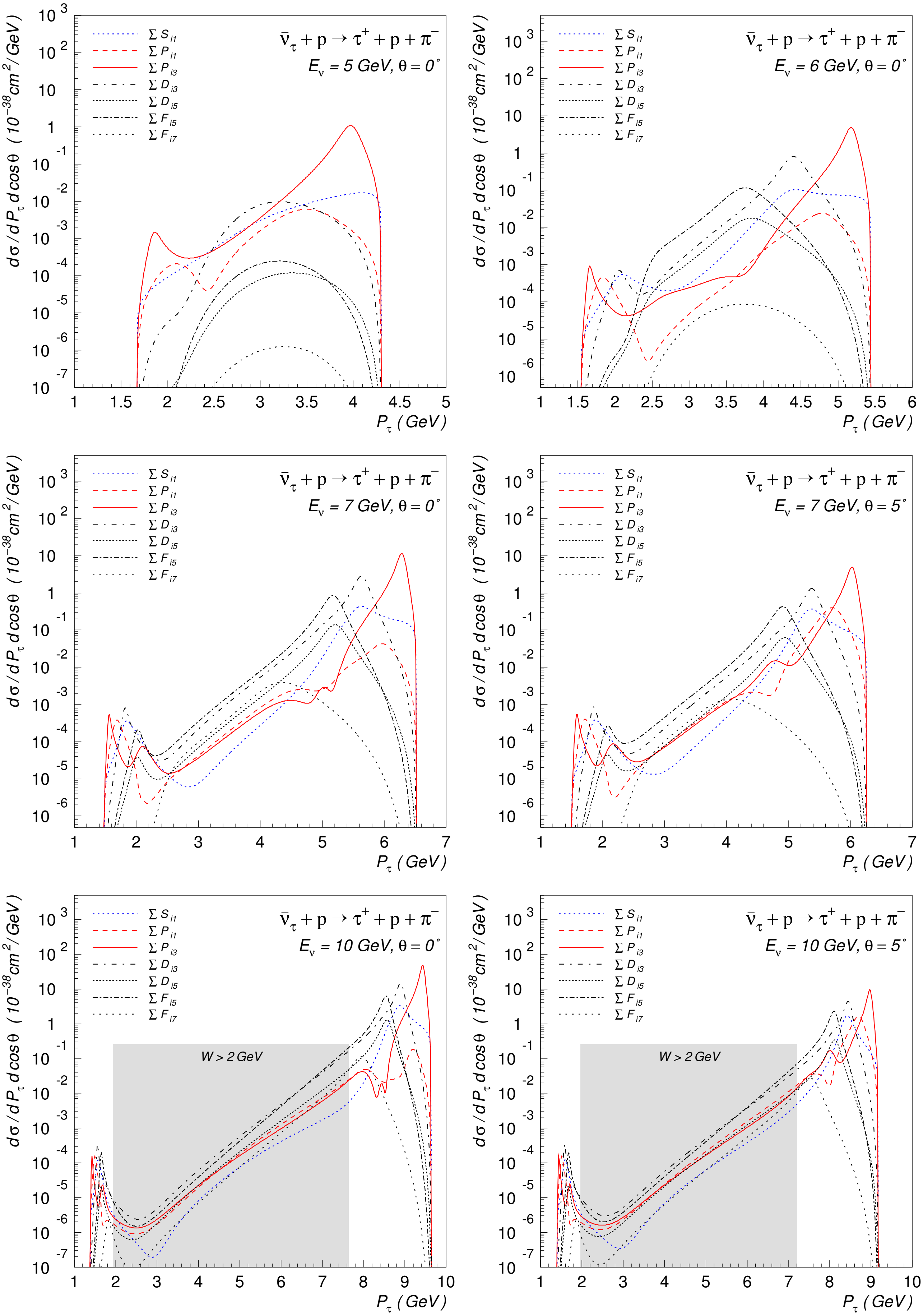

Figure 6.32: Contributions of different resonasnces to the double differential cross sections for the reaction $\overline{\nu}_\tau p \to \tau^+ p \pi^-$ at three neutrino energies and two scattering angles.

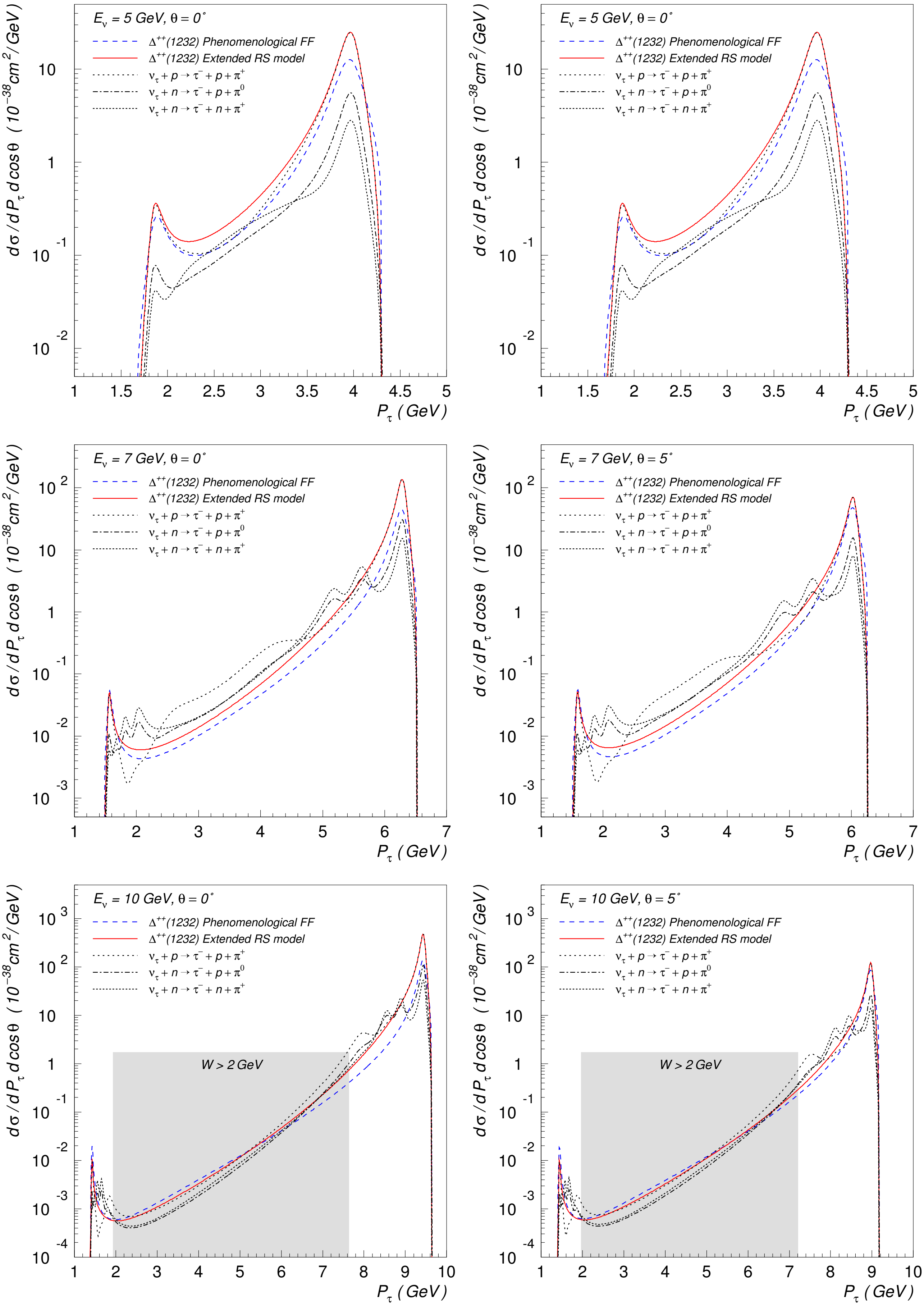

Figure 6.33: Comparison of the double differential cross sections for different ν_τ induced CC1π reactions at three energies and two scattering angles. Also shown are the cross sections for $\Delta^{++}(1232)$ production.

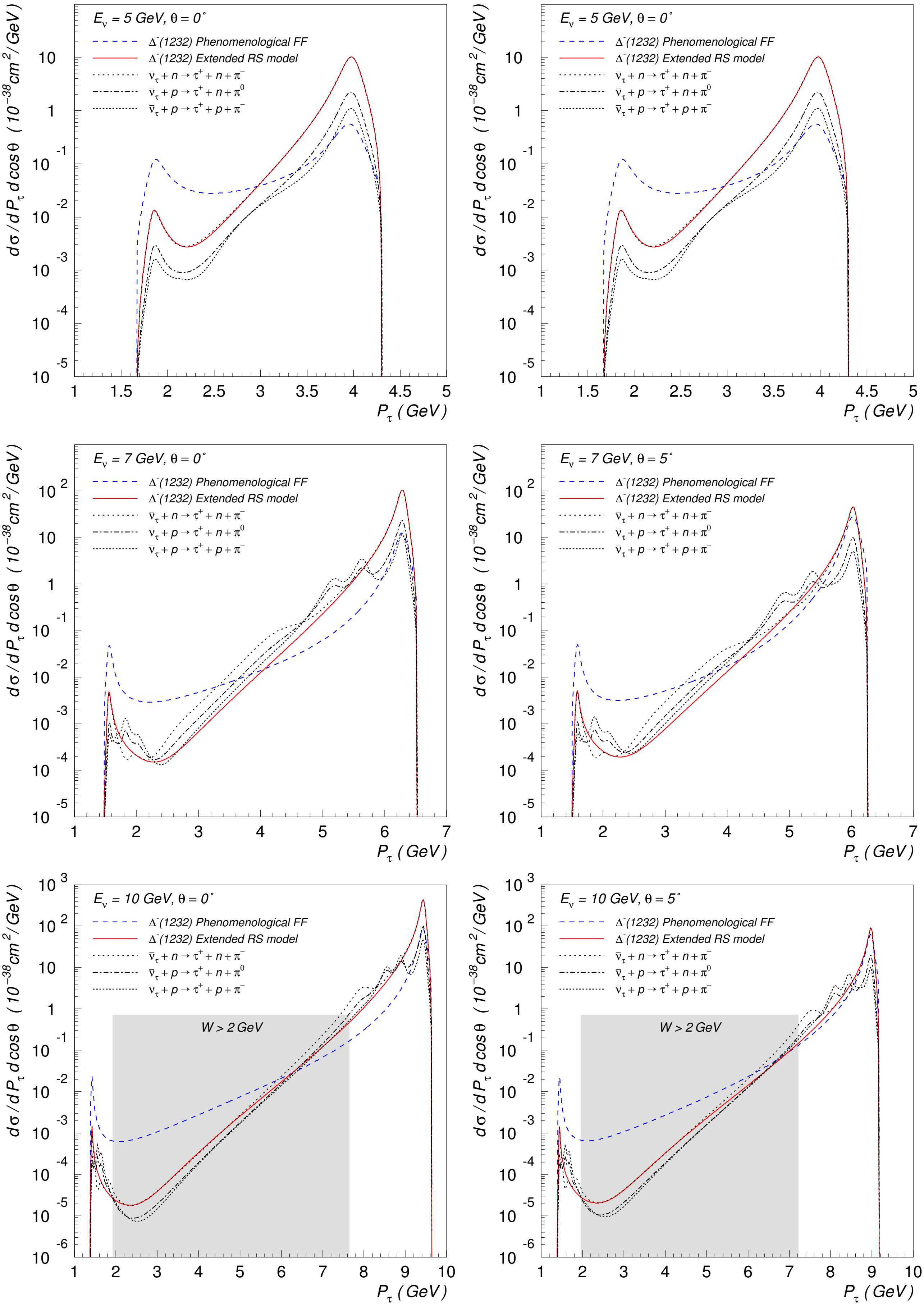

Figure 6.34: Comparison of the double differential cross sections for different $\overline{\nu}_\tau$ induced CC1π reactions at three energies and two scattering angles. Also shown are the cross sections for $\Delta^-(1232)$ production.

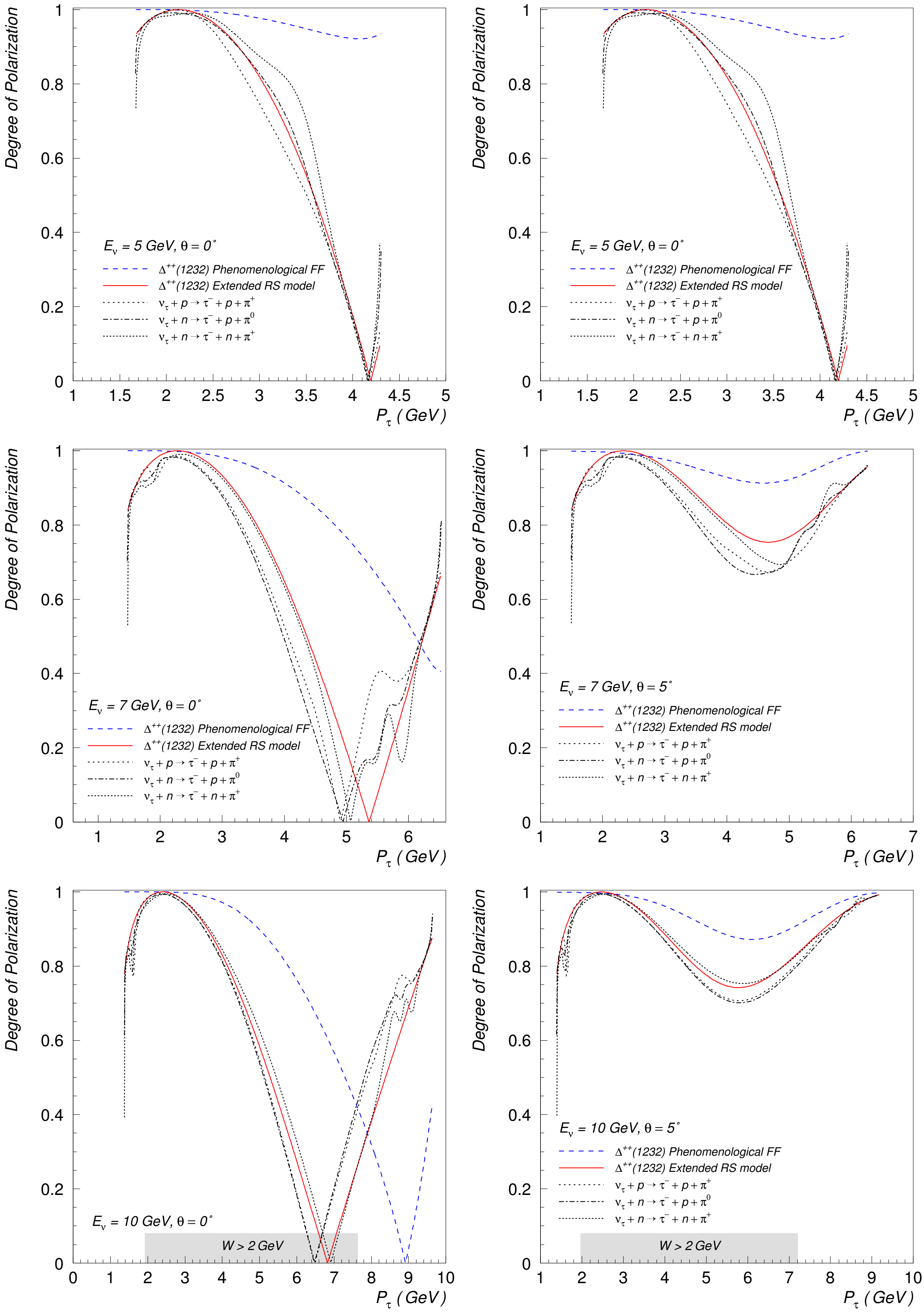

Figure 6.35: Comparison of the degree of polarization of τ^- lepton for different ν_τ induced CC1π reactions at three energies and two scattering angles. Also shown are the τ^- degrees of polarization for $\Delta^{++}(1232)$ production.

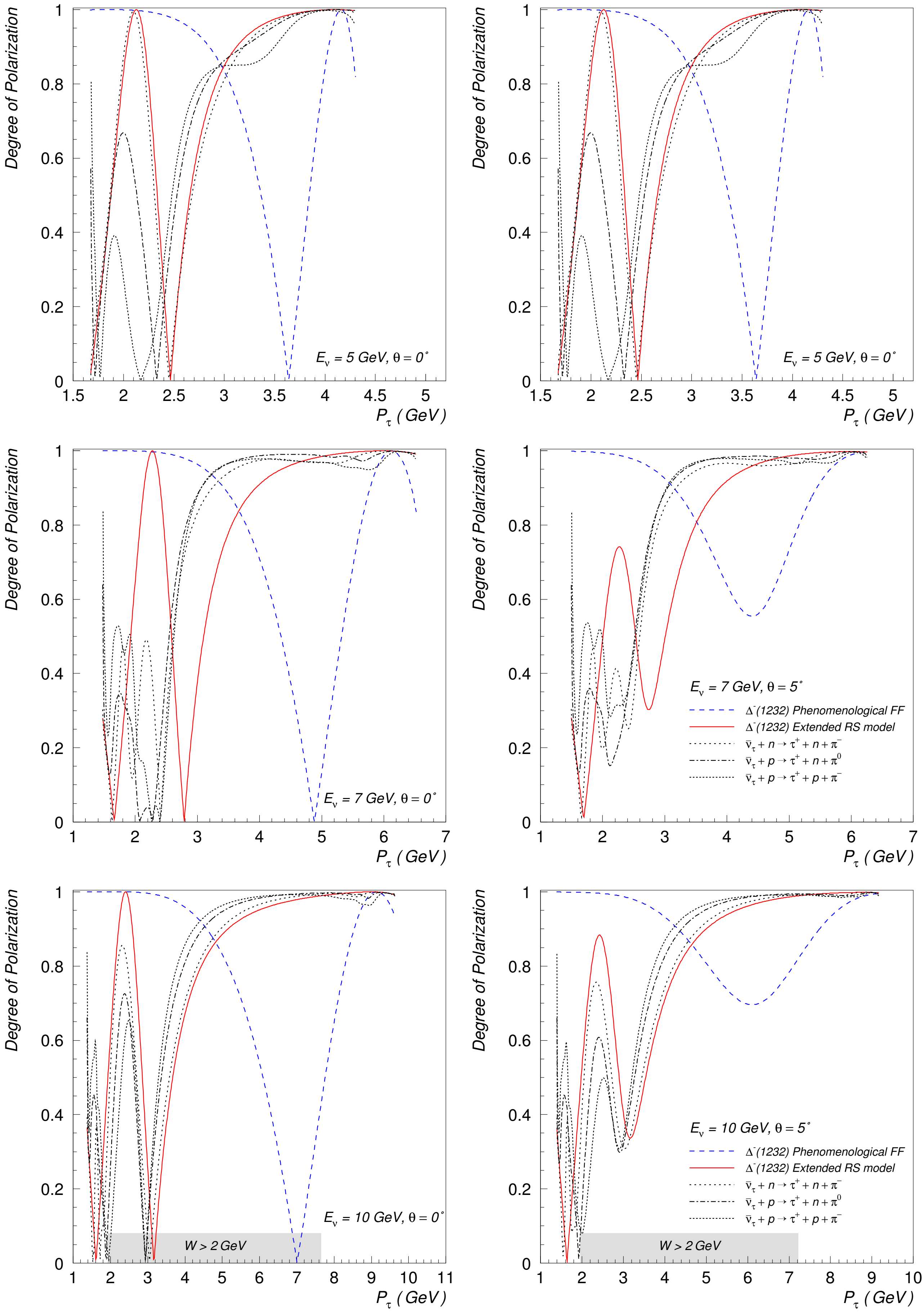

Figure 6.36: Comparison of the degree of polarization of τ^+ lepton for different $\overline{\nu}_\tau$ induced CC1π reactions at three energies and two scattering angles. Also shown are the τ^+ degrees of polarization for $\Delta^-(1232)$ production.

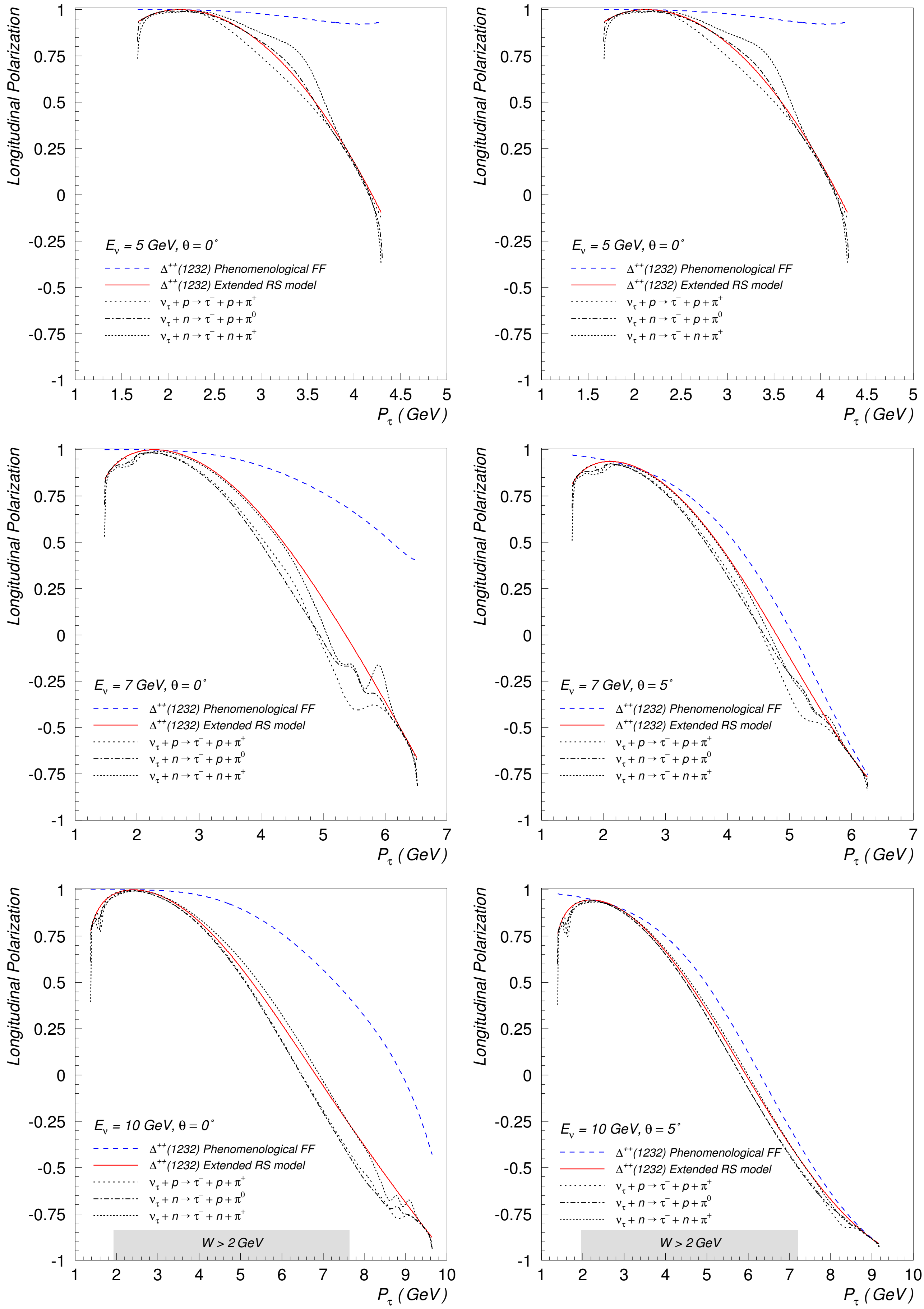

Figure 6.37: Comparison of the longitudinal polarization of τ^- lepton for different ν_τ induced CC1π reactions at three energies and two scattering angles. Also shown are the longitudinal polarizations of τ^- for $\Delta^{++}(1232)$ production.

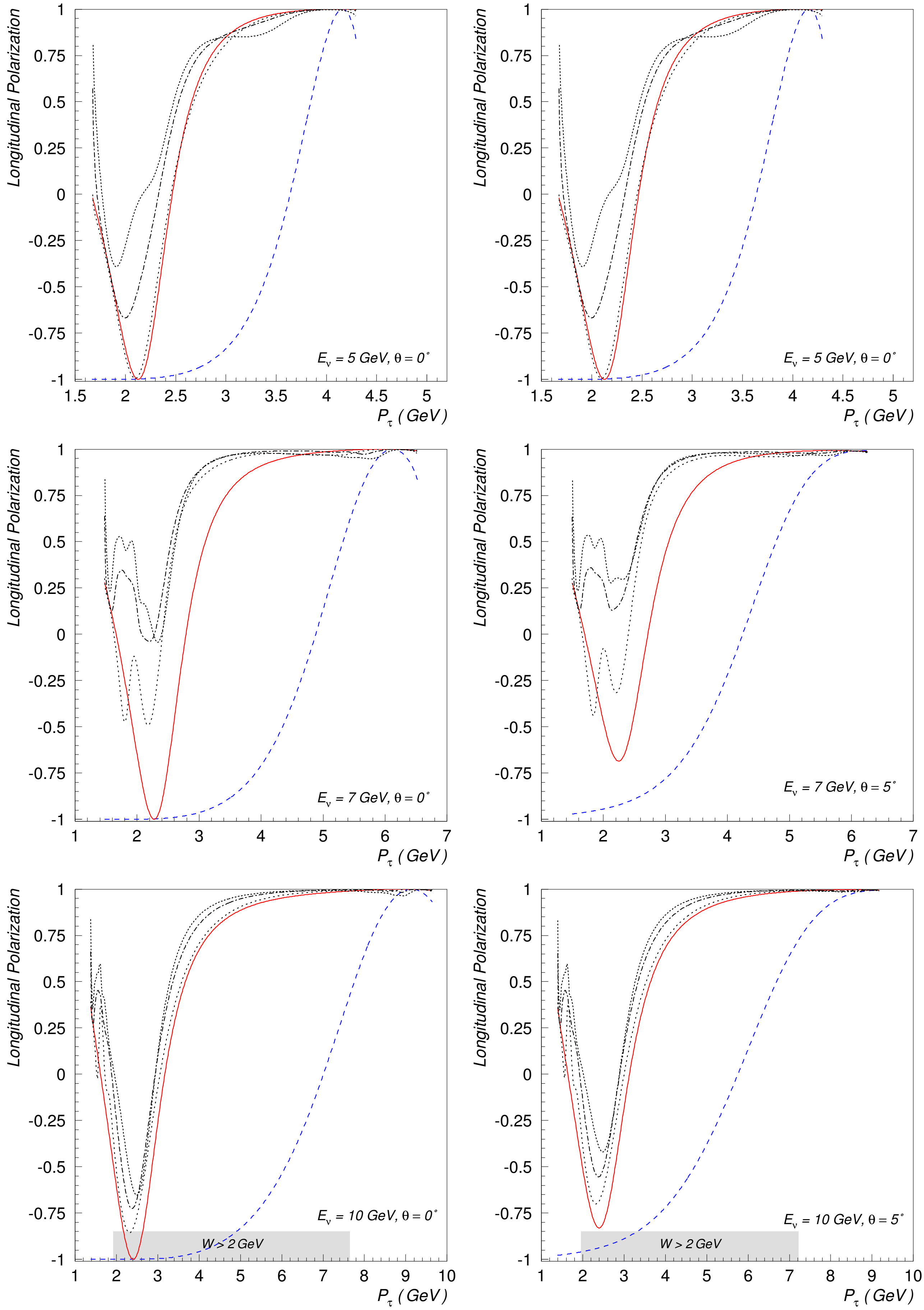

Figure 6.38: Comparison of the longitudinal polarization of τ^+ lepton for different $\overline{\nu}_\tau$ induced CC1π reactions at three energies and two scattering angles. Also shown are the longitudinal polarizations of τ^+ for $\Delta^-(1232)$ production.

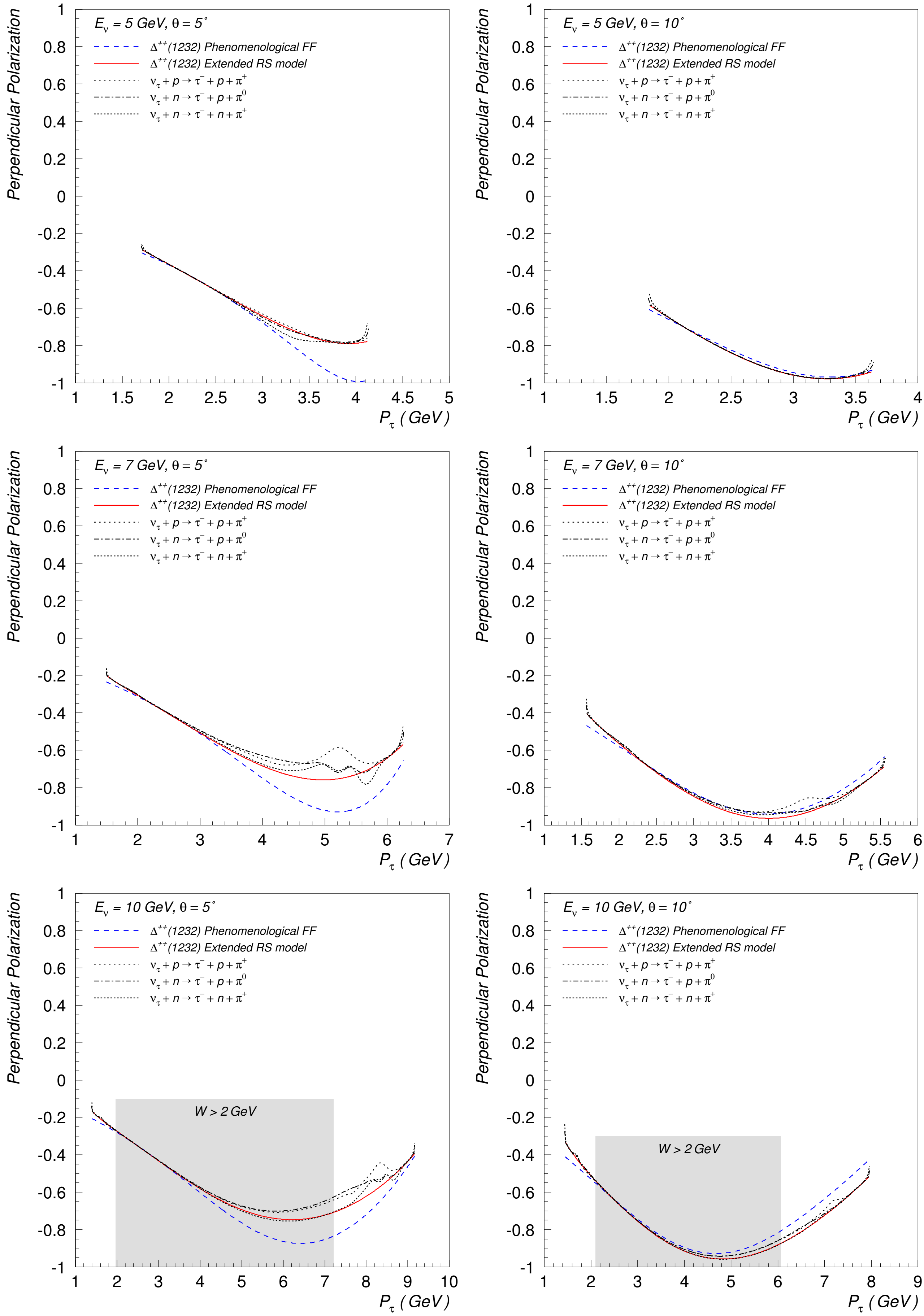

Figure 6.39: Comparison of the perpendicular polarization of τ^- lepton for different ν_τ induced CC1π reactions at three energies and two scattering angles. Also shown are the perpendicular polarizations of τ^- for $\Delta^{++}(1232)$ production.

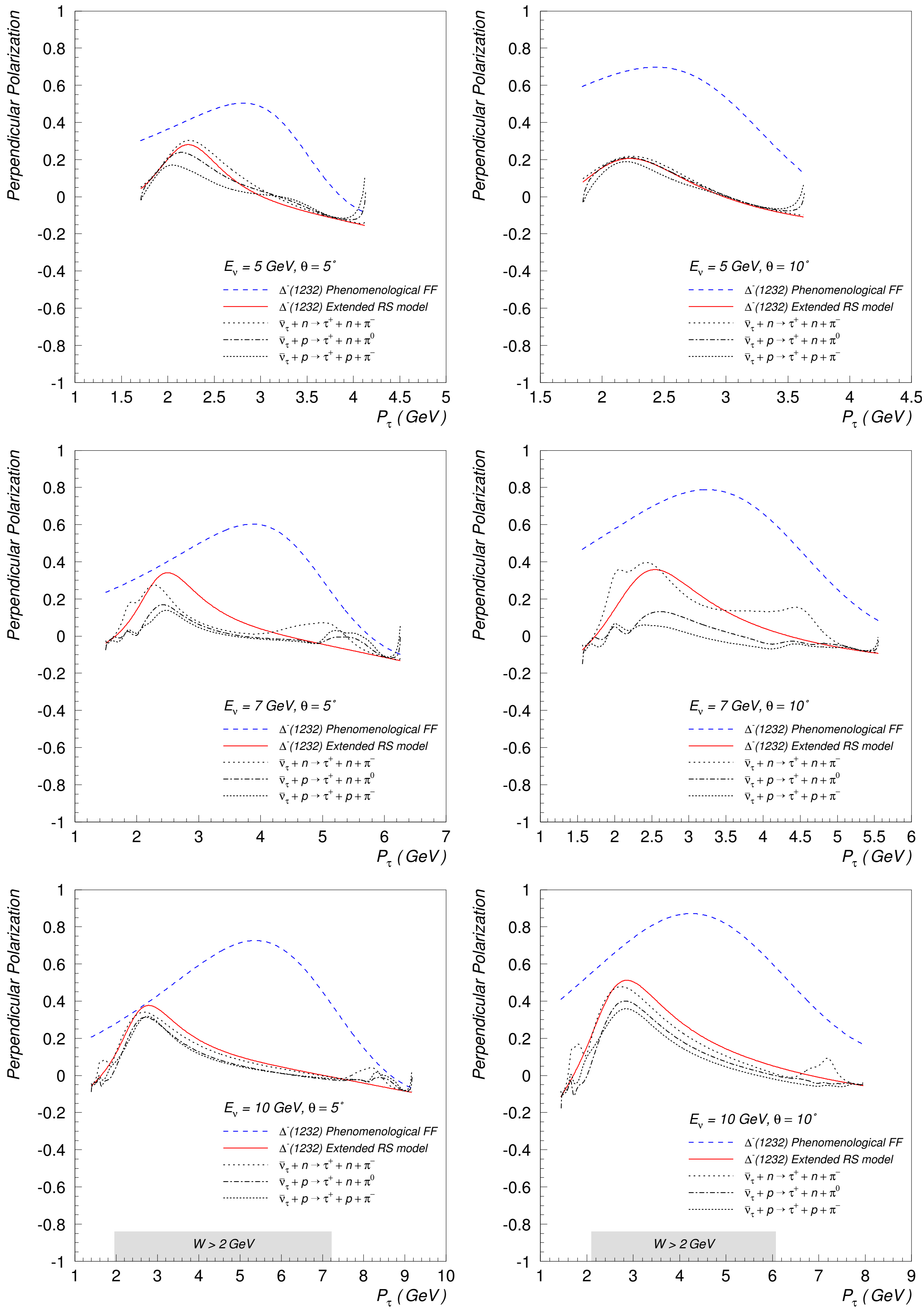

Figure 6.40: Comparison of the perpendicular polarization of τ^+ lepton for different $\overline{\nu}_\tau$ induced CC1π reactions at three energies and two scattering angles. Also shown are the perpendicular polarizations of τ^+ for $\Delta^-(1232)$ production.

6.5 Deep inelastic scattering

6.5.1 Generic formulas

$$dxdy = \left|\frac{\partial\left(x,y\right)}{\partial\left(\cos\theta, E_\ell\right)}\right| dE_\ell d\cos\theta = \frac{P_\ell dE_\ell d\cos\theta}{MyE_\nu},$$

$$\frac{d^2\sigma^{CC}}{dxdy} = \frac{G_F^2 My}{2\pi} L^{\alpha\beta} W_{\alpha\beta} = \frac{G_F^2 ME_\nu}{\pi}\sum_{i=1}^{5} A_i F_i,$$

$$\begin{aligned}
A_1 &= y\left(xy + \frac{m^2}{2ME_\nu}\right), \\
A_2 &= 1 - y - \frac{M}{2E_\nu}xy - \frac{m^2}{4E_\nu^2}, \\
A_3 &= \pm y\left[x\left(1-\frac{y}{2}\right) - \frac{m^2}{4ME_\nu}\right], \\
A_4 &= \frac{m^2}{2ME_\nu}\left(xy + \frac{m^2}{2ME_\nu}\right), \\
A_5 &= -\frac{m^2}{2ME_\nu}.
\end{aligned}$$

The structure functions $W_i^{\text{(DIS)}}\left(x, Q^2\right)$ are ....

6.5.2 Altarelli–Martinelli relation

The Altarelli–Martinelli relation [193] reads

6.5.3 Charm production, target mass correction, etc.

In this section we follow the approach by Kretzer and Reno [194–198].

The charm production contribution to the cross section is represented by the structure functions F_i^c. Kretzer and Reno [194] introduce "theoretical structure functions" ($i = 1, \ldots, 5$)

$$\mathcal{F}_i^c\left(x, Q^2\right) = (1 - \delta_{i4}) s'(\bar{\eta}, \mu^2) + \frac{\alpha_s(\mu^2)}{2\pi} \mathcal{I}_i^c\left(x, Q^2\right) \tag{6.45}$$

for scattering off the CKM-rotated weak eigenstate

$$s' = \left|V_{s,c}\right|^2 s + \left|V_{d,c}\right|^2 d \tag{6.46}$$

and its QCD evolution partner

$$g' \equiv \left(\left|V_{s,c}\right|^2 + \left|V_{d,c}\right|^2\right) g. \tag{6.47}$$

Here

$$\begin{aligned}
\mathcal{I}_i^c\left(x, Q^2\right) &= \int_{\bar{\eta}}^1 \frac{d\xi}{\xi} \left[H_i^q\left(\frac{\bar{\eta}}{\xi}, \kappa, \lambda\right) s'\left(\xi, \mu^2\right) + H_i^g\left(\frac{\bar{\eta}}{\xi}, \kappa, \lambda\right) g'\left(\xi, \mu^2\right)\right] &(6.48a)\\
&\equiv \int_{\bar{\eta}}^1 \frac{d\xi}{\xi} \left[H_i^q\left(\xi, \kappa, \lambda\right) s'\left(\frac{\bar{\eta}}{\xi}, \mu^2\right) + H_i^g\left(\xi, \kappa, \lambda\right) g'\left(\frac{\bar{\eta}}{\xi}, \mu^2\right)\right], &(6.48b)
\end{aligned}$$

$$\bar{\eta} = \eta\left(1 + \frac{m_c^2}{Q^2}\right) = \frac{\eta}{\lambda}, \quad \lambda = \left(1 + \frac{m_c^2}{Q^2}\right)^{-1}, \quad \kappa = \frac{Q^2}{\mu^2},$$

$$\eta \equiv x_N = \frac{Q^2}{2M^2 x}\left(\sqrt{1 + \frac{4M^2x^2}{Q^2}} - 1\right) = \frac{2x}{1 + \sqrt{1 + 4M^2x^2/Q^2}}$$

is the Nachtmann variable and μ is the factorization scale.

Equation (6.48b) (which seems to be more convenient for numerical integration) has been obtained from Eq. (6.48a) by the change variable of integration $\xi \to \bar{\eta}/\xi$.

Symbol $[]_+$.

According to Ref. [199], for any $h(x)$, the corresponding distribution $[h(x)]_+$ is defined by its convolutions with the arbitrary functions $f(x)$

$$\int_x^1 \frac{d\xi}{\xi} f(\xi)\left[h\left(\frac{x}{\xi}\right)\right]_+ = \int_x^1 \frac{d\xi}{\xi}\left[f(\xi) - \frac{x}{\xi} f(x)\right] h\left(\frac{x}{\xi}\right) - f(x)\int_0^x d\xi h(\xi), \tag{6.49}$$

or, equivalently,

$$\int_x^1 \frac{d\xi}{\xi} f\left(\frac{x}{\xi}\right)[h(\xi)]_+ = \int_x^1 \frac{d\xi}{\xi} f\left(\frac{x}{\xi}\right) h(\xi) - f(x)\int_0^1 d\xi h(\xi). \tag{6.50}$$

Functions H_i^q.

$$\begin{aligned}
H_{i=1,2,3,5}^q\left(\xi, \kappa, \lambda\right) &= P_{qq}^{(0)}(\xi) \ln\frac{\kappa}{\lambda} + h_i^q(\xi, \lambda),\\
H_{i=4}^q(\xi, \kappa, \lambda) = H_4^q(\xi, \lambda) &= \frac{4\lambda(1-\xi)\xi\left[1 + (1-2\lambda)\xi\right]}{3(1-\lambda\xi)^2},
\end{aligned}$$

$$\begin{aligned}
P_{qq}^{(0)}(\xi) &= \frac{4}{3}\left[\frac{1+\xi^2}{1-\xi}\right]_+,\\
h_i^q(\xi, \lambda) &= \frac{4}{3}\left\{h^q + A_i\delta(1-\xi) + B_{1,i}\left[\frac{1}{1-\xi}\right]_+ + B_{2,i}\left[\frac{1}{1-\lambda\xi}\right]_+ + B_{3,i}\left[\frac{1-\xi}{(1-\lambda\xi)^2}\right]_+\right\},\\
h^q &= -\left(4 + \frac{1}{2\lambda} + \frac{\pi^2}{3} + \frac{1+3\lambda}{2\lambda}K_A\right)\delta(1-\xi) - \frac{(1+\xi^2)\ln\xi}{1-\xi} + (1+\xi^2)\left[\frac{2\ln(1-\xi) - \ln(1-\lambda\xi)}{1-\xi}\right]_+,\\
K_A &= \left(\frac{1}{\lambda} - 1\right)\ln(1-\lambda).
\end{aligned}$$

Functions H_i^g.

$$
\begin{aligned}
H^g_{i=\,^{1,2,5}_{\;\;3}}(\xi,\kappa,\lambda) &= P^{(0)}_{qg}(\xi)\left(\pm L_\lambda + \tilde{L}_\lambda + \ln\frac{\kappa}{\lambda}\right) + \tilde{h}^g_i(\xi,\lambda),\\
H^g_{i=4}(\xi,\kappa,\lambda) &= H^g_4(\xi,\lambda) = 2\lambda\xi\left[1-\xi-(1-\lambda)\xi\, L_\lambda\right],
\end{aligned}
$$

$$
\begin{aligned}
P^{(0)}_{qg}(\xi) &= \frac{1}{2} - \xi(1-\xi),\\
\tilde{h}^g_i(\xi,\lambda) &= C_{1,i}\xi(1-\xi) + C_{2,i} + (1-\lambda)\xi L_\lambda\left(C_{3,i} + \lambda\xi C_{4,i}\right),\\
L_\lambda &= \ln\left[\frac{1-\lambda\xi}{(1-\lambda)\xi}\right],\\
\tilde{L}_\lambda &= \ln\left[\frac{(1-\xi)^2}{\xi(1-\lambda\xi)}\right].
\end{aligned}
$$

Light quark limit.

Let's consider the limit $\lambda \to 1$ with the simplest choice $\mu^2 = Q^2$.

$$
\begin{aligned}
&H^q_i(\xi,\kappa,\lambda) \to C^{(1)}_{F,i}(\xi),\\
&H^g_i(\xi,\kappa,\lambda) \to C^{(1)}_{F,i}(\xi) = \lim_{\lambda\to 1}\left\{H^g_i(\xi,\kappa,\lambda) + \zeta_i\left(1-\delta_{i4}\right)P^{(0)}_{qg}(\xi)\ln[\kappa(1-\lambda)]\right\}_{\kappa=1},
\end{aligned}
$$

where $\zeta_{i\neq 3} = 1$ and $\zeta_3 = -1$. The limits can be derived straightforwardly:

$$
\begin{aligned}
C^{(1)}_{F,1}(\xi) &= \frac{4}{3}h^q_1 + 2(1-2\xi)\left[\frac{1}{1-\xi}\right]_+,\\
C^{(1)}_{F,2}(\xi) &= \frac{4}{3}h^q_1 + 2\left[1-\frac{2}{3}(1+2\xi)\right]\left[\frac{1}{1-\xi}\right]_+,\\
C^{(1)}_{F,3}(\xi) &= \frac{4}{3}h^q_1 + \frac{2}{3}\left[1+2\xi(1+\xi)\right]\left[\frac{1}{1-\xi}\right]_+,\\
C^{(1)}_{F,4}(\xi) &= \frac{4}{3}\xi,\\
C^{(1)}_{F,5}(\xi) &= \frac{4}{3}h^q_1 + 2\left[1-\frac{2}{3}(1+2\xi)\right]\left[\frac{1}{1-\xi}\right]_+;
\end{aligned}
$$

$$
h^q_1 = -\left(\frac{9}{2}+\frac{\pi^2}{3}\right)\delta(1-\xi) - \frac{(1+\xi^2)\ln\xi}{1-\xi} + (1+\xi^2)\left[\frac{\ln(1-\xi)}{1-\xi}\right]_+,
$$

$$
\begin{aligned}
C^{(1)}_{G,1}(\xi) &= \left[1-2\xi(1-\xi)\right]\ln\left(\frac{1-\xi}{\xi}\right) + 4\xi(1-\xi) - 1,\\
C^{(1)}_{G,2}(\xi) &= \left[1-2\xi(1-\xi)\right]\ln\left(\frac{1-\xi}{\xi}\right) + 8\xi(1-\xi) - 1,\\
C^{(1)}_{G,3}(\xi) &= 0,\\
C^{(1)}_{G,4}(\xi) &= 2\xi(1-\xi),\\
C^{(1)}_{G,5}(\xi) &= \left[1-2\xi(1-\xi)\right]\ln\left(\frac{1-\xi}{\xi}\right) + 8\xi(1-\xi) - 1.
\end{aligned}
$$

6.5.4 Numerical results

Comments to Table 6.3:

1. **Barish *et al.*, ANL 1979:** "In this paper we present results $< \ldots >$ from an experiment using $< \ldots >$ bubble chamber filled with hydrogen and deuterium." "The σN total cross section, defined as the mean of the νn and νp cross sections, is given in Fig. 29(a) $< \ldots >$ $\sigma_T(10^{-38}\text{cm}^2/\text{nucleon})$"

2. **Barish *et al.*, ANL 1977:** "Fig. 1(c) Total νN cross section measured as the mean for νn and νp cross sections. $< \ldots >$ $\sigma_T(10^{-38}\text{cm}^2/\text{nucleon})$".

3. **Baker *et al.*, BNL 1982:** "The resulting nucleon total cross section $\sigma_T(\nu N) = 1/2[\sigma_T(\nu n) + \sigma_T(\nu p)]$ is plotted as function of energy $< \ldots >$"

Table 6.3: Explanation of signs for DIS experimental data. F and R – tick ✓ indicates that the total cross sections have been corrected for Fermi motion and for radiative corrections. I – ticks ✓ or ✓ indicate that the total cross sections have been corrected for an isoscalar nucleus or isoscalar nucleon (that is neutron or proton excess in the matter of detector), irrespectively. The ✗ sign indicates that there is unambiguous information in the cited document that this effect has not been taken into account. The sign ? means there is no information in the cited document.

Experiment	Year	Refs.	Detector working medium	F	R	I
Barish *et al.*, ANL	1979	[61]	H_2, D_2	?	?	✓
Barish *et al.*, ANL	1977	[147]	H_2, D_2	?	?	✓
Baker *et al.*, BNL	1982	[152]	H_2, D_2	?	?	✓
Baltay *et al.*, BNL	1980	[150]	Ne-H_2	?	?	✓
Naples, NuTeV	2003	[182]	Fe	?	✓	✓
Taylor *et al.*, FNAL	1983	[167]	Ne-H_2	?	?	✓
Baker *et al.*, FNAL	1983	[166]	Ne-H_2	?	?	✓
Kitagaki *et al.*, FNAL	1982	[164]	D_2	?	?	✓
Barish *et al.*, CITF	1975	[158]	Fe	?	?	✓
Benvenuti *et al.*, HPWF	1974	[156]	Fe	?	?	✓
Barish *et al.*, CITFR	1977	[159]	D_2	?	?	✓
Seligman, CCFR	1997	[181]	Fe	?	?	?
Auchincloss *et al.*, CCFR	1990	[169]	Fe	?	?	✓
MacFarlane *et al.*, CCFRR	1984	[168]	Fe	?	?	?
Barish *et al.*, CCFR	1981	[163]	Fe	?	✓	✓
Aderholz *et al.*, BEBC	1986	[135]	Ne-H_2	?	?	✓
Parker *et al.*, BEBC	1984	[132]	Ne-H_2	?	?	✓
Allasia *et al.*, BEBC	1984	[133]	Be	✓	✓	✓
Bosetti *et al.*, BEBC	1982	[131]	Ne-H_2	?	?	✓
Colley *et al.*, BEBC	1979	[130]	Ne-H_2	?	?	✓
Groot *et al.*, CDHS	1979	[123]	Fe	?	?	?
Berge *et al.*, CDHSW	1987	[127]	Fe	?	?	✓
Abramowicz *et al.*, CDHS	1983	[124]	Fe	?	?	?
Allaby *et al.*, CHARM	1988	[146]	Fe	?	?	✓
Morfin *et al.*, GGM	1981	[143]	C_3H_8-CF_3Br	✓	✗	✓
Ciampolillo *et al.*, GGM	1979	[142]	C_3H_8-CF_3Br	?	?	✓
Erriquez *et al.*, GGM	1979	[141]	C_3H_8-CF_3Br	?	?	✓
Eichten *et al.*, GGM	1973	[136]	C_3H_8-CF_3Br	?	?	✓
Vovenko *et al.*, IHEP-ITEP	1979	[174]	Fe	?	?	✓
Asratyan *et al.*, IHEP-ITEP	1978	[170]	Fe	?	?	✓
Anikeev *et al.*, IHEP-JINR	1996	[178]	Al	?	?	✓
Asratyan *et al.*, IHEP-ITEP	1984	[33]	Ne-H_2	✓	?	✓
Baranov *et al.*, SKAT	1979	[173]	CF_3Br	?	?	✓

4. **Baltay *et al.*, BNL 1980:** "The bubble chamber chamber was filled with heavy Ne-N_2 mixture (62 at % Ne) $< \ldots >$" "The charged current cross sections per nucleon are $< \ldots >$".

5. **Naples, NuTeV 2003:** "Corrected to isoscalar target. Iron$(N - Z)/A = 0.0567$" "Radiative corrections applied before F_2 fits performed D. Yu. Bardin and V. A. Dokuchaeva, JINR-E2-86-260 (1986)"

6. **Taylor *et al.*, FNAL 1983:** "The present result $< \ldots >$ for an isoscalar target". "The 15-ft bubble chamber filled with a Ne/H_2 mixture $< \ldots >$"

7. **Baker *et al.*, FNAL 1983:** "The 15-ft bubble chamber was filled with a 59% atomic-neon-hydrogen mixture which is almost an isoscalar target, with a 3.4% proton excess." "To express the cross section slope for an isoscalar target, one has to correct for the slight proton excess of the neon-hydrogen mixture. With use of $2\sigma_{\nu p} = \sigma_{\nu n}$, the final result $< \ldots >$ was obtained."

8. **Kitagaki *et al.*, FNAL 1982:** "We have studied the total cross section for charged-current reactions in hight-energy neutrino-deuterium interactions." "The total charged-current cross section per nucleon on isoscalar target is calculated by $< \ldots >$. The factor of 2, representing the number of nucleons in the deuterium nucleus, is included to ensure that σ_t is a cross section per nucleon."

9. **Barish *et al.*, CITF 1975:** "The total cross sections data for $\nu_\mu(\overline{\nu}_\mu)$ incident on iron nuclei were obtained $< \ldots >$". "The total neutrino cross section per nucleon was obtained from the relation $\sigma_{tot} = T/FB\epsilon$ where T is the total

number of observed interacting neutrinos with measured final muon energy, ϵ is the efficiency for the muon to traverse the magnet, F is the total number of incident neutrinos, and $B = 3.087 \times 10^{27}$ nucleons/cm^2."

10. **Benvenuti *et al.*, HPWF 1974:** "Fig. 3(a) $< \ldots >$ $\sigma_\nu \times 10^{38}$ (cm^2/nucleon)".

11. **Barish *et al.*, CITFR 1977:** "Fig. 2 $< \ldots >$ σ_ν (cm^2/nucleon)".

12. **Seligman, CCFR 1997:**

13. **Auchincloss *et al.*, CCFR 1990:** "The quantity α^ν at fixed E_ν may be written in experimental terms as $\sigma^\nu/E_\nu = N_{e\nu}/(\rho_N E_\nu \Phi_\nu)$, where $N_{e\nu}$ represents the fully corrected event sample, ρ_N the density of the target in nucleons per cm^{-2} $< \ldots >$". "Finally, the cross section was corrected for the fact that the mostly iron target contained an excess of neutrons over protons. $< \ldots >$ The final cross section results were multiplied by 0.9755 and 1.0212 fora neutrinos and antineutrinos, respectively $< \ldots >$ to give the cross section for an isoscalar target."

14. **MacFarlane *et al.*, CCFRR 1984:**

15. **Barish *et al.*, CCFR 1981:** "$< \ldots >$ parametrization was used to convert our results from cross-section/nucleon on an iron target to cross-section/nucleon on a pure isoscalar target $< \ldots >$". "The analysis for both CDHS and this experiment $< \ldots >$ corrects for neutron excess in iron, strange sea quarks with $2s/(\overline{u} + \overline{d}) = 0.35$, and radiative corrections".

16. **Aderholz *et al.*, BEBC 1986:** "In table 2 the values for the cross section ratios from this analysis are compared with similar measurements from other experiments; all values shown have been corrected for the non-isoscalarity of the target".

17. **Parker *et al.*, BEBC 1984:** "Applying the 8.4% to the Ne sample, after making a small correction for non-isoscalarity of the target $< \ldots >$". "Our data agree better with the aluminium and deuterium results than with the total absence of nuclear effects, although the latter is not excluded. However it seems that in our data any dependent nuclear correction factors are about the same size as the statistical errors, while the overall correction is small."

18. **Allasia *et al.*, BEBC 1984:** "Table 1 summarizes the average values for the corrections applied. $< \ldots >$ radiative corrections $1.010(\overline{\nu})$ $1.009(\nu)$ $< \ldots >$ The first three corrections were applied for each event individually". "Deep inelastic events were generated by means of a Monte Carlo program $< \ldots >$ Changes in the generated particle momenta were introduced to account for the Fermi motion of the target".

19. **Bosetti *et al.*, BEBC 1982:** "The observed event rates shown in table 1 had to be corrected for: $< \ldots >$ (e) The 7.4% proton excess in the Ne/H_2 mixture. This correction (assuming $\sigma^{\nu n}/\sigma^{\nu p} = \sigma^{\overline{\nu}p}/\sigma^{\overline{\nu}n} = 2$) is done so that the cross section data refer to an isoscalar target nucleus". "$< \ldots >$ total cross sections for charged-current interactions of neutrinos and antineutrinos with an isoscalar target nucleus have been measured $< \ldots >$"

20. **Colley *et al.*, BEBC 1979:** "BEBC was filled with a 74 mole % NE-H_2 mixure $< \ldots >$" "Fig. 4. Neutrino and antineutrino interaction cross sections, divided by the mean value of energy, calculated for an isoscalar target." "Table 1. Cross sections, in units of 10^{-38} cm^2/GeV/nucleon, are corrected for an isoscalar target."

21. **Groot *et al.*, CDHS 1979:**

22. **Berge *et al.*, CDHSW 1987:** "Assuming σ/E to be constant, the values corrected for non-isoscalarity are $< \ldots >$ cm^2/(GeV $\cdot$ nucleon) $< \ldots >$" "The values corrected for the neutron excess in iron (non-isoscalarity correction: -2.5% for ν, +2.3% for $\overline{\nu}$) are $< \ldots >$"

23. **Abramowicz *et al.*, CDHS 1983:**

24. **Allaby *et al.*, CHARM 1988:** "New measurements of the total cross sections of charged current interactions of muon neutrinos and antineutrinos on isoscalar nuclei have been performed." "$< \ldots >$ a corresponding number of nucleons per cm^2 of $N = 9.24 \cdot 10^{26}$ nucleons/cm^2 $< \ldots >$" "The total cross sections slope σ/E is obtained by dividing the observed event sample by the product of the energy-weight neutrino flux and number of nucleons/cm^2 of the detector." "A small correction for non-isoscalarity of the target has been applied (=0.2% for σ^ν and -0.2% for $\sigma^{\overline{\nu}}$)."

25. **Morfin *et al.*, GGM 1981:** "In addition, the effects of Fermi motion and the non-isoscalar nature of the target have been taken into account". "As the radiative corrections have been estimated to be less than 5% for $x < 0.8$, using the method of the Rujula et al.[7], they have not been applied to the data.

26. **Ciampolillo *et al.*, GGM 1979:** "Table 2. Total cross section per nucleon for an isoscalar target."

27. **Erriquez *et al.*, GGM 1979:** "The chamber was filled with a mixture of propane (C_3H_8) and heavy freon (CF_3Br) $< \ldots >$" "With a simplified nuclear model the ratio of cross sections on neutrons and protons has been estimated $< \ldots >$ "$< \ldots >$ the charged current total cross section for antineutrino on nucleons has been determined $< \ldots >$"

28. **Eichten *et al.*, GGM 1973:** “The liquid filling was heavy freon $\mathrm{CF_3Br} < \ldots >$” “The ν and $\overline{\nu}$ nucleon total cross sections have been determined $< \ldots >$”

29. **Vovenko *et al.*, IHEP-ITEP 1979:**

30. **Asratyan *et al.*, IHEP-ITEP 1978:** “The results were recalculated for the isoscalar target assuming $\sigma^{\nu n}/\sigma^{\nu p} = \sigma^{\overline{\nu} p}/\sigma^{\overline{\nu} n} = 2$ (2% correction)”.

31. **Anikeev *et al.*, IHEP-JINR 1996:** “Measured dependence of total cross section σ_{tot}/E for the ν_μ and $\overline{\nu}_\mu$ interactions with nucleon versus neutrino energy $E < \ldots >$”

32. **Asratyan *et al.*, IHEP-ITEP 1984:** “The energy distribution of inelastic events was corrected for Fermi motion $< \ldots >$” “Fig. 2. Antineutrino interaction cross section divided by the mean energy value, calculated for isoscalar target.”

33. **Baranov *et al.*, SKAT 1979:** “Fig. 3. Neutrino-nucleon total cross section as a function of the neutrino energy $< \ldots > \sigma(\mathrm{cm}^2/\mathrm{nucleon})$.

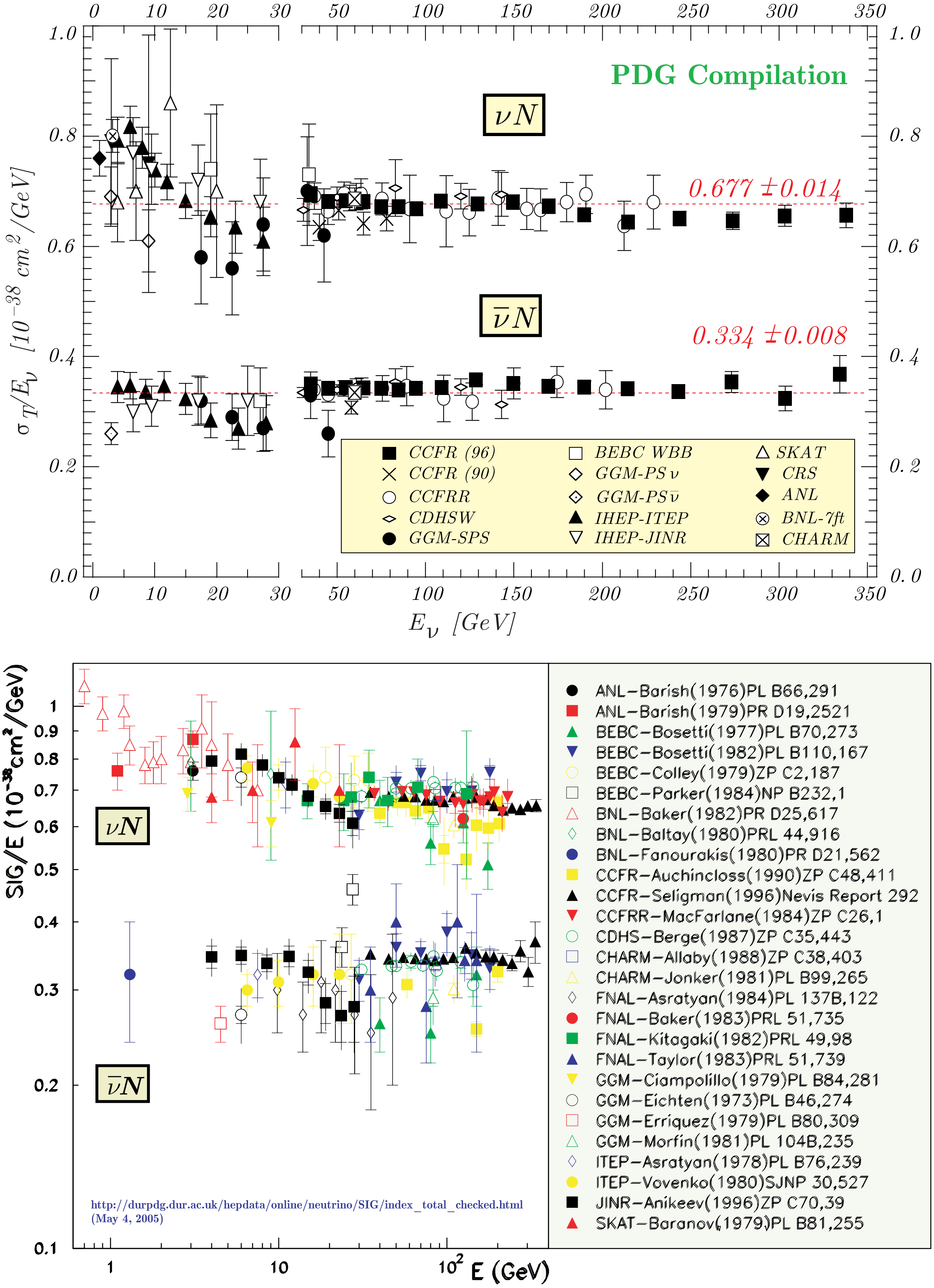

Figure 6.41: Experimental data on $\nu_\mu N$ and $\overline{\nu}_\mu N$ CC total cross sections compiled by PDG [4] (top panel) and Durham HEP Database (bottom panel).

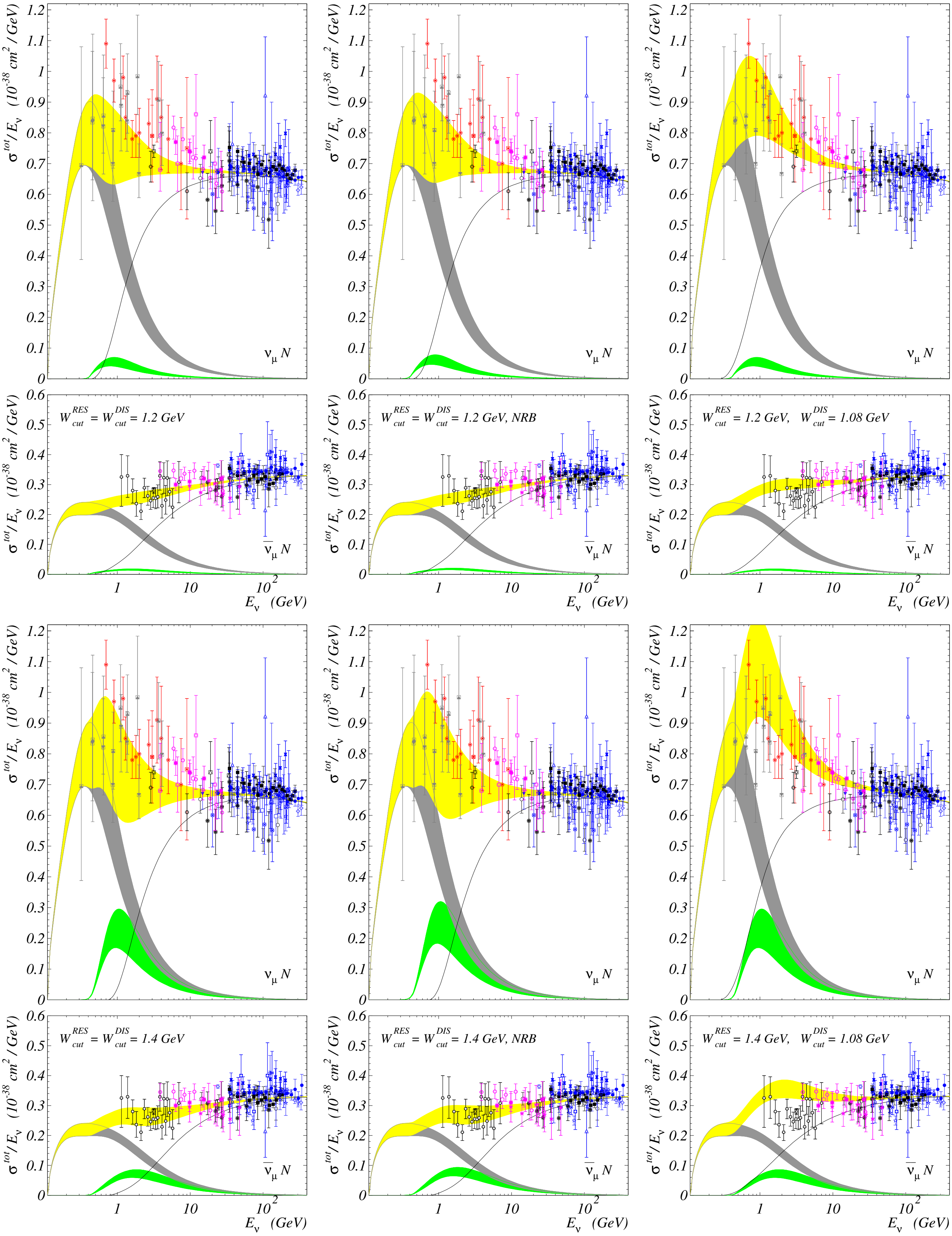

Figure 6.42: CC $\nu_\mu N$ and $\overline{\nu}_\mu N$ total cross sections calculated with $W_{\rm cut}^{\rm RES} = 1.2$ and 1.4 GeV.

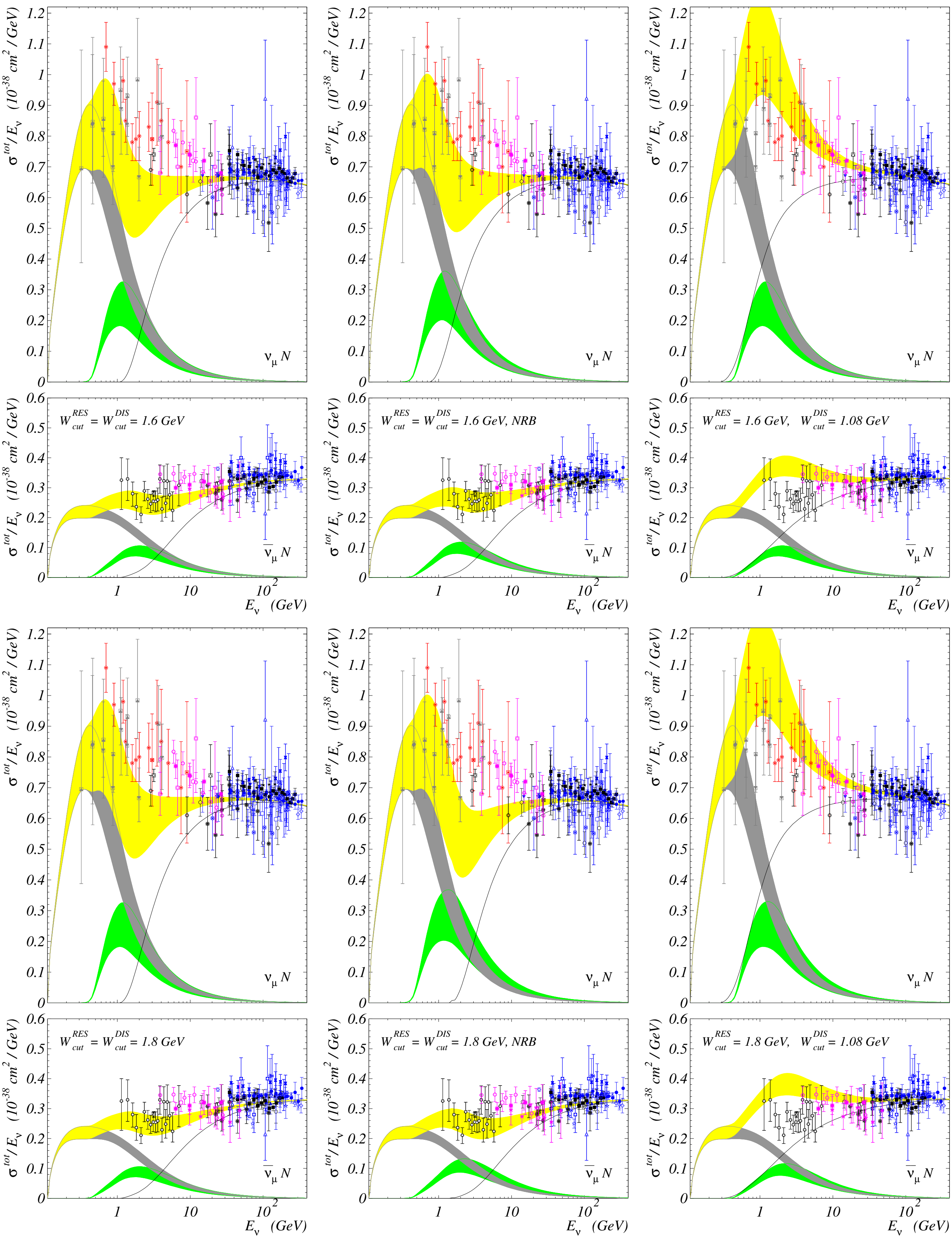

Figure 6.43: CC $\nu_\mu N$ and $\overline{\nu}_\mu N$ total cross sections calculated with $W_{\rm cut}^{\rm RES} = 1.6$ and 1.8 GeV.

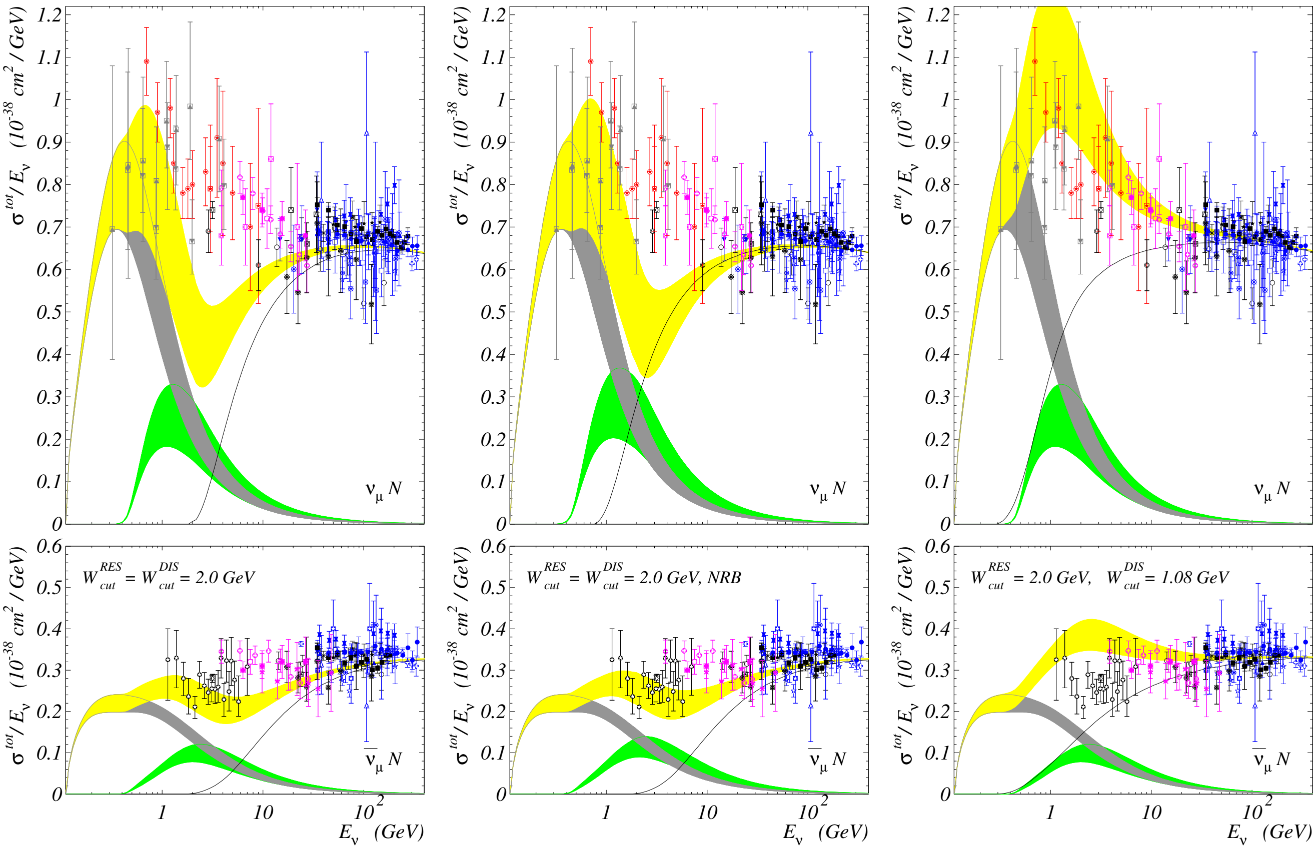

Figure 6.44: CC $\nu_\mu N$ and $\overline{\nu}_\mu N$ total cross sections calculated with $W_{\rm cut}^{\rm RES} = 2.0$ GeV.

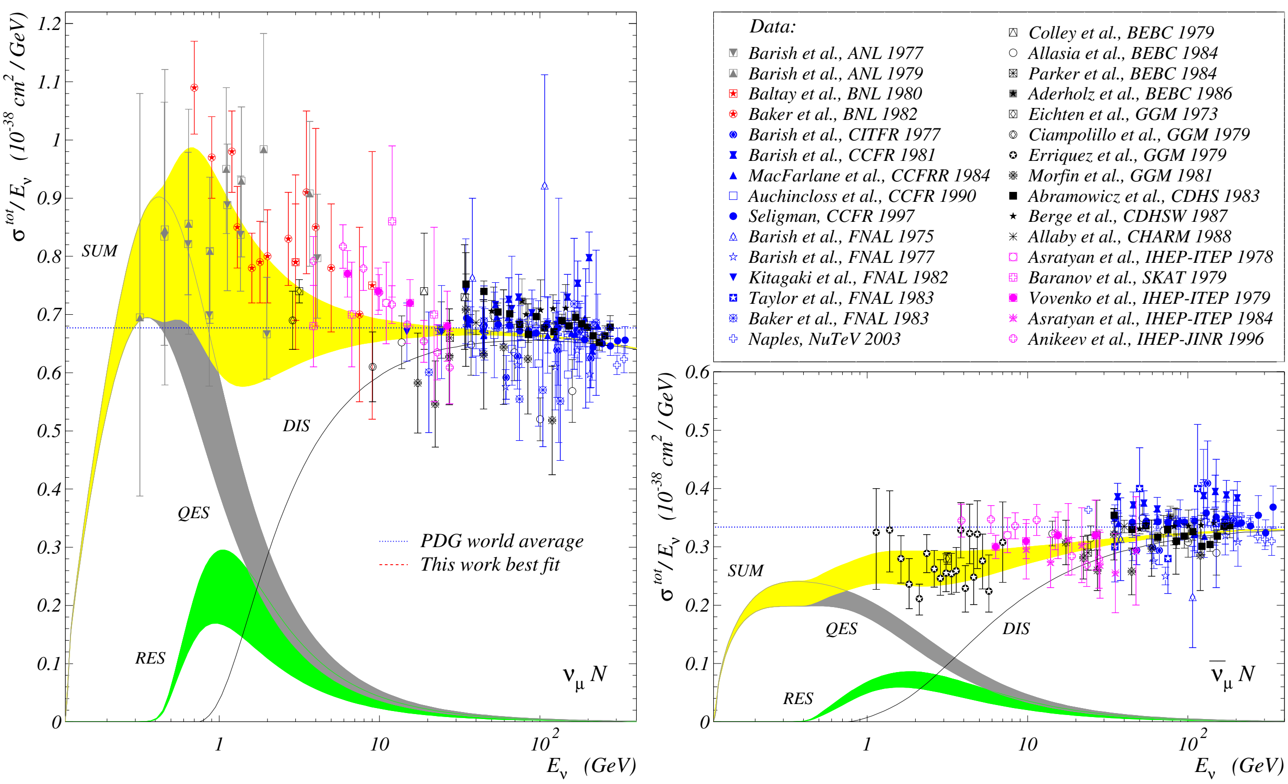

Figure 6.45: CC $\nu_\mu N$ and $\overline{\nu}_\mu N$ total cross sections calculated with the best fit walues of $W_{\rm cut}^{\rm RES}$ and $W_{\rm cut}^{\rm DIS}$.

Chapter 7

Leptonic τ decay

7.1 $\tau_{\ell 3}$ decay kinematics

$$\begin{array}{lrr}
v_\tau <\overset{*}{v}{}^{\max}, & -1 \le \cos\theta \le 1, & m_\mu \le E' \le E' \le E'^{+}, \\
E_\tau < E_\tau^0, & & 0 \le P' \le P' \le P'^{+}; \\
 & & \\
v_\tau >\overset{*}{v}{}^{\max}, & \cos\theta^{\max} \le \cos\theta \le 1, & E'^{-} \le E' \le E'^{+}, \\
E_\tau > E_\tau^0, & & \max(0, P'^{-}) \le P' \le P'^{+}.
\end{array}$$

Here $\overset{*}{v}{}^{\max}$ is the maximum muon velocity in τ lepton rest frame; E_τ^0 is the boundary τ lepton energy approximate 15 GeV; $\theta^{\max}$ is the extreme scattering angle of muon, at energy of our interest $\cos\theta^{\max}$ is closely approximated from 1 and muon is scattered only forward.

$$E_\tau^0 = \frac{m_\tau^2 + m_\mu^2}{2m_\mu}, \quad \cos\theta^{\max} = \frac{E_\tau E' - \overset{*}{E}{}^{\max} m_\mu}{P_\tau P'} \approx 1 - \frac{m_\tau^2 + m_\mu^2}{2P_\tau P'}.$$

$$E_\tau^{\pm} = \left(1 + \frac{1}{r}\right)\frac{E'}{2} \mp \left(1 - \frac{1}{r}\right)\frac{P'}{2}, \qquad E'^{\pm} = \frac{1+r}{2}E_\tau \pm \frac{1-r}{2}P_\tau,$$

$$P_\tau^{\pm} = \left(1 - \frac{1}{r}\right)\frac{E'}{2} \mp \left(1 + \frac{1}{r}\right)\frac{P'}{2}, \qquad P'^{\pm} = \frac{1-r}{2}E_\tau \pm \frac{1+r}{2}P_\tau,$$

$r = m_\mu^2/m_\tau^2$.

7.2 Energy spectra of secondaries

The differential probability of $\tau_{\mu 3}$ decay is

$$\frac{d\Gamma}{dE'} = \frac{G_F^2}{96\pi^4}\frac{P'}{E_\tau} d\cos\theta d\phi \left\{k^2\left(p_\tau p'\right) + 2\left(p_\tau k\right)\left(p'k\right) - m_\tau\left[k^2\left(p' s_\tau\right) + 2\left(p'k\right)\left(s_\tau k\right)\right]\right\},$$

where G_F is the Fermi constant, $d\phi$ is the phase size, p_τ, p' and k are 4-momenta of τ-lepton, μ and neutrino, s_τ is the 4-vector of τ polarization. The double differential probability of decay is

$$\begin{aligned}
d\Gamma = \frac{G_F^2}{96\pi^3}\frac{dE'ds}{E_\tau P_\tau} & \left\{\left(m_\tau^2 - m_\mu^2\right)^2 + \left(m_\tau^2 + m_\mu^2\right)s - 2s^2 \right. \\
& \left. - \frac{\mathcal{P}_L}{2v_\tau}\left[m_\mu^4 - m_\tau^4 + 2m_\tau^2\left(m_\tau^2 - m_\mu^2\right)\frac{E'}{E_\tau} + \left(m_\mu^2 + 3m_\tau^2 - 4m_\tau^2\frac{E'}{E_\tau}\right)s - 2s^2\right]\right\},
\end{aligned}$$

where $s = \left(p_\tau - p_\mu\right)^2$, v_τ is the τ-lepton velocity, $\mathcal{P}_L$ is the longitudinal component of τ lepton polarization vector.
$\star$ In the region $\{-1 \le \cos\theta' \le 1,\ \ m_\mu \le E' \le E'^{-},\ \ 0 \le P' \le P'^{-}\}$, the muon energy spectrum is

$$\begin{aligned}
\frac{d\Gamma_1}{dE'} = \frac{G_F^2}{36\pi^3}\frac{P'}{E_\tau} & \left\{9\left(m_\tau^2 + m_\mu^2\right)E_\tau E' - 12E_\tau^2 E'^2 - 4P_\tau^2 P'^2 - 6m_\tau^2 m_\mu^2 \right. \\
& \left. - \frac{\mathcal{P}_L}{v_\tau}\left[3\left(m_\tau^2 + 3m_\mu^2\right)E_\tau E' - 12E_\tau^2 E'^2 - 4E_\tau^2 P'^2\right]\right\}.
\end{aligned}$$

$\star$ In the region $\{\cos\theta^{\max} \le \cos\theta \le 1,\ \ E'^{-} \le E' \le E'^{+},\ \ \max(0, P'^{-}) \le P' \le P'^{+}\}$, the muon spectrum is

$$\frac{d\Gamma_2}{dE'} = \frac{G_F^2}{36\pi^3}\frac{1}{E_\tau P_\tau}\Bigg\{\frac{3}{8}\left(m_\tau^4 - m_\mu^4\right)\left(m_\tau^2 - m_\mu^2\right) - \frac{1}{16}\left(m_\tau^2 + m_\mu^2\right)^3 + 3m_\tau^2 m_\mu^2\left(E_\tau E' - P_\tau P'\right)$$
$$- \frac{9}{4}\left(m_\tau^2 + m_\mu^2\right)\left(E_\tau E' - P_\tau P'\right)^2 + 2\left(E_\tau E' - P_\tau P'\right)^3$$
$$- \frac{\eta_{\tau\pm}^{\|}}{v_\tau}\Bigg[\frac{1}{16}\left(m_\tau^2 + m_\mu^2\right)^2\left(5m_\mu^2 - m_\tau^2\right) - \frac{3}{4}\left(m_\tau^2 + 3m_\mu^2\right)\left(E_\tau E' - P_\tau P'\right)^2$$
$$+ 2\left(E_\tau E' - P_\tau P'\right)^3 - \frac{3}{2}m_\tau^2 m_\mu^2\left(m_\tau^2 + m_\mu^2\right)\frac{E'}{E_\tau}$$
$$+ \frac{3}{2}m_\tau^2\left(m_\tau^2 + 3m_\mu^2\right)\left(E_\tau E' - P_\tau P'\right)\frac{E'}{E_\tau} - 3m_\tau^2\left(E_\tau E' - P_\tau P'\right)^2\frac{E'}{E_\tau}\Bigg]\Bigg\}.$$

$$\chi = \eta + \frac{r}{\eta}, \quad \eta = \frac{E' + P'}{E_\tau + P_\tau}, \quad \xi = \frac{E_\tau + P_\tau}{E_\tau - P_\tau},$$

$$E_\tau E' - P_\tau P' = \frac{m_\tau^2}{2}\chi, \quad \frac{E'}{E_\tau} = \frac{\eta^2\xi + r}{\eta\left(\xi + 1\right)}, \qquad r \le \eta \le 1.$$

In thus terms kinematic bounds are

$$\begin{array}{lll} \eta^0 \le \eta \le \eta^-: & m_\mu \le E' \le E'^{-}, & 0 \le P' \le P'^{-}, \\ \eta^- \le \eta \le \eta^+: & E'^{-} \le E' \le E'^{+}, & P'^{-} \le P' \le P'^{+}, \\ \widetilde{\eta}^- \le \eta \le \eta^+: & E'^{-} \le E' \le E'^{+}, & \max(0, P'^{-}) \le P' \le P'^{+}. \end{array}$$

$$\eta^0 = \frac{m_\mu}{E_\tau + P_\tau}, \quad \eta^- = \frac{1}{\xi}, \quad \eta^+ = 1, \quad \widetilde{\eta}^- = r.$$

For detectors with high energy threshold of muon registration muon decay spectrum is only second region spectrum and it is convenient to write

$$\frac{1}{\Gamma}\frac{d\Gamma_2}{dE'} = \frac{1}{3gP_\tau}\Bigg\{5\left(1 + r^3\right) - 9r\left(1 + r\right) + 24r\chi - 9\left(1 + r\right)\chi^2 + 4\chi^3$$
$$- \frac{\eta_{\tau\pm}^{\|}}{v_\tau}\Bigg[(5r - 1)\left(1 + r\right)^2 - 3\left(1 + 3r\right)\chi^2 + 4\chi^3 - 12\frac{\eta^2\xi + r}{\eta\left(\xi + 1\right)}\left[2r\left(1 + r\right) - \left(1 + 3r\right)\chi + \chi^2\right]\Bigg]\Bigg\}.$$

As is well known, the terms proportional to $\eta_\tau^{\|}$ not make contribution to full width. The full width of $\tau_{\mu 3}$ with non zero lepton mass decay is

$$\Gamma = \frac{G_F^2}{192\pi^3}\frac{m_\tau^6}{E_\tau}\left[\left(1 - r^2\right)\left(1 - 8r + r^2\right) - 12r^2\ln r\right] = \frac{G_F^2}{192\pi^3}\frac{m_\tau^6}{E_\tau}g.$$

$$\frac{1}{\Gamma}\frac{d\Gamma}{dE'} = \frac{1}{\Gamma}\left(\frac{d\Gamma_1}{dE'} + \frac{d\Gamma_2}{dE'}\right) = \frac{16}{3m_\tau^6 g}\left(P'_\mu\frac{d\tilde{\Gamma}_1}{dE'} + \frac{1}{P_\tau}\frac{d\tilde{\Gamma}_2}{dE'}\right).$$

For further calculation of the neutrino regeneration the neutrino spectral functions in $\tau_{\mu 3}$ decay are essential. All neutrino spectral functions are depended of dimensionless expression

$$\eta = \frac{2E_\nu}{E_\tau + P_\tau}, \qquad \frac{E_\nu}{E_\tau} = \frac{\eta}{2}\left(1 + \beta\right),$$

$$t^- = m_\tau^2\left(1 - \eta\xi\right), \qquad t^{\min} = m_\mu^2, \qquad t^+ = m_\tau^2\left(1 - \eta\right).$$

$$\frac{d\Gamma}{dE_\nu} = \frac{G_F^2}{96\pi^3}\frac{dt}{E_\tau P_\tau}\Bigg\{m_\tau^2\left(1 + 3r\right)t - 2t^2 + \frac{m_\tau^6}{t}r^2\left(3 - r\right) - \frac{m_\tau^4 m_\mu^4}{t^2}\left(3 + r\right) + \frac{2m_\tau^4 m_\mu^6}{t^3} + m_\tau^4\left(1 - 3r\right)$$
$$- \frac{\eta_{\tau\pm}^{\|}}{v_\tau}\Bigg\{m_\tau^2\left(3 - 4\frac{E_\nu}{E_\tau} + 3r\right)t - 2t^2 - \frac{m_\tau^6}{t}r^2\left(3 + r\right) + \frac{m_\tau^4 m_\mu^4}{t^2}\left[3\left(1 - 2\frac{E_\nu}{E_\tau}\right) + r\left(3 - 2\frac{E_\nu}{E_\tau}\right)\right]$$
$$- \frac{2m_\tau^4 m_\mu^6}{t^3}\left(1 - 2\frac{E_\nu}{E_\tau}\right) - m_\tau^4\left(1 + 3r\right)\left(1 - 2\frac{E_\nu}{E_\tau}\right)\Bigg\}\Bigg\}.$$

$\star$ In the region $\{-1 \le \cos\theta_\nu \le 1,\ \ t^- \le t \le t^+,\ \ 0 \le E_\nu \le E_\nu^-\}$, the neutrino spectral function is

$$F_\nu = \frac{P_\tau}{\Gamma}\frac{d\Gamma}{dE_\nu} = \frac{1}{3g}\Bigg\{9\left(\xi^2-1\right)\eta^2 - 4\left(\xi^3-1\right)\eta^3 - 9r\left(\xi^2-1\right)\eta^2 - 18r^2\left(\xi-1\right)\frac{\eta}{\left(1-\eta\right)\left(1-\xi\eta\right)}$$
$$+ 6r^3\left(\xi-1\right)\frac{\eta\left(1-\xi\eta^2\right)}{\left(1-\eta\right)^2\left(1-\xi\eta\right)^2} + 6r^2\left(3-r\right)\ln\frac{1-\eta}{1-\xi\eta} - \frac{\eta^{\parallel}_{\tau\pm}}{v_\tau}\left[3\frac{\left(\xi-1\right)^3}{\xi+1}\eta^2 - 4\left(\xi-1\right)^3\eta^3 - 9r\frac{\left(\xi-1\right)^3}{\xi+1}\eta^2\right.$$
$$+ 18r^2\left(\xi-1\right)\frac{\eta}{\left(1-\eta\right)\left(1-\xi\eta\right)}\left(1-\frac{2\xi}{\xi+1}\eta\right)$$
$$\left. + 6r^3\left(\xi-1\right)\frac{\eta}{\left(1-\eta\right)^2\left(1-\xi\eta\right)^2}\left[1-2\xi\eta+3\xi\eta^2-2\frac{\eta\left(\xi^2\eta^2+1\right)}{y+1}\right] - 6r^2\left(3+r\right)\ln\frac{1-\eta}{1-\xi\eta}\right]\Bigg\},$$

$\star$ In the region $\{\cos\theta_\nu^{\max} \le \cos\theta_\nu \le 1,\ \ t^{\min} \le t \le t^+,\ \ E_\nu^- \le E_\nu \le E_\nu^+\}$, the neutrino spectral function is

$$F_\nu = \frac{P_\tau}{\Gamma}\frac{d\Gamma}{dE_\nu} = \frac{1}{3g}\Bigg\{5 - 9\eta^2 + 4\eta^3 - 9r\left(3-\eta^2\right) + 9r^2\frac{3-\eta}{1-\eta} - r^3\frac{5-4\eta+5\eta^2}{\left(1-\eta\right)^2} + 6r^2\left(3-r\right)\ln\frac{1-\eta}{r}$$
$$- \frac{\eta^{\parallel}_{\tau\pm}}{v_\tau}\left[3\frac{3\xi-1}{1+\xi}\eta^2 - 4\frac{2\xi-1}{1+\xi}\eta^3 - 1 + 9r\left(1-\frac{3\xi-1}{\xi+1}\eta^2\right) + 9r^2\left(3-\frac{2}{1-\eta}+\frac{4\xi}{1+\xi}\frac{\eta^2}{1-\eta}\right)\right.$$
$$\left. - r^3\left[5+\frac{12}{\left(1-\eta\right)^2} - 18\frac{\eta}{\left(1-\eta\right)^2} + \frac{12\xi}{1+\xi}\frac{\eta^2}{\left(1-\eta\right)^2}\right] - 6r^2\left(3+r\right)\ln\frac{1-\eta}{r}\right]\Bigg\}.$$

$$u^- = m_\tau^2\left(1-\xi\eta\right), \qquad u^{\min} = m_\mu^2, \qquad u^+ = m_\tau^2\left(1-\eta\right).$$

$$\frac{d\Gamma}{dE_{\overline{\nu}}} = \frac{G_F^2}{16\pi^3}\frac{du}{E_\tau P_\tau}\Bigg\{m_\tau^2\left(1+2r\right)u - u^2 + \frac{m_\tau^2 m_\mu^4}{4} - m_\tau^4 r\left(2+r\right)$$
$$- \frac{\eta^{\parallel}_{\tau\pm}}{v_\tau}\left[m_\tau^2\left(1+2r-2\frac{E_{\overline{\nu}}}{E_\tau}\right)u - u^2 + \frac{m_\tau^2 m_\mu^4}{u}\left(1-2\frac{E_{\overline{\nu}}}{E_\tau}\right) - m_\tau^4 r\left(2+r-4\frac{E_{\overline{\nu}}}{E_\tau}\right)\right]\Bigg\}.$$

$\star$ In the region $\{-1 \le \cos\theta_{\overline{\nu}} \le 1,\ \ u^{\min} \le u \le u^+,\ \ 0 \le E_{\overline{\nu}} \le E_{\overline{\nu}}^-,\ \ 0 \le \eta \le \eta^-\}$, the antineutrino spectral function is

$$F_{\overline{\nu}} = \frac{P_\tau}{\Gamma}\frac{d\Gamma}{dE_{\overline{\nu}}} = \frac{2}{g}\Bigg\{3\eta^2\left(\xi^2-1\right) - 2\eta^3\left(\xi^3-1\right) - 6r\eta^2\left(\xi^2-1\right) - 6r^2\left[\eta\left(\xi-1\right) - \ln\frac{1-\eta}{1-\xi\eta}\right]$$
$$- \frac{\eta^{\parallel}_{\tau\pm}}{v_\tau}\left[3\frac{\left(\xi-1\right)^3}{\xi+1}\eta^2 - 2\left(\xi-1\right)^3\eta^3 - 6r\frac{\left(\xi-1\right)^3}{\xi+1}\eta^2 - 6r^2\left[\left(\xi-1\right)\eta - \left(1-\frac{2\xi}{\xi+1}\eta\right)\ln\frac{1-\eta}{1-\xi\eta}\right]\right]\Bigg\}.$$

$\star$ In the region $\{\cos\theta_{\overline{\nu}}^{\max} \le \cos\theta_{\overline{\nu}} \le 1,\ \ u^{\min} \le u \le u^+,\ \ E_{\overline{\nu}}^- \le E_{\overline{\nu}} \le E_{\overline{\nu}}^+,\ \ \eta^- \le \eta \le \eta^+\}$, the antineutrino spectral function is

$$F_{\overline{\nu}} = \frac{P_\tau}{\Gamma}\frac{d\Gamma_2}{dE_{\overline{\nu}}} = \frac{2}{g}\Bigg\{1 - 3\eta^2 + 2\eta^3 - 6r\left(1-\eta^2\right) + 3r^2\left(1+2\eta+2\ln\frac{1-\eta}{r}\right) + 2r^3$$
$$- \frac{\eta^{\parallel}_{\tau\pm}}{v_\tau}\left[1 - 6\frac{\xi\eta}{\xi+1} + 3\eta^2\frac{3\xi-1}{\xi+1} - 2\eta^3\frac{2\xi-1}{\xi+1} - 6r\left(1-\frac{4\xi\eta}{\xi+1}+\frac{3\xi-1}{\xi+1}\eta^2\right)\right.$$
$$\left. + 3r^2\left[1-2\frac{2\xi-1}{\xi+1}\eta + 2\left(1-\frac{2\xi\eta}{\xi+1}\right)\ln\frac{1-\eta}{r}\right] + 2r^3\right]\Bigg\}.$$

Appendix A. Some details of calculation of the polarization density matrix by the HMY approach [223]

In this Appendix, we collect useful details of calculation of the polarization density matrix by the noncovariant method suggested by Hagiwara, Mawatari and Yokoya [223] ("HMY approach").

It is convenient to use the lab. frame whose z axis is directed along the neutrino momentum $\mathbf{k}$ and the (x, z) plane coincides with the scattering plane. In this frame, the particle 4-momenta are

$$\begin{aligned} k &= (E_\nu, 0, 0, E_\nu)\,, \\ p &= (M, 0, 0, 0)\,, \\ k' &= (E_\ell, P_\ell \sin\theta, 0, P_\ell \cos\theta)\,. \end{aligned}$$

In order to simplify formulas, we denote $C = \cos(\theta/2)$ and $S = \sin(\theta/2)$. Then

$$CS = \frac{\sin\theta}{2}, \quad C^2 = \frac{1+\cos\theta}{2} = \frac{a_+}{2}, \quad S^2 = \frac{1-\cos\theta}{2} = \frac{a_-}{2}, \quad C^2 - S^2 = \cos\theta.$$

Let a_α and b_β be the components of some 4-vectors. Then

$$\begin{aligned} L^{\alpha\beta} a_\alpha b_\beta = \; & L^{00} a_0 b_0 + L^{01} a_0 b_1 + L^{02} a_0 b_2 + L^{03} a_0 b_3 + \\ & L^{10} a_1 b_0 + L^{11} a_1 b_1 + L^{12} a_1 b_2 + L^{13} a_1 b_3 + \\ & L^{20} a_2 b_0 + L^{21} a_2 b_1 + L^{22} a_2 b_2 + L^{23} a_2 b_3 + \\ & L^{30} a_3 b_0 + L^{31} a_3 b_1 + L^{32} a_3 b_2 + L^{33} a_0 b_3 \quad , \end{aligned}$$

The general form of the hadronic tensor is

$$\begin{aligned} W_{\alpha\beta} = & -g_{\alpha\beta} W_1 + \frac{p_\alpha\, p_\beta}{M^2} W_2 - \frac{i\,\epsilon_{\alpha\beta\gamma\delta}\, p^\gamma\, q^\delta}{2M^2} W_3 \\ & + \frac{q_\alpha\, q_\beta}{M^2} W_4 + \frac{p_\alpha\, q_\beta + q_\alpha\, p_\beta}{2M^2} W_5 + i\, \frac{p_\alpha\, q_\beta - q_\alpha\, p_\beta}{2M^2} W_6\,. \end{aligned}$$

Therefore, taking into account the identities

$$L^{00} = L^{03} = L^{30} = L^{33}, \quad L^{11} = L^{22}, \quad L^{10} = L^{13}, \quad L^{01} = L^{31}, \quad L^{02} = L^{32},$$

we have to calculate the following convolutions

$$\begin{aligned} L^{\alpha\beta} g_{\alpha\beta} &= -2L^{11}\,, \\ L^{\alpha\beta} p_\alpha\, p_\beta &= M^2 L^{00}\,, \\ L^{\alpha\beta} \epsilon_{\alpha\beta\gamma\delta}\, p^\gamma\, q^\delta &= M\left[q^3\left(L^{12} - L^{21}\right) + q^1\left(L^{23} - L^{32}\right)\right]\,, \\ L^{\alpha\beta} q_\alpha\, q_\beta &= (q_0 + q_3)\left[(q_0 + q_3)\, L^{00} + q_1 L^{10}\right] + q_1\left[(q_0 + q_3)\, L^{01} + q_1 L^{11}\right]\,, \\ L^{\alpha\beta}\left(p_\alpha\, q_\beta + q_\alpha\, p_\beta\right) &= M\left[2\,(q_0 + q_3)\, L^{00} + q_1\left(L^{01} + L^{10}\right)\right]\,, \\ L^{\alpha\beta}\left(p_\alpha\, q_\beta - q_\alpha\, p_\beta\right) &= M q_1\left(L^{01} - L^{10}\right)\,. \end{aligned}$$

All these convolutions are collected in Table 1. The upper and lower signs in that table refer to neutrino and antineutrino tensor, respectively; and $a_\pm = 1 \pm \cos\theta$.

Table 1: Structures $L^{\alpha\beta}_{\lambda\lambda'}A_{\alpha\beta}$ involved into the convolution of leptonic and hadronic tensors.

$A_{\alpha\beta}$	$++$	$+-$	$-+$	$--$
	$2E_\nu\,(E_\ell \mp P_\ell)$	$2E_\nu m\dfrac{\sin\theta}{2}$	$2E_\nu m\dfrac{\sin\theta}{2}$	$2E_\nu\,(E_\ell \pm P_\ell)$
$-g_{\alpha\beta}$	$a_\pm$	∓ 2	∓ 2	$a_\mp$
$\dfrac{p_\alpha\,p_\beta}{M^2}$	$\dfrac{a_\mp}{2}$	± 1	± 1	$\dfrac{a_\pm}{2}$
$-i\dfrac{\epsilon_{\alpha\beta\gamma\delta}\,p^\gamma\,q^\delta}{2M^2}$	$\pm\dfrac{E_\nu \mp P_\ell}{2M}a_\pm$	$-\dfrac{E_\nu}{M}$	$-\dfrac{E_\nu}{M}$	$\pm\dfrac{E_\nu \pm P_\ell}{2M}a_\mp$
$\dfrac{q_\alpha\,q_\beta}{M^2}$	$\dfrac{(E_\ell \pm P_\ell)^2}{2M^2}a_\mp$	$\pm\dfrac{m^2}{M^2}$	$\pm\dfrac{m^2}{M^2}$	$\dfrac{(E_\ell \mp P_\ell)^2}{2M^2}a_\pm$
$\dfrac{p_\alpha\,q_\beta + q_\alpha\,p_\beta}{2M^2}$	$-\dfrac{E_\ell \pm P_\ell}{2M}a_\mp$	$\mp\dfrac{E_\ell}{M}$	$\mp\dfrac{E_\ell}{M}$	$-\dfrac{E_\ell \mp P_\ell}{2M}a_\pm$
$-i\dfrac{p_\alpha\,q_\beta - q_\alpha\,p_\beta}{2M^2}$	0	$+i\dfrac{P_\ell}{M}$	$-i\dfrac{P_\ell}{M}$	0

For calculations, we used the explicit form of the leptonic currents given in by Hagiwara et al. [223]. According to Ref. [223], the leptonic tensor for ℓ^- production is $L^{\alpha\beta}_{\lambda\lambda'} = j^\alpha_\lambda \overset{*}{j}{}^\beta_{\lambda'}$, where

$$
\begin{aligned}
j^\alpha_+ &= \sqrt{2E_\nu\,(E_\ell - P_\ell)}\,(\quad S\,, -\,C\,,\ \ iC\,,\quad S)\ ,\\
\overset{*}{j}{}^\alpha_+ &= \sqrt{2E_\nu\,(E_\ell - P_\ell)}\,(\quad S\,, -\,C\,, -iC\,,\quad S)\ ,\\
j^\alpha_- &= \sqrt{2E_\nu\,(E_\ell + P_\ell)}\,(\quad C\,,\quad S\,, -iS\,,\quad C)\ ,\\
\overset{*}{j}{}^\alpha_- &= \sqrt{2E_\nu\,(E_\ell + P_\ell)}\,(\quad C\,,\quad S\,,\ \ iS\,,\quad C)\ .
\end{aligned}
$$

$$
\begin{aligned}
L^{\alpha\beta}_{++} &= 2E_\nu\,(E_\ell - P_\ell)\begin{pmatrix} S^2 & -\,CS & -iCS & S^2\\ -\,CS & C^2 & iC^2 & -\,CS\\ iCS & -iC^2 & C^2 & iCS\\ S^2 & -CS & -iCS & S^2 \end{pmatrix},\\
L^{\alpha\beta}_{+-} &= 2E_\nu m^2 \begin{pmatrix} CS & S^2 & iS^2 & CS\\ -\,C^2 & -\,CS & -iCS & -C^2\\ iC^2 & iCS & -\,CS & iC^2\\ CS & S^2 & iS^2 & CS \end{pmatrix},\\
L^{\alpha\beta}_{--} &= 2E_\nu\,(E_\ell + P_\ell)\begin{pmatrix} C^2 & CS & iCS & C^2\\ CS & S^2 & iS^2 & CS\\ -iCS & -iS^2 & S^2 & -iCS\\ C^2 & CS & iCS & C^2 \end{pmatrix},\\
L^{\alpha\beta}_{-+} &= 2E_\nu m^2 \begin{pmatrix} CS & -\,C^2 & -iC^2 & CS\\ S^2 & -\,CS & -iCS & S^2\\ -iS^2 & iCS & -\,CS & -iS^2\\ CS & -\,C^2 & -iC^2 & CS \end{pmatrix}.
\end{aligned}
$$

The leptonic tensor for ℓ^+ production is $\overline{L}^{\alpha\beta}_{\lambda\lambda'} = \overline{j}^{\alpha}_{\lambda}\overset{*}{\overline{j}}{}^{\beta}_{\lambda'}$, where

$$\begin{aligned}
\overline{j}^{\alpha}_{+} &= \sqrt{2E_\nu\,(E_\ell+P_\ell)}\,(C,\ S,\ iS,\ C)\ ,\\
\overset{*}{\overline{j}}{}^{\alpha}_{+} &= \sqrt{2E_\nu\,(E_\ell+P_\ell)}\,(C,\ S,\ -iS,\ C)\ ,\\
\overline{j}^{\alpha}_{-} &= \sqrt{2E_\nu\,(E_\ell-P_\ell)}\,(-S,\ C,\ iC,\ -S)\ ,\\
\overset{*}{\overline{j}}{}^{\alpha}_{-} &= \sqrt{2E_\nu\,(E_\ell-P_\ell)}\,(-S,\ C,\ -iC,\ -S)\ .
\end{aligned}$$

$$\begin{aligned}
\overline{L}^{\alpha\beta}_{++} &= 2E_\nu\,(E_\ell+P_\ell)\begin{pmatrix} C^2 & CS & -iCS & C^2\\ CS & S^2 & -iS^2 & CS\\ iCS & iS^2 & S^2 & iCS\\ C^2 & CS & -iCS & C^2\end{pmatrix},\\
\overline{L}^{\alpha\beta}_{+-} &= 2m^2E_\nu\begin{pmatrix} -CS & C^2 & -iC^2 & -CS\\ -S^2 & CS & -iCS & -S^2\\ -iS^2 & iCS & CS & -iS^2\\ -CS & C^2 & -iC^2 & -CS\end{pmatrix},\\
\overline{L}^{\alpha\beta}_{--} &= 2E_\nu\,(E_\ell-P_\ell)\begin{pmatrix} S^2 & -CS & iCS & S^2\\ -CS & C^2 & -iC^2 & -CS\\ -iCS & iC^2 & C^2 & -iCS\\ S^2 & -CS & iCS & S^2\end{pmatrix},\\
\overline{L}^{\alpha\beta}_{-+} &= 2m^2E_\nu\begin{pmatrix} -CS & -S^2 & iS^2 & -CS\\ C^2 & CS & -iCS & C^2\\ iC^2 & iCS & CS & iC^2\\ -CS & -S^2 & iS^2 & -CS\end{pmatrix}.
\end{aligned}$$

Appendix B. Coefficients V_i^{jk}, A_i^{jk}, K_i^{jk}

$$W_i^{(\mathrm{RES})} = \frac{2\cos^2\theta_C M M' W \Gamma(W)}{3\pi\left[\left(W^2 - M'^2\right)^2 + W^2\Gamma^2(W)\right]} \sum_{jk} \left(V_i^{jk} C_j^V C_k^V + A_i^{jk} C_j^A C_k^A + 2K_i^{jk} C_j^V C_k^A \right).$$

Here $i = 1,2,3,4,5$, $j,k = 3,4,5,6$. The coefficients V_i^{jk}, A_i^{jk} and K_i^{jk} are found to be cubic polynomials over the invariant dimensionless variables

$$w = \frac{(pq)}{M^2} = \frac{E_\nu - E_\ell}{M} \quad \text{and} \quad x = \frac{-q^2}{2(pq)} = \frac{2E_\nu\left(E_l - P_l\cos\theta\right) - m^2}{2M\left(E_\nu - E_l\right)}$$

and over the parameter $\zeta = M/M'$. The nonzero coefficients are

$$\begin{aligned}
V_1^{33} &= \zeta^3(1-2x)^2w^3 + \zeta[1+\zeta^2(1-2x)^2]w^2 + 2(1+\zeta)xw,\\
V_1^{34} &= \zeta^2(1-2x)^2w^3 + [1-\zeta(2-\zeta)(1-2x)](1-2x)w^2,\\
V_1^{35} &= \zeta^2(1-2x)w^3 + [1-\zeta(2-\zeta)(1-2x)]w^2,\\
V_1^{44} &= \zeta(1-2x)^2w^3 - (1-\zeta)(1-2x)^2w^2,\\
V_1^{45} &= 2\zeta(1-2x)w^3 - (1-\zeta)(1-4x)w^2,\\
V_1^{55} &= \zeta w^3 - (1-\zeta)w^2;
\end{aligned}$$

$$\begin{aligned}
V_2^{33} &= 2\zeta^3xw^2 + 2\zeta(1+\zeta^2)xw,\\
V_2^{34} &= 2\zeta^2xw^2 + 2(1-\zeta)^2xw,\\
V_2^{35} &= 2\zeta^2(1+2x)xw^2 + 2(1-\zeta)^2xw,\\
V_2^{44} &= 2\zeta xw^2 - 2(1-\zeta)xw,\\
V_2^{45} &= 4\zeta xw^2 - 4(1-\zeta)xw,\\
V_2^{55} &= 4\zeta^3x^2w^3 + 2\zeta[1-2\zeta(1-\zeta)x]xw^2 - 2(1-\zeta)xw;
\end{aligned}$$

$$\begin{aligned}
V_4^{33} &= 2\zeta^3(1-x)w^2 + 2\zeta^3(1-x)w - 1 - \zeta,\\
V_4^{34} &= 2\zeta^2(1-x)w^2 + [1-2\zeta(2-\zeta)(1-x)]w,\\
V_4^{35} &= 2\zeta^2w^2 - \zeta(2-\zeta)w,\\
V_4^{36} &= -2\zeta^2xw^2 - (1-\zeta)^2w,\\
V_4^{44} &= 2\zeta(1-x)w^2 - 2(1-\zeta)(1-x)w,\\
V_4^{45} &= 2\zeta w^2 - 2(1-\zeta)w,\\
V_4^{46} &= -2\zeta w^2 + 2(1-\zeta)w,\\
V_4^{55} &= \zeta^3w^3 - \zeta^2(1-\zeta)w^2,\\
V_4^{56} &= 2\zeta^3(1-2x)w^3 - 2\zeta\left[1+\zeta(1-\zeta)(1-2x)\right]w^2 + 2(1-\zeta)w,\\
V_4^{66} &= \zeta^3(1-2x)^2w^3 - \zeta\left[\zeta(1-\zeta)(1-2x)^2 - 2x\right]w^2 - 2(1-\zeta)xw;
\end{aligned}$$

$$\begin{aligned}
V_5^{33} &= 2\zeta^3w^2 + 2\zeta(1+\zeta^2)w,\\
V_5^{34} &= 2\zeta^2w^2 + 2(1-\zeta)^2w,\\
V_5^{35} &= 2\zeta^2(1+2x)w^2 + 2(1-\zeta)^2w,\\
V_5^{36} &= -4\zeta^2x^2w^2 - 2(1-\zeta)^2xw,\\
V_5^{44} &= 2\zeta w^2 - 2(1-\zeta)w,\\
V_5^{45} &= 4\zeta w^2 - 4(1-\zeta)w,\\
V_5^{46} &= -4\zeta xw^2 + 4(1-\zeta)xw,\\
V_5^{55} &= 4\zeta^3xw^3 + 2\zeta[1-2\zeta(1-\zeta)x]w^2 - 2(1-\zeta)w,\\
V_5^{56} &= 4\zeta^3(1-2x)xw^3 - 4\zeta[\zeta(1-\zeta)(1-2x)+1]xw^2 + 4(1-\zeta)xw;
\end{aligned}$$

$$\begin{aligned}
A_1^{33} &= \zeta^3(1-2x)^2w^3 + \zeta[1+\zeta^2(1-2x)^2]w^2 - 2(1-\zeta)xw,\\
A_1^{34} &= \zeta^2(1-2x)^2w^3 + [1+\zeta(2+\zeta)(1-2x)](1-2x)w^2,\\
A_1^{35} &= \zeta^2(1-2x)w^2 + [1+\zeta(2+\zeta)(1-2x)]w,\\
A_1^{44} &= \zeta(1-2x)^2w^3 + (1+\zeta)(1-2x)^2w^2,\\
A_1^{45} &= 2\zeta(1-2x)w^2 + 2(1+\zeta)(1-2x)w,\\
A_1^{55} &= \zeta w + 1 + \zeta;
\end{aligned}$$

$$\begin{aligned}
A_2^{33} &= 2\zeta^3xw^2 + 2\zeta(1+\zeta^2)xw,\\
A_2^{34} &= 2\zeta^2xw^2 + 2(1+\zeta)^2xw,\\
A_2^{35} &= 2\zeta^2xw,\\
A_2^{44} &= 2\zeta xw^2 + 2(1+\zeta)xw,\\
A_2^{55} &= \zeta^3w + \zeta^2(1+\zeta);
\end{aligned}$$

$$\begin{aligned}
A_4^{33} &= 2\zeta^3(1-x)w^2 + 2\zeta^3(1-x)w + 1 - \zeta,\\
A_4^{34} &= 2\zeta^2(1-x)w^2 + [1+2\zeta(2+\zeta)(1-x)]w,\\
A_4^{35} &= 2\zeta^2w + \zeta(2+\zeta),\\
A_4^{36} &= -2\zeta^2xw^2 - (1+\zeta)^2w,\\
A_4^{44} &= 2\zeta(1-x)w^2 + 2(1+\zeta)(1-x)w,\\
A_4^{45} &= 2\zeta w + 2(1+\zeta),\\
A_4^{46} &= -2\zeta w^2 - 2(1+\zeta)w,\\
A_4^{55} &= \zeta^3w + \zeta^2(1+\zeta),\\
A_4^{56} &= 2\zeta^3(1-2x)w^2 + 2\zeta[\zeta(1+\zeta)(1-2x) - 1]w - 2(1+\zeta),\\
A_4^{66} &= \zeta^3(1-2x)^2w^3 + \zeta[\zeta(1+\zeta)(1-2x)^2 + 2x]w^2 + 2(1+\zeta)xw;
\end{aligned}$$

$$\begin{aligned}
A_5^{33} &= 2\zeta^3w^2 + 2\zeta(1+\zeta^2)w,\\
A_5^{34} &= 2\zeta^2w^2 + 2(1+\zeta)^2w,\\
A_5^{35} &= 2\zeta^2(1+x)w + (1+\zeta)^2,\\
A_5^{36} &= -4\zeta^2x^2w^2 - 2(1+\zeta)^2xw,\\
A_5^{44} &= 2\zeta w^2 + 2(1+\zeta)w,\\
A_5^{45} &= 2\zeta w + 2(1+\zeta),\\
A_5^{46} &= -4\zeta xw^2 - 4(1+\zeta)xw,\\
A_5^{55} &= 2\zeta^3w + 2\zeta^2(1+\zeta),\\
A_5^{56} &= 2\zeta^3(1-2x)w^2 + 2\zeta^2(1+\zeta)(1-2x)w;
\end{aligned}$$

$$\begin{aligned}
K_3^{33} &= -2\zeta^3(1-2x)^2w^2 + 2\zeta(2-3x)w,\\
K_3^{34} &= -\zeta^2(1-2x)^2w^2 + 2(1+\zeta)(1-2x)w,\\
K_3^{35} &= -\zeta^2(1-2x)w + 2(1+\zeta),\\
K_3^{43} &= -\zeta^2(1-2x)^2w^2 + 2(1-\zeta)(1-2x)w,\\
K_3^{44} &= \zeta(1-2x)^2w^2,\\
K_3^{45} &= \zeta(1-2x)w,\\
K_3^{53} &= -\zeta^2(1-2x)w^2 - 2(1-\zeta)w,\\
K_3^{54} &= \zeta(1-2x)w^2,\\
K_3^{55} &= \zeta w.
\end{aligned}$$

Appendix C. Partonic Cross Sections

The elementary cross sections $d\sigma/dxdy$ for νq, $\nu\overline{q}$, $\overline{\nu}q$, and $\overline{\nu q}$ CC scattering are listed in Table 2 borrowed from Ref. [190].

Table 2: The "naive" parton model cross sections for proton and neutron targets.

Process	p	n	Process	p	n
$\nu d \to \ell^- u$	$\sigma_c^d(x)$	$\sigma_c^u(x)$	$\overline{\nu d} \to \ell^+ \overline{u}$	$\sigma_c^{\overline{d}}(x)$	$\sigma_c^{\overline{u}}(x)$
$\nu s \to \ell^- u$	$\sigma_s^s(x)$	$\sigma_s^s(x)$	$\overline{\nu s} \to \ell^+ \overline{u}$	$\sigma_s^{\overline{s}}(x)$	$\sigma_s^{\overline{s}}(x)$
$\nu \overline{u} \to \ell^- \overline{d}$	$\overline{\sigma}_c^{\overline{u}}(x)$	$\overline{\sigma}_c^{\overline{d}}(x)$	$\overline{\nu} u \to \ell^+ d$	$\overline{\sigma}_c^u(x)$	$\overline{\sigma}_c^d(x)$
$\nu \overline{u} \to \ell^- \overline{s}$	$\overline{\sigma}_s^{\overline{u}}(x)$	$\overline{\sigma}_s^{\overline{d}}(x)$	$\overline{\nu} u \to \ell^+ s$	$\overline{\sigma}_s^u(x)$	$\overline{\sigma}_s^d(x)$
$\nu d \to \ell^- c$	$\sigma_s^d(z) + \varsigma_s^d$	$\sigma_s^u(z) + \varsigma_s^u$	$\overline{\nu d} \to \ell^+ \overline{c}$	$\sigma_s^{\overline{d}}(z) + \varsigma_s^d$	$\sigma_s^{\overline{u}}(z) + \varsigma_s^{\overline{u}}$
$\nu s \to \ell^- c$	$\sigma_c^s(z) + \varsigma_c^s$	$\sigma_c^s(z) + \varsigma_c^s$	$\overline{\nu s} \to \ell^+ \overline{c}$	$\sigma_c^{\overline{s}}(z) + \varsigma_c^s$	$\sigma_c^{\overline{s}}(z) + \varsigma_c^{\overline{s}}$
$\nu \overline{c} \to \ell^- \overline{d}$	$\overline{\sigma}_s^{\overline{c}}(z) + \varsigma_s^{\overline{c}}$	$\overline{\sigma}_s^{\overline{c}}(z) + \varsigma_s^{\overline{c}}$	$\overline{\nu} c \to \ell^+ d$	$\overline{\sigma}_s^{\overline{c}}(z) + \varsigma_s^c$	$\overline{\sigma}_s^{\overline{c}}(z) + \varsigma_s^c$
$\nu \overline{c} \to \ell^- \overline{s}$	$\overline{\sigma}_c^{\overline{c}}(z) + \varsigma_c^{\overline{c}}$	$\overline{\sigma}_c^{\overline{c}}(z) + \varsigma_c^{\overline{c}}$	$\overline{\nu} c \to \ell^+ s$	$\overline{\sigma}_c^{\overline{c}}(z) + \varsigma_c^c$	$\overline{\sigma}_c^{\overline{c}}(z) + \varsigma_c^c$

The following notation has been used in the Table:

$$\sigma_c^q(x) = \left(\frac{G_F^2 sx}{\pi}\right) \cos^2\theta_C\, q(x), \quad \overline{\sigma}_c^q(x) = \left(\frac{G_F^2 sx}{\pi}\right) \cos^2\theta_C\, q(x)(1-y)^2,$$
$$\sigma_s^q(x) = \left(\frac{G_F^2 sx}{\pi}\right) \sin^2\theta_C\, q(x), \quad \overline{\sigma}_s^q(x) = \left(\frac{G_F^2 sx}{\pi}\right) \sin^2\theta_C\, q(x)(1-y)^2,$$
$$\varsigma_c^q = \left(\frac{G_F^2 sx}{\pi}\right) \cos^2\theta_C\, q(x)(z-x)(1-y),$$
$$\varsigma_s^q = \left(\frac{G_F^2 sx}{\pi}\right) \sin^2\theta_C\, q(x)(z-x)(1-y).$$

Here $q(x)$ is the quark density specified in respect to proton and z is the momentum fraction of the scattering parton which is defined in Ref. [190] through the condition $(q+zp)^2 = m_c^2$. The formal positive solution to this equation is given by

$$z = \frac{Q^2}{2M^2x}\left[\sqrt{1+\frac{4M^2x^2}{Q^2}\left(1+\frac{m_c^2}{Q^2}\right)}-1\right] = \frac{2x\left(1+\frac{m_c^2}{Q^2}\right)}{1+\sqrt{1+\frac{4M^2x^2}{Q^2}\left(1+\frac{m_c^2}{Q^2}\right)}}. \tag{1}$$

As is easy to see from this equation, $z = x_N$ (where x_N is the Nachtmann variable) in the limit $m_c = 0$. Any case, the authors do not even mention Eq. (1) but use its approximation,

$$z \approx x\left(1+\frac{m_c^2}{Q^2}\right),$$

which is valid at $Q^2 \gg 4M^2x^2$. Therefore the (approximate) z is just the scaling variable used by Hagiwara et al. [223]. Clearly it has no physical meaning when $Q^2 \lesssim 4M^2x^2$.

Let us study a bit the properties of the *exact* variable z. First we note that

$$\frac{\partial z}{\partial x} = \frac{z}{x}\left(1+\frac{2M^2xz}{Q^2}\right)^{-1} > 0 \quad \text{and} \quad \frac{\partial z}{\partial Q^2} = \frac{x-z}{Q^2}\left(1+\frac{2M^2xz}{Q^2}\right)^{-1}.$$

Next, the condition $z = x$ holds if and only if $x = m_c/M$. Since $m_c > M$ and z/x is a monotonically *decreasing* function of x, it is easy to see that $z \geq x$ at any Q^2 and the equality only holds in the limit $Q^2 \to \infty$. Therefore z is a monotonically *decreasing* function of Q^2. Finally $0 \leq z \leq 1$ when

$$0 \leq x \leq \left(1+\frac{m_c^2-M^2}{Q^2}\right)^{-1}.$$

[Compare this with Eq. (5.2).]

Appendix D. Distributions etc.

Here we derive some trivial formulas for the distributions. Let $F(E_\nu)$ be the neutrino energy spectrum and x be some kinematic variable (E_ℓ, $\cos\theta$, Q^2, $\ldots$). The number of events per unit time,[1] caused by neutrinos with energies from E_ν to $E_\nu + dE_\nu$ in the interval $(x, x+dx)$ is equal to

$$dN(E_\nu, x) = \frac{d\sigma(E_\nu, x)}{dx} F(E_\nu) dE_\nu dx.$$

The sum over the spectrum of the number of events in the same interval $(x, x+dx)$ is

$$\langle dN(E_\nu, x)\rangle = dx \int_0^\infty \frac{d\sigma(E_\nu, x)}{dx} F(E_\nu) dE_\nu,$$

whence

$$\left\langle \frac{dN(E_\nu, x)}{dx} \right\rangle = \int_0^\infty \frac{d\sigma(E_\nu, x)}{dx} F(E_\nu) dE_\nu,$$

Let the measurements be made on a finite interval (x_1, x_2).[2] Then the total number of events is

$$N = \int \langle dN(E_\nu, x)\rangle = \int_{x_1}^{x_2} \left\langle \frac{dN(E_\nu, x)}{dx} \right\rangle dx = \int_{x_1}^{x_2} dx \int_0^\infty \frac{d\sigma(E_\nu, x)}{dx} F(E_\nu) dE_\nu,$$

Let's assume that the cross section $d\sigma(E_\nu, x)/dx$ is always defined so that it is zero outside the kinematically admissible region of the variables E_ν and x. Then, *assuming that the interval* (x_1, x_2) *is wide enough*,[3]

$$\int_{x_1}^{x_2} dx \frac{d\sigma(E_\nu, x)}{dx} = \sigma(E_\nu)$$

is the total cross section. Hence

$$N = \int_0^\infty \sigma(E_\nu) F(E_\nu) dE_\nu. \tag{2}$$

Then the normalized distribution of the numbers of events on the variable x is

$$\frac{d\rho}{dx} = \left\langle \frac{1}{N} \frac{dN(E_\nu, x)}{dx} \right\rangle = \frac{\int_0^\infty \frac{d\sigma(E_\nu, x)}{dx} F(E_\nu) dE_\nu}{\int_0^\infty \sigma(E_\nu) F(E_\nu) dE_\nu} = \frac{\langle d\sigma(E_\nu, x)/dx\rangle}{\langle \sigma(E_\nu)\rangle}. \tag{3}$$

This is what we usually call the distribution and denote simply $\langle dN/dx\rangle$. This value is only approximately equal to

$$\left\langle \frac{1}{\sigma(E_\nu)} \frac{d\sigma(E_\nu, x)}{dx} \right\rangle. \tag{4}$$

The value of (3) itself is generally defined only approximately, since in a real experiment the interval (x_1, x_2) experiment, strictly speaking, the interval (x_1, x_2) can never be wide enough – something is always undercounted and undermeasured. But we always assume that the experimenters know all this and make the necessary corrections.[4] Thus, the correct formula for distribution is (3), not (4)... Unless experimenters specifically state that their data should be understood as (4) (i.e., for some reason the data have been recalculated to that quantity) – which I generally don't recall. It's useful to do calculations in individual fits using the formulas (3) and (4), to see how different these values can be. In the case of QES, we should expect the differences to be small at high energies and large at low energies, with the difference being larger for antineutrinos at high energies than for neutrinos. In general, the differences will affect both the form of the $d\rho/dx$ distribution dependence on x, and in the normalization of N_0 determined from fit.,[5] as well as in the value of χ^2. Note also that at first glance it may seem that the value $d\rho/dx$ is rather poorly measured, since rather crude approximations are used in its determination. Let me reassure you (as one of Zadornov's characters used to say): for obvious reasons, the sections themselves are defined even worse...

---

[1] Tha is count rate.

[2] That is, x_1 is the left boundary of the leftmost experimental bin, and x_2 is the right boundary of the rightmost experimental bin.

[3] Which, of course, is by no means always the case, and which is mainly due to the difficulty of conversion of the measured count rates into the cross sections, distributions, etc.

[4] Since the main errors due to undercounting are concentrated in the extreme x bins, these bins are the least reliable and clever experimenters should not even show them.

[5] The letter N is used in every way imaginable. I hope there will be no confusion here. We almost always have an unknown normalization for both normalized and non-normalized distributions, because the value (2) is always defined with an error.

Appendix E. Additional notes

Integration over x and y for DIS.

Davaj akkuratno napishem formulu dlja $d\sigma^{\rm DIS}_{\nu N\to lhX}/dy$. Ya nadejus', chto uzhe posle etogo vse stanet yasno. Tem ne menee ya vypshu i formulu dlja polnogo sechenija. Nizhe ya budu ispol'zovat' oboznachenija iz svoego faila Nachtmann.pdf (vozmozhno, ne slishkom udachnye) s uchetom popravki, kotoraja v nem ne byla otrazhena, no o kotoroj ty znaesh. Dlja polnoty ya napomnju osnovnye oboznachenija i vvedu po hodu dela neskol'ko novyh. Ves' etot konglomerat gromozdkih oboznachenij ne dlja stat'i, konechno, a dlja togo lish, chtoby ne voznikalo neodnoznachnostej v ponimanii. Dlja toj-zhe celi tekst pishetsja na English (v otsutstvie kirillicy - on bolee odnoznachen).

Correct integration over Bjorken x.

First, let us remind ourselfs that the DIS physical boundary is given by the equation

$$\left(Q^2+m_\ell^2\right)^2+\frac{2Q^2E_\nu}{M_Nx}\left(Q^2+m_\ell^2\right)-4Q^2E_\nu^2=0$$

and its solution for the Bjorken variable y consists of two branchs

$$y^\pm=y^\pm(x,E_\nu)=\frac{1-\dfrac{m_\ell^2}{2E_\nu^2}\left(1+\dfrac{E_\nu}{M_Nx}\right)\pm\sqrt{\left(1-\dfrac{m_\ell^2}{2M_NxE_\nu}\right)^2-\dfrac{m_\ell^2}{E_\nu^2}}}{2\left(1+\dfrac{M_Nx}{2E_\nu}\right)}.$$

This solution exists if

$$x\geq x^-=\frac{m_\ell^2}{2M_N(E_\nu-m_\ell)}.$$

Therefore the full DIS physical region is given by the inequalities

$$x^-\leq x\leq 1,\quad y^-\leq y\leq y^+,\quad E_\nu\geq\frac{\left(M_N+m_\ell\right)^2-M_N^2}{2M_N}.$$

The equation $W=M_h$ written in terms of variables x and Q^2 is

$$(1-x)Q^2=\left(M_h^2-M_N^2\right)x.$$

Here M_h is the total mass of the final state hadron system h and we assume below that $M_h>M_N$ ($M_h=M_N+m_\pi$,$M_h=M_N+2m_\pi$, etc.).

Now we enumerate the main definitions.

1. The points of intersection between the DIS physical boundary and the curve $W=M_h$ are

$$x=x_h^\pm=\frac{a_h\pm b_h}{2c_h},$$

where

$$a_h=1-\frac{\left(M_h^2-M_N^2-m_\ell^2\right)\left[\left(M_h^2-M_N^2\right)E_\nu+m_\ell^2M_N\right]}{2M_N\left(M_h^2-M_N^2\right)E_\nu^2},$$

$$b_h^2=\left[1-\frac{\left(M_h-m_\ell\right)^2-M_N^2}{2M_NE_\nu}\right]\left[1-\frac{\left(M_h+m_\ell\right)^2-M_N^2}{2M_NE_\nu}\right],$$

$$c_h=1+\frac{\left(M_h^2-M_N^2-m_\ell^2\right)^2}{4\left(M_h^2-M_N^2\right)E_\nu^2}.$$

Clearly $b_h^2\geq 0$ (and thus the physical solution there exists) when

$$E_\nu\geq E_\nu^h=\frac{\left(M_h+m_\ell\right)^2-M_N^2}{2M_N}$$

and E_ν^h is exactly the *threshold neutrino energy* for the inclusive raction $\nu N\to lhX$.

A little bit more compact formula for $x_h^\pm$ is

$$x_h^\pm=1-\frac{a_h'\mp b_h}{2c_h},$$

where

$$a_h'=2c_h-a_h=1+\frac{(M_h^2-M_N^2-m_\ell^2)(E_\nu+M_N)}{2M_NE_\nu}.$$

2. The boundary values of the Bjorken variable in the points $x = x_h^{\pm}$:

$$y_h^{\pm}(E_\nu) = \frac{M_h^2 - M_N^2}{2M_N\left(1 - x_h^{\pm}\right)E_\nu}.$$

3. The value of $y^{\pm}$ in the point $x = x^-$:

$$y_0 = y^-(x^-, E_\nu) = y^+(x^-, E_\nu) = \frac{1 - \dfrac{m_\ell^2}{2E_\nu^2}\left(1 + \dfrac{E_\nu}{M_N x^-}\right)}{2\left(1 + \frac{M_N x^-}{2E_\nu}\right)} = \frac{m_\ell}{E_\nu}\left(\frac{E_\nu - m_\ell}{2E_\nu - m_\ell}\right).$$

By using the above definitions we can write the differential cross section

$$\frac{d\sigma_{\nu N\to lhX}^{\text{DIS}}(y, E_\nu)}{dy} = \int_{x_h^{\min}}^{x_h^{\max}} \frac{d^2\sigma_{\nu N\to l+\text{anyth}}(x, y, E_\nu)}{dxdy}\,dx \tag{5a}$$

$$= \left(x_h^{\max} - x_h^{\min}\right)\int_0^1 \frac{d^2\sigma_{\nu N\to l+\text{anyth}}(x, y, E_\nu)}{dxdy}\,dx'. \tag{5b}$$

The new variable of integration x' in Eq. (5b) is given by the equation

$$x = \left(x_h^{\max} - x_h^{\min}\right)x' + x_h^{\min};$$

and the limits of integration in Eq. (5a) are

$$x_h^{\min} = \begin{cases} x^- & \text{if} \quad y_h^- \le y_0, \\ x_h^- & \text{if} \quad y_h^- > y_0, \end{cases} \qquad x_h^{\max} = x_h^+. \tag{6}$$

Obviously the $d\sigma_{\nu N\to lhX}^{\text{DIS}}/dy$ is nonzero under the conditions

$$E_\nu > E_\nu^h = \frac{(M_h + m_\ell)^2 - M_N^2}{2M_N}, \qquad y_h^- < y < y_h^+.$$

Correct integration over Bjorken y.

This is already a trivial task:

$$\sigma_{\nu N}^{\text{DIS,tot}}(E_\nu) = \int_{y_h^-(E_\nu)}^{y_h^+(E_\nu)} \frac{d\sigma_{\nu N\to lhX}(y, E_\nu)}{dy}\,dy \tag{7a}$$

$$= \left[y_h^+(E_\nu) - y_h^-(E_\nu)\right]\int_0^1 \frac{d\sigma_{\nu N\to lhX}(y, E_\nu)}{dy}\,dy'. \tag{7b}$$

The new variable of integration y' in Eq. (7a) is given by

$$y = \left[y_h^+(E_\nu) - y_h^-(E_\nu)\right]y' + y_h^-(E_\nu).$$

The total cross section is nonzero for

$$E_\nu > E_\nu^h = \frac{(M_h + m_\ell)^2 - M_N^2}{2M_N}.$$

Hadronic Tensor (must be translated)

Otkuda voobshe berutsja novye (po sravneniju s bezmassovym sluchaem) struktury v adronnom tenzore? V sluchae nepoljarizovannoj misheni iz impul'sov p i q (indeks N opuskaju), tenzora $g_{\alpha\beta}$ i psevdotenzora $\epsilon_{\alpha\beta\gamma\delta}$ mozhno sostavit' tol'ko 6 nezavisimyh tenzornyh kombinacij:

$$g_{\alpha\beta}, \quad p_\alpha p_\beta, \quad p_\alpha q_\beta, \quad q_\alpha p_\beta, \quad q_\alpha q_\beta, \quad \epsilon_{\alpha\beta\gamma\delta} p^\gamma q^\delta.$$

Pri etom, vmesto 3-ej i 4-oj struktur udobno ispol'zovat' ih simmetrichnuju i antisimmetrichnuju kombinacii $p_\alpha q_\beta \pm q_\alpha p_\beta$.

V bezmassovom sluchae adronnyj tenzor ortogonalen vektoru q, t.k. CC tok sohranjaetsja. Mozhno poostroit' lish 3 ortogonal'nye kombinacii:

$$\frac{q_\alpha q_\beta}{q^2} - g_{\alpha\beta}, \quad \widetilde{p}_\alpha \widetilde{p}_\beta, \quad \epsilon_{\alpha\beta\gamma\delta} p^\gamma q^\delta, \tag{8}$$

gde

$$\widetilde{p}_\alpha = p_\alpha - \frac{pq}{q^2} q_\alpha.$$

T.o., v obshem sluchae imeem:

$$\begin{aligned} W_{\alpha\beta} = & -g_{\alpha\beta} W_1 + \frac{p_\alpha p_\beta}{M^2} W_2 - i \frac{\epsilon_{\alpha\beta\gamma\delta} p^\gamma q^\delta}{2M^2} W_3 \\ & + \frac{q_\alpha q_\beta}{M^2} W_4 + \frac{p_\alpha q_\beta + q_\alpha p_\beta}{2M^2} W_5 - i \frac{p_\alpha q_\beta - q_\alpha p_\beta}{2M^2} W_6. \end{aligned} \tag{9}$$

Obrati vnimanie na mnozhiteli. Ya pishu ih v tochnosti kak v obzore [6].

Mozhno zapisat' to-zhe samoe ispol'zuja struktury (8):

$$\begin{aligned} W_{\alpha\beta} = & \left(\frac{q_\alpha q_\beta}{q^2} - g_{\alpha\beta} \right) W_1 + \frac{\widetilde{p}_\alpha \widetilde{p}_\beta}{M^2} W_2 - i \frac{\epsilon_{\alpha\beta\gamma\delta} p^\gamma q^\delta}{2M^2} W_3 \\ & + \frac{q_\alpha q_\beta}{M^2} \widetilde{W}_4 + \frac{p_\alpha q_\beta + q_\alpha p_\beta}{2M^2} \widetilde{W}_5 - i \frac{p_\alpha q_\beta - q_\alpha p_\beta}{2M^2} W_6. \end{aligned} \tag{10}$$

Strukturnye funkcii $W_{4,5}$ i $\widetilde{W}_{4,5}$ svjazany sootnoshenijami

$$W_4 = \widetilde{W}_4 + \frac{M^2}{q^2} W_1 + \left(\frac{pq}{q^2} \right)^2 W_2, \quad W_5 = \widetilde{W}_5 - 2 \left(\frac{pq}{q^2} \right) W_2. \tag{11}$$

Kak pokazano v rabotah [L14] i [D7], citiruemyh v obzore Llewellyn Smith [6], funkcii $W_{1,2}$ neotricatel'ny. Ostal'nye funkcii W_i udovletvorjajut neravenstvam[6] iz kotoryh sleduet, chto vse oni veshestvenny i nesinguljarny pri $q^2 \to 0$. Togda iz Eq. (11) vidno, chto funkcii $\widetilde{W}_{4,5}$ singuljarny pri $q^2 \to 0$. Poetomu oni nikoim obrazom ne mogut byt' linejnymi kombinacijami kvarkovyh plotnostej s postojannymi koefficientami i etim ves'ma neudobnu dlja nashih celej.

T.o., vyrazhenie (9), ispol'zuemoe v rabote [222], a takzhe formuly, svjazyvajushie W_i s F_i sovershenno pravil'ny (chego nel'zja skazat' o konechnyh rezul'tatah [222], ravno ravno kak i [6]). Starkov [221] etogo ne ponjal i napisal nepravil'nye svjazi mezhdu $\widetilde{W}_i$ i F_i. Krome togo, on pochti vo vseh vkladah nadelal oshibok. Koroche, ego stat'ju – na pomojku...

Eshe odno trivila'noe zamechanie dlja polnoty. V predele $m_l^2 \to 0$ slagaemye v (9), soderzhashie $W_{4,5,6}$ ischezajut. Poetomu mozhno zapisat'

$$W_{\alpha\beta} = -g_{\alpha\beta} W_1 + \frac{p_\alpha p_\beta}{M^2} W_2 - i \frac{\epsilon_{\alpha\beta\gamma\delta} p^\gamma q^\delta}{2M^2} W_3$$

ili, chto ekvivalentno dlja rascheta sechenij,

$$W_{\alpha\beta} = \left(\frac{q_\alpha q_\beta}{q^2} - g_{\alpha\beta} \right) W_1 + \frac{\widetilde{p}_\alpha \widetilde{p}_\beta}{M^2} W_2 - i \frac{\epsilon_{\alpha\beta\gamma\delta} p^\gamma q^\delta}{2M^2} W_3.$$

Razumeetsja, dlja rascheta poljarizacionnoj matricy leptona obe eti formy neprigodny. No ih obobshenie na sluchaj poljarizovannoj misheni, napisannoe u Efremova i Ko [12], vpolne prigodno dlja reakcij s electronnym i muonnym (anti)nejtrino. Tak chto v PDG net oshibok v etom meste.

[6] Eti neravenstva mozhno poluchit' iz uslovija, chto vse minory matricu $\| W_{\alpha\beta} \|$ neotricatel'ny [6].

Bibliography

[**Marginal notes**:]

Reference marked by ★ reminds that the paper is absent from our database and it would be good to obtain its hard copy and scan it for a soft copy; the more stars the more we are in need of the paper.
Reference marked with D or F contains useful tabulated data or figures.
Reference marked with d or f contains the data which must be recalculated or low-quality figures inconvenient to extract the data.
The large tick ✓ means that the data from the paper are already included in our database and utilized in our figures or tables.
The small tick ✓ means that we will not use the data from the paper by some reasons (normally mentioned in the corresponding comment).

GENERAL

[1] L. B. Okun, "Leptons and quarks," Moscow, "Nauka", 1981.

[2] D. Bardin and G. Passarino, "The standard model in the making," Oxford University Press, 1999.

[3] K. Hagiwara *et al.* (Particle Data Group), "Review of particle physics," Phys. Rev. D **66** (2002) 010001 and the 2003 web edition (URL: http://pdg.lbl.gov/).

[4] S. Eidelman *et al.* (Particle Data Group), "Review of particle physics," Phys. Lett. B **592** (2004) 1–1109.

NEUTRINO–NUCLEON INTERACTIONS

Reviews

[5] A. Pais, "Weak interactions at high energies," Annals Phys. **63** (1971) 361–392; erratum – *ibid*. **69** (1972) 604–605.

[6] C. H. Llewellyn Smith, "Neutrino reactions at accelerator energies," Phys. Rept. **3** C (1972) 261–379.
Comment: the preprint of this paper [SLAC-PUB-958 (1971)] is full of errors and typos.

[7] B. C. Barish, "Recent high energy electron, muon, and neutrino experiments," in Proc. of the Div. of Particles and Fields Meeting, American Physical Society, Williamsburg, September 5 – 7, 1974, pp. 1–21 [see also preprint CALT-68-477].
Comment: figures with some (probably) obsolete data.

[8] F. J. Gilman, "Deep inelastic scattering and the structure of hadrons" (Rapporteur's talk), in Proc. of the 17th International Conference on High Energy Physics, London, England, July 1–10, 1974, edited by J. R. Smith (Chilton, Rutherford Lab., 1974), p. IV-149 [preprint SLAC-PUB-1455].
Comment: figures with some (probably) obsolete data.

[9] B. C. Barish, "Experimental aspects of high energy neutrino physics," Phys. Rept. **39** (1978) 279–360.
Comment: figures with some data; maybe useful.

[10] D. Theriot, "Recent experimental measurements of the neutrino charged current cross-cections," in Proc. of the International Symposium on Lepton and Photon Interactions at High Energies, Batavia, Ill., Fermilab, August 23–29, 1979, edited by T. B. W. Kirk and H. D. I. Abarbanel, p. 337 [preprint FERMILAB-CONF-79-079-EXP].
Comment: figures with some data; maybe useful.

[11] J. Steinberger, "Experiments with high-energy neutrino Beams," Rev. Mod. Phys. **61** (1989) 533–545.

[12] M. Anselmino, A. Efremov, and E. Leader, "The theory and phenomenology of polarized deep inelastic scattering," Phys. Rept. **261** (1995) 1–124; erratum – *ibid*. **281**(1997) 399 [arXiv:hep-ph/9501369].

[13] J. M. Conrad, M. H. Shaevitz, and T. Bolton, "Precision measurements with high energy neutrino beams," Rev. Mod. Phys. **70** (1998) 1341–1392 [arXiv:hep-ex/9707015].

Quasielastic scattering (experiment)

CERN Early experiments

[14] M. M. Block *et al.*, "Neutrino interactions in the CERN heavy liquid bubble chamber," Phys. Lett. **12** (1964) 281–285.
Comment: $M_A = 1.0^{+0.5}_{-0.3}$ GeV (obsolete).

[15] I. Budagov *et al.*, "A study of the elastic neutrino process $\nu + n \to \mu^- + p$," Lett. Nuovo Cim. **2** (1969) 689–695.
Comment: $M_A = 0.7 \pm 0.2$ GeV.

[16] O. Erriquez *et al.*, "Production of strange particles in antineutrino interactions at the CERN PS," Nucl. Phys. B **140** (1978) 123–140.
Comment: $M_A = 0.883 \pm 0.243$ GeV (from $\overline{\nu}p \to \mu^+\Lambda$).

CERN BEBC (Experiment WA25)

[17] D. Allasia *et al.* (WA25 Collaboration), "Investigation of exclusive channels in $\nu/\overline{\nu}$-deuteron charged current interactions," Nucl. Phys. B **343** (1990) 285–309.
Durham Reaction Data: http://www.slac.stanford.edu/cgi-hepdata/hepreac/2325837.
Comment: $M_A = 1.08 \pm 0.08$ GeV.

CERN Gargamelle

[18] S. Bonetti *et al.*, "Study of quasielastic reactions of neutrino and antineutrino in Gargamelle," Nuovo Cim. A **38** (1977) 260–270.
Durham Reaction Data: http://www.slac.stanford.edu/cgi-hepdata/hepreac/501778.
Comment: Two versions.

[19] M. Dewit (for the Aachen-Bruxelles-CERN-Ecole Polytechnique-Orsay-Padova Collaboration), "Experimental study of the reaction $\nu n \to \mu^- p$," in Proc. of the Topical Conf. on Neutrino Physics at Accelerators, Oxford, England, July 4 – 7, 1978, edited by A. G. Michette and P. B. Renton, pp. 75–77.
Comment: $M_A = 0.87 \pm 0.05 \pm 0.17$ GeV (σ) or $M_A = 0.99 \pm 0.12 \pm 0.17$ GeV ($d\sigma/dQ^2$). Probably is overlapped by Ref. [20]

[20] M. Pohl *et al.* (Gargamelle Neutrino Propane Collaboration), "Experimental study of the reaction $\nu n \to \mu^- p$," Lett. Nuovo Cim. **26** (1979) 332–336.
Durham Reaction Data: http://www.slac.stanford.edu/cgi-hepdata/hepreac/616206.
Comment: $M_A = 0.87 \pm 0.05 \pm 0.17$ GeV (σ) or $M_A = 0.99 \pm 0.12$ GeV ($d\sigma/dQ^2$).

[21] N. Armenise *et al.* "Charged current elastic antineutrino interactions in propane," Nucl. Phys. B **152** (1979) 365–375.
Comment: $M_A = 0.91 \pm 0.04$ GeV for $M_V = 0.84$ GeV or $M_A = 0.94 \pm 0.07$ GeV, $M_V = 0.81 \pm 0.03$ GeV in simultaneous fit.

CERN NOMAD

[22] V. V. Lyubushkin, D. V. Naumov, and B. A. Popov, "A study of quasi-elastic neutrino interactions in the NOMAD experiment," NOMAD Internal Memo, 2004-04.

ANL

[23] R. L. Kustom *et al.*, "Quasielastic neutrino scattering," Phys. Rev. Lett. **22** (1969) 1014–1017.
Comment: $M_A = 0.7 \pm 0.15$ or 1.05 ± 0.2 GeV.

[24] W. A. Mann *et al.*, "Study of the reaction $\nu + N \to \mu^- + p$," Phys. Rev. Lett. **31** (1973) 844–847.
Comment: $M_A = 0.95 \pm 0.12$ GeV.

[25] S. J. Barish *et al.*, "Study of neutrino interactions in hydrogen and deuterium: description of the experiment and study of the reaction $\nu + d \to \mu^- + p + p_s$," Phys. Rev. D **16** (1977) 3103–3121.
Durham Reaction Data: http://www.slac.stanford.edu/cgi-hepdata/hepreac/233870.
Comment: $M_A = 0.95 \pm 0.09$ GeV.

[26] K. L. Miller *et al.*, “Study of the reaction $\nu + d \to \mu^- + p + p_s$,” Phys. Rev. D **26** (1982) 537–542; see also K. L. Miller, “A study of the weak axial-vector form factor in the quasi-elastic reaction $\nu + d \to \mu^- + p + p_s$,” Ph. D. Thesis (Carnegie–Mellon University, September 1980), UMI 82-09392. ★
Comment: $M_A = 1.00 \pm 0.05$ GeV.

BNL

[27] G. Fanourakis *et al.*, “Study of low-energy antineutrino interactions on protons,” Phys. Rev. D **21** (1980) 562–568.
Durham Reaction Data: http://www.slac.stanford.edu/cgi-hepdata/hepreac/608734.
Comment: $M_A = 0.9^{+0.4}_{-0.3}$ GeV (from $\overline{\nu}p \to \mu^+ p\pi^-$).

[28] N. J. Baker *et al.*, “Quasielastic neutrino scattering: a measurement of the weak nucleon axial vector form factor,” Phys. Rev. D **23** (1981) 2499–2505.
Durham Reaction Data: http://www.slac.stanford.edu/cgi-hepdata/hepreac/891070.
Comment: $M_A = 1.07 \pm 0.06$ GeV.

[29] L. A. Ahrens *et al.*, “A study of the axial-vector form factor and second-class currents in antineutrino quasielastic scattering,” Phys. Lett. B **202** (1988) 284–288.
Comment: $M_A = 1.09 \pm 0.03 \pm 0.02$ GeV.

FNAL

[30] T. Kitagaki *et al.*, “High-energy quasielastic $\nu_{mu} n \to \mu^- p$ scattering in deuterium,” Phys. Rev. D **28** (1983) 436–442.
Durham Reaction Data: http://www.slac.stanford.edu/cgi-hepdata/hepreac/1149580.
Comment: $M_A = 1.06^{+0.12}_{-0.16}$ GeV.

IHEP

[31] V. V. Makeev *et al.*, “Quasielastic neutrino scattering $\nu_\mu n \to \mu^- p$ at 2 to 20 GeV in bubble chamber SKAT,” Zh. Eksp. Teor. Fiz. Pisma **34** (1981) 418–421 [see also preprint IFVE-81-144].

[32] S. V. Belikov *et al.*, “Quasielastic $\nu_\mu n$ scattering at 3–30 GeV energy,” Yad. Fiz. **35** (1982) 59–63 [Sov. J. Nucl. Phys. **35** (1982) 35–38].
Durham Reaction Data: http://www.slac.stanford.edu/cgi-hepdata/hepreac/816663.
Comment: $M_A = 1.00 \pm 0.07$ GeV.

[33] A. E. Asratian *et al.*, “Antineutrino quasielastic scattering in neon and total cross sections in the energy interval 10–50 GeV,” Yad. Fiz. **39** (1984) 619–625 [Sov. J. Nucl. Phys. **39** (1984) 392–395];
Durham Reaction Data: http://www.slac.stanford.edu/cgi-hepdata/hepreac/1291769.
A. E. Asratyan *et al.*, “Total antineutrino–nucleon charged current cross section in the energy range 10–50 GeV,” Phys. Lett. B **137** (1984) 122–124.
Durham Reaction Data: http://www.slac.stanford.edu/cgi-hepdata/hepreac/1246240.
Comment: $M_A = 0.99 \pm 0.11$ GeV.

[34] S. V. Belikov *et al.*, “Quasielastic neutrino and antineutrino scattering total cross-sections, axial-vector form-factor,” Z. Phys. A **320** (1985) 625–633.
Durham Reaction Data: http://www.slac.stanford.edu/cgi-hepdata/hepreac/1160230.
Comment: $M_A = 1.00 \pm 0.04$ GeV.

[35] H. J. Grabosch *et al.* (SKAT Collaboration), “Investigation of quasielastic neutrino and antineutrino reactions in the energy range below 20 GeV,” preprint PHE 86-11.

[36] H. J. Grabosch *et al.* (SKAT Collaboration), “Study of the quasielastic reactions $\nu n \to \mu^- p$ and $\overline{\nu} p \to \mu^+ n$ in the SKAT bubble chamber at energies 3–20 GeV,” Yad. Fiz. **47** (1988) 1630–1634 [Sov. J. Nucl. Phys. **47** (1988) 1032–1034].

[37] J. Brunner *et al.* (SKAT Collaboration), “Quasielastic nucleon and hyperon production by neutrinos and antineutrinos with energies below 30 GeV,” Z. Phys. C **45** (1990) 551–555.
Durham Reaction Data: http://www.slac.stanford.edu/cgi-hepdata/hepreac/2070456.
Comment: $M_A = 1.06 \pm 0.05 \pm 0.14$ GeV (from ν) and $M_A = 0.71 \pm 0.10 \pm 0.20$ GeV (from $\overline{\nu}$).

[38] V. V. Ammosov *et al.* (SKAT Collaboration), “Investigation of neutrino interactions using the bubble chamber SKAT,” EChAYa **23** (1992) 648–720. [Sov. J. Part. Nucl. **23** (1992) 283–316].
Comment: A review of the SKAT results.

Quasielastic scattering (theory)

[39] S. L. Adler, “Polarization effects at high-energy weak interactions,” Nuovo Cim. **30** (1963) 1020–1039; erratum – *ibid*. **32** (1964) 509.

[40] P. Vogel and J. F. Beacom, “Angular distribution of neutron inverse beta decay, $\overline{\nu}_e + n \to e^- + p$,” Phys. Rev. D **60** (1999) 053003 [arXiv:hep-ph/9903554].

[41] A. Strumia and F. Vissani, “Precise quasielastic neutrino nucleon cross section,” Phys. Lett. B **564** (2003) 42–54 [arXiv:astro-ph/0302055].

[42] H. Budd, A. Bodek, and J. Arrington, “Modeling quasi-elastic form factors for electron and neutrino scattering,” arXiv:hep-ex/0308005 [Presented at the 2nd International Workshop on Neutrino–Nucleus Interactions in the Few GeV Region (NuInt 02), Irvine, California, December 12 – 15, 2002; to be published in Nucl. Phys. B (Proc. Suppl.)]

[43] A. Bodek, H. Budd, and J. Arrington, “Modeling neutrino quasielastic cross sections on nucleons and nuclei,” AIP Conf. Proc. **698** (2004) 148–152 [arXiv:hep-ex/0309024].

[44] A. Burrows, S. Reddy, and T. A. Thompson, “Neutrino opacities in nuclear matter,” arXiv:astro–ph/0404432.

Radiative corrections

[45] P. Vogel, “Analysis of the antineutrino capture on protons,” Phys. Rev. D **29** (1984) 1918–1922.

[46] S. A. Fayans, “Radiative corrections and recoil effects in the reaction $\overline{\nu}_e + p \to n + e^+$ at low energies,” Yad. Fiz. **42** (1985) 929–940 [Sov. J. Nucl. Phys. **42** (1985) 590–597].

[47] D. H. Wilkinson, “G_V, CKM, unitarity, neutron decay; W_R?,” Z. Phys. A **348** (1994) 129–138.

[48] A. Sirlin, in *Precision tests of the Standard Model*, edited by P. Langacker (World Scientific, Singapore, 1995), pp. 766–785.

[49] A. Kurylov, M. J. Ramsey-Musolf, and P. Vogel, “Radiative corrections in neutrino–deuterium disintegration,” Phys. Rev. D **65** (2002) 055501 [arXiv:nucl-th/0110051].

[50] A. Kurylov, M. J. Ramsey-Musolf, and P. Vogel, “Radiative corrections to low-energy neutrino reactions,” Phys. Rev. D **67** (2003) 035502 [arXiv:hep-ph/0211306].

[51] M. Fukugita and T. Kubota, “Radiative corrections to neutrino–nucleon quasielastic scattering,” Acta Phys. Polon. B **35** (2004) 1687–1732 [arXiv:hep-ph/0403149].

Resonance single pion production (experiment)

BNL

[52] N. J. Baker *et al.*, “Study of the isospin structure of single pion production in charged current neutrino interactions,” Phys. Rev. D **23** (1981) 2495–2498.

[53] N. J. Baker *et al.*, “Strange particle production from neutrino interactions in the BNL 7-foot bubble chamber,” Phys. Rev. D **24** (1981) 2779–2786.

[54] T. Kitagaki *et al.*, “Charged-current exclusive pion production in neutrino–deuterium interactions,” Phys. Rev. D **34** (1986) 2554–2565.

[55] T. Kitagaki *et al.*, “Study of $\nu d \to \mu^- p p_s$ and $\nu d \to \mu^- \Delta^{++} n_s$ using the BNL 7-foot deuterium-filled bubble chamber,” Phys. Rev. D **42** (1990) 1331–1338.
Comment: Only RES to QES ratio.

[56] K. Furuno *et al.*, “BNL 7-foot bubble chamber experiment – neutrino deuterium interactions,” KEK preprint 2003-48; to be published in Proc. of the 2nd International Workshop on Neutrino–Nucleus Interactions in the Few-GeV Region (“NuInt’02”), Irvine, California, December 12 – 15, 2002.

ANL

[57] J. Campbell *et al.*, “Study of the reaction $\nu p \to \mu^- \pi^+ p$,” Phys. Rev. Lett. **30** (1973) 335–339.
Comment: Cited by Fogli & Nardulli [93].

[58] S. J. Barish *et al.*, "Study of the isospin properties of single-pion production by neutrinos," Phys. Rev. Lett. **36** (1976) 179–183.

[59] S. J. Barish *et al.*, "Study of the isospin properties of single-pion production by neutrinos," Phys. Rev. Lett. **36** (1976) 179–183.
Comment: Cited by Fogli & Nardulli [93]. The same data with improved statistics are given in Ref. [60].

[60] V. E. Barnes *et al.*, "Study of the isospin properties of single-pion production by neutrinos," in Proc. of the International Conf. on Neutrino Physics and Astrophysics, "Neutrino'78", Purdue University, April 28 – May 2, 1978, edited by E. C. Fowler (Purdue University Press, West Lafayette, Indiana, 1978), pp. C 56–C 63; see also preprints PURDUE COO-1428-450, ANL-HEP-CP-78-21.
Comment: Cited by Fogli & Nardulli [93].

[61] S. J. Barish *et al.*, "Study of neutrino interactions in hydrogen and deuterium. II. Inelastic charged-current reactions," Phys. Rev. D **19** (1979) 2521–2542.
Durham Reaction Data: http://www.slac.stanford.edu/cgi-hepdata/hepreac/325783.
Comment: Data for single-pion production are obsolete (see Ref. [62]).

[62] G. M. Radecky *et al.*, "Study of single-pion production by weak charged currents in low-energy νd interactions," Phys. Rev. D **25** (1982) 1161–1173; erratum – *ibid.* D **26** (1982) 3297; see also G. M. Radecky, "Study of single-pion production by the weak charged current," Ph. D. Thesis, Purdue University, December 1980, UMI 81-13740 (unpublished).
Comment: Supersedes Ref. [61]

CERN HLBC

[63] I. Budagov *et al.* "Single pion production by neutrinos on free protons," Phys. Lett. B **29** (1969) 524–528.
Comment: Cited by Fogli [95]

CERN BEBC

[64] P. C. Bosetti (for the Aachen-Bonn-CERN-Munich-Oxford and Aachen-Bonn-CERN-London-Saclay Collaborations), "Resonance production in νp interactions," in Proc. of the Topical Conf. on Neutrino Physics at Accelerators, Oxford, England, July 4 – 7, 1978, edited by A. G. Michette and P. B. Renton (Rutherford Pub.), pp. 82–89.
Comment: Multiparticle production. No too interesting for the moment.

[65] B. Conforto (for the Aachen-Bonn-CERN-Munich-Oxford Collaboration), "Preliminary results on the reaction $\nu p \to \mu^- \Delta^{++}$ from a neutrino experiment in hydrogen at SPS energies," in Proc. of the Topical Conf. on Neutrino Physics at Accelerators, Oxford, England, July 4 – 7, 1978, edited by A. G. Michette and P. B. Renton (Rutherford Pub.), pp. 90–93 [see also preprint CERN/EP/PHYS 78-26].
Comment: Cited by Fogli & Nardulli [93]. There are data on Δ^{++} production in figure.

[66] P. Allen *et al.* (Aachen-Bonn-CERN-Munich-Oxford Collaboration), "Single π^+ production in charged current neutrino–hydrogen interactions," Nucl. Phys. B **176** (1980) 269–284.

[67] P. Allen *et al.* (Aachen-Birmingham-Bonn-CERN-London-Munich-Oxford Collaboration), "A study of single-meson production in neutrino and antineutrino charged-current interactions on protons," Nucl. Phys. B **264** (1986) 221–242.

[68] W. Wittek *et al.* (BEBC WA59 Collaboration), "Production of π^0 mesons and charged hadrons in $\overline{\nu}$ Neon and ν Neon charged current interactions," Z. Phys. C **40** (1988) 231–251; see also preprint MPI-PAE-EXP-EL-188 (1988).
Comment: No data on σ.

[69] G. T. Jones *et al.* (WA21 Collaboration), "Experimental test of the PCAC hypothesis in the reactions $\nu_\mu p \to \mu^- p \pi^+$ and $\overline{\nu}_\mu p \to \mu^+ p \pi^-$ in the $\Delta(1232)$ region," Z. Phys. C **43** (1989) 527–540.
Comment: No data on σ.

[70] See Ref. [17]

CERN Gargamelle

[71] W. Lerche *et al.*, "Experimental study of the reaction $\nu_\mu p \to \mu^- p \pi^+$ (Gargamelle Neutrino Propane experiment)," Phys. Lett. B **78** (1978) 510–514.

[72] O. Erriquez *et al.*, "Single-pion production in antineutrino–induced neutral current interactions," Phys. Lett. B **73** (1978) 350–354.

[73] T. Bolognese, J. P. Engel, J. L. Guyonnet, and J. L. Riester, “Single pion production in antineutrino induced charged current interactions,” Phys. Lett. B **81** (1979) 393–396 [see also preprint CRN/HE 78-26]; T. Bolognese, “Study of antineutrino interactions with charged current pion production,” Ph. D. Thesis (Strasbourg University, 1978); preprint CRN/HE 78-22 (unpublished).
Durham Reaction Data: http://www-spires.dur.ac.uk/hepdata/index.html.

[74] M. Pohl (for the Aachen-Bruxelles-CERN-Ecole Polytechnique-Orsay-Padova Collaboration), “Experimental study of one pion production by the weak charged current,” in Proc. of the Topical Conf. on Neutrino Physics at Accelerators, Oxford, England, July 4 – 7, 1978, edited by A. G. Michette and P. B. Renton (Rutherford Pub.), pp. 78–82.
Comment: Cited by Fogli & Nardulli [93] but probably overlapped by Ref. [75].

[75] M. Pohl *et al.* (Gargamelle Neutrino Propane Collaboration), “Experimental study of single pion production in charged current neutrino interactions,” Lett. Nuovo Cim. **24** (1979) 540–544.

[76] D. Allasia *et al.* (Amsterdam-Bologna-Padova-Pisa-Saclay-Torino Collaboration), “Single pion production in charged current $\overline{\nu}D$ interactions at high energies,” Z. Phys. C **20** (1983) 95–100.
Comment: Only data for νD.

FNAL

[77] B. P. Roe (for the Fermilab-Michigan-Berkeley-Hawaii Collaboration), “Examination of the reaction $\nu p \to \mu^- p\pi^+$,” in Proc. of the Topical Conf. on Neutrino Physics at Accelerators, Oxford, England, July 4 – 7, 1978, edited by A. G. Michette and P. B. Renton, pp. 94–98.
Comment: Cited by Fogli & Nardulli [93]; there are useful data if figures.

[78] J. Bell *et al.*, “Cross-section measurements for the reactions $\nu p \to \mu^- \pi^+ p$ and $\nu p \to \mu^- K^+ p$ at high energies,” Phys. Rev. Lett. **41** (1978) 1008–1011.
Durham Reaction Data: http://www.slac.stanford.edu/cgi-hepdata/hepreac/308838.

[79] J. Bell *et al.*, “Study of the reaction $\nu p \to \mu^- \Delta^{++}$ at high energies and comparisons with theory,” Phys. Rev. Lett. **41** (1978) 1012–1015.
Comment: Only $d\sigma/dQ^2$.

[80] S. J. Barish *et al.*, “Study of the reaction $\overline{\nu}p \to \mu^+ p\pi^+$,” Phys. Lett. B **91** (1980) 161–164.
Durham Reaction Data: http://www.slac.stanford.edu/cgi-hepdata/hepreac/394793.

Serpukhov-SKAT

[81] H. J. Grabosch *et al.* (SKAT Collaboration), “Cross-section measurement for the reaction $\nu_\mu p \to \mu^- p\pi^+$ in the energy range below 30 GeV,” preprint PHE 87-06 (unpublished).

[82] V. V. Ammosov *et al.* (SKAT Collaboration), “Study of the reaction $\nu p \to \mu^- \Delta^{++}$ at energies 3–30 GeV,” Yad. Fiz. **50** (1989) 106–110 [Sov. J. Nucl. Phys. **50** (1989) 67–69]; see also preprint IFVE-88-122.
Durham Reaction Data: http://www-spires.dur.ac.uk/hepdata/index.html.

[83] H. J. Grabosch *et al.* (SKAT Collaboration), “Cross-section measurements of single pion production in charged current neutrino and antineutrino interactions,” Z. Phys. C **41** (1989) 527–531; see also preprint PHE-88-9.
Durham Reaction Data: http://www-spires.dur.ac.uk/hepdata/index.html.

Resonance single pion production (theory)

[84] C. .H. Albright and Lu Sun Liu, “N^* production by neutrinos,” Phys. Rev. Lett. **13** (1964) 673–676.

[85] C. .H. Albright and Lu Sun Liu, “N* production by neutrinos,” in Proc. of the Informal Conf. on Experimental Neutrino Physics, CERN, January 20 – 22, 1965, edited by C. Franzinetti, pp. 89–96.

[86] S. L. Adler, “Photoproduction, electroproduction and weak single pion production in the (3,3) resonance region,” Annals Phys. **50** (1968) 189–311.

[87] R. P. Feynman, M. Kislinger, and F. Ravndal, “Current matrix elements from a relativistic quark model,” Phys. Rev. D **3** (1971) 2706–2732.

[88] F. Ravndal, *Nuovo Cim.* **18A**, 385 (1973).

[89] P. A. Schreiner and F. Von Hippel, “Neutrino production of the $\Delta(1236)$,” Nucl. Phys. B **58** (1973) 333–362.

[90] P. A. Schreiner and F. Von Hippel, "$\nu p \to \mu^- \Delta^{++}$: comparison with theory," Phys. Rev. Lett. **30** (1973) 339–342.

[91] E. H. Monsay, "Single-pion production by the weak neutral current," Phys. Rev. D **18** (1978) 2277–2289.

[92] E. H. Monsay, "Remarks on single-pion production by the weak neutral current," Phys. Rev. Lett. **41** (1978) 728–731.

[93] G. L. Fogli and G. Nardulli, "A new approach to the charged current induced weak one-pion production," Nucl. Phys. B **160** (1979) 116–150.

[94] G. L. Fogli and G. Nardulli, "Neutral current induced one-pion production: a new model and its comparison with the experiment," Nucl. Phys. B **165** (1980) 162–184.

[95] G. L. Fogli, "Total cross sections in a new model of ν and $\overline{\nu}$ charged current induced one-pion production," Phys. Lett. B **87** (1979) 75–79.

[96] G. L. Fogli, "$I = 1/2$ resonant contribution to the high-energy CC-induced weak one pion production," Phys. Lett. **90 B** (1980) 155–158.

[97] G. Nardulli, "Study of the reaction $\nu n \to \nu p \pi^-$," Lett. Nuovo Cim. **28** (1980) 533–537.

[98] G. L. Fogli, "Resonance background interference in CC neutrino induced π^+ production," Nuovo Cim. A **66** (1981) 173–204.

[99] G. L. Fogli, "Evidence of $I = 1/2$ resonant states in charged current induced weak one-pion production," Phys. Rev. D **25** (1982) 1436–1439.

[100] D. Rein and L. M. Sehgal, "Neutrino excitation of baryon resonances and single pion production," Annals Phys. **133** (1981) 79–153.

[101] D. Rein, "Angular distribution in neutrino–induced single pion production processes," Z. Phys. C **35** (1987) 43–64.

[102] L. Alvarez-Ruso, S. K. Singh, and M. J. Vicente Vacas, "$\nu d \to \mu^- \Delta^{++} n$ reaction and axial vector $N - \Delta$ coupling," Phys. Rev. C **59** (1999) 3386–3392 [arXiv:nucl-th/9804007].

[103] J. T. Sobczyk, J. A. Nowak, and K. M. Graczyk, "WroNG – Wroclaw Neutrino Generator of events for single pion production," arXiv:hep-ph/0407277.

Coherent and diffractive scattering (reviews)

[104] P. Marage, "Hadronic component in neutrino interactions," in Proc. of the 17th International Symposyum on Multiparticle Dynamics, Seewinkel, Austria, June 16 – 20, 1986, edited by M. Markytan *et al.* (Singapore, World Scientific, 1987); a shorter version in Proc. of the 12th International Conf. on Neutrino Physics and Astrophysics, "Neutrino'86", Sendai, Japan, June 3 – 8, 1986 (World Scientific, Singapore, 1986) [see also preprint IIHE-86.04].

[105] P. Marage, "Tests of PCAC and coherent interactions on nuclei," in Proc. of the 13th International Conf. on Neutrino Physics and Astrophysics, "Neutrino'88", Boston, MA, June 5 – 11, 1988, edited by J. Schneps *et al.* (World Scientific, 1989), pp. 231–242 [see also preprint IIHE-88.09].

[106] P. Marage, "Low Q^2 neutrino interactions and hadronic component," in Proc. of the 10th International Seminar on High Energy Physics Problems, Relativistic Nuclear Physics and Quantum Chromodynamics, Dubna, USSR, September 24 – 29, 1990, pp. 382–391 [see also preprint IIHE-90.06].

Coherent and diffractive scattering (experiment)

[107] H. Faissner *et al.* (Aachen–Padova Collaboration), "Observation of neutrino and antineutrino induced coherent neutral pion production off Al^{27}," Phys. Lett. **125 B** (1983) 230–236.

[108] P. Marage *et al.* (BEBC WA59 Collaboration), "Observation of coherent diffractive charged current interactions of antineutrinos on neon nuclei," Phys. Lett. B **140** (1984) 137–141.

[109] E. Isiksal, D. Rein, and J. G. Morfin, "Evidence for neutrino and antineutrino–induced coherent π^0 production," Phys. Rev. Lett. **52** (1984) 1096–1099.

[110] P. Marage *et al.* (BEBC WA59 Collaboration), "Coherent single pion production by antineutrino charged current interactions and test of PCAC," Z. Phys. C **31** (1986) 191–197.

[111] H. J. Grabosch *et al.* (SKAT Collaboration), "Coherent π meson production in neutrino and antineutrino interactions on freon nuclei," preprint IFVE-86-117.
Durham Reaction Data: http://www.slac.stanford.edu/cgi-hepdata/hepreac/1595326.

[112] H. J. Grabosch *et al.* (SKAT Collaboration), "Coherent pion production in neutrino and antineutrino interactions on nuclei of heavy freon molecules," Z. Phys. C **31** (1986) 203–211 [see also preprint PHE 85-12].
Durham Reaction Data: http://www.slac.stanford.edu/cgi-hepdata/hepreac/1595326.

[113] P. Marage *et al.* (BEBC WA59 Collaboration), "Coherent production of π^+ mesons in neutrino–neon interactions," Z. Phys. C **43** (1989) 523–526; see also preprint IIHE-88-06.

[114] M. Aderholz *et al.* (E632 Collaboration), "Coherent production of π^+ and π^- mesons by charged current interactions of neutrinos and antineutrinos on neon nuclei at the Tevatron," Phys. Rev. Lett. **63** (1989) 2349–2352.

Coherent and diffractive scattering (theory)

[115] K. S. Lackner, "Coherent meson production as a test for neutral weak currents of exotic space-time structure," Nucl. Phys. B **153** (1979) 526–545.

[116] D. Rein and L. M. Sehgal, "Coherent production of photons by neutrinos," Phys. Lett. B **104** (1981) 394–398; erratum – *ibid.* **106**(1981) 513.

[117] D. Rein and L. M. Sehgal, "Coherent π^0 production in neutrino reactions," Nucl. Phys. B **223** (1983) 29–44.

[118] D. Rein, "Diffractive pion production in neutrino reactions," Nucl. Phys. B **278** (1986) 61–77.

[119] H. C. Kim, S. Schramm, and C. J. Horowitz, "Delta excitations in neutrino–nucleus scattering," Phys. Rev. C **53** (1996) 2468–2473 [arXiv:nucl-th/9507006].

[120] N. G. Kelkar, E. Oset, and P. Fernandez de Cordoba, "Coherent pion production in neutrino nucleus collision in the 1 GeV region," Phys. Rev. C **55** (1997) 1964–1971 [arXiv:nucl-th/9609005].

[121] E. A. Paschos and A. V. Kartavtsev, "Coherent neutrino–nucleus scattering," arXiv:hep-ph/0309148.

CC deep inelastic scattering (experiment)

CERN HLBC

[122] I. Budagov *et al.*, "Measurement of structure factors in inelastic neutrino scattering," Phys. Lett. B **30** (1969) 364–368.
Comment: freon 1963/64 and propane 1967 data on $\sigma_{\rm tot}$ are plotted. Probably obsolete.

CERN CDHS (WA-01 Experiment)

The CDHS neutrino experiment at CERN was a collaboration of CERN, Dortmund, Heidelberg and Saclay (later joined by Warsaw) led by Jack Steinberger.

[123] J. G. H. de Groot *et al.* (CDHS Collaboration), "Inclusive interactions of high-energy neutrinos and antineutrinos in iron," Z. Phys. C **1** (1979) 143–162.
IHEP-Protvino Data: see in SPIRES "KEY 341681.
Comment: obsolete data (see Ref. [124])

[124] H. Abramowicz *et al.* (CDHS Collaboration), "Neutrino and antineutrino charged-current inclusive scattering in iron in the energy range $20 < E_\nu < 300$ GeV," Z. Phys. C **17** (1983) 283–307 [see also preprint CERN-EP/82-210].
Durham Reaction Data: http://www.slac.stanford.edu/cgi-hepdata/hepreac/1023179.

[125] H. Abramowicz *et al.* (CDHS Collaboration), "Measurement of neutrino and antineutrino structure functions in hydrogen and iron," Z. Phys. C **25** (1984) 29–43 [see also preprint CERN-EP/84-57].
Comment: data on $\sigma_{\rm tot}/E_\nu$ for proton target (Table 3) but with no information on average energy in bins.

[126] H. Wachsmuth, "Total cross-sections for charged current neutrino interactions in Fe, Ne and H_2," in Proc. of the 12th International Conf. on Neutrino Physics and Astrophysics, "Neutrino'86", Sendai, Japan, June 3 – 8, 1986, edited by T. Kitagaki and H. Yuta, pp. 330–339. [see also preprint CERN-EP/86-168].

[127] P. Berge *et al.*, "Total neutrino and antineutrino charged current cross section measurements in 100, 160, and 200 GeV narrow band beams," Z. Phys. C **35** (1987) 443–452 [see also preprint CERN-EP/87-09].
Durham Reaction Data: http://www.slac.stanford.edu/cgi-hepdata/hepreac/1687654.

[128] P. Berge *et al.*, "A measurement of differential cross-sections and nucleon structure functions in charged-current neutrino interactions on iron," Z. Phys. C **49** (1991) 187–223 [see also preprint CERN-EP/89-103].
Durham Reaction Data: http://www.slac.stanford.edu/cgi-hepdata/hepreac/2058162.

CERN BEBC (Experiments WA21/WA59)

[129] P. C. Bosetti *et al.* (Aachen-Bonn-CERN-London-Oxford-Saclay Collaboration), "Total cross sections for charged-current neutrino and antineutrino interactions in BEBC in the energy range 20–200 GeV," Phys. Lett. B **70** (1977) 273–277.
Durham Reaction Data: http://www.slac.stanford.edu/cgi-hepdata/hepreac/250600.
Comment: preliminary data, see Ref. [131] for the final result.

[130] D. C. Colley *et al.*, "Cross-sections for charged current neutrino and antineutrino interactions in the energy range 10 to 50 GeV," Z. Phys. C **2** (1979) 187–190.
Durham Reaction Data: http://www.slac.stanford.edu/cgi-hepdata/hepreac/378186.

[131] P. Bosetti *et al.* (Aachen-Bonn-CERN-Democritos-London-Oxford-Saclay Collaboration), "Total cross sections for ν_μ and $\overline{\nu}_\mu$ charged-current interactions between 20 and 200 GeV," Phys. Lett. B **110** (1982) 167–172.
Durham Reaction Data: http://www.slac.stanford.edu/cgi-hepdata/hepreac/866067.
Comment: The data have been revised in Ref. [134].

[132] M. A. Parker *et al.* (BEBC TST Neutrino Collaboration), "A comparison of charged current cross sections and structure functions for neutrino and antineutrino beams on hydrogen and neon," Nucl. Phys. B **232** (1984) 1–20.
Durham Reaction Data: http://www.slac.stanford.edu/cgi-hepdata/hepreac/1117050.

[133] D. Allasia *et al.* (Amsterdam-Bergen-Bologna-Padova-Pisa-Saclay-Torino Collaboration), "Measurement of the ν_μ and $\overline{\nu}_\mu$ nucleon charged-current total cross sections, and the ratio of ν_μ neutron to ν_μ proton charged-current total cross sections," Nucl. Phys. B **239** (1984) 301–310.
Comment: there is a figure, no table.
Durham Reaction Data: .

[134] P. N. Shotton, W. Venus, and H. Wachsmuth, "Revised total cross sections in neon for ν_μ and $\overline{\nu}_\mu$ charged-current interactions between 20 and 200 GeV," CERN/EP/NBU 85-2; see also P. N. Shotton, "A measurement of the proton structure functions in neutrino–hydrogen and antineutrino–hydrogen charged-current interactions," Ph. D. Thesis (RAL Chilton, 1985).

[135] M. Aderholz *et al.* (BEBC WA21 and WA25 Collaborations), "Measurement of total cross sections for neutrino and antineutrino charged-current interactions in hydrogen and neon," Phys. Lett. B **173** (1986) 211–216.
Durham Reaction Data: http://www.slac.stanford.edu/cgi-hepdata/hepreac/1477471.

CERN Gargamelle

[136] T. Eichten *et al.*, "Measurement of the neutrino–nucleon and antineutrino–nucleon total cross sections," Phys. Lett. B **46** (1973) 274–280.
Durham Reaction Data: http://www.slac.stanford.edu/cgi-hepdata/hepreac/2160650.

[137] T. Eichten *et al.*, "High energy electronic neutrino (ν_e) and antineutrino ($\overline{\nu}_e$) interactions," Phys. Lett. B **46** (1973) 281–284.
Comment: there are some numbers.

[138] G. Myatt *et al.* (Gargamelle Collaboration), Acta Phys. Polon. **5** (1974) 799.

[139] P. Musset and J. P. Vialle, "Neutrino physics with Gargamelle," Phys. Rept. **39** (1978) 1–130.

[140] M. Rollier (for the Gargamelle antineutrino Collaboration), "Recent results from the Gargamelle $\overline{\nu}$ Propane Experiment at the CERN-PS," in Proc. of the Topical Conf. on Neutrino Physics at Accelerators, Oxford, England, July 4 – 7, 1978, edited by A. G. Michette and P. B. Renton, pp. 68–74.
Comment: Data on DIS and QE (including Λ production).

[141] O. Erriquez *et al.*, "Antineutrino–nucleon total cross section and ratio of antineutrino cross section on neutrons and protons," Phys. Lett. B **80** (1979) 309–313.
Durham Reaction Data: http://www.slac.stanford.edu/cgi-hepdata/hepreac/584665.

[142] S. Ciampolillo *et al.* (Gargamelle Neutrino Propane Collaboration), "Total cross section for neutrino charged current interactions at 3 GeV and 9 GeV," Phys. Lett. B **84** (1979) 281–284.
Durham Reaction Data: http://www.slac.stanford.edu/cgi-hepdata/hepreac/362069.

[143] J. G. Morfin *et al.* (Gargamelle SPS Collaboration), "Total cross sections and nucleon structure functions in the Gargamelle SPS neutrino/antineutrino experiment," Phys. Lett. B **104** (1981) 235–238.
Durham Reaction Data: http://www.slac.stanford.edu/cgi-hepdata/hepreac/814636.

[144] F. Rahimi, "Experimental study of the high-energy reactions $\overline{\nu}_\mu e^- \to \overline{\nu}_\mu e^-$, $\overline{\nu}_\mu N \to \mu^+ X$ in the Gargamelle bubble chamber," Ph. D. Thesis (University of Strasbourg, December 1982), Report CRN/HE 84-13 [in French.]
Comment: there is a table of data reported in Ref. [143] and a table with many data of earlier experiments.

CERN CHARM

[145] M. Jonker *et al.* (CHARM Collaboration), "Experimental study of neutral-current and charged-current neutrino cross sections," Phys. Lett. B **99** (1981) 265–270; erratum – *ibid.* B **100** (1981) 521; erratum – *ibid.* B **103** (1981) 469.
Durham Reaction Data: http://www.slac.stanford.edu/cgi-hepdata/hepreac/718866.
Comment: obsolete data (see Ref. [146]).

[146] J. V. Allaby *et al.* (CHARM Collaboration), "Total cross sections of charged-current neutrino and antineutrino interactions on isoscalar nuclei," Z. Phys. C **38** (1988) 403–410.
Durham Reaction Data: http://www.slac.stanford.edu/cgi-hepdata/hepreac/179162.

ANL

[147] S. J. Barish *et al.*, "Inclusive νp and νn charged-current neutrino reactions below 6 GeV," Phys. Lett. B **66** (1977) 291–294. [see also preprint ANL-HEP-PR-76-66]
Durham Reaction Data: http://www.slac.stanford.edu/cgi-hepdata/hepreac/150100.

[148] See Ref. [61].

BNL

[149] See Ref. [27].
Comment: only data for proton target.

[150] C. Baltay *et al.*, "Cross sections and scaling-variable distributions of neutral- and charged–current neutrino–nucleon interactions from a low-energy narrow band beam," Phys. Rev. Lett. **44** (1980) 916–919.
Durham Reaction Data: http://www.slac.stanford.edu/cgi-hepdata/hepreac/752088.

[151] M. J. Murtagh, "Recent results from BNL neutrino experiments and plans for the future," in Proc. of the International Conf. on Neutrino Physics and Astrophysics, "Neutrino'81", Wailea, Hawaii, July 1 – 8, 1981, edited by R. J. Cence, E. Ma and A. Roberts, Vol. **1**, pp. 388–410 [see also preprint BNL-30082].
Comment: the same data as in Ref. [152].

[152] N. J. Baker *et al.*, "Total cross sections for $\nu_\mu n$ and $\nu_\mu p$ charged-current interactions in the 7-foot bubble chamber," Phys. Rev. D **25** (1982) 617–623.
Durham Reaction Data: http://www.slac.stanford.edu/cgi-hepdata/hepreac/914398.

FNAL

[153] A. C. Benvenuti *et al.*, "Early observation of neutrino and antineutrino events at high energies," Phys. Rev. Lett. **30** (1973) 1084–1087.
Comment: no data on cross section.

[154] J. J. Aubert, in Proc. of the 17th International Conference on High Energy Physics, London, England, July 1–10, 1974, edited by J. R. Smith (Chilton, Rutherford Lab., 1974), p. ? ★★
Comment: Most probably the data are obsolete. Good resolution figure is available from Ref. [8].

[155] B. C. Barish, "Results from the Caltech-Fermilab experiment," in Proc. of the 17th International Conference on High Energy Physics, London, England, July 1–10, 1974, edited by J. R. Smith (Chilton, Rutherford Lab., 1974), pp. IV-111–113. [preprint D75-05503]. ★★
Comment: Most probably the data are obsolete. Good resolution figure is available from Ref. [8].

[156] A. C. Benvenuti *et al.*, "Measurements of neutrino and antineutrino cross-sections at high energies," Phys. Rev. Lett. **32** (1974) 125–128.
IHEP-Protvino Data: see in SPIRES "KEY 318078. Comment: figure with the data (probably obsolete).

[157] B. C. Barish, "Recent results from the Caltech-Fermilab neutrino experiment," Lecture presented at the International School of Subnuclear Physics, Erice, Sicily, July 11 – 31, 1975 [see also preprint CALT-68-510].
Comment: figures with data (obsolete).

[158] B. C. Barish *et al.* (FNAL-E-0021 Experiment) “Measurement of neutrino and antineutrino total cross sections at high energy,” Phys. Rev. Lett. **35** (1975) 1316–1320.
IHEP-Protvino Data: see in SPIRES ”KEY 90360”.
Comment: there is table.

[159] B. C. Barish *et al.* (CITFR Collaboration), “Measurements of ν_μ and $\overline{\nu}_\mu$ charged-current total cross sections,” Phys. Rev. Lett. **39** (1977) 1595–1598.
Durham Reaction Data: http://www.slac.stanford.edu/cgi-hepdata/hepreac/256552.

[160] B. C. Barish *et al.* (CITFR Collaboration), “Total cross-sections and mean y from charged current ν_μ and $\overline{\nu}_\mu$ collisions,” in Proc. of the 8th International Symposium on Lepton and Photon Interactions at High Energies, Hamburg, Germany, August 25 – 31, 1977, edited by F. Gutbrod, pp. 239–258 [see also preprint CALT-68-626 (1977)].
Comment: figure with data.

[161] B. Barish, “Flux normalized charged current neutrino cross sections up to neutrino energies of 260 GeV,” in Proc. of the International Conf. on Neutrinos, Weak Interactions and Cosmology, “Neutrino’79,” June 18 – 22, 1979, Bergen, Norway (Bergen, Norway, Bergen University), edited by A. Haatuft and C. Jarlskog, Vol. **2**, pp. 272–278.

[162] B. Barish *et al.* (CFRR Collaboration), “Recent results from the CFRR neutrino experiment at Fermilab,” in Proc. of the 8th SLAC Summer Inst. on Particle Physics (the Weak Interactions), Stanford, California, July 28 – August 5, 1980, edited by A. Mosher, pp. 475–486 [see also preprint CALT-68-802 (1980)].
Comment: obsolete, see Ref. [163].

[163] B. Barish *et al.* (CFRR Collaboration), “Recent results on total neutrino and antineutrino cross sections by the CFRR collaboration,” in Proc. of the 9th SLAC Summer Inst. on Particle Physics (the Strong Interactions), Stanford, California, July 27 – August 4, 1981, edited by A. Mosher, pp. 641–661. [see also preprint FERMILAB-conf-81/80-EXP 7420.616].
Comment: figure.

[164] T. Kitagaki *et al.*, “Neutrino flux and total charged-current cross sections in high-energy neutrino–deuterium interactions,” Phys. Rev. Lett. **49** (1982) 98–101.
Durham Reaction Data: http://www.slac.stanford.edu/cgi-hepdata/hepreac/1014706.

[165] R. Blair *et al.* “Measurement of the rate of increase of neutrino cross sections with energy,” Phys. Rev. Lett. **51** (1983) 343–346.
Durham Reaction Data: http://www.slac.stanford.edu/cgi-hepdata/hepreac/1138758.Comment: obsolete, see Ref. [168].

[166] N. J. Baker *et al.*, “Measurement of the ν_μ charged-current cross section,” Phys. Rev. Lett. **51** (1983) 735–738.
Durham Reaction Data: http://www.slac.stanford.edu/cgi-hepdata/hepreac/1033263.

[167] G. N. Taylor *et al.*, “$\overline{\nu}_\mu$-nucleon charged-current total cross section for 5–250 GeV,” Phys. Rev. Lett. **51** (1983) 739–742.
Durham Reaction Data: http://www.slac.stanford.edu/cgi-hepdata/hepreac/1172743.

[168] D. MacFarlane *et al.*, “Nucleon structure functions from high energy neutrino interactions with iron and QCD results,” Z. Phys. C **26** (1984) 1–12 [see also preprint FERMILAB-PUB-83-108-EXP].
Durham Reaction Data: http://www.slac.stanford.edu/cgi-hepdata/hepreac/1163744.

[169] P. S. Auchincloss *et al.*, “Measurement of the inclusive charged current cross section for neutrino and antineutrino scattering on isoscalar nucleons,” Z. Phys. C **48** (1990) 411–432.
Durham Reaction Data: http://www.slac.stanford.edu/cgi-hepdata/hepreac/2198835.

IHEP

[170] A. E. Asratyan *et al.*, “Charged current neutrino interactions below 30 GeV,” Phys. Lett. B **76** (1978) 239–242.
A. E. Asratyan *et al.*, “The total cross sections for neutrino and antineutrino interactions in the energy range 3 – 30 GeV,” Yad. Fiz. **28** (1978) 424–428 [Sov. J. Nucl. Phys. **28** (1978) 214–216];
Durham Reaction Data: http://www.slac.stanford.edu/cgi-hepdata/hepreac/303305.

[171] V. V. Makeev, “Study of CC interactions of neutrino and antineutrino in bubble chamber SKAT at 2–30 GeV,” in Proc. of the International Conf. on Neutrinos, Weak Interactions and Cosmology, “Neutrino’79,” June 18 – 22, 1979, Bergen, Norway, edited by A. Haatuft and C. Jarlskog, Vol. **2**, pp. 297–305.

[172] A. I. Mukhin, "Energy dependence of total cross-sections for neutrino and antineutrino interactions at energies below 35 GeV," in Proc. of the International Conf. on Neutrinos, Weak Interactions and Cosmology, "Neutrino'79," June 18 – 22, 1979, Bergen, Norway, edited by A. Haatuft and C. Jarlskog, Vol. **2**, pp. 306–313.

[173] D. S. Baranov *et al.*, "Measurement of the total cross section for interaction of neutrinos in the energy region 2–30 GeV in the SKAT chamber," Yad. Fiz. **29** (1979) 1203–1205 [Sov. J. Nucl. Phys. **29** (1979) 620–621];
D. S. Baranov *et al.*, "Measurements of the $\nu_\mu N$ total cross section at 2–30 GeV in a SKAT neutrino experiment," Phys. Lett. B **81** (1979) 255–257.
Durham Reaction Data: http://www.slac.stanford.edu/cgi-hepdata/hepreac/303585.

[174] A. S. Vovenko *et al.*, "Energy dependence of total cross sections for neutrino and antineutrino interactions at energies below 35 GeV," Yad. Fiz. **30** (1979) 1014–1017 [Sov. J. Nucl. Phys. **30** (1979) 527–529].
Durham Reaction Data: http://www.slac.stanford.edu/cgi-hepdata/hepreac/374687.

[175] See Ref. [33].

[176] V. V. Ammosov *et al.*, "Study of neutrino (antineutrino) interactions with nuclei at 3 to 30 GeV," preprint IFVE-85-107 (unpublished).
Durham Reaction Data: http://www.slac.stanford.edu/cgi-hepdata/hepreac/1417800.

[177] V. V. Ammosov *et al.*, "Neutrino (antineutrino) interaction cross section ratio in neutral and charged current channels up to 30 GeV," preprint IFVE-85-110 (unpublished).
Durham Reaction Data: http://www.slac.stanford.edu/cgi-hepdata/hepreac/1435663.

[178] V. B. Anikeev *et al.*, "Total cross section measurements for ν_μ, $\overline{\nu}_\mu$ charged current interactions in 3–30 GeV energy range with IHEP–JINR neutrino detector" Z. Phys. C **70** (1996) 39–46 [see also preprint IFVE-95-50 (1985)].
Durham Reaction Data: http://www.slac.stanford.edu/cgi-hepdata/hepreac/3232182.

[179] A. S. Vovenko, "Total cross section measurements for ν_μ, $\overline{\nu}_\mu$ interactions in 3–30 GeV energy range with IHEP–JINR detector and future plans," Nucl. Phys. B (Proc. Suppl.) **112** (2002) 116–123.
Comment: the same data as in Ref. [178].

NuTeV[7]

[180] See Ref. [215].

[181] W. G. Seligman, "A Next-to-leading-order QCD analysis of neutrino–iron structure functions at the Tevatron," Ph. D. Thesis, Nevis Report No. 292 [see also FERMILAB-THESIS-1997-21], 448 pp. (unpublished); the thesis errata can be found at URL: <http://www.nevis.columbia.edu/∼seligman/weblinks.html#physpart> (last updated on October 18, 1999).
Durham Reaction Data: http://www.slac.stanford.edu/cgi-hepdata/hepreac/3532135.

[182] D. Naples (for the NuTeV Collaboration), "NuTeV structure functions results," talk at the XI International Workshop on Deep Inelastic Scattering "DIS'03", St. Petersburg, 23–27 April, 2003.

[183] S. B. Boyd *et al.* (NuTeV Collaboration), "Cross section measurements and charm production in the NuTeV experiment," talk at the 8th Conference on the Intersections of Particle and Nuclear Physics "CIPANP 2003", New York, 19–24 May, 2003 (for short version see AIP Conf. Proc. **698** (2004) 95–99).

[184] M. Tzanov (for the NuTeV Collaboration), "Precise measurement of the differential cross section for $\nu-$ Fe and $\overline{\nu}-$ Fe scattering," talk at the Annual Meeting of the Division of Particles and Fields of the American Physical Society "DPF 2004", Riverside, California, 26–31 August, 2004 (to be published in Int. J. Mod. Phys. A).

[185] V. A. Radescu (for the NuTeV Collaboration), "Differential cross section results from NuTeV," talk at the 12th International Workshop on Deep Inelastic Scattering "DIS 2004", Štrbské Pleso, High Tatras, Slovakia, 14–18 April, 2004; (for short version see hep-ex/0408006).

[7] *Preliminary* data on the total νN and $\overline{\nu}N$ cross sections were reported at several meetings [182–185] but absent from the published versions. The slides of the full talks are available from URL <http://www-nutev.phyast.pitt.edu/results_2004/nutev_sf.html>.

Deep inelastic scattering (theory)

Scaling variables and slow rescaling

[186] O. Nachtmann, "Positivity constraints for anomalous dimensions," Nucl. Phys. B **63** (1973) 237–247;
O. Nachtmann, "Is there evidence for large anomalous dimensions?" Nucl. Phys. B **78** (1978) 455–467.

[187] H. Georgi and H. D. Politzer, "Precocious scaling, rescaling and ξ scaling," Phys. Rev. Lett. **36** (1976) 1281–1284; erratum – *ibid*. **37** (1976) 68;
H. Georgi and H. D. Politzer, "Freedom at moderate energies: masses in color dynamics," Phys. Rev. D **14** (1976) 1829–1848.

[188] A. De Rujula, H. Georgi, and H. D. Politzer, "Trouble with ξ scaling?," Phys. Rev. D **15** (1977) 2495–2490.

[189] A. De Rujula, H. Georgi, and H. D. Politzer, "Demythification of electroproduction, local duality and precocious scaling," Annals Phys. **103** (1977) 315–353 [see also preprint HUTP-76/A155 (1976)].

[190] F. N. Ndili and G. C. Chukwumah, "Threshold effects of charm production in neutrino interactions," Phys. Rev. D **15** (1977) 1227–1239.

[191] X. Song, "Modified Wandzura-Wilczek relation with the Nachtmann variable," Phys. Rev. D **63** (2001) 094019 [arXiv:hep-ph/0008104].

[192] S. R. Kelner and D. A. Timashkov, "Proton structure functions in the quasielastic limit," Yad. Fiz. **64** (2001) 1802–1808 [Phys. Atom. Nucl. **64** (2001) 1722–1728].

[193] G. Altarelli and G. Martinelli, "Transverse momentum of jets in electroproduction from quantum chromodynamics," Phys. Lett. B **76** (1978) 89–94.

[194] S. Kretzer and M. H. Reno, "Tau neutrino deep inelastic charged current interactions," Phys. Rev. D **66** (2002) 113007 [arXiv:hep-ph/0208187].

[195] S. Kretzer, "Mass corrections and neutrino DIS," Acta Phys. Polon. B **33** (2002) 2953–2958 [arXiv:hep-ph/0207140].

[196] S. Kretzer and M. H. Reno, "Deep inelastic neutrino interactions," arXiv:hep-ph/0306307.

[197] S. Kretzer and M. H. Reno, "Target mass corrections to electro-weak structure functions and perturbative neutrino cross sections," Phys. Rev. D **69** (2004) 034002 [arXiv:hep-ph/0307023].

[198] S. Kretzer and M. H. Reno, "$\sigma_{DIS}(\nu N)$, NLO perturbative QCD and O(1 GeV) mass corrections," Nucl. Phys. B (Proc. Suppl.) **139** (2005) 134–139 [arXiv:hep-ph/0410184].

[199] M. Glück, E. Reya, and A. Vogt, "Parton distributions for high-energy collisions," Z. Phys. C **53** (1992) 127–143.

NC reactions (experiment)

ANL

[200] M. Derrick *et al.*, "Study of the reaction $\nu n \to \nu p\pi^-$," Phys. Lett. B **92** (1980) 363–366 erratum – *ibid*. **96** (1980) 461.

[201] M. Derrick *et al.*, "Study of single-pion production by weak neutral currents in low-energy νd interactions," Phys. Rev. D **23** (1981) 569–575.

BNL

[202] H. H. Williams, "Study of neutrino interactions at Brookhaven using counter techniques," in Proc. of the International Symposium on Lepton and Photon Interactions at High Energies, Hamburg 1977, pp. 205–216.
Comment: Cited by Fogli & Nardulli [93].

[203] W. Y. Lee *et al.*, "Single pion production in neutrino and antineutrino reactions," Phys. Rev. Lett. **38** (1977) 202–204.
Comment: NC to CC ratio.

[204] N. J. Baker *et al.*, "The exclusive neutral current reaction $\nu_\mu n \to \nu_\mu p\pi^-$ in the BNL 7-foot deuterium bubble chamber," Phys. Rev. D **28** (1983) 2900–2902.

[205] L. A. Ahrens *et al.*, "Measurement of neutrino–proton and antineutrino–proton elastic scattering," Phys. Rev. D **35** (1987) 785–809.
Durham Reaction Data: http://www.slac.stanford.edu/cgi-hepdata/hepreac/1525735.
Comment: $M_A = 1.06 \pm 0.05$ GeV.

FNAL

[206] B. C. Barish *et al.*, "Observation of single pion production by a weak neutral current," Phys. Rev. Lett. **33** (1974) 448–451.
Durham Reaction Data: http://www.slac.stanford.edu/cgi-hepdata/hepreac/35815.

[207] B. C. Barish *et al.*, "Neutral currents in high-energy neutrino collisions: an experimental search," Phys. Rev. Lett. **34** (1975) 538–541.

CERN

[208] W. Krenz *et al.* (Neutrino Propane Gargamelle Collaboration), "Experimental study of exclusive one-pion production in all neutrino–induced neutral current channels," Nucl. Phys. B **135** (1978) 45–65.

[209] M. Pohl *et al.*, "Study of neutrino proton elastic scattering in the "Gargamelle" freon experiment," Phys. Lett. B **72** (1978) 489–492.

[210] M. Pohl *et al.* (Gargamelle Neutrino Propane Experiment), "Measurement of the ratio of neutral current $\nu + p$ and $\nu + n$ inelastic cross sections below 10 GeV," Phys. Lett. B **79** (1978) 501–504.

[211] S. Bonetti *et al.* ($\nu - \overline{\nu}$ Propane Gargamelle Collaboration), "Comparison of single π^0 production by ν and $\overline{\nu}$ neutral currents," Phys. Lett. **82 B** (1979) 461–463.

[212] O. Erriquez *et al.*, "Experimental results on one pion neutral current reaction in all channels induced by antineutrinos at CERN PS," Nucl. Phys. B **176** (1980) 37–50; see also preprint CRN-HE-80-5.

[213] H. Faissner *et al.*, "Measurement of elastic muon-neutrino scattering off protons," Phys. Rev. D **21** (1980) 555–561.

[214] G. T. Jones *et al. et al.* (BEBC WA21 and WA25 Collaborations), "Measurement of the neutral to charged current cross-section ratios for neutrino and antineutrino interactions on protons," Phys. Lett. B **178** (1986) 329–334.

Bodek–Yang prescription

[215] U. K. Yang, "A measurement of differential cross sections in charged-current neutrino interactions on iron and a global structure functions analysis," Ph. D. Thesis; FERMILAB-THESIS-2001-09.

[216] A. Bodek and U. K. Yang, "Modeling deep inelastic cross sections in the few GeV region," Nucl. Phys. B (Proc. Suppl.) **112** (2002) 70–76 [arXiv:hep-ex/0203009].

[217] A. Bodek and U. K. Yang, "Higher twist, ξ_w scaling, and effective LO PDFs for lepton scattering in the few GeV region," J. Phys. G **29** (2003) 1899–1906 [arXiv:hep-ex/0210024].

[218] A. Bodek and U. K. Yang, "Modeling neutrino and electron scattering cross sections in the few GeV region with effective LO PDFs," AIP Conf. Proc. **670** (2003) 110–117 [arXiv:hep-ex/0301036].

[219] A. Bodek and U. K. Yang, "Modeling neutrino and electron scattering cross sections in the few GeV region with effective LO PDFs," arXiv:hep-ex/0308007 [Presented at the 2nd International Workshop on Neutrino–Nucleus Interactions in the Few GeV Region (NUINT 02), Irvine, California, December 12 – 15, 2002; to be published in Nucl. Phys. B (Proc. Suppl.)]

[220] A. Bodek, I. Park, and Un ki Yang, "Improved low Q^2 model for neutrino and electron nucleon cross sections in few GeV region," Nucl. Phys. B (Proc. Suppl.) **139** (2005) 113–118 [arXiv:hep-ph/0411202].

τ ($L^{\pm}$) lepton production

[221] N. I. Starkov, "The kinematic features of the tau-neutrino–nucleon interaction," J. Phys. G **27** (2001) L81–L85.

[222] E. A. Paschos and J. Y. Yu, "Neutrino interactions in oscillation experiments," Phys. Rev. D **65** (2002) 033002 [arXiv:hep-ph/0107261].

[223] K. Hagiwara, K. Mawatari, and H. Yokoya, "Tau polarization in tau-neutrino nucleon scattering," Nucl. Phys. B **668** (2003) 364–384; erratum – *ibid.* B **701** (2004) 405 [arXiv:hep-ph/0305324].

[224] K. S. Kuzmin, V. V. Lyubushkin, and V. A. Naumov, “Lepton polarization in neutrino nucleon interactions,” in Proc. of the 10th International Workshop on High-Energy Spin Physics (SPIN 03), Dubna, Russia, September 16 – 20, 2003 [arXiv:hep-ph/0312107].

[225] K. S. Kuzmin, V. V. Lyubushkin, and V. A. Naumov, “Polarization of tau leptons produced in quasielastic neutrino–nucleon scattering,” in Proc. of the 8th Scientific Conf. for Young Scientists and Specialists (SCYSS 04), Dubna, Russia, February 2 – 6, 2004 [arXiv:hep-ph/0403110].

[226] K. Hagiwara, K. Mawatari, and H. Yokoya, “Pseudoscalar form factors in tau-neutrino nucleon scattering,” Phys. Lett. B **591** (2004) 113–118 [arXiv:hep-ph/0403076].

[227] C. Bourrely, J. Soffer, and O. V. Teryaev, “Positivity constraints for lepton polarization in neutrino deep inelastic scattering,” Phys. Rev. D **69** (2004) 114019 [arXiv:hep-ph/0403176].

[228] K. M. Graczyk, “Tau polarization in charge current neutrino–nucleon deep inelastic scattering,” arXiv:hep-ph/0407283.

[229] K. M. Graczyk, “Tau polarization in quasielastic charge-current neutrino(antineutrino)–nucleus scattering,” arXiv:hep-ph/0407275.

L^0 production

[230] D. Rein, L. M. Sehgal, and P. M. Zerwas, “Signatures of neutral heavy leptons in neutrino–induced dilepton events,” Nucl. Phys. B **138** (1978) 85–108.

Nuclear effects

[231] R. A. Smith and E. J. Moniz, “Neutrino ractions on nuclear targets,” Nucl. Phys. B **43** (1972) 605–622; erratum – *ibid*. **101** (1975) 547.

Parton density functions

Experiment

[232] C. Adloff *et al.* (H1 Collaboration), “Deep-inelastic inclusive ep scattering at low x and a determination of $\alpha(s)$,” Eur. Phys. J. C **21** (2001) 33–61 [arXiv:hep-ex/0012053].

GRV

[233] M. Glück, E. Reya, and A. Vogt, “Dynamical parton distributions of the proton and small x physics,” Z. Phys. C **67** (1995) 433–448; see also preprint DO-TH-94-24.

[234] M. Glück, E. Reya, and A. Vogt, “Dynamical parton distributions revisited,” Eur. Phys. J. C **5** (1998) 461–470 [arXiv:hep-ph/9806404].

[235] M. Gluck, C. Pisano, and E. Reya, “Probing the perturbative NLO parton evolution in the small-x region,” arXiv:hep-ph/0412049.

NUCLEON FORM FACTORS (G_E, G_M)

Reviews

[236] M. Gourdin, “Weak and electromagnetic form factors of hadrons,” Phys. Rept. **11** (1974) 29–98.

[237] G. G. Petratos, “An experimental review of the nucleon electromagnetic form factors,” Nucl. Phys. A **666** (2000) 61c–74c.

[238] M. Garcon and J. W. Van Orden, “The deuteron: Structure and form factors,” Adv. Nucl. Phys. **26** (2001) 293–378 [arXiv:nucl-th/0102049].

[239] H. Gao, “Nucleon electromagnetic form factors,” Int. J. Mod. Phys. E **12** (2003) 1–40; erratum – *ibid*. 567 [arXiv:nucl-ex/0301002].

[240] H. Schmieden, “Form factors of the nucleon,” Nucl. Phys. A **737** (2004) 147–155.

[241] H. Gao, “Neutron electromagnetic form factors,” arXiv:nucl-ex/0411015.

Experimental data

Jefferson Lab

[242] M. K. Jones *et al.* (Jefferson Lab Hall A Collaboration), "G_{Ep}/G_{Mp} ratio by polarization transfer in $\mathbf{e}p \to e\mathbf{p}$," Phys. Rev. Lett. **84** (2000) 1398–1402 [arXiv:nucl-ex/9910005];
M. K. Jones (for the Jefferson Lab Hall A Collaboration), "Measurement of the ratio of the proton's electric to magnetic form factors by Recoil Polarization," Fizika B **8** (1999) 59–63.

[243] J. Hansen (for the Jefferson Lab E95-001 Collaboration), "Precise measurement of the transverse asymmetry in quasielastic $^3\overrightarrow{\mathrm{He}}\,(\mathbf{e}, e')$ and the neutron magnetic form factor," Nucl. Phys. A **663** (2000) 409c–412c. *f*

[244] W. Xu *et al.*, "The transverse asymmetry $A_{T'}$ from quasielastic polarized $^3\overrightarrow{\mathrm{He}}\,(\mathbf{e}, e')$ process and the neutron magnetic form factor," Phys. Rev. Lett. **85** (2000) 2900–2904 [arXiv:nucl-ex/0008003]. DF

[245] H. Zhu *et al.* (Jefferson Lab E93-026 Collaboration), "A measurement of the electric form-factor of the neutron through $\mathbf{d}\,(\mathbf{e}, e'n)\,p$ at $Q^2 = 0.5$ (GeV$/c)^2$," Phys. Rev. Lett. **87** (2001) 081801 [arXiv:nucl-ex/0105001]. DF

[246] H. Gao "Measurement of the neutron magnetic form factor from a polarized ^{3}He target," Nucl. Phys. A **684** (2001) 139c–147c. *f*

[247] O. Gayou *et al.* (Jefferson Lab Hall A Collaboration), "Measurements of the elastic electromagnetic form factor ratio $\mu_p G_{Ep}/G_{Mp}$ via polarization transfer," Phys. Rev. C **64** (2001) 038202. DF

[248] O. Gayou *et al.* (Jefferson Lab Hall A Collaboration), "Measurement of G_{Ep}/G_{Mp} in $\mathbf{e}p \to e\mathbf{p}$ to $Q^2 =$ 5.6 GeV^2," Phys. Rev. Lett. **88** (2002) 092301 [arXiv:nucl-ex/0111010]. DF

[249] N. Savvinov (for the Jefferson Lab E93-026 Collaboration), "Measurement of the charge form factor of the neutron G_E^n from $\mathbf{d}(\mathbf{e}, e'n)p$ at $Q^2 = 0.5$ and 1.0 (GeV$/c)^2$," AIP Conf. Proc. **675** (2003) 630–633 [arXiv:nucl-ex/0210035]. *f*

[250] M. K. Jones (for the Jefferson Lab Hall A Collaboration), "New results on the electric form factor of the proton," Nucl. Phys. A **699** (2002) 124c–127c. *f*

[251] W. Xu *et al.* (Jefferson Lab E95-001 Collaboration), "Plane-wave impulse approximation extraction of the neutron magnetic form factor from quasi-elastic $^3\overrightarrow{\mathrm{He}}\,(\mathbf{e}, e')$ at $Q^2 = 0.3$ (GeV$/c)^2$ to 0.6 (GeV$/c)^2$," Phys. Rev. C **67** (2003) 012201 [arXiv:nucl-ex/0208007]. DF

[252] L. Penchev *et al.* (Jefferson Lab Hall A and G_{Ep} (III) Collaborations), "Measurements of the proton electric form factor at Jefferson Lab," in Proc. of the International Conf. on High-Energy Interactions: Theory and Experiment (Hadron Structure'02), September 22 – 27, 2002, Herlany, Slovakia, edited by J. Urban and J. Vrlakova (Kosice University, 2003), pp. 287–293.

[253] C. F. Perdrisat and V. Punjabi, the Jefferson Lab Hall A and G_{Ep}/G_{Mp} Collaborations, "The JLab polarization transfer measurements of proton elastic form factor," Pramana **61** (2003) 827–835.

[254] V. Punjabi, C. F. Perdrisat, and the Jefferson Lab Hall A and G_{Ep} (III) Collaborations, "Measurements of the electromagnetic form factor of the proton at JLab," arXiv:nucl-ex/0307001; *f*

[255] J. Arrington (for the Jefferson Lab E01-001 Collaboration), "New measurement of G_E/G_M for the proton," arXiv:nucl-ex/0312017.

[256] R. Madey *et al.* (Jefferson Lab E93-038 Collaboration), "Measurements of G_E^n/G_M^n from the ^{2}H$(\mathbf{e}, e'\mathbf{n})^1$H reaction to $Q^2 = 1.45$ (GeV$/c)^2$," Phys. Rev. Lett. **91** (2003) 122002 [arXiv:nucl-ex/0308007]; DF
R. Madey *et al.*, "Neutron electric form factor up to $Q^2 = 1.47$ (GeV$/c)^2$," Eur. Phys. J. A **17** (2003) 323–327. F

[257] T. Reichelt *et al.* (Jefferson Lab E93-038 Collaboration), "Measurement of the neutron electric form factor via recoil polarimetry," Eur. Phys. J. A **18** (2003) 181–183. F

[258] G. Warren *et al.* (Jefferson Lab E93-026 Collaboration), "Measurement of the electric form factor of the neutron at $Q^2 = 0.5$ and 1.0GeV^2/c^2," Phys. Rev. Lett. **92** (2004) 042301 [arXiv:nucl-ex/0308021]. DF

[259] D. Day (for the Jefferson Lab E93-026 Collaboration), "Measurement of the neutron electric form factor G_E^n in $\mathbf{d}(\mathbf{e}, e'n)p$ quasielastic scattering," Eur. Phys. J. A **17** (2003) 329–334. DF

[260] M. E. Christy *et al.* (Jefferson Lab E94-110 Collaboration), "Measurements of electron proton elastic cross sections for $0.4 < Q^2 < 5.5$ (GeV$/c)^2$," arXiv:nucl-ex/0401030. DF

[261] I. A. Qattan *et al.* (Jefferson Lab E01-001 Collaboration), "Precision Rosenbluth measurement of the proton elastic form factors," arXiv:nucl-ex/0410010. DF

CEA

[262] J. R. Dunning *et al.*, "Quasi-elastic electron-deuteron scattering and neutron form factors," Phys. Rev. **141** (1966) 1286–1297. *df*

[263] M. Goitein *et al.*, "Measurements of elastic electron-proton scattering at high momentum transfer by a coincidence technique," Phys. Rev. Lett. **19** (1967) 1016–1018.

[264] R. J. Budnitz *et al.*, "Neutron form factors from quasielastic electron deuteron scattering," Phys. Rev. **173** (1968) 1357–1390.

[265] L. E. Price *et al.*, "Backward-angle electron-proton elastic scattering and proton electromagnetic form factors," Phys. Rev. D **4** (1971) 45–53.

[266] K. M. Hanson *et al.*, "Large angle quasielastic electron-deuteron scattering," Phys. Rev. D **8** (1973) 753–778.

SLAC

[267] E. B. Hughes *et al.*, "Neutron form factors from inelastic electron-deuteron scattering," Phys. Rev. 139 (1965) B458–B471;
E. B. Hughes *et al.*, "Neutron form factors from a study of inelastic electron spectra in the electrodisintegration of deuterium," Phys. Rev. 146 (1966) 973–979.

[268] T. Janssens *et al.*, "Proton form factors from elastic electron-proton scattering," Phys. Rev. **142** (1966) 922–931.

[269] D. H. Coward *et al.*, "Electron-proton elastic scattering at high momentum transfers," Phys. Rev. Lett. **20** (1968) 292–295.
Comment: The data are obsolete.

[270] J. Litt *et al.*, "Measurement of the ratio of the proton form factors, G_E/G_M, at high momentum transfers and the question of scaling," Phys. Lett. B **31** (1970) 40–44.

[271] F. A. Bumiller *et al.*, "Form factor ratio G_{En}/G_{Ep} at low momentum transfers," Phys. Rev. Lett. **25** (1970) 1774–1778.

[272] S. Rock *et al.*, "Measurement of elastic electron-neutron cross sections up to $Q^2 = 10(\mathrm{GeV}/c)^2$," Phys. Rev. Lett. **49** (1982) 1139–1142.

[273] R. G. Arnold *et al.*, "Measurements of transverse quasielastic electron scattering from the deuteron at high momentum transfers," Phys. Rev. Lett. **61** (1988) 806–809;
R. G. Arnold *et al.*, "Measurement of elastic electron scattering from the proton at high momentum transfer," Phys. Rev. Lett. **57** (1986) 174–177.
Comment: The data are obsolete.

[274] P. E. Bosted *et al.*, "Measurement of the deuteron and proton magnetic form factors at large momentum transfers" Phys. Rev. C **42** (1990) 38–64.

[275] P. E. Bosted *et al.*, "Measurement of the electric and magnetic form factors of the proton $Q^2 = 1.75$ to $8.83(\mathrm{GeV}/c)^2$" Phys. Rev. Lett. **68** (1992) 3841–3844.

[276] A. Lung *et al.*, "Measurements of the electric and magnetic form-factors of the neutron from $Q^2 = 1.75$ to $4(\mathrm{GeV}/c)^2$," Phys. Rev. Lett. **70** (1993) 718–721.

[277] A. F. Sill *et al.*, "Measurements of elastic electron-proton scattering at large momentum transfer," Phys. Rev. D **48** (1993) 29–55.

[278] P. Markowitz *et al.*, "Measurement of the magnetic form factor of the neutron," Phys. Rev. C **48** (1993) R5–R9.

[279] R. C. Walker *et al.*, "Measurement of the proton elastic form factors for $Q^2 = 1 - 3(\mathrm{GeV}/c)^2$," Phys. Lett. B **224** (1989) 353–358; erratum – *ibid*. B **240** (1990) 522.

[280] R. C. Walker *et al.*, "Measurements of the proton elastic form factors for $1 \le Q^2 \le 3(\mathrm{GeV}/c)^2$ at SLAC," Phys. Rev. D **49** (1994) 5671–5689.

[281] L. Andivahis *et al.*, "Measurements of the electric and magnetic form factors of the proton from $Q^2 = 1.75$ to $8.83(\mathrm{GeV}/c)^2$," Phys. Rev. D **50** (1994) 5491–5517;
L. Andivahis *et al.*, "Measurements of the nucleon form factors at large momentum transfers," Nucl. Phys. A **553** (1993) 713–716.

MAMI

[282] F. Borkowski *et al.*, "Electromagnetic form factors of the proton at low four-momentum transfer," Nucl. Phys. B **93** (1975) 461–478.

[283] M. Meyerhoff *et al.*, "First measurement of the electric form factor of the neutron in the exclusive quasielastic scattering of polarized electrons prom polarized ^{3}He," Phys. Lett. B **327** (1994) 201–207.

[284] C. Herberg *et al.*, "Determination of the neutron electric form factor in the $D(e,e'n)p$ reaction and the influence of nuclear binding," Eur. Phys. J. A **5** (1999) 131–135. *DF*

[285] J. Becker *et al.*, "Determination of the neutron electric form factor from the reaction ^{3}He$(e,e'n)$ at medium momentum transfer," Eur. Phys. J. A **6** (1999) 329–344. *DF*

[286] D. Rohe *et al.*, "Measurement of the neutron electric form factor G_{En} at 0.67 (GeV$/c)^2$ via $^3\overrightarrow{\mathrm{He}}(\mathbf{e},e'n)$," Phys. Rev. Lett. **83** (1999) 4257–4260. *DF*

[287] M. Ostrick *et al.*, "Measurement of the neutron electric form factor G_{En} in the quasifree ^{2}H$(\mathbf{e},e'\mathbf{n})p$ reaction," Phys. Rev. Lett. **83** (1999) 276–279; *DF*
M. Ostrick, "Recent results on G_{En} from MAMI," Nucl. Phys. A **666** (2000) 100c–105c. *f*

[288] S. Dieterich *et al.*, "Polarization transfer in the ^{4}He$(\mathbf{e},e'\mathbf{p})^3$H reaction," Phys. Lett. B **500** (2001) 47–52 [arXiv:nucl-ex/0011008]. *df*

[289] D. Rohe (for the MAMI A1 Collaboration), "Recent results on neutron electromagnetic form factors," Nucl. Phys. A **663** (2000) 413c–416c. *f*

[290] J. Jourdan (for the MAMI A1 Collaboration), "Recent results on neutron electromagnetic form factors," Nucl. Phys. A **689** (2001) 425c–428c. *f*

[291] T. Pospischil *et al.* (MAMI A1 Collaboration), "Measurement of G_{Ep}/G_{Mp} via polarization transfer at $Q^2 = 0.4$(GeV$/c)^2$," Eur. Phys. J. A **12** (2001) 125–127. *DF*

[292] U. Muller and M. Seimetz (for the MAMI A1 Collaboration), "Measurement of the neutron electric form factor," Prog. Part. Nucl. Phys. **50** (2003) 483–485.

[293] J. Jourdan (for the MAMI A1 Collaboration), "Recent results of neutron electromagnetic form factors," Nucl. Phys. A **721** (2003) 395c–400c. *F*

[294] U. Muller and M. Potokar (for the MAMI A1 Collaboration), "Revisiting the axial form factor of the nucleon from low Q^2 pion electroproduction," Nucl. Phys. A **721** (2003) 425c–428c.

[295] J. Bermuth *et al.*, "The neutron charge form factor and target analyzing powers from $^3\overrightarrow{\mathrm{He}}(\mathbf{e},e'n)$ scattering," Phys. Lett. B **564** (2003) 199–204 [arXiv:nucl-ex/0303015]. *DF*

[296] D. I. Glazier *et al.* (MAMI A1 Collaboration), "Measurement of the electric form factor of the neutron at $Q^2 = 0.3 - 0.8\,$(GeV$/c)^2$," arXiv:nucl-ex/0410026

Bonn

[297] C. Berger *et al.*, "Electromagnetic form factors of the proton at squared four-momentum transfers between 10 and 50 fm^{-2}," Phys. Lett. B **35** (1971) 87–89; *df*
C. Berger *et al.* "Electromagnetic form factors of the proton between 5 and 50 fm^{-2}," Phys. Lett. B **28** (1968) 276–278. *df*

[298] E. E. W. Bruins *et al.*, "Measurement of the neutron magnetic form factor," Phys. Rev. Lett. **75** (1995) 21–24. *DF*

DESY

[299] W. Bartel *et al.*, "Small-angle electron-proton elastic scattering cross sections for squared momentum transfers between 10 and 105 F^{-2}," Phys. Rev. Lett. **17** (1966) 608–611. *df*

[300] W. Albrecht *et al.*, "Elastic electron-proton scattering at momentum transfers up to 245 F^{-2}," Phys. Rev. Lett. **17** (1966) 1192–1195. *df*

[301] W. Albrecht *et al.*, "Some recent measurements of proton form factors," Phys. Rev. Lett. **18** (1967) 1014–1015. *df*

[302] W. Albrecht *et al.*, "Quasi-elastic electron-deuteron scattering between $q^2 = 18$ fm^{-2} and 100 fm^{-2}," Phys. Lett. B **26** (1968) 642–644. *df*

[303] W. Bartel *et al.*, "Electromagnetic proton form factors at squared four momentum transfers between 1 and 3 $(\mathrm{GeV}/c)^2$," Phys. Lett. B **33** (1970) 245–248. *df*

[304] S. Galster *et al.*, "Elastic electron-deuteron scattering and the electric neutron form factor at four momentum transfers $5\mathrm{fm}^{-2} < q^2 < 14\mathrm{fm}^{-2}$," Nucl. Phys. B **32** (1971) 221–237. *f*

[305] W. Bartel *et al.*, "Electromagnetic form factors of the neutron at squared four-momentum transfers of $1.0 \mathrm{and} 1.5 (\mathrm{GeV}/c)^2$," Phys. Lett. B **39** (1972) 407–410;
W. Bartel *et al.*, "Measurement of proton and neutron electromagnetic form factors at squared four momentum transfers up to $3(\mathrm{GeV}/c)^2$," Nucl. Phys. B **58** (1973) 429–475.

[306] R. Felst, "Phenomenological fits to the nucleon electromagnetic form factors based on vector meson dominance," preprint DESY 73/56 (unpublished).

MIT-Bates LAC

[307] T. Eden *et al.*, "Electric form factor of the neutron from the $^2\mathrm{H}(\mathbf{e}, e'\mathbf{n})^1\mathrm{H}$ reaction at $Q^2 = 0.255(\mathrm{GeV}/c)^2$," Phys. Rev. C **50** (1994) R1749–R1753;
A. K. Thompson *et al.*, "Quasielastic scattering of polarized electrons from polarized ^{3}He and measurement of the neutron's form factors," Phys. Rev. Lett. **68** (1992) 2901–2904;
Comment: The data are obsolete.
C. E. Jones-Woodward *et al.*, "Determination of the neutron electric form factor in quasielastic scattering of polarized electrons from polarized ^{3}He," Phys. Rev. C **44** (1991) R571–R574.
Comment: The data are obsolete.

[308] H. Gao *et al.*, "Measurement of the neutron magnetic form factor from inclusive quasielastic scattering of polarized electrons from polarized ^{3}He," Phys. Rev. C **50** (1994) R546–R549.

[309] B. D. Milbrath *et al.* (MIT-Bates FPP Collaboration), "A comparison of polarization observables in electron scattering from the proton and deuteron," Phys. Rev. Lett. **80** (1998) 452–455; erratum – *ibid.* **82** (1999) 2221 [arXiv:nucl-ex/9712006].

[310] H. Gao (for the MIT-Bates 88-25 Collaboration), "Precise measurement of the neutron magnetic form factor from quasielastic $^3\overrightarrow{\mathrm{He}}(\mathbf{e}, e')$," Nucl. Instrum. Meth. A **402** (1998) 277–283.

NIKHEFF

[311] H. Anklin *et al.*, "Precision measurement of the neutron magnetic form factor," Phys. Lett. B **336** (1994) 313–318.

[312] J. Jourdan, "Precise determinations of the neutron magnetic form factor," Prog. Part. Nucl. Phys. **34** (1995) 211–212.

[313] H. Anklin *et al.*, "Precise measurements of the neutron magnetic form factor," Phys. Lett. B **428** (1998) 248–253.

[314] I. Passchier *et al.*, "The charge form factor of the neutron from $^2\overrightarrow{\mathrm{H}}(\mathbf{e}, e'n)p$," Nucl. Phys. A **663** (2000) 421c–424c [arXiv:nucl-ex/9908002];
I. Passchier *et al.*, "The charge form factor of the neutron from the reaction $^2\overrightarrow{\mathrm{H}}(\mathbf{e}, e'n)p$," Phys. Rev. Lett. **82** (1999) 4988–4991 [arXiv:nucl-ex/9907012].

[315] D. J. Boersma (for the NIKHEFF 9405 Collaboration), "Neutron electric form factor from $^3\overrightarrow{\mathrm{He}}(\mathbf{e}, e'n)$," Nucl. Phys. A **663** (2000) 417c–420c [arXiv:nucl-ex/9908003].

[316] G. Kubon *et al.*, "Precise neutron magnetic form factors," Phys. Lett. B **524** (2002) 26–32 [arXiv:nucl-ex/0107016].

SLEA

[317] S. Platchkov *et al.*, "Deuteron $A(Q^2)$ structure function and the neutron electric form factor," Nucl. Phys. A **508** (1990) 343c–348c;
S. Platchkov *et al.*, "Deuteron $A(Q^2)$ structure function and the neutron electric form factor," Nucl. Phys. A **510** (1990) 740–758.

Cornell Electron Synchrotron

[318] P. Stein *et al.*, "Measurements of neutron form factors," Phys. Rev. Lett. **16** (1966) 592–594.

LA of the Faculty of Sciences of the University of Paris

[319] P. Lehmann, R. Taylor, and R. Wilson. "Electron-proton scattering at low momentum transfers," Phys. Rev. **126** (1962) 1183–1188.

LEA of Orsay

[320] B. Grossetete, S. Jullian, and P. Lehmann, "Electrodisintegration of the deuteron around $q^2 = 3.5$ F^{-2}," Phys. Rev. **141** (1966) 1435–1440. *d*

[321] D. Benaksas, D. Drickey, and D. Frerejacque, "Deuteron electromagnetic form factor for 3 F^{-2} $< q^2 <$ 6 F^{-2}," Phys. Rev. **148** (1966) 1327–1331.

Analysis of experimental data

[322] G. Hohler *et al.*, "Analysis of electromagnetic nucleon form factors," Nucl. Phys. B **114** (1976) 505–534. *df*

[323] Ulf-G. Meißner "Baryon form factors: model-independent results," Nucl. Phys. A **666** (2000) 51c–60c.

[324] J. J. Kelly, "Nucleon charge and magnetization densities from Sachs form factors," Phys. Rev. C **66** (2002) 065203 [arXiv:hep-ph/0204239]. *dF*

[325] J. Arrington, "How well do we know the electromagnetic form factors of the proton?," Phys. Rev. C **68** (2003) 034325 [arXiv:nucl-ex/0305009]; *DF*
J. Arrington, "How well do we know the electromagnetic form factors of the proton?," Eur. Phys. J. A **17** (2003) 311–315 [arXiv:hep-ph/0209243]; *F*
J. Arrington, "Are recoil polarization measurements of G_E^p/G_M^p consistent with Rosenbluth separation data?" arXiv:nucl-ex/0205019. *F*

[326] H. Schmieden, "Electromagnetic form factors of the nucleon," arXiv:nucl-ex/0302027. *f*

[327] M. M. Mustafa *et al.*, "Extracting a value of the slope of the neutron form factor $G_{En}(q^2)$ at $q^2 = 0$ by reanalysis of the experimental data," arXiv:nucl-th/0308070.

Theoretical description and semiempirical models

[328] M. N. Rosenbluth, "High energy elastic scattering of electrons of protons," Phys. Rev. **79** (1950) 615–619.

[329] F. Iachello, A. D. Jackson, and A. Lande, "Semiphenomenological fits to nucleon electromagnetic form factors," Phys. Lett. B **43** (1973) 191–196. *f*

[330] R. G. Arnold, C. E. Carlson, and F. Gross, "Polarization transfer in elastic electron scattering from nucleons and deuterons," Phys. Rev. C **23** (1981) 363–374.

[331] M. F. Gari and W. Krüempelmann, "The electric neutron form factor and the strange quark content of the nucleon," Phys. Lett. B **274** (1992) 159–162; erratum – *ibid*. B **282** (1992) 483.

[332] P. E. Bosted, "An empirical fit to the nucleon electromagnetic form factors," Phys. Rev. C **51** (1995) 409–411.

[333] G. Holzwarth, "Electro-magnetic nucleon form factors and their spectral functions in soliton models," Z. Phys. A **356** (1996) 339–350 [arXiv:hep-ph/9606336]. *f*

[334] E. E. W. Bruins, "The magnetic form factor of the neutron," arXiv:nucl-ex/9611004. *f*

[335] F. Klein and H. Schmieden (for the MAMI A3 Collaboration), "Electromagnetic nucleon form factors in the space-like region," Nucl. Phys. A **623** (1997) 323c–332c. *f*

[336] H. Gao, "Effective neutron targets," Nucl. Phys. A **631** (1998) 170c–189c. *f*

[337] W. M. Alberico *et al.*, "Neutrino (antineutrino)-nucleon scattering and strange form factors of the nucleon," Nucl. Phys. A **663** (2000) 833c–836c.

[338] E. J. Brash *et al.*, "New empirical fits to the proton electromagnetic form factors," Phys. Rev. C **65** (2002) 051001 [arXiv:hep-ex/0111038]. *DF*

[339] R. Schiavilla and I. Sick, "Neutron charge form factor at large q^2," Phys. Rev. C **64** (2001) 041002 [arXiv:nucl-ex/0107004]. *F*

[340] I. Sick, “Elastic electron scattering from light nuclei,” Prog. Part. Nucl. Phys. **47** (2001) 245–318 [arXiv:nucl-ex/0208009].

[341] E. L. Lomon, “Effect of recent R_p and R_n measurements on extended Gari–Krüempelmann model fits to nucleon electromagnetic form factors,” Phys. Rev. C **66** (2002) 045501 [arXiv:nucl-th/0203081].

[342] A. F. Krutov and V. E. Troitsky, “Extraction of the neutron charge form factor from the charge form factor of deuteron,” Eur. Phys. J. A **16** (2003) 285–290 [arXiv:hep-ph/0202183].

[343] A. W. Thomas *et al.*, “Progress in the calculation of nucleon form factors and parton distribution functions,” Nucl. Phys. A **721** (2003) 915c–921c.

[344] K. de Jager, “Nucleon form factors,” Nucl. Phys. A **721** (2003) 66c–75c.

[345] Fayyazuddin, “Structure of proton,” arXiv:hep-ph/0306149.

[346] J. Arrington, “Implications of the discrepancy between proton form factor measurements,” Phys. Rev. C **69** (2004) 022201 [arXiv:nucl-ex/0309011].

[347] See Ref. [42].

[348] S. Boffi *et al.*, “Covariant electroweak nucleon form factors in a chiral constituent-quark model,” Eur. Phys. J. A **14** (2002) 17–21.

[349] “Nucleon form factors from generalized parton distributions” M. Guidal, M. V. Polyakov, A. V. Radyushkin, and M. Vanderhaeghen, arXiv:hep-ph/0410251.

Neutron charge radius

[350] P. Grabmayr and A. J. Buchmann, “Moments of the neutron charge form factor and the $N \to \Delta$ quadrupole transition,” Phys. Rev. Lett. **86** (2001) 2237–2240 [arXiv:hep-ph/0104203].

[351] S. Kopecky *et al.*, “New measurement of the charge radius of the neutron,” Phys. Rev. Lett. **74** (1995) 2427–2430.

[352] S. Kopecky *et al.*, “Neutron charge radius determined from the energy dependence of the neutron transmission of liquid ^{208}Pb and ^{209}Bi,” Phys. Rev. C **56** (1997) 2229–2237.

Miscellanea

[353] P. Stoler, “Connection between the elastic G_{Ep}/G_{Mp} and $p \to \Delta$ form factors,” Phys. Rev. Lett. **91** (2003) 172303 [arXiv:hep-ph/0210184].

NUCLEON FORM FACTORS (F_A, F_P)

Reviews

[354] V. Bernard, L. Elouadrhiri, and Ulf-G. Meißner, “Axial structure of the nucleon,” J. Phys. G **28** (2002) R1–R35 [arXiv:hep-ph/0107088].

[355] H. Budd, A. Bodek, and J. Arrington, “Vector and axial form factors applied to neutrino quasielastic scattering,” Nucl. Phys. B (Proc. Suppl.) **139** (2005) 90–95 [arXiv:hep-ex/0410055].

Experimental data

JINR Phasotron

[356] V. Brudanin *et al.*, “Measurement of the induced pseudoscalar form factor in the capture of polarized muons by Si nuclei,” Nucl. Phys. A **587** (1995) 577–595.

Saclay

[357] G. Bardin *et al.*, “Measurement of the ortho-para transition rate in the $p\mu p$ molecule and deduction of the pseudoscalar coupling constant,” Phys. Lett. **104**B (1981) 320–324.

[358] S. Choi *et al.*, “Axial and pseudoscalar nucleon form-factors from low energy pion electroproduction,” Phys. Rev. Lett. **71** (1993) 3927–3930; See also V. Bernard, N. Kaser, and Ulf-G. Meißner, ”Comment on ’Axial and pseudoscalar nucleon form factors from low energy pion electroproduction’,” Phys. Rev. Lett. **72** (1994) 2810.

TRIUMF cyclotron

[359] G. Jonkmans *et al.*, "Radiative muon capture on hydrogen and the induced pseudoscalar coupling," Phys. Rev. Lett. **77** (1996) 4512–4515 [arXiv:nucl-ex/9608005].

Theoretical description and semiempirical models

[360] K.-F. Liu, S.-J. Dong, T. Draper, and W. Wilcox, "πNN and pseudoscalar form factors from lattice QCD," Phys. Rev. Lett. **74** (1995) 2172–2175 [arXiv:hep-lat/9406007].

[361] K. Khosonthongkee, V. E. Lyubovitskij, T. Gutsche, A. Faessler, K. Pumsa-ard, S. Cheedket, and Y. Yan, "Axial form factor of the nucleon in the perturbative chiral quark model," J. Phys. G **30** (2004) 793–810 [arXiv:hep-ph/0403119].

[362] T. Sato and T. S. Lee, "Dynamical model of electroweak pion production reaction," arXiv:hep-ph/0411182.

SECOND CLASS CURRENTS

Neutrino experiments

[363] J. Bell *et al.*, "Diffractive production of vector mesons in high-energy neutrino interactions," Phys. Rev. Lett. **40** (1978) 1226–1229.
Comment: Fermilab 15-ft bubble chamber, ν_μ beam with $\langle E_\nu \rangle = 15$ GeV.

[364] Other limits on SCC from neutrino experiments are given in Refs. [28] (ν_μ beam with $\langle E_\nu \rangle = 1.6$ GeV), [151] (ν_μ beam with $E_\nu = 0.3 - 6$ GeV), [34] (ν_μ and $\overline{\nu}_\mu$ beams with $E_\nu = 3 - 30$ GeV) and [29] ($\overline{\nu}_\mu$ beam with $\langle E_\nu \rangle = 1.2$ GeV).

Beta Decay & Muon Capture experiments

Osaka

Theory (general)

[365] S. Weinberg, "Charge symmetry of weak interactions," Phys. Rev. **112** (1958) 1375–1379.

[366] B. R. Kim and R. Rodenberg, "Implications of second class currents for neutral weak currents and gauge models," Phys. Rev. D **10** (1974) 2234.

[367] K. Kubodera, J. Delorme, and M. Rho, "Second-class currents," Phys. Rev. Lett. **38** (1977) 321–324.

[368] N. Samsonenko, Y. Cumar, and M. Suvorov, "Effets des courants faibles de seconde classe dans les processes semileptoniques," (Effects of second class weak currents in semileptonic processes)," Annales Poincare Phys. Theor. A **36** (1982) 239–255.

[369] L. Grenacs, "Induced weak currents in nuclei," Ann. Rev. Nucl. Part. Sci. **35** (1985) 455–500.

[370] H. Shiomi, "Second class current in QCD sum rules," Nucl. Phys. A **603** (1996) 281–302 [arXiv:hep-ph/9601329].

[371] H. Shiomi, "Second class current in QCD sum rules," J. Korean Phys. Soc. **29** (1996) S378–S380. ★

[372] D. H. Wilkinson, "Limits to second-class nucleonic and mesonic currents," Eur. Phys. J. A **7** (2000) 307–315.

[373] D. H. Wilkinson, "Limits to second-class nucleonic currents," Nucl. Instrum. Meth. A **455** (2000) 656–659.

[374] D. H. Wilkinson, "Second-class currents and Δs in $\nu(\overline{\nu})p$ elastic scattering," Nucl. Instrum. Meth. A **469** (2001) 286–291.

[375] M. D. Slaughter, "Connection between second class currents and the $\Delta N \gamma$ form factors $G^*_M(q^2)$ and $G^*_E(q^2)$," arXiv:hep-ph/0412161.

Theory (νN)

[376] B. R. Holstein, "Second-class currents and analog processes," Phys. Rev. C **4** (1971) 764–775.

[377] H. Pietschmann and H. Rupertsberger, "Weak Mesonic Currents ff Second Class," Phys. Lett. B **40** (1972) 662–664.

[378] M. Zh. Shmatikov, "Restrictions on the second-kind currents from deep-inelastic νN scattering," Yad. Fiz. **21** (1975) 1278–1280 [Sov. J. Nucl. Phys. **21** (1976) 660–661].

[379] B. R. Holstein and S. B. Treiman, "Second-class currents," Phys. Rev. D **13** (1976) 3059–3066.

[380] R. Rodenberg, "Second class currents in neutrino reactions," Annalen Phys. **33** (1976) 329–340.

[381] M. S. Chen, F. S. Henyey, and G. L. Kane, "A model for charged second class currents," Nucl. Phys. B **114** (1976) 147–156.

[382] V. A. Korotkov, E. P. Kuznetsov, V. V. Makeev and Y. P. Nikitin, "On influence of second class currents on differential cross section behavior in quasielastic $\nu_\mu(\overline{\nu}_\mu)N$ scattering," Yad. Fiz. **26** (1977) 601–604 [Sov. J. Nucl. Phys. **26** (1977) 318–320].

[383] E. H. Monsay, "Second-class currents in weak pion production," Phys. Rev. D **16** (1977) 609–621.

[384] G. A. Lobov, "Second class axial current and neutrino and antineutrino scattering processes," preprint ITEP-84-1978.

[385] B. K. Kerimov and N. V. Samsonenko, "Effects of second-class currents in the direct and inverse β decay processes," Izv. Akad. Nauk SSSR, Ser. Fiz. **43**, No. 11 (1979) 2449–2453.

[386] R. Rodenberg and C. Stamm, "Implications of Higgs bosons on second class currents in neutrino reactions," Nuovo Cim. A **56** (1980) 159–186.

[387] B. K. Kerimov, D. Ishankuliev, and N. V. Samsonenko, "Currents of the second kind in the neutrino splitting of a deuteron," Izv. VUZ, Fiz. **24**, No. 9 (1981) 48–52 [Sov. Phys. J. **24**, No. 9 (1982) 824–828].

[388] N. V. Samsonenko, C. L. Katkhat, and A. D. Nevsky, "Second class currents in the processes of inverse beta decay $\overline{\nu}_e + {}^3\mathrm{He} \to {}^3\mathrm{H} + e^+$ and $\nu_e + {}^3\mathrm{He} \to {}^3\mathrm{H} + e^-$ at low neutrino energy," Izv. Ross. Akad. Nauk Ser. Fiz. **57**, No. 1 (1993) 2–7.

[389] N. V. Samsonenko and A. D. Nevsky, "Second class currents in inverse beta decay of polarized ^{3}H and ^{3}He nuclei," Izv. Akad. Nauk SSSR, Ser. Fiz. **57**, No. 9 (1993) 72–76 [Bull. Acad. Sci. USSR, Phys. Ser. **57** (1993) 1545–1548].

[390] N. V. Samsonenko, M. A. Usman, A. D. Nevsky, and A. Rivasplata, "Currents of the second kind in quasielastic scattering of ν ($\overline{\nu}$ by free polarized nucleons," Izv. VUZ, Fiz. **36**, No. 1 (1993) 36–40 [Russ. Phys. J. **36**, No. 1 (1993) 29–32].

Theory (β decay, muon capture, etc.)

[391] B. R. Holstein and S. B. Treiman, "Tests for second-class currents in nuclear beta decay," Phys. Rev. C **3** (1971) 1921–1926.

[392] M. Oka and K. Kubodera, "Determination of upper limits to second class currents," Phys. Lett. B **90** (1980) 45–49.

[393] I. Kumar and N. V. Samsonenko, " Polarization effects of currents of the second kind during beta decay," Izv. Akad. Nauk SSSR, Ser. Fiz. **46**, No. 5 (1982) 921–924 [Bull. Acad. Sci. USSR, Phys. Ser. **46** (1982) 83–87].

[394] B. R. Holstein, "Limit on second class polar vector couplings in semileptonic weak interactions," Phys. Rev. C **29** (1984) 623–627.

[395] N. V. Samsonenko, A. L. Samgin, and C. L. Katkhat, "Influence of meson exchange currents of the second kind on the characteristics of the $\beta^\pm$ decay of light nuclei," Yad. Fiz. **47** (1988) 348–354 [Sov. J. Nucl. Phys. **47** (1988) 220–223].

[396] C. L. Katkhat, " Second class meson exchange currents and neutrino mass in μ^- capture by light nuclei," Izv. Akad. Nauk SSSR, Ser. Fiz. **53**, No. 1 (1989) 103–110 [Bull. Acad. Sci. USSR, Phys. Ser. **53**, No. 1 (1989) 100–107].

[397] N. V. Samsonenko, A. L. Samgin, M. I. Suvorov, and E. V. Brilev, "Second class currents and neutrino mass in beta decay processes $\mathrm{Ne}^{19} \to \mathrm{Fe}^{19} + e^+ + \nu_e$ and $n \to p + e^- + \overline{\nu}_e$," Izv. Akad. Nauk SSSR, Ser. Fiz. **53**No. 11 (1989) 2110–2115 [Bull. Acad. Sci. USSR, Phys. Ser. **53**, No. 11 (1989) 47–53].

[398] N. V. Samsonenko, A. L. Samgin, C. L. Katkhat, and A. P. Loginov, "Study of the beta decay of ^{6}He with allowance for second class currents and the anti-neutrino mass," Izv. VUZ, Fiz. **32**, No. 9 (1989) 62–67 [Sov. Phys. J. **32**, No. 9 (1989) 723–727].

[399] N. V. Samsonenko, C. L. Kathat, and A. L. Samgin, "Second class currents and neutrino mass in mirror transitions," Nucl. Phys. A **491** (1989) 642–651.

[400] C. L. Kathat and N. V. Samsonenko, “Second-class currents and the muon-neutrino rest mass in the muon capture by ^{6}Li and ^{3}He,” Nucl. Phys. A **500** (1989) 669–680.

[401] S. Gardner and C. Zhang, “Sharpening low-energy, standard-model tests via correlation coefficients in neutron β decay,” Phys. Rev. Lett. **86** (2001) 5666–5669 [arXiv:hep-ph/0012098].

MUON INTERACTIONS

General

[402] Y. M. Andreev and E. V. Bugaev, “Radiative energy losses of muons in the ground,” Izv. Akad. Nauk SSSR Ser. Fiz. **42**, N. 7 (1978) 1475–1478 [Bull. Russ. Acad. Sci. Phys. **42**, N. 7 (1978) 112–115].

[403] R. P. Kokoulin and A. A. Petrukhin, “Muon interactions and consequences in underground physics,” in Proc. of the Vulcano Workshop 1996, “Frontier Objects in Astrophysics and Particle Physics,” Vulcano, May 27 – June 1, 1996, Edited by F. Giovannelli and G. Mannocchi, Vol. **57**, pp. 379–392.

[404] D. E. Groom, N. V. Mokhov, and S. I. Striganov, “Muon stopping power and range tables 10 MeV to 100 TeV,” Atom. Data Nucl. Data Tabl. **78** (2001) 183–356.

Ionization and excitation

[405] R. M. Sternheimer, M. J. Berger, and S. M. Seltzer, “Density effect for the ionization loss of charged particles in various substances,” Atom. Data Nucl. Data Tabl. **30** (1984) 261.

Multiple Coulomb scattering

[406] D. Theriot, “Muon shielding: Multiple Coulomb scattering of muons with energy loss,” preprint FERMILAB-TM-0261.

[407] A. V. Butkevich, R. P. Kokoulin, G. V. Matushko, and S. P. Mikheyev, “Comments on multiple scattering of high-energy muons in thick layers,” Nucl. Instrum. Meth. A **488** (2002) 282–294 [arXiv:hep-ph/0108016].

Direct pair production

[408] S. R. Kelner and Y. D. Kotov, “A contribution to the problem of electron and muon pair production by cosmic ray muons,” Yad. Fiz. **9** (1969) 1210–1211 [Sov. J. Nucl. Phys. **9** (1969) 708].

[409] D. Ivanov, E. A. Kuraev, A. Schiller, and V. G. Serbo, “Production of e^+e^- pairs to all orders in $Z\alpha$ for collisions of high-energy muons with heavy nuclei,” Phys. Lett. B **442** (1998) 453–458 [arXiv:hep-ph/9807311].

[410] S. R. Kelner, “Pair production in collisions between muons and atomic electrons,” Yad. Fiz. **61** (1998) 511–519 [Phys. Atom. Nucl. **61** (1998) 448–456].

[411] S. R. Kelner, R. P. Kokoulin, and A. A. Petrukhin, “Muon pair production by high energy muons and muon bundles underground,” in Proc. of the 26th International Cosmic Ray Conf. , Salt Lake City, Utah, August 17 – 25, 1999, edited by D. Kieda, M. Salamon and B. Dingus, Vol. **2**, pp. 20–23.

[412] S. R. Kelner, R. P. Kokoulin, and A. A. Petrukhin, “Direct production of muon pairs by high-energy muons,” Yad. Fiz. **63** (2000) 1690–1698 [Phys. Atom. Nucl. **63** (2000) 1603–1611].

[413] V. A. Kudryavtsev and O. G. Ryazhskaya, “Muon pair production by muons and narrow muon bundles underground,” Nuovo Cim. **21 C** (1998) 171–176.

[414] V. A. Kudryavtsev, E. V. Korolkova, and N. J. Spooner, “Narrow muon bundles from muon pair production in rock,” Phys. Lett. B **471** (1999) 251–256 [arXiv:hep-ph/9911493].

Bremsstrahlung

[415] Y. M. Andreev, L. B. Bezrukov, and E. V. Bugaev, “Excitation of a target in muon bremsstrahlung,” Yad. Fiz. **57** (1994) 2146–2154 [Phys. Atom. Nucl. **57** (1994) 2066–2074].

[416] Y. M. Andreev and E. V. Bugaev, “Muon bremsstrahlung on heavy atoms,” Phys. Rev. D **55** (1997) 1233–1243.

[417] S. R. Kelner, R. P. Kokoulin, and A. A. Petrukhin, “Bremsstrahlung from muons scattered by atomic electrons,” Yad. Fiz. **60** (1997) 657–665 [Phys. Atom. Nucl. **60** (1997) 576–583].

[418] S. R. Kelner and A. M. Fedotov, "Diffractive corrections to bremsstrahlung from muons," Yad. Fiz. **62** (1999) 307–315 [Phys. Atom. Nucl. **62** (1999) 272–280].

[419] S. R. Kelner and A. M. Fedotov, "Varying charge ratio in muons passing through matter," Izv. Ross. Akad. Nauk. **63**, N. 3 (1999) 574–576 [Bull. Russ. Acad. Sci. Phys. **63**, N. 3 (1999) 465–467].

Photonuclear interactions

[420] A. V. Butkevich and S. P. Mikheyev, "The cross-section of muon nuclear inelastic interaction," arXiv:hep-ph/0109060.

[421] E. V. Bugaev and Y. V. Shlepin, "Photonuclear interaction of high energy muons and tau leptons," Phys. Rev. D **67** (2003) 034027 [arXiv:hep-ph/0203096].

MUON DECAY

[422] T. Bergfeld *et al.* (CLEO Collaboration), "Observation of radiative leptonic decay of the tau lepton," Phys. Rev. Lett. **84** (2000) 830–834 [arXiv:hep-ex/9909050].

ATMOSPHERIC MUON POLARIZATION

[423] S. Hayakawa, "Polarization of cosmic-ray μ mesons: theory," Phys. Rev. **108** (1957) 1533–1537.

[424] G. W. Clark and J. Hersil, "Polarization of cosmic-ray μ mesons: experiment," Phys. Rev. **108** (1957) 1538–1544; erratum – *ibid*. **110** (1958) 1485.

[425] C. S. Johnson, "Polarization of cosmic-ray muons at sea level," Phys. Rev. **122** (1961) 1883–1890.

[426] H. V. Bradt and G. W. Clark, "Polarization of cosmic-ray μ mesons," Phys. Rev. **132** (1963) 1306–1316.

[427] R. Turner, C. M. Ankenbrandt, and R. C. Larsen, "Polarization of cosmic-ray muons," Phys. Rev. D **4** (1971) 17–23.

[428] M. Yamada *et al.* (Kamiokande Collaboration), "Measurements of the charge ratio and polarization of 1.2 TeV/c cosmic-ray muons with the Kamiokande II detector," Phys. Rev. D **44** (1971) 617–621.

RELEVANT PROJECTS

Reviews

[429] T. Tabarelli de Fatis, "Future projects on atmospheric neutrinos," Nucl. Phys. B (Proc. Suppl.) **118** (2003) 118–125 [arXiv:hep-ex/0209053].

[430] C. Yanagisawa, "Super-K, K2K, JHFnu and UNO: Past, present and future," talk at the International Workshop on Astroparticle and High-Energy Physics (AHEP-2003), Valencia, Spain, October 14 – 18, 2003; JHEP Proceedings, AHEP2003/062

[431] A. Rubbia, "Very massive underground detectors for proton decay searches," Invited talk at the 11th International Conf. on Calorimetry in High Energy Physics (CALOR'04), Perugia, Italy, March 28 – April 2, 2004, arXiv:hep-ph/0407297.

[432] A. Rubbia, "Neutrino detectors for future experiments," arXiv:hep-ph/0412230.

BooNE and MiniBooNE

[433] J. L. Raaf (for the BooNE Collaboration), "MiniBooNE Status," arXiv:hep-ex/0408008.

NuMI–MINOS

[434] A. Weber, "MINOS: The Main Injector Neutrino Oscillation Search," Nucl. Phys. B (Proc. Suppl.) **98** (2001) 57.

[435] V. Paolone (for the MINOS Collaboration), "Status of The MINOS Experiment," Nucl. Phys. B (Proc. Suppl.) **100** (2001) 197–199.

[436] K. Lang (for the MINOS Collaboration), "MINOS detectors for neutrino interactions," Nucl. Instrum. Meth. A **461** (2001) 290–292.

[437] E. Buckley-Geer (for the MINOS Collaboration), "Status of the MINOS experiment," Nucl. Instrum. Meth. A **503** (2001) 122–123.

[438] R. Saakian (for the MINOS Collaboration), "Status of the MINOS experiment," Nucl. Phys. B (Proc. Suppl.) **111** (2002) 169–174.

[439] D. Michael, "The MINOS experiment," Prog. Part. Nucl. Phys. **48** (2002) 99–109.

[440] M. V. Diwan (for the MINOS Collaboration), "Status of the MINOS experiment," Nucl. Phys. B (Proc. Suppl.) **123** (2003) 272–278 [arXiv:hep-ex/0211026].

[441] M. O. Wascko, "Measuring ν_μ charged-current interactions in MiniBooNE," arXiv:hep-ex/0412008.

FINeSSE

[442] L. Bugel *et al.* (FINeSSE Collaboration), "A Proposal for a near detector experiment on the booster neutrino beamline: FINeSSE: Fermilab intense neutrino scattering scintillator experiment," arXiv:hep-ex/0402007.

[443] S. Brice *et al.*, "The FINeSSE detector," Nucl. Phys. B (Proc. Suppl.) **139** (2003) 317–322.

[444] S. Boyd (for the MINERνA Collaboration), "MINERνA: A high statistics neutrino scattering experiment in the NuMI neutrino beam," Nucl. Phys. B (Proc. Suppl.) **139** (2003) 311–316.

[445] D. Drakoulakos *et al.* (MINERνA Collaboration), "Proposal to perform a high-statistics neutrino scattering experiment using a fine-grained detector in the NuMI beam," arXiv:hep-ex/0405002.

[446] D. A. Harris *et al.* (MINERνA Collaboration), "Neutrino scattering uncertainties and their role in long baseline oscillation experiments," arXiv:hep-ex/0410005

[447] L. Bartoszek *et al.* "FLARE, Fermilab Liquid Argon Experiments (Letter of Intent)," arXiv:hep-ex/0408121.

MONOLITH

[448] N. Y. Agafonova *et al.* (MONOLITH Collaboration), "MONOLITH: A massive magnetized iron detector for neutrino oscillation studies," LNGS-P26-2000.

[449] A. Geiser (for the MONOLITH Collaboration), "The MONOLITH project," Nucl. Instrum. Meth. A **472** (2000) 464–469 [arXiv:hep-ex/0008067].

[450] A. A. Petrukhin (for the MONOLITH Collaboration), "Present status of the MONOLITH project," Part. Nucl. Lett. **109** (2001) 32–42.

[451] F. Terranova (for the MONOLITH Collaboration), "MONOLITH: A massive magnetized tracking calorimeter for the study of atmospheric neutrino oscillations," Int. J. Mod. Phys. A **16 S1B** (2001) 736–738.

[452] A. Geiser (for the MONOLITH Collaboration), "The MONOLITH experiment at Gran Sasso," Phys. Scripta **T 93** (2001) 86–90.

[453] P. Antonioli (for the MONOLITH Collaboration), "MONOLITH: A next generation experiment for atmospheric neutrinos," Nucl. Phys. B (Proc. Suppl.) **100** (2001) 142–144 [arXiv:hep-ex/0101040].

[454] T. Tabarelli de Fatis (for the MONOLITH Collaboration), "Sensitivity to oscillation parameters of the MONOLITH experiment," Nucl. Phys. B (Proc. Suppl.) **110** (2002) 352–354.

ICARUS

[455] P. Cennini *et al.* (ICARUS Collaboration), "ICARUS II: A second generation proton decay experiment and neutrino observatory at the Gran Sasso laboratory: Proposal," LNGS-94/99, Vol. **I** (1993) & Vol. **II** (1994). ★

[456] P. Aprili *et al.* (ICARUS Collaboration), "The ICARUS experiment: A second-generation proton decay experiment and neutrino observatory at the Gran Sasso laboratory (addendum to the LNGS proposal LNGS-94/99 [455])," CERN/SPSC 2002-027.

[457] F. Arneodo *et al.* (ICARUS Collaboration), "ICARUS: An innovative detector for underground physics," Nucl. Instrum. Meth. A **461** (2001) 324–326.

[458] F. Arneodo *et al.* (ICARUS Collaboration), "The ICARUS experiment, a second-generation proton decay experiment and neutrino observatory at the Gran Sasso Laboratory," arXiv:hep-ex/0103008.

[459] J. Rico (for the ICARUS Collaboration), "Status of ICARUS," arXiv:hep-ex/0205028.

[460] A. Badertscher (for the ICARUS Collaboration), "The ICARUS project: a 3000 t LAr TPC for neutrino physics and a search for nucleon decays," Nucl. Instrum. Meth. A **535** (2004) 129–133.

NOE

[461] M. Ambrosio *et al.* (*NOE* Collaboration), "The *NOE* detector for a long baseline neutrino oscillation experiment," INFN/AE-98-09 (1998).

[462] G. C. Barbarino *et al.*, "*NOE* : A long baseline neutrino detector," Nucl. Phys. B (Proc. Suppl.) **66** (1998) 428–431.

[463] G. C. Barbarino *et al.*, "The *NOE* detector for a long baseline neutrino oscillation experiment," Nucl. Phys. B (Proc. Suppl.) **70** (1999) 223–226.

[464] E. Scapparone (for the *NOE* Collaboration), "*NOE* : A neutrino experiment for the CERN – Gran Sasso long base line project," Nucl. Phys. B (Proc. Suppl.) **76** (1999) 471–476 [arXiv:hep-ex/9902025].

[465] G. Osteria (for the *NOE* Collaboration), "The *NOE* detector for a long baseline neutrino oscillation experiment," Nucl. Phys. B (Proc. Suppl.) **78** (1999) 401–406.

ICANOE

[466] F. Arneodo *et al.* (ICARUS and *NOE* Collaborations), "*ICANOE* : Imaging and calorimetric neutrino oscillation experiment: A proposal for a CERN-GS long baseline and atmospheric neutrino oscillation experiment," INFN/AE-99-17 (1999).

[467] A. Rubbia (for the ICARUS and NOE Collaborations), "*ICANOE* : Imaging and calorimetric neutrino oscillation experiment," arXiv:hep-ex/0001052; see also Ref. [468].

[468] A. Rubbia, "*ICANOE* and OPERA experiments at the LNGS/CNGS," Nucl. Phys. B (Proc. Suppl.) **91** (2000) 223–229 [arXiv:hep-ex/0008071].

Super-ICARUS

OPERA

[469] M. Guler *et al.* (OPERA Collaboration), "Experiment Proposal OPERA: An appearance experiment to search for $\nu_\mu \to \nu_\tau$ oscillations in the CNGS beam," CERN/SPSC 2000-028.

[470] See Ref. [468].

UNO

[471] C. K. Jung, "Feasibility of a next generation underground water Cherenkov detector: UNO," in Proc. of the International Workshop on Next Generation Nucleon Decay and Neutrino Detector (NNN 99), Stony Brook, New York, September 23 – 25, 1999, pp. 29–34 [arXiv:hep-ex/0005046].

[472] M. Goodman *et al.* (UNO Proto-collaboration) The UNO whitepaper, "Physics Potential and Feasibility of UNO", edited by D. Casper *et al.*, preprint # SBHEP 01-3, June 2001 (available from URL http://ale.physics.sunysb.edu/uno/publications.shtml).

TITAND (TITANIC)

[473] Y. Suzuki (for the TITAND Working Group), "Multi-Megaton water Cherenkov detector for a proton decay search TITAND (former name: TITANIC)," arXiv:hep-ex/0110005.

Hyper-Kamiokande

[474] K. Nakamura(for the MONOLITH Collaboration), "Hyper-Kamiokande – a next generation water Cherenkov detector," Int. J. Mod. Phys. A **18** (2003) 4053–4063.

Aqua-RICH

[475] P. Antonioli *et al.*, "The AQUA-RICH atmospheric neutrino experiment," Nucl. Instrum. Meth. A **433** (1999) 104–120.

LANNDD and Mini-LANNDD at WIPP

[476] D. B. Cline and F. Sergiampietri, "A super beam to the LANNDD detector at the Carlsbad Underground Laboratory," in Proc. of the APS/DPF/DPB Summer Study on the Future of Particle Physics (Snowmass 2001), ed. by N. Graf, eConf **C010630** (2001) E107.

[477] D. B. Cline, K. Lee, Y. Seo, and P. F. Smith, "Study of the backgrounds for the search for proton decay to 10^{35} Y at the WIPP site with the LANNDD detector," arXiv:astro-ph/0208381.

[478] D. B. Cline, F. Sergiampietri, J. G. Learned, and K. McDonald, "LANNDD: A massive liquid argon detector for proton decay, supernova and solar neutrino studies, and a neutrino factory detector," Nucl. Instrum. Meth. A **503** (2003) 136–140 [arXiv:astro-ph/0105442].

[479] D. B. Cline, S. Otwinowski, and F. Sergiampietri, "Mini-LANNDD: A very sensitive neutrino detector to measure $\sin^2\big(2\theta_(13)\big)$," J. Phys. G **29** (2003) 1893–1898 [arXiv:astro-ph/0206124].

[480] D. B. Cline, Y. H. Seo, and F. Sergiampietri, "Mini-LANNDD T40: A detector to measure the neutrino argon cross section and the nu/e contamination in the off-axis NuMI beam," arXiv:astro-ph/0301545.

3M

[481] A. K. Mann, "Megaton modular multi-purpose neutrino detector," arXiv:hep-ex/0108036.

[482] M. V. Diwan *et al.*, "Megaton modular multi-purpose neutrino detector for a program of physics in the Homestake DUSEL," arXiv:hep-ex/0306053.

SCIPIO

INO

[483] G. Rajasekaran, "India-based neutrino observatory," arXiv:hep-ph/0402246.

[484] D. Indumathi (for the INO Collaboration), "India-based Neutrino Observatory (INO)," Pramana **63** (2004) 1283–1293.

NEUTRINO PROPAGATION THROUGH MATTER

[485] V. A. Naumov, "High-energy neutrino oscillations in absorbing matter," Phys. Lett. B **529** (2002) 199–211 [arXiv:hep-ph/0112249].

[486] V. A. Naumov and L. Perrone, "Neutrino propagation through dense matter," Astropart. Phys. **10** (1999) 239–252 [arXiv:hep-ph/9804301].

ATMOSPHERIC NEUTRINOS

[487] T. Nakaya (for the Super-Kamiokande Collaboration), "Atmospheric and long baseline neutrino," eConf **C020620** (2002) SAAT01 [arXiv:hep-ex/0209036].

POSSIBLE APPLICATIONS

Neutrino oscillations

[488] V. D. Barger *et al.*, "Neutrino oscillation parameters from MINOS, ICARUS and OPERA combined," Phys. Rev. D **65** (2002) 053016 [arXiv:hep-ph/0110393].

[489] T. K. Gaisser and T. Stanev, "Charge ratio of muons from atmospheric neutrinos," Phys. Lett. B **561** (2003) 125–129 [arXiv:astro-ph/0210512].

[490] G. L. Fogli, E. Lisi, A. Marrone, and D. Montanino, "Status of atmospheric $\nu_\mu \to \nu_\tau$ oscillations and decoherence after the first K2K spectral data," Phys. Rev. D **67** (2003) 093006 [arXiv:hep-ph/0303064].

Proton decay

[491] D. Rein, “Neutrino induced pion production and proton decay,” Phys. Rev. D **28** (1983) 1800–1801.

Dark matter WIMPs

[492] S. Desai *et al.* (Super-Kamiokande Collaboration), “Search for dark matter WIMPs using upward through-going muons in Super-Kamiokande,” arXiv:hep-ex/0404025. See also S. Desai, “High energy neutrino astrophysics with Super-Kamiokande,” Ph. D. Thesis (Boston University, 2004).

Tomography of the earth

[493] A. Nicolaidis, M. Jannane, and A. Tarantola, “Neutrino tomography of the Earth,” J. Geophys. Res. **96 (B13)** (1991) 21811–21817.

[494] B. Kahle, “Tomography of the earth by oscillation of atmospheric neutrinos,” Ph. D. Thesis (Hamburg University, April 2002).

[495] M. M. Reynoso and O. A. Sampayo, “On neutrino absorption tomography of the Earth,” arXiv:hep-ph/0401102.

RELEVANT AND IRRELEVANT

[496] S. R. Kelner, R. P. Kokoulin, and A. A. Petrukhin, “Radiation logarithm in the Hartree–Fock model,” Yad. Fiz. **62** (1999) 2042–2048 [Phys. Atom. Nucl. **62** (1999) 1894–1898].

[497] A. E. Asratyan *et al.*, “Neutral strange particle production in antineutrino–induced neutral current interactions,” Phys. Lett. B **140** (1984) 127–129.

[498] R. R. Horgan, “The $(56, 1-)$ $N = 3$ baryonic multiplet and the spin averaged mass of the Δ resonance sector,” CERN-TH-2916; “Spin-averaged mass formulas and the mass spectrum of low lying Δ resonances in harmonic-oscillator-like quark models,” Z. Phys. C **13** (1982) 25–33.

[499] P. Langacker, “Grand unification,” Comments Nucl. Part. Phys. **15** (1985) 41–67.

[500] S. Weinberg, “Precise relations between the spectra of vector and axial-vector mesons,” Phys. Rev. Lett. **18** (1967) 507–509.

Papers from the KEK Library

[140], [19], [20], [64], [65], [77], [85], [48], [60] [171], [172], [161], [126]

[501] H. Pietschmann, “Second class currents in weak interactions,” in Proc. of the European Neutrino Conf. , “Neutrino’72”, Balatonfured, Hungary, June 11 – 17, 1972, edited by A. Frenkel and G. Marx, Vol. **1**, pp. 239–246.
Comment: See References

[502] B. Eman and D. Tadić, “Induced tensor interactions and second-class surrents,” in Proc. of the European Neutrino Conf. , “Neutrino’72”, Balatonfured, Hungary, June 11 – 17, 1972, edited by A. Frenkel and G. Marx, Vol. **1**, pp. 247–260.
Comment: See References

[503] E. Vatai, “Nuclear beta-decay experiments and second-class weak currents,” in Proc. of the European Neutrino Conf. , “Neutrino’72”, Balatonfured, Hungary, June 11 – 17, 1972, edited by A. Frenkel and G. Marx, Vol. **1**, pp. 261–267.
Comment:

[504] B. C. Barish *e*t al., “Measuremens of $\nu_\mu N$ and $\overline{\nu}_\mu N$ charged current total cross-sections,” in Proc. of the International Conf. on Neutrino Physics and Astrophysics, “Neutrino’77”, Baksan Valley, USSR, June 18 – 24, 1977, edited by M. A. Markov *e*t al., Vol. **2**, pp. 33–39.

[505] A. E. Astrayan *e*t al., “Charged current interactions at neutrino energies 6–30 GeV,” in Proc. of the International Conf. on Neutrino Physics and Astrophysics, “Neutrino’77”, Baksan Valley, USSR, June 18 – 24, 1977, edited by M. A. Markov *e*t al., Vol. bf2, pp. 52–57.

[506] P. C. Bosetti *e*t al., “Total csoss sections for charged-current neutrino and antineutrino interactions in BEBC,” in Proc. of the International Conf. on Neutrino Physics and Astrophysics, “Neutrino’77”, Baksan Valley, USSR, June 18 – 24, 1977, edited by M. A. Markov *e*t al., Vol. **2**, pp. 58–67.

[507] R. A. Singer, "High energy antineutrino–proton interactions," in Proc. of the International Conf. on Neutrino Physics and Astrophysics, "Neutrino'77", Baksan Valley, USSR, June 18 – 24, 1977, edited by M. A. Markov *e*t al., Vol. **2**, pp. 68–94.

[508] R. A. Singer, "Study of the reaction $\nu n \to \mu^- p$," in Proc. of the International Conf. on Neutrino Physics and Astrophysics, "Neutrino'77", Baksan Valley, USSR, June 18 – 24, 1977, edited by M. A. Markov *e*t al., Vol. **2**, pp. 95–104.

[509] H. Mulkens *e*t al., "Further results from the Gargamelle experiment," in Proc. of the International Conf. on Neutrino Physics and Astrophysics, "Neutrino'77", Baksan Valley, USSR, June 18 – 24, 1977, edited by M. A. Markov *e*t al., Vol. bf2, pp. 105–112.

[510] V. E. Barnes, "Review of charged current deep inelastic scaling distributions from the fermilab 15-foot bubble chamber," in Proc. of the International Conf. on Neutrino Physics, "Neutrino'78", Lafayette, Indiana, April 28 – May 2, 1978, edited by E. C. Fowler, pp. 217–242.
Comment: See Table I for deciphering code of Fermilab Experimental groups and Collaborations.

[511] R. T. Ross, "A study of the rection $\nu p \to \mu^- \pi^+ p$," in Proc. of the International Conf. on Neutrino Physics, "Neutrino'78", Lafayette, Indiana, April 28 – May 2, 1978, edited by E. C. Fowler, pp. 929–938.

[512] P. Schmid (Aachen-Bonn-CERN-Munich-Oxford Collaboration), "First results from a νp experiment in BEBC," in Proc. of the International Conf. on Neutrino Physics, "Neutrino'78", Lafayette, Indiana, April 28 – May 2, 1978, edited by E. C. Fowler, pp. .939–949.

[513] K. Myklebost (Gargamelle-Bari-Bergen-Milano-Strasbourg-Torino-London Collaboration), "Quasi-elastic production of lambda hyperons in antineutrino interactions at the CERN PS," in Proc. of the International Conf. on Neutrino Physics, "Neutrino'78", Lafayette, Indiana, April 28 – May 2, 1978, edited by E. C. Fowler, pp. C 37–C 41.

[514] M. Jonker *et al.* (Amsterdam-CERN-Hamburg-Moscow-Rome Collaboration), "Measurement of the cross section of neutrino scattering on electrons with a digitized calorimeter," in Proc. of the International Conf. on Neutrinos, Weak Interactions and Cosmology, "Neutrino'79", Bergen, Norway, June 18 – 22, 1979, edited by A. Haatuft and C. Jarlskog, pp. 219–229.

[515] N. J. Baker *e*t al., "Measurement of the ν_μ charged current cross section," in Proc. of the International Conf. on Neutrino Physics, "Neutrino'82", Balatonfured, Hungary, June 14 – 19, 1982, edited by A. Frenkel and L. Jenik, Suppl. to Vol. **2**, pp. 69–79.

[516] G. N. Taylor *e*t al., "Anti-neutrino–nucleon charged current interaction cross sections measured by the Fermilab 15' Ne-H_2 bubble chamber in a dichromatic beam," in Proc. of the International Conf. on Neutrino Physics, "Neutrino'82", Balatonfured, Hungary, June 14 – 19, 1982, edited by A. Frenkel and L. Jenik, Suppl. to Vol. **2**, pp. 81–85.

[517] C. Baltay, "Charm production by neutrinos as seen in hadronic final states," in Proc. of the International Conf. on Neutrino Physics, "Neutrino'82", Balatonfured, Hungary, June 14 – 19, 1982, edited by A. Frenkel and L. Jenik, Suppl. to Vol. **2**, pp. 109–138.

[518] A. E. Astrayan *e*t al., "Antineutrino quasielastic scattering in neon and total cross section for the charged current interactions in the energy range 10 to 50 GeV," in Proc. of the International Conf. on Neutrino Physics, "Neutrino'82", Balatonfured, Hungary, June 14 – 19, 1982, edited by A. Frenkel and L. Jenik, Suppl. to Vol. **2**, pp. 139–142.

[519] T. Kitagaki *e*t al., "Nuclear effect in neutrino interactions; comparison of the ν-Fe and ν-D interactions," in Proc. of the 12th International Conf. on Neutrino Physics and Astrophysics, "Neutrino'86", Sendai, Japan, June 3 – 8, 1986, edited by T. Kitagaki and H. Yuta, pp. 381–391.

[520] R. C. Allen *e*t al., "A study of $\nu_e e^-$ elastic scattering," in Proc. of the 12th International Conf. on Neutrino Physics and Astrophysics, "Neutrino'86", Sendai, Japan, June 3 – 8, 1986, edited by T. Kitagaki and H. Yuta, pp. 392–401.

[521] N. J. Baker *e*t al., "Strange particle production in neutrino–neon charged current interactions," in Proc. of the 12th International Conf. on Neutrino Physics and Astrophysics, "Neutrino'86", Sendai, Japan, June 3 – 8, 1986, edited by T. Kitagaki and H. Yuta, pp. 513–524.

[522] T. Kitagaki *e*t al., "Comparison of quasielastic scattering $\nu_\mu N \to \mu^- p$ and Δ^{++} production reaction $\nu_\mu p \to \mu^- \Delta^{++}$ in the BNL 7-foot deuterium bubble chamber," in Proc. of the 12th International Conf. on Neutrino Physics and Astrophysics, "Neutrino'86", Sendai, Japan, June 3 – 8, 1986, edited by T. Kitagaki and H. Yuta, pp. 525–539.

[523] G. T. Jones *e*t al., (Birmingham-CERN-Munich-Oxford-London Collaboration), "A measurement of the proton structure functions from neutrino–hydrogen and antineutrino–hydrogen charged current interactions," Z. Phys. C **44** (1989) 379–384.

[524] W. Wittek *e*t al. (BEBC WA59 Collaboration), “Production of $\rho^{+,-,0}(770)$, $\eta(550)$, $\omega(783)$ and $f_2(1270)$ mesons in $\overline{\nu}$ neon and ν neon charged current interactions,” Z. Phys. C **44** (1989) 175–186.

[525] G. T. Jones *e*t al., (Birmingham-CERN-Munich-Oxford-London Collaboration), “Inclusive $\rho^0(770)$ meson production in $\mathcal{N}p$ and $\overline{\nu}p$ charged current interactions,” Z. Phys. C **51** (1991) 11–24.

[526] M. Y. Safin, B. K. Kerimov and D. Ishankuliev, “On the role of polarization effects in elastic lepton-nucleon scattering as a test of gauge theories,” Yad. Fiz. **32** (1980) 765–775 [Sov.J.Nucl.Phys. **32** (1980) 394–399].

[527] L. A. Mikaelyan and S. A. Fayans, “Elastic scattering of neutrinos by nuclei,” Yad. Fiz. **32** (1980) 748–755 [Sov. J. Nucl. Phys. **32** (1980) 385–389].

[528] S. I. Bilenkaya, Y. M. Kazarinov, and L. I. Lapidus, “Protom form factors,” Zh. Eksp. Teor. Fiz. **60** (1971) 460–467 [Sov. Phys. J. Exp. Theor. Phys. 33 (1971) 247–250].

[529] S. I. Bilenkaya, Y. M. Kazarinov, and L. I. Lapidus, “Protom electromagnetic form factors,” Zh. Eksp. Teor. Fiz. **61** (1971) 2225–2230 [Sov. Phys. J. Exp. Theor. Phys. **34** (1972) 1192–1194].

[530] S. I. Bilenkaya, S. M. Bilenky, Y. M. Kazarinov, and L. I. Lapidus, “The proton electromagnetic form-factor and heavy hypothetical particles,” Zh. Eksp. Teor. Fiz. Pisma **19** (1974) 613–616 [JETP Lett. **19** (1974) 317].

[531] S. I. Bilenkaya, N. B. Skachkov, and I. L. Solovtsov, “Proton electromagnetic form factor in the vector dominance model with modifications at small distances,” Yad. Fiz. **26** (1977) 1051–1057 [Sov. J. Nucl. Phys. **26** (1977) 556–559]; see alpso preprint JINR-E2-10-404.

[532] S. I. Bilenkaya and Y. M. Kazarinov, “Neutron form factors (analysis of data on elastic ed scattering),” Yad. Fiz. **32** (1980) 742–747 [Sov. J. Nucl. Phys. **32** (1980) 382–385]; see also preprint JINR-P1-80-59.

[533] S. I. Bilenkaya and N. P. Nedelcheva, “Elastic scattering of neutrino and antineutrinos by protons in the Weinberg-Salam theory,” Yad. Fiz. **36** (1982) 487–493 [Sov. J. Nucl. Phys. **36** (1982) 285–288]; see also preprint JINR-E2-81-763.

[534] S. I. Bilenkaya, S. Dubnicka, A. Z. Dubnickova, and P. Strizenec, “Towards the results of global analyses of data on nucleon electromagnetic structure,” Nuovo Cim. A **105** (1992) 1421–1434; see also preprint JINR-E2-91-475.

[535] D. Y. Bardin and V. A. Dokuchaeva, “On radiative corrections to the process $\nu N \to \nu X$,” Yad. Fiz. **36** (1982) 482–486 [Sov. J. Nucl. Phys. **36** (1982) 282–284]; see also preprint JINR-P2-81-552.

[536] D. Y. Bardin and V. A. Dokuchaeva, “On the radiative corrections to the neutrino deep inelastic scattering,” preprint JINR-E2-86-260 (unpublished).
Comment: Cited by Seligman [181].